

LEVEL II

1

AGARD-LS-110

AGARD-LS-110

AGARD

ADVISORY GROUP FOR AEROSPACE RESEARCH & DEVELOPMENT

7 RUE ANCELLE 92200 NEUILLY SUR SEINE FRANCE

AD A 087976

AGARD LECTURE SERIES No. 110

**Atmospheric Electricity –
Aircraft Interaction**

DTIC
ELECTE
AUG 19 1980
S D C

NORTH ATLANTIC TREATY ORGANIZATION



FILE COPY

DISTRIBUTION AND AVAILABILITY
ON BACK COVER

① 11 AGARD-LS-110

NORTH ATLANTIC TREATY ORGANIZATION
ADVISORY GROUP FOR AEROSPACE RESEARCH AND DEVELOPMENT
(ORGANISATION DU TRAITE DE L'ATLANTIQUE NORD)

AGARD Lecture Series No. 110

④
ATMOSPHERIC ELECTRICITY – AIRCRAFT INTERACTION

④
1234
DTIC
ELECTE
AUG 19 1980

4000
The material in this publication was assembled to support a Lecture Series under the sponsorship of the Avionics Panel and the Consultant and Exchange Programme of AGARD, presented on 9–10 June 1980 in London, UK; 12–13 June 1980 in Munich, Germany and 24–25 June 1980 at Menlo Park, California, USA.

This document has been approved

THE MISSION OF AGARD

The mission of AGARD is to bring together the leading personalities of the NATO nations in the fields of science and technology relating to aerospace for the following purposes:

- Exchanging of scientific and technical information;
- Continuously stimulating advances in the aerospace sciences relevant to strengthening the common defence posture;
- Improving the co-operation among member nations in aerospace research and development;
- Providing scientific and technical advice and assistance to the North Atlantic Military Committee in the field of aerospace research and development;
- Rendering scientific and technical assistance, as requested, to other NATO bodies and to member nations in connection with research and development problems in the aerospace field;
- Providing assistance to member nations for the purpose of increasing their scientific and technical potential;
- Recommending effective ways for the member nations to use their research and development capabilities for the common benefit of the NATO community.

The highest authority within AGARD is the National Delegates Board consisting of officially appointed senior representatives from each member nation. The mission of AGARD is carried out through the Panels which are composed of experts appointed by the National Delegates, the Consultant and Exchange Programme and the Aerospace Applications Studies Programme. The results of AGARD work are reported to the member nations and the NATO Authorities through the AGARD series of publications of which this is one.

Participation in AGARD activities is by invitation only and is normally limited to citizens of the NATO nations.

The content of this publication has been reproduced
directly from material supplied by AGARD or the authors.

Published May 1980

Copyright © AGARD 1980

All Rights Reserved

ISBN 92-835-1361-4



Printed by Technical Editing and Reproduction Ltd
Harford House, 7-9 Charlotte St, London, W1P 1HD

FOREWORD

This AGARD Lecture Series No. 110 on Atmospheric Electricity – Aircraft Interaction is sponsored by the Avionics Panel of AGARD and is implemented by the Consultant and Exchange Programme.

The potential susceptibility of aircraft to atmospheric electricity hazards (such as lightning and static charging phenomena) appears as an increasing threat to future aircraft for two reasons: on the one hand, more and more sensitive solid-state electronics and micro-processors will be used in the future on flight critical equipment, as can be anticipated from advanced guidance and control hardware developments; on the other hand, new structural materials, such as dielectrics and composites, will be extensively used for aircraft, leading to potential problems due to surface charges and reducing the electromagnetic shielding protection offered by the conventional metallic skins on present-day vehicles.

Starting with fundamentals of atmospheric electricity phenomena, the Lecture Series reviews the hazards, criteria, testing and avionics protection, and provides insights from both pilot and design perspectives. In view of the above, this Lecture Series should be of interest to aircraft manufacturers, airline operators, government and industrial research establishments, and avionics engineers.

G.A. DuBRO
Lecture Series Director

Accession For	
NTIS GRA&I	<input checked="checked" type="checkbox"/>
DOC TAB	<input type="checkbox"/>
Unannounced	<input type="checkbox"/>
Justification	
By	
Distribution/	
Availability Codes	
Dist	Avail and/or special
A	

LIST OF SPEAKERS

Lecture Series Director: Mr G.A.DuBro
US Air Force Flight Dynamics
Laboratory
Wright-Patterson Air Force Base
Dayton, Ohio 45433
USA

SPEAKERS

Mr D.W.Clifford
P.O.Box 516
McDonnell Aircraft Company
St.Louis, Missouri 63166
USA

Dr P.F.Little
UKAEA Culham Laboratory
Lightning Studies Unit
Abingdon, Oxfordshire OX14 3DB
UK

Prof. Dr Ing. R.P.Muhleisen
Institute of Astronomy
University of Tübingen
Aussenstelle Weissenau
7980 Ravensburg/Rasthalde
Germany

Dr J.Nanevicz
Electromagnetic Sciences Laboratory
Stanford Research Institute International
333 Ravenswood Avenue
Menlo Park, California 94025
USA

Mr J.A.Plumer
Lightning Technologies Incorporated
560 Hubbard Avenue
Pittsfield, Massachusetts 01201
USA

Dr J.Taillet
ONERA
29 Avenue de la Division Leclerc
92320 Chatillon-sous-Bagneux
France

CONTENTS

	Page
FOREWORD	iii
LIST OF SPEAKERS	iv
	Reference
ATMOSPHERIC ELECTRICITY INTERACTIONS WITH AIRCRAFT – AN OVERVIEW by G.A.DuBro	1
AIRCRAFT MISHAP EXPERIENCE FROM ATMOSPHERIC ELECTRICITY HAZARDS by D.W.Clifford	2
PHENOMENOLOGY OF LIGHTNING/AIRCRAFT INTERACTION by R.P.Mühleisen	3
SUSCEPTIBILITY OF AVIONICS TO LIGHTNING INDIRECT EFFECTS by J.A.Plumer	4
MODELS FOR ASSESSING HAZARDS DUE TO LIGHTNING by P.F.Little	5
LIGHTNING TEST CRITERIA FOR AIRCRAFT AVIONICS SYSTEMS by D.W.Clifford	6
LIGHTNING TESTING FOR AIRCRAFT AVIONICS SYSTEMS by D.W.Clifford	7
THE COUPLING OF LIGHTNING FIELDS INTO AIRCRAFT AND CABLES by P.F.Little	8
PROTECTION OF AIRCRAFT AVIONICS FROM LIGHTNING INDIRECT EFFECTS by J.A.Plumer	9
LIGHTNING EFFECTS ON AIRCRAFT: A COCKPIT PERSPECTIVE by J.A.Plumer	10
BASIC PHENOMENOLOGY OF ELECTRICAL DISCHARGES AT ATMOSPHERIC PRESSURE by J.Taillet	11
STATIC CHARGING EFFECTS ON AVIONIC SYSTEMS by J.E.Nanevicz	12
ALLEVIATION TECHNIQUES FOR EFFECTS OF STATIC CHARGING ON AVIONICS by J.E.Nanevicz	13
AIRCRAFT STATIC CHARGING TESTING by J.Taillet	14
BIBLIOGRAPHY	B

ATMOSPHERIC ELECTRICITY INTERACTIONS WITH AIRCRAFT: AN OVERVIEW

by

Gary A. DuBro
Air Force Wright Aeronautical Laboratories
Wright-Patterson Air Force Base, Ohio 45433
USA

SUMMARY

Concern for the vulnerability of aircraft flight-critical and mission-critical avionics to atmospheric electricity hazards has increased over the last fifteen years. The major hazards of concern are lightning and static electrification. Two primary factors have contributed to a potentially increased threat to new generation aircraft: (1) increasingly widespread use of sensitive microelectronics in flight-critical and mission-critical electronic and electrical systems; and (2) the reduced electromagnetic shielding afforded by many advanced aircraft structural materials.

In this paper, a description of the atmospheric electricity interaction with aircraft and the manner in which it impacts the aircraft avionics is summarized. Key areas of pertinent research and development are identified and the present state-of-the-art in each of these key areas is presented.

INTRODUCTION

Have you ever stood outside, mesmerized by an approaching thunderstorm? It's a show as spectacular as any you might see. Just close your eyes and picture it—the dark swirling clouds circling overhead, the crack of some phantom thunder whip, the darting path of lightning streaking across the sky. Its awesomeness is indeed something to behold.

To aircraft pilots, such acts of nature are also something to avoid if at all possible. The effects of lightning, hail, and turbulence have caused a considerable amount of damage to aircraft, with the integrity of flight itself a critical concern to smaller aircraft. With foresight to the future trends of modern aircraft design, the concern will manifest itself to all classes of vehicles, unless appropriate protection is incorporated. Of those hazards noted, atmospheric electrical phenomena pose the most severe threat to the new generation of sophisticated aircraft now emerging. Such is the topic for this lecture series—the interaction of aircraft with atmospheric electrical phenomena. A special emphasis will be placed on the impact of such phenomena as they affect aircraft avionics and the associated electrical systems.

With respect to the adverse impact to modern-day aircraft, there are two primary naturally-occurring electrical phenomena—lightning, and static electrification. The most familiar and dramatic of these is, of course, the lightning flash. Indeed, since the beginnings of mankind, lightning has aroused man's curiosity of the world about him, and imparted to him the omnipresence of his deities and a feeling of his own being and smallness. Lightning certainly represents one of nature's most ostentatious shows of power. It has, to many, connotated a world of the occult, of black-garmented magicians and sorcerers, of Merlin himself, beckoning evil spirits, or of the great Norse God "Thor" grasping a thunderbolt in each hand. The spectacle of lightning has been seen almost everywhere in the world. At any one instant, there may be several thousand lightning discharges occurring over the surface of the earth. Over the centuries, lightning has spawned the efforts of many scientists and engineers to study its grandeur, and its impact on mankind. Much has been done to dispel the sanctity of its mystery. From the eighteenth century experiments of Benjamin Franklin and his famous kite to the more recent electromagnetic measurements from around the world and the rocket-lightning triggerings in Florida¹ and St. Privat D'Allier², man has actively reached out to understand. Be this as it may, his present knowledge of the subject still remains far from complete or adequate.

LIGHTNING

The detailed description of what is presently known, as well as those present ongoing efforts to characterize the phenomenon will be discussed at great lengths later in the lecture series, however, as a matter of introduction, a short description will now be presented. Suffice it to say the occurrence of lightning is usually associated with some form of charge separation process in a cloud, and the subsequent creation of positive and negative charge centers. When the local potential near one of the charge centers exceeds the threshold for atmospheric breakdown, a discharge results. If the event occurs within a cloud, it is called an intra-cloud lightning; if the event occurs between clouds, it is called an inter-cloud event. Another common circumstance is that during the charge separation process, the base of the cloud becomes negatively charged. In opposition to this, an image charge of opposite polarity develops on the earth. As in the inter- and intra-cloud events, when the local conditions are such to support atmospheric breakdown, a discharge occurs. A lightning channel will be formed which in some random step-wise fashion propagates to the ground. This will be followed by a luminous high current surge through the already-established ionized channel. This entire process is called cloud-to-ground lightning.

Figure 1 illustrates the cloud-to-ground process including the attachment to an aircraft. In the first scene (Figure 1a), the initial lightning discharge has been initiated. This portion of the event is called the stepped-leader phase. It is seen that as the lightning path approaches the aircraft, "streamers" emanate from the aircraft extremities. In Figure 1b, the lightning stepped-leader has attached to one of the streamers and subsequently enters the aircraft skin. The current levels associated with the stepped-leader phase are on the order of a thousand amperes, however, the time rate of change of the local electric field may be exceptionally high. In the next scene (Figure 1c), the lightning channel leaves the aircraft at some extremity and jaggedly winds its path towards the earth. As in the case of the aircraft, upward streamers from the ground can be observed. In scene 1d, contact between the stepped-leader and the upward ground streamer has taken place, and a large current surge races back up the established ionized path. This is referred to as the "return stroke". The average current magnitude associated with this phase of the event is approximately 30,000 amperes, with some small percentage of return strokes having been recorded at in excess of 200,000 amperes. Recent measurements indicate a characteristic rise time of the return stroke to reach peak current on the order of 100 nanoseconds³. Eventually, the return stroke will reach the cloud; however, the lightning event is not yet complete. As the return stroke reaches into the cloud to neutralize nearby charge centers, considerably more branching and diffusion occurs as the process becomes one of neutralization over a considerably larger volume. The current levels of this phase are much less than those experienced during the return stroke phase, say, on the order of hundreds of amperes. The initial portion of this phase is called the intermediate current phase, and the later portion is referred to as the continuing current phase. As the process taps new charge centers in the cloud, a repeat of the entire process occurs, except that an ionized channel already exists. The repeat process is referred to as the "restrike" and usually occurs several times. An idealized waveform is shown in Figure 2 with the significant phases of the lightning event identified.

STATIC ELECTRIFICATION AND DISCHARGE PROCESSES

The second type of atmospheric electrical activity which is to be discussed in this lecture series is that of static electrification, and the subsequent resulting discharge processes. Static electrification comes about as the result of two materials coming into contact, and then being separated. As a result of this contact and separation, a charge separation process occurs, and the two materials become oppositely charged. This is indeed the situation when an aircraft comes in contact with precipitation or particulate matter during flight.

Precipitation, such as ice or rain, impacts the aircraft. As the process is continued, the charge on the skin of the aircraft is increased, thereby increasing the aircraft potential. When the localized potential exceeds the threshold for atmospheric breakdown, discharges may occur, usually at the aircraft extremities and antenna ends. These discharges can produce a continuous ultraviolet glow, particularly visible at night, called St. Elmo's Fire or corona. Figure 3 illustrates corona phenomena on a laboratory model of an aircraft. Static electricity will be the topic of four papers within this lecture series, and will not be discussed in depth in this paper.

HAZARDS TO AIRCRAFT

Atmospheric electricity interactions with aircraft can result in numerous types of damage. For the case of lightning, the lightning channel will generally attach to an aircraft extremity, and subsequently pass the current through the aircraft skin. Such an event can result in damage of two basic types. The most obvious type is that of physical damage resulting from a direct attachment. Such damage is characterized by burning, eroding, blasting, etc., and is a consequence of either the extreme heat loading, an accompanying acoustic shock wave, or deforming magnetic forces, all of which are associated with the high current aspects of lightning. Such effects have been commonly referred to as "direct effects". Since attachment occurs at aircraft extremities, direct damage is usually observed at radomes, pitot booms, external antennas, and wing lights. Figure 4 is an example of direct effects damage to an aircraft radome. On rare occasions the currents have penetrated the skin via an attached internal electrical cable or via the burn-through of the aircraft skin. Potentially, more serious damage can result, such as avionics burnout or even more seriously, fuel tank explosions. In general, however, direct physical damage does not pose a safety of flight concern, although it is indeed a maintenance concern. Technology to address the current penetration issue is well developed, and is now in common usage in aircraft design.

With the passage of significant electrical current magnitude through the aircraft skin, and as a result of localized arcing and electrical streamers, fast changing electric and magnetic fields are produced. Nearby lightning also produces electromagnetic fields which intercept the aircraft. In either case, these fields can couple voltage transients into the internal aircraft wiring, and subsequently to the aircraft avionics. The voltage levels of such transients may be sufficient to cause damage and/or upset to the newer generation avionics systems. The type of damage which can occur to sensitive microelectronic components as the result of transient overvoltage is shown in the photomicrograph (Figure 5). Effects associated with this type of interaction are aptly referred to as "indirect effects". Static discharges can likewise cause transient overvoltage problems as is the case with lightning. It is this type of damage, i.e., "indirect effects", which poses the most severe threat to avionics, and which is to be emphasized throughout the lecture series. The specific types of damage to aircraft, the resulting causes, and identification as to the potential criticality of such damage to the aircraft are noted

in Table I. Both direct and indirect effects damage are listed in that table. It has been reported that the incidence of lightning to commercial aircraft is approximately once in 3000 hours of flight¹, or in more practical terms, about once per year. US Air Force experience suggests a rate somewhat less, about one strike every 20,000 hours. In the time frame 1963 to 1978, no less than nine US aircraft have been lost as the result of a lightning strike. The point to be made here is that from an aircraft designer's or an aircraft pilot's perspective, lightning is not an infrequent occurrence. It should be noted that as a result of these losses, various design changes have been made.

Over the last decade, outstanding improvements in aircraft performance have been realized. This progress is, to a great degree, attributable to two fast-advancing technologies: microelectronics and advanced structural materials. Consistent with the use of these emerging technologies has been a change in aircraft design philosophy, so as to take fullest advantage of the benefits that the technologies might offer. Concepts such as fly-by-wire, digital engine controls, and propulsion/flight control integration, to name out a few, have become a reality. The trend to the future promises even greater capabilities. However, the incorporation of these technologies in the new generation aircraft is not without some attendant concern. As pertains to atmospheric electricity hazards, the concern has prompted a comprehensive examination of the impact of electromagnetic coupling on advanced systems.

The concerns are three-fold. First, the avionics and electrical systems use microelectronics which operate at substantially lower power levels than earlier electronic components, and hence, are more sensitive to transient overvoltage. Such overvoltage could result in system upset or malfunction, or even component burnout. Secondly, newer materials such as graphite or boron-epoxy composites do not provide the same degree of electromagnetic shielding in the 10 kHz to 1 MHz frequency band as has been afforded by conventional all-aluminum aircraft. Within the specified frequency band, the use of composites subjects the internal avionics subsystems to higher levels of electromagnetic energy. And thirdly, the microelectronics are being incorporated into flight critical systems, systems that, if affected, could jeopardize the aircraft safety. To reiterate, it would appear that advanced-electronics flight-critical and mission-critical avionics which are to be utilized in advanced aircraft are inherently more sensitive to upset/malfunction or physical damage, and are to be used in airframes which allow increased levels of coupling energy to pass through the skin to those internal avionics. Indeed, appropriate protection techniques must be integrated to remove the possible hazard.

APPROACH TO THE PROBLEM

In order to address the problem, i.e., to insure the safety of flight of advanced technology aircraft in an adverse atmospheric electromagnetic environment, a systematized approach has been developed. There are four basic areas of effort. The relationship between these areas is schematically treated in Figure 6. The first basic area is the hazard characterization area and determination of the intrinsic hardness levels of electronics and materials. The inputs from accident investigations provide some assistance in the identification of aircraft vulnerability to the atmospheric electricity hazards. However, the major effort is in understanding the hazard itself, specifically in those ways it may effect the aircraft. The second primary area is that of assessment methodology. This area has two complementary facets—testing/simulation and analytics. The work in this area is concentrated on increasing the general understanding of the physics of the aircraft-lightning interaction and on developing specific laboratory threat simulation testing techniques. The prime objective of this testing development activity is to provide design inputs for aircraft protection as well as for qualification for safety of flight. This area is coupled closely with the characterization area in that the input source driver for simulations is an output of characterization research. The third area concerns the identification of hardening options for potentially vulnerable subsystems. This includes the baseline definition for hardness for state-of-the-art avionics and subsystems and determination of the effectiveness of the various hardening options. The aircraft protection and hardening area is also tied to the assessment/methodology area in that once the impact of the hazard has been assessed, an input to more effectively design appropriate level of protection may be made. The fourth and final area is that of optimized hardening and qualification. This includes establishing trade-offs between hardening options as dictated by system performance, hardening efficiency, system criticality, cost, maintainability and reliability, and ease of incorporation. The development of generic guidelines based upon the above-noted trade-offs and validation of the optimization are follow-on steps. Subsequent to all four major areas will be the establishment of standards and specifications for the testing of aircraft to atmospheric electrical hazard threats. Major aspects of the technology roadmap are summarized below.

CHARACTERIZATION OF THE THREAT

A rather extensive data base has been established over the past forty years, most of which has been taken from ground-based stations. These measurements have been obtained worldwide by noted atmospheric electricity phenomenologists. From their work has come most of what is known of the mechanism by which thunderstorms develop, and of the detailed progress of a lightning flash.

In addition to the ground-based data, there have been airborne measurement programs. Fitzgerald made the initial measurements in the early 1960's in the US Air Force Rough Rider Program². The major problem with the above-noted measurements, both airborne and ground-based, was the lack of instrumentation sufficiently responsive in the time/frequency

domains of interest i.e., the primary resonance frequency of the aircraft. It has only been recently that the state-of-the-art in sensing and recording instruments necessary to characterize lightning in the frequency domain of maximum coupling to aircraft has been possible.

The first such program to utilize the high speed equipment was a joint NASA/Air Force Flight Dynamics Laboratory (AFFDL) program conducted in association with the 1976 Thunderstorm Research International Program (TRIP 76)^{6,7}. Because of numerous reasons, up until that time it had been surmised by the aircraft/lightning community that the threat posed to aircraft via electromagnetic coupling was a relatively low frequency phenomena. The work by Cianos and Pierce⁸ had analyzed considerable amounts of data from many investigators to define the power spectral density of lightning. The results of the analysis showed the peak to occur in the 1-20 kHz range, and the associated energy to fall off as $1/f$ or $1/f^2$. The TRIP 76 experience clearly demonstrated that lightning has significant high frequency content which could couple into the aircraft and its associated avionics. Up until that time, the energy acceptance of the aircraft was considered to be a low frequency phenomenon. The TRIP 76 results quite definitely showed that the aircraft indeed, acts as an antenna, and accepts energy in a frequency range dependent on the aircraft configuration; both the external structure and the internal wire lengths. AFFDL has continued to pursue the characterization effort since TRIP 76, and has made steady progress in developing the instrumentation system so that a clearer understanding of threat is known⁹. Similar efforts are presently underway by NASA Langley Research Center¹⁰, and in France¹¹.

Added information may be obtained as a result of lightning triggering experiments. This approach has been successfully demonstrated by Newman¹ in the USA, and Fleux and Gary² of St. Privat D'Allier in France, using rockets with trailing wires. Such experiments may provide a controlled means of studying lightning, but at present, more attention is being directed toward the triggering process itself, rather than the measurement of lightning characteristics.

ASSESSMENT METHODOLOGY

The assessment function is viewed as having three purposes: (1) understanding the physics of the interaction, (2) establishing engineering design and protection criteria, and (3) qualifying specified test objects to some threat level. Two complementary approaches are used in the assessment process—experimentation and analytics, both of which will be discussed at length in the lecture series. Active research is presently being pursued with both approaches.

SIMULATION AND TESTING

A complete simulation of a natural lightning flash cannot be achieved in the laboratory, thus it is necessary to develop tests which reproduce only portions of the event. This is accomplished with the aid of high voltage or high current generators. The high voltage characteristics of lightning have been shown to establish probable attachment points, likely breakdown paths, and streamer effects; high currents are used in the assessment of direct and indirect effects.

In an attempt to standardize test procedures and test waveforms for the aerospace community, a special committee under the Society of Automotive Engineers (SAE) was established in the 1970's. The committee, called the AE4L, developed a document describing waveforms and tests criteria. The document was aptly titled "Lightning Test Waveforms and Techniques for Aerospace Vehicles and Hardware".¹² A similar document was generated in the UK.¹³ The information presented in these reports is based on the best available knowledge of the natural lightning environment coupled with the practical consideration of state-of-the-art laboratory equipment and techniques.

Both direct effects and indirect effects testing procedures are specified. An excellent review of the state-of-the-art in lightning testing can be found in the proceedings of the "Conference on Certification of Aircraft for Lightning and Atmospheric Electricity Hazards".¹⁴ A brief description of these tests now follows:

Full Size Hardware Attachment Point Tests

This attachment point test is conducted on full size structures that include dielectric surfaces in order to determine the detailed attachment points on the external surface. If the entire surface is nonmetallic, however, the test determines the path taken by the lightning arc in reaching a metallic structure. A high voltage impulse generator, such as a Marx-type generator, is used for this test. The gap spacing between the generator and the test object is critical as is the waveshape of the applied wave. Since the test specification is based on information now known on the natural phenomena, it cannot be stressed enough that all new and future measurements of lightning acquired by in-flight as well as ground based measurements will benefit simulation testing in accuracy and validity.

Direct Effects - Structural

These tests determine the direct effects which lightning currents may produce in structures. Simulated lightning current waveforms are applied. The attachment points are established before testing, and it is the waveshape magnitude and

dwelt time that are important in this type of test.

Direct Effects - Combustible Vapor Ignition Via Skin or Component Puncture, Hot Spots or Arcing

The objective of these tests is to ascertain the possibility of combustible vapor ignition as a result of skin or components puncture, hot spot formation, or arcing in or near fuel systems or other regions where combustible vapors may exist.

Tests are run on full scale fuel tanks, wings, or mockups of both to determine ignition sources. Photography is the means to determine if sparking is present inside the test chamber.

Direct Effects - Streamers

Electrical streamers initiated by high electric fields represent a possible ignition source for combustible vapors. The objective of this test is to determine if streamers may be produced in regions where vapors exist.

Direct and Indirect Effects - External Electrical Hardware

The objective of the direct effects tests is to determine the amount of physical damage which may be experienced by externally mounted electrical components, such as pitot tubes, antennas, navigation lights, etc., when directly struck by lightning. The indirect effects test is performed to determine the conducted currents and surge voltages, and induced voltages on these electrical components.

Model Aircraft Lightning Attachment Point Test

The objective of the model test is to determine the locations on the vehicle that direct lightning strikes are likely to attach. Size of the models (1/30 to 1/10 full scale) is important, as is placement of the high voltage electrode distance from the model and the waveform risetime.

Full Size Hardware Attachment Point Test—Swept Stroke Test

It is possible when lightning attaches to an aircraft for the arc to sweep across the surface of the wing or fuselage, attaching and re-attaching, as the aircraft moves forward relative to the lightning channel.

- The dwell time of an arc is a function of the lightning flash characteristics, surface properties of the aircraft skin, and aircraft speed. Swept stroke attachment point and dwell time phenomena are of interest for two main reasons. First, if there is a nonmetallic surface along the path over which the arc may be swept, the swept stroke phenomena may determine whether the nonmetallic surface will be punctured or whether the arc will pass harmlessly across it to the next metallic surface. Second, the dwell time of an arc on a metallic surface is a factor in determining if sufficient heating may occur at a dwell point to burn a hole or form a hot spot capable of igniting combustible mixtures or causing other damage.

Indirect Effects - Complete Vehicle

The objective of this test is to measure induced voltages and currents in electrical wiring within a complete vehicle. Complete vehicle tests are intended to identify circuits which may be susceptible to lightning induced effects.

The test involves the application of a scaled down unidirectional waveform representative of a natural lightning stroke or a damped oscillatory current waveform. The results of these tests are then scaled up to full threat level to determine the actual threat to the system measured. Other test procedures which accomplish the same objective are presently being examined, but as yet, have not been incorporated into the SAE-AE4L document.

ANALYTICS

It should first be recognized that electromagnetically, an aircraft is a very complex structure, and hence, does not easily lend itself to a precise prediction of induced effects. Analytical efforts complement experimental research programs in determining the governing physics, and hence, give the aircraft/lightning community a direction for aircraft qualification and engineering testing, and assist in the selective integration of hardening options.

Three specific aspects of the lightning aircraft interaction have been addressed by the analytical community. These include (1) the lightning arc channel itself, (2) the ground-based lightning simulation tests, and (3) the electromagnetic coupling to internal electrical wiring. The primary objectives of these efforts have been to understand the physical processes involved in the complex coupling process.

Until recently, only a paucity of work on the various aspects of lightning arc channel modeling had been reported. A renewed interest has been spawned recently in an attempt to more accurately quantify not only the physics of the channel propagation, but the

associated time and frequency characteristics, the influence of altitudes on waveform, the generation of electromagnetic fields, and the impact of an aircraft within the channel.

The technical area of ground-based simulation testing for induced coupling effects has in itself been developed for only a decade, with by far the greatest effort going into understanding by laboratory experimentation. The work accomplished at AFFDL by McCormick, et al.,¹⁵ and at Culham by Burrows¹⁶ represents analytical efforts to examine justification for testing. The major questions which have plagued this area include linearity, scaling, facility effects, and aircraft effects. Additional work on the influence of ground effects and static charging has also been accomplished. The Air Force Weapons Laboratory has conducted extensive work in the related area of nuclear electromagnetic pulse testing, but until very recently has provided minimal input into analytics for the lightning test area. Some analytical treatment has been accomplished in other aspects of testing—specifically fuel volatility to spark ignition, long arc attachments, and puncture on metal skins.

The third major area of effort has been directed toward the understanding of the governing physical process for the electromagnetic coupling of fields generated by lightning strokes through aircraft skins and outer structures. Some initial efforts were reported by Fisher, et al. (1973, 1977), Strawe, et al. (1978),¹⁹ and Burrows (1975, 1977).^{16, 20} The earliest work addressed diffusive and aperture coupling via magnetic field coupling. Magnetic field coupling was pursued because, initially, the major degree of coupling was thought to be low frequency dominated, and the influence of the aircraft configuration on the level of coupling was assumed negligible. Subsequently, through extensive ground tests and the results of the TRIP 76 AFFDL/NASA effort, capacitive effects/electric field coupling at the aircraft electromagnetic resonant frequencies (1-30 MHz) were investigated. The discovery of transmission line effects also prompted some additional analytical research. As in the testing area, AFWL has developed a vast data base in electromagnetic coupling to aircraft within the frequency range of interest, but as yet, has had little impact in the lightning analytics area.

HARDENING

The heart of whether an aircraft is vulnerable to an atmospheric electricity threat, is the adequacy of protection put into the aircraft. However, the incorporation of advanced microelectronics into flight critical systems has significantly complicated the design approach to the previously noted threats. There is no one method applicable to all situations or configurations. The hardening process must be carefully blended with other design considerations—criticality of the system being protected, aircraft performance, life-cycle considerations, effectiveness of the hardening options, and ease of implementation. There are numerous options to each requirement, but one must optimally choose the option which satisfies the trade-off considerations.

For the case of protection against direct effects, technology has been continually evolving for thirty years. External hardware (e.g., air data probes, antennas, radomes, navigation lights, windshields, canopies and other objects mounted on the external surface of the aircraft) have had to be designed to safely conduct lightning currents, and to prevent surges from being coupled into associated electrical wiring, if present. Arc surge suppressors and shielded cables have been developed to limit induced voltages caused by lightning surge currents. Metal diverter strips have been applied to radomes and canopies to prevent puncture of dielectric covers from lightning strikes. Fuel system hardware (e.g., fuel tanks, access doors, filler caps, quantity probes, drains, vents, plumbing and other components in contact with fuel) have received special attention because of the catastrophic consequences of fuel vapor ignition that can be caused by arcing, sparking, and hot spots due to lightning attachment. In some cases flame arrester and surge tank protection are used to minimize the danger from sparking. Flight control hardware (e.g., control surface hinges and bearings, actuators, and cables) must be capable of conducting lightning surge currents without damage or freeze-up.

For indirect effects, hardening techniques have generally been divided into two complementary types: (1) topological and (2) functional. The first type is the protection provided at various layers of an aeronautical system (e.g., hull, compartments, cables, and subsystems). Techniques include ports-of-entry closures, isolation devices, shielding, suppression, and terminal protection devices. The objective is to reduce the induced lightning transients to a level such that neither upset nor damage is a problem. The second type is protection provided against both upset and damage by selecting components, design redundancy (component, circuit, and subsystems), coding and signal processing techniques, circumvention techniques, and designing to increase failure thresholds for subsystems.

A LOOK TO THE FUTURE

Great strides have been taken by the technical community over the last decade in addressing the basic concern of avionics susceptibility to lightning and static electricity hazards. First and foremost has been the identification of the key research areas required to resolve the problem and the establishment of meaningful interrelationships between these areas. One perception of the research areas and those interrelationships has been presented in this paper as a technology roadmap. Within the guidelines of the prescribed roadmap, it would appear that the "lightning" community is on the threshold of establishing the critical parameters and their associated magnitudes. Three major airborne programs and numerous ground measurement programs are presently underway; essential to the successful accomplishment of these efforts is the incorporation of high frequency

recording capabilities.

Efforts to understand the electromagnetic coupling to internal aircraft wiring have seen a blended approach between theory and experiment. This is recognized as a very challenging problem, and the application of basic elements from nuclear electromagnetic pulse (NEMP) protection technology development is presently being pursued. As regards testing, a set of standardized test procedures is under review by many countries and by NATO. The elements of these test standards have been developed within the last decade. Efforts to establish a more firm scientific basis for many of the testing procedures are likewise underway.

Hardening technology is available for most atmospheric electricity indirect effects problems; however, the issue is how to optimally use the available options, and selectively integrate those options to minimize impact on cost, performance, and design, and at the same time, guarantee integrity of flight in advanced technology aircraft. The incorporation of new technologies such as fiber optics should see widespread use in the future, and greatly aid in hardening efforts.

As has been seen in this paper, the solution to those problems posed by the atmospheric electricity interactions with advanced state-of-the-art aircraft requires the blending of many diverse disciplines so that aircraft can be operational in an all-weather environment.

It is paramount that one not lose sight of the basic objectives of the research discussed herein. We wish to encourage and support the maximum utilization of the newly emerging technologies of microelectronics and advanced structural materials. Indeed, these technologies could significantly advance aircraft operational capabilities. The effort of the "lightning/aerospace" community is intended to guarantee that no compromise of flight safety will occur as a result of the incorporation of such technologies. However, an equally significant goal, not to be forgotten, is to insure that the safety guarantee be accomplished in such a manner as to minimally impact the benefits derived from the opportunities provided by such technology.

REFERENCES

1. Newman, M.M., Stahmann, J.R., and Robb, J.D., "Experimental Study of Triggered Natural Lightning Discharges", 1967, Federal Aviation Administration Reprint No. DS-67-3.
2. Fieux, R.P., Gary, C.H., Hutzler, B.P., Eybert-Berand, A.R., Hubert, P.L., Perroud, P.H., Hamelin, J.H., and Person, J.M., "Research on Artificially Triggered Lightning in France", IEEE Transactions on Power Apparatus and Systems, Volume PAS-97, #3, May/June 1978, p. 725-733.
3. Uman, M.A., Clifford, D.W., and Krider, E.P., "A Case for Submicrosecond Rise Time Lightning Current Pulses for Use in Aircraft Induced Coupling Studies", IEEE International Symposium on Electromagnetic Compatibility, 1979, p. 143-149.
4. Fisher, F.A. and Plumer, J.A., "Lightning Protection of Aircraft", 1977, NASA Reference Publication 1008, p. 71.
5. Fitzgerald, D.R., "USAF Flight Lightning Research", Lightning and Static Electricity Conference, 1968, AFAL-TR-68-290, Part II, p. 123-134.
6. Nanevicz, J.E., Adamo, R.C., and Bly, R.T., "Airborne Measurement of Electromagnetic Environment Near Thunderstorm Cells (TRIP-76)", 1977, AFFDL-TR-77-62.
7. Djak, J.T., "Airborne Measurements of Transient Electric Fields and Induced Transients in Aircraft Due to Close Lightning", 1977, AFFDL-TR-77-64.
8. Cianos, N. and Pierce, E.T., "A Ground-Lightning Environment for Engineering Use", 1972, Stanford Research Institute Project 1834.
9. Baum, R.K., "Airborne Lightning Characterization", 1980, Symposium on Lightning Technology, NASA Langley Research Center, Hampton, Virginia.
10. Thomas, Robert M., "Expanded Interleaved Solid State Memory for a Wide Bandwidth Transient Waveform Recorder", 1980, Symposium on Lightning Technology, NASA Langley Research Center, Hampton, Virginia.
11. Taillet, J., private communication
12. Society of Automotive Engineers, Committee AE4L, "Lightning Test Waveforms and Techniques for Aerospace Vehicles and Hardware", 1978.
13. Phillpott, J., "Recommended Practice for Lightning Simulation and Testing Techniques for Aircraft", 1977, United Kingdom Atomic Energy Authority Report, CLM-R163.
14. ———, "Conference on Certification of Aircraft for Lightning and Atmospheric Electricity Hazards, Proceedings", 1978, Office National D'Etudes et de Recherches Aérospatiales, Paris.

15. McCormick, W., Maxwell, K.J., and Finch, R., "Analytical and Experimental Validation of the Lightning Transient Analysis Technique", 1978, AFFDL-TR-78-47.
16. Burrows, B.J.C., "Induced Voltages, Measurement Techniques and Typical Values", Lightning and Static Electricity Conference, 1975, Royal Aeronautical Society, London.
17. Maxwell, K.J., Fisher, F.A., Plumer, J.A., and Rogers, P.R., "Computer Programs for Prediction of Lightning Induced Voltages in Aircraft Electrical Circuits", 1975, AFFDL-TR-75-36, Volume I.
18. Fisher, F.A., "Analysis and Calculations of Lightning Interactions with Aircraft Electrical Circuits", 1978, AFFDL-TR-78-106.
19. Strawe, D.F., O'Byrne, M., and Sandberg, S., "Electromagnetic Coupling Analysis of a Learjet Aircraft", 1978, AFFDL-TR-78-121.
20. Burrows, B.J.C., Luther, C., and Pownall, P., "Induced Voltages in Full-Sized Aircraft at 10" A/S", IEEE International Symposium on Electromagnetic Compatibility, 1977, p. 207-214.

Table 1 - Atmospheric electricity threats to aircraft

<u>Hazard</u>	<u>Cause</u>	<u>Hazard Criticality</u>
Malfunction/failure of electronic control systems	Low tolerance to electrical transients caused by direct/induced lightning or static electrification effects. May simultaneously affect parallel 'redundant' system.	Minor to catastrophic
Fuel tank fire or explosion	Fuel vapor ignition caused by static electricity or lightning effects.	Minor to catastrophic
Loss of engine power	Possible lightning acoustic shock at engine inlet, or electrical transient effects on engine controls.	Minor to catastrophic
Inadvertent release/ignition of external stores	Premature activation caused by lightning or static electrification effects.	Serious to catastrophic
Radome, canopy, and windshield damage	Direct lightning strikes; arc discharge caused by static electricity buildup.	Minor to serious
Instrumentation problems/communications, navigation & landing system interference	Transient effects caused by static electricity buildup & direct and nearby lightning strikes.	Minor to catastrophic
Structural damage	Direct lightning attachment to aircraft.	Minor to serious
Physiological effects on crew	Flash blindness & distracting or disabling electrical shock caused by direct & near lightning strikes.	Minor to catastrophic

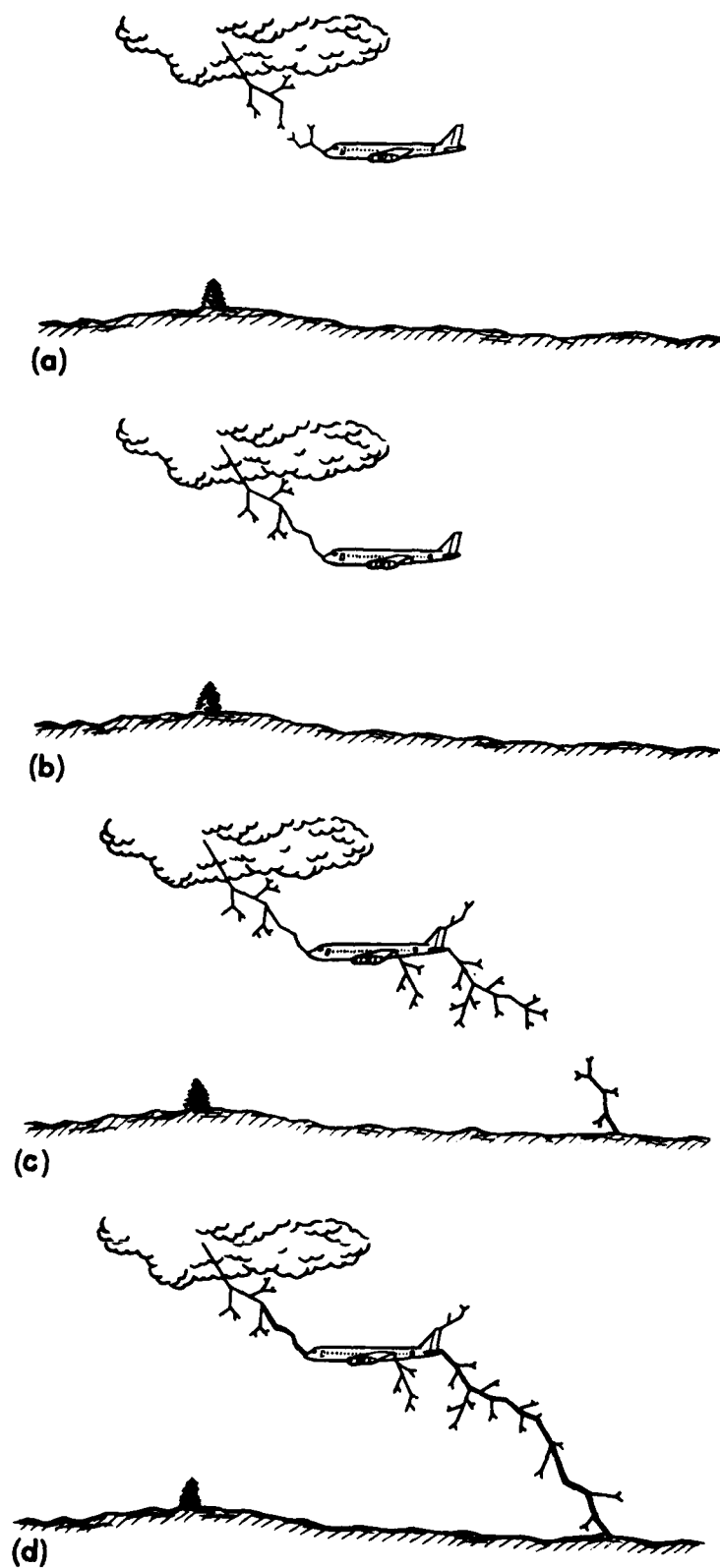


Figure 1. Lightning Aircraft Interaction^a
 (a) Stepped-leader approaching aircraft
 (b) Stepped-leader attachment to aircraft
 (c) Stepped-leader approaching the ground
 (d) Return-stroke through the aircraft

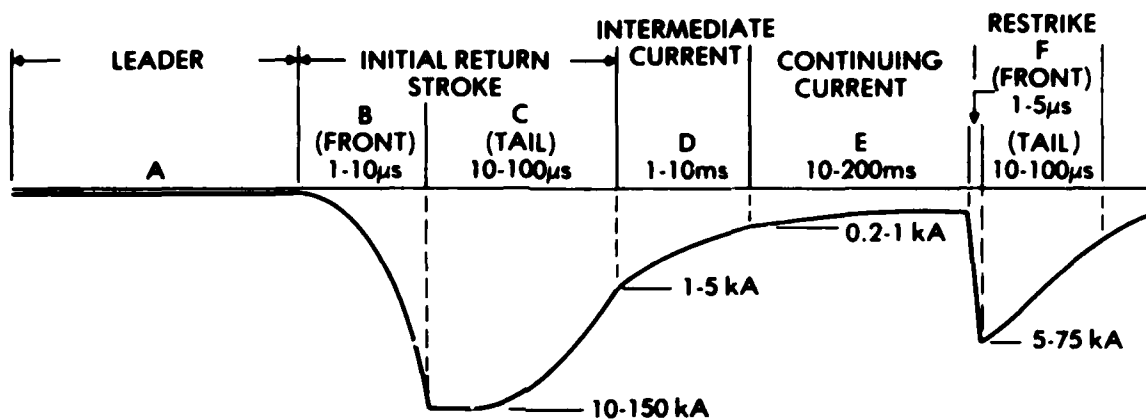


Figure 2. Generalized waveshape of current in negative cloud-to-ground lightning. (Note that drawing is not to scale.)"

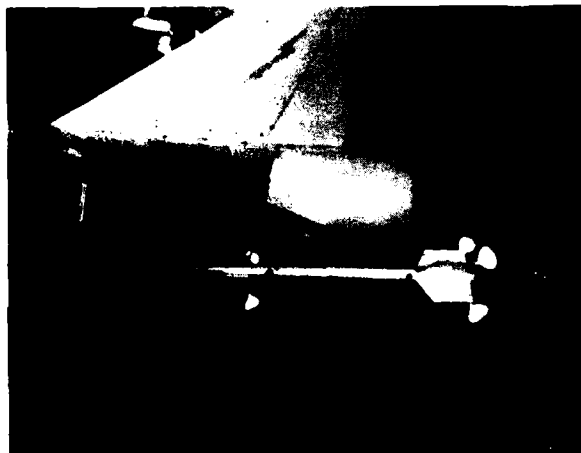


Figure 3. Example of corona on an aircraft model.



Figure 4. Example of "direct effects" damage.

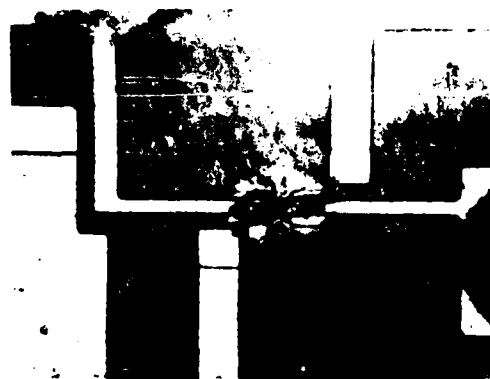


Figure 5. Photomicrograph of "indirect effects" damage to an integrated circuit caused by transient over-voltage.

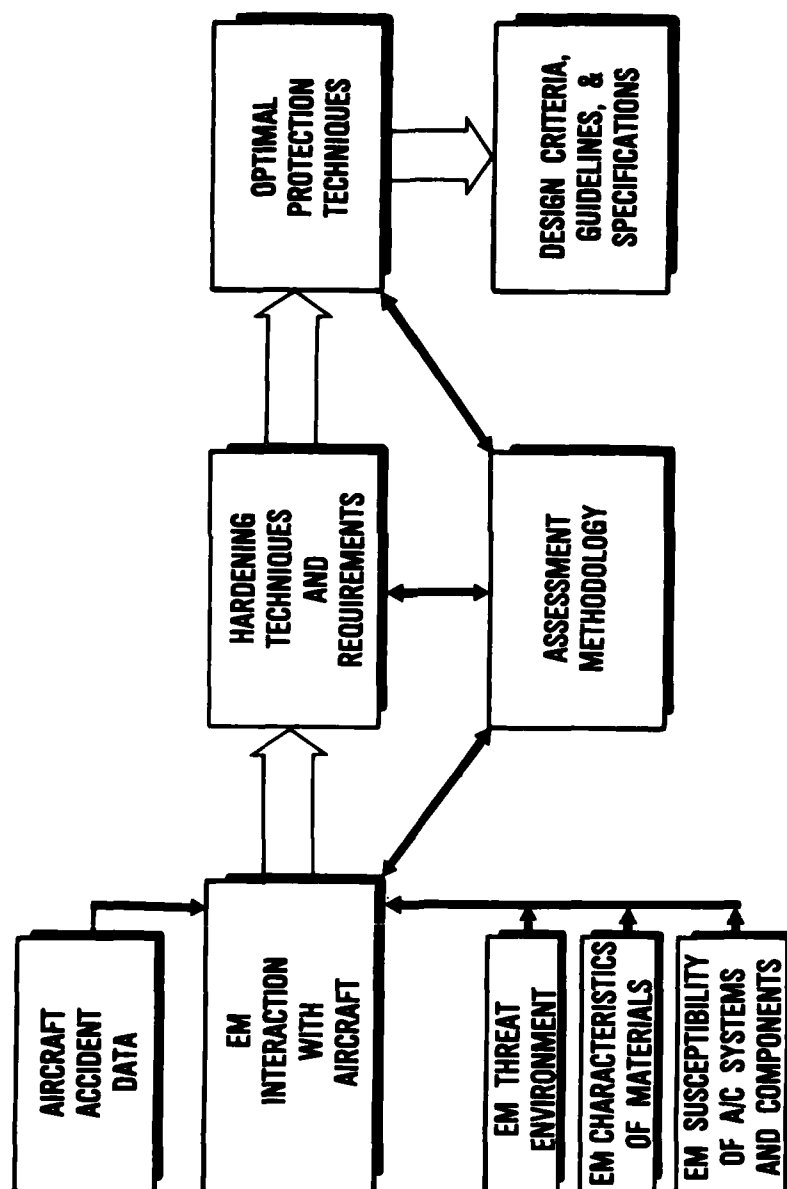


Figure 6. Technology Roadmap for Atmospheric Electricity Hazards to Aircraft

AIRCRAFT MISHAP EXPERIENCE FROM ATMOSPHERIC ELECTRICITY HAZARDS

Don W. Clifford
McDonnell Aircraft Company
St. Louis, Missouri

SUMMARY

Aircraft mishaps resulting from in-flight lightning strikes can range from inconsequential to catastrophic, although even the inconsequential mishaps can be alarming until it is determined that no damage has been done. Lightning discharges to aircraft in flight are not uncommon. Usually, however, little or no damage results from the strike. Nonetheless, occasional incidents of major, and even catastrophic proportions do occur, and therefore care must be taken to ensure that the lightning hazard is well understood and accounted for in the manufacture and operation of modern aircraft.

This paper seeks to establish a basic understanding of how lightning affects aircraft, based upon both military and commercial experience. Pilot reports of some representative incidents will be described in some detail, illustrating how the various atmospheric conditions and interaction mechanisms have affected aircraft operations. A summary of in-flight mishap conditions will then be presented describing the range of flight circumstances under which aircraft are usually struck. Finally, the interaction of high current arcs with structural and external electrical hardware, the effects of electromagnetic coupling to interior avionics and the effects of corona and high voltage sparking will be discussed.

INTRODUCTION

Lightning strikes to aircraft occur over a wide range of atmospheric and flight conditions and produce a variety of effects on all types of aircraft. The purpose of this paper is to establish some perspective on the problem by reviewing the statistics of the number and types of lightning related mishaps that occur, and then by describing some actual flight incidents. The in-flight weather conditions most likely to be present will be summarized; then the physical interaction processes involved and the resulting effects on aircraft struck by lightning will be described.

MISHAP EXPERIENCE

Lightning Mishap Statistics

In Reference 1, P.B. Corn reports the following U.S. Air Force statistics as of February 1979. "More than half of all Air Force weather-related aircraft mishaps are caused by lightning strikes. The USAF financial loss incurred in such mishaps exceeds 21 million dollars in the past five years, besides two aircraft lost with eight lives in 1978 alone. In the past ten years, seven USAF aircraft losses have been confirmed as lightning-related, two others ascribed to lightning as a likely cause, and over 150 serious mishaps reported. Imputed mechanisms include pilot disorientation and instrument failure (F-101, F-106), flight control failure after high current penetration (F-111F), fuel tank explosion, dual engine flameouts with electrical failure (F-4), fuel tank burn-through and explosion (C-130E), and failure of unprotected nonmetallic rotor blades (HH-33). A probable lightning-associated fuel ignition caused the loss of an Imperial Iranian Air Force 747 aircraft on 9 May 1976 near Madrid, Spain," Figure 1, reprinted from Reference 2, shows the percent of Air Force mishaps by aircraft type.

A total of 773 documented USAF lightning strikes was reported in this ten-year period. A recent study performed by the Air Force inspection and Safety Center indicates that because of damage cost thresholds for reporting, actual strikes probably exceed those reported by at least a factor of three. Corn also reports that requirements are expanding for USAF in-weather capability to meet European conditions, which will increase aircraft exposure to the lightning strike environment.

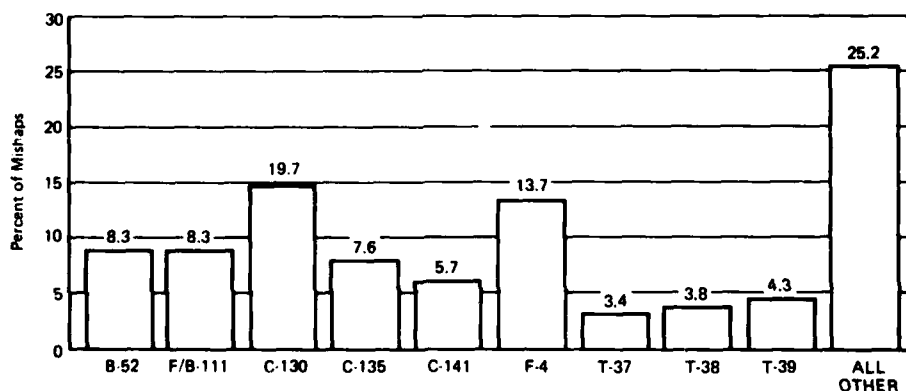


FIGURE 1
PERCENT OF MISHAPS BY AIRCRAFT TYPE - FROM REF (2)
(1973-1977)

It has been estimated that in the past about 20% of all strikes to aircraft result in the outage of some electrical or avionics equipment. As future aircraft become more heavily equipped with solid state avionics, that percentage can be expected to increase dramatically. Tables 1 and 2 are taken from Corn's summary of Air Force mishaps.⁽³⁾ Table 1 summarizes the extent of the lightning hazard to aircraft avionics. The hazards listed in Table 2 show that at least half relate to effects on electrical and avionic systems.

Commercial aircraft data given by Fisher and Plumer⁴ indicate that reported strikes to this aviation sector average about one every 2,930 flight hours, or 34 per 100,000 hours. This is about one strike to each airliner annually. Several trends in commercial aviation are likely to cause even greater future exposure to lightning. These include increased time in congested holding patterns and more intermediate stops on former nonstop routes. The increasing use of radar and other navigation aids in general aviation aircraft, will allow a larger portion of in-weather flight for that segment of the aviation world also. Recent general aviation mishap experience is reviewed by Plumer.⁵

TABLE 1
TEN YEAR HISTORY OF USAF LIGHTNING INCIDENTS - FROM REF (3)

A/C	Structure	Electrical, Instruments	Fuel	Others	Catastrophic	Major	Minor
F101	1	4		1	1	7	3
F102				3			3
F106	3	5			1	2	5
F-111	3	15		6	1	1	22
F-4	14	26	4	6	2	1	47
F-15	1	1					2
T-29	3	2		1			6
T-38	2	1					3
C119		1			1		
C124	1						1
C130	4	6	1	1	1		11
C131	3	2					5
KC135	8	5	1		1		13
C141	3	3					6
Other	7	5					12
B-52	12	2		1		1	14
HH-43	1				1		
	<u>66</u>	<u>78</u>	<u>6</u>	<u>19</u>	<u>9</u>	<u>7</u>	<u>153</u>

GP01 0146 3

TABLE 2
LIGHTNING AND STATIC ELECTRICITY THREATS TO AIRCRAFT - FROM REF (3)

Hazard	Cause	Hazard Criticality
Malfunction/Failure of Electronic Control Systems	Low Tolerance to Electrical Transients Caused by Direct/Induced Lightning or Static Electrification Effects. May Simultaneously Affect Parallel "Redundant" System	Minor to Catastrophic
Fuel Tank Fire or Explosion	Fuel Vapor Ignition Caused by Static Electricity or Lightning Effects	Minor to Catastrophic
Loss of Engine Power	Possible Lightning Acoustic Shock at Engine Inlet, or Electrical Transient Effects on Engine Controls	Minor to Catastrophic
Inadvertent Release/Ignition of External Stores	Premature Activation Caused by Lightning or Static Electrification Effects	Serious to Catastrophic
Radome, Canopy, and Windshield Damage	Direct Lightning Strikes; Arc Discharge Caused by Static Electricity Buildup	Minor to Serious
Instrumentation Problems/Communications, Navigation and Landing System Interference	Transient Effects Caused by Static Electricity Buildup and Direct and Nearby Lightning Strikes	Minor to Catastrophic
Structural Damage	Direct Lightning Attachment to Aircraft	Minor to Serious
Physiological Effects on Crew	Flash Blindness and Distracting or Disabling Electrical Shock Caused by Direct and Nearby Lightning Strikes	Minor to Catastrophic

GP01 0146 4

The higher commercial aircraft strike rates compared with Air Force rates apparently reflect the constraints of airline fixed routes and rigid schedules. This is supported by the considerably higher strike rates experienced by aircraft operating in Europe, apparently due in part both to higher lightning incidence and to the political airspace constraints imposed there.

Pilot Descriptions of Lightning

In a 1965 United Airline Report entitled "UAL Turbojet Experience with Electrical Discharges,"⁶ the practical experience of numerous pilots, with many thousands of hours of flying experience, was summarized and reported as they responded to questions about their experience with lightning. The pilots almost unanimously agreed that there are two distinct classes of lightning observed in flight. The most common variety usually occurs while flying in precipitation at temperatures near freezing. This type is preceded by a buildup of static noise in the communication gear and the presence of corona (St. Elmo's fire) can be observed if the flight is at night. The buildup may continue for several seconds before the discharge (lightning strike?) occurs. The discharge terminates the static and corona.

The second variety occurs abruptly with no warning. It is most likely to be encountered in or near thunderstorms, in contrast to the former variety which is more likely to be experienced in precipitation that has no connection with thunderstorms. Pilots tend to believe that the slow buildup type of discharge is not a true lightning strike but rather a discharge of excess charge built up on the aircraft by flying through the precipitation. This non-thunderstorm type greatly outnumbers the other. Both kinds can create a brilliant flash and a boom which can be heard throughout the airplane.

The response of scientists to the pilot's static discharge theory has been universally negative. They insist that insufficient charge can be stored on an aircraft to produce a discharge which looks and sounds like lightning. Scientists are even more emphatic that insufficient energy could be contained in such a static charge buildup to produce any visible evidence such as burn marks, pitting or other damage on the aircraft. Yet, the pilots continue to insist that the aircraft is discharging and that the discharges do manifest themselves by bright noisy arcs and (not all pilots are sure about this) visible damage. The controversy has been characterized as a difference in view between scientists of long standing and pilots of long sitting.

Clifford addresses this issue in Ref. (7). In a paper entitled "Another Look at Aircraft Triggered Lightning", he discounts the static discharge theory but then notes that there is positive evidence that a rapidly moving aircraft charged to high potentials by triboelectric processes can trigger lightning discharges by passage through freezing precipitation. The freezing zone in a nonstormy rain cloud is shown to be an electrically volatile region because of the potent charge exchange mechanisms which are active in agitated mixtures of super-cooled water droplets and ice. Several intensifying effects are suggested which can be produced by the passage of an aircraft through this precipitation, resulting in a highly-ionized wake which acts like a trailing conductor. If weak charge centers are present in the cloud, the ionized wake acts to short out the gradient field resulting in very high potentials at the aircraft. The high potentials explain the electrical activity at the aircraft described by pilots, including intense corona, sparks and radio interference terminating in a loud discharge. Lightning strikes to naval aircraft towing gunnery targets at the end of long steel cables are described, showing that the same triggering mechanism may be involved in those cases. Recommendations are made to include triggering experiments in government flight programs now in progress.

Some "Typical Severe" Incidents

The following actual incidents illustrate some of the types of mishaps that may be experienced when lightning strikes aloft.

An example of an unusual lightning strike to a military aircraft occurred as an Air Force fighter was on "enroute descent" in clouds and descending through 6,550 feet. The pilot noticed a lightning flash off the left wing, then corona buildup on the pitot boom. This was followed by a bright flash and a jolt to the aircraft. Immediately both fire-warning lights came on and stayed on. The back seat crew member suffered mild shock and was unconscious for a few seconds. The pilot applied power and climbed to 14,000 feet to VFR conditions. During the climb, he found that he had lost all UHF comm, heading indicators, INS and airspeed indications. The climb was continued using power, ADA, and the attitude indication. Approach control was contacted on an auxiliary VHF radio and the aircraft was vectored back to the air base. Descent was made through a break in the clouds. With the field in sight, the gear and flaps were lowered which caused the aircraft to yaw and roll to the left. Both gear and flaps indicated down, but the aircraft was difficult to turn left. The fire lights were still on and a large amount of smoke was coming from both sides of the cockpit. At this time, cabin pressure was dumped and 100 percent oxygen was selected. At three miles out on final approach, all instrument lights went out. The back seater was advised to prepare to eject. However, final approach was continued with power, attitude indicator (emergency floodlight was turned on) and "seat of the pants" as the only references. The aircraft landed, barrier engagement was accomplished, and engines were secured as crash equipment arrived. Upon post-flight inspection, 13 electronic components were found to be damaged and four circuit breakers were thrown. No evidence of fire was found. There was no evidence reported of lightning entering the electrical system through damage to external components.

In 1975 an Air Force F-4 fighter flying at 37,000 feet and 0.86 Mach number experienced an in-flight explosion that resulted in separation of the left wing and loss of the aircraft. According to verbal reports, the crew had reported visual sighting of lightning ahead and was attempting to contact the area controller when they heard a loud explosion. The aircraft went into a roll to the left and the pilot tried to correct and assess the damage but the high G forces caused him to lose consciousness. The second crew member ejected immediately after hearing fragments of statements from the pilot to "leave the aircraft." The pilot remained with the aircraft until an altitude of 5,000 feet before he regained consciousness and successfully ejected. The left wing impacted into a swamp miles from the point of aircraft impact, but the flyers were safely rescued. Recovery of the left wing and parts of the right wing allowed the accident investigation team to determine that ignition of fuel vapors occurred in the right integral fuel tank. The ignition front propagated into the left wing tank, rupturing the center rib panel separating the tanks. The pressure rose in the left tank, resulting in an explosion that separated the left wing from the aircraft.

Positive evidence of a lightning strike was found on the aircraft. Attachment points were found on the navigation lights on both wing tips, both stabilators, and the rudder. The left wing navigation light showed one attachment point. The right wing light had three attachment point on the tips, and there were two on the rudder, one at the top rear tip, and the second on the trailing edge near the bottom. All of these attachment points show the typical characteristics of pitting and molten metal.

Although the aircraft was lost because of a fuel vapor explosion, this incident is of interest to aircraft electrical and avionics engineers because the possible ignition sources in such cases include electrical equipment such as fuel quantity probes or electrically actuated valves or pumps in the fuel volume. In this particular incident, the accident investigation board determined that the most probable cause of ignition was fuel probe arcing or breakdown.

As a matter of fact, many catastrophic aircraft losses have been attributed to lightning initiated fuel explosions, including the Elkton commercial 707 incident in 1963 with a loss of 81 lives. Of five such documented aircraft losses, although lightning burn marks were evident on areas of the wing tips away from the fuel volume, no direct evidence of lightning arcing could be found on any of the metal surrounding the fuel volume. In only one of those cases (C-130E, November 1978) was arc penetration into the fuel volume observed. In the other cases, the most probable causes cited were arcing in electrical equipment located in the fuel volume, or streamer arcing at fuel vents.

Another incident, which was not fuel related, involved the RF-4C shown in Figure 2. It was being flown on a routine training mission when the aircraft experienced a dual lightning strike. In addition to the radome damage which is evident in the photo, all primary flight instruments were lost after the second strike and the attitude and vertical velocity indicators were fluctuating wildly. After declaring an emergency and taking the necessary precautionary measures, the crew aided by another RF-4C, made a successful landing. The incident occurred in Europe in 1970 and the weather conditions at the time of the incident were: ceiling 1200 foot overcast, visibility 2 miles, and temperature 6°C.

Although the extensive radome damage experienced in this incident is rare, the incident illustrates how lightning can gain access to the electrical system through externally mounted electrical equipment (the radar antenna or pitot mast in most radome cases) resulting in widespread damage to other electrical equipment.

The unusual events described are examples of some of the malfunctions that can occur as a result of lightning strikes to aircraft. As shown in Table 2, many other effects are common, such as turbine engine compressor stalls, temporary flash blindness, inadvertent jettison of external stores, and various other electrical malfunctions. The mechanisms of lightning interaction with aircraft will be discussed in the last section of this paper, leading to a description of how the observed effects are produced. The following section deals with the weather and flight conditions in which aircraft/lightning mishaps have been recorded.

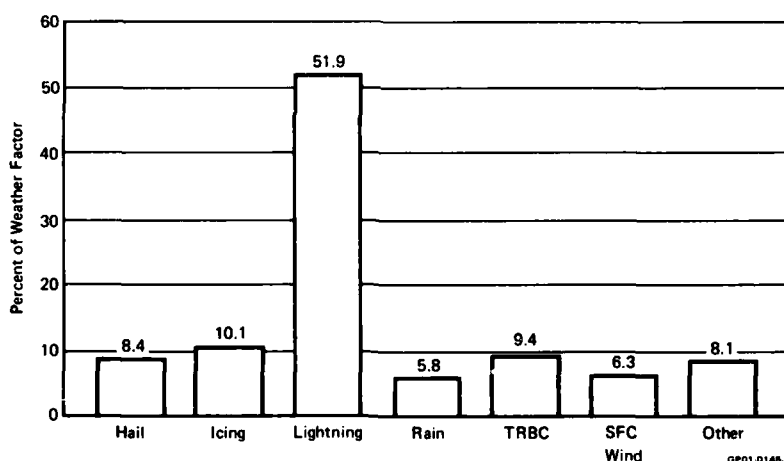
WEATHER AND FLIGHT FACTORS

Although weather factor mishaps are caused by a variety of weather phenomena, U.S. Air Force statistics indicate that lightning strikes are the most frequent cause. Figure 3 from Reference 2 shows that over one-half of all weather related mishaps are related to lightning.



GP01 0148-2

FIGURE 2
RF-4C AFTER DIRECT NATURAL LIGHTNING STRIKE TO RADOME



GP01 0148-5

FIGURE 3
MISHAP CAUSES - FROM REF (2)
(1972-77)

The vulnerability of aircraft to lightning hazards depends on several factors. The operating parameters, i.e. normal cruise altitude, number of missions relative to other aircraft, and the operating theatre all have a bearing. It is also becoming apparent that aircraft size is a factor in the likelihood of being struck. Commercial airlines report that the jumbo jets are logging more strikes than their smaller predecessors. It is also notable that numerous cases of strikes to aircraft flying in formation have been noted; the same strike passing through each aircraft in the group. It is also notable that aircraft trailing long wire antennas or towing gunnery targets have received a large number of lightning strikes. All of these incidents imply that size can be a factor in lightning strike incidents.

Fisher and Plumer have published in their book *Lightning Protection of Aircraft*⁴, a helpful summary of atmospheric and flight conditions under which aircraft have been struck by lightning. Their summary is based upon reporting projects conducted by a number of individuals and organizations throughout the world. Their data include findings reported by the Lightning and Transients Research Institute (LTRI) (Reference 8), Plumer and Hourihan of General Electric (Reference 9), Anderson and Kroninger of South Africa (Reference 10), Perry of the British Civil Aviation Authority (Reference 11), and Trunov of the USSR National Research Institute for Civil Aviation (Reference 12). Strike incidence data, based largely on commercial turbojet or turboprop aircraft, is usually summarized according to the following categories:

- Altitude
- Flight path (i.e., climb, level flight, descend, etc.)
- Meteorological conditions
- Outside air temperature

Figure 4 from Chapter 3 of Fisher and Plumer's book shows the altitudes at which the reporting projects show aircraft are being struck, as compared with a typical cumulonimbus (thunder) cloud. The turbojet and turboprop data from the four summaries are in close agreement. For comparison, the data from the earlier piston aircraft survey of Newman are also presented. Cruise altitude for jet

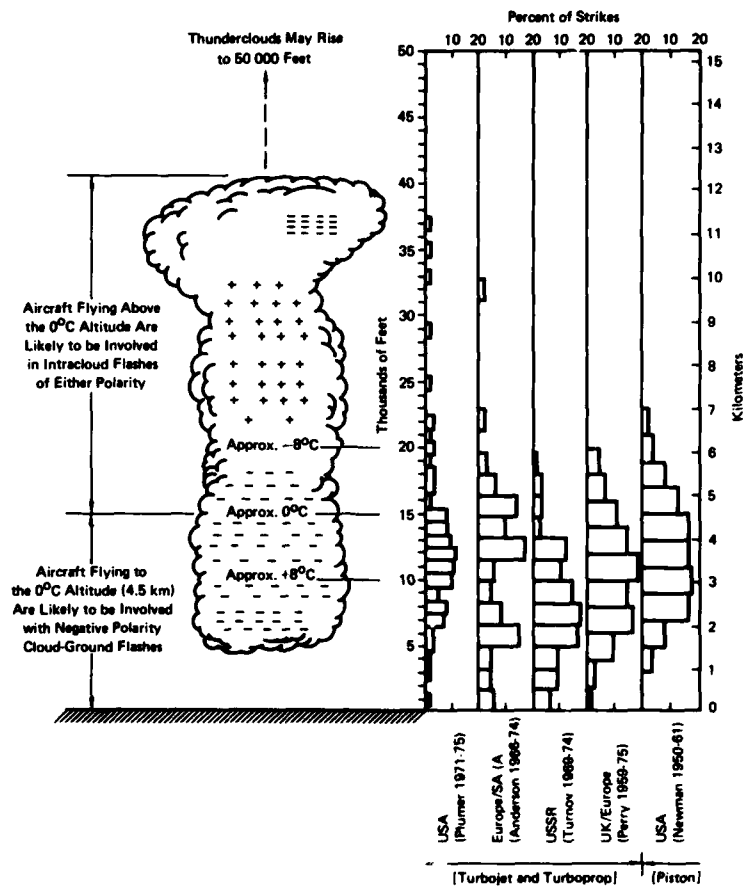


FIGURE 4
AIRCRAFT LIGHTNING-STRIKE INCIDENTS vs ALTITUDE-FROM REF (4)

aircraft is considerably higher (10 km) than that of earlier piston aircraft, which flew at about 4 to 5 km; yet Figure 4 shows the altitude distribution of lightning-strike incidents to be nearly the same. This fact indicates (1) that there are more lightning flashes to be intercepted below about 6 km than above this altitude, and (2) that very likely jet aircraft are being struck at lower than cruise altitudes; that is, during climb, descent, or hold operations. Flight regime data obtained from the jet projects confirm this.

If the strike altitudes shown in Figure 4 are compared with the electrical charge distribution in the typical thundercloud shown in the figure, it is evident that strikes which occur above about 3 km result from intracloud flashes between positive and negative charge centers in the cloud (or between adjacent clouds), whereas strikes below about 3 km probably result from cloud-to-ground flashes. Strike incidents occurring above 6 km are less common because of the absence of concentrated charge centers at the higher altitudes and because aircraft at these altitudes can more easily divert around thunderclouds than can aircraft at lower altitudes.

By way of comparison, Shaeffer¹³ reports a somewhat different distribution with altitude for the F-4 aircraft. The F-4 distribution, shown in Figure 5, indicates significantly more strikes below 3 km than in the commercial case, but also more strikes at higher altitudes. Another interesting comparison from Shaeffer is shown in Figure 6 where the rate of lightning strikes to various F-4 models is shown as a function of the operating theatre. Notice that a clearly higher incidence rate is noted for European operations than for Asian or American operations, for all models. Both weather patterns, the types of missions flown, and political air space constraints in Europe are likely contributors to the observed F-4 strike patterns.

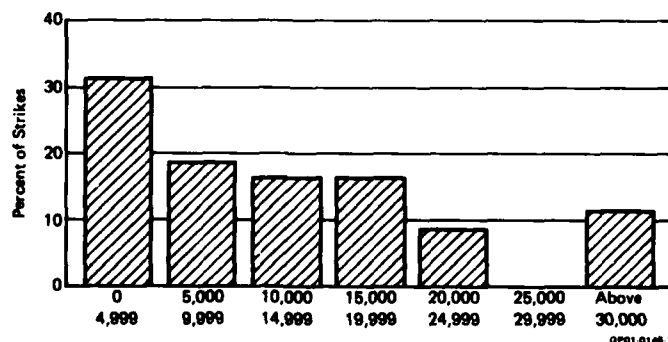


FIGURE 5
LIGHTNING STRIKES TO F-4 AIRCRAFT AS A
FUNCTION OF ALTITUDE - FROM REF (13)

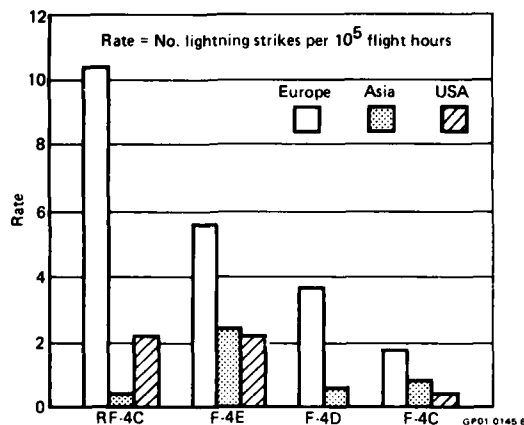


FIGURE 6
RATES OF LIGHTNING STRIKES TO F-4s - FROM REF (13)

It is interesting to note that although aircraft are sometimes struck while penetrating active thunderclouds (almost always inadvertently), aircraft generally avoid thunderclouds by a wide margin. Most reported strikes occur to aircraft flying through inactive clouds, in light rain and in light turbulence. Figure 7 illustrates the environmental conditions at the time of strike for 214 strikes reported by Plumer and Hourihan⁽⁹⁾. Notice that strikes sometimes occur in the clear. Aircraft have reported strikes as far as 25 miles from the nearest cloud. In fact, occasionally a "bolt out of the blue" is reported with no clouds anywhere around. Such reports are usually greeted with skepticism, however, because it is difficult to conceive of a charge separation mechanism capable of producing regions of charge large enough to support a discharge, with no cloud activity present.

Figure 8 indicates the temperature distribution over which lightning strikes occur as reported by Plumer. A summary of the prevailing synoptic meteorological conditions for 99 UAL lightning incidents is shown in Table 3 from H. T. Harrison (Reference 6).

Harrison has summarized this data by saying that any conditions which will cause precipitation may also be expected to cause electrical discharges (lightning), although he adds that no strikes were reported in the middle of warm front winter snowstorms.

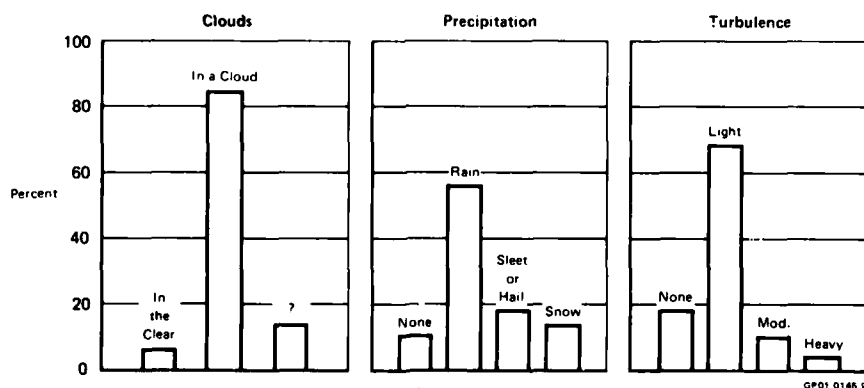


FIGURE 7
ENVIRONMENTAL CONDITIONS AT TIME OF STRIKE - FROM REF (4)

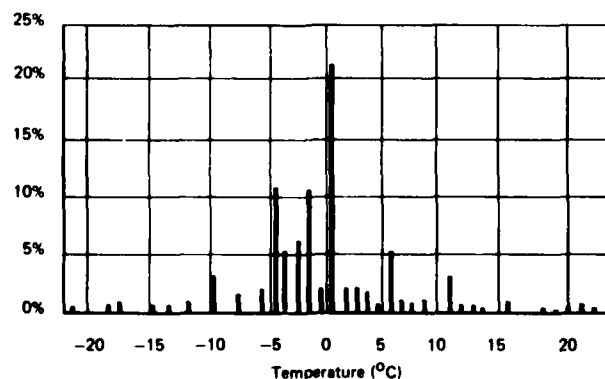


FIGURE 8
LIGHTNING STRIKES TO AIRCRAFT AS A FUNCTION OF TEMPERATURE - FROM REF (4)

TABLE 3
SYNOPTIC TYPES INVOLVED WITH 99 ELECTRICAL DISCHARGES - FROM REF (6)
July 1963 to June 1964

Synoptic Type	Percentage
Airmass Instability	27
Stationary Front	18
Cold Front	17
Warm Front	9
Squall Line or Instability Line	9
Orographic	6
Cold LOW or Filling LOW	5
Warm Sector Apex	3
Complex or Intense LOW	3
Occluded Front	1
Pacific Surge	1

GP01 0146 11

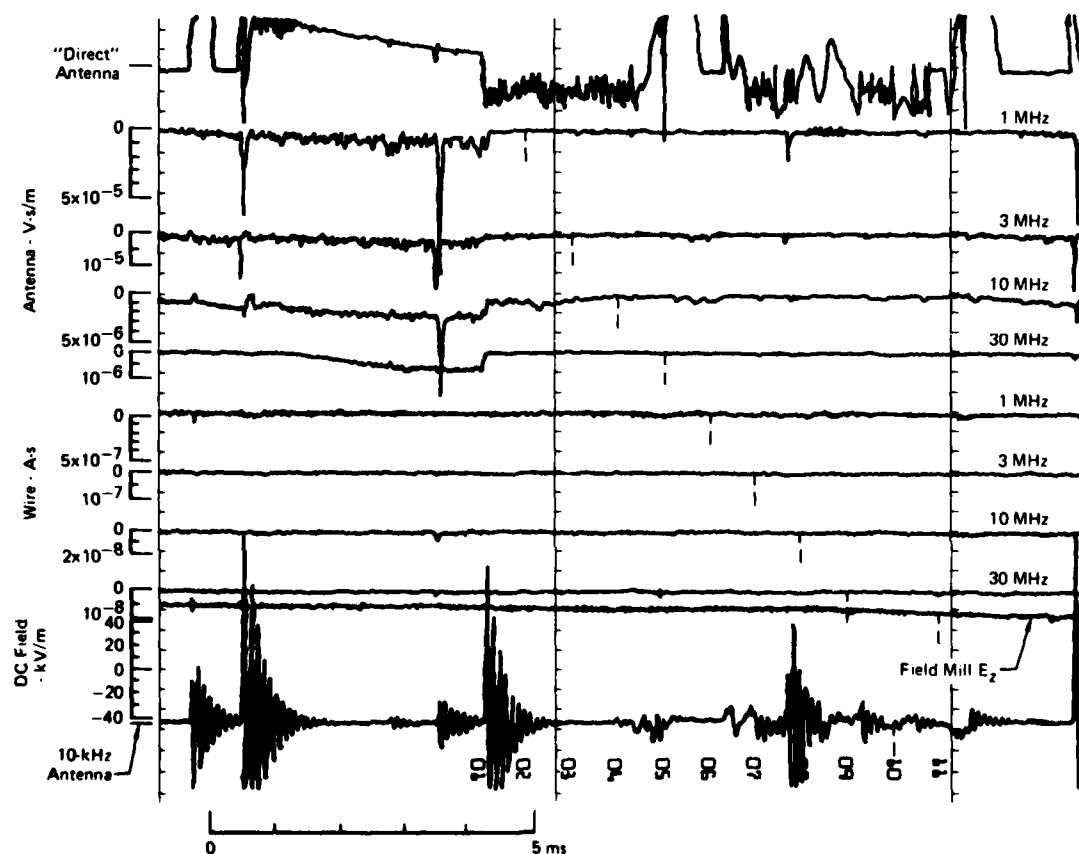
LIGHTNING INTERACTION WITH AIRCRAFT

The mechanisms and processes of lightning have been described in a previous lecture in this series, and elsewhere⁽¹⁴⁾. The presence of an aircraft in the high field region where a lightning stepped leader is propagating may intercept the leader and become established as a small portion of the channel. The interaction of lightning with the aircraft therefore begins with the buildup of high electric fields and continues through the stepped leader attachment, return strike phase and subsequent stroke activity. It also includes the effects of fast changing fields from nearby lightning activity.

Broadly speaking, the interaction mechanisms can be categorized as radiated field effects, high voltage effects, and high current effects. Traditionally, however, the actual effects on aircraft are defined on a more localized basis as direct effects, related to visible mechanical damage and indirect effects, related to electromagnetically coupled transients in electrical and avionics systems. Before dealing with the localized effects, however, some of the broader interaction processes will be discussed.

Radiated Fields (Nearby Lightning)

An aircraft flying in a thunderstorm environment will experience rapid and numerous fluctuations in the ambient electric and magnetic field environment. This field environment is not at all well defined at flight altitudes. Nanevich, et. al.,⁽¹⁵⁾ reported in-flight measurements during Lear jet flights around Florida thunderstorms in 1977. Though limited, the results were very informative. Figures 9 and 10, taken from the Nanevich report, illustrate the complexity and extensive duration of the activity. References 16 and 17 also report results of recent in-flight measurement programs. Extensive ground-based measurements have been made of lightning field activity, mostly by Uman, Krider and their co-workers^(18,19,20) but measurements at ground level may not reflect the actual field environment at altitude.



GP01 0146 12

FIGURE 9
AUGUST 10 RUN 19 NEARBY LIGHTNING - FROM REF (15)

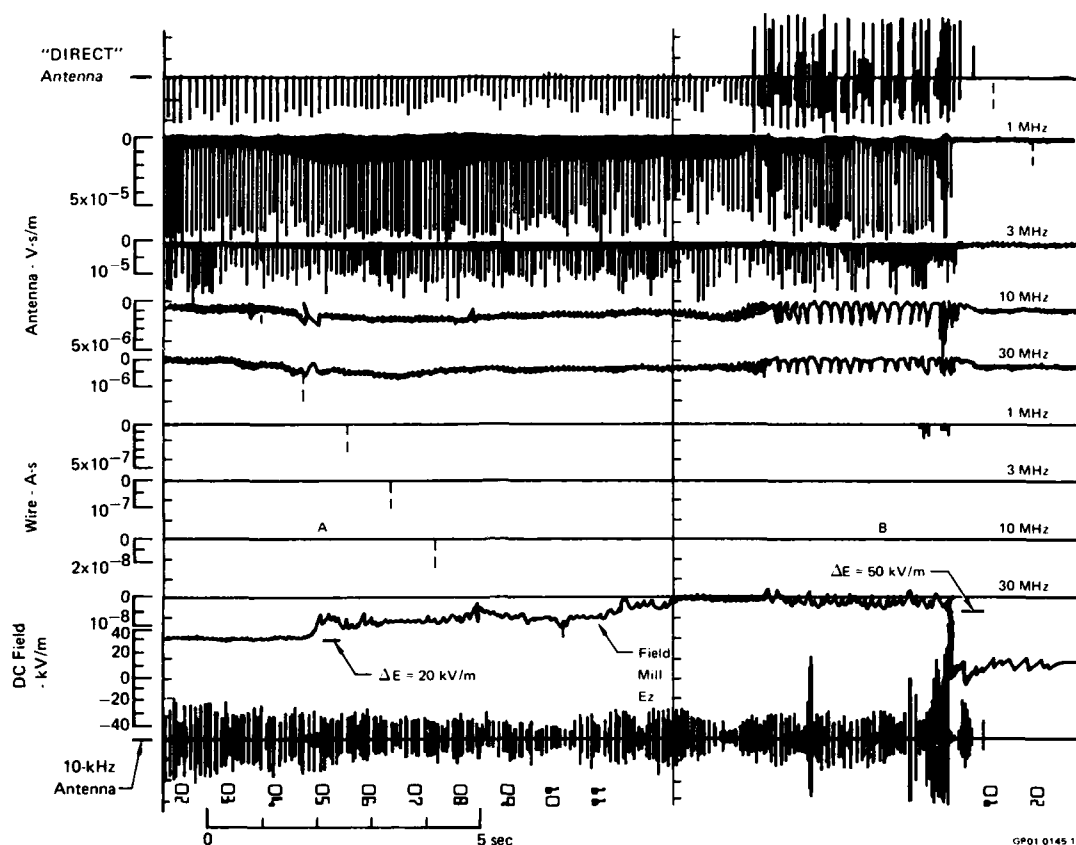


FIGURE 10
"INCIPIENT STREAMERS" FOLLOWED BY "LIGHTNING OBSERVED" - FROM REF (15)

An aircraft flying in this field environment acts like a large antenna, having displacement currents excited on the surface and inducing transients or internal electrical wiring. The extent of electrical transients produced by nearby lightning activity is a subject of current debate. No serious avionics problems have been reported in the past as a result of nearby activity, but there is concern that future aircraft will be equipped with avionics which are both more sensitive to electrical upset and more critical to flight safety. These concerns are amplified by the uncertainties introduced by the expanding use of advanced composite materials.

Nanevici¹⁵ reported transients measured on a hastily constructed internal wire loop during some of the Lear jet flights mentioned earlier. The aircraft was actually struck by lightning once during the flight program. The transient measured on the internal wire during that strike was not much larger than other transients measured as a result of nearby lightning. The authors concluded that on the basis of the observed data, nearby lightning may constitute an induced transient threat of the same approximate magnitude as a direct strike.

High Voltages

(Pre-Return Stroke Phase) - The process of a lightning strike to an aircraft in flight is depicted in Figure 11. The aircraft will first experience an intensification of the ambient electric field as the lightning stepped leader approaches the aircraft, carrying with it the high potential of the cloud. Since the leader is propagating at an average velocity of 0.1 - 0.2 meter/ μ sec, the intensification process will take place over a brief interval of a few milliseconds.

The highest electric fields about the aircraft will occur around extremities such as the nose and wing tips, and sometimes smaller protrusions, such as antennas or probes. When the leader approaches to the point where the field adjacent to an aircraft extremity is increased to about 30 kV/cm, the air will breakdown and electrical corona will form at the sharpest extremities extending in the direction of the oncoming leader. Extensions of the corona, called streamers, occur simultaneously from opposite extremities of the aircraft, as shown in Figure 11A. One of these streamers will meet the nearest branch of the advancing leader and form a conductive path from the cloud charge center to the aircraft. Thus, when the aircraft is close enough to influence the direction of the leader propagation, it will very likely become attached to a branch of the leader system (Figure 11B).

As the stepped leader contacts the aircraft, the aircraft is raised to the potential of the leader channel, which may be of the order of 50 to 100 million volts. Virtually all external conductive surfaces can then be expected to issue corona and streamers radially outward until the vehicle is surrounded by a plasma sheath (as the rest of the arc channel is) extending out several meters from the aircraft. This condition will occur quickly and will persist until the highly charged arc channel is discharged by the passage of the return stroke (again a few milliseconds, depending on the proximity of the aircraft to the charge centers).

It should be noted that an aircraft may become a part of a branch off the main channel rather than a part of the main channel itself. In fact since there are many branches off the main channel it would appear that the likelihood would be much higher of being "struck" by a branch than by the main channel. The consequences may be indistinguishable to occupants of the aircraft. There would still be a bright flash and a loud boom as the branch channel discharges into the main channel. The peak current amplitude would be lower, there would be no continuing current and there would be no restrikes. Any direct damage effects should therefore be minimal but sparking problems and interference with avionics systems may still be significant. The possibility exists that a percentage of the strikes reported each year are branch discharges rather than main channel strikes, including the Lear jet strike in Reference 15. No voltage or current waveforms have been defined for branch discharges.

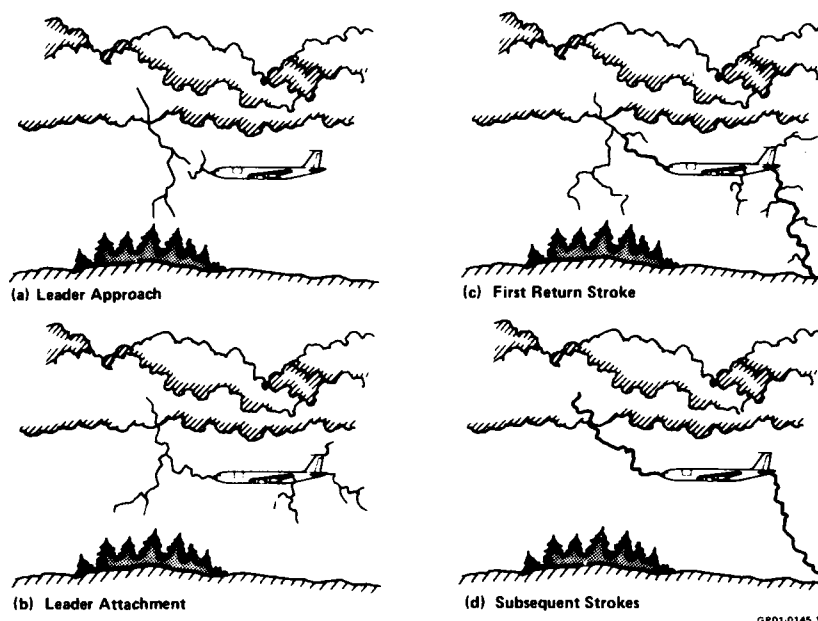


FIGURE 11
THE LIGHTNING STRIKE PROCESS - FROM REF (4)

The effects produced on the aircraft by the various high voltage processes involved in the lightning arc channel attachment are not well defined or understood. However, it is certain that the rapid redistributions of charge will result in very fast changing magnetic fields and the high potentials will ensure that very high electric fields will be produced. Therefore, electrical and avionics equipment will most likely be subjected to significant transient voltages during this period whose total duration is a few milliseconds.

The stepped leader and aircraft streamer formation process will stress dielectric materials in the high field regions. Therefore, the puncture or flashover of radomes or other dielectric structures will be determined during this period. The detailed behavior of the electric fields as seen by the aircraft have not been measured. Therefore, the design and testing of protection measures addressing the high voltage mechanisms must be done on the basis of other considerations, using worst case assumptions where no other criteria, such as in-flight damage comparisons exist. For example, it is known that fast changing voltage pulses will puncture dielectric materials more readily than slowly rising pulses. The slow rising voltages tend to flashover the surface because of the longer time allowed for streamers to develop across the surface from surrounding metal structures. Therefore, simulation tests are conducted using fast rising pulses, since the condition thus simulated is worst case.

The high voltages associated with the pre-return stroke events may also lead to active sparking in the form of corona and streamers in unshielded regions. This activity is primarily a problem only in areas where flammable mixtures of fuel vapors and air exist, e.g., fuel vents or dump openings.

High Current Interactions (Return Stroke Phase)

For design and test purposes, the conservative approach is to assume a worst case cloud to ground strike. In this case, the return stroke current will be higher, there is a high probability of multiple restrikes, and there may be heavy continuing currents associated with one or more of the return strokes. The total duration of the flash may last a half of a second or more. Figure 12 is a representation of the current waveforms proposed by Cianos and Pierce(21) as a severe lightning model for engineering test purposes.

The rather long interval over which a multiple-stroke flash may persist, coupled with the movement of the aircraft at a velocity of 50 to 80 meters per second, leads to the dynamic interaction process known as the swept stroke phenomenon. If lightning attaches initially at a forward point on the aircraft such as the forward fuselage, or to the front of wing mounted engines or stores, or possibly even the leading edge of a wing, the arc attachment point will effectively sweep back across the surface as the aircraft flies through the stationary arc channel. The principal complication of this sweeping action is that inboard surfaces of the aircraft in low-field regions may become exposed to lightning arc attachment with continuing currents and restrikes, although lightning would never attach there initially. Consequently the design specification for external electrical hardware must consider where the component is located on the aircraft.

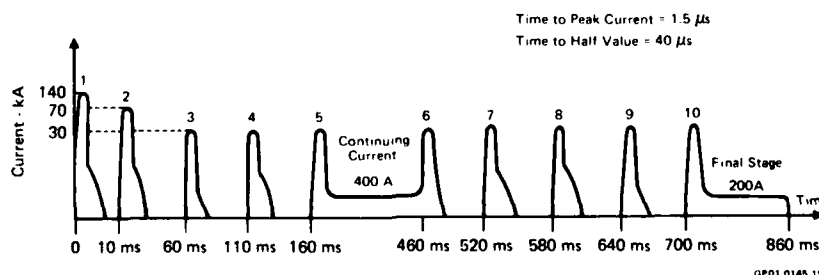


FIGURE 12
TIME HISTORY OF SEVERE (BASIC) LIGHTNING MODEL - FROM REF (21)

Lightning attachment zones on aircraft are defined to help identify the lightning threat by location. Zone 1 regions are the high field regions such as wing tips, vertical fin, nose, etc. where there is a high probability of direct attachment. Zone 2 covers the regions aft of Zone 1 attachments where lightning arc attachments may sweep; Zone 3 covers the other regions of the aircraft where there is a low probability of any arc attachment but where lightning currents may pass enroute between attachment points. Zones 1 and 2 are further divided into A and B regions. A regions are forward points where the arc can sweep off easily. B regions are trailing edges where the arc has nowhere to go and will, therefore, remain attached and not sweep.

EFFECTS ON AIRCRAFT

Lightning effects on aircraft are classified as "Direct Effects" or "Indirect Effects." Direct effects include the physical damage produced at the point of arc attachment and damage produced directly by current flow between arc attachment points. Indirect effects are electromagnetically induced by field coupling to wires or avionics equipment. Direct effects may include both high voltage and high current effects on hardware. Since this paper is oriented to avionics considerations, the principal direct effects of concern are those associated with externally mounted electrical hardware and the attached avionics equipment. Indirect effects are of concern only to avionics and electrical systems.

Other than direct and indirect effects, physiological effects on the crew such as flash blindness and loss of consciousness from electrical or acoustical shock are of concern. These effects are usually temporary, lasting perhaps up to 30 seconds or longer. Effects such as fuel vapor ignition or engine outages may be caused by either direct or indirect effects and may or may not be associated with electrical or avionics systems. They will be discussed further in this section.

Direct Effects on Electrical Systems

The direct effects of lightning are the burning, eroding, blasting and structural deformation caused by lightning arc attachment, as well as damage produced by the high-pressure shock waves and magnetic forces produced by the high currents. Structural damage effects are typically localized to the immediate area of the arc attachment point or points since the current density is highest there. As the current enters a conductive structure, it rapidly spreads so that the current density is quickly reduced to harmless levels. This localization effect is particularly true for the lower level continuing current phases of a strike.

Damage may be more far reaching if current dispersion is prevented or if there is limited current-carrying capacity in the path taken by the lightning currents. For example, if the lightning arc attaches to a nose radome mounted pitot mast, the only current path to the main structure may be through the heater wires attached to the pitot probe. These wires would not typically be able to carry a heavy lightning current without explosively vaporizing. The resulting vaporization pressure could rupture the radome causing extensive damage to the radome and possibly serious aerodynamic effects. The lightning currents can also then find their way into the heater power supply and from there into the main electrical distribution system causing widespread electrical problems.

Other examples of inadequate current-carrying capacity might include bonding straps, adhesively bonded structures, or high resistance coatings of the type designed for prevention of static charge buildup. When an electric current passes through a material a certain amount of energy is converted to heat because of the electrical resistance of the conducting material. When the material heats, its resistance also changes. Complicating the matter still further is the fact that the current is transient in nature. Neglecting resistance changes due to temperature, the Joule heating developed can be represented mathematically as

$$H = \int_0^t R I^2(t) dt$$

Where:

- H = heat developed in test part (Joules)
- t = time (seconds)
- R = electrical resistance (ohms)
- $I(t)$ = electrical current (amps) as a function of time.

When the electric current is introduced into the conducting material (assume a flat metal plate) by means of an electric arc, an even more complex situation arises. Heat is generated in the material due to normal Joule heating and to heating at the arc/metal interface. If the current is fast rising, the initial current will essentially remain on the surface of the metal (skin effect), but as the current continues, the current and the heat will diffuse and spread into the material. This can be compared to an arc weld except that electrical currents are several orders of magnitude greater for lightning and the time can be several orders of magnitude shorter.

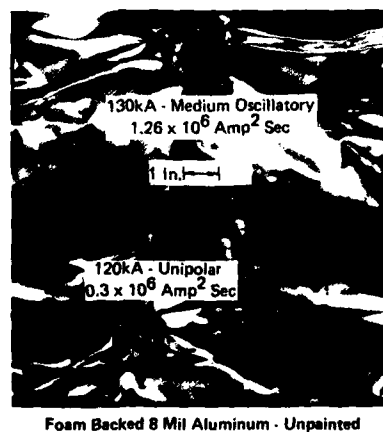
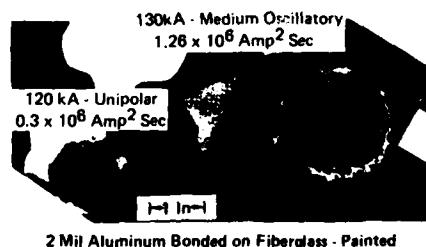
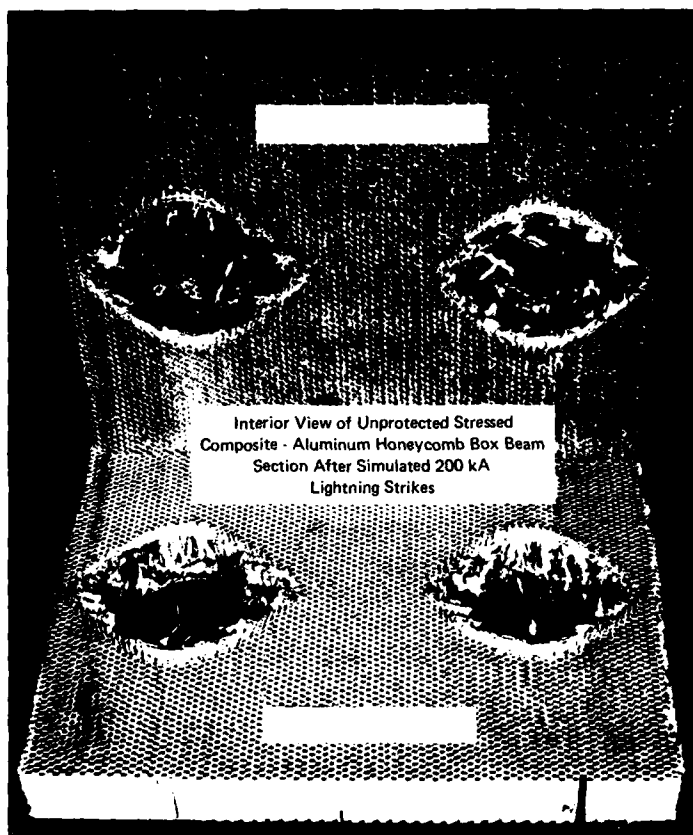
The nature of localized structural damage to electrical hardware is dependent upon the construction and geometry of the part as well as on the type of lightning current flowing. The high peak current surge exerts shock and mechanical bending forces because of the intense magnetic fields and the explosive channel. However, on sturdy conductors such as thick aluminum, very little effect is noted; typically just small pits or etch marks on the surface. Figure 13 illustrates very little high peak current damage to thin metal coatings on fiberglass, but extensive damage to confined honeycomb structure. Conversely, the continuing current phase is capable of melting sizable holes through relatively thick, metal parts if allowed to deposit its energy at one point for a few tenths of a second (see Figure 14).

The shock and blast effects of the high peak current phase may shatter light coverings or lenses, allowing the current direct access to the electrical system. The high peak currents tend to flow in straight lines so conductors with sharp bends will either be magnetically distorted (unbent) or the lightning may flash across the corner or find an alternate path. Magnetic forces are proportional to the square of the current producing them and the damage produced is related both to the magnetic forces and to the response time of the affected system.

In areas where the current density is high, such as at the attachment of protective bonding jumpers or at an arc root, the magnetic forces can become extremely large. This problem has been previously addressed by James and Phillpott.²² They determined that an arc rising in a few microseconds to a peak current of 200 kA will have a diameter of about 2 mm and hence its maximum magnetic field will be about 40 Tesla producing a magnetic pressure approaching $6.3 \times 10^8 \text{ N/M}^2$ (150,000 lbs/in.²).

Externally mounted electrical components most frequently experiencing the direct effects of lightning include various types of lights, antennas, probes, windshield heaters and radomes. Radomes are frequently located in prime lightning attach points (nose or wing tips). Therefore, particular attention should be paid to the mechanisms of high voltage breakdown and high current damage which they may experience.

An excellent example of the direct effects of lightning to an aircraft electrical system was reported by Fisher and Plumer.¹¹



GP01 0146 16

FIGURE 13
EXAMPLES OF HIGH PEAK CURRENT EFFECTS ON EXPOSED,
PAINTED AND ENCLOSED SURFACES

A strike to a general aviation aircraft of the type shown in Figure 15 was analyzed extensively resulting in the following findings.

This aircraft, flying at about 900 m (3,000 ft), was experiencing light rain and moderate turbulence when it was struck by lightning. The pilots had seen other lightning flashes in the vicinity before their aircraft was struck, and embedded thunderstorms had been forecast enroute, but there had been no cells visible on the air traffic control (ATC) radar being used to vector the aircraft, which had no weather radar of its own.

The strike entered one wing tip and exited from the other. It sounded to the pilot reporting like a rifle going off in the cabin, and the cabin immediately filled with smoke. Other effects follow.

- The No. 1 VHF communication set burned out.
- Seventy-five percent of the circuit breakers were popped, of which only 50% could be reset later.
- The left wing tip fuel tank quantity indicator was disabled.
- The right main fuel tank quantity indicator was badly damaged.
- Several instrument lights were burned out.
- The navigation light switch and all lights were burned out.

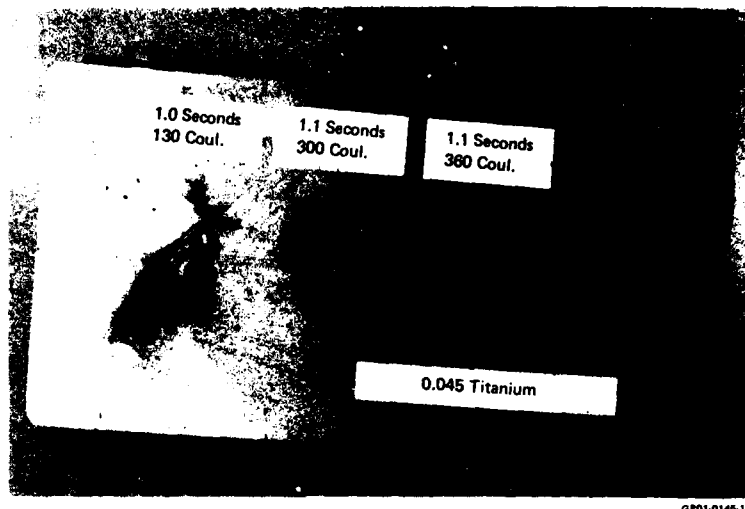


FIGURE 14
CONTINUING CURRENT BURNTHROUGH OF .045 INCH TITANIUM PLATE

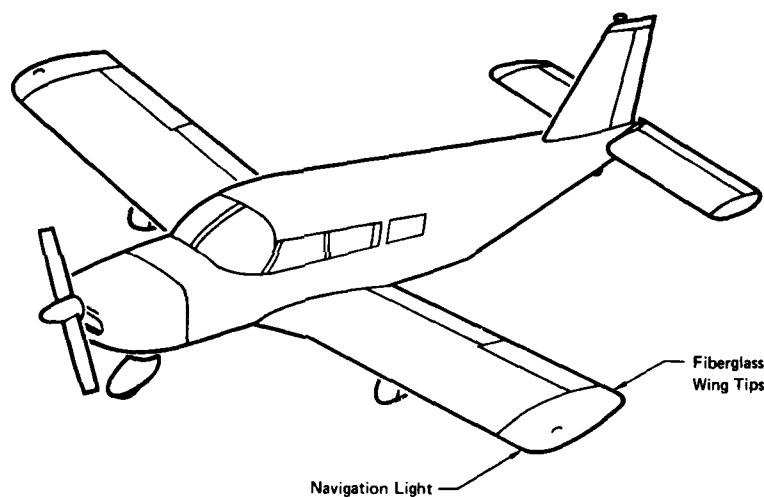


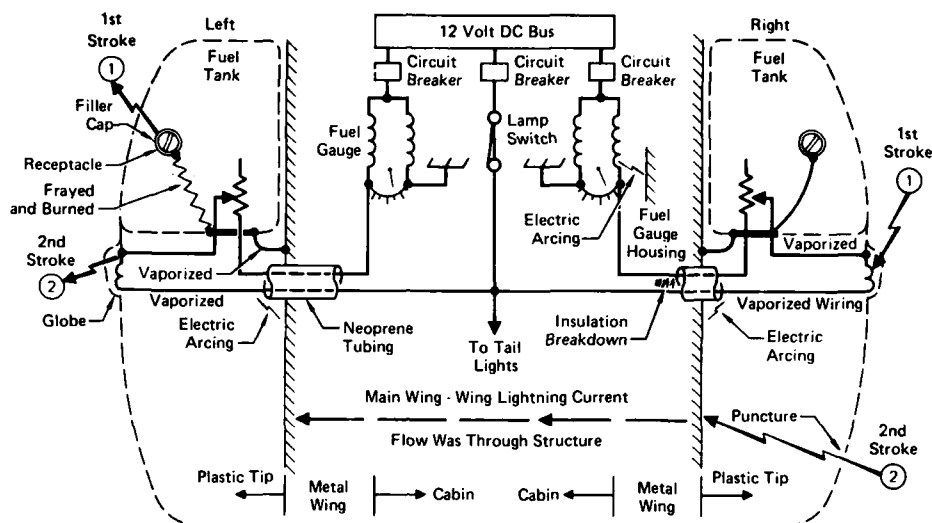
FIGURE 15
GENERAL AVIATION AIRCRAFT WITH PLASTIC WING TIPS - FROM REF (4)

The evidence suggests that the flash included two or more strokes separated by a few milliseconds of continuing current. Assuming, for purposes of explanation that the original lightning flash approached the right wing tip, the probable sequence of events was as follows: (refer to Figure 16 electrical schematic). The initial point of attachment was the right wing tip navigation light housing. Current from this stroke entered the housing ground wire and exploded both sections of it on the way to the right outboard metallic rib, as evidenced by the absence of these wires and the blackened interior. Current continued through the airframe to the left outboard rib and out the sender unit ground wire to the sender unit. From there, the current followed the filler cap ground braid and exited the aircraft at the filler cap. The current exploded the sender unit ground wire but not the heavier filler cap ground braid, which was only frayed. Sparks undoubtedly occurred inside the fuel tank along the ground braid and between the filler cap and its receptacle, but the fuel-air mixture in the ullage of these half-full tanks was probably too rich to support ignition.

Blast forces from stroke No. 1 at the right navigation light housing also shattered the lamp globe and bulb. This shattering allowed a portion of the first stroke current to enter the right navigation light power wire, exploding it between the lamp and the outer rib, where the current jumped to the rib and continued through the rest of the airframe to the left sender unit ground wire.

Lightning current flowing in the navigation lamp power wire elevated its voltage to several thousand volts with respect to the airframe, a voltage high enough to break down the insulation at the outer rib feed-through point, as shown in Figure 16. Until breakdown occurred here (a few microseconds after the first stroke began), the wire was at sufficiently high voltage to break down the insulation to the neighboring sender wire. This breakdown occurred all along the wire inside the right wing. The portion of current arcing into the sender wire caused a large voltage to build up across the right wing tip tank fuel gauge magnet inductance, to which this wire connects. This voltage in turn sparked over the gap between the gauge terminal and the nearest grounded housing wall, the arcing badly damaging the gauge unit. While the left navigation light power wire was also exploded, it is probable that this did not occur until the second stroke.

Since the aircraft was moving forward, the entry and exit points of the second stroke were farther aft on both wing tips than the points of the first stroke. Since no other metallic components were present aft of the first stroke attach point on the right wing tip, the second stroke punctured a hole in the fiberglass trailing edge and contacted the metallic outboard rib. As shown in Figure 16 current from this stroke proceeded through the airframe to the left wing tip, where by this time the stroke had swept aft adjacent to the navigation lamp from which point the stroke current exited. Current from stroke No. 2 thus probably arced between the left outer rib to the navigation lamp power wire (the ground wire having been vaporized by the first stroke), which it followed to the lamp housing. The power wire was vaporized by the second stroke current flowing in it.



GP01 0145 19

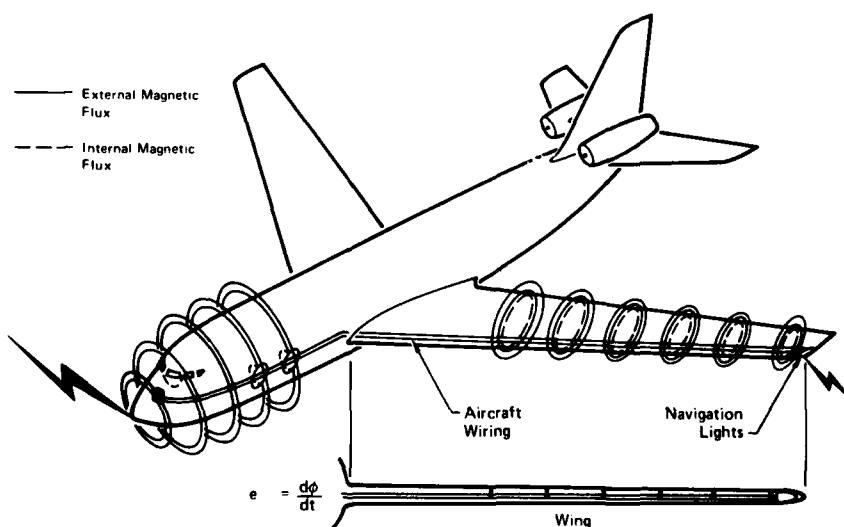
FIGURE 16
PLASTIC WING TIPS AND ASSOCIATED ELECTRIC CIRCUITS AND
LOCATIONS OF LIGHTNING EFFECTS - FROM REF (4)

Both left and right navigation lamp power wires were connected together in the cabin and to both the 12 V dc bus and the tail light. The voltage and current surges which entered the lamp power wires inboard of the outer rib feedthroughs were also conducted to the tail light, burning it out, and to the 12 V dc bus. The surge on the bus, of course, was immediately imposed on all of the other electrical equipment powered from this bus, or all of the electrical equipment in this aircraft. Arcing undoubtedly occurred in a number of components, causing circuit breakers to pop. Because circuit breakers, however, react much too slowly to prevent passage of a lightning surge, at least one piece of equipment (the No. 1 VHF communication set) and several instrument lamps were burned out.

Indirect Effects on Electrical System

Indirect effects result from the interaction of the electromagnetic fields accompanying lightning with electrical equipment in the aircraft. Hazardous indirect effects could, in principle, be produced by a lightning flash that did not directly contact the aircraft and hence could produce none of the direct effects described earlier. In some cases both direct and indirect effects may occur to the same component of an aircraft. An example would be an antenna which is physically damaged but which also couples damaging voltages into the transmitter or receiver connected to the antenna.

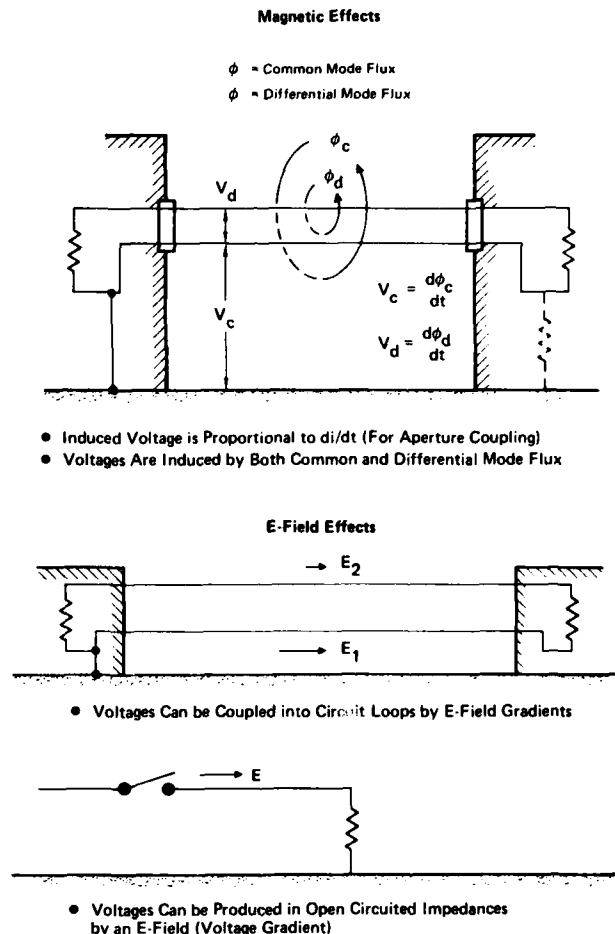
The mechanism whereby lightning currents induce voltages in aircraft electrical circuits is illustrated in Figure 17. As lightning current flows through an aircraft, strong magnetic fields surround the conducting aircraft and change rapidly in accordance with the fast-changing lightning-stroke currents. Some of this magnetic flux may leak inside the aircraft through apertures such as windows, radomes, canopies, seams, and joints. Other fields may arise inside the aircraft when lightning current diffuses to the inside surfaces of skins. In either case these internal fields pass through aircraft electrical circuits and induce voltages in them proportional to the rate of change of the magnetic field. These magnetically induced voltages may appear between both wires of a two-wire circuit, or between either wire and the airframe. The former are often referred to as line-to-line, or differential-mode voltages and the latter as common-mode voltages.



GP01 0145 20

FIGURE 17
MAGNETIC FLUX PENETRATION AND INDUCED
VOLTAGES IN ELECTRICAL WIRING - FROM REF (4)

In addition to these induced voltages, there may be resistive voltage drops along the airframe as lightning current flows through it. If any part of an aircraft circuit is connected anywhere to the airframe, these voltage drops may appear between circuit wires and the airframe, as shown in Figure 18. For metallic aircraft made of highly conductive aluminum, these voltages are seldom significant except when the lightning current must flow through resistive joints or hinges. However, the resistance of titanium is 10 times that of aluminum, and that of composite materials many hundred times that of aluminum, so the resistive voltages in future aircraft employing these materials may be as much as hundreds of times higher.



GP01-0148 21

FIGURE 18
ELECTRICAL AND MAGNETIC FIELD COUPLING TO ELECTRICAL CIRCUITS

Until the advent of solid state electronics in aircraft, indirect effects from external environments, such as lightning and precipitation static, were not much of a problem and received relatively little attention. No airworthiness criteria are available for this environment. There is increasing evidence, however, of troublesome indirect effects. Incidents of upset or damage to avionic or electrical systems, for example, without evidence of any direct attachment of the lightning flash to an electrical component are showing up in airline lightning-strike reports. Table 4 summarizes the reports of interference or outage of avionic or electrical equipment reported by a group of U.S. airlines for the period June 1971 to November 1974 (Reference 9).

The incidents reported in Table 4 occurred in 20% of the total of 214 lightning-strike incidents reported during the period. U.S. military aircraft have had similar experience. This experience is probably a result of the increasing sensitivity of miniaturized solid state electronics to transient voltages, a trend which necessarily would not have posed a problem in older, less sophisticated equipment. In any one incident, only a few electronic components are affected; others are not. Yet laboratory tests have shown that lightning-induced voltages appear in all aircraft electric wiring at once. Thus it is evident that surges reach higher values in some circuits than in others or that some electronics are less tolerant of such surges than others.

Indirect effects were evident in about 20% of all the incidents reported, while outages were reported in only about 10% of all incidents. Since severe strokes also occur in only about 10 to 20% of all flashes, it is possible that a severe stroke may be required to cause noticeable effects.

While the indirect effects are not presently a major safety hazard, there are four trends in aircraft design and operations which could increase the potential problem. These include the following:

- Increasing use of plastic or composite skin.
- Further miniaturization of solid state electronics.
- Greater dependence of electronics to perform flight-critical functions.
- Greater congestion in terminal airways, requiring more frequent flight through adverse weather conditions at altitudes where lightning strikes frequently occur.

TABLE 4
EVIDENCE OF INDIRECT EFFECTS IN COMMERCIAL AIRCRAFT - FROM REF (4)
 (214 Strikes)

	Interference	Outage
HF Communication Set	—	5
VHF Communication Set	27	3
VOR Receiver	5	2
Compass (All Types)	22	9
Marker Beacon	—	2
Weather Radar	3	2
Instrument Landing System	6	—
Automatic Direction Finder	6	7
Radar Altimeter	6	—
Fuel Flow Gauge	2	—
Fuel Quantity Gauge	—	1
Engine rpm Gauges	—	4
Engine Exhaust Gas Temperature	—	2
Static Air Temperature Gauge	1	—
Windshield Heater	—	2
Flight Director Computer	1	—
Navigation Light	—	1
AC Generator Tripoff	(6 Instances of Tripoff)	—
Autopilot	1	—

GP01-0146 22

Engine Mishaps

Reported lightning effects on turbojet engines show that these effects are limited to temporary interference with engine operation. Flameouts, compressor stalls, and roll-backs (reduction in turbine rpm) have been reported after lightning strikes to aircraft with fuselage-mounted engines. This type includes military aircraft with internally mounted engines and fuselage air intakes or other military and civil aircraft with engines externally mounted on the fuselage. There have been no attempts to duplicate these events with simulated lightning in a laboratory, and there has been no other qualitative analysis of the interference mechanism.

An extensive survey was undertaken by workers at McDonnell Aircraft Co. to determine the extent of the lightning-induced turbine engine outage problem. Contacts were made with the Air Force and Navy Safety Operations Offices, the Air Force and Navy Propulsion Laboratories, the FAA, the major engine manufacturers and representatives from the UK, France and Germany. The results of the survey indicated that there have been 22 reported incidents in the U.S. between 1968 and 1978 of engine problems and/or flameouts as a result of a lightning strike. However, it is believed that there are at least two to five times more cases that are not reported because the FAA does not require mandatory reporting of such incidents if there is no injury. Individual pilots interviewed have had flameouts resulting from lightning strikes who have not filed reports of the incidents. Of the reported cases, none of the lightning strikes has resulted in extensive engine damage and none has resulted in loss of life. However, there have been instances where one engine flamed out on a twin-engine aircraft and where the pilot was unable to restart the engine in flight. He was forced to resort to emergency landing procedures. There have also been incidents on two engine aircraft where both engines have stalled simultaneously, but in each of these cases, one or both were restarted in flight.

Almost all of the reported incidents of engine problems were associated with lightning strikes to small aircraft, either fighters or business-type aircraft, rather than to large aircraft. This uneven distribution of events may be due to the inability of the smaller engines to adequately compensate for temperature and pressure fluctuations associated with lightning strikes; or on the larger aircraft it may be due to the dying out of the lightning channel before it reaches the rear-mounted engines because of the long distance from the nose to the tail.

The results of the literature search and discussions with cognizant personnel revealed that there is a potential hazard to single-engine jet fighters. However, there are many other causes for compressor stalls which present more immediate problems to propulsion engineers.

Fuel Ignition Related to Electrical Systems

Potentially, aircraft fuel systems represent the most critical lightning hazard to flight safety. An electric spark produced by only 0.2 millijoule (mJ) of energy is sufficient to ignite a propagating flame in a near stoichiometric mixture of hydrocarbon fuel and air (Reference 23), yet lightning-flash currents may deposit several thousand joules of energy in an aircraft.

There are several jet and turbojet transport accidents on record which have been attributed to lightning ignition of fuel. Although the exact location of ignition in each case remains obscure, the most prevalent opinion is that lightning ignited fuel vapor at the wing tip vent outlets of these aircraft or that sparking occurred somewhere inside a fuel tank as lightning currents flowed through the aircraft. The inflight loss of at least two military aircraft also has been attributed to lightning ignition of fuel, and there is a report of lightning strike igniting fuel in another military aircraft parked on the ground. Lightning-induced voltages in aircraft electrical wiring are believed to have resulted in sparks across a capacitance-type fuel probe or some other electrical object inside fuel tanks of several military aircraft, resulting in loss of external tanks in some cases and the entire aircraft in others. Capacitance-type fuel probes are designed to preclude such occurrences. The voltage required to spark a typical capacitance-type probe is many times greater than the voltage thought to be induced in fuel gauge circuits by lightning. However, other situations involving unenclosed circuits, such as externally mounted fuel tanks, exist wherein induced voltages may be much higher than those found in circuits completely enclosed by an airframe.

The accidents mentioned above prompted extensive research into the lightning effects on and protection of all aircraft fuel systems. Improved bonding, lightning-protected filler caps and access doors, active and passive vent flame suppression devices, flame-retardant foams, and safer (i.e., less flammable) fuels are examples of developments which have resulted from this research. In addition, government airworthiness requirements now include lightning protection for aircraft fuel systems and specify requirements and tests that must be passed to demonstrate compliance prior to aircraft certification. As a result of these safety measures, lightning strikes present fewer hazards to the fuel systems aboard modern transport aircraft than to those of older aircraft, and properly certificated aircraft may expect to experience lightning strikes with no adverse effects on fuel systems. Continued changes in airframe designs and materials, however, make it mandatory that care and diligence in fuel system lightning protection not be relaxed in the future.

SUMMARY AND CONCLUSIONS

Lightning mishaps to aircraft in flight occur periodically to aircraft of all types under many different weather conditions. Incidents occur most frequently at medium altitudes and at temperatures near the freezing point. An evaluation of pilot reports indicated that lightning may strike unexpectedly or there may be a buildup of static noise and corona before the strike. Pilots contend that the latter type of strike far outnumbers the former and some think that this type can be avoided by reducing the velocity of the aircraft. An examination of the lightning initiation process raises the additional question of whether some reports of aircraft being "struck" might involve a branch of the flash rather than the main channel to ground, or lightning triggered by the aircraft.

Effects of lightning on aircraft electrical systems include physical damage to electrical wiring and associated avionics equipment as a result of lightning currents finding their way into the wiring through the external hardware. Indirect effects can result in the loss or temporary malfunction of avionics equipment due to electromagnetic coupling of lightning produced fields onto internal wiring and equipment.

Instances of turbine engine lightning-induced outages may sometimes be related to indirect effects on the electrical control system. Indirect lightning effects may also be implicated in some of the fuel vapor explosions which have resulted in catastrophic losses of aircraft.

It is obvious that lightning strikes to aircraft occur in only a very small percentage of flights and only a small fraction of the lightning incidents are major problems. However, because of the very large number of aircraft in the air at all times and the large number of storms around the globe at any instant in time, the total number of lightning strikes to aircraft per year is not a small number. It is not our task to prevent the strikes altogether because most are unavoidable. It is rather our task to maintain the lightning problem at or below the nuisance level. That is, to ensure that the incidents are minor, that damage is minimized, and that both military and domestic flight operations can proceed safely without undue fear of the natural lightning hazard.

REFERENCES

1. P. B. Corn, "Lightning as a Hazard to Aviation" presented at the American Meteorological Society's 111th Conference on Severe Local Storms, 3-5 Oct 1979, Kansas City, Missouri
2. F. L. Guiberson, "Weather Factor Mishaps," Aerospace Safety, June 1978.
3. P. B. Corn, "Lightning Hazards Overview - Aviation Requirements and Interests," presented at the NASA/UTSI Workshop on the Need for Lightning Measurements from Space, University of Tennessee Space Institute, Tullahoma, Tenn., February 1979.
4. F. A. Fisher and J. A. Plumer, "Lightning Protection of Aircraft," NASA RP-1008, October 1977.
5. J. A. Plumer, "Lightning Effects on General Aviation Aircraft," Proceedings of the FAA/FIT Workshop on Grounding & Lightning Technology, March 6-8, 1979, Melbourne, Fla.
6. H. T. Harrison, "UAL Turbojet Experience with Electrical Discharges," UAL Meteorological Circular No. 57, United Airlines, Chicago, Ill., January 1965.
7. D.W. Clifford, "Another Look at Aircraft Triggered Lightning", presented at the FAA/NASA/FIT Symposium on Symposium on Lightning Technology, Virginia, April 22-24, 1980.
8. M. M. Newman and J. D. Robb, "Aircraft Protection from Atmospheric Electrical Hazards," USAF Report ASD-TR 61-493, December 1961.
9. B. I. Hourihan, "Data from the Airlines Lightning Strike Reporting Project, June 1971 to November 1974," Summary Report GPR-75-004, High Voltage Laboratory, General Electric Company, Pittsfield, Mass., March 1975.
10. R. B. Anderson and H. Kroninger, "Lightning Phenomena in the Aerospace Environment: Part II, Lightning Strikes to Aircraft," Proceedings of the 1975 Conference on Lightning and Static Electricity, Culham Laboratory, England, April 1975.
11. J. A. Plumer and B. L. Perry, "An Analysis of Lightning Strikes in Airline Operation in the USA and Europe," Proceedings of the 1975 Conference on Lightning and Static Electricity, Culham Laboratory, England, April 1975.
12. O. K. Trunov, "Conditions of Lightning Strikes in Air Transports and Certain General Lightning Protection Requirements", Proceedings of the 1975 Conference on Lightning and Static Electricity, Culham Laboratory, England, April 1975.
13. J. F. Shaeffer, "Aircraft Initiation of Lightning", Proceeding of the 1972 Lightning and Static Electricity Conference, Las Vegas, Nevada, December 1972.
14. M. A. Uman, Lightning, McGraw Hill, New York, 1969.
15. J. E. Nanevicz, R. C. Adamo and R. T. Bly, Jr., "Airborne Measurements of Electromagnetic Environment Near Thunderstorm Cells (TRIP-76)," Final Report to NASA JSC, Contract NAS9-15101, March 1977.
16. J. T. Dijack, "Airborne Measurements of Transient Electric Fields and Induced Transients in Aircraft Due to Close Lightning," U.S. Air Force Report AFFDC-TR-77-64, June 1977.
17. R. K. Baum, "Airborne Lightning Characterization," presented at the FAA/NASA/FIT Symposium on Lightning Technology, Hampton, Virginia, April 22-24, 1980.
18. E. P. Krider and G. J. Radda, "Radiation Field Waveforms Produced by Lightning Stepped Leaders," Journal of Geophysical Research, Vol. 80, No. 18 (1975), pp. 2653-2657.
19. Y. T. Lin, M. A. Uman, J. A. Tiller, R. D. Brantley, R. P. Krider and C. D. Weidman, "Characterization of Lightning Return Stroke Electric and Magnetic Fields from Simultaneous Two-Station Measurements," Journal of Geophysical Research (March 1979).

20. M. A. Uman, D. K. McLain, R. J. Fisher and E. P. Krider, "Electric Field Intensity of the Lightning Return Stroke," *Journal of Geophysical Research*, Vol. 78 (1973), pp. 3530-3537.
21. N. Cianos and E. T. Pierce, "A Ground-Lightning Environment for Engineering Usage," Stanford Research Institute Technical Report No. 1, Project 1834 (August 1972).
22. T. E. James and J. Phillpott, "Simulation of Lightning Strikes to Aircraft," Culham Laboratory Report CLM-R111, Abingdon, Oxfordshire, U.K. 1971.
23. "Fire Protection and Research Program for Supersonic Transport," U.S. Air Force Report APL TDR-64-105, October 1964.

PHENOMENOLOGY OF LIGHTNING/AIRCRAFT INTERACTION

R.P. Mühleisen
Astronomisches Institut
der Universität Tübingen
7980 Ravensburg-Rasthalde

SUMMARY

Lightning aircraft interaction depends on the behaviour of the lightnings as well as on the aircraft shape and material used for the skin and for the interior of the aircraft. The paper deals mainly with the lightnings themselves.

Two types of lightning discharges have different characteristics:

- 1) Intracloud and cloud to cloud discharges and
- 2) Cloud to ground discharges.

First it will be tried to introduce the many hypotheses of thundercloud electrification. It is unknown which of these gives the right explanation for the charge separation in the clouds which produces high electric fields. Just so unknown is the initiation of the discharges themselves. But the parameters of lightnings can be enumerated much better.

Calculation results and graphs are given due to the electric field strength around thunderclouds. The distortion of these fields by aircraft bodies and the initiation of triggered lightnings are described. One problem due to the effect of the jet exhaust on the field distortion could be solved by experiments and considerations. It seems that the exhaust has no influence.

1. SURVEY OF THE ELECTRIFICATION THEORIES AND HYPOTHESES AND CRITICALS REMARKS.

Lightnings occur in the atmosphere if the electric field strength in cloud exceeds a critical value of about 10 kV/m and if the potential difference in a small volume of the cloud exceeds some million Volts. Such electric fields are developed only in thunderclouds. Because of the difficulties of measurements inside such clouds due to the strong dynamics and turbulence the knowledge of the electric phenomena and the electrification processes are not satisfactory.

Many laboratory investigations yielded a great number of electric charge separation effects. It is necessary to distinguish between electric effects in small bodies as water droplets, ice pellets or snowflakes, electric effects on the solid-liquid interface of hydrometeors and the gravitational separation of different particles with charges of different polarities within the large space of a thundercloud in the updraughts and in the downdraughts. Namely the distribution of charge in the entire thundercloud requires beside microphysical electrification mechanisms an extended separation of charges. This separation can be achieved in the up-wind and downdraughts either if the charges are deposited on particles of different size and mass or if the charges of the one polarity reach the up-wind meanwhile the other particles with the charges of the opposite polarity remain in the downdraught.

Another hypothesis deals with the electrical charging by induction in a ionized atmosphere and a charge separation by vertical air streams which is similar as a Van de Graf-generator. Now to the first class of hypotheses: I mention by name the authors Find-eisen (1940), Workman-Reynolds (1950), Latham and Mason (1961) among others. They all explain from their experiments charging processes by the micro-physics of the lattice of solid and liquid bodies. Either temperature gradients and diffusion of positive protons inside the bodies or double layers on the surface of droplets are the reason for charge separation in the bodies. A series of hypotheses postulates electric volta potential differences between the liquid and the solid phase of droplets even when the supercooled droplets collide with others or with ice pellets. Because of many lightning strikes on aircraft occur near the region where the air temperature is between + or - 5°C, it is likely to be justified to assume that the strongest charge separation processes take place connected with the collision of solid and liquid particles. In this region graupel came down and collide with supercooled droplets; one part of the water freezes on the graupel nucleus, the other part flies upwards in the up-wind. During the contact there exists a potential difference in the solid-liquid interface according to the temperature gradient. An older hypothesis of Workman and Reynolds (1950) explains the charge separation by electrolytic potentials. The disappearing water droplets are therefore electrically charged. One problem is the polarity of the charges; they depend on the solution of impurities in the water. Recently this hypothesis is questionable because the impurities in the form of condensation nuclei are different from place to place so the polarity is uncertain.

The hypothesis of Latham and Mason explains the charging process in the solid-liquid interface by temperature gradient in the ice. The falling ice pellets are colder than the environment; during the contact with super-cooled water droplets the surface of the ice will accept the temperature of the melting point so that a temperature difference between the surface and the interior of the ice pellet results. By the temperature difference a electrical voltage is generated in the ice therefore the waterskin on the surface will be charged and will leave the surface charged. Both authors show by calculation that about 1 Cb/km² min is produced.

Another process of charging is described by Dinger and Gunn (1946). The charging occurs during the melting of down coming ice particles. This process will be able to produce charges in the air and on the water droplets with different polarities. The earlier finding of Findeisen (1940) can be explained by one of this mentioned hypothesis.

A quite different hypothesis is the induction-hypothesis of Vonnegut and others (1958). He assumes that the upcurrent in the developing thundercloud sucks air with positive space charges from near the earth surface and carries these charges up to the top of the cumulonimbus cloud; these charges attract negative charges from the outside air which attach onto the outer cloud particles and remain on these. Because of the down-draughts of the outer parts of the cloud the negative charges descend whereas the positive charges ascend and are concentrated in the upper part of the cloud in the anvil. This induction mechanism will be intensified when the space charge production near the ground is increased by corona discharges which have the positive sign also. Then the maximum of the charge production culminates simultaneously with the maximum of the up-wind, that means with the dynamical climax. Later on the charge production ceases in the final stage of the thundercloud. Many experts doubt this hypothesis.

It is very probable that many processes work together inside a thundercloud. Therefore one has to keep in mind that the electric field configuration will be very complicated and complex and simple theoretical descriptions or incidental measurements of the electrical features give no complete picture of the electrical conditions which vary in space and time so immense.

A general view about the hypotheses for precipitation electrification is presented in figure 1. For detail it is necessary to look into the original papers of the authors.


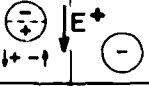

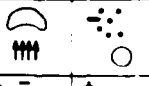





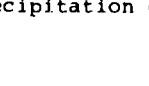
author	presupposition	process of charge separation before later on	experimental evidence	charge productivity
Elster-Geitel 1913	electric field		-	?
Wilson 1929 (Wall 1948)	electric field + ions		+	$10^{-1} \text{Cb/km}^3 \text{min}$
Vonnegut 1955	space charges at ground		-	?
Simpson 1909 Lenard 1892	$t > 0^\circ \text{C}$ up-wind		+	$9 \cdot 10^{-2} \text{Cb/km}^3 \text{min}$
Frenkel 1944	$t \approx 0^\circ \text{C}$ ions		-	?
Findeisen 1940	$t < 0^\circ \text{C}$		+	$10^{-15} \text{Cb/cm}^2 \text{sec}$
Findeisen	$t < 0^\circ \text{C}$		+	$10^{-14} \text{Cb/cm}^2 \text{sec} (?)$
Findeisen	$t < 0^\circ \text{C}$		+	$10^{-12} \text{Cb/cm}^2 \text{sec}$
Latham-Mason 1961 Reynolds 1957	$t < 0^\circ \text{C}$		+	$1 \text{Cb/km}^3 \text{min}$
Workman-Reynolds 1950	$t \leq 0^\circ \text{C}$		+	$> 1 \text{Cb/km}^3 \text{min}$

Fig. 1: Hypotheses for precipitation electrification

2. ELECTRIC FIELDS AROUND THUNDERCLOUDS.

It is an open question if the strong electric fields inside and around thunderclouds begin with the precipitation processes or earlier with the beginning of up and downdraughts. The author believes that the first assumption is right. With the precipitation the charge separation processes over large vertical distances starts and by this the electric fields of a thundercloud are generated. Under the simplified assumption of a separation of positive and negative charges of 15 C located in 2.5 km, resp. 7.5 km altitude above ground and under the assumption of a weak conducting atmosphere one can calculate the field distribution around a thundercloud; taking into account the mirror image charges under the earth surface one gets pictures of the distribution of the electric field strength, the vertical and horizontal components as shown in fig. 2 a-c.

Normally it is unknown which charges really exist in a thundercloud and how the real distribution of charges in the entire cloud is; so the calculated field configurations in fig. 2 are only a first approximation for a normalized cloud case. Also many observations and measurements point to a small pocket of positive charge near the base of a thundercloud. This would modify and change considerably the picture of field strengths in the lower altitudes. Another reason for an extremely important change of the picture is the frequent neighbourhood of other thundercloud cells. Then mainly the horizontal component of the electric field is enhanced and occurs in a much larger area.

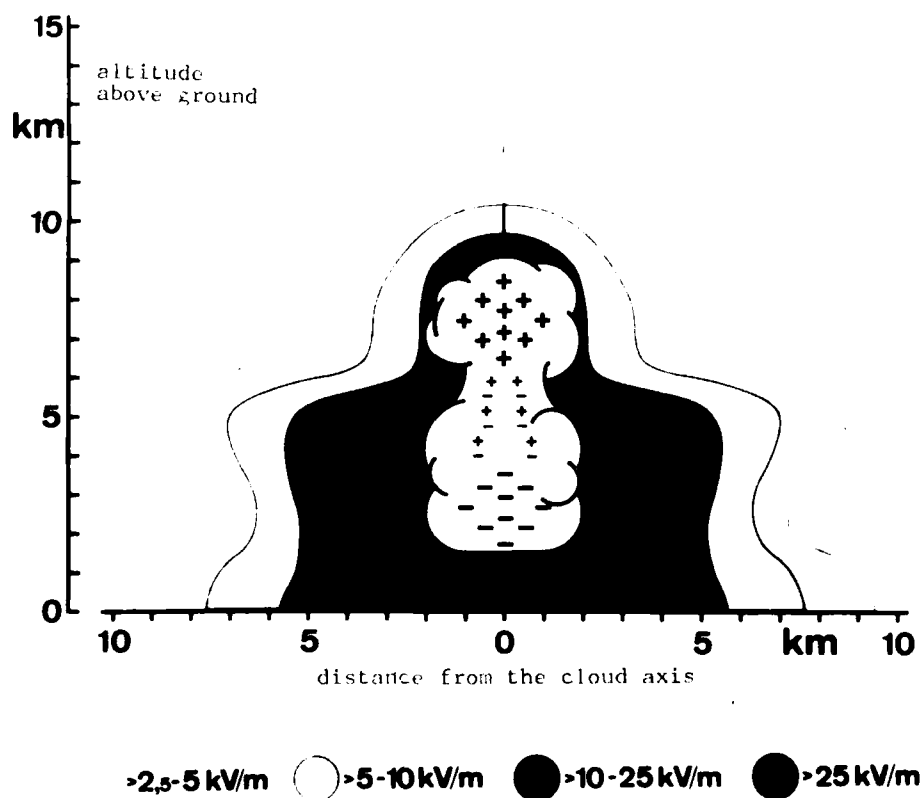


Fig. 2a: Air electric field strength in function of altitude and distance from cloud axis.

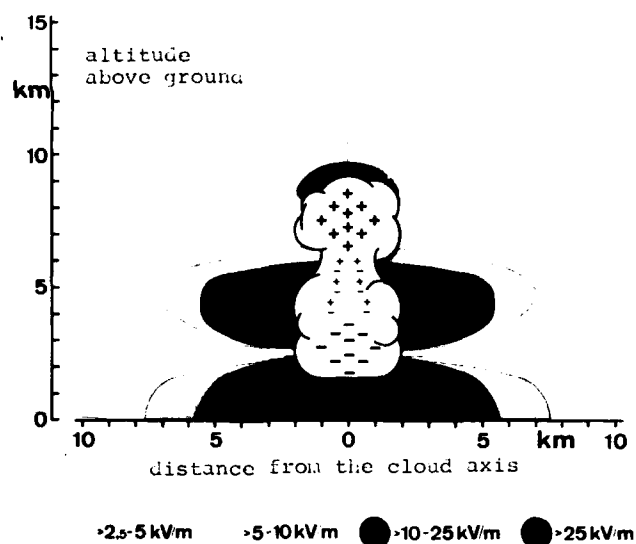


Fig. 2b: Vertical component of air electric field strength in function of altitude and distance from the cloud axis.

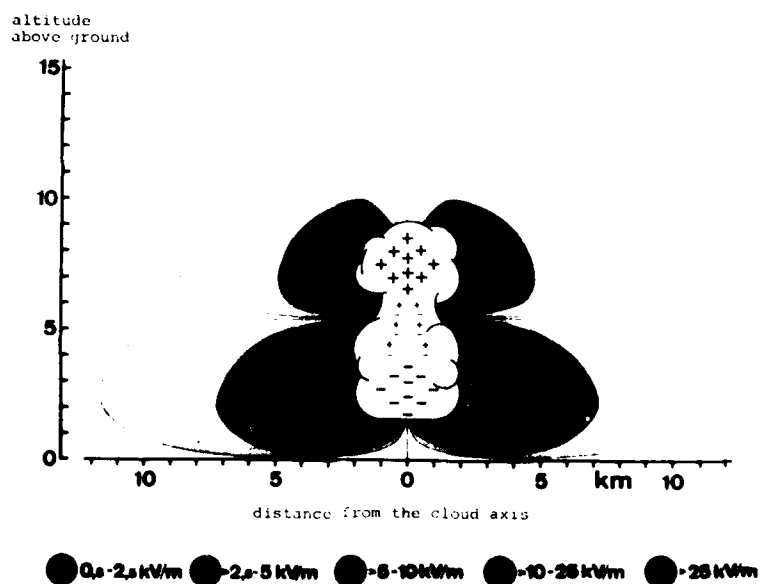


Fig. 2c: Horizontal component of air electric field strength in function of altitude and distance from the cloud axis.

3. INFLUENCES OF AIRCRAFT ON THE ATMOSPHERIC ELECTRIC FIELD

The natural electric field in the atmosphere will be distorted in the surroundings of an aircraft. The distortion depends mainly on the geometric form of the aircraft body. For an idealized form of an ellipsoid the outer electric field E is enlarged by a factor k depending on the ratio a/b where a is the length of the longer axis and b is the length of the transverse axis of the ellipsoid.

Values of k are given in table 1

table 1

a/b	2	5	10	20	50	100
k	5,8	16	49	148	694	2330

In the case of longer extremities as antennas or Pitot-valves the factor k is magnified furthermore. In the case of a jet aircraft one has to put on the basic ellipsoid with the axis a and b another half ellipsoid with the diameter or the small axis $2r$ and the length or the long half axis s imitating a rod, an antenna or a Pitot-valve. If the aircraft flies in an atmosphere with a horizontal undisturbed electric field E_a and has a self charge Q on its body then the fieldstrength on the uttermost point is:

$$E_s = (E_a \cdot k_{a,b} - \frac{Q}{4\pi \cdot \epsilon_0 \cdot b^2}) \cdot k_{s,r}$$

With mean values of a/b of 10 and a ratio s/r of about 20 one achieves a critical value for the enlarged fieldstrength E_s of more than 1000 kV/m with a outer horizontal field E_a of about 500 V/m. Much less is the enlargement faktor k for a vertical field, namely about 2-4 for $k_{a,b}$ and for $k_{s,r}$ too.

The enlargement of the electric field on the surface of the aircraft body has the following consequences:

First corona discharges are generated if the surface fieldstrength exceed a certain value, about 3-10 kV/cm or 300-1000 kV/m. Second if a charge has been generated on the aircraft itself by precipitation particles or by the exhaust, then the self produced electric field around the aircraft is enlarged too on the surfaces with strong curvature by the same factor k . For this reason very small charges on the aircraft (several μC) are able to produce corona discharges. Therefore such self charges cannot exceed a threshold charge of several μC .

Aircraft are able to trigger lightnings or they can be located in the path of a natural lightning. Because of the lack of measurements of the courses of the fieldstrength and currents in the case of lightning strokes to aircraft no credible hypothesis could be found in the literature which describes the transition from a corona discharge into a lightning discharge. The condition that on the top of a discharge channel the fieldstrength is always large enough for breakdown has to be fulfilled for the development of a streamer or a pilot leader. In addition to this the current in the streamer has to be so great that

- a) the freshly formed part of the channel is filled with charges,
- b) space charges of opposite sign can be neutralised,
- c) all losses from corona discharges of the channel wall itself can be filled up.

From all of them one can derive that the main condition for the development of a lightning stroke is the concentration of a large amount of charges in a great volume of cloudy air. Therefore only in thundercloud in its mature stage lightning strokes can originate.

4. LIGHTNING PARAMETERS

The most important parameters of lightning are

- l = length of the lightning channel,
- I_{max} = maximum lightning current,
- $\frac{dI}{dt}/_{max}$ = maximum current rise rate,
- t_s = duration of single strokes,
- n = number of strokes,
- t_f = entire duration of lightning flash,
type of the discharge:

First to the last point: one has to distinguish between

- 1) Intracloud and cloud to cloud discharges,
- 2) Cloud to ground discharges.

In middle latitudes about half of the lightnings belong to each type. The length of lightning channels varies from several km to 20 km. Partly they are orientated vertically, partly horizontally. Most of the cloud to ground flashes have long extensions inside the clouds. The lightning currents vary between 100 A and several 100 kA. Values above 100 A belong exclusively to the ground flashes as far as one knows for the time being. The current rise rate is also variable between 1 to 100 kA/ μs and less of this in the case of intracloud or cloud to cloud flashes. Sometimes continuous currents occur for some 10-100 milliseconds with values of about 100 A. The entire duration of a flash depends on the number of strokes. One flash has normally 1-3 strokes, the maximum is about 25 strokes. A single flash has a duration of several msec. A multistroke flash lasts about 100-1000 msec. The intervals between successive strokes in one flash amount to 3-100 msec.

5. EFFECT OF THE EXHAUST ON THE ELECTRIC FIELD DISTORTION

Many experts in the field of lightnings believe that the exhaust of an airplane or of a rocket causes a fictitious electric enlargement of the conducting body of the aircraft. This would cause a further increase of the distortion of the ambient electric field and so an increase of the probability to trigger lightnings. This hypothesis came up with the lightning events during the launch of the Apollo 12.

In the meantime we did some theoretical and experimental work to investigate this case (Mühleisen and Fischer 1976). The result was that the exhaust of a rocket or a jet engine cannot achieve an electrical enlargement of the aircraft body. The reason is that the velocity of ions in the exhaust is larger than the drift in a naturally possible electric field: that means

$$E \times b < v_{\text{exhaust}}$$

E = electric fieldstrength,

b = mobility of ions,

v_{exhaust} = velocity of the gas molecules in the exhaust.

If this is correct then no ion is able to transport any charge backwards to the aircraft body. Therefore no current can flow in the exhaust as an effect of the external electric field. The exhaust has therefore not to be considered as an enlargement of the conducting body of an aircraft.

REFERENCES

- (1) Dinger, J.E. and R. Gunn, "Electrical effects associated with a change of state of water." Terr. Magn. a Atm. Electricity, Vol. 51, 1946, pp. 477 - 494.
- (2) Elster, J. und H. Geitel, "Zur Influenztheorie der Niederschlagselektrizität." Phys. Zeitschr. Vol. 14, 1913, pp 1287 - 1292.
- (3) Findeisen, W. "Über die Entstehung der Gewitterelektrizität." Meteorol. Zeitschr. Vol. 57, 1940, pp. 201 - 215.
- (4) Frenkel, Y.I., "A theory of the fundamental phenomena of atmospheric electricity." Journ. Phys. Moscow, Vol. 8, 1944, pp. 285 - 304.
- (5) Latham, J. and B. Mason, "Electric charge transfer associated with temperature gradients in ice." Proc. of the Roy. Soc. A, Vol. 260, 1961, pp. 523 - 536.
- (6) Latham, J. and B. Mason, "Generation of electric charge associated with the formation of soft hail in thunderclouds." Proc. of the Roy. Soc. A, Vol. 260, 1961, pp. 537 - 549.
- (7) Mühleisen, R. and H.-J. Fischer, "Blitzgefährdung von Strahlflugzeugen." BMVg-FBWT 76 - 14, 1976, pp. 1 - 42.
- (8) Pierce, E.T., "Triggered lightning and its application to rockets and aircraft." 1972 Lightning and static electricity conference, 12 - 15 Dec. 72. Air Force Avionics. Lab. and SAE Committee AE-4 on Electromagnetic Compatibility, AFAL-TR-72-325, pp. 180 - 188.
- (9) Simpson, G.C., "On the electricity of rain and its origin in thunderclouds." Phil. Trans. A, Vol. 209, 1909, pp. 379 - 413.
- (10) Vonnegut, B. and Ch.B. Moore, "Giant electrical storms." Recent Advances Atmosph. Electr., Pergamon Press, New York: 1958, pp. 399 - 411.
- (11) Wilson, C.T.R., "Some thundercloud problems." Journ. of Franklin Inst. Vol. 208. 1929, pp. 1 - 12.
- (12) Workman, E.J. and S.E. Reynolds, "Electrical phenomena occurring during the freezing of dilute aqueous solution." Phys. Rev. Vol. 78, 1950, pp. 254.

SUSCEPTIBILITY OF AVIONICS TO LIGHTNING INDIRECT EFFECTS

by
J. Anderson Plumer
Lightning Technologies, Inc.
560 Hubbard Avenue
Pittsfield, Massachusetts 01201
U.S.A.

SUMMARY

The use of sensitive, solid-state avionic equipment to perform flight critical functions requires that this equipment be adequately protected from the transient voltage and current surges induced in aircraft electrical circuits by lightning strikes. Design of protection requires, first, that the nature of the lightning-induced transients that may appear at the terminals of aircraft avionic equipment be known. This paper describes ways that lightning currents may flow in an airframe and basic mechanisms whereby these currents may induce transient voltages and currents in typical aircraft electrical circuits. Examples of induced voltages and currents measured during simulated lightning tests are presented and significant aspects of them are discussed, together with estimates of the ranges of induced voltages to be expected in typical circuits. Examples of the magnetic fields that are responsible for some of these induced effects are also presented. The paper concludes with a discussion of the basic damage effects that lightning-induced voltages may have on typical solid-state electronic components. Methods of protection against these effects are treated in a subsequent paper.

INTRODUCTION

In contrast to the physical damage effects that lightning strikes may cause to an aircraft structure which are termed the *direct effects*, the effects on aircraft electrical and avionic systems are termed *indirect effects*. The indirect effects refer to the temporary upset or permanent damage to electrical and avionic equipment that results from lightning flashes. These effects may range from tripped circuit breakers to computer upset, or to physical damage to input or output circuits of electronic equipment. There may be other indirect effects of lightning flashes that pertain to aircraft safety, such as flash blindness of the crew or acoustic shock waves, but these effects are not treated here. Included in this definition and discussed here are the voltages and currents induced by lightning on the electrical wiring of the aircraft, regardless of whether or not such voltages and currents cause damage or upset of electrical equipment.

To date, occurrence of induced voltages in aircraft has been evidenced by occasional upset or damage to aircraft avionics and flight instruments during lightning strike events. Sometimes this has resulted in curtailment of a flight mission, but there are very few records of an aircraft being lost due to indirect effects. The increasing use of more sensitive electronics however, and the housing of these within nonmetallic structures implies that induced voltages may be more severe and hazardous in the future if left unchecked. It is therefore important for designers to be aware of their existence, and of ways to estimate their magnitude and design adequate protection.

Analysis of indirect effects to be expected in a particular aircraft can be divided into several stages. The overall task is to determine how the lightning current, I_L , leads to voltages and currents on the internal wiring. The individual tasks are as follows:

- To determine the amplitude and waveform of lightning currents flowing in the aircraft structure. This current may be different from the undisturbed lightning current.
- To determine the magnitude of voltages and currents induced on aircraft electrical circuits.
- To determine how these currents and voltages affect the electrical equipment in the aircraft.

LIGHTNING CURRENTS IN THE AIRCRAFT

The problem of how the aircraft as a whole responds to the passage of lightning current is illustrated in Figure 1. There are two parts of this problem, one involving a direct flash to the aircraft and the other involving a nearby flash. While it is generally true that the indirect effects produced by a direct flash are more severe than those produced by a nearby flash, they are not necessarily so, since the response of the aircraft

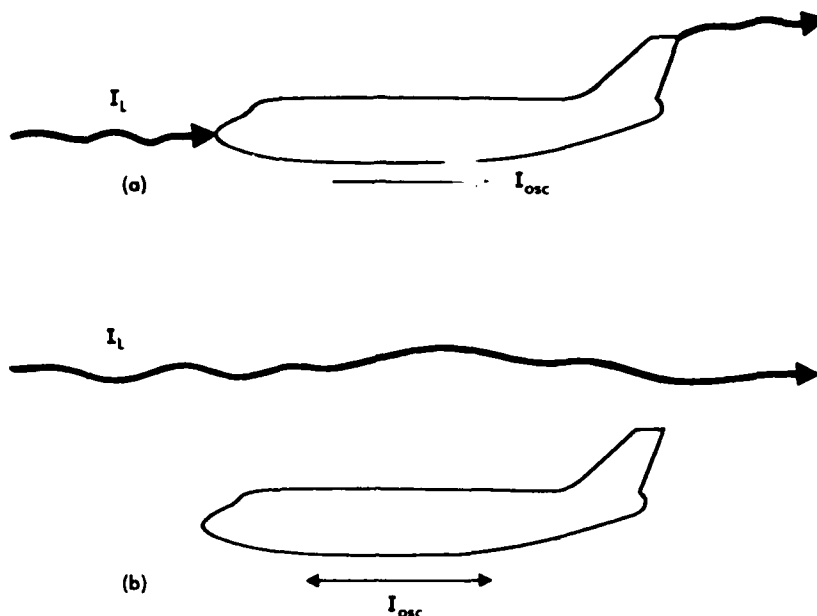


Figure 1 - Response of the Structure to the Lightning Current.
 (a) To a direct flash
 (b) To a nearby flash

Consider first a direct hit on the aircraft. The return stroke current enters the aircraft at one extremity, flows through it, and exits from the other end. As a result of the different impedances of the lightning channel and the aircraft, the current flowing through the aircraft may undergo some distortion in waveform. The result is that the waveform of the current leaving the aircraft may be different from that entering the aircraft. Typically, the exit current rises to crest over a longer time than does input current.

The phenomena involved are shown in Figure 2. A waveform is shown traveling along the conductor having surge impedance Z_1 . Surge impedance is defined as

$$Z = \sqrt{L/C} \quad (1)$$

where

Z = surge impedance (ohms)
 L = inductance (henries) per unit length
 C = capacitance (farads) per unit length

at the point under consideration. At some point the current encounters a transition point between the conductor having surge impedance Z_1 and a different conductor of surge impedance Z_2 . At this transition point, part of the incident current is transmitted onto the second conductor, but part of it is reflected back in the direction from which it came. The magnitudes of the transmitted and reflected components of voltage or current at this transition point are given by the values of transmission and reflection operators, α and β for voltage and λ and δ for current, shown in Figure 2(a).

If there are two discontinuities, as in the case of Figure 2(b), there will be reflections at each discontinuity with currents traveling back and forth, and thus oscillating, in the intermediate conductor. The amplitudes of these oscillatory currents will diminish as energy is transmitted from the intermediate conductor to the conductors on either end.

The geometry of Figure 2(b) approximates that of a lightning current entering an aircraft, since the surge impedance of the lightning channel is probably higher than the surge impedance of the aircraft. When account is taken of all the reflections and transmissions at the various transition points, the result is that the current waveforms will appear as shown in Figure 2(c). If the entering lightning current has a fast front and a slower decay, the current at the entrance of the low-impedance section (in the aircraft) will exhibit an overshoot. The current at the center of the aircraft will have an oscillatory component superimposed upon a waveform fundamentally like that of the input current, and the current leaving the aircraft will have a slower rise time than that of the incident lightning current.

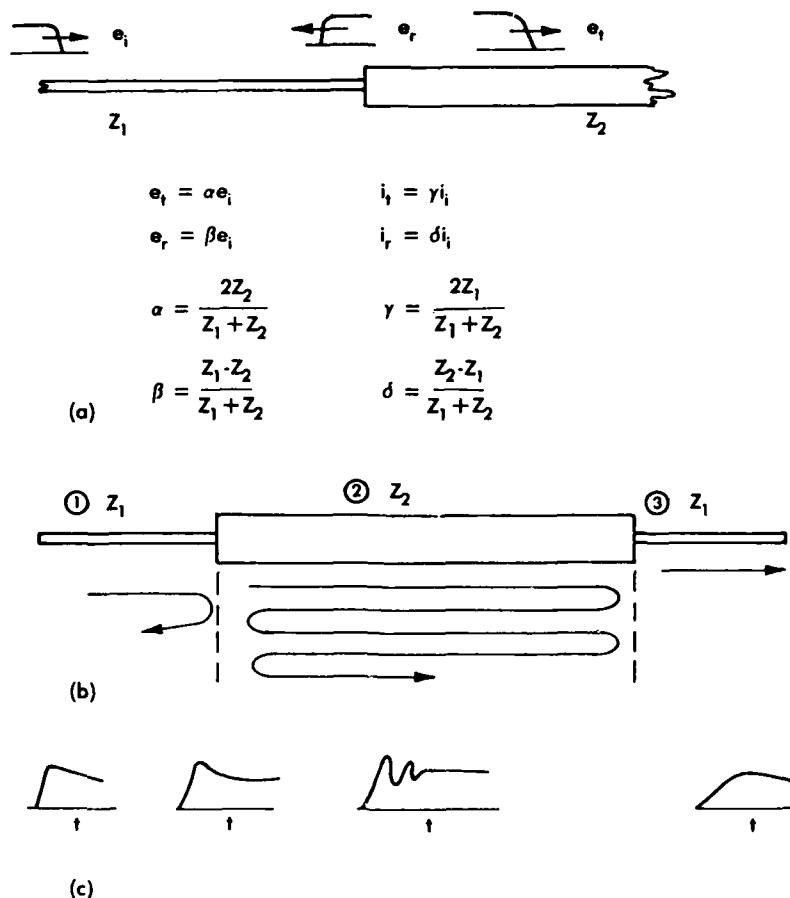


Figure 2 - Surge Propagation at Transition Points.
 (a) A single transition point
 (b) Two transition points
 (c) Waveshapes

A way in which one can tally the various reflected and transmitted currents is through the use of the lattice diagram shown in Figure 3.

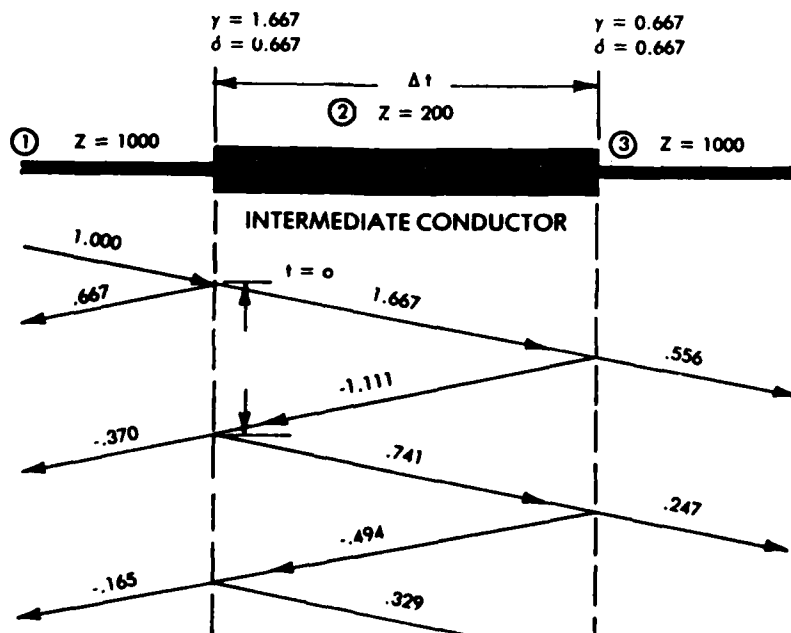


Figure 3 - Lattice Diagram Showing Amplitude of Reflections.

A current wave of unit amplitude enters from the left, sees the transition point, and is partly transmitted and partly reflected. Since Z_2 is less than Z_1 , the exiting (leaving) current is of higher amplitude than the entering current. In the limit, a current wave traveling on a conductor and encountering a short circuit ($Z_2 = 0$) would double at that discontinuity. The transmitted current then passes along the low impedance conductor and after a time delay of Δt encounters the discontinuity at the exit end. Here part of the current on conductor 2 is again reflected. Since the impedance of conductor 3 is greater than the impedance of conductor 2, the transmitted current is less than the incident current. A limiting condition of this would consist of a current wave traveling on a conductor and then encountering an open circuit. The current transmitted into the open circuit is of course zero.

The current amplitude at any point is then the algebraic sum of the reflected and transmitted components at that point. For example, the current leaving the intermediate conductor is 0.556 at $1\Delta t$ after the current enters the left-hand portion of it, 0.803 after $2\Delta t$, and 0.913 after $3\Delta t$, etc. The exit current thus rises more slowly than does the incident current. At the center of the low-impedance intermediate conductor, the current is oscillatory.

If instead of a step function a current wave of finite rise time encounters the transition, there will be a less pronounced oscillation of current in the intermediate conductor and less difference between the waveforms of the entering and exiting currents.

An example of this effect was demonstrated on a simple model of the NASA Space Shuttle. A two-dimensional outline of the Shuttle was cut from metal foil and the outline split in the center so that the two halves could be slightly separated. The model was suspended in the air and connected to a fine wire; a pulse current was passed along the wire, through the model, and along the rest of the fine conductor wire to a termination resistor. The fine wire represented the channel of the lightning arc. The input and output currents and the current at the center of the model were measured with small transformers.

Typical results are shown in Figure 4. One significant point about the results was that fast-rising incident currents excited a higher degree of oscillation of the aircraft than did slower rising currents. The second significant point demonstrated was that in most cases the waveform of the lightning current passing through the center of the aircraft was sufficiently similar to the waveform of the basic lightning current that the oscillatory component superimposed as a result of the change in impedance between the arc channel and the aircraft was not significantly large.

In the case of a nearby lightning flash, the electric field from the flash will excite a dipole oscillation of the aircraft. In terms of Figure 3, the effect could be viewed as one in which the impedance of conductors 1 and 3 was infinite, leading to complete reflection and no transmission at the entry and exit points on a low-impedance aircraft. A dipole kind of oscillation excited on an aircraft structure would be the typical response considered if one were evaluating the effect on aircraft of the electromagnetic fields produced by nuclear explosions. The period of oscillation would be proportional to the length of the aircraft; thus, large aircraft would tend to ring at lower frequencies and higher amplitudes than would shorter aircraft.

While the response of aircraft and missile systems to the rapidly changing electromagnetic fields produced by nuclear explosions has been extensively studied, there have not been corresponding studies of the response of aircraft to the electric fields associated with the passage of a nearby lightning flash. Accordingly, the case of the nearby lightning flash will not be treated further, except to add the cautionary statement that it has not been proven finally that the indirect effects associated with a nearby lightning flash are necessarily lower than those associated with a lightning flash that contacts the aircraft. In the case of a nearby lightning flash it would appear that the aircraft structure would be subjected to currents of much lower amplitude but currents much more oscillatory in nature. These lower amplitude-higher frequency currents might lead to more upsets of some types of electronic circuits than would currents of higher amplitude and lower frequency.

FIELDS WITHIN AN AIRCRAFT

A metallic aircraft is often viewed as a Faraday Screen, a concept from electrostatics which implies that the electrical environment inside the aircraft is separate and distinct from the environment outside. To some extent this is true for the electrical environment inside the structure: the environment is not nearly as harsh as is the external environment. There are, however, some important mechanisms by which electrical energy couples to the interior of the aircraft.

The basic coupling mechanisms are shown in Figure 5. The first of these relates to the electric field produced along the inner surface of the aircraft. This coupling mechanism might be defined as a resistive voltage drop. In some cases a definite resistance will be involved, though frequently the resistance will be of a distributed nature and probably frequency- or time-dependent.

The second coupling mechanism involves magnetic fields in the interior volume of the aircraft. The most common and important type of magnetic field is that drawn through apertures from the outside of the aircraft to the interior, as shown in Figures 5 and 6.

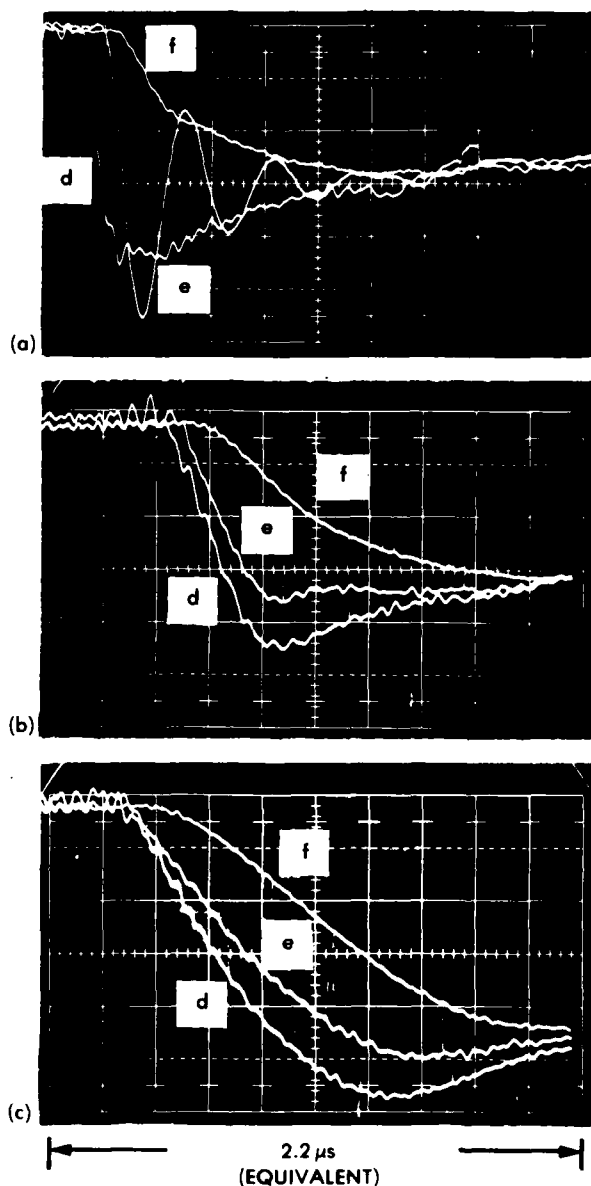


Figure 4 - Dipole oscillation of an aircraft excited by the passage of lightning current.

- | | |
|-----------------------------|--|
| (a) Fast rise of current | On each oscillogram |
| (b) Average rise of current | d is the current entering the aircraft |
| (c) Slow rise of current | e is the current at the center of the aircraft |
| | f is the current leaving the aircraft |

This is frequently called the *aperture field*. There will also be magnetic fields produced by the diffusion of lightning currents to the inside surfaces of the aircraft skins. These are referred to as the *diffusion fields*. The diffusion fields are also related to the frequency-dependent properties of the resistively generated electric field. Because some of the concepts involved in the study of the diffusion fields are central to an understanding of other effects, particularly with respect to the response of shielded wires, they will be discussed in detail before fields of other origins are considered.

The third type of coupling involves electric fields passing directly through apertures, such as windows or canopies, to the interior of the aircraft. In metal aircraft this coupling is entirely through apertures, since virtually any thickness of metal provides comparatively good shielding. Aperture-type electric field coupling is shown in Figures 5 and 7.

The most easily understood mechanism by which the passage of lightning current gives rise to voltages on aircraft electrical circuits is that in which the current, flowing through joint resistances, produces a voltage by the elementary IR voltage drop. Such a case is shown in Figure 8. Here lightning is shown contacting a wing tip navigation light. The lightning current flowing through the resistance of the mechanical mounting structure of the lamp housing produces a voltage across that resistance. The voltage drop across the resistance will have the same waveform as that of the lightning current.

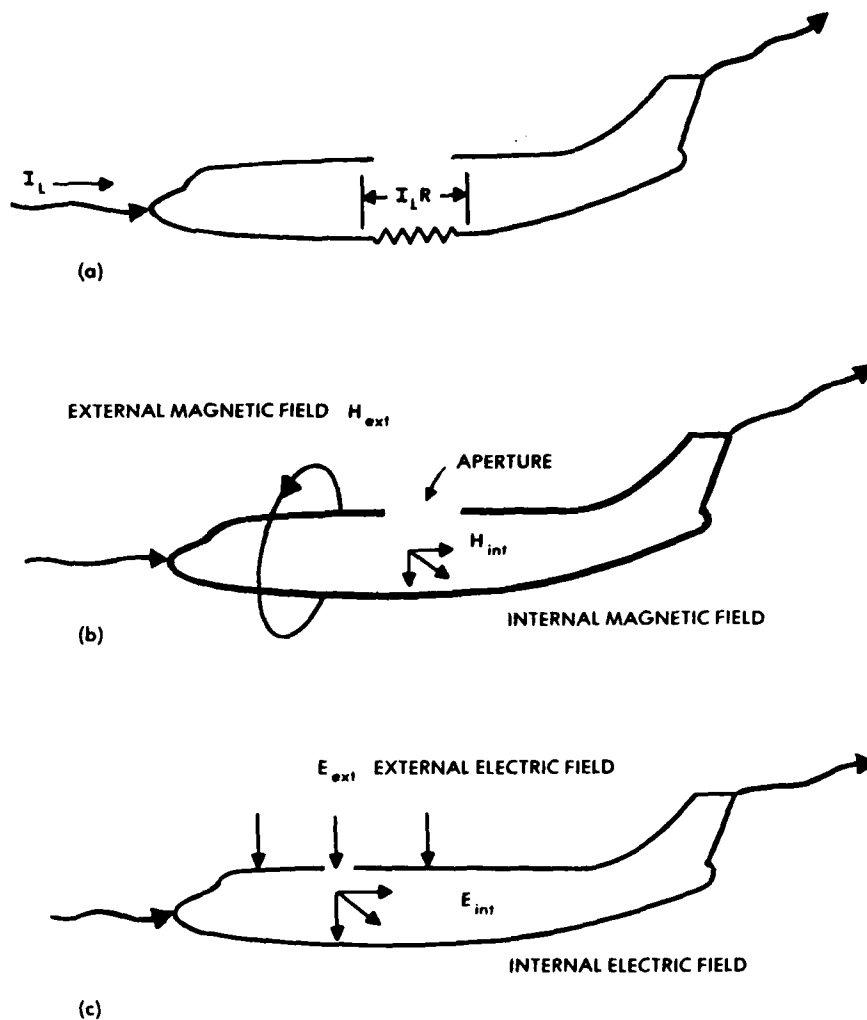


Figure 5 - Coupling Mechanisms. (a) Resistive, (b) Magnetic Fields, (c) Electric Fields.

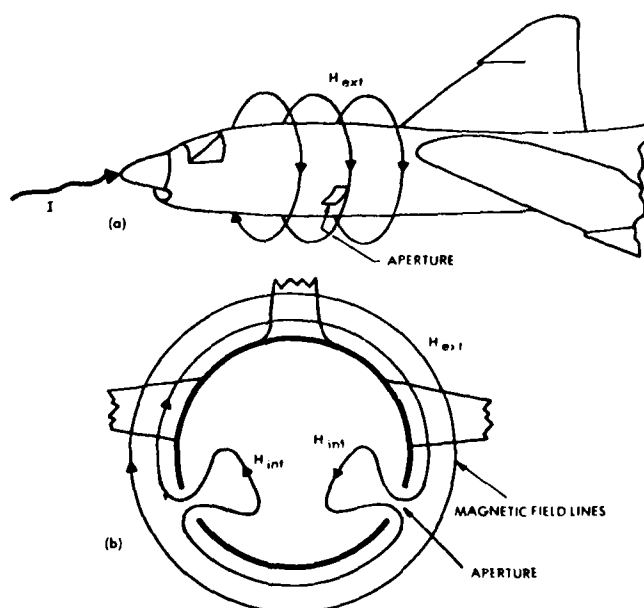


Figure 6 - Aperture-type Magnetic Field Coupling.
 (a) External field patterns
 (b) Internal field patterns

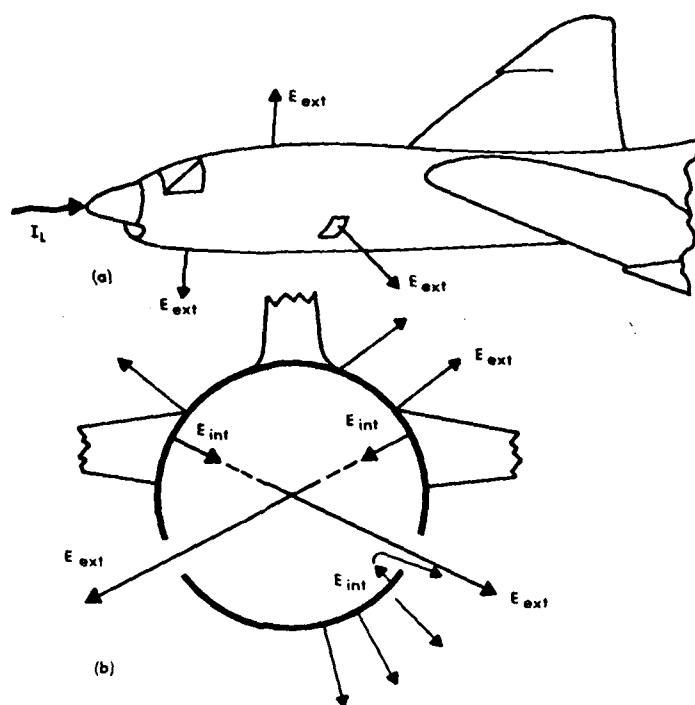


Figure 7 - Aperture-type Electric Field Coupling.
 (a) External field patterns
 (b) Internal field patterns

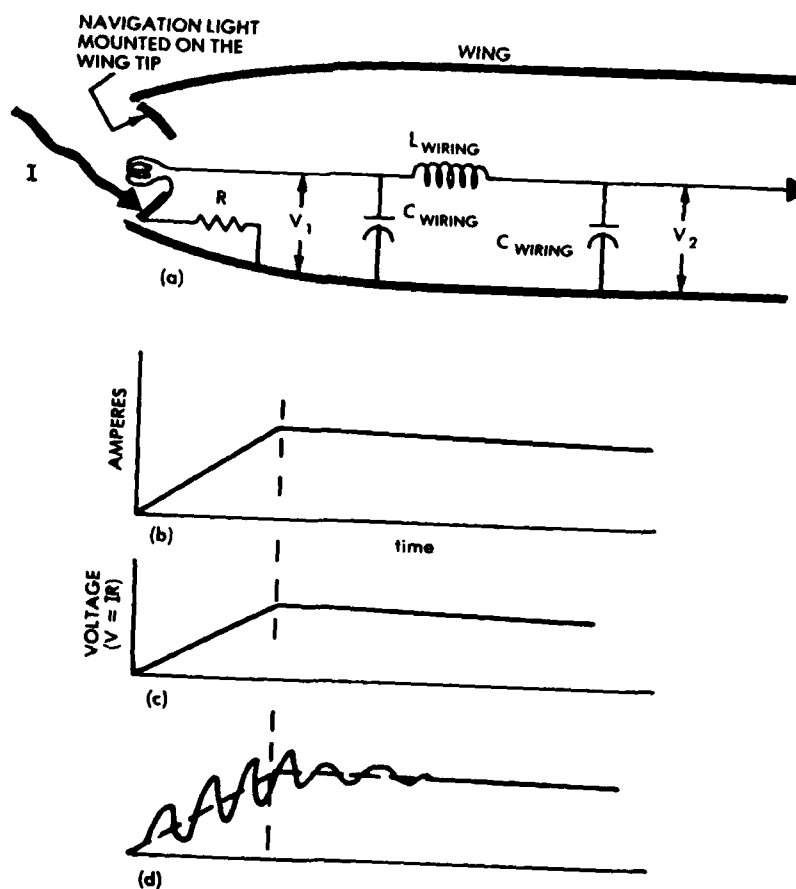


Figure 8 - Resistive Voltages.
 (a) Physical structure, (b) Current waveshape, (c) V_1 , (d) V_2

The voltage at some remote point, however, may not have the same waveform, since the distributed inductance and capacitance of the wire supplying power to the filament of the light will be set into oscillation superimposed upon the basic IR voltage.

Figure 9 shows two other examples of cases in which resistive voltages might be encountered. The first would be at the pylons for mounting external stores, shown in Figure 9(a). If lightning current were to contact such external stores, it would have to flow through the pylons to enter the aircraft. The pylons, not generally designed as current-carrying members and being points where the lightning current would be concentrated, might have a high voltage developed across them. Another example might be the structural bolts attaching a large segment of the airframe, such as the vertical stabilizer shown in Figure 9(b).

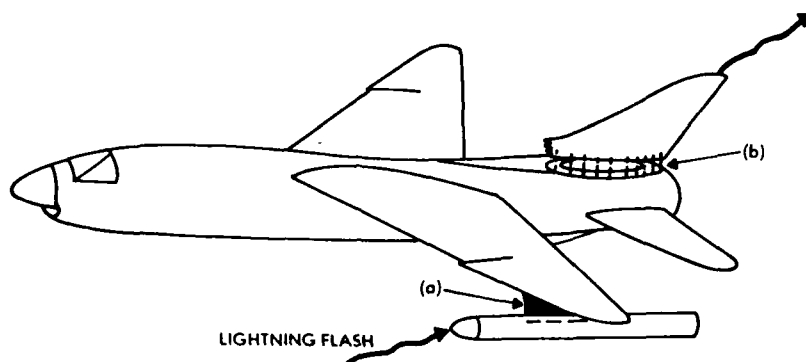


Figure 9 - Other Examples of Resistance.

- (a) The pylons for external stores
- (b) Joints in structural members

The effects of joint resistance on circuits are strongly influenced by the manner in which circuits are grounded, as shown in Figure 10. Current flowing across the joint resistance, R , produces a driving voltage: $V = IR$. Since the circuit across which V_1 is measured employs the structure as a ground-return path, the circuit couples all of this voltage; thus V_1 would be high. A circuit employing a single-point ground does not include this resistive drop; hence V_2 would be low. The use of a single-point ground, however, does not eliminate the voltage, since in this latter case the voltage at the source end of the circuit, V_3 , would be high.

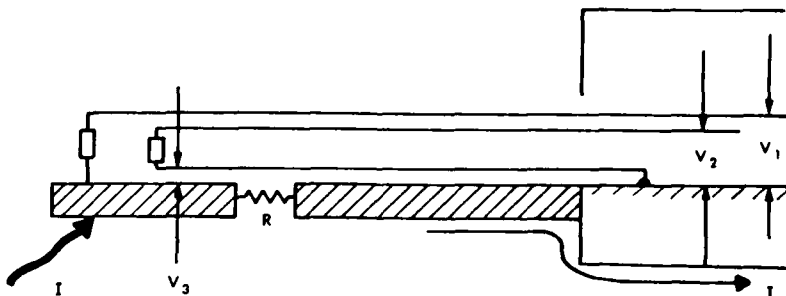


Figure 10 - Effects of Grounding.

- (a) Structural return, $V_1 = IR$
- (b) Single-point ground, $V_2 = \text{low}$
- (c) Single-point ground, $V_3 = IR$

These elementary descriptions of joint resistance should not be relied upon to predict coupling into circuits extending throughout the entire aircraft. The more massive the joint and the lower the DC resistance, the greater will be the dependence of resistance on the waveform and frequency content of the lightning current, and the greater will be the proportionate effects of changing magnetic fields. While these effects will be discussed in more detail in other paragraphs, one common oversimplification, shown in Figure 11, should be pointed out here. If the total end-to-end resistance of the aircraft were $2.5 \text{ m}\Omega$ and a lightning current of $200,000 \text{ A}$ were flowing through the aircraft, the end-to-end voltage on any circuit should not be depended upon to be less than 500 V , the product of the lightning current and the DC resistance. Magnetic field coupling may induce voltages of equal or greater magnitude.

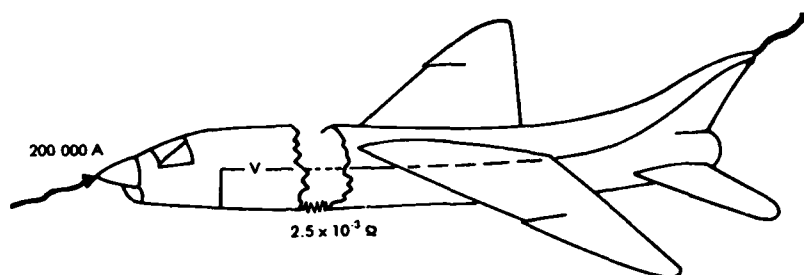


Figure 11 - An Oversimplified Model.

- Maximum voltage is not determined only by total end-to-end resistance.

Due to the complex geometry of an airplane and of its internal electrical circuits, it is not yet possible to accurately determine the magnitude and waveshape of lightning-induced voltages by analytical means. Thus, most of what is known about lightning-induced voltages in typical aircraft electrical circuits has been derived from simulated lightning test data.

LIGHTNING-INDUCED VOLTAGES IN TYPICAL AIRCRAFT ELECTRICAL CIRCUITS

There have been several sets of tests made in which simulated lightning currents were conducted through the aircraft and the resultant voltages and currents induced in the aircraft wiring measured. A few examples of these measurements will be given in the following paragraphs, and an attempt will be made to indicate some of the important facts learned from these tests.

Full Scale Lightning-Induced Voltage Measurements

The first set of tests to be discussed (Reference 2) was one in which high lightning-like currents were injected into one wing of an F-89J aircraft. During the test, represented in Figure 12, the wing was fastened onto a screened instrument enclosure, which may be viewed as representing the fuselage of the aircraft. Lightning-like currents of up to 40,000 A were injected into the wing or into the external wing tip tank from a high-current surge generator, allowed to flow along the wing to the outer wall of the screened instrument enclosure, and then to ground. An example of one of the types of current injected into the wing is shown in Figure 12(b). In order to obtain maximum current, the surge generator was operated in a mode that essentially allowed the production of only one cycle of a damped oscillatory current, unlike a typical lightning current, which would rise to crest fast and decay at a much slower rate. The shape of the current wave must be considered when observing the waveshape of some of the voltages that will be discussed. In particular, note that at about 20 μ s appears a major discontinuity in waveshape. This discontinuity in current waveshapes is reflected in the induced voltages.

Within the wing there were a number of electrical circuits, such as those to navigation lights, fuel gauges, pumps, relays, and switches indicating position of flaps. Some of these ran in the leading edge of the wing and were well shielded from many electromagnetic effects, while others ran along the trailing edge between the main body of the wing and the wing flaps. These latter were most exposed to the electromagnetic fields. All of the circuits were relatively independent of each other; they were not, as a general rule, bundled together in one large cable bundle, a practice that provides maximum coupling from one circuit to another and makes analysis difficult.

The first circuit that will be discussed, shown in Figure 13, was a circuit supplying power to a position light mounted on the external fuel tank. An electrical diagram of the circuit, shown in Figure 13(b), shows that the circuit consisted of one wire supplying power to the filament of the position light with the return circuit for the light being through the wing structure. Accordingly, if the lightning current contacts the external tank, that circuit will be influenced by the resistance R_1 of the hangers fastening the tank to the wing, by R_2 , the inherent resistance of the wing, and by magnetic flux arising from the flow of current.

Typical results for the stroke position shown are given in Figure 13(c) and 13(d). The basic waveform of the open circuit voltage is seen to rise rapidly to its crest and to decay more rapidly than does the injected current shown in Figure 12(b). As a result, the open circuit voltage appears to be the time derivative of the basic lightning current waveform and thus was responding primarily to the magnetic flux associated with this current. A high frequency oscillatory voltage is also superimposed on the first several microseconds of the basic voltage waveform. This voltage is attributable to the traveling wave reflections in the airframe and will be discussed further in subsequent paragraphs.

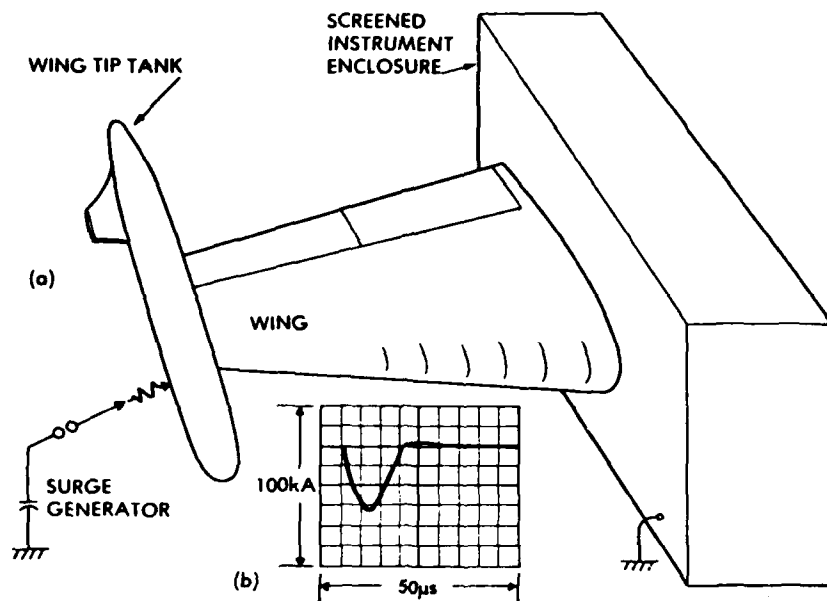


Figure 12 - High Current Injection Tests on the Wing from an F-89J.
(a) Test arrangement (b) Waveshape of injected current

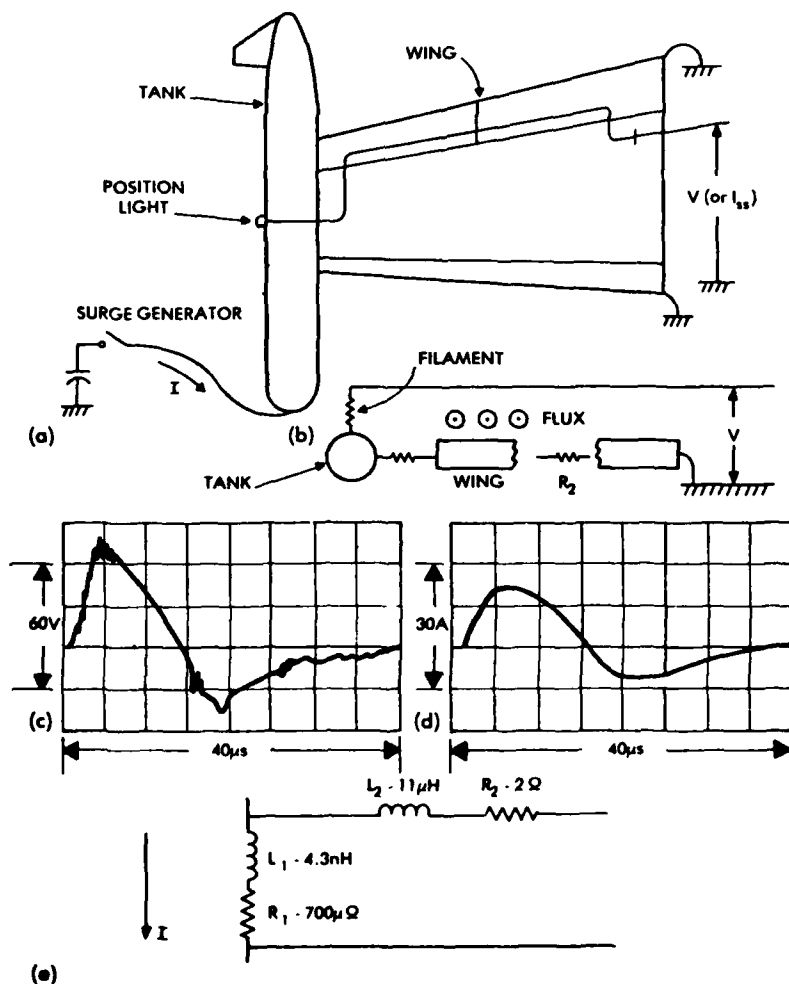


Figure 13 - A Wing Tip Circuit. (a) Circuit orientation, (b) Electrical details of circuit.
(c) Open circuit voltage, (d) Short circuit current, (e) Equivalent circuit.

When the conductor was shorted to ground at the instrument enclosure, the short circuit current rose to its crest in approximately the same length of time as did the injected current and displayed much the same waveshape as the injected current.

Figure 13(e) shows an approximate equivalent circuit that might be derived. L_1 and R_1 represent a transfer impedance between the current flowing in the wing and the voltage developed on the circuit. L_2 and R_2 represent the inherent inductance and resistance of the wires between the fuselage and the light. The transfer inductance and resistance, which it should be emphasized do not necessarily represent any clearly definable resistance or inductance of the wing, are merely those values which, when operated upon by the external lightning current, produced the observed open circuit voltage.

A different type of circuit is that shown in Figure 14. In this circuit a conductor ran through the leading edge of the wing and terminated in an open circuit on a pylon mounted underneath the wing. In the electrical detail circuit shown in Figure 14(b), it can be seen that this circuit would not respond to the voltage developed across the resistance between the tank and the wing. The circuit would respond in some measure to some fraction of the wing resistance and to some fraction of the magnetic field set up by the flow of current in the wing, but since the circuit was only capacitively coupled to the wing, the total coupling impedance should have been, and was, less than that of the circuit shown in Figure 13. The purpose of the conductor shown in Figure 14 was to supply power to a relay and to explosive bolts in the pylon used to hold a weapon.

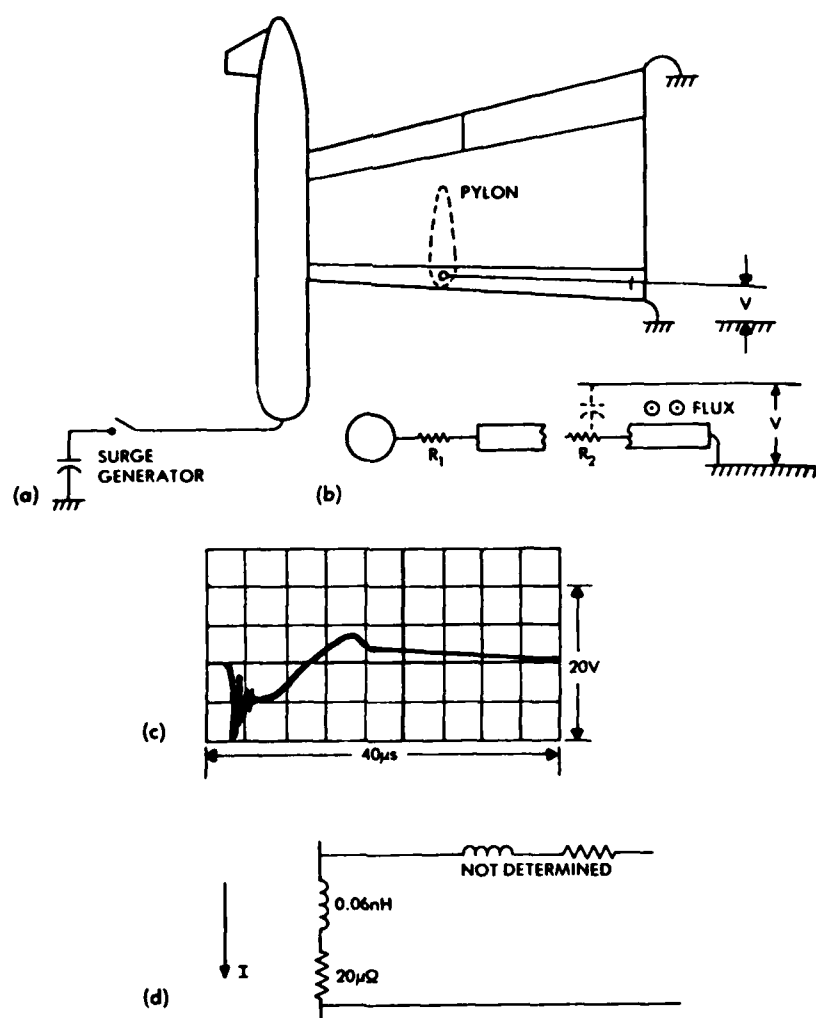


Figure 14 - A Pylon Circuit - Open at Pylon.

- (a) Circuit orientation
- (b) Electrical details of circuit
- (c) Open circuit voltage
- (d) Equivalent circuit

In Figure 14 the pylon was not installed, so there was no load on the conductor. Figure 15 shows the results when that pylon was installed, when the conductor was connected to a relay with a return through the aircraft structure, and when the lightning flash was allowed to contact the pylon. The combination of a structural return path for the circuit and a lightning flash terminating upon the pylon and thus including the resistive drop across R_3 , the resistance between the pylon and the wing, served to make the voltage much greater than it was when the conductor was open circuited. No attempt was made to completely analyze from which area the total amount of magnetic flux was coming or whether the flux ϕ_1 , representing that in the pylon, or ϕ_2 , representing the flux within the wing, was the larger.

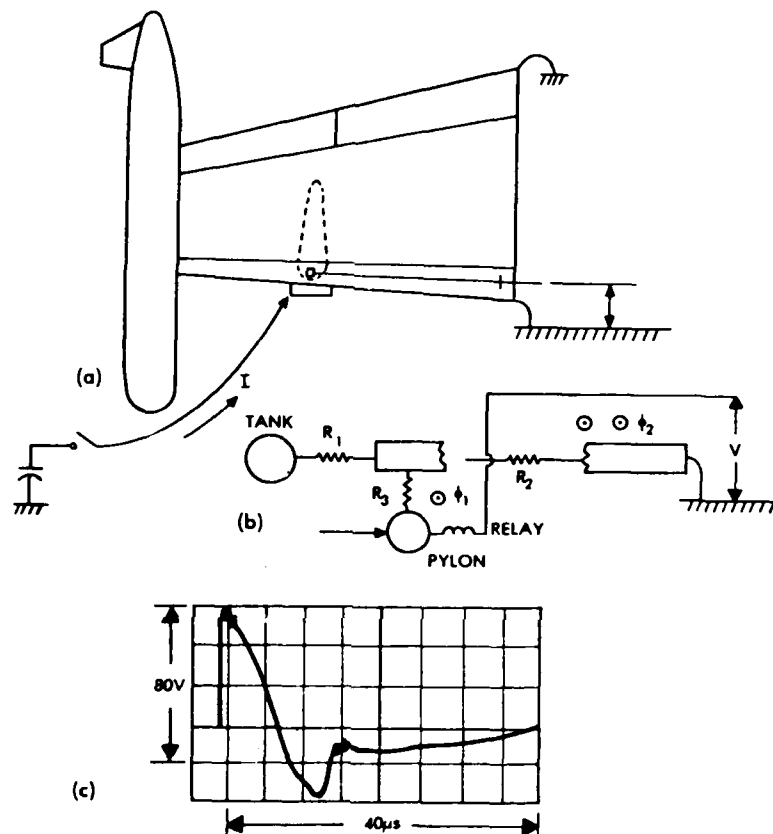


Figure 15 - A Pylon Circuit-Loaded at Pylon.

- (a) Circuit orientation
- (b) Electrical details of circuit
- (c) Open circuit voltage

Several significant things were learned from these measurements. The first was that the voltages induced in a typical circuit within the wing consisted of a magnetically induced component and a component proportional to the resistance of the current path through the airframe. Also, the location at which the lightning flash contacted the wing had an important effect on the magnitude of voltages developed on different circuits.

Lightning Transient Analysis Measurements

These induced voltage measurements (Reference 3) were made on an F-8 aircraft fitted with a fly-by-wire control system. The fly-by-wire controls, shown in Figure 16, consisted of a primary digital system, a backup analog system, and a common set of power actuators operating the control surfaces. The major components of the control system were located in three locations: the cockpit, where sensors coupled to the control stick provided signals for the control systems; an area behind the cockpit, where there was located the digital computer; and a compartment behind and below the cockpit on the left side of the aircraft. This latter compartment was one that would normally have been occupied by guns; accordingly, it will be referred to as the "gun bay". In this gun bay were located the interface and control assemblies.

Several hydraulic actuators were located at each of the major surfaces. These were interconnected to the fly-by-wire control systems through wire bundles that ran under the wings. The control systems did not depend upon the aircraft structure as a return path; the system had a single-point ground, located at a panel in the gun bay. By and large, none of the control wiring in the aircraft was shielded.

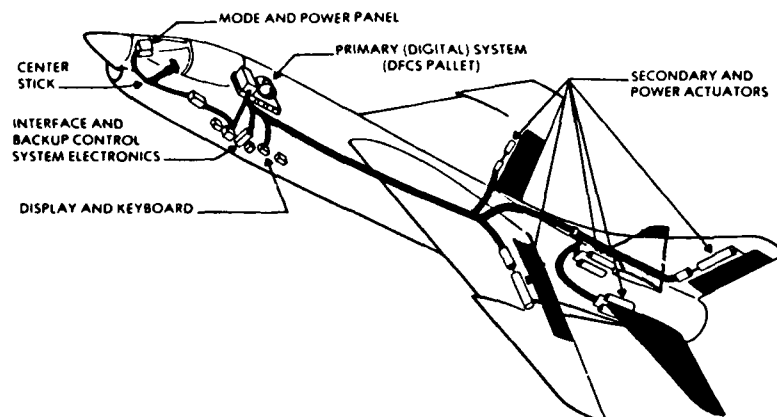


Figure 16 - Location of Fly-by-wire Control System Hardware and Wiring Bundles in F-8 Aircraft.

In contrast to the tests on the wing of the F-89J aircraft, in which high amplitude currents were injected into the wing from a high-power surge generator, the tests on the complete F-8 aircraft were made with what has been called the *transient analysis* technique, in which a portable and relatively low-power surge generator is used, capable of injecting currents of a waveform similar to that found in lightning, but of a much lower, and nondestructive level. During the tests on the F-8, the injected current was about 300 A. It was a current rising to crest in about 3 μ s and decaying to half value in about 16 μ s. This waveform is shown in Figure 17.

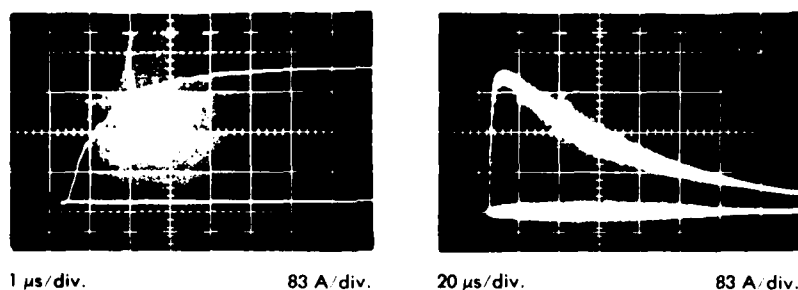


Figure 17 - Simulated Lightning Test Waveform.

The first set of measurements to which reference will be made was that on a set of spare conductors running between an interface box in the gun bay and a disconnect panel located near the leading edge of the vertical stabilizer. The routings of the circuit and the induced voltage waveforms are shown in Figure 18. The voltage measured between the conductor and ground consisted of a high-amplitude oscillatory component and a much lower amplitude but longer duration component. The oscillatory component was excited by magnetic flux leaking inside the aircraft, while the longer duration component was produced by the flow of current through the structural resistance of the aircraft. The voltage measured between conductors (the line-to-line voltage) was much lower in amplitude than the voltage measured between either of the conductors and the airframe (the line-to-ground voltage) as would be expected in a well-balanced circuit.

The second set of measurements was made on a circuit running from the interface control unit in the gun bay to a wing position indicator switch located underneath the leading edge of the wing. The wing on the F-8 aircraft could be raised or lowered around a pivot point towards its rear in order to change the angle of attack during landing and takeoff. The purpose of the switch was to indicate the position of the wing. The voltages induced on that switch circuit are shown in Figure 19. The voltages measured from line to airframe were higher than those measured from line to line, but is is significant that the line-line voltages, while of a somewhat different waveshape, were not much lower than the line-to-ground voltages. The reason for this lay in the fact that the load impedances in the interface box in the gun bay were different from each other on the two

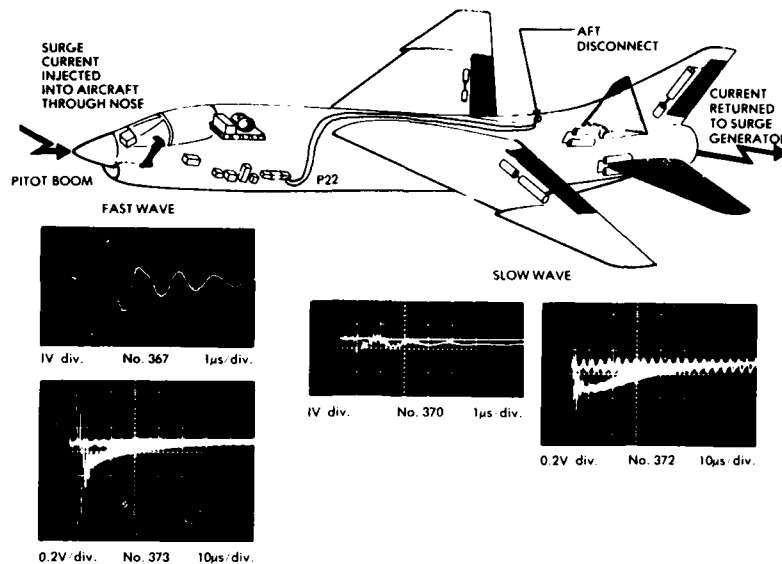


Figure 18 - Spare Conductor Measurements on P22 (Pin 24 to airframe).

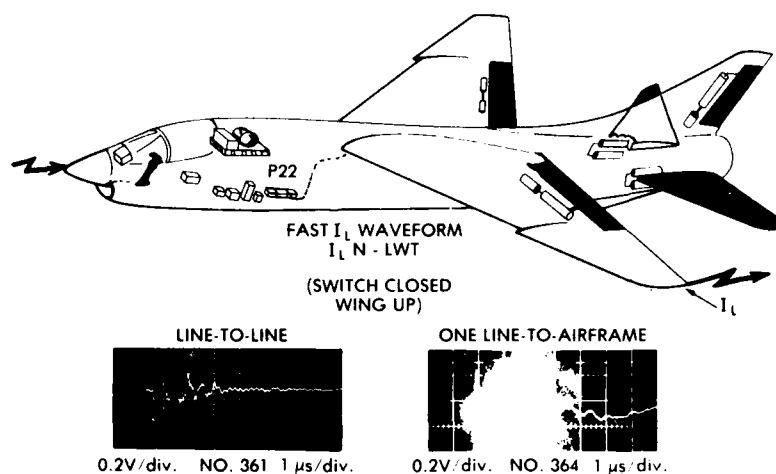


Figure 19 - Voltages Induced in Wing Position Indicator Switch Circuit at Open Plug P22.

sides of the circuit. One side connected to a power supply bus, while the other side probably connected to an emitter follower. Another significant feature about these voltages was that they were again of an oscillatory nature. They were apparently excited by the leakage of magnetic flux inside the aircraft and were not excited by the drop in potential along the structural resistance of the aircraft.

Figures 20 and 21 show voltages measured on two different circuits going to actuators, one (Fig. 20) going to the left pitch actuator and the other (Fig. 21) going to the left roll actuator. In both cases the voltages displayed were the output of the driver amplifier used to control the servo valve in the actuator. Both of these were line-line voltage measurements. The significant feature about these measurements was, again, that the characteristic response was oscillatory and apparently excited by the leakage of magnetic flux inside the aircraft.

On the F-8, as is typical of most aircraft, the control wires were laced together into fairly large bundles. The routing of some typical bundles in the gun bay housing the backup and interface electronic control boxes is shown in Figure 22. While it was not possible to measure the current on individual wires within these cable bundles because of limitations of measurement technique and because of the large number of wires within the bundles, it was possible to measure the total current flowing on the various bundles. This was done by clamping around the bundle a current transformer have a split core.

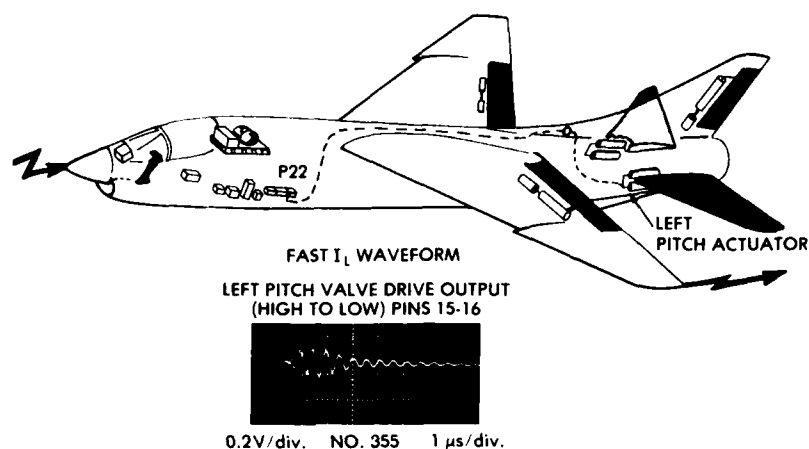


Figure 20 - Left Pitch Valve Drive Output (high to low) at Plug 22 (system battery powered).

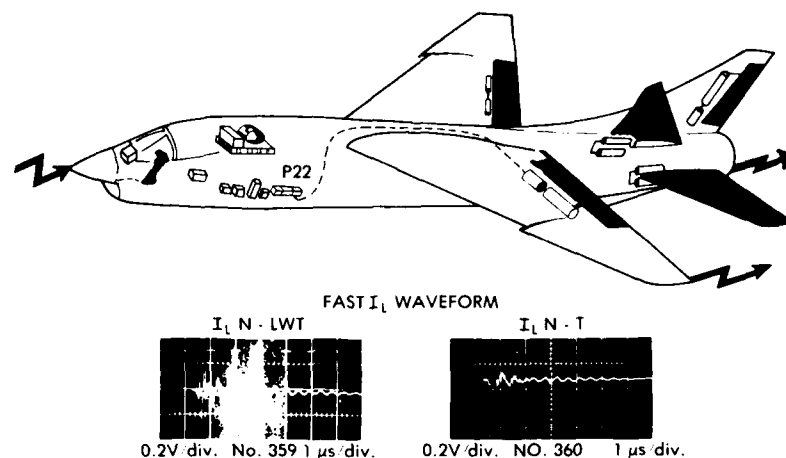


Figure 21 - Voltages Induced in Left Roll Valve Drive Output Circuit (Pins 44-45) at Open Plug P22.

The bulk cable currents were also found to be oscillatory, just as were the voltages on conductors described earlier. Since the flight control wiring did not make use of multiple ground points within the aircraft, it follows that none of the currents in these cable bundles would exhibit any of the long time response characteristic of multiple-grounded conductors.

Figure 23 shows a statistical distribution of the peak amplitude of currents in all of the cable bundles upon which measurements were made. The distribution is shown both for the actual current amplitudes injected into the aircraft and in terms of what those currents would be if the results were scaled up to currents representative of actual lightning flashes. In terms of an average-amplitude lightning flash of 30,000 A, the total current on most cable bundles would have been on the order of 20 to 100 A.

Measurements were also made of the amplitude and waveshape of the magnetic field at a number of points in and around the aircraft. One location upon which attention was concentrated was the cockpit, since the cockpit is an inherently unshielded region and one in which many control wires would be subjected to changing magnetic fields. The positions at which fields were measured, the peak amplitude of the fields, and the predominant orientation of the fields are shown in Figure 24. A significant feature about these measurements is that there was no orientation of the magnetic field probe that resulted in a zero output, which indicated that the orientation of the magnetic field was not uniform with respect to time. The field produced at any one point was the sum of the field produced by oscillatory current in the various structural members as the current in those structural members changed with time.

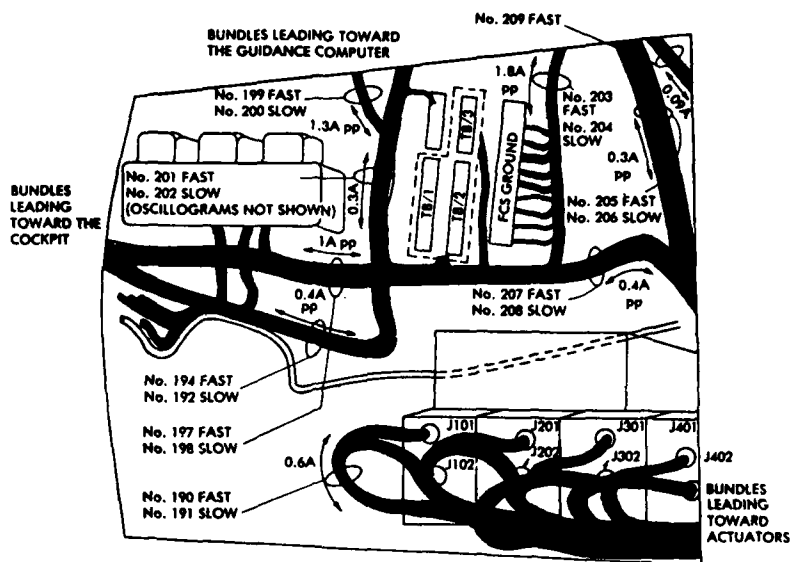


Figure 22 - Cable Bundles within the Gun Bay.

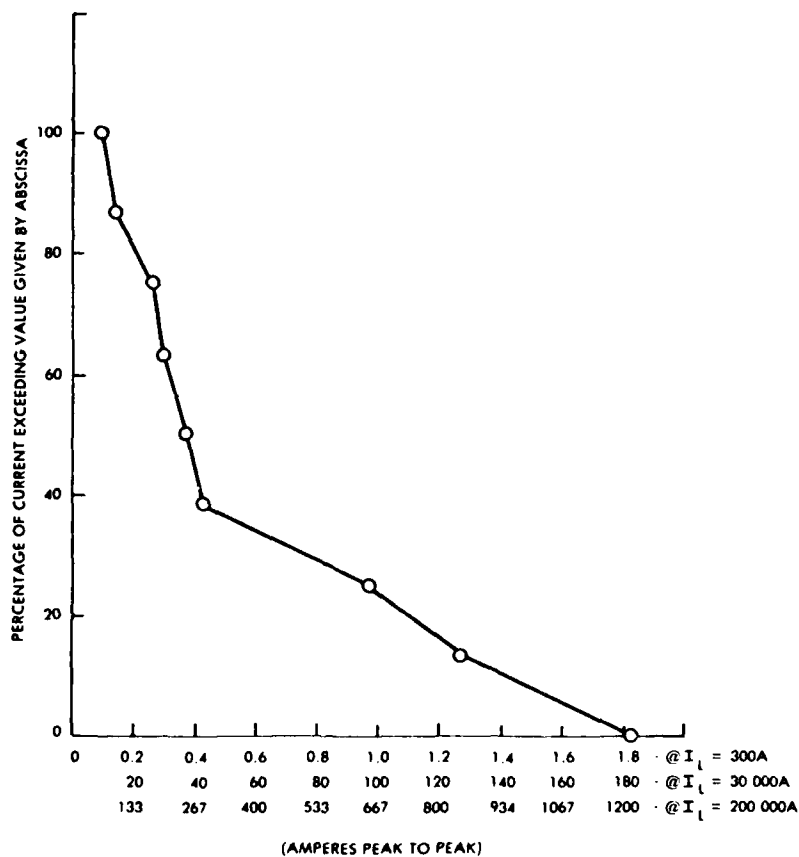


Figure 23 - Distribution of Amplitudes of Cable Bundle Currents (measured in left gun bay).

Some measurements of the magnetic fields within the fuselage are shown in Figure 25. The measurements showed first some oscillatory magnetic field, followed by a field which rose to crest at a time much longer than the crest time or even the duration of the lightning current that was injected into the aircraft. Oscillogram No. 452 in Figure 25 indicated the rate of change of field as falling to zero at about 400 μs . This would indicate that the field itself reached its crest value in about 400 μs .

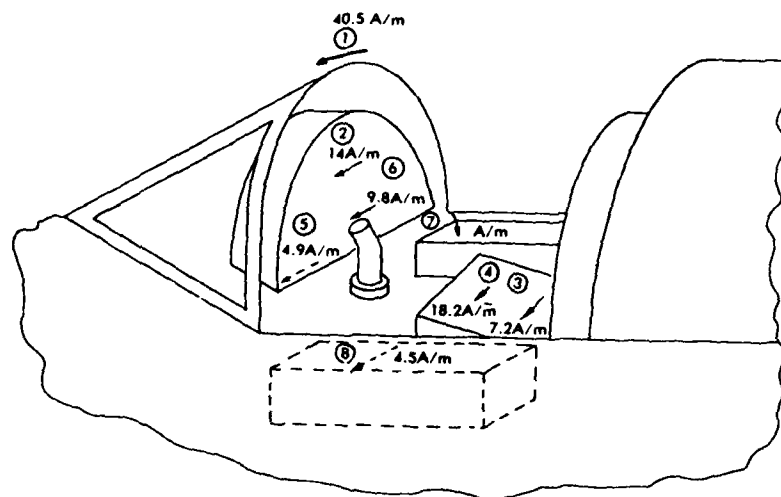
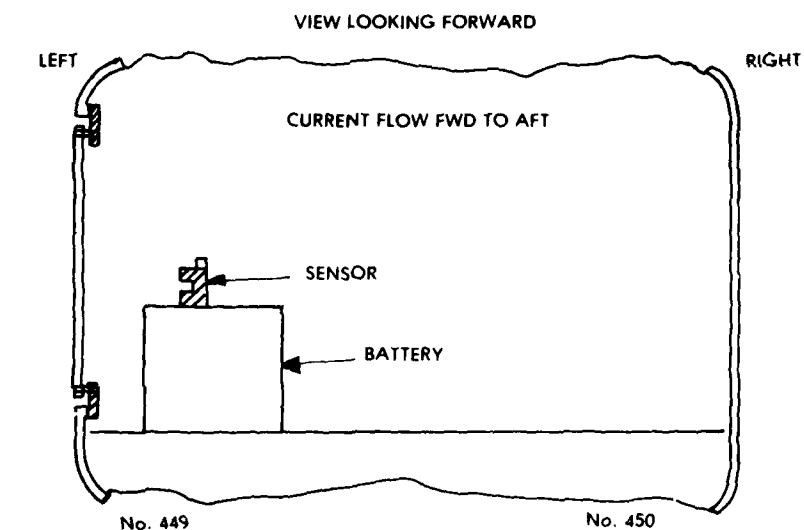
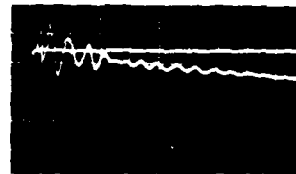


Figure 24 - Magnetic Field Measurements in the Cockpit.



1.5A/m div. 1 μ s div.
(COVER REMOVED)

No. 451



0.15A m div. 1 μ s div.
(COVER IN PLACE)

No. 452



0.15A/m div. 20 μ s div.
(COVER IN PLACE)



0.15A m div. 100 μ s div.
(COVER IN PLACE)

Figure 25 - Magnetic Fields Inside the F-8 Fuselage.

Some of the significant points about the results of tests on this aircraft may be summarized here. The first was that the use of a single-point ground system did not eliminate all transient voltages produced by the flow of lightning current through the structure of the aircraft. It minimizes the amount of voltage appearing between each wire of a circuit, but a much larger induced voltage may still appear between either wire and ground at the ungrounded end of the circuit. The ranges of induced voltages measured in various flight control circuits in the F-8 airplane, extrapolated to correspond to full threat conditions, are presented in Table I.

TABLE I - Ranges of Peak Induced Voltages Measured in the NASA F-8.

<u>Circuit</u>	<u>Location and Connector No.</u>	<u>Induced Voltages Scaled to $i_L = 200$ kA</u> <u>Fast i_L Waveform</u>
<u>FUSELAGE</u>		
FCS Grd. to A/C Grd: (in Gun Bay)		420-653
28 VDC Busses		213-346
Interface Elec- tronics Test Receptacle		160-519
DFCS (AGC)	J25	353-1059
Pitch, Roll and Yaw Servos	J2	286-559
<u>COCKPIT</u>		
Mode and Power Control Panel	J14	206-932
<u>WING AREA</u>		
Primary Circuits to Left Roll Actuator	J105	286-1039
Backup (Channel 2) Circuit to Left Roll Actuator	J205	127-1172
<u>TAIL AREA</u>		
Primary Circuits to Yaw Actuator	J107	280-1705
Backup (Channel 3) Circuits to Yaw Actuator	J307	84-2005

Another significant point is that the total current on the cable bundles was of the order of 20 to 100 A for an average lightning flash. This bulk cable current was again oscillatory, with a frequency tending to correspond to the length of the cable bundle. The equipment bays in this aircraft, not being designed for electromagnetic shielding qualities, allowed significant amounts of magnetic flux to develop within those bays. This is particularly true of those bays intended for ease of access.

SEMICONDUCTOR FAILURE MECHANISMS

Failure of an avionic system to function properly may result from damage to a single component device when it is subjected to a transient voltage or current. Systems vulnerability evaluation therefore requires that one know the failure thresholds for devices subjected to transients. Simulation of failure resulting from transients at the component level can be conveniently performed in the laboratory by means of high-voltage generators. Information from such simulation can then be correlated with the lightning-induced voltages by analytical techniques. Semiconductor electronic components are generally more vulnerable under pulse conditions than are nonsemiconductor components; therefore, most of the discussion of this section will be devoted to semiconductors.

In addition to the theoretical correlations just described, experimental data have been used in the development of empirical relations which are obtained from two models of semiconductor junction devices - the junction capacitance model and the thermal resistance model. These models provide a framework from which the power failure threshold of an untested device can be estimated from the quantities listed in a data sheet description prepared by manufacturers for a diode or a transistor.

Semiconductor Breakdown Modes

There are two principal breakdown modes for semiconductor PN junctions, as follows:

1. Surface damage around the junction as a result of arcing.
2. Damage to the junction region as a result of elevated temperatures.

Surface damage refers to the establishment of a high-leakage path around the junction which effectively eliminates any junction action. The junction itself is not necessarily destroyed, since, if it were possible to etch the conducting material away from the surface, the device might be able to return to its normal operating state. This is not practical, of course, in an operational semiconductor. It is likely that the formation of any surface leakage path would be the result of excessive heat formation in the bulk of the material, and this would typically be an irreversible phenomenon. It is very difficult to predict analytically the conditions which will lead to surface damage because they depend upon many variables, such as the geometrical design and the details of the crystal structure of the surface. The theoretical prediction of surface arcing under pulse conditions is not practical (Reference 4). It should be cautioned that surface damage, in the general case, may occur in devices at power levels which are orders of magnitude below those sustainable by devices in which bulk damage occurs (Reference 5).

Bulk damage, which results in a permanent change in the characteristic electrical parameters of the junction, indicates some physical change in the structure of the semiconductor crystal in the region of the junction. The most significant change is melting of the junction as a result of high temperatures. Other types of change may involve the impurity concentrations, the formation of alloys of the crystal materials, or a large increase in the number of lattice imperfections, either crystal dislocations or point defects.

The simplest structure to analyze is a diode, as shown in Figure 26. In this diode a current is assumed to flow as a result of some outside stimulus and, in doing so, to produce a voltage across the diode. This voltage may be the forward bias voltage (0.5 to 1.5 V), or it may be the reverse breakdown voltage if the outside stimulus has biased the diode in the reverse direction. Assume that I is a square wave and that V is not a function of time, as it might be if V depended upon the junction temperature. The instantaneous power dissipated in the diode is then a square pulse of magnitude:

$$P = IV \quad (2)$$

and the total energy produced is

$$W = \int_0^t P dt = IVt \quad (3)$$

Both experimental and theoretical analyses indicate that the power (or energy) required to cause failure depends on pulse width: the narrower the pulse, the greater the power required to cause failure. Over a broad range of times, typically between 0.1 μ s and 100 μ s, the power required to cause failure is inversely proportional to the square root of time. For very short pulse durations the power required to cause failure is inversely proportional to the first power of time and for very long pulse durations the power required to cause failure is a constant. These relations may be expressed by the following equations:

$$Pt = C \quad t < T_0 \quad (4)$$

$$Pt^{\frac{1}{2}} = K \quad T_0 < t < 100 \mu s \quad (5)$$

$$P = \text{Constant} \quad t > 100 \mu s \quad (6)$$

where T_0 generally lies between 10 ns and 1 μ s.

Figure 27 (Reference 6) shows an example for a 10 W diode. The most important region is the center region, where

$$P = Kt^{-\frac{1}{2}} \quad (7)$$

Junctions are less susceptible to burnout when operated with forward bias: first, because the power produced by a given current is lower when flowing through the low forward bias voltage V_{BD} , and, second, because the current is more uniformly distributed across the junction in the forward direction. Accordingly, it requires more power in the forward direction to cause failure. An example is shown in Figure 28 (Reference 7). The 2N2222 transistor is a 0.5 W NPN silicon high-speed switch.

Damage Constants

From curves such as those of Figure 28, the value of a damage constant, K , can be determined and tabulated for a variety of devices. The appropriate threshold damage curve can then be reproduced as desired from a single damage characterization number, the damage constant K . It is convenient to express K in $\text{kW} \cdot \mu\text{s}^{\frac{1}{2}}$, since the value of K in these units then becomes numerically equal to the power necessary for failure, dissipated by a square pulse of 1 μ s duration. If this point is located on a log-log graph (Figure 27 or Figure 28), then a curve of slope, $-\frac{1}{2}$ drawn through this point reconstructs the curve fit to the data for a particular device, and the power for failure at other pulse durations can be read directly from such a graph. Ideally, the K factor should be

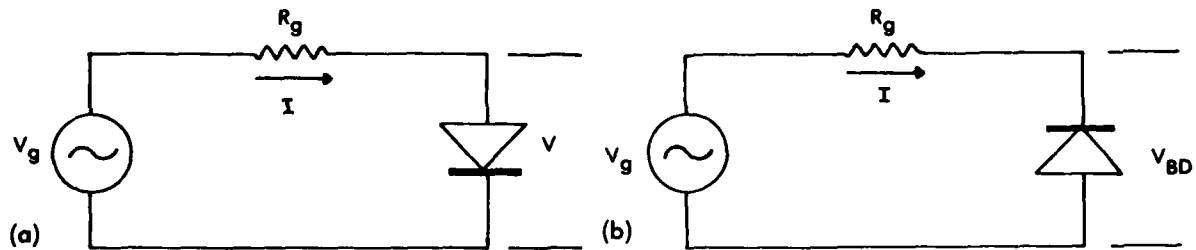


Figure 26 - Voltage and Current through a Diode Junction.

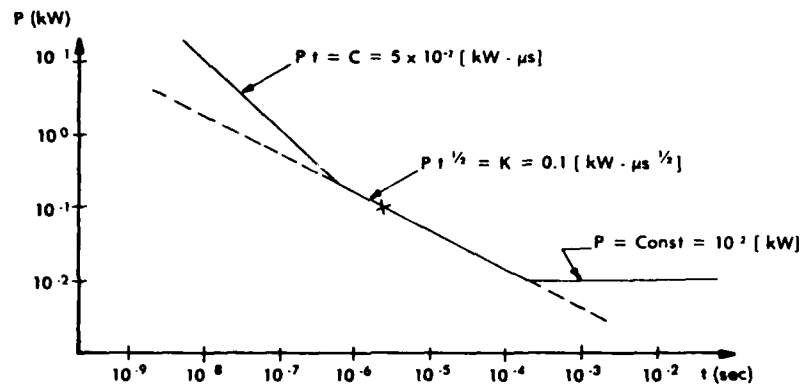


Figure 27 - Expected Time Dependence of Pulse Power Failure: Threshold for an Example 10 W Diode.

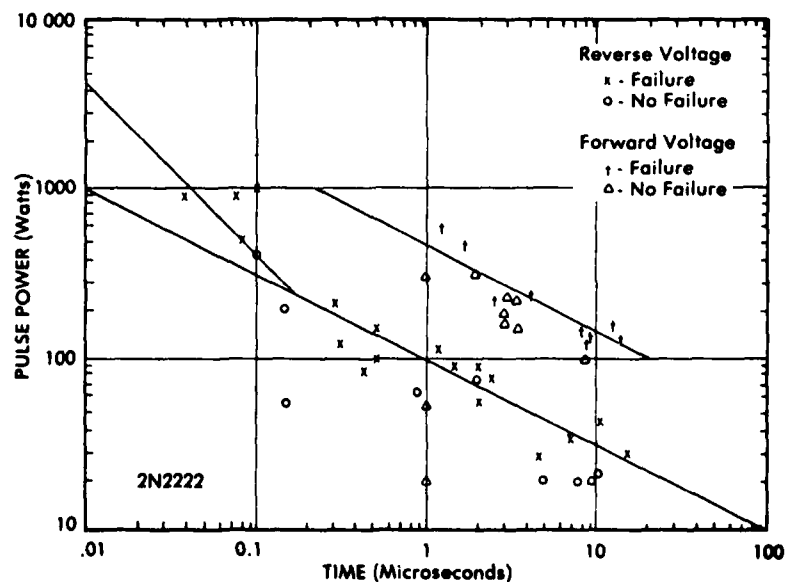


Figure 28 - Experimental Data Points for Failure of the Base-emitter: Junction of a 2N-2222 Transistor for Forward and Reverse Polarity Voltage Pulses.

known for both the forward bias and the reverse bias conditions. Generally, only the K factor for the reverse bias condition is known. This limitation gives conservative answers, since K for the reverse bias condition is almost always lower than is K for the forward bias condition.

The magnitude of the damage constant depends upon the type of junction under consideration: broadly speaking, it is larger for large junctions and smaller for small junctions. Figure 29 (Reference 8) shows the range of the damage constant for typical diodes and transistors. These damage constants have been termed "K factors".

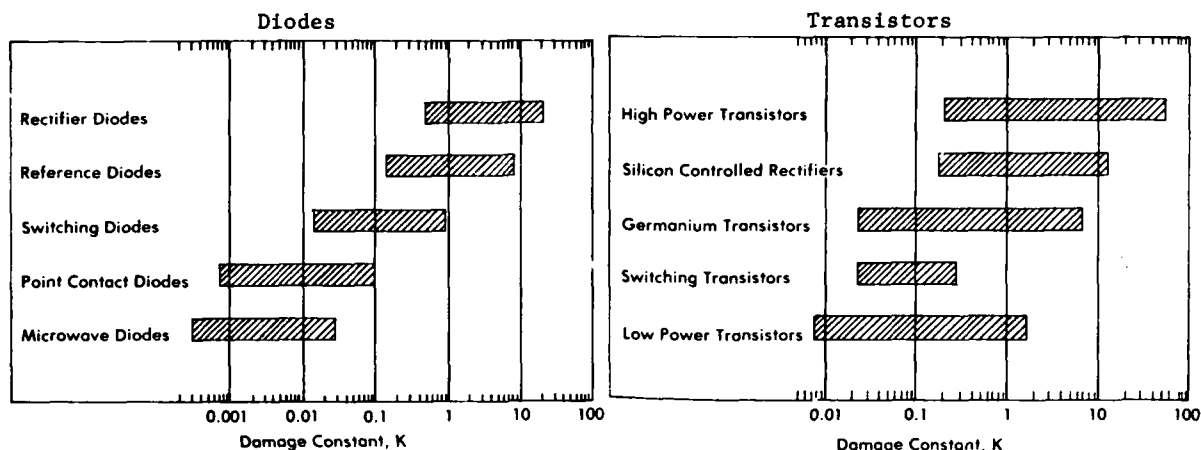


Figure 29 - Ranges of Pulse Power Damage Constant for Diodes and Transistors.

K Factors Determined Experimentally

Experimentally the K factor is determined by injecting power pulses into the semiconductor junction, starting at low levels and increasing the levels until either failure or significant degradation of the junction occurs. Devices would normally be pulsed in both the forward and reverse directions.

The K Factors and breakdown voltages for a large number of semiconductors are given in Reference 9. In the case of transistors, the K factor listed generally refers to the base-emitter junction, since this is generally the junction most susceptible to burnout. In all the cases the K factor refers to the reverse bias direction.

K Factor as Determined from Junction Area

If the K factor is not measured, it may be estimated by one or more of three methods. The most accurate of the indirect methods involves a knowledge of the area of the junction. If the area is known, the K factor may be estimated from the following relations (Reference 10):

$$\text{Diodes: } K = 0.56A \quad (8)$$

$$\text{Transistors: } K = 0.47A \quad (9)$$

$$K \text{ in kW} \cdot \mu\text{s}^{\frac{1}{2}}$$

$$A \text{ in cm}^2$$

For transistors, the junction area to be used is that of the base-emitter region. This is generally the weaker junction (lower breakdown voltage), and it is that for which the experimental average value for $K(A)$ was obtained.

This method is of course limited by the availability of information on junction area, but where such information is available, the method yields damage constants accurate to within a factor of two. For planar devices, the junction area can often be measured on the silicon chip.

K Factor as Determined from Junction Capacitance

The next most reliable method of determining the damage constant is from a knowledge of the capacitance (C_j) and breakdown (V_{BD}) of the junction. For three different categories of devices, the relations are (Reference 11):

$$\text{Category 1 - insufficient data} \quad (10)$$

$$\text{Category 2 - } K = 4.97 \times 10^{-3} C_j V_{BD}^{0.57} \quad (11)$$

$$\text{Category 3 - } K = 1.66 \times 10^{-4} C_j V_{BD}^{0.992} \quad (12)$$

The different categories are

- Category 1 - Germanium diodes and germanium transistors
- Category 2 - Silicon diodes, all silicon transistor structures except planar and mesa
- Category 3 - Silicon planar and mesa transistors

If the junction is a transistor base-emitter junction, the capacitance used should be taken at a reverse bias of approximately 1V. If it is a collector-base junction or a diode junction, the value should be taken at the reverse bias of approximately 5 to 10V.

Integrated Circuit Failure Data

A limited amount of data relating voltage and current durations to the breakdown of integrated circuits is available. Figures 30 (Reference 12), 31 (Reference 13) and 32 (Reference 14) show the results of measurements on SN55107 line receivers, SN55109 line drivers, and CD4050 AE hex buffers.

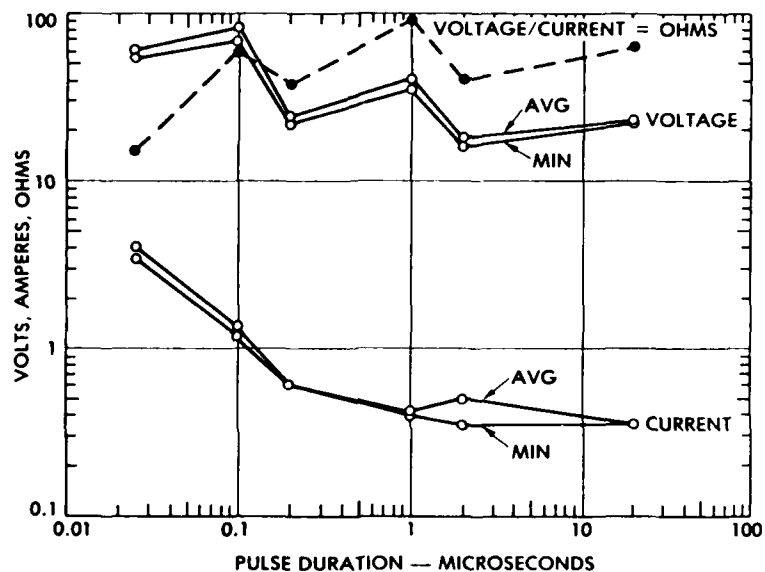


Figure 30 - Damage Thresholds of SN 55107 Line Receivers.

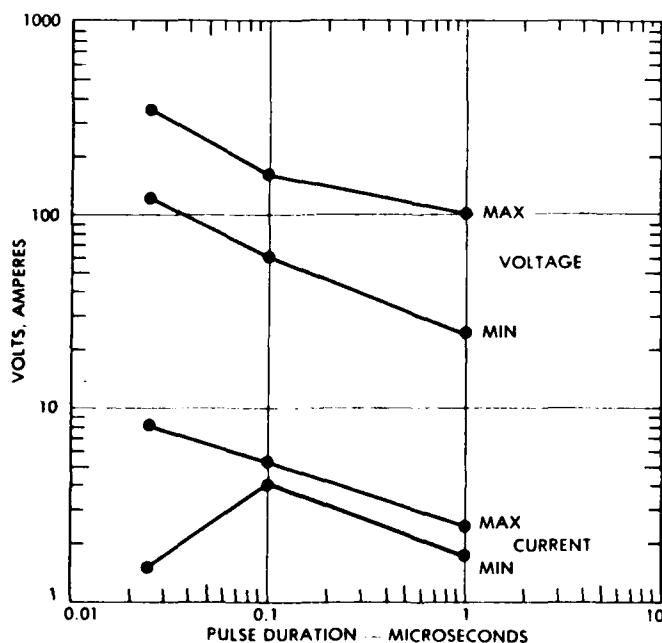


Figure 31 - Damage Thresholds of SN 55109 Line Drivers.

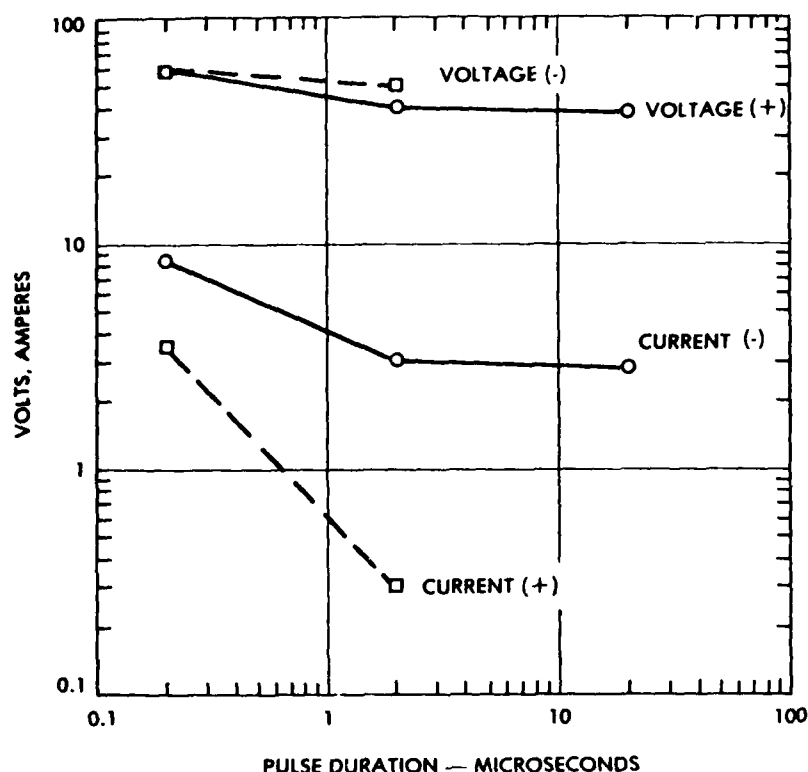


Figure 32 - Damage Thresholds of CD 4050 AE Hex Buffers.

CAPACITOR FAILURE MECHANISMS

Capacitors fail by a mechanism different from that of semiconductors. The mechanism of capacitor failure depends upon the type of dielectric. Capacitors with solid dielectrics - paper, Mylar, or ceramics - will, when subjected to nonrepetitive transients, either fail by puncture of the dielectric or not fail at all. Typically, a capacitor can withstand short-duration transient voltages several times greater than the DC rating of the insulation. The pulse-breakdown rating of the dielectric, however, is not a constant ratio to the DC voltage rating, nor is it normally part of any manufacturer's specification. Accordingly, it is safest to consider that such a capacitor is in danger of failure if the pulse voltage exceeds the DC rating of the capacitor.

Electrolytic capacitors, on the other hand, do not experience abrupt failure when exposed to short-duration transients. If the voltage across the capacitor exceeds the voltage used to form the dielectric film, the dielectric film begins to conduct. After the pulse has disappeared, the dielectric returns to nearly its normal state. During the transient period the dielectric film can carry substantial transient current without permanent or catastrophic degradation. Transients, however, may lead to increased leakage currents. An example of data that is available relates to a series of tests made on tantalum electrolytic capacitors of value 0.47 μF , 0.047 μF , and 0.0047 μF with a DC voltage rating of 350 V (Reference 15). The data indicate that failure (defined as a substantial increase in the leakage current at voltages of less than 350 V) can generally be associated with the time during which internal conduction occurs. For these components, conduction was initiated at 3 to 4 times the voltage rating. Leakage current increased continuously with time of conduction, from initial values of a few nanoamperes through milliamperes. The value of the capacitance determines how quickly the voltage across the capacitor reaches the breakdown voltage range, 90 to 140 V, which then relates to the time of conduction and the extent of damage. Figure 33 (Reference 16) shows the data for the nine 0.0047 μF capacitors tested. For a particular pulse duration of 5 μs , an increase in leakage current is expected; for pulse voltages of 100 to 150 V and for pulses of 150 to 200V, an increase in leakage current to several milliamperes is possible.

EXAMPLES OF USE OF DAMAGE CONSTANTS

Some examples of how the preceding material may be used to determine whether or not a given transient will cause damage to semiconductors follow. The first circuit chosen for analysis is shown in Figure 34 and is a simple remote-controlled relay. Across the

terminals of the relay coil there is a diode which would be exposed to the same transients as those to which the coil is exposed. The analysis approach that will be taken is first to calculate the current level that would cause the diode to fail and then to see whether or not the transient voltage source could supply that current. It will be assumed that the oscillatory pulse is a transient of 1 MHz frequency or 1 μ s period. At this frequency the inductive reactance of the relay coil would be sufficiently large that the relay could be neglected. The current required to cause failure at time, t , would be (from equation 13):

$$I_F = \frac{P_F}{V_{BD}} = \frac{Kt^{-\frac{1}{2}}}{V_{BD}} \quad (13)$$

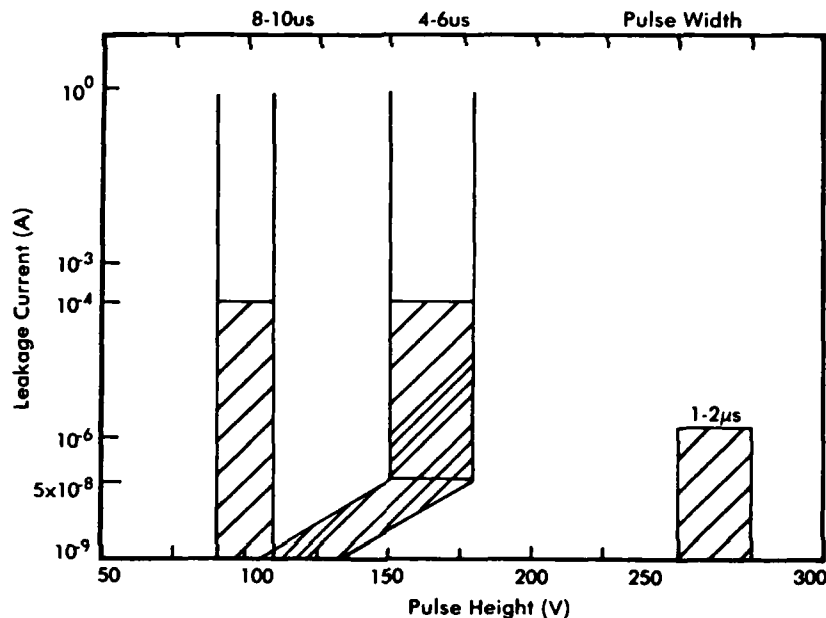


Figure 33 - Representation of Pulse Test Data for Sprague 0.0047 μ F Electrolytic Capacitors.

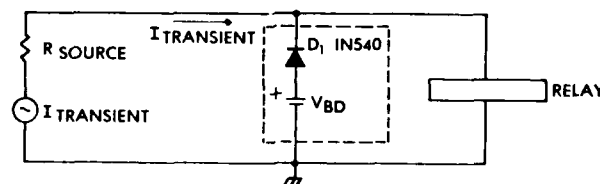


Figure 34 - Simple Remote-controlled Relay.

For a 1N540 diode, the reverse breakdown voltage, V_{BD} , is 400 V and the damage constant, K , is 0.93 (Reference 17). If a 200 ns pulse is used to approximate at 1 MHz damped sine wave, the failure current for the diode would be

$$I_F = \frac{0.93(2 \times 10^{-7})^{-\frac{1}{2}}}{400} \quad (14)$$

$$I_F = 5.2 \text{ A}$$

Assume now that the impedance of the source from which the voltage transient generates is 10 Ω . The voltage required to produce a current of 5.2 A through the diode would be

$$\begin{aligned} V_{\text{Transient}} &= V_{BD} + I_{\text{Transient}} R_{\text{Source}} \\ &= (400\text{V}) + (5.2\text{A})(10\Omega) \end{aligned} \quad (15)$$

$$V_{\text{Transient}} = 452 \text{ V}$$

Therefore, a 452 V pulse, 200 ns wide or a 1 MHz damped sine wave having a peak amplitude of 452 V would cause the diode to fail.

The second circuit chosen for analysis is the simple phase-splitter amplifier shown in Figure 35. The first step in determining the input current required for damage is to simplify the circuit. Again assume that the voltage source producing the transient is a damped sine wave of 1 MHz frequency. At such a frequency the reactances of capacitors C1 and C2 will be so small that they may be neglected. Likewise the 12V power supply line can be considered to be at AC ground potential. The resultant circuit after simplification is shown in Figure 36. The circuit can be further simplified by determining the equivalent resistances for the base and for collector circuits. The base-emitter junction and the base-collector junction can also be replaced by their diode equivalents to represent operation in the breakdown regions. This simplified circuit is shown in Figure 37. Also shown in Figure 37 are the breakdown voltages and damage constants for the 2N706B.

The circuit is now simplified to the point where it lends itself easily to hand analysis. The next step is to determine which junction will fail and what the failure mode is. The passive components are generally able to withstand higher energies for short-duration pulses than can transistors. Therefore, the transistor is the first element to consider for damage. Failure is also assumed to occur in the reverse biased direction.

Using the Wunsch damage model ($P = Kt^{-\frac{1}{2}}$), a calculation is made to see whether the emitter-base junction or the collector-base junction will fail first.

$$P_{EB} = K_{EB} t^{-\frac{1}{2}} = 17 \text{ W} \quad (16)$$

$$P_{CB} = K_{CB} t^{-\frac{1}{2}} = 130 \text{ W} \quad (17)$$

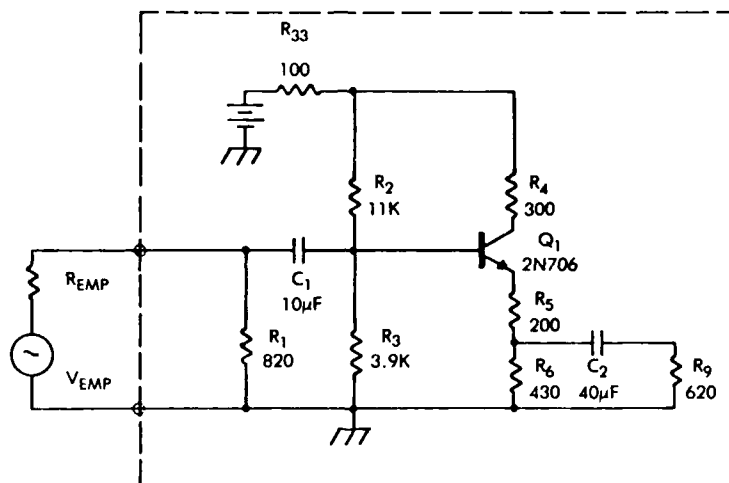


Figure 35 - Phase-splitter Circuit.

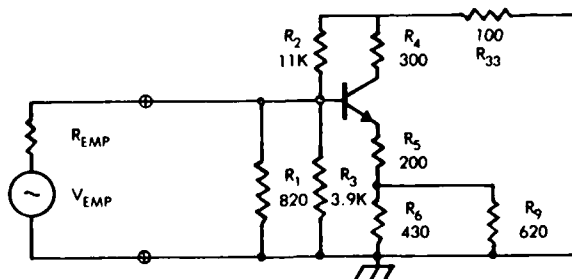


Figure 36 - Simplified Phase-splitter Circuit.

This calculation shows that the emitter-base junction is the more susceptible. The current required to fail the emitter-base junction would be

$$I_{JF} = \frac{P_{EB}}{V_{BD}} = 3.4 \text{ A} \quad (18)$$

The voltage from the base to ground is

$$V_{BASE} = BV_{EBO} + I_{JF} R_{EQ2} = 1.5 \text{ kV} \quad (19)$$

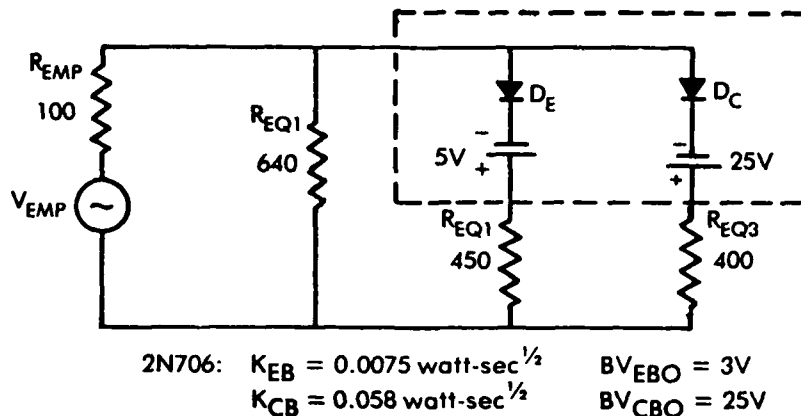


Figure 37 - Further Simplification of Phase-splitter Circuit.

The current through the collector-base junction is

$$I_{CB} = \frac{V_{BASE} - BV_{CBO}}{R_{EQ3}} = 3.7A \quad (20)$$

The power dissipated in the collector-base junction is

$$P_{CB} = BV_{CBO} I_{CB} = 93W \quad (21)$$

which is below its failure-threshold power.

The total current into the circuit is then

$$I_{Transient} = I_{jF} + I_{CB} + \frac{V_{BASE}}{R_{EQ1}} = 9.4A \quad (22)$$

and the $I_{Transient}$ voltage required to cause failure is

$$V_{Transient} = V_{BASE} + I_{Transient} R_{Source} = 2.5 \text{ kV} \quad (23)$$

Therefore (assuming a 100 Ω source impedance) a 2.5 kV pulse, 200 ns wide, will cause the transistor to fail.

Limitations to the Above Techniques

Certain limits to the accuracy and application of the theoretical and empirical damage models just described exist and must be noted in estimating component device vulnerability. The models have been verified only for diodes and bipolar transistors. Other devices, such as FETS and unijunction transistors, have been tested in insufficient numbers for definite conclusions to be drawn as to their conformance with the model. Also, the results and models which are presented apply strictly only to an isolated device—that is, not to a device in a circuit. In the case of a multiple-terminal device, they apply only to the two terminals connected for test, with any other terminals open.

The assumptions made about junction heating and transfer of heat in the derivation of the models limit their applicability to the region of pulse durations of approximately 0.1 to 20 μs . For longer times, appreciable heat transfer may take place away from the junction area during the pulse input. For short pulses the power levels are so high (1 to 10 kW) that very large currents flow; consequently, the joule heating in the bulk materials is appreciable. The transition behavior between these three regions of pulse duration is not well defined and may vary from one device type to another. Examination of available data indicates the transition region generally between 100 ns and 1 μs .

Still another limitation is fundamental to the work summarized in this section: it applies only to junction burnout. Other modes of device failure, such as metallization burnout and internal arcing, are not treated here. Based on the results obtained in studies of junction burnout, it would seem that other effects, such as metallization burnout, occur at higher power input levels than those input levels sufficient to damage the junction.

REFERENCES

1. F.A. Fisher, General Electric Co., "Analysis of Lightning Current Waveforms through the Space Shuttle," Aircraft Lightning Protection Note 75-1, National Aeronautics and Space Administration, Lyndon B. Johnson Space Center, Houston, Texas, (1975).
2. K.J. Lloyd, J.A. Plumer, and L.C. Walko, General Electric Co., "Measurements and Analysis of Lightning-Induced Voltages in Aircraft Electrical Circuits," NASA CR-1744, National Aeronautics and Space Administration, Lyndon B. Johnson Space Center, Houston, Texas (1971).
3. J.A. Plumer, F.A. Fisher and L.C. Walko, General Electric Co., "Lightning Effects on the NASA F-8 Digital-Fly-by-Wire Airplane," NASA CR2524, National Aeronautics and Space Administration, Lewis Research Center, Cleveland, Ohio (1975).
4. R.L. Davies and F.E. Gentry, "Control of Electric Field at the Surface on PN Junctions," IEEE Transactions of Electron Devices, ED-11, Institute of Electrical and Electronics Engineers, New York, New York (1964): pp. 313-23.
5. H.S. Velorie and M.P. Prince, "High-Voltage Conductivity-Modulated Silicon Rectifier," The Bell System Technical Journal, July 1957, pp. 975-1004.
6. F.A. Fisher and J.A. Plumer, General Electric Co., "Lightning Protection of Aircraft" National Aeronautics and Space Administration Reference Publication 1008, 1977, p. 455.
7. Fisher and Plumer, NASA RP 1008, p. 455.
8. Fisher and Plumer, NASA RP 1008, p. 456.
9. Fisher and Plumer, NASA RP 1008, pp. 470-491.
10. Fisher and Plumer, NASA RP 1008, p. 457
11. Fisher and Plumer, NASA RP 1008, p. 458
12. E. Keuren, R. Hendrickson, and R. Magyarics, "Circuit Failure Due to Transient-Induced Stresses," First Symposium on Electromagnetic Compatibility, Montreux, Switzerland, May 1975, IEEE EMC Conference Record 75 CH10124, Institute of Electrical and Electronics Engineers, New York, New York (1975), pp. 500-505.
13. Keuren, Hendrickson, and Magyarics, "Circuit Failure," p. 504.
14. Keuren, Hendrickson, and Magyarics, "Circuit Failure,"
15. Fisher and Plumer, NASA RP 1008, p. 463.
16. Fisher and Plumer, NASA RP 1008, p. 466.
17. Fisher and Plumer, NASA RP 1008, p. 472.

MODELS FOR ASSESSING HAZARDS DUE TO LIGHTNING

P.F. Little
Culham Laboratory
Abingdon Oxfordshire

SUMMARY

The characteristics of lightning current pulses and the radiated fields produced by lightning are summarised. The transmission-line model of the ground flash is considered and the derivation of the parameters of the line from the physical processes taking place is treated in various degrees of approximation. Changes in the shape of the current pulse occur as the return stroke is propagating, and the implications of these changes in waveform are discussed. The transition from leader channel to return stroke channel may be regarded as a shock front, and this aspect is explored also in respect of the leader advance. The coupling of fields and currents due to lightning into the aircraft when it forms part of the return stroke channel and when it is close to an independent stroke are considered in the light of these physical models.

1. INTRODUCTION

The general characteristics of lightning discharges have been described in earlier lectures. A brief review of the most important features of the higher-frequency components of the current pulse and the radiated spectrum is presented here, together with some comments about the effects of the complex shape of the lightning channel itself. The return stroke phase is then considered as a transmission line, with the aircraft behaving as an inserted section of different characteristic impedance. It becomes clear that the greatest rates of rise of current are likely to occur at the point where a leader from cloud or ground meets an opposing leader, and the gap between cloud and ground is bridged. Intracloud discharges are compared with ground flashes on this model. The progress of the leader itself, and the advance of the return stroke along the pre-ionised leader channel, appear to involve shock wave phenomena in the electron fluid which forms one constituent of the plasma of the arc channel. The shock wave picture is outlined, and its application to leaders and return strokes described. The interaction of lightning with aircraft is then considered in comparison with the effects of the electromagnetic pulse from a nuclear explosion, which has been intensively studied. The relevance to effects from nearby strikes which do not attach directly to the aircraft is obvious, though some differences exist. A direct strike to an aircraft defines the net current flow rather than the amplitude of an incident electromagnetic wave, but the coupling from given skin currents and surface charges to internal wiring and electronic systems is the same no matter what the origin of these currents or charges. The approaches developed during studies of nuclear electromagnetic radiation are applicable to direct attachments and to nearby strikes when this part of the coupling problem is being considered.

2. SUMMARY OF LIGHTNING CHARACTERISTICS

2.1 Current Pulse Waveforms

Flashes lowering negative charge predominate in nature, and those lowering positive charge often begin with an upward-going leader from a high point at ground potential (Anderson and Eriksson, 1979). All Berger's (1978) measurements of positive discharges (San Salvatore) are of upward discharges. Downward negative flashes have been most recently analysed by Anderson and Eriksson, from whose data Table 1 has been extracted.

Table 1
Characteristics of Negative Downward Flashes

Parameter	Position in Flash	Number of Cases	Percentage of Cases Exceeding Tabulated Value		
			95%	50%	5%
Maximum di/dt (kA/ μ s)	First Return Stroke	75	9.1	24	65
	Subsequent Strokes	113	7.5	38	190
Rise Time, 30%-90% (μ s)	First Return Stroke	75	0.9	2.3	5.8
	Subsequent Strokes	113	0.07	0.35	1.8

The average shapes of the current pulse for these two classes of stroke are compared in Figure 1. The initial rise is concave, with the maximum rate of rise occurring at about 80% of the peak amplitude. Subsequent strokes rise much faster than first return strokes.

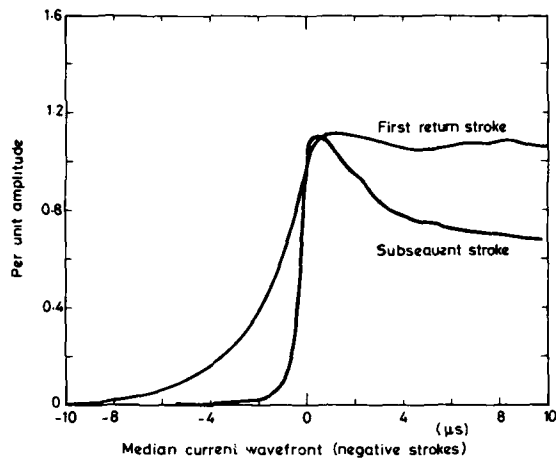


Figure 1. Lightning current pulse shapes

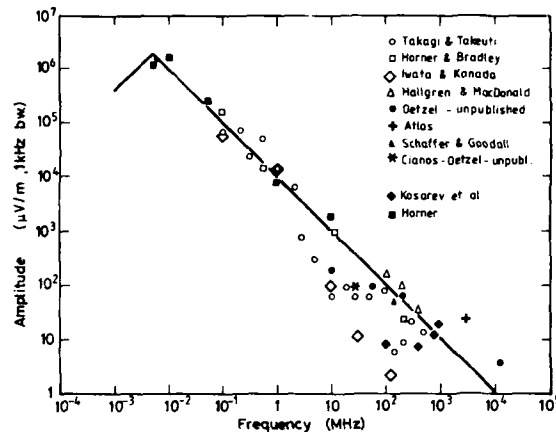


Figure 2. Spectrum of lightning flash at 10km

Positive flashes display current pulses that rise more slowly and fall much more slowly than the negative flash pulses. Usually only one positive stroke appears, giving a current pulse typically 250μs long at half-amplitude, compared to 80μs for negative first strokes and 30μs for negative subsequent strokes (Golde, 1977). High frequency energy is less likely to be generated with positive strokes from this data. The highest frequencies to be expected, from less than 5% of subsequent strokes with rise-times of 0.07μs, lie in the region of 2 MHz. This rise-time limit may be instrumental however. It should be noted that all the information is derived from ground-based measurements.

2.2 Observations of Radiation from Lightning Flashes

(a) Scope

We are concerned here only with nearby flashes, usually termed 'close' lightning although the radiation or 'far-field' component is dominant.

Measurements of the E- and B-fields due to a lightning flash are made either by measuring RF radiation in various frequency bands or by recording the magnitude of the total field changes. We consider here only the E-field values obtained in both ways: the B-fields are consistent with these.

Slow E-field changes, which we shall not discuss, occur in times of order 0.1 s during the whole flash, with fast changes superimposed. The rise-time of the fast E-field pulses is of order 5μs or less, and their duration 100μs or less. The spectrum of the RF radiation emitted peaks at about 5 kHz and extends beyond 10 GHz in frequency.

(b) RF Radiation

The radiated field intensity due to lightning is inversely proportional to the distance from the flash if that distance is greater than 10 km approximately. This scaling holds for individual sources of radiation down to distances of 500 m for frequencies above 100 kHz if the sources are much less than 500 m in extent. Since the radiation from a travelling current pulse behaves as if emitted from the ends of a straight conducting channel, or from bends in a tortuous channel, the sources are likely to be small compared to 500 m. They may be distributed over distances of several kilometres.

Amplitude spectra for the RF radiation emitted at a frequency of f Hz ($f > 10^5$) from a ground flash are approximately represented (see Figure 2) by the expression.

$$E = \frac{10^4}{f} \quad \text{V/m for 1 kHz bandwidth}$$

at a distance of 10 km. Above 300 kHz a cloud flash behaves similarly. The scaling of E with bandwidth W depends on the pulse repetition rate. As an approximation for an extremely low rate $E \propto W$; for very high rates $E \propto W^{1/2}$.

Some features of the RF radiation spectrum emitted during the initial breakdown phase and the leader development are described in Figure 3. The mechanism of the radiation is still under investigation.

Below 300 kHz single RF pulses appear, associated with a return stroke (about 4 per flash) or a K-change (about 40 per flash). Above 300 kHz the number of pulses per flash increases. Pulses are emitted during the breakdown processes associated with the movement of leaders in the cloud, recoil streamers (perhaps propagating along twisted channels) and leaders to ground. The average rate of pulse emission rises from $2 \times 10^3 \text{ s}^{-1}$ at 3 MHz to a maximum near 10^4 s^{-1} at 300 MHz. Signals at HF and VHF are partly quenched after return strokes and K-changes, probably because probing streamers are absent after charged pockets have been neutralised by these events. Above 10 MHz and in the VHF band (to 300 MHz) dart leaders and recoil streamers (K-changes) are the strongest sources of radiation. Above 300 MHz the pulse emission rate continues to fall and return strokes become more important again. At 10 GHz few pulses appear, each being associated with a return stroke. Figure 4 shows the general structure of signal observed.

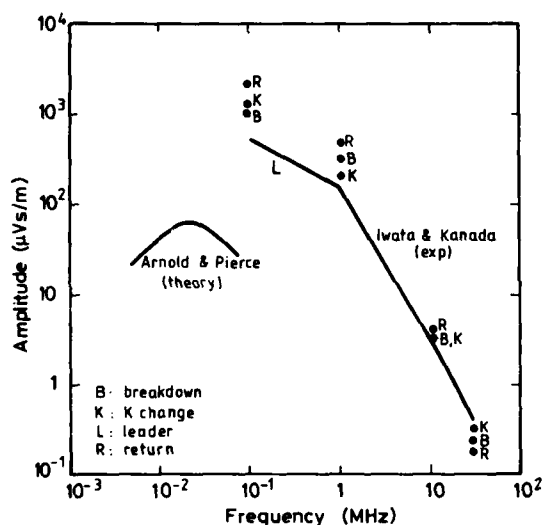


Figure 3. Spectrum of lightning phases at 10 km.

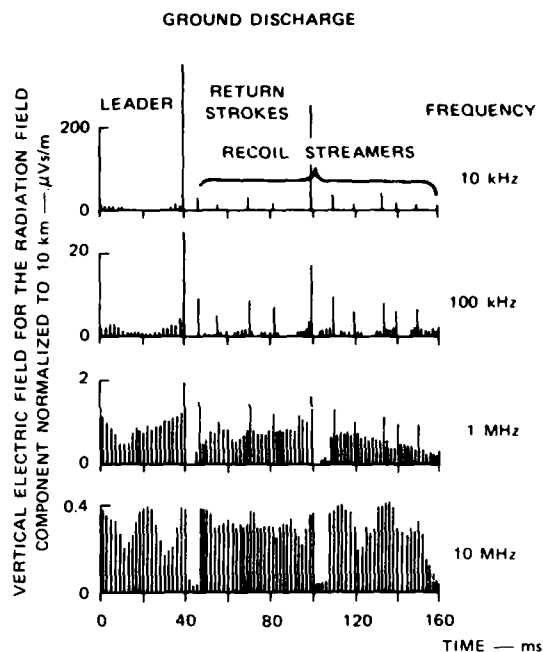


Figure 4. Schematic description of the structure of lightning radiation.

The observed rate of emission depends upon receiver characteristics, and the variation between discharges is large. Cloud flashes produce somewhat more pulses than ground flashes.

(c) Fast E-Field Changes

The amplitude of these pulses from a return stroke 10 km distant is typically 50 V/m, with approximately a log-normal distribution. When the signals are expressed relative to the median value in dB the deviation is about 7dB. Pulses lowering negative charge are defined as positive pulses by the observers.

The pulse shape is initially concave, rising slowly for about 5μs when the source is the first return stroke and for about 1μs with subsequent strokes. The final rise to the peak is very fast, occurring in a time of order 0.1μs or less. This difference is reminiscent of the difference in the current waveforms themselves (Figure 1). The decay time is approximately 50μs for the first stroke and 20μs for subsequent strokes, but the pulse shape is complex. Several subsidiary maxima appear after the main peak (see Figure 5).

First return strokes are preceded by a stepped leader, and the pulsed currents of this leader generate a train of unipolar E-field pulses. Their rise times are less than 1μs, and typically about 0.3μs; the lower limit is not known. The pulse width is 0.5μs and the amplitudes increase just before the return stroke, reaching 10 V/m (10 km distance). Subsequent return strokes may be preceded by a dart-stepped leader, which produces a similar train of fast E-field pulses: dart leaders yield no such train, but the fast part of the return stroke pulse following these leaders is typically 80 V/m in amplitude.

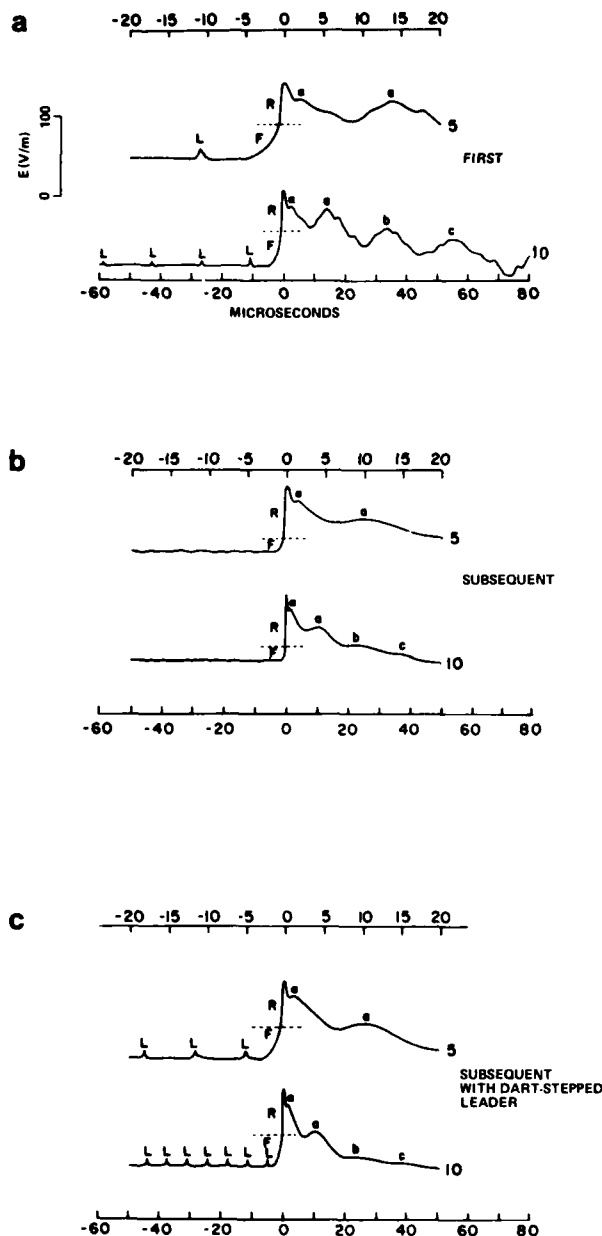


Figure 5. Sketches of radiation fields at 10km from (a) first return stroke, (b) subsequent stroke after dart leader, (c) subsequent stroke after dart-stepped leader.

In contrast to the unipolar form of the pulses produced by return strokes and leaders to ground, the basic wave shape of large pulses from a cloud process is bipolar. The initial half-cycle is usually positive if the event is a precursor to a ground flash, and usually negative if an isolated cloud discharge is developing (see Figure 6). Several faster, nearly unipolar pulses of the same sign as the first half cycle may be superimposed upon it or precede it. These pulses have about half the amplitude of the main bipolar pulse. A typical amplitude for the main pulse is about 20 V/m at 10km distance, and the total duration is about 50 μ s with approximately equal positive and negative sections. The time intervals between the fast unipolar pulses superimposed on the first half cycle are approximately 8 μ s for positive and 15 μ s for negative waveforms. Their rise times are less than 0.2 μ s, widths about 1 μ s and amplitudes about 10 V/m. They resemble the pulses produced by stepped leaders to ground.

Quite regular sequences of fast, approximately unipolar pulses similar to those just described may appear without the bipolar pulse at times, in intracloud discharges. A single sequence may last 100 - 400 μ s.

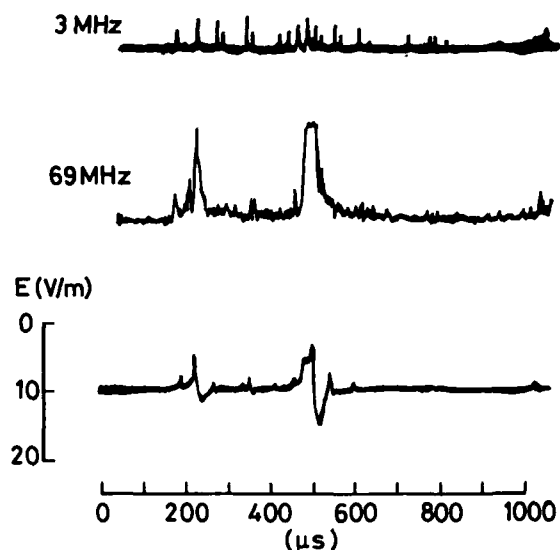


Figure 6. Example of RF and fast E-field pulses during intracloud discharge.

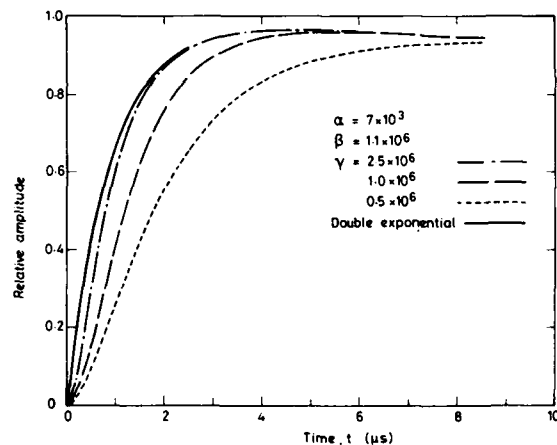


Figure 7. Waveforms of double-exponential and triple-exponential pulses.

(d) Relation between E-field Pulses and RF Radiation

During large intracloud events the RF radiation and fast E-field pulse are nearly simultaneous, reaching a maximum usually in the initial negative half-cycle. In contrast, the RF radiation during first return strokes in Florida storms reaches a maximum 10 - 30 μ s after the start of the E-field pulse. During subsequent return strokes the delay is between 200 and 600 μ s. Obviously different mechanisms obtain for the two types of discharge, but these have not been described in detail.

(e) Parameters of the Current Pulse

From observations of the radiation patterns it is deduced that the rates of current rise in a leader step lie in the range of 0.6 - 2.6 kA/ μ s or 6 - 24 kA/ μ s according to different authors. The current amplitudes lie between 2 - 8 kA. In return strokes the mean rate of rise is estimated to be 35 - 40 kA/ μ s, comparable with the values measured directly.

3. DIPOLE MODEL OF RETURN STROKE

3.1 The Dipole Field

The return stroke has been intensively studied as a source of EM radiation, with the emphasis frequently on effects at very great distances of 100 km or more. The channel length is then relatively short, so that the whole can be regarded to a first approximation a single dipole. It may be treated as a series of shorter dipoles placed end-to-end if the fields very close to the channel are of interest.

The vertical electric field $E(t, d)$ and horizontal magnetic flux density $B_\phi(t, d)$ at a time t and distance d from a channel length $l(t)$ carrying a current $I(t)$ is described to a good approximation by the variation in the current moment $M(t) = 2I(t)l(t)$, according to

$$E(t + \frac{d}{c}, d) = \frac{1}{4\pi\epsilon_0} \left[\int_0^t \frac{M(\tau) d\tau}{d^3} + \frac{M(t)}{cd^2} + \frac{1}{c^2 d} \frac{dM(t)}{dt} \right] \quad (1)$$

$$B_\phi(t + \frac{d}{c}, d) = \frac{\mu_0 c}{4\pi} \left[\frac{M(t)}{cd^2} + \frac{1}{c^2 d} \frac{dM(t)}{dt} \right] \quad (2)$$

where $c = (\mu_0 \epsilon_0)^{-1/2}$, the velocity of light in free space: (Uman 1969). Note that the fields depend on currents at earlier times, allowing for propagation delay. Electric and magnetic field wave shapes are clearly identical except at very short distances. The equations are valid provided both

$$\text{and} \quad \begin{aligned} d &\gg l \\ \frac{1}{2}\lambda &\gg l \text{ or } f \ll \frac{c}{2l} \end{aligned}$$

where f and λ are the frequency and wavelength of an emitted disturbance. These restrictions permit the radiating channel to be considered as a small coherent element, giving the simple forms (1) and (2). The three terms in the electric field equation are known as the electrostatic, induction, and radiation fields respectively, and are equal at a distance $d_0 = c/2\pi f_0$. For $d \gg d_0$ and $f \ll f_0$ or $f \gg f_0$ and $d \ll d_0$ the radiation or 'far' field term dominates. For a return stroke channel of length 2 km or more, equations (1) and (2) will only be valid for distances above 20 km. To obtain fields close to the channels, it is necessary to perform an integral summing radiation from elements along the whole length. This approach is desirable to include the variation of current along the channel.

Fields due to shorter radiating elements may be scaled to closer distances.

3.2 Empirical Representation of Current Waveforms

One of the earliest and most widely used empirical approximations to the return stroke current waveform at ground is due to Bruce and Golde (1941):

$$I(t) = I_0(e^{-\alpha t} - e^{-\beta t}) \quad (3)$$

where $I_0 = 20$ kA, $\alpha = 2 \times 10^4 \text{ s}^{-1}$, $\beta = 2 \times 10^6 \text{ s}^{-1}$ for the first return stroke, and $I_0 = 10$ kA, $\alpha = 2 \times 10^4 \text{ s}^{-1}$ and $\beta = 6 \times 10^6 \text{ s}^{-1}$ for subsequent strokes.

Dennis and Pierce (1964) included the variation of channel current with height, which removed the assumption that charge was transferred instantaneously from ground to the current wavefront. Only the far fields were calculated, and these are in good agreement with experimental data at low frequencies.

The far field radiation from K-changes, which has also been modelled in this way (Arnold and Pierce 1964, Cianos and Pierce 1972, Pierce 1977) is in fair agreement with experimental data for the low frequency amplitude spectrum. K-pulses of 3 Vm^{-1} at 10km are predicted (Pierce 1977).

The Bruce-Golde waveform can be criticised for its poor representation of the initial rise to peak current. Currents measured at ground show an initial concave rise (see Section 1.5) rounding only near the peak current, while the double exponential form commences at maximum slope and has a convex rise to peak: the high frequency content of these will be different. One way to introduce a concave initial rise with zero slope at $t=0$ is to add a multiplying term to form a triple-exponential pulse (Figure 7):

$$I = I_0(e^{-\alpha t} - e^{-\beta t})(1 - e^{-\gamma t}) \quad (4)$$

This waveform is closer to reality at the initial rise and its Fourier spectrum is reduced at high-frequencies compared to the Bruce-Golde waveform (3). It ignores all fine structure in the current pulse, so predictions made from (4) would underestimate the high-frequency components. The waveform (3) introduces such components in an unrepresentative way, but it is a simple form of great value in predicting the field of the return stroke.

4. TRANSMISSION LINE MODELS OF A RETURN STROKE

4.1 Introduction

The return stroke of a lightning discharge in a cloud-to-ground flash can be represented in a very simple way if the charge on the initiating leader channel is ignored. The capacitance of the cloud then contains all the electrical charge present, and the leader channel is a resistive and inductive element in a simple series LCR circuit. The final step of the leader acts as a switch which completes the circuit. The representation cannot, of course, provide any information about the progress of the return stroke current pulse along the leader channel. The current pulse shape is regarded as identical at all points along the channel.

Prinz (1977) discussed this model and evaluated its self-consistency in terms of the relationship between known parameters for natural lightning. The action integrals calculated are two to three times larger than those observed in natural lightning strokes. This is good agreement for such a simple model. The overestimate arises because actual lightning pulses are more peaked than the exponential decaying form produced by a discharging capacitor.

If the charge on leader channel is included in the model, the final step is equivalent to a switch connecting a charged transmission line to a terminating resistance (Figure 8). When the channel connects to the ground, usually through a short answering leader propagating from ground level, the charge on the channel flows to ground and contributes to the current pulse. Neglect effects due to the ground streamer for the moment. Because the channel charge is closer to the ground than the cloud charge, the inductance of its connecting path is lower. The channel then will contribute a fast-rising current pulse. The charge from the cloud contributes only to the later current flow.

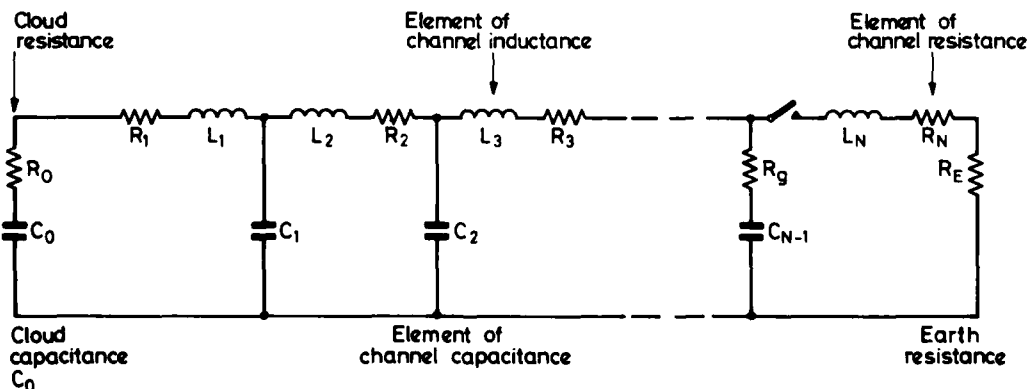


Figure 8. Lumped parameter transmission line as a representation of a lightning return stroke.

This modification clearly allows peak currents of shorter duration to appear, and thus should lead to more realistic values of the action integral. The leader channel may be treated as a uniform transmission line as a first step. Price and Pierce (1977) describe the development of this model (neglecting the cloud capacitance) from the first discussions of a line excited by a source at the base by Bruce and Golde (1941). They consider finally a finite, lossy, uniform transmission line terminated in its characteristic impedance and initially charged to a uniform potential. The current at the ground is found to rise instantaneously to a maximum value and then decay, exponentially at first. A similar onset is predicted for current flow at all points of the channel, but the magnitude of the current peak falls as the height above ground increases.

The behaviour of the current at ground level is in general accord with observation, though peak values of dI/dt occur at $t=0$, whereas there is a delay before this peak occurs in real lightning. At very long times the current falls as t^{-2} and this has some correspondence with the intermediate current often observed.

The fact that the line is lossy is important, since a loss-free line produces a current in its terminating resistances that is constant between abrupt step-changes. Such a current waveform is not typical of lightning current pulses. Resistance reduces the importance of reflections, and any model of a lightning channel must include resistance if a realistic current pulse at ground level is to be reproduced. The effective channel resistance per metre R^* is often taken to be constant with time, but in nature the lightning channel resistance varies very greatly during the pulse. It is difficult to assess a useful mean value.

The inductance per metre L^* and capacitance per metre C^* of the uniform line can be chosen to give the observed velocity of propagation of the return stroke (2×10^7 to $1.1 \times 10^8 \text{ m s}^{-1}$) (Price and Pierce 1977, Schonland 1956, Berger 1977).

It is desirable to derive all the line elements from physical arguments rather than from any matching of propagation velocities, making simplifying assumptions where possible. We consider only the return stroke.

4.2 Capacitance elements

If the leader channel is regarded as a vertical charged conductor of small radius extending toward the ground and at the same potential as the cloud, the electric field and therefore the linear charge density is greatest at tip - Golde (1973) assumed an exponential form for the decay of charge density with height as an approximate description.

An accurate solution for the field distribution between the complex electrode formed by the cloud and the channel combined and the ground plane can be found by numerical methods. The POTENT code at Culham Laboratory uses a finite-difference method to find solutions for such problems (Thomas 1974) and similar codes exist in many establishments. Then from the electrostatic field E around the channel at a radius r the charge on the channel per unit length λ can be determined if it is regarded as a cylindrical conductor, since $\lambda = 2\pi r \epsilon_0 E$. Thus the capacitance per metre C^* can be calculated from the potential V ; $C^* = \lambda/V$. The tip nearest the ground may be regarded as a hemispherical cap carrying a charge $Q = 2\pi r^2 \epsilon_0 E$ where E is now the field at a distance r from the tip. The additional capacitance is found as before and added to the last section of the channel. Figure 9 shows some typical results (Little 1978).

The charge distribution is determined by the geometry of the cloud and the channel, but the general shape of the field lines around the channel always appears as in Figure 10(a).

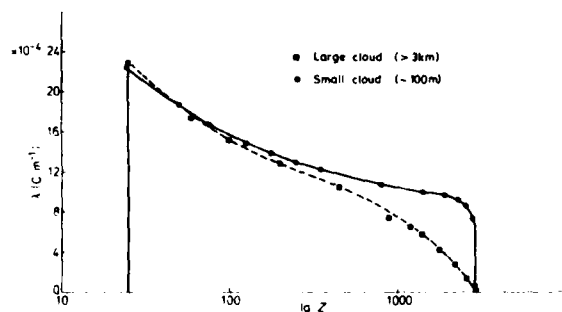


Figure 9. Distribution of linear charge density λ along a 3km lightning channel for two cloud models.

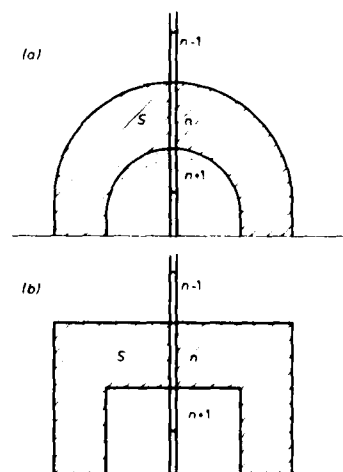


Figure 10. Field lines around a lightning channel.

For each channel segment the geometrical capacitance is now known at the beginning of the return stroke. These values may be used as approximations throughout the pulse, introducing some inaccuracies. The passage of the return stroke releases more charge on the channel, however, and this extra charge has not been calculated. It is available from the leader channel because roughly equal amounts of positive (largely nitrogen) ions and negative oxygen ions are present throughout the leader channel. After a pulse of leader current (electron flow) the electrons attach to oxygen molecules and their space charge is neutralised by the positive ions present. After the connection to ground is complete the high electric fields at the tip of the advancing return stroke detach the electrons once more, and they are free to participate in the return stroke current pulse.

On the transmission-line model, an underestimate of the stored charge means that C^* is underestimated. This implies that the velocity of a current pulse along the line will be too high.

4.3 Inductance Elements

When current flows from any segment to ground, displacement current flows in the space between the segment and ground. If the field distribution is assumed to be stationary this current ($\epsilon_0 dE/dt$) flows along the field lines already calculated. The inductance associated with this flow is determined by the area under the field lines. This is shown by the sum of the shaded and dotted zones in Figure 10 for the n^{th} element at the beginning of the return stroke.

The total inductance associated with the next lowest element ($n+1$) is determined in a similar way by the area shown by the dotted zone in Figure 10. It is appropriate then to associate the difference between these two inductances, determined by the flux in the hatched area S of Figure 10 with n^{th} line segment. This defines the inductance L_n of the n^{th} loop of the ladder network of the computer model.

The exact shape of the outer boundaries of S is not critical. Circular or rectangular approximations (Figure 10(b)) within the same limits give essentially the same values for L_n . The inductance of a line segment may be estimated by regarding it as the inner of a coaxial line whose outer conductor is remote, so making L_n constant during the pulse.

4.4 Resistance Elements

The effective resistance per metre R^* is a complex function of height and time. At a given height $R^* = R^*(t)$ may be estimated from the physics of a uniform arc column, if the current waveform is known. Hill (1971) calculated the heating of an arc column for the Bruce-Golde current waveform, and from his work $R^*(t)$ is found to fall from about $500\Omega/\text{m}$ to about $1\Omega/\text{m}$ in the first $10\mu\text{s}$ (Little 1979). This rapid variation means that great inaccuracies would be introduced by the use of an average value. $R^*(t)$ needs to be calculated for each element of the ladder, network at each time-step for a self-consistent current waveform.

Strawe (1979) used the spark channel model of Braginskii (1958). This relatively simple model assumes that a conducting channel has been established prior to the initiation of the spark by prebreakdown streamer, and/or leader processes. The resultant arc radius, temperature, pressure, etc. are determined from the spark current time history. The current is assumed to heat (i^2R loss) the initially conducting arc plasma to higher temperatures and tens of atmospheres of pressure. This condition produces a hydro-dynamic shock wave in the air surrounding the spark channel resulting in rapid channel expansion. Braginskii uses the strong shock approximation to simplify the physical picture of the expansion process. This picture produces an essentially uniform electrical conductivity determined from channel temperature and pressure which is nearly constant in time. The channel resistance per unit length is determined from the conductivity and the arc radius $a(t)$.

Braginskii ultimately assumes σ to be independent of time and temperature so that only $a(t)$ need be determined to calculate the resistance R . He neglects radiation in favour of conduction losses, and thus arrives at excessively high temperature estimates. Strawe uses these assumptions in his Model I computation. A second Model II is developed from Model I by modifying the basic equations to include the effect of lost and reabsorbed thermal radiation from the channel, the variation of thermal and electrical conductivity with time, and a closer account of the momentum transfer.

For both models, the final equations are solved numerically at each time-step of the time-domain code CIRCUS. This code can deal with large numbers of the ladder sections used to represent a transmission line, and Strawe ensures that his results are independent of the number of line segments chosen by making this number very large, about 100. Earlier calculations used far fewer sections and thus cannot in principle be as accurate.

4.5. Terminations

The resistance of a hemispherical earth conductor as computed by Weisinger is (Prinz 1977)

$$R_E = 8.9 \frac{\rho}{I_{\max}} \quad (5)$$

where ρ is the specific resistivity of the ground. This gives $R_E = 10 - 100\Omega$ for $I_{\max} = 10 - 100$ kA as the ground termination. No inductance or capacity is present.

At the cloud a resistance in series with a capacitor may be used as the terminating impedance. The resistance is uncertain, and the capacitance varies with the size of the charge pockets in the cloud.

4.6 Initial Conditions

Usually the capacitors on the transmission line are assumed to be charged to a uniform potential in the range of 10 MV to 100 MV to represent the charged leader column. To represent the answering leader from ground in the commonly-occurring negative stroke the capacitor in the lower elements of the line are left uncharged. At $t=0$ a switch connection is made between the upper and lower sections and a current pulse travels in both directions away from the junction point. The height of the switch can be chosen at will; it is usually placed between 25 m and 100 m.

It should be noted (Little 1979) that a switch can be positioned close to the cloud to represent the result of a leader initiated at ground level. Positive discharges usually are associated with long ground leaders (Berger 1978) as we remarked in Section 2.1. A positive stroke is described then by a long section of line at earth potential and a short section at cloud potential. The electrostatic charge distribution is then very different from that used to determine C^* for a negative stroke. However, in view of the additional charge held by negative and positive ions within the column the same values of C^* may be appropriate for both types of stroke to a good approximation.

It has been suggested (Anderson 1971) that there is a substantial voltage gradient along the leader column at the time when the junction to ground is made. This would have a significant influence on the velocity of the return stroke, because it would affect the heating of the column and hence the variation of R^* with time at all heights.

4.7 Possible Improvements to the Model

Some complicating factors have been omitted from this model of the return stroke which could have considerable influence.

(a) The branching of the leader channel results in the creation of additional charged transmission-lines, capacitatively-coupled to the main channel as well as directly-connected to it. This introduces additional fast pulses into the main current pulse as it moves along the channel, making the form of the pulse more complex with extra high-frequency components.

(b) The main channel is not precisely vertical, but may be nearly horizontal, or even fall rather than rise. This range of directions is important in assessing the fields due to the channel. The tortuous nature of the channel should also be recognised.

(c) The junction between the cloud leader and the ground leader is not well understood. The high-frequency current components initiated at this point are expected to represent the upper limit of the frequencies in the current pulse.

(d) The physics of the process by which the tip of the return stroke advances has not been adequately represented. This seems to be dependent on some form of shock wave (Section 6)

(e) The arc channel, carrying heavy currents, is likely to experience significant magnetic pinching forces. This has not been included yet in any analysis.

5. RESULTS OF THE TRANSMISSION LINE MODEL

5.1 Solution of the Circuit Problem

The circuit elements of the lumped-parameter ladder network are established from physical arguments or by assigning L^* and C^* from the observed return stroke velocities. The behaviour of this network under the chosen initial conditions can be followed by analogue or digital computations. Digital codes of varying degrees of complexity exist in many institutions and analogue computers, usually less flexible, are also available. It is not difficult to handle up to ten segments of a ladder network, and this is sufficient for a simple analysis that gives the main features. Accurate results require many more segments, but the physical basis of the model used must also then be more accurate to justify the computing effort needed.

5.2 The Current Waveform

It is generally agreed (Kim et al 1977, Little 1978, Strawe 1979) that the highest peak value of the current pulse in the channel occurs at the point of intersection of the cloud leader with the answering leader from ground. The details of this junction process have not been described sufficiently well to allow an accurate assignment of $R^*(t)$ (or indeed C^* or L^*) to the line segment which includes the junction point near $t=0$, but the uncertainties here do not affect this general conclusion.

The peak values of dI/dt also appear at the junction point. These are independent of $R^*(t)$, since at $t=0$, $I=0$ and

$$\frac{dI}{dt} = \frac{V}{L}$$

where V is the potential across the gap and L is the gap inductance. If $L = 2 \mu\text{H/m}$ (a typical value) and $V = 20 \text{ MV}$ for a gap of 50 m then

$$\frac{dI}{dt} = 200 \text{ kA}/\mu\text{s}$$

which is near the extreme upper limit of observed values. As the current pulse propagates, the peak value of dI/dt falls much more rapidly than the peak value of the current itself. Figure 11 shows some results of Little (1978) for a simple eight-section representation of a 3 km channel where R^* was taken to be constant. The peak dI/dt value falls by about two orders of magnitude as the distance from the junction point increases. The current falls only by a factor three approximately along the channel, and becomes much smoother in form.

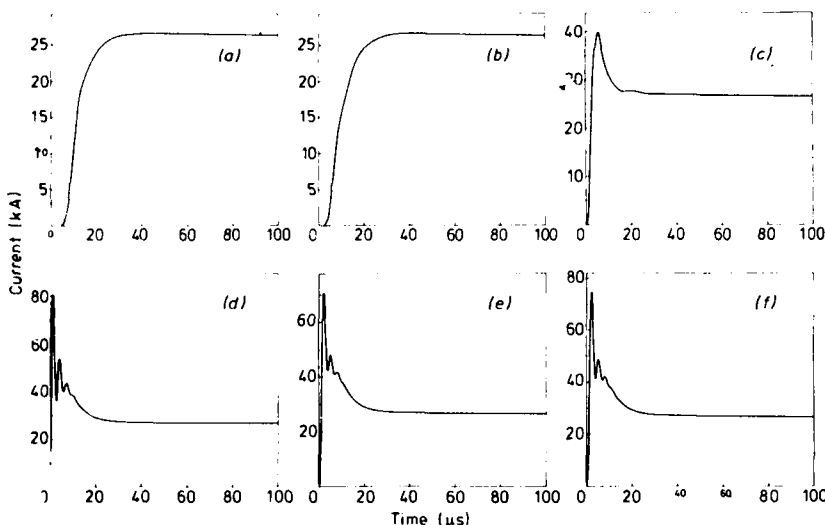


Figure 11

Current waveforms in a 3 km lightning channel at (a) 2950, (b) 1950, (c) 900 (d) 450, (e) 250 (f) 70m. Leader junction height at 250m within the channel element (e).

This implies that the greatest threat to aircraft appears near the junction point as far as induced voltages are concerned. For a negative stroke this is near ground level. For the rarer positive stroke, the greatest threat is near the cloud or at a great height. Intra-cloud discharges may perhaps have similar values for the maximum dI/dt at the junction of a probing streamer with a charge pocket (onset of K-change) because the ratio V/L determining this value should be comparable with that for earth strokes. The peak currents are lower, however (1 kA rather than 30 kA).

The difference in the waveform of positive and negative strokes observed at ground level is explained by the difference between the heights of the junction point. When a negative stroke is observed the current pulse is seen close to the switching point: for positive strokes the pulse is seen after transmission along the larger part of the column. Figure 11 indicates the effect of distance on Little's model, and Figure 12 from Strawe (1979) shows the difference in pulse shape (on his accurate calculation) at different heights along a 9.6 km channel when the junction point is 100 m above ground. The increase in rise time with height is clear: Strawe derives values of 87 kA/ μs at 50 m and 0.87 kA/ μs at 9 km. These conclusions are similar to those of Little (1978). Positive strokes observed at ground would be expected then to show slower rise times and a much smoother profile than negative strokes.

If the aircraft actually forms part of the lightning channel it will carry the current pulse without affecting the current waveform, provided that the rise time of the pulse is slow compared to the period of the lowest resonance frequency of the aircraft. The discontinuity in the transmission line due to the presence of the aircraft will excite oscillations in the skin currents if this condition is violated. Resonance frequencies would be expected to be within the range 2 MHz - 20 MHz, so that rise times below 0.2 μs

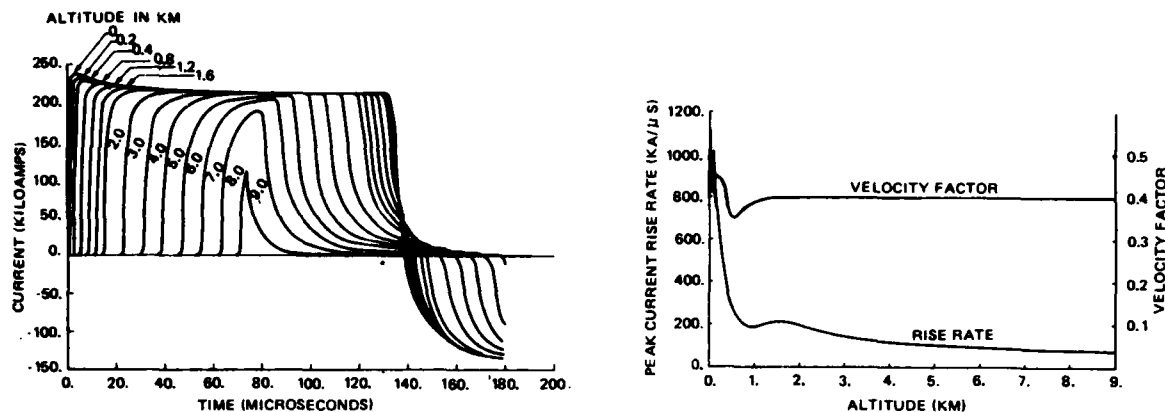


Figure. 12. Calculated current pulse shapes (a), rates of current rise and ratio of return stroke velocity to the velocity of light (b), as a function of height

should excite airframe resonances. Such fast rise times are observed in radiated E-field pulses produced during the breakdown phase, and by leader pulses, in K-changes and in the fast portions of the E-field pulses due to return strokes. This suggests that current pulses in intracloud and in ground discharges are fast enough to excite airframe resonances.

Measurements on negative flashes at ground (Anderson and Eriksson 1979) show that for first return strokes about 2% have rise times faster than 1 μ s, and for subsequent strokes 85% have such rise times. Indeed, 15% have rise times faster than 0.1 μ s. Aircraft struck near the ground by a negative stroke, or near the junction point of the leaders for any stroke, are likely to display current oscillations at their fundamental frequency. A crude calculation (Little 1979) suggests that oscillating currents of about 1 kA amplitude may appear in an aircraft 50 m long. The corresponding potential difference along it would approach 1 MV if its inductance is about 50 μ H and the frequency about 3 MHz. At a point on the channel remote from the leader junction no such oscillations would be excited, because the current pulse rises too slowly.

5.3 Fields Near a Lightning Channel

Transmission-line models have been derived on the basis of radiated fields measured at great distances (20 - 50 km) from the flash, largely by Uman and his co-workers (see Uman et al 1973 and references). Currents so obtained are more sharply peaked than those observed directly (Berger et al 1975, Golde 1977, Berger 1978). The radiation field at one point does not give a unique solution for the current waveform, and further the electric field at distances under 10 km calculated in this way displays features which are not observed experimentally (Uman, Brantley et al 1975). Figure 13 shows their calculated fields at 1 km distance (curve U). The insert shows the E-field and B-field pulses observed at about 2 km distance.

An improvement in modelling the near field waveform is due to Price and Pierce (1977), who consider the channel as an initially charged transmission line which is suddenly terminated by its characteristic impedance at ground. The resulting disturbance which propagates up the channel is subject to resistive losses. The far field obtained in this way is similar to that of Uman, but the near field now follows that observed quite closely after the initial rise, as shown in Figure 13 for a stroke 1 km aw. (curve P & P). There is scope for extending this work to include the first sharp change in electric field when the current surge just begins. Its omission means that the high frequency content is very poorly simulated. The step rise is accompanied by a peak in natural lightning pulses.

We present also a diagram from Pierce (1975) which models the frequency spectrum of electric and magnetic fields at 300 m distance from severe ground and intracloud discharges (Figure 14). Details of this work are lacking, but it seems that a transmission line model was employed. Values at high frequencies are not unreasonable by comparison with far field radiation amplitudes (compare Figure 2).

It is well-known that a conducting filament carrying a travelling current pulse radiates as if the fields emanated from the ends of the filament. Uman, McLain and Krider (1975) used this result without taking into account the tortuous nature of the return stroke channel. In a real strike radiation will appear from every point where the channel changes direction. Le Vine and Meneghini (1978) included this effect and found that the electric field changes observed can be better accounted for as a function of time. The spectrum radiated is also better described (Le Vine 1978; Oetzel and Pierce 1969; Horner 1964). The effects of the tortuous channel have not yet been included in calculations of the fields near the return stroke. Fields so calculated might lead to more accurate values of induced currents in aircraft.

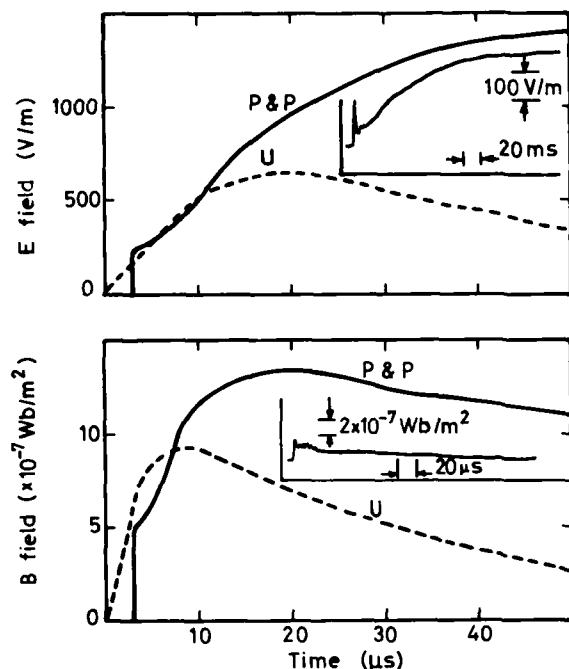


Figure 13. Electric and magnetic field pulses at 1km distance from a return stroke, computed from models by Uman et al (U) and Price and Pierce (P&P). Inset: observed pulses at 2km distance approx.

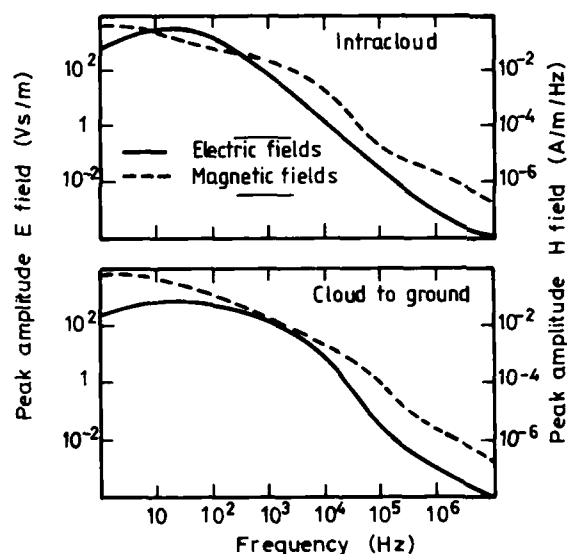


Figure 14. Frequency spectrum at 300m distance from intracloud and ground strokes according to Pierce.

The model of Uman, Brantley et al (1975) has been used by Perala, Cook and Lee (1979) to deduce the electric fields 20 m from a 200 kA return stroke, as shown in Figure 15. The maximum E-fields occur horizontally, reaching 800 kV/m. Experience with laboratory long sparks suggests that 500 kV/m is the greatest field (averaged across a gap) when virgin air breaks down. The greatest vertical field found by Perala et al is 100 kV/m.

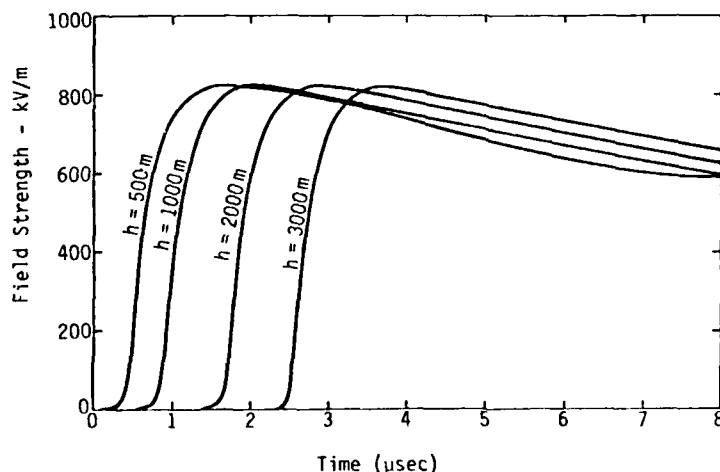


Figure 15

Computed field strength (horizontal) due to severe lightning stroke at 18m distance.

At distances of 2 km, observations suggest that E is of order 300 V/m (Figure 13). Inverse scaling with distance to 20 m (which is unjustified) would lead to E-fields of order 30 kV/m, but it is not likely that the stroke creating these fields was carrying 200 kA. If it was an average stroke (30 kA) then E-fields of 200 kV/m in the severe stroke considered by Perala would be expected by simple inverse scaling. This leads to some slight independent support for the order of magnitude of the fields derived: if other terms than the radiation term dominate at short distances, they must exceed 100 kV/m. The computed pulses are fast enough to be capable of stimulating airframe resonances in some aircraft.

The unipolar pulses due to stepped leaders (Figure 5) observed by Krider et al (1977) at distances of 10 - 20 km form the basis of another extrapolation by Perala (1979). He estimated fields of 10 kV/m close to the leader channel.

It seems unlikely that a stroke could approach an aircraft as closely as 20 m without forming a direct attachment to the aircraft. Normal leader steps are about 50 m, and streamering from the aircraft in the high ambient fields near a thunderstorm is very likely to occur. The closest nearby strikes should probably be regarded as at least 50 m away from the aircraft.

The size of the aircraft should have some influence on the minimum separation S needed to allow a leader to pass it without attachment. The geometrical disturbance of the electrostatic field due to the induced charges on the aircraft extends over a distance proportional to the aircraft's dimensions; however, any streamer activity taking place increases the effective size of the aircraft. Some guidance as to the value of S may be obtained from the generally accepted striking distances S_0 to ground structures (Golde 1977a). These are known to be correlated with the current in the return stroke following. If the peak current is 20 kA, $S_0 \approx 30$ m; if the peak current is 100 kA, $S_0 \approx 120$ m. For severe strokes the values of S near 100 m would seem appropriate.

No computations have been published dealing with fields near a transmission-line model of a lightning channel carrying self-consistently-derived current pulses in the manner described in the previous section. Thus the basic physics of the discharge has not been taken into account in much detail. The current pulse description, however it is arrived at, can be inserted into the general expressions for the electric and magnetic fields due to a straight vertical channel of length H (McLain and Uman 1971).

6. FUTURE DEVELOPMENTS

The numerical model of the channel as a transmission line has employed either a prescribed current pulse or constant line elements in most of the work. The calculation of time-dependent elements and current pulses in a self-consistent manner with a sufficiently large number of line segments is beginning to give more realistic answers. In the future more of the physics of the arc channel should be included.

The breakdown process, including the advance of the leader, requires to be better represented and so does the transition from leader to return stroke. Shock waves in the electron fluid (Fowler 1974, 1976) need to be considered. Electrons advance under forces due to their own pressure as well as the electric field, and when the electron temperature or density is changing rapidly the pressure differences may dominate. In this advance more electrons are created by ionisation of the gas present, whether this is previously conducting or not. A shock condition exists at the leading edge between the neutral gas and a region where the electric field E and electron fluid velocity v change rapidly while the gas temperature T and electron density n vary slowly. Behind this region E and v are zero, but T and n are still variable.

This theory leads to the conclusion that in breakdown conditions where the direction of the electric force on the electrons is in the same direction as the wave propagation (proforce waves) the speed of advance is proportional to the electron mobility, and determined directly by E at the leading edge. For breakdown propagation in the opposite direction (antiforce waves) the shock speed is proportional to the electron pressure which in turn is proportional to E . Numerical results agree well for wave speeds above 3×10^6 m/s with experiments on shock tubes and with observations on lightning, both leaders and return strokes. Photoionisation is not thought to be important except at low pressures.

In a negative stroke the (proforce) leader moves in steps. From a shock tube model standpoint we have a self creating shock tube growing steadily longer, along which successive shocks are launched as the apparatus becomes charged up to permit them. The initial wave hypothesized to exist by Schonland (1938), and named the pilot leader, is a necessary feature. Its nature must be a weak discontinuity proforce shock wave whose velocity should be close to that observed in the laboratory by Wagner (1966) for proforce avalanches.

When the column reaches a distance above ground slightly longer than one step, it is usual for an antiforce wave (the leader from ground) to leave a sharp point on the ground and move to the column to make the final connection. Again the wave is a shock wave, and it derives its large speed from the fact that its local potential is essentially the same but of opposite sign to that end of the column, while its radius is very small because its electron needs are met by a solid electrode. It is, in fact, of the same character as a long spark in the laboratory.

This small radius, fast moving, antiforce wave not only reaches the column, but penetrates it, taking advantage of the large amount of energy stored during formation in the column by radial diffusion and attachment. These electrons and the energy which their charge separation represents are easily available to the strong electric fields generated by the return stroke via collisional detachment, so the stroke can proceed from ground to cloud at speeds up to 2×10^8 ms⁻¹ driven by a wave field $\sim 10^6$ volts/m-torr.

Restrikes behave like the first return stroke, if the leader is stepped. Dart leaders are very similar to the rekindling waves, in speed and every other aspect. Their behaviour, however, furnishes one more point of contact with theory. Because the channel is extremely hot after the passage of the previous return stroke current pulse theory predicts and the experiment confirms that no breakdown wave is possible until it cools. During the interval it will conduct freely any charge supplied at the upper end - the continuing current.

All these processes seem to be describable by a shock theory which uses the fluid dynamics of electrons that multiply by collision processes. This shock-wave model provides a physical basis yet to be exploited for developing a theory of the processes which lead to the appearance of sub-microsecond rise-time in the EM pulses radiating from lightning leaders and return strokes.

7. COMPARISON WITH ELECTROMAGNETIC PULSES FROM NUCLEAR EXPLOSIONS

The electromagnetic radiation pulses emitted from a nuclear explosion induce skin currents in nearby aircraft which may create significant voltages and currents in the electrical systems of the aircraft. Hazards created by nuclear electromagnetic pulses (NEMP) have been intensively studied, but the field has developed largely in isolation from the work on lightning hazards. Part of the reason for this is that the direct effects of lightning current pulses were emphasised in the early work, and damage of this type occurs only when the aircraft is struck. Also, early work on lightning testing was generally restricted to frequencies below about 300 kHz, and this was another reason for separate development. Part of the analysis pursued in order to understand NEMP involves a study of the coupling from skin currents into interior circuits which is relevant to direct strikes.

More obviously, the skin currents induced in aircraft near a lightning stroke can be analysed in much the same way as the currents induced in aircraft near a nuclear explosion. We may refer to EMP from lightning as LEMP as distinct from NEMP.

For both direct strikes and nearby strikes it is necessary to describe the distribution of skin currents, magnetic fields and electric fields around the aircraft. These disturbances can couple into the interior of the aircraft in a variety of ways, which are discussed in a later lecture.

ACKNOWLEDGEMENTS

This lecture was prepared with the support of the Procurement Executive of the UK Ministry of Defence.

REFERENCES (first mention only)

- SECTION 2.1**
R.B. Anderson and A.J. Eriksson (1979), Lightning Parameters for Engineering Applications, Discussion Paper for CIGRE Committee 33, Roumania Colloquium: CSIR Special Report ELEK 170.
K. Berger (1978), Blitstrom Parameter von aufwärts Blitzen, Bull. S.E.V. 69 353-360.
R.H. Golde (1977), Lightning Currents and Related Parameters, Chap. 9, Lightning (Ed. R.H. Golde) Academic Press: London
- SECTION 3.1**
M.A. Uman (1969), Lightning, McGraw Hill, New York.
- SECTION 3.2**
C.E.R. Bruce and R.H. Golde (1941), The Lightning Discharge, J. Inst. Electr. Eng. 88, 487-520.
A.S. Dennis and E.T. Pierce (1964), The Return Stroke of the Lightning Flash to Earth as a Source of V.L.F. Atmospherics, Radio Sci. 68D 777-794.
R.R. Arnold and E.T. Pierce (1964), Leader and Junction Processes in the Lightning Discharge as a Source of V.L.F. Atmospherics, Radio Sci. 68D, 771-776.
M. Csanos and E.T. Pierce (1972), A Ground Lightning Environment for Engineering Usage, Stanford Research Institute Report: Project 1834.
E.T. Pierce (1977), Atmospherics and Radio Noise, Chap. 10 of Lightning (Ed. R.H. Golde), Academic Press.
- SECTION 4.1**
R. Prinz (1977), A Description of the Lightning Discharge using Four Parameters (in German), Bull. SEV/VSE 68, 600-603.
G.H. Price and E.T. Pierce (1977), The Modelling of Channel Current in the Lightning Return Stroke, Radio Sci. 12, 381-388.
B.F.J. Schonland (1956), The Lightning Discharge, in Encycl. of Physics, Vol. 22, pp 576-628 (Springer-Verlag, Berlin).
K. Berger (1977), The Earth Flash, Chap. 5 of Lightning (Ed. R.H. Golde), Academic Press.
- SECTION 4.2**
R.H. Golde (1973), Lightning Protection (Arnold: London).
C.L. Thomas (1974) in Software for Numerical Mathematics (Ed. D.J. Evans) pp 315-36 (Academic Press, London).
P.F. Little (1978), Transmission Line Representation of a Lightning Return Stroke, J. Phys. D. 11, 1893-1910.
- SECTION 4.4**
R.D. Hill (1971), Channel Heating in Return Stroke Lightning, J. Geophys. Res. 76, 537.
P.F. Little (1979), The Effects of Altitude on Lightning Hazards to Aircraft, 15th European Conference on Lightning Protection, Uppsala.
- D.F. Strave (1979), Non-Linear Modelling of Lightning Return Strokes, FAA-FTT Workshop on Grounding and Lightning Technology, Melbourne pp 9-15.
S.I. Braginski (1958), Theory of the Development of a Spark Channel, Soviet Phys. JETP 7 1068-1074.
- SECTION 4.6**
R.B. Anderson (1971), The Lightning Discharge (Part 1), Ph.D Thesis CSIR, Special Report, ELEK 12.
- SECTION 5.2**
D.G. Kim, G.A. Dubro, L.T. Tessler and R.L. Boggess (1977), IEE International Symp. EMC, Seattle, pp 215-222.
- SECTION 5.3**
M.A. Uman, D.K. McLain, R.J. Fisher and E.P. Krider (1973).
(1) Electric Field Intensity of the Lightning Return Stroke.
(2) Currents in Florida Lightning Return Strokes, J. Geophys. Res. 78, 3523-3529 and 3530-3537.
K. Berger, R.B. Anderson and M. Kroninger (1975), Parameters of Lightning Flashes, Electra - CIGRE 41, 23-47.
M.A. Uman, R.D. Brantley, Y.T. Lin, J.A. Tiller, E.P. Krider, D.K. McLain (1975), Correlated Electric and Magnetic Fields from Lightning Return Strokes, J. Geophys. Res. 80, 373-376.
E.T. Pierce (1975), Natural Lightning Parameters and their Simulation in Laboratory Tests, Lightning and Static Electricity Conference (1975), Culham, UK.
M.A. Uman, D.K. McLain and E.P. Krider (1975), The Electromagnetic Radiation from a Finite Array, Amer. J. Phys. 43, 33-38.
D.M. Le Vine and R. Meneghini (1978), Simulation of Radiation from Lightning Strokes: the Effects of Tortuosity, Radio Sci. 13, 801-809.
G.W. Oetzel and E.T. Pierce (1969), Radio Emission from Close Lightning, in Planetary Electrodynamics, Ed. S.C. Coroniti.
F. Horner (1964), Radio Noise from Thunderstorms, Advances in Radio Research, (J.A. Saxton, Ed) 2, 121-204, Academic Press.
R.A. Perala, K. Lee and R. Cook (1979), Induced Effects of Lightning on an All-Composite Aircraft, Proc. IEEE Internat. Symp. EMP, Rotterdam, Holland.
E.P. Krider, C.D. Weidman and R.C. Noggle (1977), The Electric Fields Produced by Lightning Stepped Leaders, J. Geophys. Res. 82, 951-960.
R.H. Golde (1977a), The Lightning Conductor, Chap. 17, Lightning (Ed. R.H. Golde) Academic Press, London.
D.K. McLain and M.A. Uman (1971), Exact Expression and Moment Approximation for the Electric Field Intensity of the Lightning Return Stroke, J. Geophys. Res. 81, 2101-2105.
- SECTION 6**
R.G. Fowler (1974), Non-Linear Electron Acoustic Waves, Part I: Adv. Electronics Electr. Phys. 35, 1-86.
R.G. Fowler (1976), Non-Linear Electron Acoustic Waves, Part II: Adv. Electronics Electr. Phys. 41, 1-72.
B.F.J. Schonland (1958), Proc. Roy. Soc. Lond. A164, 132.
R.H. Wagner (1966), Studies of Electron Avalanche Development in Plasma Breakdown with an Image Converter. (In German). Z. Phys. 189, 465-575.

LIGHTNING TEST CRITERIA FOR AIRCRAFT AVIONICS SYSTEMS

Don W. Clifford
McDonnell Aircraft Company

SUMMARY

Lightning testing of aerospace systems and avionics equipment is governed by various test specification documents in the United States and in Europe. A new generation of criteria documents has been developed in the last few years, each of which attempts to set forth test criteria in terms of the various current and voltage waveforms to be used in lightning tests. The simulation waveforms are based upon statistical summaries of the natural lightning environment. Modern test criteria documents account for the dynamic nature of the lightning interaction with aircraft by using the zonal concept to more accurately identify the threat to specific systems and equipment. Test techniques can affect simulated lightning test results and the modern criteria documents include recommended practices for achieving accurate and consistent results.

The evolutionary history of the new criteria is presented, along with a summary of the salient features and the rationale for selection of the parameters specified in the modern documents. Some predictions of future evolutionary changes in the criteria documents are made on the basis of information about the lightning threat based upon recent measurements of natural lightning.

INTRODUCTION

Laboratory simulation tests have been used for many years to evaluate the effects of lightning strikes to aircraft systems and equipment. However, because of the complexity of lightning phenomena and the difficulty of the simulation task, there needs to be generally accepted and standardized criteria for conducting such tests. Standardized criteria help to ensure the highest reasonable level of accuracy in testing and also serve to produce consistent test results among different test facilities.

Significant efforts have been underway in NATO countries during the past several years to standardize lightning testing by generating accepted test criteria documents. The purpose of this lecture is to identify and describe the various test criteria which have been established, and to discuss the rationale used in their selection. The discussion focuses upon the selection of test waveforms and the associated lightning/aircraft interaction criteria which determine their application. Specific test techniques will be addressed in a separate lecture, as will detailed discussions of the natural environment.

Background and History

Until recent years the only governing criterion for lightning tests in the U.S. was Military Specification MIL-B-5087B¹, except in a very few cases where criteria documents were written to govern the testing of specific systems or components. For example, FAA Advisory Circular AC 20-53² (which superseded AC 25-3A) and Military Specifications MIL-F-38363B³ and MIL-C-38373⁴ concern the protection and testing of aircraft fuel systems against lightning. Also, MIL-A-9094D⁵ specifies strenuous simulation tests of lightning arrestors which are to be used with radio receiving and transmitting antenna systems. MIL-STD-461A⁶ and MIL-STD-462⁷ identify general electromagnetic interference design and test requirements. However, the only specification document governing the design and testing of lightning protection for aircraft and other military systems in general was MIL-B-5087B.

MIL-B-5087B concerns electrical bonding and lightning protection for aerospace systems. Paragraph 3.3.4, entitled "Class L bonding (lightning protection) (except for antenna systems)" addresses the lightning protection and testing requirement. It is quoted in its entirety below. (Based on Amendment 2 dated 31 August 1970).

"Lightning protection shall be provided at all possible points of lightning entry into the aircraft and shall be proven by test.

- | | |
|-----------------------|---|
| (a) Navigation lights | (f) Antennas (see 6.3.1) |
| (b) Fuel filler caps | (g) Radomes |
| (c) Fuel gage covers | (h) Canopies |
| (d) Refueling booms | (i) Pitot-static booms |
| (e) Fuel vents | (j) Wiring not protected by metal or body structure |

The following bonding requirements are designed to achieve protection against lightning discharge current carried between the extremities of an airborne vehicle without risk of damaging flight controls or producing sparking or voltages within the vehicle in excess of 500 volts. These requirements are based upon a lightning current waveform of 200,000 amperes peak, a width of 5 to 10 microseconds at the 90-percent point, not less than 20 microseconds width at the 50-percent point, and a rate of rise of at least 100,000 amperes per microsecond. When flight safety is not a factor, 100,000 amperes peak with a rate-of-rise of 50,000 amperes per microsecond may be used at the discretion of the procuring activity."

Other paragraphs in MIL-B-5087B deal briefly with lightning protection design considerations, but the paragraph quoted above has been the sole governing criterion for lightning testing of aerospace systems, other than the specifications for particular subsystems mentioned earlier.

The "A" version, MIL-B-5087A, dated 30 July 1954, specified a basic peak current of 100,000 amperes, but the value was raised to 200,000 when the "B" version was released in 1964. It is interesting to note that the peak current values used in this specification were not based on the measured values of natural lightning which were available at the time the specification was written. Rather, the values were based upon the damage observed on aircraft struck by lightning and the laboratory test currents which were necessary to reproduce the damage.⁸ The 200,000 ampere value has carried over to the modern criteria documents and is now seen to be at the 99 percentile level (one percent of all strikes are higher than 200,000 amps).

The Need for New Criteria

As aircraft technology expanded during the 60's and early 70's, pressure mounted within the industry to develop more adequate criteria for lightning protection and verification. Expanded research efforts, which were prompted by new technologies such as advanced composite materials and computerized flight control systems, led to improved testing techniques and to a better understanding of many of the lightning/aircraft interaction processes. It was soon realized that peak current is only one factor in the production of physical damage. The energy dissipated is also a major factor and is represented by the "action integral". The value of the integral over time of the current squared ($\int i^2 dt$) represents the potential energy of the current pulse. In addition, other aspects of the lightning current flow such as the continuing current and intermediate currents were shown to be very significant in the design and protection of some systems. It was later recognized that the actual threat from lightning is different for different regions of the aircraft and that fact also needed to be accounted for.

The actual waveform specified by MIL-B-5087B is virtually impossible to produce experimentally in any realistic test object. A test waveform constructed from the information specified is shown in Figure 1. The fast rise to peak coupled with the slow decay and the unipolar requirement are all difficult to simulate. A criteria document was needed which spelled out reasonable test waveforms and criteria for applying them. In addition, testing techniques needed to be standardized because widely varying test results were being reported from different laboratories.

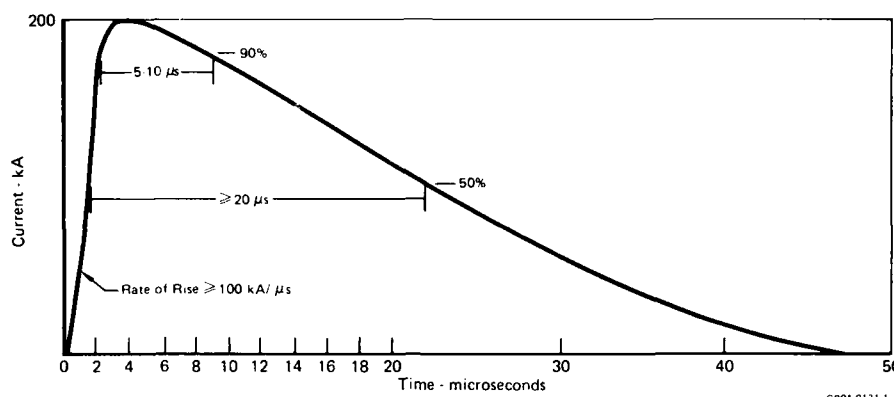


FIGURE 1
HIGH CURRENT WAVEFORM SPECIFIED BY MIL-B-5087B

In regards to the protection and testing of avionics equipment, the adage of "keep the current on the outside of the aircraft and all will be well" no longer generated much confidence. The "500 volt maximum" criterion specified by "5087" is not generally acceptable for modern solid state equipment, and the questionable shielding qualities of new materials does not ensure that even the 500 volt limit will be realized on all circuits. In fact, the need for full scale vehicle tests was being expressed as the potential problems related to induced or indirect coupling were realized.

The Development of New Criteria Documents

In 1972, a committee of government and industry workers was formed in the U.S. under the aegis of the SAE Committee AE-4 to draft a new lightning test criteria document. Soon after, lightning specialists at Culham Laboratory in the U.K. were commissioned to develop a similar document for Great Britain. Cooperation between the SAE committee and the British team led to the development of two separate, but generally consistent test documents. Growing out of the U.S. and British work, a NATO Standardization Agreement (STANAG) was proposed in 1978 and is now being circulated among member countries for review and comment. Similarly, a new U.S. Military Standard based upon the NATO document is also in the review process.

The proposed NATO STANAG and U.S. Military Standard address only those lightning tests which simulate the better understood and non-controversial aspects of the lightning environment. The tests in these documents are considered to be Qualification or Demonstration tests, as opposed to Engineering or R&D tests. The SAE and U.K. documents address not only the Qualification tests, but also other lightning simulation techniques which are not as standardized, but which still provide valuable engineering information.

Within the U.S. there have been other criteria documents developed over the same time period, independent of the SAE effort, which address a specific program or system. Two of these are noteworthy because they attempt to carry the specification criteria further than the other documents mentioned. The NASA Space Shuttle Criteria document⁹ attempts to specify or define interpretive guidelines for evaluating electrical transients on internal wiring systems. "Transient Control Levels" are defined which establish margins of safety based upon the degree of analysis and test performed. The Air Force MX missile program has accounted for the most recent measurements of fast rising lightning current waveforms in their criteria document¹⁰ and has specified a 200-nanosecond, 100,000-ampere first return stroke current pulse for the design and testing of the MX missile.

Other than the specific differences mentioned above, the criteria documents which have been developed for specific programs are generally very similar to the four general documents mentioned earlier. Therefore, the remainder of this lecture will be concerned with the development and description of the four related criteria documents. These four documents are further identified as:

1. NATO Draft STANAG 3659AE dated 20 August 1978, Subject: Lightning Qualification Test Techniques for Aircraft and Hardware
2. Proposed U.S. Military Standard MIL-STD-XXXX, "Lightning Qualification Test Techniques for Aerospace Vehicles and Hardware"
3. J. Phillpott, "Recommended Practice for Lightning Simulation and Testing Techniques for Aircraft", UKAEA Report CLM-R163, 1977
4. "Lightning Test Waveforms and Techniques for Aerospace Vehicles and Hardware", report of SAE Committee AF4L, June 1978

NATURAL LIGHTNING PARAMETERS

The selection of lightning test criteria for aerospace systems must be based upon three factors: a) our best understanding of the natural lightning environment as it impacts the operation of systems, b) the physics of its interaction with aerospace systems, and c) the limitations and capabilities of laboratory equipment used to simulate the interaction processes. Each of these factors is very complex and difficult to fully understand and characterize. Yet the importance of the problem requires that attempts be made to standardize testing at the highest level of simulation which is economically reasonable.

A large number of measurements of natural lightning parameters have been made and reported in the literature. However, in establishing the values of parameters to be used in lightning testing, it is desirable to consider a statistical summary of all the various parameters which might impact aircraft operation. In recognition of this need, a most helpful summary and analysis of measured lightning parameters was published in 1972 by Cianos and Pierce. Their report, entitled "A Ground-Lightning Environment for Engineering Usage"¹¹ presents statistical summaries of all the major return stroke parameters such as peak current, charge transfer, rate of rise and restrike values. Examples of their statistical summaries are shown in Figure 2 for peak currents, continuing current charge transfer, rates of rise, and decay time to half value. As an end result of their summary, Cianos and Pierce proposed the severe negative lightning flash current waveform shown in Figure 3. The Cianos and Pierce report summarized published measurements of cloud-to-

ground return stroke current pulses which have been assumed as the principal threat to aerospace systems operation. Table 1 summarizes the parameters of the Cianos and Pierce severe current waveform.

Another important source of information on the natural environment is Uman's book "Lightning",¹² and Golde's recent two volume work by the same name.¹³ Table 2 reproduced from Uman's book summarizes many of the important lightning parameters besides return stroke current and their range of values. These books and others in the literature provide the aerospace community with reasonably up-to-date knowledge of all aspects of the lightning environment which may be of concern to the operation of airborne equipment.

Since the publication of the referenced summaries, much new information has been developed which is of particular interest to the operation of avionics equipment. Measurements of submicrosecond risetime current pulses,¹⁴ high frequency emanations from inter-cloud precursor events¹⁵ and stepped leader activity¹⁶ indicate that these sources of electromagnetic activity may well excite significant transients in sensitive aircraft avionics systems. However, such data are still scarce and much additional work is required to establish statistical distributions of parameters such as frequency spectra, amplitude and energy content before any standardized test criteria can be established. Therefore, lightning test criteria are seen to be in a state of change, particularly as far as the factors affecting electromagnetic coupling to avionics systems are concerned. Despite this consideration, however, the well established return stroke current threat and the precursor voltages are still an important factor in the design and operation of avionics components and equipment. These threats are the ones which will be addressed in the remainder of this paper.

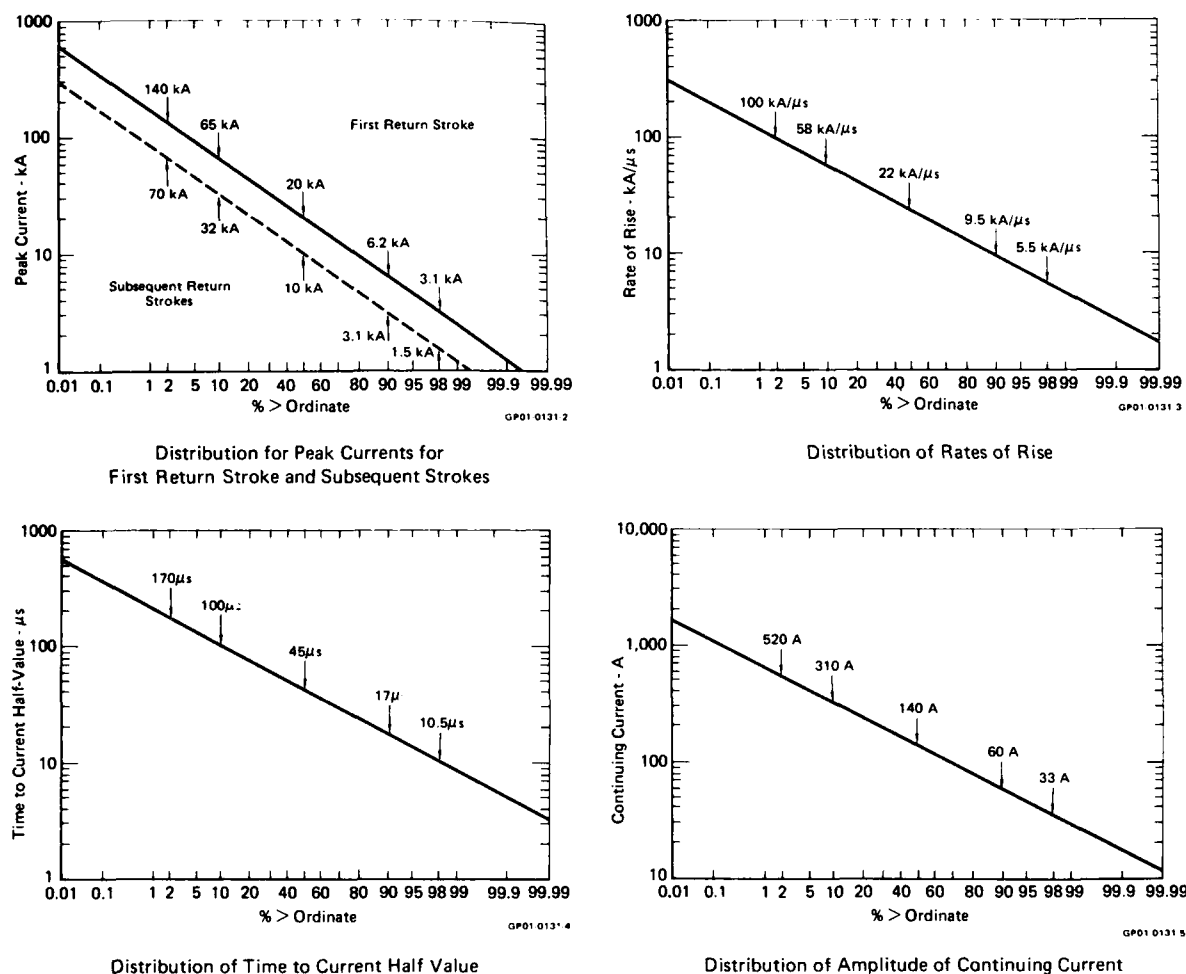


FIGURE 2
STATISTICAL SUMMARIES OF RETURN STROKE PARAMETERS - FROM REF (11)

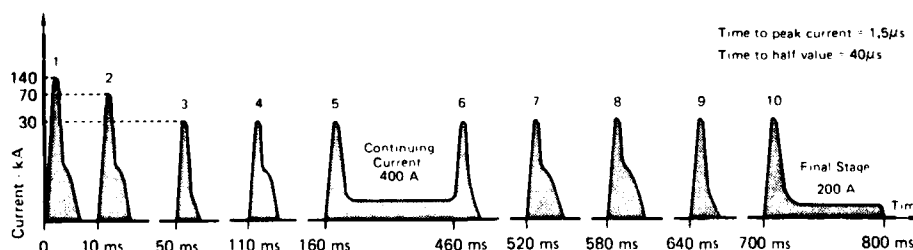


FIGURE 3
TIME HISTORY OF SEVERE (BASIC) LIGHTNING MODEL - FROM REF (11)

TABLE 1
SEVERE-LIGHTNING-MODEL PARAMETERS (BASIC MODEL) - FROM REF (11)

Stroke Order	Peak Current (kA)	Charge (C)	Time Between Strokes (ms)	Model Current, I_0 (kA)	Intermediate Current Model		Continuing Current
					I_i (kA)	Charge (C)	
1	140	~8		144	4	4	Continuing Current [†]
2	70	~4	10	72	4	4	
3	30	~2	60	31	0	0	
4	30	~2	60	31	4	4	
5	30	~2	60	31	0	0	
6	30	~2	300	31	0	0	
7	30	~2	60	31	4	4	
8	30	~2	60	31	4	4	
9	30	~2	60	31	0	0	
10	30	~2	60	31	0	0	Final Stage ^{§§}

Totals: Charge transferred = 200 C
Duration = 0.9 s
Action integral = 10^6 A²-s

GP01 0131 6

† Continuing current = 400 A, duration = 300 ms, charge transfer = 120 C
§ Final-stage continuing current = 200 A, duration = 160 ms, charge transfer = 32 C.

TABLE 2
DATA FOR A NORMAL CLOUD-TO-GROUND LIGHTNING DISCHARGE
BRINGING NEGATIVE CHARGE TO EARTH*

	Minimum**	Representative	Maximum**
Stepped Leader			
Length of Step, m	3	50	200
Time Interval Between Steps, μ s	30	50	125
Average Velocity of Propagation of Stepped Leader, m/s†	1.0×10^5	1.5×10^5	2.6×10^6
Charge Deposited on Stepped-Leader Channel, Coul	3	5	20
Dart Leader			
Velocity of Propagation, m/s†	1.0×10^6	2.0×10^6	2.1×10^7
Charge Deposited on Dart-Leader Channel, Coul	0.2	1	6
Return Stroke			
Velocity of propagation, m/s†	2.0×10^7	5.0×10^7	1.4×10^8
Current Rate of Increase, kA/ μ s [‡]	< 1	10	> 80
Time to Peak Current, μ s §	< 1	2	30
Peak Current, kA §		10-20	110
Time to Half of Peak Current, μ s	10	40	250
Charge Transferred Excluding Continuing Current, Coul	0.2	2.5	20
Channel Length, km	2	5	14
Lightning Flash			
Number of Strokes per Flash	1	3-4	26
Time Interval Between Strokes in Absence of Continuing Current, ms	3	50	100
Time Duration of Flash, sec	10^{-2}	0.2	2†
Charge Transferred Including Continuing Current, Coul	3	25	90

* From Uman, Ref 12

GP01 0131 12

** The words maximum and minimum are used in the sense that most measured values fall between these limits.

† Velocities of propagation are generally determined from photographic data and thus represent "two-dimensional" velocities. Since many lightning flashes are not vertical, values stated are probably slight underestimates of actual values.

First return strokes have slower average velocities of propagation, slower current rates of increase, longer times to current peak, and generally larger charge transfer than subsequent return strokes in a flash.

§ Current measurements are made at the ground.

¶ A lightning flash lasting 15 to 20 sec has been reported by Goddington (1896).

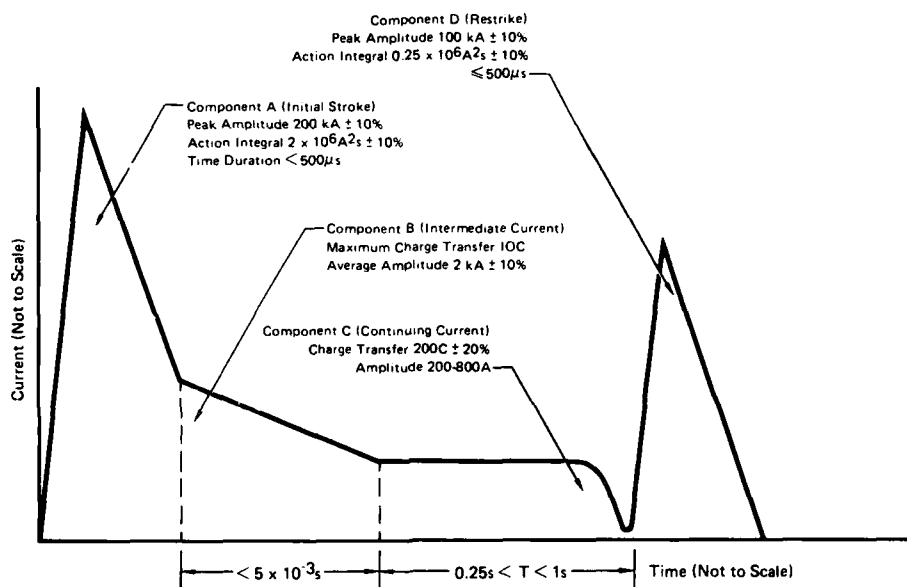
TEST WAVEFORMS

Return Stroke Current Simulation

If the severe lightning current waveform proposed by Cianos and Pierce and shown in Figure 3 represents accurately the critical lightning threat to aircraft avionics systems, then the question of how best to simulate that threat in practical terms must be answered. Is it necessary to faithfully reproduce every detail of the waveform including each individual current pulse with the specified time intervals and duration? Or, can the important features of the threat be summarized in a simple waveform which could be more readily used in design analysis and test planning?

For testing purposes, it is immediately obvious that complete natural lightning flashes cannot be duplicated in the laboratory; particularly the rapid sequence of many high current pulses. However, most of the characteristics of an individual lightning current pulse can be duplicated by laboratory generators. Therefore, as a result of the complex nature of natural lightning discharges and the limitations of laboratory facilities, it is necessary to define an equivalent lightning waveform for test purposes that contains the major destructive features of natural lightning.

For airworthiness purposes, a four component severe model waveform has been agreed upon as a waveform which will give direct damage effects equivalent to those produced by the most severe natural lightning. The idealized (straight line) waveform is shown schematically in Figure 4. The waveform comprises four components designated as Current Components A, B, C and D. The waveform parameters for each component are listed in the figure.



GP01 0131 B

FIGURE 4
IDEALIZED CURRENT WAVEFORM COMPONENT FOR QUALIFICATION TESTS

The following comments may help to clarify some of the rationale for stating that this waveform is equivalent for damage testing to the multiple component waveform in Figure 3. First of all, note that Figure 4 is not a test waveform. It is a straight-line schematic representation or idealization which may help to visualize the relative character of the various components. It is not drawn to scale either in amplitude or in time. Rather, it is the component parameter values called out in the figure which govern the actual design and testing.

Note that Component A, representing the initial return stroke current pulse, has a magnitude of 200 kA. This value is in keeping with the traditional severe threat level used in the U.S. for many years. By itself, it represents the 99 percentile level of peak current amplitudes, as opposed to the 140 kA, 98 percentile level chosen by Cianos and Pierce. However, it is rationalized that by selecting the 200 kA level, the multiple restrikes at levels below 70 kA can be ignored and need not be included in the simulation.

One high peak current restrike is included in the model waveform because many times the mechanisms of interaction of lightning with the aircraft will result in exposure of some portions of aircraft to subsequent strokes, but not to initial strokes. The intent is not to require both initial and restrike components in the same discharge for all cases. As with the other components of the model waveform, the restrike is of importance primarily to structural and fuel systems.

The concern for avionics systems from the current components in Figure 3 is in the possible damage to externally-mounted electrical hardware, and in the introduction of lightning currents via electrical wiring directly into the avionics equipment. In addition, for avionics system concerns, induced electromagnetic transient effects related to the return stroke current waveform can be produced by resistive voltage drops along the length of the current flow path and by magnetic flux linkage generated by fast changing current pulses. Therefore, the peak current values associated with Current Components A and D can produce indirect effects without getting directly onto internal wiring. The magnetic coupling effects are proportional to the rate of change of current, di/dt , a parameter which is not specified in the model waveform of Figure 4.

Induced (Indirect) Coupling Test Criteria

An additional test criterion has been developed for magnetic coupling effects. Rather than specify rate-of-rise or time-to-peak on the model waveform, a severe rate-of-rise threat of $100 \text{ kA}/\mu\text{sec}$ has been established for indirect effects testing. This value is shown as the 98 percentile level in the statistical distributions of Cianos and Pierce. As discussed in Reference 14, however, the Cianos and Pierce summary is based on average rates of rise which may be 3 to 10 times lower than the maximum rate which occurs during the fast transition portion of the pulse.

For testing purposes, it is recognized that very fast rising current pulses cannot be produced at the peak current threat levels in most test articles of interest because of the electrical impedance of the test articles and the limited driving voltages produced by laboratory generators. In order to overcome this difficulty, the linearity of the magnetic coupling phenomenon is employed to allow testing to be conducted at reduced peak currents and rates of current rise. Measured transients can then be extrapolated to the full 100 kA/ μ sec threat.

An auxiliary fast rate-of-rise current waveform has been defined in the four criteria documents mentioned earlier for induced (indirect) effects qualification testing of electrical components. The waveform and its derivative are shown in Figure 5 with the parameter values of interest. Note that this waveform is an actual waveform for test purposes. The amplitude of 50 kA was selected because it is within the capabilities of most lightning test laboratories when testing small electrical components, and it requires only a factor of 4 extrapolation. The U.K. criteria document specifies a 100 kA peak, presumably because the Culham facility is able to produce that level in the range of test article impedances which they anticipate.

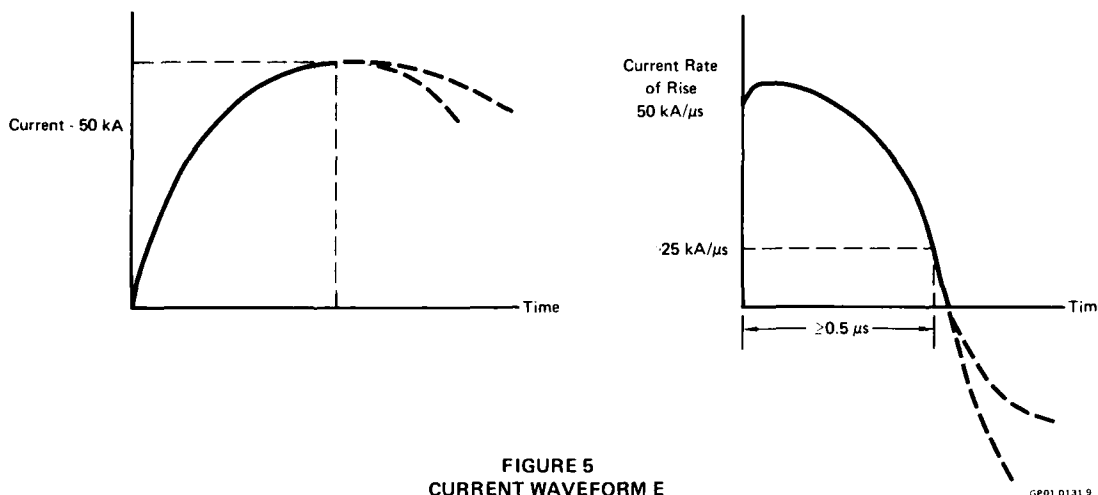


FIGURE 5
CURRENT WAVEFORM E

Current Waveform E is defined with a minimum rate-of-rise requirement of 25 kA/ μ sec, and that minimum rate must persist for at least 0.5 μ sec. The minimum duration is specified because of the response time of both the test instrumentation and the equipment under test. The induced voltages produced by this waveform must be extrapolated to threat level by multiplying the peak induced voltage by the ratio of 100 kA/ μ sec to the actual rate-of-rise measured on the test waveform. Note that current waveform E is a minimum waveform. Test facilities are encouraged to test with a waveform as close to the actual threat waveform as possible. However, in order to limit the range of extrapolation, the minimum values of peak current and rate-of-rise are established.

Some test facilities may be able to meet the minimum requirements of Current Waveform E with the same generator used to produce Current Components A and D described earlier. Therefore, provisions are made in the criteria documents to allow induced effects to be measured during the direct effects test if the minimum rate-of-rise criterion is met.

Full Scale Vehicle Testing

Current Waveform E is specified for qualification level testing of components. Recognizing the need to conduct ground tests on full scale operational aircraft, an attempt has been made in the S.A.E. and U.K. documents to define waveforms which can be used for engineering evaluations. It is realized that the large electrical impedance of full scale aircraft will prevent fast rising high peak current pulses from being used. It is also realized that there are many complexities to full scale vehicle testing which are not present at the component level. However, with the rapid introduction of flight critical avionics equipment into new technology fighter aircraft, there is a pressing need to conduct whatever reasonable test is possible.

Consequently, two optional approaches have been defined in the U.S. SAE document for engineering evaluation purposes. The first approach employs a double exponential (unipolar) $2 \times 50 \mu$ sec current pulse with a minimum amplitude of 250 amps. This waveform is designated as Current Waveform F and is shown in Figure 6. This waveform is passed through the aircraft structure and the resulting transients produced on internal wiring systems of interest are simultaneously measured. This $2 \times 50 \mu$ sec waveform is a miniature version of Current Components A and D. In this case, the measured transients may be extrapolated on the basis of peak current only, as long as the time-to-peak is held constant.

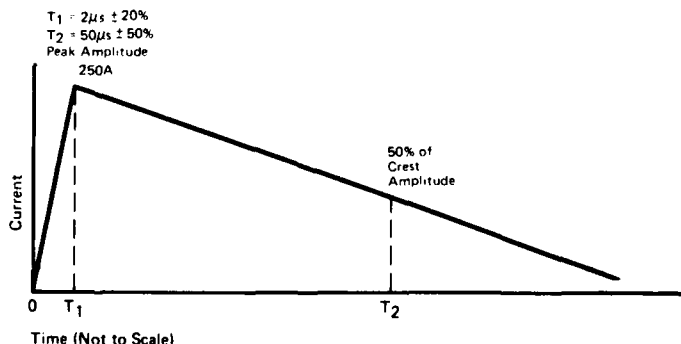


FIGURE 6
CURRENT WAVEFORM F

The second approach employs a pair of damped oscillatory waveforms designated Current Waveforms G_1 and G_2 (Figure 7). Waveform G_1 is a low frequency waveform for assessing diffusion flux effects and G_2 is a high frequency waveform for evaluating aperture coupled effects. Extrapolation of measured induced transients is again necessary with the basis for extrapolation being peak current in the case of G_1 and rate-of-rise in the case of G_2 .

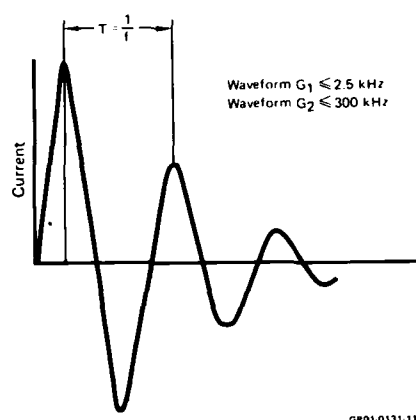


FIGURE 7
CURRENT WAVEFORMS G_1 AND G_2

The U.K. document does not define specific waveforms for full vehicle tests but only recommends that minimum current amplitudes of 4 kA and minimum rates-of-rise of 2 kA/ μ sec be observed.

Because of the uncertainties which are present in full scale vehicle tests, they are not included in the proposed NATO STANAG or the U.S. Military specification documents.

Voltage Waveform Simulation - Qualification Tests

As illustrated by the Cianos and Pierce statistical summary, the current waveforms associated with lightning return strokes have been studied extensively and are therefore fairly well characterized. However, it is apparent from observations of aircraft damage that the high voltages associated with lightning are also capable of producing significant effects on aircraft. The high fields experienced at the aircraft as the stepped leader approaches give rise to corona and streamering activity which are the basis for establishing lightning attachment points on the aircraft, flashover vs punch-through or rupture of dielectric surfaces, and possible ignition of fuel vapors.

Unfortunately, the precursor voltages and fields of lightning are not well characterized at all. In fact, little is known beyond the kind of information summarized in Table 2. Therefore, it is difficult to specify voltage waveform criteria which can be rigorously defended on the basis of natural lightning measurements. At the same time, it is obvious that the voltage effects must be accounted for in the design and testing of aircraft systems.

Of particular concern to the avionics engineer is the knowledge of whether lightning will attach to electrical components on the aircraft and how dielectric materials such as radomes or light covers will withstand puncture and subsequent damage.

In specific instances such as these, it is possible to approach the voltage waveform definition problem from the standpoint of test conservatism and the knowledge of how systems will respond to different waveform parameters. In particular, for qualification testing of electrical components incorporating dielectric materials, it is known that fast-rising voltages stress the dielectric more than slow rising pulses. Therefore, to ensure a conservative, or worst-case test, a very fast rising voltage pulse can be specified. This approach has been taken in all of the subject criteria documents.

The Voltage Waveform A, shown in Figure 8, is specified for testing full scale hardware. It is only identified by the 1000 kV/ μ sec rate of rise. No peak voltage or decay time is specified because the ramp will terminate itself when flashover or puncture occurs. To ensure that the arc closes before the peak is reached, either the air gap between the test object and the high voltage electrode, or the peak voltage can be adjusted. A 1 meter gap is recommended, which would require around 0.7-1.0 megavolt peak voltage to ensure arc closure on the wavefront. Whether or not lightning fields as seen on the aircraft will change as fast as 1000 kV/ μ sec is not at issue. It is thought to be unlikely, however, that they will change much faster than that.

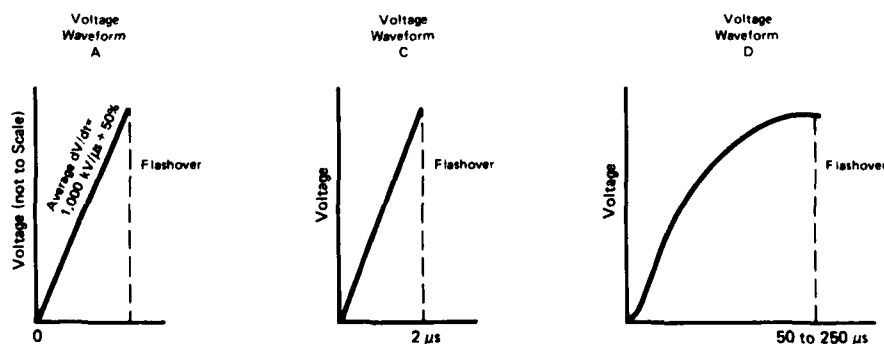


FIGURE 8
IDEALIZED HIGH VOLTAGE WAVEFORMS

Voltage waveform A is also specified for full-scale hardware attachment tests where it is desired to learn where lightning may attach to the detail geometry of a part. This test application is not universally accepted, however, because it is known that slow rising voltage waveforms will produce a wider range of attachment points than will fast rising pulses. Therefore, the U.K. document recommends a 200 x 2000 long-front wave for attachment testing.

Scale Model Attach Point Testing - Engineering Test

Long spark testing of aircraft models is used to determine probable lightning attachment points on aircraft. As mentioned earlier, the characteristics of natural lightning voltages and field changes have not been measured. However, the parameters of the test voltage waveform can have a significant effect on the results of the test. Figure 9 illustrates how fast and slow fronted voltage waves might produce different attachment patterns on a model aircraft.

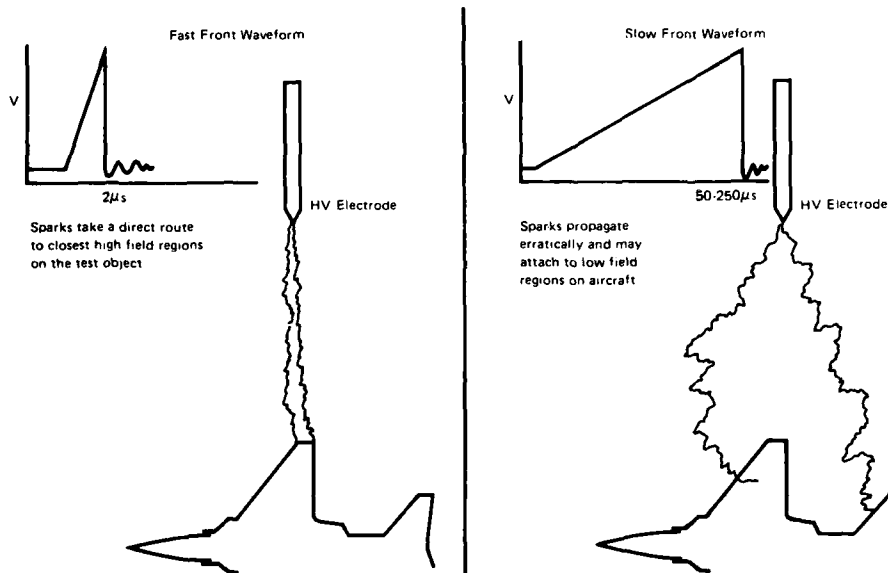


FIGURE 9
VOLTAGE WAVEFORM EFFECTS ON ATTACHMENT BEHAVIOR

GP01 0131 14

In the full-scale hardware dielectric punchthrough/flashover test, the test waveform was set to give the worst case results, thus ensuring a conservative test. This approach has also been recommended for model attach point testing, and for this reason, the U.K. document recommends a 200 x 2000 μ sec slow front waveform for model testing. However, the U.S. SAE document has selected a fast-fronted wave as the primary waveform because the observed test results using fast waves appear to agree better with in-flight experience. A slow front waveform is also included as an optional approach if very conservative results are desired. These two test waveforms are shown in Figure 8 as Voltage Waveforms C and D. (Voltage Waveform B is used for fuel ignition tests and is not addressed here).

Because of the waveform uncertainties and other factors (such as questions about the validity of scaling the attachment process) the model attach point test is not included in the NATO STANAG nor in the U.S. Mil standard documents. The test is for engineering information and is not a final verification. It is therefore included in the Engineering Test section of the SAE document.

LIGHTNING/AIRCRAFT INTERACTION

Swept Stroke Phenomenon

In most cases the question of how lightning interacts with the aircraft is the subject of, and the reason for, laboratory tests. However, there are some a priori effects which should be taken into consideration before defining the tests to be conducted on specific pieces of equipment. The most important of these considerations is what is referred to as the "Swept Stroke" phenomenon.

During the return stroke phase of a lightning strike to an aircraft in flight, the lightning channel is effectively stationary in space with the aircraft becoming locally part of the channel. However, due to its forward speed, the aircraft moves relative to the stationary channel during the duration of the strike. When lightning attaches initially to a forward extremity such as a nose or wing mounted engine pod, the aircraft moves through the lightning channel. Thus with respect to the aircraft the lightning channel is swept back over the surface, as illustrated in Figure 10.

The basic mechanism of arc sweeping, is shown in Figure 11. The arc first attaches to point A and then as a result of the movement of the aircraft, the arc distends along the surface until the configuration shown in Figure 11 is produced. There is then a possibility of a re-attachment to the surface at point B if the voltage across the gap BC is sufficient to break down the air gap and any insulating coating on the surface. The dwell time at any one point is therefore a complex function, of the local geometry, nature of the surface, the current waveform and the speed of the aircraft. Consequently, the attachment point may dwell at various surface locations for differing periods of time thus resulting in a skipping action across the surface of the aircraft. The other initial attachment point often occurs to a trailing edge and therefore carries the full current associated with the flash.

The amount of damage produced at any point in a swept stroke region is related to the type of material, the arc dwell time at that point and the waveform of the lightning current. Both high peak current restrikes with intermediate current components and continuing currents may be experienced. Restrikes typically produce re-attachment of the arc at a new point because:

- a) the magnitude of the voltage across gap BC is large due to the large inductive voltage developed by the restrike current buildup, and
- b) if the flash is discontinuous for a brief period a new (dart) leader will travel along the previous channel since it will still be hot. Consequently, a high electric stress can be produced at the aircraft surface. The resulting voltage could be higher than the inductive voltage produced by the changing current and consequently puncture of non-metallic surfaces or dielectric coating is more likely to occur.

When the lightning arc has been swept back to a trailing edge it may remain attached at that point for the remaining duration of the flash. If an initial attachment point occurs at a trailing edge then of course that particular attachment point cannot sweep.

The significance of the swept stroke phenomena is that portions of the aircraft that would not be targets for the initial attachment of a lightning flash may nevertheless be involved in the lightning flash process as a result of the rearward sweeping action. Under these circumstances it should be noted that except at trailing edges it is unlikely that the total energy associated with the flash will flow into one point. For this reason it is convenient to divide the aircraft surface into zones for damage and assessment purposes. The following zonal definitions have been incorporated into each of the modern criteria documents.

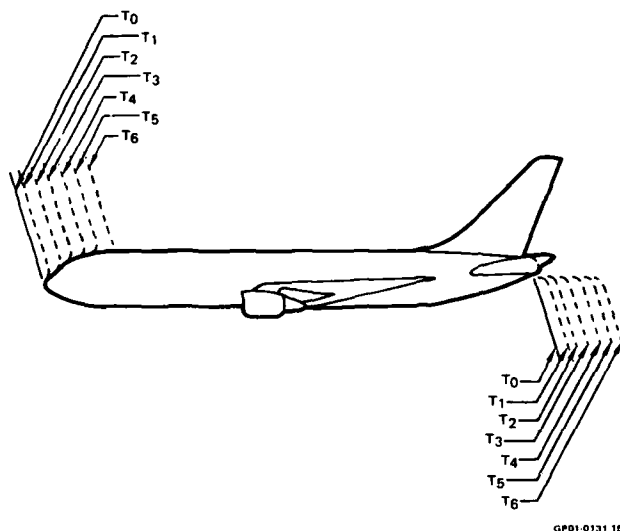


FIGURE 10
AIRCRAFT AERODYNAMIC INTERACTION WITH LIGHTNING CHANNEL

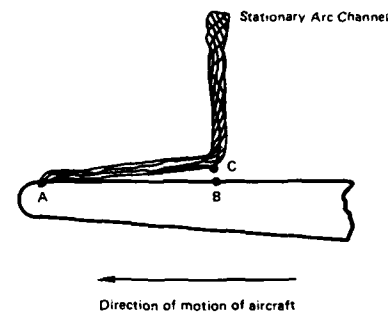


FIGURE 11
MECHANISM OF SWEEPED STROKE ACTION

Lightning Attachment Zones

Aerospace vehicle surfaces are divided into three zones, with each zone having different lightning attachment and/or transfer characteristics. These are defined as follows:

ZONE 1: Surfaces of the vehicle for which there is a high probability of initial lightning flash attachment.

ZONE 2: Surfaces of the vehicle across which there is a high probability of a lightning flash being swept by the airflow from a Zone 1 point of initial flash attachment.

ZONE 3: Zone 3 includes all of the vehicle areas other than those covered by Zone 1 and Zone 2 regions. In Zone 3 there is a low probability of any direct attachment of the lightning flash arc. Zone 3 areas may carry substantial amounts of electric current, but only by conduction between some pair of initial or swept stroke attachment points.

Zones 1 and 2 are further divided into A and B regions depending on the probability that the flash will hang on for any protracted period of time. An A type region is one in which there is low probability that the arc will remain attached and a B type region is one in which there is a high probability that the arc will remain attached. Examples of zones are as follows:

ZONE 1A: Initial attachment point with low probability of flash hang-on, such as a leading edge.

ZONE 1B: Initial attachment point with high probability of flash hang-on such as a trailing edge.

ZONE 2A: A swept stroke zone with low probability of flash hang-on, such as a wing mid-span.

ZONE 2B: A swept stroke zone with high probability of flash hang-on such as a wing inboard trailing edge."

Note that the above definitions define each zone, but do not provide dimensions or other description of where the zones are located on particular aircraft. Establishment of the zone locations is therefore the first step in design of protection for a new aircraft. The first step in this determination is to establish the initial strike points (Zone 1) on the aircraft. This determination is usually accomplished by conducting a long spark attachment test on a scale model of the aircraft.

Once the forward Zone 1 locations are identified, the Zone 2 and 3 regions are established by definition. Figure 12 shown the various zones on a commercial jet aircraft.

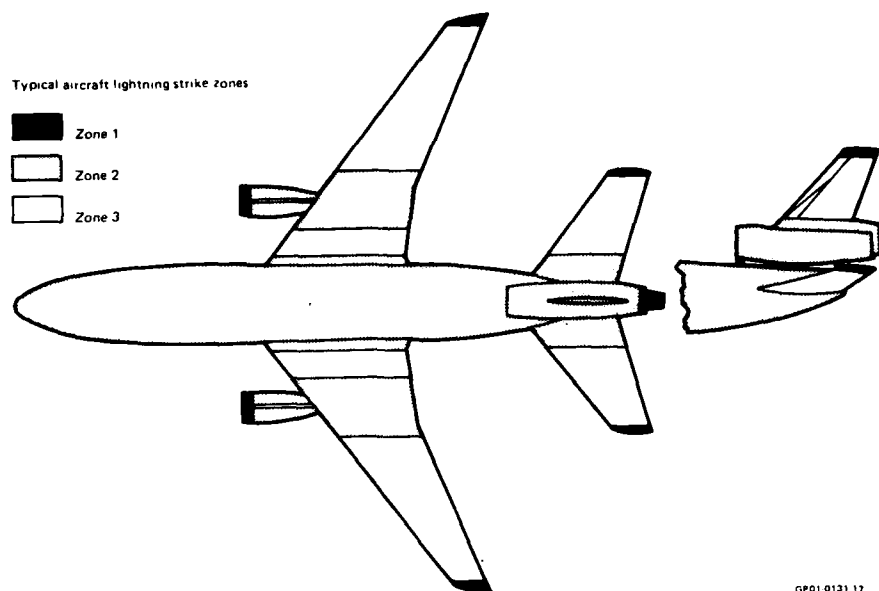


FIGURE 12
SWEEP STROKE ZONES ON A LARGE AIRCRAFT

APPLICATION OF WAVEFORMS

In the earlier section of this paper, the natural lightning threat was established and criteria were defined for simulating the lightning current and voltage waveforms. In addition, aircraft zones were defined which now allow the local threat at different points on the aircraft to also be defined. That is, the proper test waveforms to be applied to any specific piece of externally mounted electrical equipment, depending upon its location on the aircraft, can be specified.

The application of waveforms is defined and summarized in Table 3. The type of test is identified in the first column, the total location of the equipment to be tested is listed in Column 2, and the test waveform to be used is indicated in the appropriate waveform column. Table 3 has been adapted from the criteria documents and has been tailored to exclude those tests which do not directly relate to avionics or electrical systems tests.

The table identifies the current components that can flow through an aircraft structure or component in each zone. There may be some cases, however, where not all of the components specified in the table will contribute significantly to the failure of the part. Therefore, in principle, the non-contributing component(s) can be omitted from the test. If components are to be omitted from a test because they are deemed to be non-contributory, the proposed test revision should be agreed upon with the cognizant regulatory authority.

The test matrix in Table 3 makes it clear that not every waveform and test described in the new criteria documents should be applied to every system requiring verification tests. The documents are written so that the specific aspects of the environment can be called out for each specific program as dictated by the vehicle design, performance, and mission constraints. The decision of which systems or equipment should be tested is left to the cognizant regulatory authority or contracting agency. So is the determination of pass/fail criteria. The criteria documents seek to give guidance only on how equipment is to be tested after it has been determined that it shall be tested.

TABLE 3
APPLICATION OF TEST WAVEFORMS FOR AVIONICS TESTS

Test	Zone	Voltage Waveform	Current Waveform
Damage Effects, Structural (Direct Effects)	1A		A, B
	1B		A, B, C, D
	2A		B, C, D
	2B		B, C, D
	3		A, C
Induced Effects, External Electrical Hardware			E*
Full-Size Hardware Attach Point Test	1A	A	
	1B	A	
Induced Effects, Complete Vehicle Test	N/A		F or
	N/A		G1, G2
Model Aircraft Attach (Fast) Point Test (Slow)	N/A	C	
	N/A	D	

* Note: Induced effects should also be measured with current components A, B, C, and D as appropriate to test zone

Test Techniques

In addition to the proper definition of test waveforms and locations where they are to be applied, the techniques of testing can also affect test results. For this reason, test techniques are defined in criteria documents to the extent necessary to ensure reliable and consistent test results. Where it has been shown that test conditions can affect results of the test, a specific approach is recommended as a guideline to new laboratories and for consistency of results between laboratories. The test techniques are kept as general as possible to allow for improved, innovative techniques and to cover as many test situations as possible.

The modern criteria documents attempt to address the test techniques appropriate to each type of test identified. The technique criteria specify test object configuration, test waveforms to be applied, the physical arrangement of current carrying conductors, test electrode configuration, spacing between electrode and test object, measurement requirements, instrumentation, and in some cases, techniques for making measurements. In a few cases, where it is felt to be important, specific test arrangements and procedures are spelled out and specified in some detail.

It is not the intention of this lecture to discuss the details of the test technique criteria. That information will be discussed in a subsequent lecture in this series. It is emphasized, however, that test technique is an important factor in obtaining accurate and meaningful test results.

FUTURE DEVELOPMENTS

It was mentioned earlier that there is much that is not known about the natural lightning environment and there are many uncertainties regarding the response of aircraft and other aerospace systems to the total lightning environment. New information is being obtained through continued research of natural lightning by the academic community. In addition, both the U.S. Air Force and NASA are initiating in-flight measurement programs aimed at characterizing the fields and voltages associated with lightning at flight altitudes.

Some data are already available indicating that aircraft electrical systems may respond to high-frequency components of radiated fields as well as to direct strike current pulses. Laboratory experiments indicate that the natural electrical resonances of aircraft can be excited by voltage and E-field changes associated with nearby lightning and by pre-return stroke events during a direct strike. For example, the attachment of the stepped leader to the aircraft and the passage of a dart leader preceding a restrike can both cause rapid changes in charge density on the aircraft. These rapid changes result in changing internal fields and subsequent induced transients on wiring systems and avionics equipment.

Recent measurements of return stroke currents indicate that submicrosecond rise times are typical. The 100 kA/ μ sec rate of rise used in the criteria documents may therefore represent a typical strike rather than a worst case condition. If rise times on the order of 200 nanoseconds are considered, then the response of a full-scale vehicle will include high-frequency oscillatory ringing because the resonances of the aircraft will then be excited.

Most observers agree that the total lightning environment must be considered in determining the threat to avionics systems performance. However, it is still too early to establish standardized criteria for specifying the high-frequency components of lightning and for defining techniques for systems testing. However, considerable research and development is now underway in both areas, and it is reasonable to expect that future modifications or additions to the criteria documents will be made in these areas within a few years.

The SAE AE-4L committee is now engaged in an attempt to define test waveforms for evaluating internal avionics equipment directly. The proposed document will specify a family of damped sinusoidal waveforms which would be representative of transient signals induced on aircraft wiring by lightning striking the vehicle. The intention is to provide the system designer with a standard set of waveforms which he can choose from to specify to his avionics suppliers. His choice will be determined by the anticipated shielding or attenuation provided by the airframe balanced against the cost of hardening the avionics equipment. Although this work is still in the early stages, it illustrates the desire of government and industry to address the problem at the earliest opportunity. Such efforts as this will eventually impact the formulation of criteria for evaluating the impact of the total lightning environment on avionics systems.

SUMMARY

This paper has attempted to summarize the criteria which have been established for lightning simulation testing. The discussion has concentrated on working from the natural lightning threat to the definition of simulation test waveforms, both for current and for voltage. Aerodynamic interaction of the aircraft with the lightning arc channel leads to definitions of zones on aircraft from which the localized threat at specific locations on the aircraft can be deduced. These considerations led to a test matrix which defines the test waveforms to be used in evaluating any particular piece of externally mounted electrical or electronic equipment on the aircraft as a function of its position or location on the aircraft surface.

For internal equipment, full-scale vehicle tests have been defined as engineering evaluation tests. These tests for induced transient levels require extrapolation of measured transients to predict actual threat level values. The full vehicle tests are still in the developmental stage and may be modified as more information is obtained about the high voltage and high frequency aspects of lightning and about the way large systems respond to various laboratory excitation sources. It is generally agreed that the new criteria documents which have been developed over the past few years represent a major improvement over the previously existing guidelines. Yet, because of the importance of new technology avionics equipment and new information about the lightning environment, it is anticipated that many changes are to come in future years. Much work remains to be done and workers in this field are encouraged to be alert for opportunities to understand and to minimize the lightning hazard to future generation aircraft.

REFERENCES

- 1 Military Specification MIL-B-5087B, "Bonding, Electrical, and Lightning Protection for Aerospace Systems" (6 February 1968).
- 2 FAA Advisory Circular No. 20-53, "Protection of Aircraft Fuel Systems Against Lightning" (October 1967).
- 3 Military Specification MIL-F-38363B (USAF), "Fuel System, Aircraft, Design, Performance, Installation, Testing and Data Requirements."
- 4 Military Specification MIL-C-38373, "Cap, Fluid Tank Filler."
- 5 Military Specification MIL-A-9094D, "Arrestor, Lightning, General Specification for" (17 March 1969).
- 6 Military Standard MIL-STD-461A, "Electromagnetic Interference Characteristics Requirements for Equipment, Subsystem and System" (9 February 1971).
- 7 Military Standard MIL-STD-462, "Electromagnetic Interference Characteristic, Measurement of" (31 July 1967).
- 8 Personal Communication with Mr. John Robb of Lightning Transients Research Institute (6 November 1979).
- 9 "Space Shuttle Program Lightning Protection Criteria Document," NASA Report No. JSC-07630, Revision A (4 December 1975).
- 10 "MX Missile Direct Strike Lightning Study," Martin Marietta Corp. Internal Report (December 1979).
- 11 N. Cianos and E.T. Pierce, "A Ground-Lightning Environment for Engineering Usage," SRI Technical Report No. 1, prepared for McDonnell Douglas Corp (August 1972).
- 12 M.A. Uman, "Lightning," McGraw Hill, New York (1969).
- 13 R.H. Golde (editor), "Lightning" Volumes 1 and 2, Academic Press, London, New York (1977).
- 14 D.W. Clifford, E.P. Krider, and M.A. Uman, "A Case for Submicrosecond Rise Time Lightning Current Pulses for Use in Aircraft Induced-Coupling Studies," presented at the 1979 IEEE International Symposium on EMC, San Diego, California (9-11 October 1979).
- 15 C.D. Weidman and E.P. Krider, "The Radiation Field Waveforms Produced by Intracloud Lightning Discharge Processes," Journal of Geophysical Research, 84 (C6), 3159-3164, 1979.
- 16 E.P. Krider, C.D. Weidman, and R.C. Noggle, "The Electric Fields Produced by Lightning-Stepped Leaders," Journal of Geophysical Research, Vol 82, No. 6 (6 February 1977) pp. 951-959.
- 17 USA Standard C68.1/IEEE Standard No. 4, "Standard Techniques for Dielectric Tests" (1979) paragraphs 2.4 and 2.6.
- 18 High-Voltage Test Techniques, IEC 60-2 (1973) Sections 4 and 6.

LIGHTNING TESTING FOR AIRCRAFT AVIONICS SYSTEMS

Don W. Clifford
McDonnell Aircraft Company
St. Louis, Missouri

SUMMARY

Laboratory tests can be used to evaluate the performance of electrical components and complete avionics systems in aircraft exposed to lightning. Direct damage tests can be conducted on externally-mounted electrical hardware such as lights, probes and antennas by applying high-current or high-voltage arcs representative of natural lightning directly to a representative component. Externally-mounted equipment is tested in this manner both to evaluate the extent of damage to the component and to determine if high transient voltages or currents are produced on internal wiring attached to the component. These tests are standardized in criteria documents and are categorized as Qualification Tests.

Tests of avionics equipment located internal to the aircraft are not well defined nor standardized. Problems exist in defining the actual threat to the equipment, taking into account the complex response of the total aircraft to lightning excitation. An accurate definition of the transient signals appearing on avionics systems wiring must be based upon analyses or tests of the electrical response of the total aircraft to lightning excitation, the degree of airframe shielding, and coupling of external fields onto internal wiring.

Despite the lack of good definition, tests of complete vehicles or large full-scale structures can be conducted to assist in determining the total avionics system responses to lightning. The high electrical impedance associated with complete aircraft precludes full threat currents from being passed through the vehicle. Present test techniques therefore use low-level current pulses through the structure to develop engineering information about the transient signals induced on internal wiring. Since these tests are not well developed yet they are categorized as "Engineering Tests."

This paper will describe the test techniques used to evaluate lightning effects on avionics equipment. The facilities necessary to produce the current and voltage waveforms specified in the criteria documents will be briefly described as will the sensors and instrumentation used to measure and record the test data. Where test setup details can affect test results, the preferred techniques will be described. Newly developed techniques for full vehicle tests will be discussed briefly as they may impact the next generation of criteria documents.

INTRODUCTION

Laboratory tests can be used to evaluate the performance of aircraft exposed to lightning. The test equipment and techniques employed specifically for tests of aircraft avionics equipment and systems are the subject of this paper. Test waveforms and application criteria are defined in recently published documents which are discussed in a companion lecture in this series. The mechanisms of electronic failures, either damage or momentary disruption, while of interest in determining the susceptibility of avionics equipment to lightning-produced transients, is outside the scope of this paper. The test techniques described herein are based solely upon considerations of natural lightning currents and voltages and the secondary fields produced internally by circulating currents on the surface of the aircraft.

Direct and Indirect Lightning Effects

The lightning effects to which aerospace vehicles are exposed and the effects which are reproduced through laboratory testing with simulated lightning waveforms are divided into "Direct Effects" and "Indirect Effects." The direct effects of lightning are the burning, eroding, blasting, and structural deformation caused by lightning arc attachment, as well as the high-pressure shock waves and magnetic forces produced by the associated high currents. The indirect effects are predominately those resulting from the interaction of the electromagnetic fields accompanying lightning, with electrical apparatus in the aircraft. Hazardous indirect effects could in principle be produced by a lightning flash that did not directly contact the aircraft and hence was not capable of producing the direct effects of burning and blasting. However, most indirect effects of importance will be associated with a lightning flash to the aircraft. In some cases both direct and indirect effects may occur to the same component of the aircraft. An example would be a lightning flash to an antenna which physically damages the antenna and also couples damaging voltages into the transmitter or receiver connected to that antenna. In this document, the physical damage to the antenna will be discussed as a direct effect and the voltages or currents coupled from the antenna into the communications equipment will be treated as an indirect effect.

Qualification Versus Engineering Tests

Two categories of lightning tests have been defined in modern US criteria documents. Qualification Tests are intended for final demonstration or verification purposes. The natural lightning waveforms and the interaction mechanisms relevant to these tests are believed to be understood adequately to standardize the test waveforms and testing methods. Qualification Tests include high-voltage and high-current physical damage tests of fuel, structural and electrical hardware as well as indirect effects associated with lightning strikes to externally-mounted electrical hardware. Engineering Tests are tests designed to provide engineering information for design purposes rather than for final demonstration purposes. Engineering Tests usually involve mechanisms or waveform parameters which are not as well defined as those for Qualification Tests, or for which widespread agreement cannot be reached. The principal engineering tests which are applicable to avionics systems are the model attach point test and full-scale vehicle indirect effects tests. A third engineering test which will not be described is the swept stroke test which is used to determine arc attachment behavior over inboard surfaces. For the purpose of this paper, it is assumed that any electrical hardware located in an inboard region will be tested for direct and indirect effects in accordance with the guidelines given in the discussion of Qualification Tests. Swept stroke tests could conceivably be conducted to determine the arc hang-on time for a protruding electrical component, but no such tests have been previously reported.

The tests categorized as Qualification Tests are included in a proposed NATO Standardization Agreement, Draft STANAG 3659AF, entitled "Lightning Qualification Test Techniques for Aircraft and Hardware," dated 20 August 1978.¹ The STANAG includes brief descriptions of recommended testing techniques for the tests covered in the document. In addition, recent criteria documents published in the US² and in the UK³ include descriptions of testing techniques for both Qualification and Engineering Tests. This paper will seek to enlarge upon those descriptions and will preface the discussion of testing techniques with a description of the general laboratory facilities and equipment used to simulate lightning effects. The paper will conclude with a brief discussion of work which is underway to develop testing methodology for evaluating electronic equipments located within aircraft to determine their susceptibility to lightning-induced waveforms.

LIGHTNING SIMULATION TECHNIQUES

The laboratory equipment used to simulate lightning effects naturally involves high-voltage and high-energy electrical discharge technology. Of these two technologies, the high-voltage laboratory techniques are well developed and documented. Numerous textbooks are available to the experimenter as well as a large body of published literature related mostly to electrical utility research and development. On the other hand, high-energy electrical discharge technology has mostly been developed over the past 30 years, and most of that work has not been published in the open literature. Much of it is related to nuclear oriented R&D, either weapons related (simulating transient phenomena) or fusion energy related, where very heavy electrical discharges are required to produce the high temperatures necessary to achieve thermonuclear reactions. Capacitor banks storing tens of megajoules of energy have been constructed for fusion energy research.

The voltage and current required for lightning effects testing are modest in relation to those associated with the equipment just referred to. However, the techniques required to accurately produce the waveforms and to accurately simulate and measure the wide variety of lightning effects of interest to aircraft designers are not trivial. Current pulses with magnitudes up to 200,000 amperes (98 percentile first return stroke) are not too difficult to produce, given the energy storage capacitors. However, the challenge of accurately simulating all of the waveform parameters of realistic lightning return stroke current waveforms is so great as to be unmet. Even a straightforward $2 \times 50 \mu\text{sec}$ current waveform (which roughly resembles a return stroke pulse) is possible only at low-current levels in most laboratories. However, a worst case first return stroke current waveform actually includes an exponentially increasing front with a rapid transition over the last 100 to 140 kiloamperes occurring in 200 nanoseconds or less.^{4,5} The rapid front of the wave is followed by a slow decay which involves a very respectable action integral (i^2t) of over $10^6 \text{ amp}^2\text{-seconds}$. The production of such a waveform, particularly through a sizable test article, may be possible. However, the cost and complexity of the required facilities are generally considered to be both prohibitive and unnecessary.

The key to an economically feasible lightning simulation program is to simulate the important effects of lightning, rather than attempting to reproduce the lightning itself. Although the effects may be many, and although they are almost certainly interrelated (to some degree synergistic), for engineering purposes they can generally be separated and simulated independently. This fact has been recognized in the formulation of recommended test waveforms in the modern criteria documents.

High Voltage Simulation

Conventional high-voltage impulse generators are used for generating high electric fields and long arcs for the purposes of determining arc attachment points on models or on full-sized aircraft components. These generators are also used for evaluating materials and components for punch-through or flashover characteristics. The voltage level and waveforms required for testing are dependent upon the type of test and the size of the test object.

The impulse generators used for transient high-voltage tests are usually Marx-surge generators which are described in high-voltage textbooks.^{6,7} These generators are fairly simple to build if the only objective is to produce a fixed waveshape pulse. Several generators of this type have been built and are in operation at lightning simulation laboratories in the U.S. and Europe. Output voltages of at least several hundred kV are necessary for long spark testing. Larger machines ranging up to 5 mV can be built economically for fixed waveform testing. A few generators are available with outputs up to 10 mV with both wave front and tail shaping capability. These generators are available at specialized high voltage facilities such as the General Electric High-Voltage Laboratory in the U.S. and similar laboratories in Europe.

Figure 1 is a typical schematic representation of a Marx system. These generators produce high voltage by charging a number of "stages" of relatively low-level capacitors (up to 100 kV per stage) in parallel and then discharging them in series through a spark gap switching arrangement. The voltage pulse produced at the output has a rise time determined essentially by the resistance and capacitance of the output and external circuit, and a decay time determined by the RC time constant of the stack capacitance and any resistance to ground. Figure 2 is a waveform showing the output of a machine with a very fast rise to peak, a slow decay as the stack capacitance decays back through the charging resistors, and then the fast drop as the air gap is closed by a long spark, dropping the total circuit resistance from thousands of ohms to tens of ohms or less. Figure 3 is a photograph of a 4.2 mV Marx generator used in aircraft testing.

Very high-voltage DC rectifier sets are used in specialized applications such as corona streamer tests on dielectric materials or high static-field generation. Moderately high-voltage DC power supplies (up to 100 kV) are used as the charging supplies for capacitor banks and Marx generators. These power supplies are very low current supplies so cannot be used for damage effects tests.

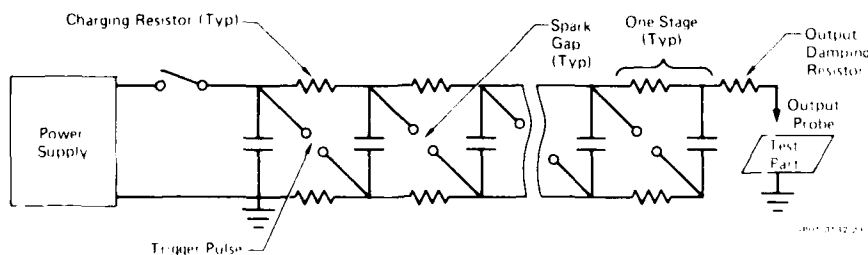


FIGURE 1
BASIC MARX SURGE GENERATOR CIRCUIT (n STAGES)

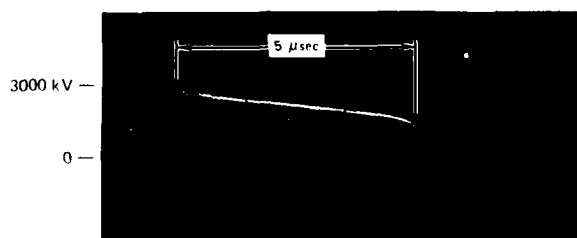


FIGURE 2
TYPICAL 3000 kV HIGH-VOLTAGE OUTPUT WAVE FORM PRODUCED BY 4.2mV GENERATOR

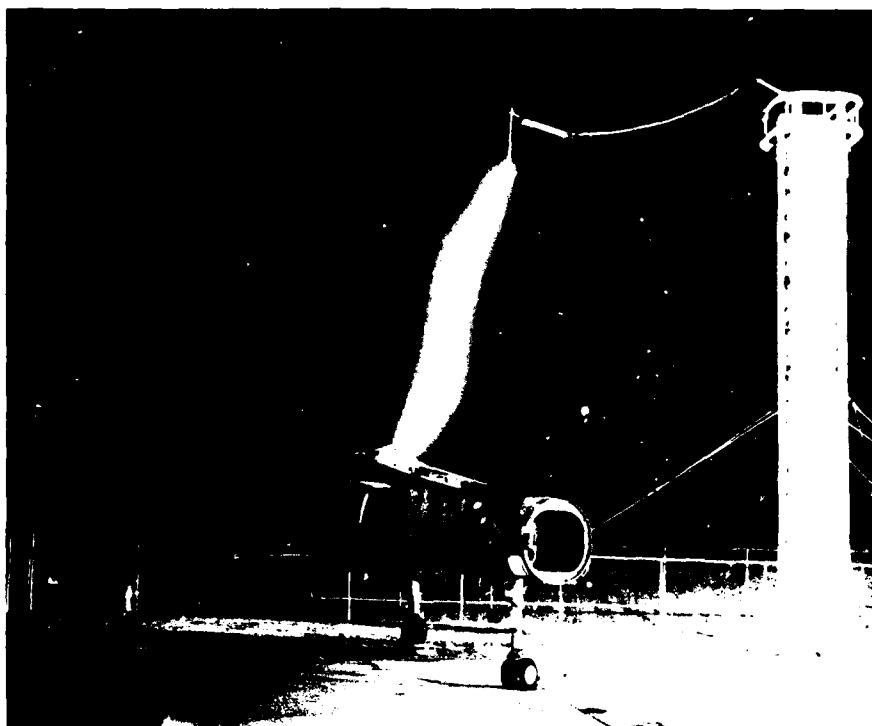


FIGURE 3
4.2 Mv TEST OF FULL SCALE AIRCRAFT TEST ARTICLE

High-Peak Current Simulation

High-current simulation is conducted separately from long spark tests, because the voltage required to break down a large gap (10^6 volts) is so high that the power necessary to generate up to 200,000 amps in the arc quickly exceeds the bounds of feasibility.

The proposed STANAG high-current waveform is presented in Figure 4. Notice that the current covers three orders of magnitude and the time scale encompasses nearly five orders of magnitude. The very high-current portions of these waveforms are generally simulated by discharging energy storage capacitors into the test sample. Large capacitor banks can be constructed easily to produce high-energy, high-current discharges in very short arcs, but, as mentioned earlier, some complexity is involved if a reasonable simulation of the actual lightning current waveform is required.

The discharge from a capacitor bank can be represented by an equivalent LRC circuit, as shown in Figure 5, and standard electrical theory can be used to predict the circuit current. The capacitance in the circuit is dominated by the capacitors; the inductance of the circuit is the combined internal inductance of the capacitors plus the external circuit; and the resistance is the combined effect of internal capacitor resistance and external circuit resistance, which includes that of the test sample. The resistance, and especially the inductance, of the test setup are often difficult to control because they are distributed quantities which are dependent upon the size and configuration of the test object.

Upon discharge, the generator simply behaves like an LRC circuit in which a capacitor is discharged through a resistor and an inductor by a switch closure. The output current waveform is then given by

$$I(t) = \frac{V}{\omega L} e^{\left[-\frac{R(t)t}{2L} \right]} \sin \omega t$$

where V is the charging voltage, ω is the resonant frequency of the circuit given by

$$\omega = \left[\frac{n}{LC_s} \frac{R^2(t)}{4L^2} \right]^{1/2}$$

$R(t)$ and L are, respectively, the bulk circuit resistance and inductance, while C_s is the capacitance of only one generator stage. The circuit inductance is principally a result of the pulse generator's internal inductance and for all practical test purposes it is unalterable. This inductance limits the rise time of the generator and the resulting discharge is generally much too slow to obtain the model waveform's specified value of current rate of rise of 100 kA μ sec.

Depending on the resistive damping, the circuit may resonate (underdamped case) or the current may be critically damped or overdamped. The underdamped case is commonly used by many laboratories to obtain the high-peak current components of the lightning waveform because it can be done easily with a minimum of equipment. However, the underdamped case is less desirable for it is difficult to control the energy in the discharge waveshape. The total discharge energy is the sum of the energy deposited during each half cycle of the oscillatory current and is carefully specified in the model waveform. If the generator has sufficient energy and output voltage, it can utilize resistive damping to eliminate oscillations, control the current and pulse width and still achieve the full peak amplitude. The single polarity pulse thus produced is more representative of a natural discharge than an oscillatory pulse. Tests have shown that a unipolar discharge often constitutes a more strenuous test condition than does an oscillatory discharge of equal peak amplitude and energy content.⁸

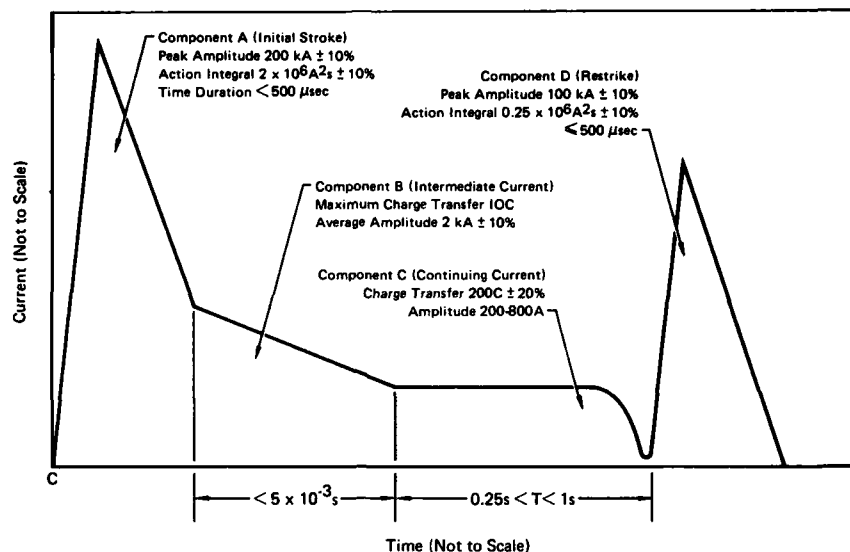


FIGURE 4
IDEALIZED CURRENT WAVEFORM COMPONENTS FOR QUALIFICATION TESTS

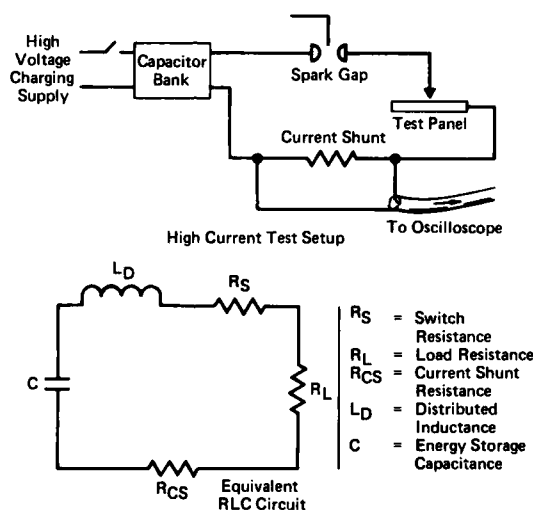


FIGURE 5
HIGH CURRENT TEST SETUP AND EQUIVALENT CIRCUIT

Inductive energy storage is used in the UK (Culham Lab) based on technology developed in their fusion energy program.⁹ The advantage of the inductive storage technique is that the large inductor acts like a fixed current generator, and in this respect is more comparable to natural lightning than a capacitor bank. In addition, less capacitance is needed to generate the action integral specified in the criteria documents. However, the inductors are large and expensive to manufacture: they must be custom built, and the associated magnetic fields are very intense, possibly requiring extra shielding of other laboratory equipment.

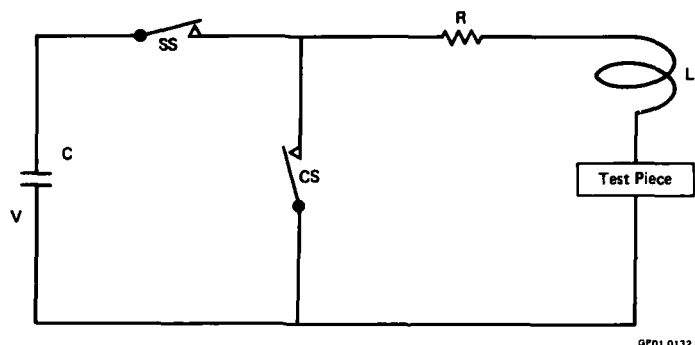
With peak currents up to 200 kA, it is both difficult and expensive to charge an inductor from conventional DC sources. To overcome this, capacitive storage can be used to charge the inductor. The simplest method of achieving this is to discharge the capacitor via the test piece into the inductor. At the first current peak, all the remaining energy is stored in the inductor, and this can be fed into the test piece by simply short circuiting the capacitor. (See Figures 6 and 7.)

This system of initial capacitance storage, discharged into inductive loads with a clamping or diverting switch, serves very well for simulation of the current component A (Figure 4) where the peak current, rise times and pulse duration permit the design of a generator having practical dimensions. The main limitation of this system, however, is the control of the rise time, which is a function of L and C. Where high charge transfers and medium currents are required (such as in current components B and C), both C and L need to be large; and this gives a very long rise time for current in the inductor. Faster rise times can be achieved by discharging the capacitor directly into the inductor, and discharging the inductor into the test piece after the transfer of stored energy from capacitor to inductor has been completed.

High-Charge Transfer Simulation

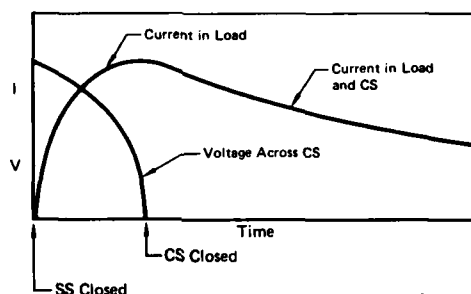
The continuing current type lightning stroke (lower level currents shown in Figure 4) has been simulated most readily by high-energy DC rectifiers or by batteries in a series-parallel combination. The STANAG specifies 200 amps for one second as a simulation requirement for fuel systems; 200-amp DC supplies are not difficult to obtain, but a complicating factor is the necessary driving voltage. Many test objects requiring high coulomb tests are resistive in nature and often even metallic materials are covered by good dielectric paints.

Consequently, the arc may extinguish or fail to strike if the sustaining voltage is too low. When resistance is a problem, or when larger arcs are needed, capacitor banks are often used because of the higher charge voltages. However, capacitor banks are limited in the total charge which can be stored. Inductive energy storage systems are particularly useful in this application.



GP01 0132 4

FIGURE 6
EQUIVALENT CIRCUIT FOR CLAMPED INDUCTOR DISCHARGE HIGH-CURRENT TEST



GP01 0132 5

FIGURE 7
CURRENT WAVEFORMS PRODUCED BY CLAMPED INDUCTOR DISCHARGE

INSTRUMENTATION

Diagnostics

The two basic measurements required in the lightning laboratory are current and voltage. Current measurements can be made by using either low inductance resistive shunts or magnetic probes, pickup coils, or Rogowski coils.

Shunts are most useful for the intermediate current and continuing current phases, where the di/dt is low, the duration relatively long, and the circuit can tolerate the shunt inductance. Sensitivities vary from 100 A or so to some tens of kiloamperes. Calibration is absolute; and the diagnostic is durable, consistent, and reliable. The shunt must be able to carry the $\int i^2 dt$ of the high current circuit, and it must be introduced at the ground point only. Care must be taken not to introduce ground loops.

Current transformers, Rogowski coils, and magnetic probes may be used for the higher peak value currents ($> 10^4$ A) and di/dt values (> 5 kA/ μ s). The Rogowski coils have the advantage of absolute calibration, but their high frequency performance is poor. These two sensors have no metallic connection with the high current circuit and, therefore, they do not require reference to ground. They are, however, more susceptible to high frequency pickup and hash originating from the very high peak current trigger pulses and other switching noises.

An extension of the Rogowski coil is the modern commercially available current transformers. These units have fair to good frequency response, depending on cost; they are well shielded against RF interference and they come in a variety of sizes for different applications. Balanced twin lead cables can again be used for connection to recording equipment.

Voltage measurements are usually accomplished by arrangement of capacitive or resistive voltage dividers. These measurements can be very difficult to accomplish with great accuracy and confidence if very high voltages with rapid rates of change are involved. This is especially true if the divider unit is exposed to radiated fields from the high voltage generator. Well-shielded cabling must again be employed. Compensated dividers are available commercially and construction techniques can be found in textbooks. 6,7

Alternatively, electric field sensors are inherently high frequency devices and can yield very accurate measurements of high-voltage waveforms. Accurate quantitative measurements of peak voltage levels are more difficult to make with field sensors because of uncertainties in field gradients generated by corona and streamering across the air gap containing the sensor.

In open arc work, photography can be employed to great advantage; either still or high-speed movies may be used as appropriate. Pressure sensors, thermocouples, infrared sensors, and other transducers have an important role to play for appropriate tests. However, with any electrical sensor, great care must be taken (because of the intense EM environment during generator discharge) to ensure that the recorded output signal is truly representative of the actual parameter to be measured.

Measurement Equipment and Techniques

Care must be taken in the arrangement of the diagnostic equipment used for induced coupling measurements. The physical circuit must be arranged to ensure that the diagnostic equipment is not influencing the system response. The discharge of laboratory generators produces intense electromagnetic fields over a wide range of frequencies. High-frequency RF energy from spark gap switches and rapidly changing electric fields accompany the magnetic fields produced by the high-peak current surges. This intense EM field environment will induce currents in any exposed electrical conductors, including exposed signal leads, building power lines, and measuring instruments. These spurious signals can easily mask the desired signal if care is not taken in the design and installation of the instrumentation system.

In addition to the problem of shielding the instrumentation system, the frequency response of the total measurement must be fast enough to detect the very sharp high-frequency transients which often occur at the instant the generator is triggered. For small component-sized test articles, system resonances and coupling modes other than magnetic or resistive are not under study. Therefore, the upper frequency limit requirement will be determined by the test waveform. For example, direct effects tests on external hardware may employ fairly slow current waveforms (10 to 20 μ sec to peak). On the other hand, indirect effects tests using Current Waveform E from the proposed STANAG will need to be able to see induced transients rising to peak in a tenth of a microsecond. Therefore, a bandwidth upper limit of at least 10 MHz should be used in those tests.

Where full-scale aircraft testing is involved, system resonances become very important. Therefore, instrumentation capabilities must be extended into the 30-MHz range, at least for small aircraft. Responses in the 100 MHz range may become viewed as important as more is learned about the coupling of lightning produced transients onto signal cables.

For component-level tests, the instrumentation may be installed in the same shielded enclosure on which the test object is mounted. Such installation requires adequate volume in the enclosure, as well as good ventilation for cooling and quick access for data retrieval. The advantages of this arrangement are that the measurement leads are short, and minimum additional effort is required in shielding of the instruments. A test of this type is illustrated in Figure 8.

In other instances, the instrumentation may be housed in a separate shielded room. The measured transient signals must then be transmitted to the shield room via signal leads of some type. In this case, precautions must be taken to ensure that spurious signals are not induced in the signal leads. The elimination of interference can be greatly facilitated by the use of balanced twin cables, in solid copper tubes. The copper tube must be kept directly against and in electrical contact with the high-current transmission line at its lowest field point, from the position of the diagnostic to the common ground point. Care must be taken, however, to ensure that long-shielded cable runs do not load down the signal, either in frequency or magnitude. Care must be taken in the design of impedance matching devices and other interface circuitry to ensure that the signal is not distorted or masked.

Other low-noise signal transmission techniques include the following:

- a. Double-shielded duplex cable and differential readout instrumentation to eliminate common mode voltages.
- b. Completely floating battery-powered instrumentation (elimination of ground loops and power line filtering).
- c. Fiber optics to isolate the readout instrumentation from both the electrical circuit under test and the transient generator (elimination of ground loops).
- d. Fiber optics and very short instrumentation cables to minimize loading effects on the test circuit.
- e. Isolation resistors at the voltage pick-off point to minimize the loading effects on the circuit under test.

Even after all these precautions have been taken, the elimination of noise in the measurement instrumentation system should be verified. This can be accomplished by delivering the test current to the shielded enclosure while monitoring the readout instrumentation with the leads disconnected from the electrical circuit under test. This should be done under two conditions:

- a. with the disconnected measurement leads open circuited, and
- b. with the disconnected measurement leads shorted.

Since fiber optic techniques are fairly new, the following paragraphs will describe their application in more detail.

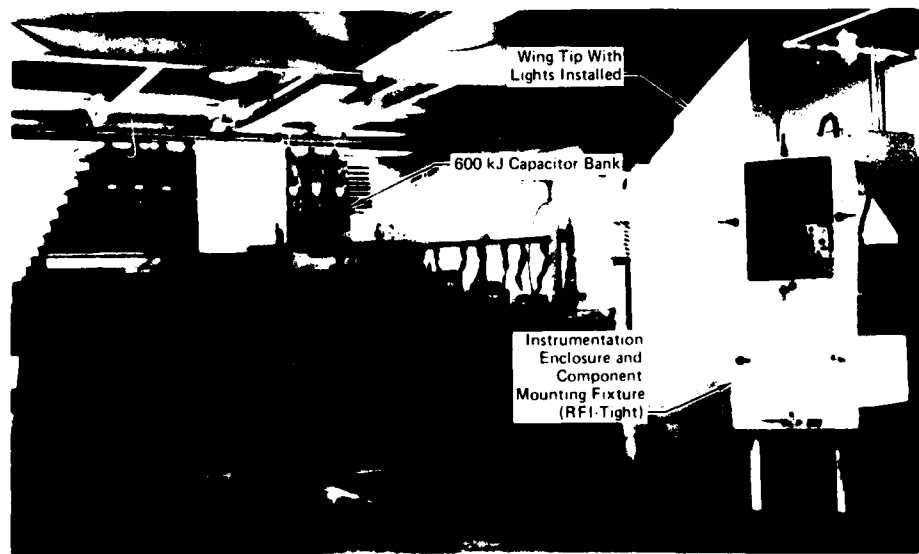
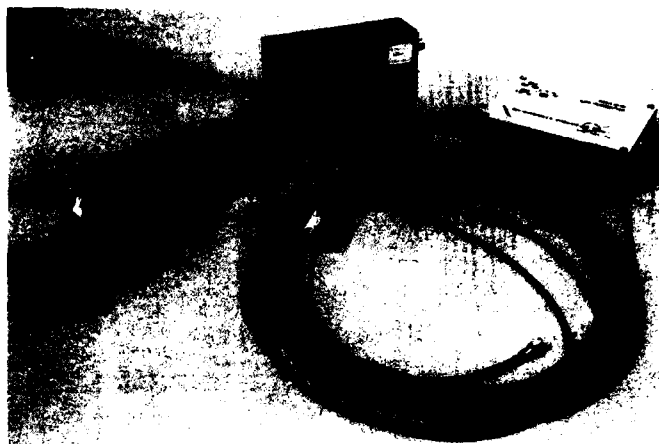


FIGURE 8
COMBINED DIRECT AND INDIRECT EFFECTS TEST SETUP FOR
EXTERNAL ELECTRICAL HARDWARE

Fiber Optic Data Links

An attractive alternative to multiply-shielded, carefully grounded signal cables has become available in the form of fiber optic data links. These units have the advantage of completely isolating the instrumentation from the test environment and eliminating the long signal leads which act as antennas to pick up unwanted fields produced by the generator upon discharge. The instrumentation can be enclosed in a shielded room with no cable penetration other than shielded filtered power lines. In addition, the data can be taken from a test article raised to very high voltages since there is no grounding of shields to worry about.

The disadvantages of fiber optics are disappearing as the technology matures. Good fidelity and linearity can be achieved in analog systems with bandwidths up to 100 MHz. A transmitter/converter receives the electrical signal, converts it to an optical encoding diode where it is transmitted as a modulated light signal via a light pipe to the instrumentation room. There it is reconverted to an electrical signal for display on an oscilloscope or for digital recording. A fiber optic data link set is shown in Figure 9.



GP01 0122 7

FIGURE 9
FIBER OPTIC DATA TRANSMITTER/RECEIVER SET

Recording and Data Processing

The recording of transient electrical signals is conventionally achieved by photographing oscilloscope traces with a Polaroid (or equivalent) camera. Most oscilloscopes designed for transient applications are equipped with face-mounted cameras. The photographs of the scope sweeps or traces have long constituted the final output data from the test.

The "scope camera" technique has disadvantages. Much time (and film) is often required to obtain the proper light levels and triggering. Many data events are missed as a result of improper triggering, wrong exposure settings, or failure to reload film in the camera. In addition, modern requirements dictate additional data processing of the measured transient. For photos of scope traces, that means manual integration or differentiation of the signal, or manually digitizing the signal for computer processing. Despite these disadvantages, the technique is still useful for verifying generator performance parameters and will likely remain popular for some time.

Transient digital recorders have many advantages for lightning-type tests and they are becoming very popular in the U.S. These units have a recirculating memory which is constantly monitoring the input data line via an analog to digital converter. The memory can be frozen at any time by triggering internally on the leading edge of the signal to be measured. By adjusting the "pretrigger time" the data record can be stored beginning a set time before the event begins. This feature prevents losing data on the leading edge of the pulse.

The commercial units are being improved rapidly, but current models have effective bandwidths up to 100 MHz and storage times out to 100 microseconds. Because the memory has a set storage capability, the time resolution is reduced as the storage time is increased. That is, a short record, say ten microseconds full scale, will have more discrete data points available to record the data per microsecond than if the record is stretched out to 100 microseconds.

Once the datum is stored in memory, it can be manipulated at will for display on different time and amplitude scales, and it can be transferred into a digital computer for further processing. A simple application of this capability is the calculation of the action integral of a high current waveform, as required by the new criteria documents. Another application where this capability is almost essential, is in the measurement of induced transients in full-scale aircraft tests. These transients are generally in the form of damped sinusoids with a mixture of different frequencies. In order to understand the coupling processes, the time-domain record must be converted to a frequency domain record by taking the Fourier transform. This operation requires a computer if any number of data events are to be analyzed.

An example of a typical data trace from a fiber optics/digital recorder system is shown in Figure 10, along with the Fourier transform. The data is typically filed on magnetic tape and plotted out with an X-Y recorder for presentation or reporting. No film or photography is involved.

The computational tasks for lightning test data processing are not extensive and can generally be met by a programmable calculator or a small laboratory microcomputer.

Summarizing the discussion of simulation and instrumentation techniques, Figure 11 is a block diagram of a One-Megajoule High-Current Damage Test facility, showing the relationship of energy storage systems for the various current components, the charging systems, the diagnostics and the instrumentation.

TEST TECHNIQUES

Having discussed the general simulation and instrumentation techniques for lightning testing, the specific procedures and rationale for different types of tests will now be described. The tests are categorized as Direct Effects or Indirect Effects tests and they are also categorized as Qualification Tests or Engineering Tests. These terms have been defined previously. The order in which the tests will be discussed follows roughly the order in which the tests would be conducted in a typical program. Thus, the first test is the model attach point test, which is an Engineering Test, followed by three Qualification tests oriented to externally-mounted electrical hardware, then concluding with the full-vehicle indirect effects test which is an Engineering Test.

Model Attach Point Test (Engineering Tests)

The initial laboratory test used in the development of lightning protection for an aircraft is often a scale model lightning attach point study. It is important for aircraft designers to know precisely where lightning may strike on a new aircraft. It is known that lightning initially attaches primarily to the extremities of the aircraft. Most attachments are to wing tips, nose, horizontal and vertical fin tips and other protuberances such as antennas, probes or external stores. However, there are questionable areas on most aircraft where a simple examination is not sufficient to determine, with any confidence, whether lightning will strike there or not. If there is a question of attachment probability, then it is likely that the probability of an attachment there is low. However, where safety of flight is concerned, even low probabilities must be considered. In such cases, more information is needed for making important design decisions regarding lightning protection. The placement of electrical hardware, the incorporation of protective measures, and the routing and shielding of critical avionics wiring may be influenced by the location of attachment points.

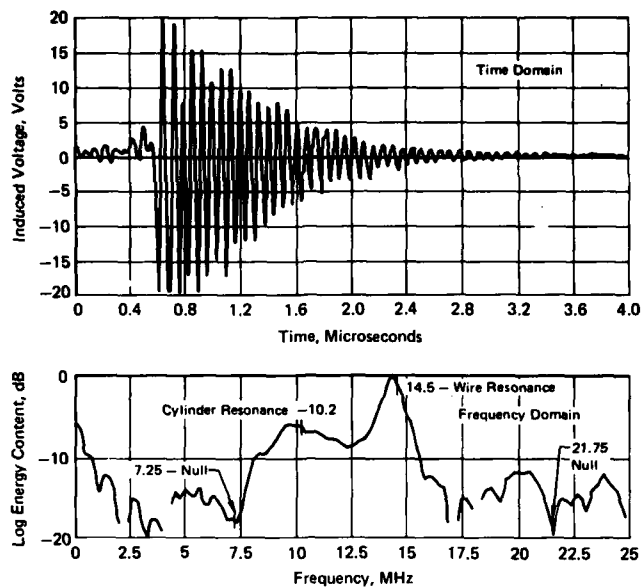


FIGURE 10
TRANSIENT DIGITAL RECORDER RECORD OF
INDUCED TRANSIENT WITH FOURIER TRANSFORM

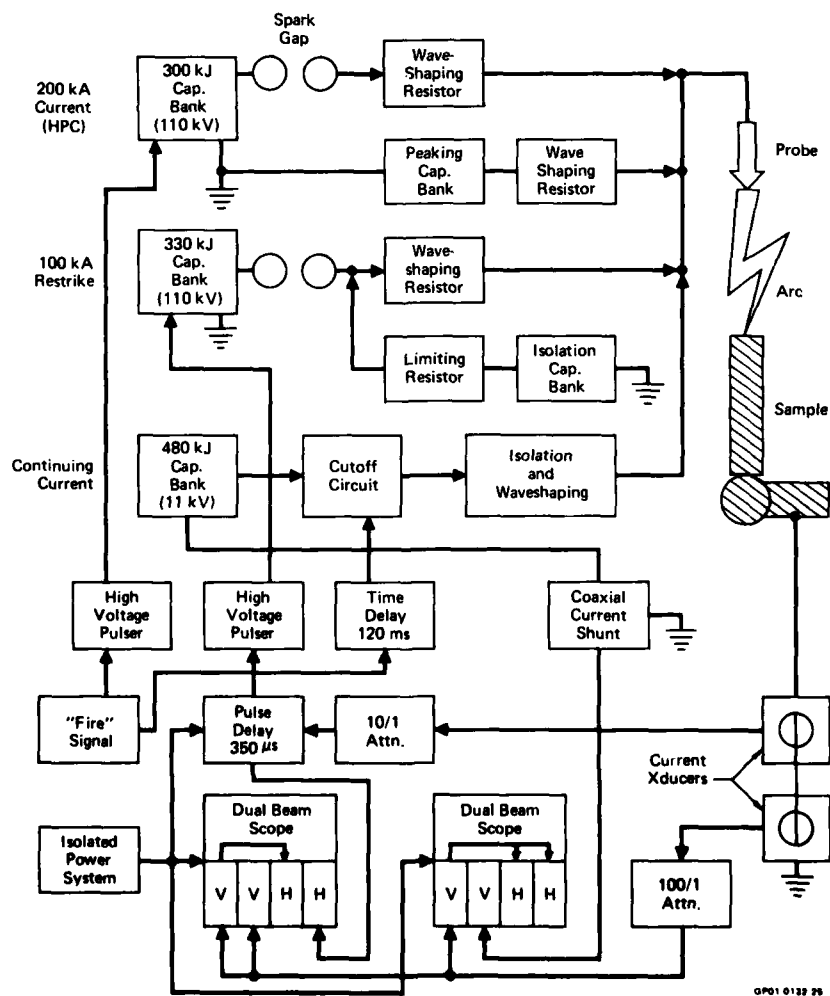


FIGURE 11
SIMPLIFIED BLOCK DIAGRAM OF IMJ HIGH-CURRENT LIGHTNING GENERATOR
CONNECTED FOR SEVERE MULTICOMPONENT LIGHTNING TEST

A scale model lightning attach point study can assist in this determination. The study is typically performed by placing a conductive model of the aircraft in an air gap between electrodes of a high-voltage impulse generator. The air gap is overvolted, causing a long spark to propagate between the electrodes. The spark is intercepted by the aircraft model, and the points on the model where the spark attaches are recorded as possible lightning attachment points. The model is rotated in small steps through all three axes of roll, pitch and yaw, and spark discharges to the model are triggered in each position. In this manner, lightning strikes to the aircraft from every direction are simulated.

Typically, three to ten shots are taken with the model in each orientation. Photographs, usually taken with two cameras positioned at right angles to each other, are used to identify and record the attachment points. Data from the photographs can then be used to tabulate all attachment points or to construct diagrams of various types showing capture angles or probability distributions.

In planning a model attach point test, a number of questions arise concerning various test parameters such as model size, construction and accuracy, air gap spacing, electrode geometry, electrode polarity, high-voltage waveform, grounding of the model and the number of discharges at each model orientation. It is difficult to specify these variables exactly, because a detailed knowledge of the mechanisms of propagation of natural lightning and the associated fields does not exist. The results of experiments which have been conducted for the purpose of determining the effects of these variables and their impact on the test are reported in References 10 and 11.

In view of the fact that model attach point tests may be relied upon to make important lightning protection design decisions, the test should be conservative, but as realistic as possible. The large number of laboratory variables which must be considered makes the establishment of a standard test procedure difficult. However, agreement has been reached on most aspects of the technique, with optional procedures defined in the principal areas of uncertainty.

The questions surrounding the proper choice of high-voltage waveshape and polarity are probably the most complex, and at the same time the most significant in terms of the effect of the choice on the results of the test. It has been shown that the use of high-voltage pulses with fast wavefronts, such as the standard 1.5/40 wave (1.5 μ sec rise, 40 μ sec decay), results in a limited distribution of attach points, mostly in high field regions. However, if slow rising waves are used, such as a 50 μ sec rise time switching pulse, then the arc propagation mechanisms are altered, and the arc tends to meander in an erratic fashion. As a result, the arc attachment points become more scattered, resulting in a larger number of attachment points, including some at inboard regions. Since the model attachment points produced by the slow wave are more scattered, the test is seen as being more conservative, thus producing greater confidence that all attach points have been considered. On the other hand, fast rising waveforms have been used in most of the previous model tests, resulting in fewer attachment points but good correlation with flight experience.

As a result of the waveform controversy, a double-option approach has been agreed upon by workers in the U.S. and Britain. Two test waveforms have been defined for model attach point testing. The first is a fast-fronted waveform which is to be used for what is termed "Fast Front Model Tests." The second waveform is a slow rising waveform which is to be used for "Slow Front Model Tests."

The voltage waveform for the fast front model test is a chopped voltage waveform in which flashover of the gap between the model under test and the test electrodes occurs at two μ sec (+50%). The amplitude of the voltage at the time of flashover and the rate-of-rise of voltage prior to breakdown are not specified. Attachment points on models obtained by tests using this waveform are all automatically designated as Zone 1 (direct attachment) regions.

The voltage waveform used for the slow front model tests has a rise time between 50 and 250 μ sec so as to produce a more erratic arc attachment behavior. It should produce a greater spread of attach points, possibly including attachments to low field regions. Therefore, the test data obtained must be analyzed by appropriate statistical methods to arrive at the definition of Zone 1 regions. In other words, some judgment must be exercised in interpreting the results of the slow front test, whereas the fast front test results are used directly. Neither criteria for judgment, nor the "appropriate statistical methods" to be employed in the slow front test analysis, have been specified.

A model attach point test on a scale model of the Space Shuttle in the launch configuration is shown in Figure 12. The simulated plumes are attached to help in determining if lightning could attach to the main engine nozzle on the Orbiter.



GPO: 01328

FIGURE 12
MODEL ATTACH POINT TEST ON SPACE SHUTTLE WITH SIMULATED PLOMES

High-Voltage Attachment Tests on Full-Scale Hardware (Qualification Test)

Electrical equipment is often mounted on the external surfaces of aircraft and many times the location is on or near extremities of aircraft where lightning flashes may attach. Many times antennas or other electrical components are covered by radomes or nonconducting fairings or glass lenses. High-voltage, long-spark tests are used to determine whether lightning can be expected to puncture dielectric covers and attach to the internal components or whether the stroke will flash over the surface of the cover and attach less harmfully to metallic structure. The tests are also used to identify detailed attachment points on complex metallic structures where it is desirable to know exact attachment points or detailed current flow paths.

A fast rate of rise voltage waveform has been defined for arc attachment tests on full-scale hardware. This waveform is designed to produce worst case results on dielectric puncture/flashover tests, but may not be worst case for attach point distributions on metallic systems. For situations where conservative test results are desired on all metal systems, an optional slow rate of rise waveform is also defined. The two waveforms, designated voltage waveforms A and D, respectively, are shown in Figure 13 along with the relevant parameters. The rationale for the definition of the test waveforms is discussed in a companion lecture in this series. An attachment test of a light/antenna group on a vertical stabilizer is shown in Figure 14.

In the fast waveform test, it is important that flashover occur on the rising front of the waveform in order to ensure that worst case stress conditions are being applied to the test article. Since a one-meter gap is also specified for the test, a high-voltage generator with a peak output voltage of one megavolt or greater is required.

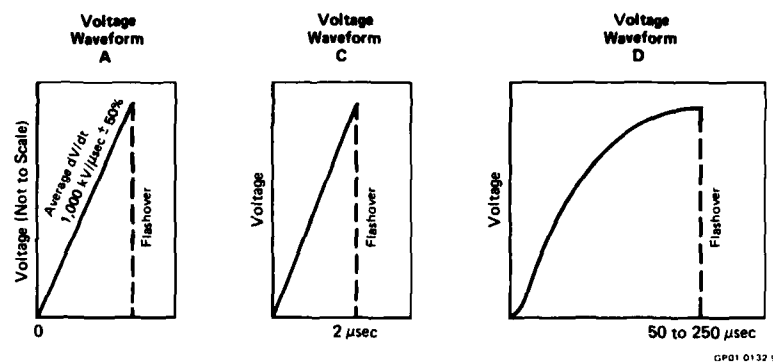


FIGURE 13
IDEALIZED HIGH VOLTAGE WAVEFORMS



FIGURE 14
LONG SPARK ATTACHMENT TEST OF LIGHT AND ANTENNA
CLUSTER ON VERTICAL FIN

The qualification test specifications which have been developed for this type of test specify the following criteria.

- This test is performed on full size structures that include nonmetallic surfaces and is used to determine the possibility of puncture and any other paths taken by the lightning current in reaching a conductive element.
- This test method is applicable to radomes, canopies, wing and empennage tips, antenna fairings, windshields and any other assemblies located in a direct strike zone and constructed of nonmetallic materials which might be vulnerable to puncture and damage from a lightning strike.
- The test apparatus required includes: A high-voltage generator capable of producing voltage waveform A with a peak voltage of at least 1.5 million volts, high voltage measuring and recording instruments, and photographic equipment for recording strike points.

- d. The test object should be a production-line hardware component or a full-scale prototype. All conducting objects within or on nonmetallic hardware that are normally connected to the vehicle when installed in the aircraft should be electrically connected to ground (the return side of the lightning generator). Surrounding external metallic vehicle structure should be simulated and attached to the test object.
- e. The test electrode to which test voltage is applied is positioned so that its tip is one meter away from the nearest surface of the test object. Dimensions of the test electrode are not critical. If model tests or field experience have indicated that lightning flashes can approach the object under test from several different directions, the tests are repeated with the test electrode oriented to create strokes to the object from these different directions.

If the test object is so small that a one-meter gap permits strokes to miss the test object, or if a one-meter gap is inappropriate for other reasons, shorter or longer gaps may be used.
- f. A typical test procedure would include the following steps:
 1. Set up the high-voltage generator, test electrode and photographic equipment.
 2. Inspect the high-voltage equipment and area for safe operation.
 3. Insert a dummy test object beneath the electrode, or place a conductive bar over the actual test object such that waveform checkout discharges cannot damage the test object.
 4. Fire a dummy discharge to the test object to check the voltage waveform and establish that the specified waveform is in fact being applied and check out the operation of the photographic equipment.
 5. Place the test object beneath the test electrode and begin the tests by firing one discharge at the test object.
 6. Fire the specified number of discharges from each position. Inspect the test object after each discharge and record the strike attachment points. This may be accomplished by moving either the electrode or the test object to cause the discharges to approach from each of the other direction(s) from which a natural lightning strike might be expected to approach. Repeat steps 5 and 6. If a change results in the air gap between the electrode and the test object, step 4 must also be repeated.
 7. Tests may be commenced with either positive or negative polarity. If test electrode positions are found from which the simulated lightning flashovers do not contact the test object or do not puncture it if it is nonmetallic, the tests from these same electrode positions should be repeated using the opposite polarity.
 8. Correlate photographs with strike attachment points observed on the test object.
- g. The data taken should include:
 1. Environmental data such as temperature and humidity;
 2. Description and photographs of the test setup;
 3. Date, personnel performing the tests, and location of the test;
 4. Test voltage waveform oscillographs;
 5. Photographs of discharges and attachment points on the test objects.

Test Rationale - The new STANAG and the SAE report (Reference 2) upon which it is based advise that tests begin with the high-voltage electrode at either polarity and suggest that tests in which no punctures occur be repeated at the other polarity to make sure that the same result holds, since either polarity may exist in flight. Plumer, in Reference 12, concurs in this recommendation, but has found, in most cases, that somewhat more punctures occur when the high-voltage electrode is at positive polarity. This is probably because streamering is more profuse from a positive electrode, permitting streamers to move closer to the test object (and apply a more intense field to it) prior to being intercepted by a streamer emanating from an external conductor.

Until recently, it was considered appropriate to apply many discharges to the test object to cover scattering effects. It is now apparent that partial breakdowns occur within some dielectrics found on aircraft, resulting in punctures after several withstands. This effect is most pronounced in fiberglass materials, including multi-ply or filament-wound laminations and foam or honeycomb-filled sandwich configurations. If such a material will withstand three discharges without puncture, it may be considered to have passed the test, since few such structures would experience more strikes than this (at the same location) during their lifetime.

If three discharges are insufficient to evaluate scatter effects, the test object should be rotated to expose an untested surface if available; otherwise, additional test objects should be used. The inside and outside surfaces of the test object should be inspected after each discharge to identify the attachment point(s) and punctures, if any. Each point should be marked so that it will not be confused with attachments produced by subsequent discharges. In addition, each discharge should be photographed so that the path taken by the flashover can be identified.

Restrike Simulation - In cases where the lightning current decays prior to a restrike, an intense electric field similar to that which preceded the original strike may be applied to the aircraft. If the aircraft has moved forward during this time, this field may be applied to surfaces aft of the original attachment point. This possibility must be assumed to occur over any surface that may experience a swept stroke (as in zone 2A). Since the dart leader preceding the restrike may follow the original path, the electric field may be most intense between points C and B beneath the channel, as shown in Figure 15.

The possibility of a puncture beneath such a restrike can be evaluated using this test technique by placing the high-voltage electrode several centimeters above the surface. The rate of voltage rise should be 100 kV/ μ s as in the initial attachment point test, but since the flashover path(s) is shorter, flashover will occur at an appropriately lower voltage.

Multiple paths are common, and care should be taken to assure that all such paths are identified. There are cases, for example, in which both a puncture and a surface flashover will occur simultaneously. A camera placed inside the test object may be utilized to identify internal streamers or punctures.

Protection Development Tests - The high-voltage test may be utilized to evaluate the performance of protective devices, such as diverter strips, or to determine the maximum separation permissible without puncture. Such tests can often be performed upon flat samples of the dielectric wall material of sufficient size to allow diverter strips to be attached and spaced similarly to the desired aircraft installation. The high-voltage probe is positioned one meter above the surface, equidistant between the diverter strips being tested, as shown in Figure 16.

Successful coordination of diverter spacing with internal conductor-to-wall spacing is achieved when the voltage and time necessary to flashover from any point on the external surface to the nearest diverter strip is lower than the voltage and time required to puncture the skin and attach to a conducting object beneath. The latter path includes the dielectric skin material as well as the air gap, but is must be remembered that the voltage withstand capability of a path through several different materials is less than the sum of the separate withstand voltages. Thus, the withstand or puncture voltage of a structure cannot normally be determined by testing its components individually. The complete structure should be tested. Further discussion of the subject is presented in Reference 12.

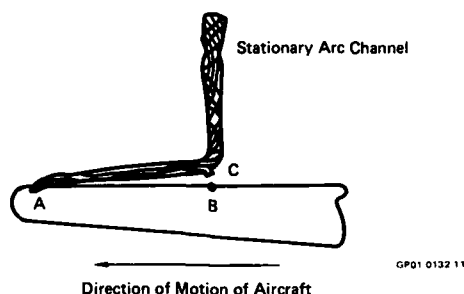


FIGURE 15
MECHANISM OF SWEEP STROKE ACTION

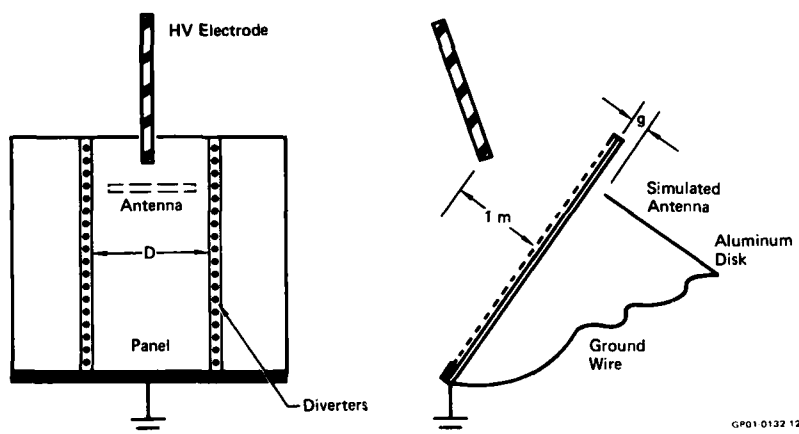


FIGURE 16
TEST ARRANGEMENT FOR DETERMINING DIVERTER SPACING (D) AS A FUNCTION
OF PROXIMITY (g) TO AN INTERNAL CONDUCTOR - FROM REF (12)

Tests to Determine Zone Boundaries - The tests described thus far have been designed to identify puncture possibilities. The fast rising test voltage, which is provided by voltage waveform A, enables the electric field to reach sufficient intensity to puncture the dielectric skin before streamers drawn from external conductors further away reach the high-voltage electrode. If the test voltage were increased at a slower rate, external flashovers would begin to predominate.

In some cases, however, it is desirable to encourage streamers from more distant, less probable locations, to identify the boundaries of a zone over which direct lightning strikes are possible. Here a slower rising test voltage is desirable. If the range of electric field rates-of-rise possible from natural lightning is as broad as the range of return stroke current amplitudes (a likely possibility since both are related to charge in the leader), voltage rates two orders of magnitude lower than waveform A may also be possible.

A voltage waveform which rises to crest in 50 microseconds has been identified as waveform C in Reference 2 for use in certain engineering tests. Waveforms with rise times of up to 250 microseconds are permitted by the definition of waveform C (50 to 250 μ s) and the particular rise time is not critical. Tests with this waveform would be used to determine how far inboard Zone 1 should extend on wing tips with large radii of curvature and to evaluate worst case attachment distributions on complex arrangements of components in Zone 1 areas.

High-Current Direct Effects (Qualification Tests)

When an aircraft is struck by lightning, high current damage effects may be produced when the aircraft forms part of the total lightning path. Lightning currents flow between the two or more attachment points on the aircraft. Direct (damage) effects are most generally produced in the localized vicinity of arc roots or attachment points, although current flow through joints or high impedance paths can produce damage away from the arc. Because of the sweeping action of the lightning arc in the windstream, arc attachment points on forward parts of the aircraft often move aft in the windstream. This sweeping action may expose externally-mounted electrical hardware to arc attachment and damage although not mounted in a direct strike zone. The high current threat characteristics depend upon location on the aircraft because of the time-varying nature of the current and the sweeping action. The direct damage effects include burning, eroding, blasting, and structural deformation caused by arc attachment, as well as high-pressure shock waves and magnetic forces produced by the associated high currents.

The severe model current waveform used in the modern criteria documents was shown previously in Figure 4, along with the numerical values of the various components (A-D). In addition, current waveform E, shown in Figure 17, may be used to test for direct effects which are dependent upon inductive effects. These effects might include sparking or surge arrestor damage, for example.

The swept stroke zones are defined in detail elsewhere. Briefly, however, Zone 1 regions are subject to direct (initial) attachment, Zone 2 regions are swept stroke zones aft of forward Zone 1 regions. Zone 3 regions have low probability of arc attachment. Category A zones have high probability of arc movement (sweeping action), whereas Category B zones have high likelihood of arc hang-on.

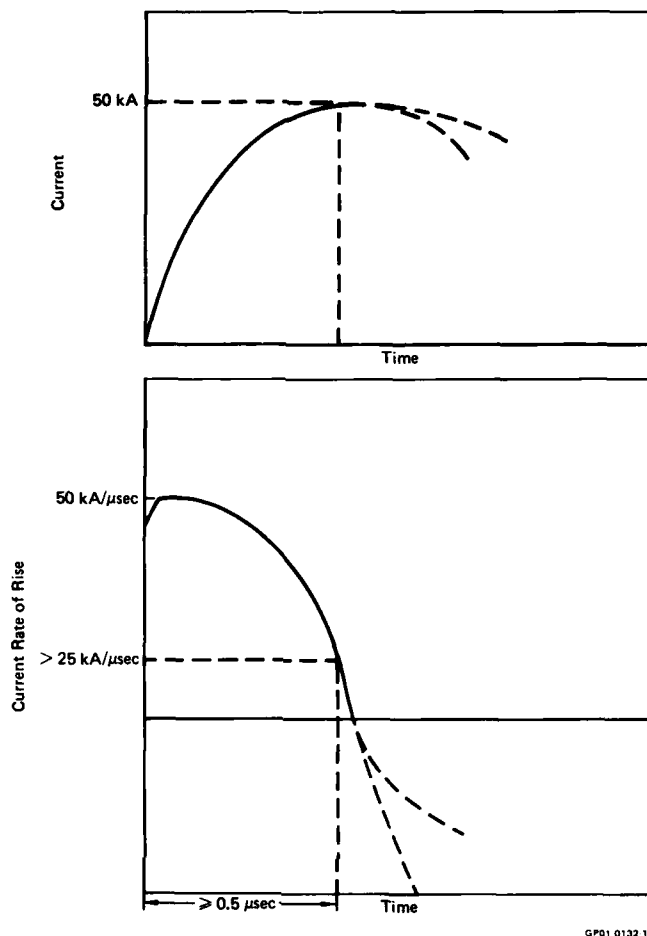


FIGURE 17
CURRENT WAVEFORM E

With this background, the proposed STANAG test specification includes a waveform application table, shown below as Table 1. The STANAG test procedure for Qualification Tests for Direct (Damage) Effects includes the following criteria:

- a. This method is used for determining the direct effects resulting from the interaction of lightning currents with aerospace vehicles and hardware.
- b. This test method is applicable to aerospace vehicle structures and components which are susceptible to lightning current attachments or transfer. This includes probes, booms, antennas, lights, and other hardware located in zones 1 or 2.
- c. The test apparatus required includes a high current generator(s) capable of producing the specified waveforms, and high current measurement and recording instruments.
- d. The test object should be a production-line hardware component or a full-scale prototype. All conducting objects within or on nonmetallic hardware that are normally connected to the vehicle when installed in the aircraft should be electrically connected to ground (the return side of the lightning generator). Surrounding external metallic vehicle structure should be simulated and attached to the test object.

The test setup should be such that the simulated lightning currents are delivered to and conducted away from the test object in a manner representative of the condition where the aircraft is struck by lightning. Care must be taken to assure that magnetic forces and other interactions which are unrepresentative of the natural situation are minimized.

CAUTION: There may be interactions between the arc and the test conductors. Care must be taken to assure that these interactions do not influence the test results.

- e. Arc-entry tests for zones 1 and 2 are conducted using electrode materials which are good electrical conductors capable of resisting the erosion produced by the test currents involved. Yellow brass, steel, tungsten, and carbon are suitable electrode materials. The electrode is a rod with a rounded end, which is firmly affixed to the generator output terminal and spaced at a fixed distance away from the test object.
- f. The gap spacing must be sufficient to ensure that arc-jet and blast pressure effects do not influence the test results. Normally the gap will be at least 50 mm for Component A or D and at least 10 mm for multiple component tests. A fine wire such as No. 30 copper wire can be used as required in the gap to assist in the current discharge of low-voltage-driven current generator(s).
- g. The electrode polarity of the Waveform Components A and D can be either positive or negative. The electrode polarity of the Waveform Components B and C must be negative.
- h. Conducted entry tests for tests of objects in zone 3: the test current is conducted directly into and out of the test object in a manner representative of the actual lightning current paths in the aircraft. This test can be combined with the zone 1 and 2 tests described earlier.

- i. Normally, the test waveforms are applied as follows:
 Zone 1A: Apply Waveform Components A and B in order.
 Zone 1B: Apply Waveform Components A, B, C, and D in order, but not necessarily in one continuous discharge.
 Zone 2A: Apply Waveform Components D, B, and C in order. The total current discharge time shall be limited to 50 milliseconds or to a time period previously determined through a swept-stroke attachment test or analysis (see Table I, Note 1).
 Zone 2B: Apply Waveform Components B, C, and D in order.
 Zone 3: Apply Waveform Components A and C in order.
- j. Lightning damage may be in the form of pit marks or burn-through holes on skin panels, weakened or distorted structural joints, structural deformation from blast pressures, puncture or delamination of composite structures, etc. Structural tests and/or nondestructive inspections may be required both before and after tests for damage evaluation.
- k. The actual test procedure will include the following steps:
 1. Set up the high-current generator, discharge circuit and diagnostic equipment.
 2. Inspect the equipment and area for safe operation.
 3. Insert a dummy test object beneath the electrode, or place a conductive bar over the actual test object such that waveform-checkout discharges cannot damage the test object.
 4. Fire a discharge to the dummy test object to check the current waveforms and establish that the specified waveform(s) is in fact being applied and check out the operation of the diagnostic equipment.
 5. Place the test object in the discharge circuit.
 6. Fire the specified number of discharges and inspect the test object after each discharge and record the results.
- l. The following data should be collected:
 1. Environmental data which may affect the test results;
 2. Description and photographs of the test setup;
 3. Date, personnel performing the tests and location of tests;
 4. Test object photographs both before and after lightning tests;
 5. Test current waveforms.
- m. It is important to ensure that the test instrumentation shall be adequately shielded from electromagnetic fields associated with the lightning test currents and other sources. In cases where inductive sparking may be a problem, a test with current waveform E may be advisable.

An example of a high-current damage test is shown in Figure 18, where both physical damage and induced voltages are being assessed. Additional clarification and rationale for some of the recommended procedures may be helpful. Hansen has discussed the importance of proper simulation of current paths and arc root and length effects. His arguments are summarized below.



FIGURE 18
COMBINED HIGH CURRENT DIRECT AND INDIRECT EFFECTS TEST
ON AN EXTERNAL FUEL TANK

Simulation of the Lightning Current Paths - In the natural environment, the charge is simply transferred from one cloud area to another, or from cloud to ground. The aircraft is therefore in free space with no return path current magnetic fields to influence the behavior of the lightning currents flowing through it. In laboratory conditions, return path conductors are always associated with the test piece, and their associated magnetic fields can influence the test results. In tests on components in zones 1 and 2 where open arcs are used, the arc path can be severely distorted by magnetic forces, and in zone 3 tests the path taken by the current through the test object can be influenced by the position of the return current conductors.

One solution to this problem is to have multi-return paths so arranged that the individual magnetic fields sum to zero in the region of the test object. In most cases this can be achieved with three or four return conductors. In some cases, only two wide transmission paths may be necessary. With very large objects, and particularly for currents with high d/dt, an assessment must be made of where the currents will flow, and how they will redistribute themselves during the pulse. The return conductor geometry may then be designed to reproduce that effect. This final design will usually be a compromise between the load inductance requirements, and the environment simulation requirements.

Arc Length and the Arc Root - In early work on arc root burn through of metal panels, the results were strongly influenced by the arc length. This was found to result from the presence of electrode jets. These jets are emitted from arc roots on both electrodes and consist of a jet of ions, neutral particles and clusters of neutral particles. High-speed cine film shows that these jets are very active for up to 50 mm from each electrode, and have a strong interaction with each other. In a natural strike to an aircraft, only the jet associated with the attachment point to the aircraft itself exists, and there is no jet corresponding to that emanating from the test electrode in a laboratory simulation. It is therefore desirable to separate the electrode jet from the current channel and direct it away from the test object. Since the electrode jet is always emitted normally to the surface of the electrode at the arc root, the jet may be directed from the test object by redirecting the arc root to a suitable angled facet of the electrode by means of a suitable insulator.

Experiments with this type of electrode have given results which are sensibly independent of arc length, indicating that the electrode jet effect has been virtually eliminated. Where this type of electrode is not used, much longer gap distances are required to avoid the effects of jet interaction. Ideally, a distance of about 150 mm is required to ensure no jet interaction, but practical difficulties of arc stabilization and driving voltage forces some compromise. The proposed STANAG recommends 50 mm for current components A and D and 10 mm for combined waveforms. This reduced length of 10 mm is in general a more severe test.

The Effects of Forward Speed - The forward speed of the aircraft causes the lightning attachment points to sweep rearward in discrete steps. For arc burn through tests in the swept stroke region, it is useful to know the maximum arc dwell times. Techniques for establishing dwell times are described by D. Clifford and P. Little in References 14 and 15. Where it is not possible to firmly establish a maximum possible dwell-time, however, a dwell-time of 50 ms should be assumed.

Experience has shown that when a restrike occurs in a swept stroke region, a new attachment point is always formed, so tests for zone 2A, therefore, have the current components applied in order of D (representing the restrike) followed by B and C (representing the subsequent intermediate and continuing currents). Tests for zone 1A require only current components A and B, as the attachment point will have swept backwards before the event of the continuing current (Component C) or the restrike (Component D). Zone 1B is an initial attachment which cannot sweep anywhere else and will, therefore, see all current components of the strike in the order in which they occur viz A, B, C, and D. Zone 2B, however, does not see the initial return stroke, but could see all the remaining components in the order in which they occur, i.e., B, C, and D.

Data to be Collected - The principal data to be collected from damage tests is a description and, in some cases, an evaluation of the damage produced, along with documentation of the actual test parameters (current waveforms, action integrals, coulombs, etc.). Generally, damage is documented by pretest and post-test photographs, but in some cases damage is not always visible and other inspection techniques may be required. For example, x-ray inspection may be necessary to determine the extent or type of damage to internal wiring or connections in a light or antenna assembly. Nondestructive testing (NDT) of structural members can sometimes reveal internal damage which is not visible to the naked eye. This is particularly true in laminated composite structures.

High-Current Indirect Effects Qualification Tests

Lightning strikes to electrical equipment mounted on the external surface of an aircraft may produce undesired currents and surge voltages on internal wiring, either by direct contact of the lightning arc to the electrical circuit or by electromagnetic coupling due to the intensive fields produced by the lightning strike. These undesired transients may not only threaten the operation of avionics equipment connected directly to the external components, but may even couple electromagnetically into other unrelated circuits and equipment within the airframe.

The objective of this test is to determine the magnitude of voltages and currents produced on aircraft wiring when lightning attaches to externally-mounted electrical hardware. The object to be tested (a production-line hardware component or an accurate prototype) is mounted on a shielded test chamber, so that access to its electrical connectors can be obtained in an area relatively free from extraneous electromagnetic fields produced by the discharge of the high-current lightning simulator. The test object is mounted on the test chamber exactly as it is mounted on the aircraft, since normal bonding impedances can contribute to the voltages induced in the electrical circuit. Inside the shielded enclosure, connectors and wiring representative of the flight installation may be used to connect the test object to either the actual equipment or to a simulated load impedance. Usually a dummy load is used since the test is designed primarily to measure the levels of voltage and current appearing on the wires. The measuring instruments may also be located in the same shielded enclosure or in a separate shielded room connected by a suitably shielded instrument cable.

A laboratory generator capable of producing the prescribed lightning waveform is used to inject simulated lightning currents into the test object at the various points where lightning can attach. The test object is grounded via the shielded enclosure so that current flows through the test object in a manner representative of the aircraft installation. The conducted and induced voltages produced in the related electrical circuit are measured at the terminals of the circuits with suitable measuring equipment. The technique is described in greater detail by Clifford in Reference 16.

It can be seen from Table 1 and from the zone definitions that electrical hardware located in either zone 1 or zone 2 will receive either current Component A or Component D, or both. Each of these current pulses in nature may exhibit very fast rates-of-rise, although the rate-of-rise is not specified in the waveform parameters for these components. Rate-of-change of current is an important parameter, since magnetic coupling effects ($\propto d\phi/dt$) are directly influenced.

Since the model waveform does not specify rates-of-rise of current, a specialized current waveform designated as Current Waveform E, Figure 15, has been defined for use in tests for induced coupling effects. Current Waveform E is not intended to resemble a particular lightning strike component in terms of energy content, and is not used, therefore, in damage effects testing. It is intended to simulate the early-time initial wavefront of the return stroke current pulse (either initial strike or restrike), where di/dt 's (rate-of-change of current) can reach 100 kA/ μ sec or higher.

As discussed earlier, undesired voltages and current surges can be produced in aircraft wiring by either arc attachment to the wiring or by induced coupling. Therefore, a complete evaluation of zone 1 or zone 2 externally-mounted electrical hardware should include tests with the proper waveform components from Table 1, plus a fast rate-of-rise test with Current Waveform E. If the Component A or D waveform actually used in the direct effects test has a fast rate-of-rise conforming to the requirements for Waveform E, the separate fast rate-of-rise test is not required. However, Current Waveform E is often used separately for induced coupling measurements because it is a low-energy waveform and can be applied repeatedly with no damage to the test article.

When the direct effects test is conducted, measurements should be made of voltages appearing on internal wiring. Even if the waveform used does not have the fast rate-of-rise required to meet the induced coupling requirement, voltage may be produced by other mechanisms. The arc may attach directly to the wiring, as discussed earlier, or the high-peak current may produce resistive voltage drops which can appear across the wiring. When a direct effects test is conducted the high-current electrode is placed a small distance from the desired arc attachment point on the test object, leaving an air gap of a few centimeters. If a separate Waveform E test is conducted, the output of the generator may be clamped directly to a point on the test object, especially when it is desirable to minimize damage to the test article.

The points of attachment are determined from separate high-voltage, long-spark attachment tests to the full-scale components. Numerous current flow patterns may be indicated by these tests, possibly leading to a requirement for several induced coupling tests to determine the worst case attachment point. The point or points thus determined can then be used in the direct effects test.

Although not required by specification, it is desirable to conduct the induced coupling test at a number of different peak current levels (maintaining the same waveshape) leading up to, or beyond, the 50 kA level. The measured voltages at each driving current level can then be plotted to verify that a linear relationship exists. This linearity is important, because it is necessary to extrapolate the measured transients to correspond to a full threat level waveform. Indirect effects measured as a result of Waveform E must be extrapolated as follows:

- a. Induced voltages dependent on resistive or diffusion flux should be extrapolated linearly to a peak current of 200 kA.
- b. Induced voltages dependent upon aperture coupling should be extrapolated linearly to a peak rate-of-rise of 100 kA/ μ sec.

Further interpretation of the measured transients and the rationale for extrapolation are given by Burrows in Reference 17, and are summarized below.

Resistive/Diffusion Flux Induced Voltages - When the construction of the test object is such that the simulated lightning current produced voltages arising from resistive volt drops in the test object or its mounting system, then the voltage so generated will be related to the current amplitude and waveshape. Extrapolation should therefore be up to 200 kA. That is, voltages and currents measured with a test pulse of say 50 kA peak should be scaled up four times to give the equivalent 200 kA value.

The important characteristics of these voltages are:

- a. There is no instantaneous jump in voltage at $t = 0+$; the waveform starts at zero and may then (1) commence to rise at finite slope similar to the current waveshape (especially in very resistive materials like carbon fiber or thin wires) or (2) show a dead time (i.e., zero slope) for a short period before rising (as would be observed in high conductivity materials like aluminum).
- b. Peak voltage does not occur at $t = 0+$, but will normally occur at or near peak current, often somewhat early when measured within carbon fiber/metal structures; and in high conductivity materials may occur late, owing to the time delay introduced by the diffusion process.

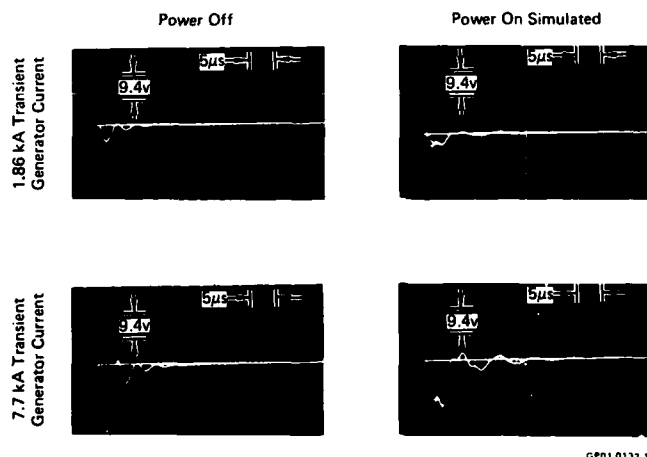
Fast Flux ("Aperture") Coupling - When the magnetic flux surrounding conductors carrying the simulated lightning pulse couples with loops (e.g., in unshielded pitot heater wires, etc.), then the induced voltages will be proportional to $d\phi/dt$ in that loop. The flux external to a conductor, and flux within apertures having insulating covers is instantaneously proportional to the current, and hence $d\phi/dt = di/dt$. Therefore, the voltage waveform will normally bear a strong resemblance to the first derivative, di/dt , of the current waveform, and therefore extrapolation will be up to 100 kA/ μ s. That is, an induced voltage of di/dt type caused by a current pulse whose peak di/dt is say 40 kA/ μ s should be multiplied by 2.5 to give the 100 kA/ μ s value.

The important characteristics of these waveforms are:

- a. A fast step in the waveform amplitude occurs at $t = 0+$, at the commencement of the current pulse. The waveform is often accompanied by 5 to 50 MHz components, and the first zero crossing will be at peak current where $di/dt = 0$.
- b. The peak voltage attained will normally occur at the initial transient at $t = 0+$. (If peak voltage occurs at or near peak current, the mechanism cannot be aperture coupling.)

Choice of Simulated Load Impedances for Indirect Effects Tests - The simulated load impedances should be chosen to make the effective load presented to the test object wiring as representative as possible over a broad frequency range. Where possible, actual circuit components should be used, or replicas thereof, so that low, medium and high frequency impedance is duplicated. It is not sufficient to load a 50 Ω antenna cable with 50 Ω . The radio receiver/transmitter unit will normally only match the cable with a 50- Ω over a small frequency range. During a lightning test, the circuit might act like a very low impedance to low frequencies if the receiver includes a shunt choke to ground, or be very high impedance if there is only a small series capacitor. Therefore, some knowledge of the real circuitry into which the feeder operates is required so that meaningful measurements might be made.

This point can be illustrated by the combined direct and indirect effects test on an aircraft anti-collision light as shown in Figure 8. The transient voltages induced in the internal wiring were first measured for a series of applied $2 \times 50 \mu$ sec current waveforms with increasing magnitudes. The induced signals are shown in Figure 19. The light is mounted near the upper tip of the vertical stabilizer and employs solid-state circuitry.



GP01 0132 15

FIGURE 19
TYPICAL 'POWER OFF' AND 'POWER ON' VOLTAGES INDUCED
IN TAIL ANTICOLLISION LIGHT CIRCUIT

Tests were performed at four low-level driving current levels to confirm linearity under these conditions:

- (1) Power off - simulating unpowered aircraft on ground or combat flying conditions.
- (2) Power on - the light was operating in a flashing mode.
- (3) Simulated power on - power in a flashing mode was simulated to simplify induced voltage measurement. It was determined that the induced voltage waveshape was almost identical to that in (2) above, although the absolute magnitude was slightly different.

The peak induced voltages are plotted in Figure 20; it is seen that these voltages must be extrapolated or "scaled" to a 200 kA peak driving current, or 100 kA/ μ sec rate-of-rise. This test shows that if the light were struck by lightning with a 200-kA peak and a time-to-peak of two μ sec, a peak induced voltage of 368 volts could be expected for a power-on condition; 606 volts would be produced in a power-off condition, because of different circuit loading characteristics. It is noted that the induced voltage in the power-on condition is lower than that obtained for the simulated power-on condition. This is believed to be due to the impedance loading effects of the flasher unit and the 400 hertz power supply, which are slightly different when the units are operating normally and when the operation is simulated. Because of observed differences such as this, it is recommended that induced voltage testing be conducted when the subject equipment is operating normally.

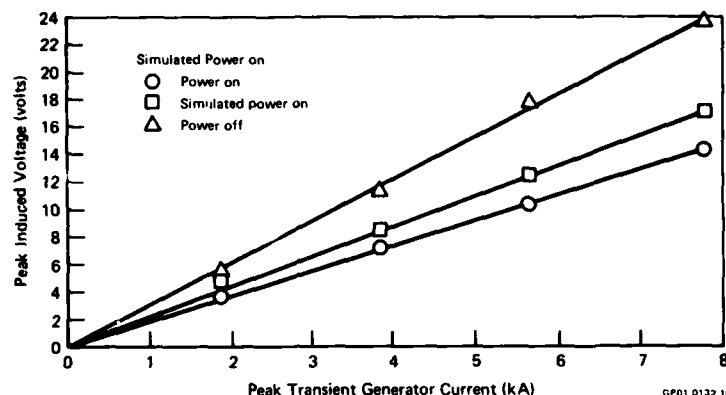


FIGURE 20
ACTUAL INDUCED VOLTAGES INTO TAIL
ANTICOLLISION LIGHT CIRCUITRY

Tests for Full-Scale Vehicle Indirect Effects (Engineering Tests)

The characteristics of electrical transients induced in aircraft wiring and avionics systems are affected by the system response of the entire aircraft to the lightning stimulus. Although induced-coupling tests may be conducted on electrical hardware and associated wiring at the component level, the final determination of voltage and current levels induced internally must take into consideration the complex response of the total structure and the subsequent coupling of magnetic and electric fields generated by currents on the external surfaces to internal regions of the aircraft. The lightning current waveform will be modified by the resonant responses of the structure.

The complexities of full-scale vehicle testing are extensive and are probably not fully appreciated, even by those working in this area. However, the rapid advent of new avionics and equipments which utilize sensitive elements leads to a real need to evaluate and verify the performance of the critical equipment as it is integrated into the total system of the vehicle. Therefore, whatever testing can reasonably be conducted now must proceed.

The electrical impedance of a full-scale aircraft precludes the use of even the 50 kA current pulse used for component indirect effects tests. Consequently, lower level current pulses must be used to evaluate the nature of transients produced by the lightning return stroke. The transients produced on internal wiring by current flow through the structure must be measured and then extrapolated to threat level conditions. For flux coupled voltages which are proportional to di/dt , the transients should be extrapolated to 100 kA/ μ sec. Resistive voltage must be extrapolated to 200 kA.

Based upon linearity arguments, Walko, et al.¹⁸ developed a test based upon the use of a very low-level $2 \times 50 \mu$ sec double exponential current pulse with a peak magnitude as low as 200 amps. This current pulse theoretically contains all of the frequency components of a 200,000-amp $2 \times 50 \mu$ sec waveform, therefore allowing induced transients to be scaled directly. The pulse is passed through the aircraft structure (from nose to tail, for example) and the resulting transients produced on critical wire runs inside the aircraft are monitored by connecting the leads of a shielded instrument cable across the circuit to be monitored. The peak values of the measured transients are then extrapolated upward to the threat current level. In the case of a 200-amp $2 \times 50 \mu$ sec test pulse, the peak levels are always multiplied by 1,000 to determine the anticipated transients for a 200,000-amp strike. Since the waveshape is the same as the threat waveform, the di/dt and peak current have the same scaling factor.

Recognizing some of the problems which could be associated with interpreting such a low-level test, the U.S. Air Force Flight Dynamics Laboratory has extended the test to higher current levels and has incorporated improved diagnostic and instrumentation equipment and techniques.¹⁹ These improvements include fiber optic data links, computerized data analysis and techniques for extracting the signal from the desired circuit without introducing more pickup on the wires. The Air Force has reported tests with current levels upwards of 30 kA with rise times of a few microseconds through a small fighter aircraft.²⁰ The technique is referred to as the Lightning Transient Analyzer (LTA) test.

Prior to the introduction of the LTA tests, a few full vehicle tests had been conducted using damped oscillatory discharges rather than a double exponential pulse. These tests were sometimes conducted with both a fast and a slow discharge whose parameters were defined by the limitations of the test generators. The fast waveform, in the 100-300 kHz range, was used to evaluate direct flux coupled transients which are dependent on di/dt . The slow waveform, in the range of a few kilohertz, was used to evaluate resistivity coupled transients and the effects of fields which diffuse through the skins.

Both the double exponential and the damped oscillatory waveforms are allowed by the modern criteria documents, and each has certain advantages. The primary advantages of the 2×50 waveform is that it is the same approximate shape as the natural lightning discharge and, therefore, presumably contains the same energy distribution in the frequency domain. The pulse is produced by discharging a capacitor bank through a resistive element, resulting in an overdamped waveform. This peak current is thereby reduced from the underdamped case, but faster times to a peak can be achieved. The underdamped (oscillatory) waveforms are simpler to produce and have the advantage that the induced transients are readily identified by the oscillatory signature. The slow wave carries considerable energy and at high peak levels are more likely to produce damage, either in the structure or in the avionics.

Each test is carried out by passing the test current through the complete vehicle while measuring the induced voltages and/or currents. If possible, the aircraft equipment should be operating on internal (battery) power so the proper impedances are present and so that operation of the systems may be observed. The addition of external power carts and other connections may alter the response of the systems. Indeed, even the connection of the test generator will modify the system response and therein lies one of the major difficulties with this test. The Culham Laboratory in the U.K. has developed a modified hookup which seeks to eliminate facility effects by the selection and placement of current returns and terminating impedance.²¹ These types of tests seem to indicate the most troublesome circuits and systems in aircraft on a qualitative basis, and that information is very valuable.

The test current should be applied between several representative pairs of attachment points such as nose-to-tail, wing tip-to-wing tip, etc. Attachment points are normally selected so as to pass current through the parts of the vehicle where circuits of interest are located. The current leads to and from the aircraft should be routed so as to minimize the biasing of current flow patterns on the vehicle. A coaxial arrangement is the most desirable. The LTA current return technique now used by the Air Force is adapted from the British work at Culham which is shown in Figures 21 and 22. The technique uses wide aluminum sheets configured around the vehicle. This approach also reduces the inductance of the test setup and allows higher peak currents to be achieved.

The instrumentation techniques are very critical for this test because of the size of the test, the high frequencies involved and the low levels of signals to be measured. The instrumentation practices described earlier should be employed. Noise-free operation of the instrumentation must be verified before testing. The sketches in Figure 23 illustrate how the aircraft grounding and generator hookup may be accomplished.

When testing operational aircraft, some care must be exercised in regard to the fuel system and any ordnance or pyrotechnic devices employed on the aircraft. Fuel tanks should be inerted by topping off and purging with nitrogen gas. Alternatively, the fuel tanks can be drained and then purged, but a lengthy purge time is then required with monitoring of the exhaust vapors to ensure a suitably low fuel vapor content. Pyrotechnic actuators should be removed or otherwise made safe. After the test, an operational check of all systems should be conducted to ensure safety and proper operation of all systems during subsequent flight.

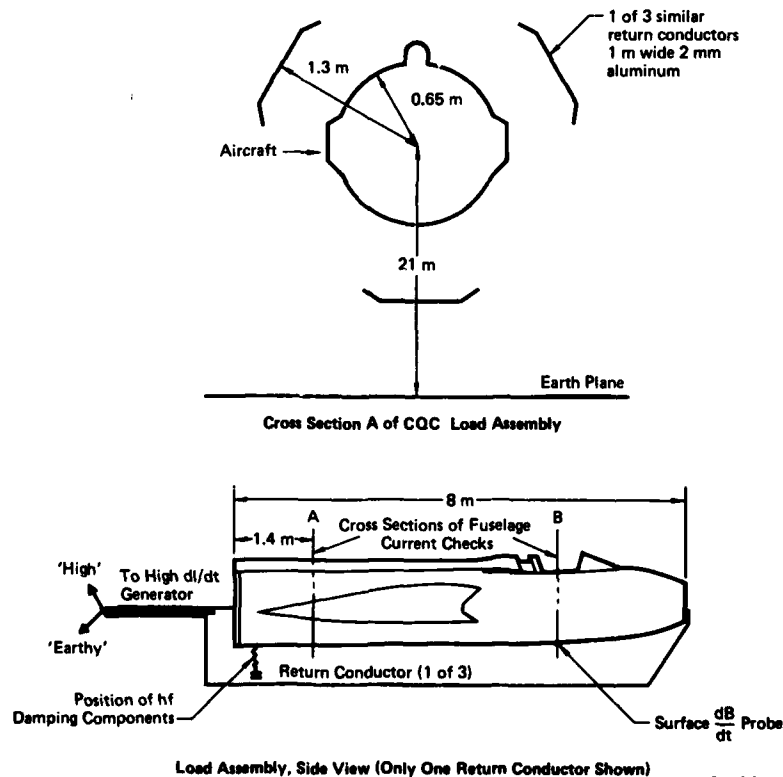
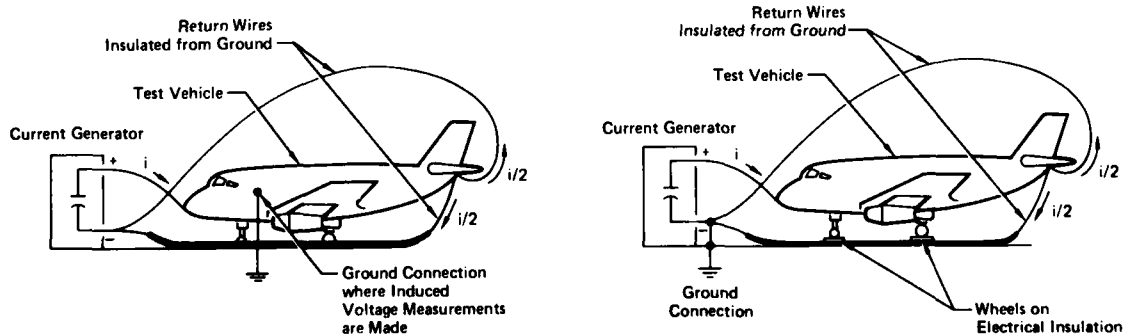


FIGURE 21
CULHAM QUASI-COAXIAL (CQC) FULL-VEHICLE INDIRECT EFFECTS TEST-FROM REF (21)



GPO1 0112 27

FIGURE 22
CULHAM QUASI-COAXIAL EXPERIMENTAL ARRANGEMENT VIEWED FROM FRONT
END OF FUSELAGE WHERE RETURN CONDUCTORS ARE JOINED TO THE NOSE
 (Photo Courtesy of Culham Laboratory, UKAEA)



GPO1 0112 18

FIGURE 23
TYPICAL SETUPS FOR COMPLETE VEHICLE TESTS

NEW TESTING DEVELOPMENTS

New test techniques which are now being developed are aimed almost entirely at the questions surrounding full scale vehicle testing for induced transient effects on avionics systems. In addition to the upgrading of the LTA technique by the U.S. Air Force, other approaches are also being proposed to address this problem. Three such techniques will be discussed briefly. They are the swept-frequency CW test, the high voltage shock excitation test, and the LEMP test.

Swept-Frequency CW Test

This test is a low-level method which is proposed by workers at the Boeing Company as a supplement to pulsed methods.²² The technique was derived from the nuclear electromagnetic pulse (NEMP) testing and analysis of military systems. The technique employs a wide range R.F. oscillator and amplifier to produce a continuous sine wave whose frequency can be changed continuously from near DC to 10 MHz. The amplitude of the current flow is typically a few amps. The swept CW current is passed through the aircraft structure and the responses of selected circuits are measured, as with the pulsed test. However, the output of the swept CW test is the transfer function of the system and circuit under test. The transfer function is in the frequency domain and thus indicates the response of the circuit as a function of frequency. A typical transfer function is shown in Figure 24 as reported in Reference 22, when the technique was applied to the wing of a 747 aircraft.

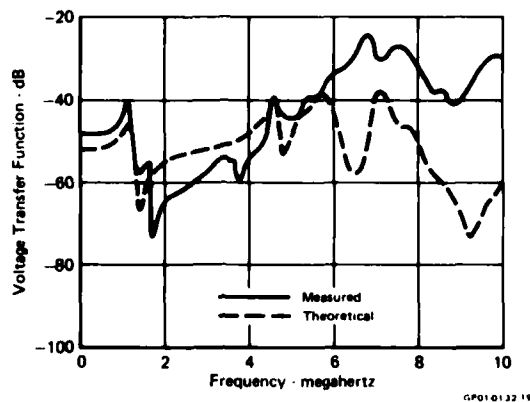


FIGURE 24
TRANSFER FUNCTION FOR COMMON MODE VOLTAGE ON 30KΩ SIGNAL LOAD
USING THE SWEPT CW TEST - FROM REF (22)

In order to utilize the measured transfer function, a considerable amount of analysis must be performed requiring a circuit analysis computer code capable of computing transients on large circuits. The analytical model is compared with the test data and then refined according to the flow diagram shown in Figure 25. Once the model successfully predicts the test results, the lightning threat waveform is folded into the model and the threat level response of the circuit is calculated. The test is therefore a tool used to refine and verify the accuracy of the analytical model. The output of the test does not yield information which directly predicts the performance of the system without the accompanying computer model which must be developed for the particular aircraft under test, and then it gives no information about nonlinearities in the physical response of the system at high current levels.

The advantages of the swept-frequency test are that it is simple and does not require specialized high voltage equipment, it clearly identifies the system/circuit resonances if properly setup, and the setup can be modified and the effects of the test setup can be identified relative to the computer model parameters. The concurrent development of an analytical model should yield additional insight into the test setup and measured data.

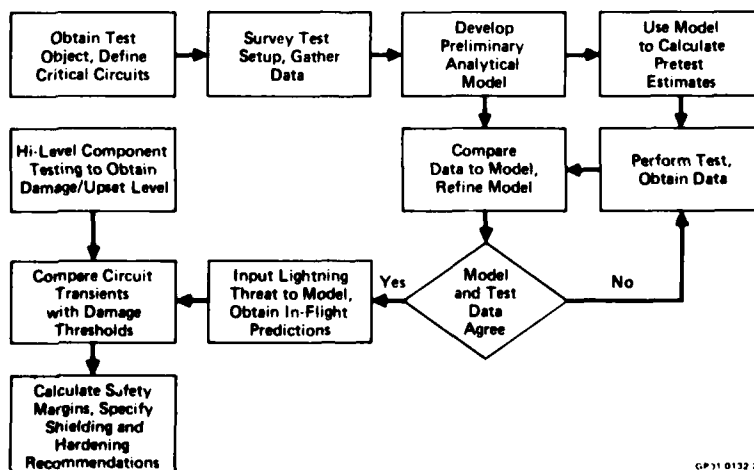


FIGURE 25
SWEPT CW ANALYSIS/TEST PROGRAM FOR INDUCED EFFECTS OF LIGHTNING - FROM REF (22)

High Voltage Shock Excitation Test

Questions surrounding some of the early LTA results led workers at the McDonnell Aircraft Company to study the induced coupling phenomena more closely by utilizing a long cylinder with an internal wire pair; a simple system which could be modeled analytically.²³ Experiments conducted on the cylinder disclosed that the coupling phenomena were very complex, involving a number of test setup effects, and at least three different excitation mechanisms. The cylinder was long enough (10 meters) to allow system resonances to be excited which were measurable with the fiber optic instrumentation being utilized.

The results of the cylinder test indicated that fast oscillatory transients observed during tests of actual aircraft are system resonances which can be excited by either a) pulsing the structure with a fast voltage step waveform, or b) passing a fast rise time current pulse through the system, or c) irradiating the structure with a fast changing E-field waveform.

In order to isolate these different driving functions, the McDonnell team has developed a test technique utilizing high voltage arcs²⁴ whose impedances can be adjusted to decouple the aircraft from the external test setup. The transients produced by each driving function are separated in time because of the finite time required for the long arcs to be established. By adjusting the circuit impedances, the transients produced by the rapid voltage changes can be separated from those produced by the current waveform. The extrapolation of transients produced by the current waveform can thereby be firmly related to the current waveform.

The interpretation of transients produced by the voltage function is more difficult and is still under study. The radiated E-field transients can be related to measured E-field changes associated with nearby lightning flashes. In most cases measured, however, those transients are small compared to the transients produced by the direct attachment voltages and currents.

The shock excitation technique highlights various phases of the lightning discharge process. Figure 26 illustrates the sequence of events associated with a long spark discharge to an isolated conductive vehicle correlated with the E-field in the vicinity of the cylinder. Figure 27 shows the differential responses of an internal wire pair to the various changes in the measured E-field. Of particular interest is the observation that the isolated test article becomes charged to the potential of the arc channel at time T_2 . At T_3 , when the leader (or streamers) contact the ground, the charge on the structure quickly discharges to ground, generating a new transient excitation source which is not present in the hardwired case. This excitation source was isolated and measured for the case of the cylinder. It was seen to have a 50 nanosecond rise time and an amplitude of several thousand amps. This fast discharge source was seen to be a major contributor to transients excited on the internal wire pair, but it is difficult to predict the effects of the analogous situation in the natural lightning case. An understanding of all of the phases of the lightning discharge and the response of airframe and avionics system is the focus of continuing research.

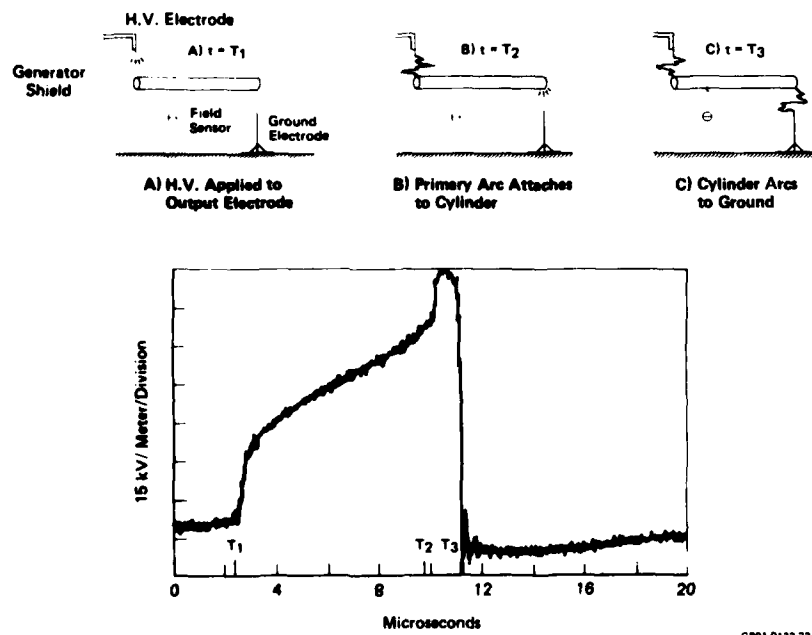
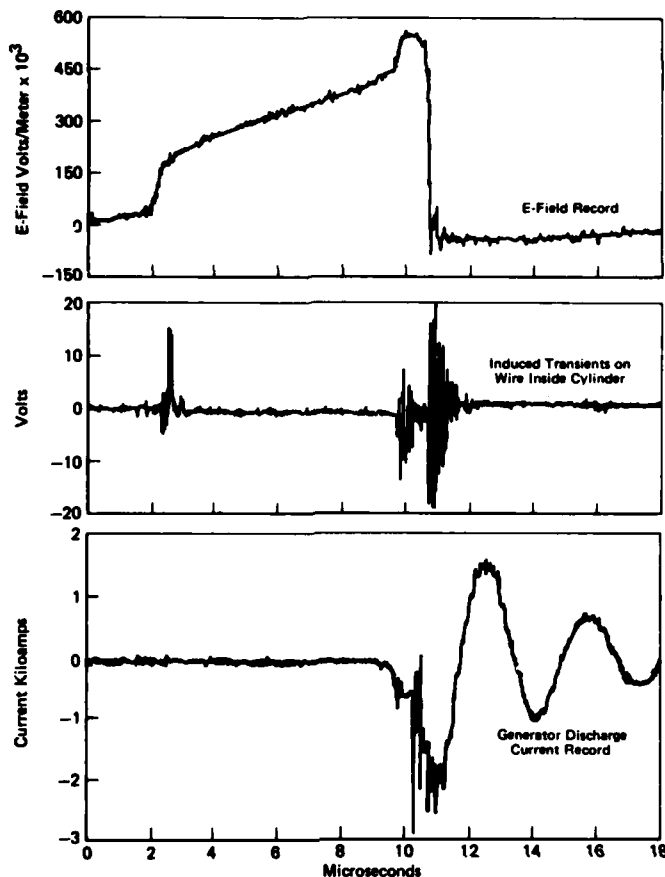


FIGURE 26
E-FIELD RECORD WITH ARC SEQUENCE



GP01-0132-21

FIGURE 27
TIME HISTORY OF TRANSIENT EVENTS

Lightning Electromagnetic Pulse (LEMP) Testing

As discussed in the previous section, transients can be produced on internal wires as a result of nearby lightning strikes. Or, more generally, aircraft resonances can be excited by rapid changes in the ambient E-field. This situation is similar to the nuclear EMP condition except that the frequencies associated with the field change are much higher in the EMP case. Extensive facilities have been developed for testing military systems for NEMP. Although the facilities have not been used for LEMP testing, the technique is well proven and could be adapted for lightning work if necessary.

The question of necessity should be addressed, however. If the aircraft has been protected and tested properly against a direct strike, the need for an LEMP test is questionable. The direct strike case should include the extreme field condition and if a long spark test is conducted on the aircraft, the EMP effects will be covered.

If, however, an existing aircraft which has not undergone high voltage testing is to be operated in a thunderstorm environment, it may be exposed to numerous nearby strikes although it may not be struck directly. In such a case, it may be desirable to conduct an LEMP test, if such a facility were available. The degree to which existing NEMP facilities would have to be modified to generate lightning type fields is not clear at this time.

By way of note, some workers have reported LEMP tests of isolated instrument packages with interconnecting cables in a small chamber. It is not clear that such a test would represent an accurate simulation of the field environment inside an aircraft. However, the test may establish LEMP susceptibility limits of electronic systems for reference to anticipated field threats.

SUMMARY

This lecture has set forth the techniques used to test aircraft avionic and electrical systems for lightning. The discussion has focused particularly on avionics system testing and has therefore not included techniques unique to other subsystems tests such as fuel vapor ignition or swept stroke attachment or damage tests. Simulation facilities and equipment were briefly described with emphasis on instrumentation practices. The techniques for conducting engineering and qualification tests as defined by the modern criteria documents were described, including model attach point testing, high voltage attachment tests on full size hardware, high current damage effects on full size hardware, indirect effects tests of components, and indirect effects on full scale aircraft. The paper concluded with a discussion of new developments in full scale vehicle test techniques.

In conclusion, the tests classified as qualification tests are considered to be well understood and well enough rationalized to be standardized as non-controversial tests. The engineering tests and the new techniques now being developed are subject to more interpretation and debate. It is clear that there is much about the nature of lightning and about the interaction of lightning with aircraft which is not well understood. This is particularly true where the voltage and field changes are concerned and where complex system interactions are involved. Lightning testing is moving from a routine engineering operation to a more sophisticated research and development activity which must be more closely coordinated with the academic studies of the natural phenomenon.

REFERENCES

- ¹NATO (MAS) Standardization Agreement Draft, "Lightning Qualification Test Techniques for Aircraft and Hardware," Draft STANAG 3659 AE, 20 August 1978.
- ²"Lightning Test Waveforms and Techniques for Aerospace Vehicles and Hardware," Report of SAE Committee AE4L, 20 June 1978.
- ³J. Phillpott, "Recommended Practice for Lightning Simulation and Testing Techniques for Aircraft," Culham Laboratory Report CLM-R163, Culham Laboratory, Abingdon, Oxfordshire, U.K., May 1977.
- ⁴D.W. Clifford, E.P. Krider, and M.A. Uman, "A Case for Submicrosecond Rise Time Lightning Current Pulses for Use in Aircraft Induced-Coupling Studies," presented at the 1979 IEEE International Symposium on EMC, San Diego, California, 9-11 October 1979.
- ⁵C.D. Weidman and E.P. Krider, "The Fine Structure of Lightning Return Stroke Waveforms," Journal of Geophysical Research, Vol. 83, No. C12, 20 December 1978, pp 6239-6247.
- ⁶J.D. Craggs and J.M. Meek, "High Voltage Laboratory Technique," published by Butterworth's Scientific Publications, Great Britain, 1954.
- ⁷L.L. Alston, "High Voltage Technology," published by Oxford University Press, Great Britain, 1968.
- ⁸E.H. Schulte, "High Current Lightning Simulation-Waveshape Evaluation," presented at the Eleventh National Conference on Environmental Effects on Aircraft and Propulsion Systems, Trenton, N.J., May 1974.
- ⁹A.W. Hanson, "Techniques of Strike Tests on Structures, Components and Materials," presented at the 1975 Lightning and Static Electricity Conference, Culham Laboratory, England, April 1975.
- ¹⁰D.W. Clifford, "Scale Model Lightning Attach Point Testing," presented at the 1975 Lightning and Static Electric Conference, Culham Laboratory, England, April 1975.
- ¹¹J. Phillpott, P. Little, E.L. White, et-al, "Lightning Strike Point Location Studies on Scale Models," presented at 1975 Lightning and Static Electricity Conference, Culham Laboratory, England, April 1975.
- ¹²J.A. Plumer, "Laboratory Test Procedures to Determine Lightning Attachment Points on Actual Aircraft Parts," Proceedings of the Conference on Certification of Aircraft for Lightning and Atmospheric Electricity Hazards, ONERA-Chatillon, France, September 1978.
- ¹³A.W. Hanson, "Laboratory Tests to Determine the Physical Damage (Direct Effects) caused by Lightning (Qualification Test)," Proceedings of the Conference on Certification of Aircraft for Lightning and Atmospheric Electricity Hazards, ONERA-Chatillon, France, September 1978.
- ¹⁴D.W. Clifford, "Laboratory Simulation of Swept Strokes (Engineering Test)," Proceedings of the Conference on Certification of Aircraft for Lightning and Atmospheric Electricity Hazards, ONERA-Chatillon, France, September 1978.
- ¹⁵P. Little, "Laboratory Simulation of Swept Strokes (Engineering Test)," Proceedings of the Conference on Certification of Aircraft for Lightning and Atmospheric Electricity Hazards, ONERA-Chatillon, France, September 1978.
- ¹⁶D.W. Clifford, "Laboratory Tests of Undesired Conducted Currents and Surge Voltages caused by Lightning (Qualification Test)," Proceedings of the Conference on Certification of Aircraft Lightning and Atmospheric Electricity Hazards, ONERA-Chatillon, France, September 1978.
- ¹⁷B. Burrows, "Laboratory Tests of Undesired Conducted Currents and Surge Voltages caused by Lightning (Qualification Test)," Proceedings of the Conference on Certification of Aircraft for Lightning and Atmospheric Electricity Hazards, ONERA-Chatillon, France, September 1978.
- ¹⁸L.C. Walko, "A Test Technique for Measurement of Lightning Induced Voltages in Aircraft Electrical Circuitry," 1972 Lightning and Static Electricity Conference, USAF Report AFAL-TR-72-32, December 1972.
- ¹⁹W. McCormick, K.J. Maxwell, and R. Finch, "Analytical and Experimental Validation of the Lightning Transient Analysis Technique," Air Force Report AFAL-TR-78-47, March 1978.
- ²⁰L.C. Walko and J.G. Schneider, "Full Scale Lightning Test Technique," presented at the FAA/NASA Symposium on Lightning Technology, Hampton, Virginia, April 1980.
- ²¹B.J. Burrows, "Induced Voltages in Full Size Aircraft at 10^{11} A/S," Proceedings of 1977 IEEE International Symposium on EMC, Seattle, Washington, August 1977.
- ²²D.E. Young, and L.D. Piszker, "The Use of CW Tests and Analysis Techniques in Lightning Vulnerability Assessment of Aircraft Systems," Proceeding of FAA/Georgia Tech Workshop on Grounding and Lightning Protection, Atlanta, Georgia, May 1978.
- ²³D.W. Clifford and K.S. Zeisel, "Evaluation of Lightning Induced Transients in Aircraft Using High-Voltage Shock Excitation Techniques," 1979 IEEE International Symposium on EMC, San Diego, California, October 1979.

THE COUPLING OF LIGHTNING FIELDS

INTO AIRCRAFT AND CABLES

P.F. Little
Culham Laboratory
Abingdon, Oxfordshire
England

S U M M A R Y

The current distribution in the skin of an aircraft struck by lightning is described and the effects of airframe resonances are noted. Nearby strikes produce initially an electromagnetic pulse which is scattered by the aircraft, creating circulating currents in the skin: this process is considered. The magnetic fields at the surface diffuse into the skin, and significant currents flow on the interior after a time lag dependent on the skin resistivity. In addition, the surface fields couple directly into the interior through breaks in the conducting skin or through insulating panels. Methods of calculating the magnetic and electric fields in the interior of the aircraft are discussed, and the effects on electrical and electronic systems described. The screening of internal cabling is reviewed.

1. INTRODUCTION

The effects of lightning arise either through a direct strike or a nearby strike which does not attach to the aircraft. In the first case, the total current flow is determined. In the second, an electromagnetic pulse (EMP) of radiation is scattered by a complex conductor, so that E-fields and B-fields are initially given and currents must be derived.

In a direct strike to an aluminium-alloy skin of normal thickness the initial fast pulse of current flows only on the outer surface of the skin, because a significant time is required for the current to diffuse into the skin. The penetration time is much less for materials of poorer conductivity such as carbon-fibre composites, titanium or stainless steel. Larger peak currents appear on the inner surface of such skins causing larger resistive voltages there. Apertures or breaks in a highly conducting skin allow the magnetic field of the surface current itself to enter the interior of the aircraft, so that around cockpits, radomes, bay doors, etc., fast-changing magnetic fields can induce voltages in the electrical circuits present. Considerable insight into the processes occurring can be obtained in a two-dimensional analysis, assuming that the conductor cross-sections are constant along its length. This is an approximate representation of many fuselage and wing sections which will be considered here.

By ignoring the length of the conductor all resonance phenomena dependent on the length are ignored. Streamers appearing before attachment, leader pulses, parts of the return stroke, and intracloud discharges can create current pulses with high-frequency components capable of exciting resonances in aircraft wings and fuselage ($f > 2\text{MHz}$ approximately). The longitudinal current distribution must be superimposed on the distribution around the periphery to obtain a full description of the surface currents. The amplitude of the resonance currents will be affected by the impedance of the attached arc channel in a direct strike, but both direct and indirect discharges can be analysed by numerical methods developed for the problem of the nuclear EMP scattering. The approaches to this problem will be reviewed, and some examples given of applications to lightning problems in actual aircraft.

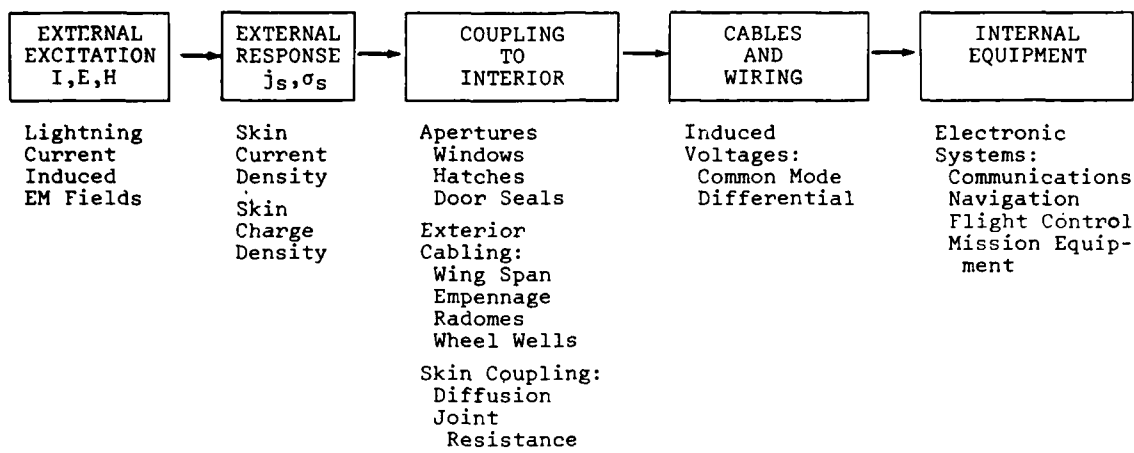
Whatever the mode of excitation of the structure as a whole, the penetration of electric and magnetic fields of a given frequency into a given aperture is independent of the remote field pattern. The surface currents and charges in the immediate vicinity, estimated from the solution to the general problem, can be used to obtain accurate solutions to two-dimensional problems or for small apertures. Simple cavities can be treated in detail over a wide frequency range, but practical examples generally are complex. Approximate methods of treating the coupling problems are considered.

Once the fields in the interior are defined, the effect on cables and wiring can be calculated. Methods of reducing the disturbances produced in the circuits are reviewed, and the importance placing the cable runs to best advantage is emphasised.

If dielectric coverings are punctured, it is possible for lightning to attach directly to aeriels or radar equipment, so injecting current immediately into the electronic system. Damage to a pitot may also permit direct injection of current into the electrical system. Even without structural damage, cables leading to the exterior of the aircraft enter a region of rapidly-changing magnetic field, and voltages may be induced in the circuits connected to them. All cable entry points present special hazards.

An overall view of the way in which interference due to lightning couples into aircraft circuits is given in Table 1, adapted from Corbin (1978).

TABLE 1



We are concerned here with the central three boxes of this table. The lightning sources, and the response of the equipment, are dealt with in other lectures.

Appropriate test procedures are discussed also in another lecture, but some of the requirements which testing procedures must satisfy are briefly surveyed here.

2. DISTRIBUTION OF CURRENTS IN CYLINDRICAL STRUCTURES

Although all aircraft fuselages and wings vary in cross-section along their length, the variation in a distance equal to the diameter is often small. To regard any section as a cylinder of uniform cross-section is then a good approximation, provided that resonances along the total length are not important. This is frequently true for lightning interactions with aircraft. We may obtain some insight into the behaviour of the aircraft from an analysis of a hollow cylindrical structure of appropriate cross-section. First we assume that the skin of the aircraft is continuous, and then treat the effect of apertures (slots) assuming that cavity resonances may be ignored.

2.1 Cylindrical Structures with Continuous Skins

Consider a hollow circular cylinder of metal, having a wall thickness h and diameter D . If this cylinder carries a step function current of amplitude I_0 Evans (1975) has shown that the field E at some point distant x from the inner surface within the tube wall is given by

$$E(t) = \frac{I_0 \rho}{\pi D h} \left[1 + 2 \sum_{n=1}^{\infty} \left(\frac{-1}{e^{t/T_M}} \right)^{n^2} \cos \left(\frac{n\pi x}{h} \right) \right] \quad (1)$$

where ρ is the metal resistivity and

$$T_M = \frac{\mu_0 h^2}{\pi^2 \rho} = 1.27 \times 10^7 h^2 / \rho \quad (2)$$

assuming that the relative permeability of the metal is unity. The form of $E(t)$ and the surface current on the inner surface ($x=0$) is given by the term in square brackets in (1) if the cosine term is omitted. Figure 1 shows the result (Burrows 1975). A delay occurs before the value of $E(t)$ rises in a time dependent on T_M .

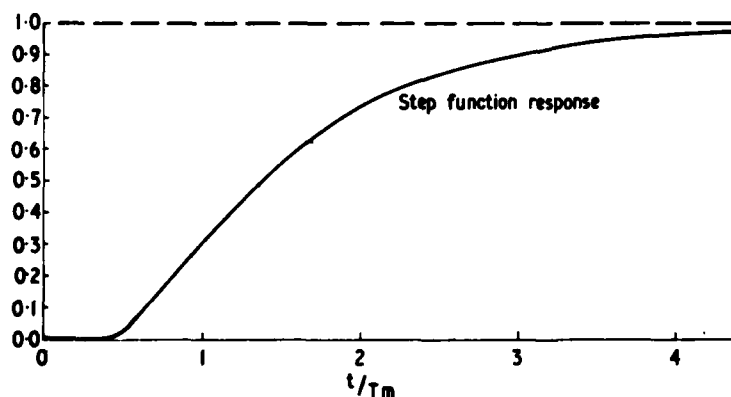


Figure 1

E-field on
inner surface
(step function
current)

For typical aluminium alloy 2mm thick $T_M \approx 10\mu s$. The E-field and the corresponding currents on the inner surface of an aluminium tube rise and fall much more slowly than the current pulse generating them. The peak amplitude appears at $t \approx 6 T_M$ or about $60\mu s$ in our example.

A current pulse of width less than T_M would obviously be much attenuated by such a tube, which would act as an excellent screen. For any waveform $I(t)$ the diffusion response $f(t, I(t), T_M)$ is given by

$$f(t, I(t), T_M) = \frac{d}{dt} \int_0^t E(t-\tau) I(\tau) d\tau \quad (3)$$

where $E(t)$ is the response to a step function defined by (1). From (3) the response to any waveform may be computed. Lightning current waveforms with rise times T_r of $5\mu s$ at most (first return stroke) are heavily attenuated because $T_r < T_M$.

Any other cross-section than circular is best analysed numerically to determine the current distribution around it. A finite-difference code that solves Laplace's equation with arbitrary boundary shapes can be applied (Thomas 1974) for example to an idealised wing geometry (Burrows 1975). Figure 2a shows the magnetic flux surfaces around such a 'wing' at $t \ll T_M$ when no skin penetration has occurred. The lines drawn are also the field lines, and the distance between the nearest line and the surface is inversely proportioned to the magnetic field strength, which in turn determines the surface current density J_s . Obviously the greatest value of J_s occurs at the sharp edge.

At times $t \gg T_M$ with a slowly falling current pulse the current will penetrate completely into the skin. It will then redistribute itself around the wing profile so that the current density is uniform, as in the steady state dc case. To do this, flux must penetrate into the surface of the wing, as shown in Figure 2b, and this makes the redistribution time very long in large structures of aluminium alloy.

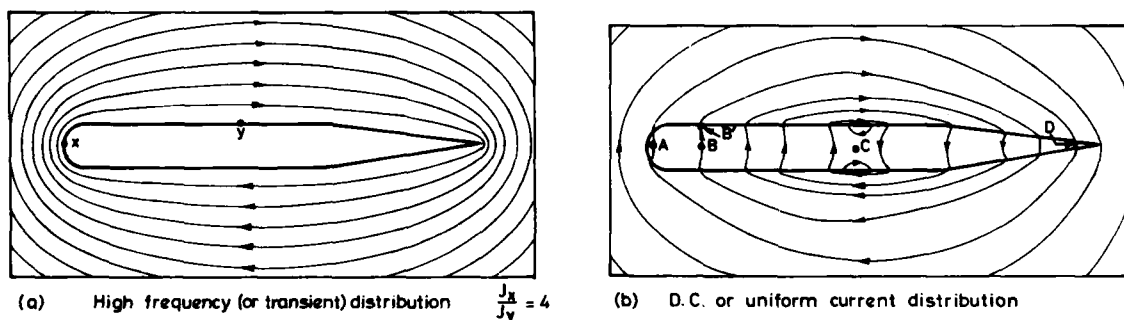


Figure 2 Magnetic flux contours (field lines) around an idealised wing.

If a wire parallel to the wing is positioned within it at points such as A, B, C, D and attached to one end-cap of the wing, the signal on the wire for times much less than the redistribution time is a measure of the E-field along the interior surface. Similar measurements can be made on a circular tube with the same known current pulse shape and in each case the response has the same form initially (Burrows 1975). The amplitude seen with the circular tube agrees with the calculated value using equation (3), and the variation in amplitude seen inside the wing is in accordance with the variation in the skin current around the wing at early times. After about $200\mu s$ significant flux penetration appears, and after about $10ms$ approximately dc conditions are established in an aluminium wing $0.8m$ wide and $0.08m$ in thickness, with a $2mm$ skin.

A calculation of the penetration time τ of a uniform magnetic field perpendicular to the axis of a circular tube (Khalafallah 1974) provides an estimate for the redistribution time of currents in non-circular conductors. If $h \ll D$ we have

$$\tau = \frac{\mu_0 D h}{4 \rho} \quad (4)$$

For a thin-walled tube of any cross-section having a total cross-sectional area A and a perimeter P it would be consistent to use

$$\tau = \frac{\mu_0 A h}{P \rho} \quad (5)$$

For the wing configuration used we find $\tau = 3.4ms$, compatible with the redistribution time observed.

The transient distribution of Figure 2a may be thought of as inductively-determined and the dc distribution of Figure 2b as resistively-determined. An alternative way of deriving the transient distributions is to represent the body by a series of long straight filaments of circular cross-section. Then we may calculate the self-inductance of each filament, and the mutual-inductance between each pair. Since the voltage across each is the same, a matrix equation can be set up and solved to give the current distribution. Results virtually identical with those obtained by the finite-difference scheme can be obtained by this finite-element approach (Burrows 1979). Using a filamentary representation removes the need to specify outer boundaries.

The arguments above apply to titanium, stainless steel or carbon-fibre reinforced plastics (CFRP). These have similar, relatively low, conductivities: for CFRP $\rho = 4 \times 10^{-5} \Omega\text{-m}$ compared to $4 \times 10^{-8} \Omega\text{-m}$ for typical aluminium alloys. A 2mm skin of CFRP has a penetration time constant $T_M = 13\text{ns}$ approximately, so that typical return stroke current pulses penetrate quickly. The redistribution time constant τ would be $3.4\mu\text{s}$ for the idealised wing structure of Figure 2(a) in CFRP, so that a resistively dominated current distribution would appear with a first return stroke (rise time $5\mu\text{s}$). The potential along the inner surface would then follow the current pulse waveform, as in a resistor. In practical structures thicker strengthening spars of CFRP, or metal spars, are normally included, and current will redistribute into these areas in times of order $1\mu\text{s}$.

If a tube is made of metal that is a good electrical conductor with a strip of CFRP forming part of the wall, it can be shown that the flux ϕ_D diffusing through the CFRP creates induced voltages $d\phi_D/dt$ of the same form as the resistive voltage along the CFRP strip. These voltages appear in loops within the structure. They are greatest for loops near to the CFRP, and least for those near to the metal wall. They may be as large as the resistive drop along the inner surface of the CFRP strip. The same general conclusions hold also for induced voltages beneath a CFRP panel mounted on the metal skin of an aircraft. The finite length of the panel and the complex form of the cavity beneath it affect only the spatial dependence of the amplitude (Burrows 1980).

All this discussion has related to a direct treatment in the time domain. It is possible to use Fourier analysis and work in the frequency domain. The electric field $E(\omega)$ on the inside of the skin is related to the current density $J_S(\omega)$ on the outer surface by the transfer impedance $Z_T(\omega)$:

$$\frac{E(\omega)}{J_S(\omega)} = Z_T(\omega) = \frac{\eta}{\sinh(\gamma h)} \quad (6)$$

where η is the intrinsic impedance of the wall material ($\eta = \sqrt{j\omega\mu_0\rho}$) and γ is the propagation constant ($\gamma = \sqrt{j\omega\mu_0/\rho}$). For small values of ω ($\omega < \rho/\mu_0 h^2$) $Z_T = \rho/h$ is purely real (resistive). This condition is met at lightning frequencies by CFRP skins of normal thickness: it is equivalent to requiring $\omega T_M < 1/\pi^2$. Hence for such skins E on the inner surface is predicted to be in phase with J_S , as seen in the experiments above. The same would be true for thin titanium or stainless steel skins. For aluminium alloy skin Z_T is complex and time-lags are predicted between E and J_S , as observed. J_S will vary around non-circular cylinders as discussed above.

2.2 Apertures in Current-Carrying Cylindrical Structures

Apertures, which take the form of slots in cylindrical geometry, allow the main external flux to couple into the interior of the hollow conductor. The fast changes in flux induce voltages proportional to dI/dt in loops within the cylinder, rather than voltages dependent on the resistive potential gradient in the wall or on flux which has diffused through the wall, as discussed in Section 2.1 for cylinders without any slots. It is assumed that the flux changes are not fast enough to excite any cavity resonances.

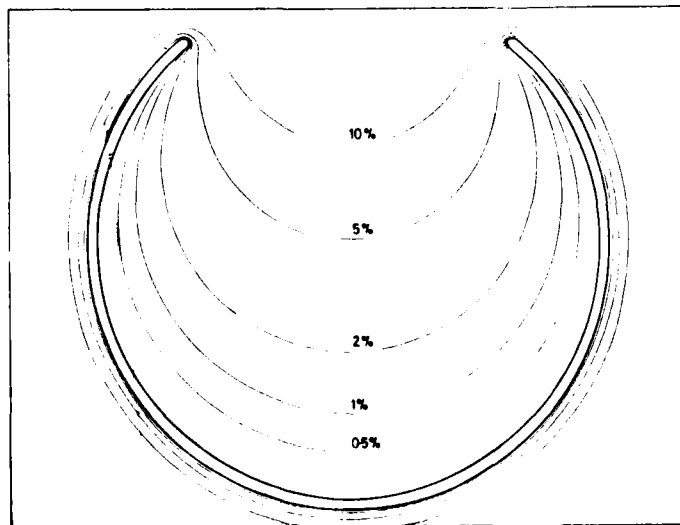


Figure 3

Flux surfaces
(field lines)
around a slotted
cylinder

The flux surfaces around a cylinder with a slot in it are shown in Figure 3. The surfaces are labelled according to the percentage of the total flux around the cylinder that appears between the cylinder and the surface. The flux outside the surface gives the ratio of the mutual inductance M for a wire at a point to the self-inductance L of the cylinder. For aircraft circuits the flux between a wire and the cylinder is important: this is given by the transfer inductance for fast-flux coupling

$$M_{TF} = L - M \quad (7)$$

For times small compared to T_M the flux does not penetrate the metal at the edges of the slot, but the effective width of the slot increases on the time-scale of the redistribution time τ . The value of L appropriate to high frequencies is needed in (7). Obviously a loop near the bottom will experience voltages about two orders of magnitude less than a similar loop near the edges of the slot. These voltages can be very large: wires in the vicinity of the slot could experience fields of 5kV/m along their length if $dI/dt = 100$ kA/ μ s.

Similar plots have been made for models of a gap at the trailing edge of a wing, with and without a central conductor, and for slots at the mid-chord of a wing (Figure 4, Burrows 1975). Correction factors to allow the calculation of voltages in slots of finite length are also given in that paper, so that voltages due to gaps down to 2mm length can be predicted. These factors are experimentally determined. The effects of cover plates are discussed.

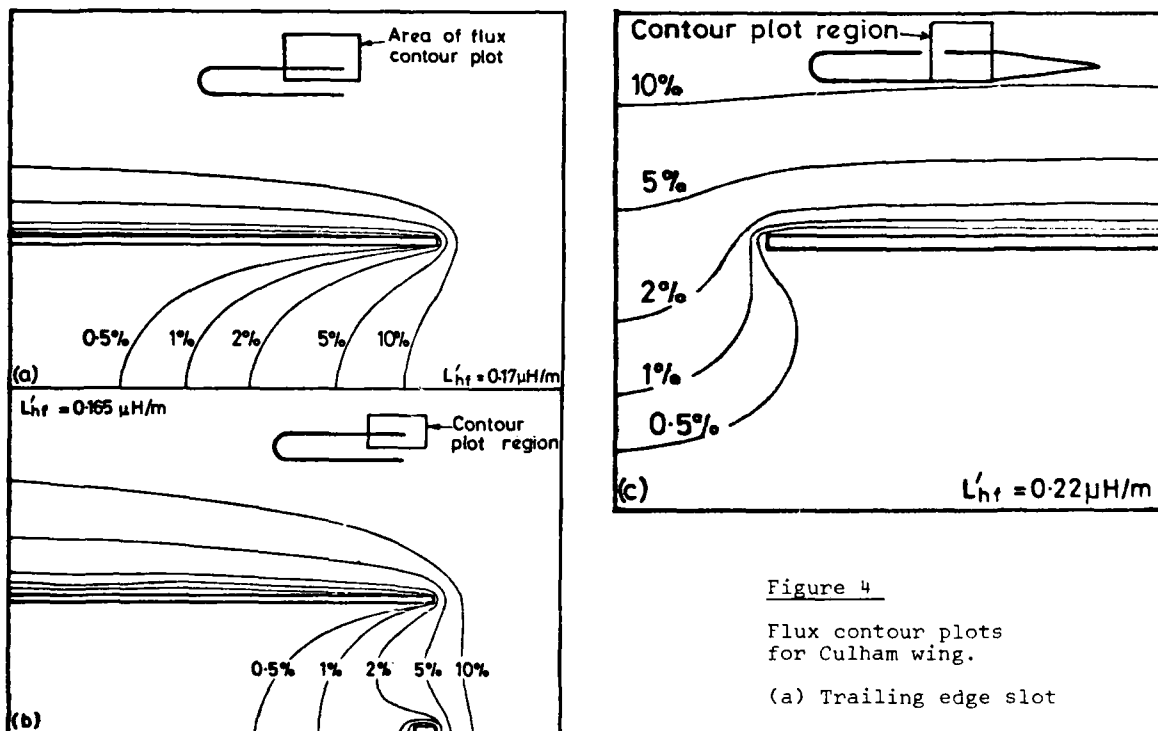


Figure 4

Flux contour plots
for Culham wing.

- (a) Trailing edge slot
- (b) As (a) with central conductor
- (c) Mid-chord slot.

3. SKIN CURRENTS IN COMPLEX STRUCTURES

3.1 Currents Induced by Incident EM Radiation

Early analytical work on the scattering of electromagnetic waves was carried through by frequency domain solutions. Scattering by perfectly conducting spheres and other simple geometric forms (see for example Born and Wolf 1959) was treated as a boundary value problem. With the advent of high speed digital computers integral-equation techniques allowed solutions in the frequency domain to be obtained for scattering from many bodies of arbitrary shape. Later time-domain solutions were developed. Either integral forms of Maxwell's equations or the equivalent differential equations can be solved directly in the time domain by numerical methods. Two types of integral equation have been derived for perfectly conducting scatterers, depending on which boundary condition is applied (either to the E-field or to the H-field at the scattering body). Bennett and Ross (1978) review this work and give many references.

The choice of approach depends on the problem and on available computing resources. The solution of Maxwell's equations in their differential form by finite-difference methods is a boundary-value problem, and resonances within the scattering body (defining one boundary) must be carefully treated. The integral equation using the E-field boundary condition is found to be well-suited to handling thin wires and open thin surfaces (plates). The integral equation using the H-field boundary condition finds difficulty in handling wires but is well-suited for problems involving closed conducting bodies. For complex shapes like aircraft, a combination of the integral equations can be applied to deal with wire aeriels or struts protruding from a closed structure.

All these types of solution have been used to compute NEMP scattering by aircraft. Further details may be found in the Special Issue (1978) of the IEEE Transactions on Antennae and Propagation, and in the US Air Force Weapons Laboratory Interaction Notes on EMP. The IEEE International Symposia on EMC should also be consulted.

One simple point can be deduced from the formulation of the magnetic integral equation. The skin current density J induced at a point on the surface includes a term $2\mathbf{n} \times \mathbf{H}_1$, where \mathbf{n} is the outward normal at the scattering surface and \mathbf{H}_1 is the field of the incident wave. The greatest value of the term is clearly $2H_1$. This is the source term, directly due to the incident wave, and it is supplemented by the effects of surface currents elsewhere on the scattering body. These however will tend to cancel out except near resonances, and thus at low frequencies the maximum skin current J_{\max} is

$$J_{\max} \approx 2 H_1 \quad (\text{A/m}) \quad (8)$$

For a pulse of radiation whose peak energy appears at a frequency below the lowest resonance of the structure this would be an approximation for J_{\max} . It is appropriate for LEMP hazards as a guide.

If a circular cylinder is illuminated by EMP radiation with the H-field perpendicular to the axis, the skin current flows in one direction up the side illuminated and down the shadowed side. This current follows the waveform of the H-field applied and its current densities will be about $2H_1$. In addition body resonances will be excited if the EMP contains appropriate frequencies. These current oscillations are superimposed on the currents in phase with the source, but at the boundary between the shadow and the illuminated side only the body resonance term exists because $\mathbf{n} \times \mathbf{H}_1 = 0$. Long, thin cylinders show the most marked resonances.

3.2 Currents Caused by a Direct Strike

These can be analysed by representing the lightning channel in the same type of way as the aircraft, according to the method of solution proposed. The driving source is modelled with appropriate impedance, and if the differential equations are to be solved, geometrical boundary conditions must be imposed. If the electric field integral equation is to be used, the lightning channel must be represented by wires connected to the wire-grid model of the aircraft; and similarly closed surfaces would be employed if the magnetic field integral equation were used.

These techniques can be employed also to model lightning simulation tests on the ground. It is an extension of the technique of representing the aircraft as part of a transmission line, where much simplification is necessary and little information about the current distribution in the skin can be obtained (Fisher and Plumer 1977).

Some examples of codes applied to LEMP and direct strike studies are given in the next sections.

3.3 The Differential Equation Approach

A solution of Maxwell's differential equations in the time domain by a finite-difference method was developed by Yee (1966) for initial boundary value problems. Merewether applied this to NEMP scattering bodies of revolution (1971) and it was later extended to three-dimensional problems by Holland (1977). An application of this finite-difference code THREDE to an all-composite design concept for an aircraft is described by Perala et al (1979). They study the effects of lightning on the Advanced Design Composite Aircraft (ADCA) for both attached strokes and LEMP. It is a very complex structure about 18m long (Figure 5).

For the NASA Space Shuttle model (1973) of the return stroke current pulse Perala et al noted that the Fourier spectrum is 80 dB down at the principal aircraft resonances near 6 MHz so that resonance phenomena should not be prominent. The results of a THREDE computation with a faster pulse (250ns rise and fall time) indeed show that the current waveform is substantially independent of position. The computed amplitudes can be used for the slower (2μs rise time) lightning current model with confidence, for resonance phenomena are much less likely to appear with this slow pulse.

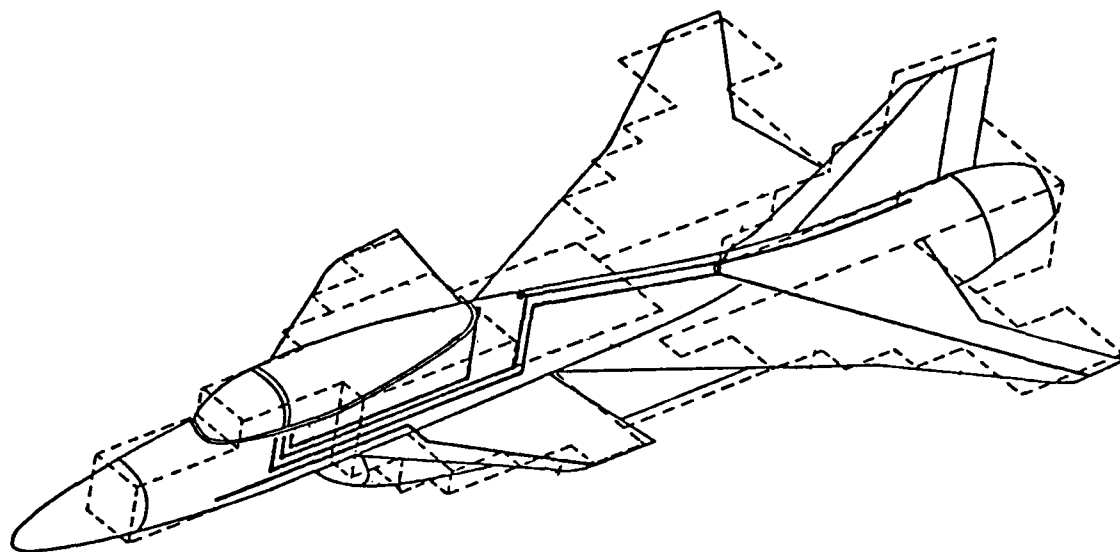


Figure 5. Overlay of the THREDE mathematical model and the structural outline of the ADCA.

The channel attachment as simulated in this computation is shown in Figure 6. The source impedances represent typical values for lightning channels (Wagner and Hileman 1962). The ground plane return distorts the current distribution around the fuselage, and an approximate correction is applied when interior coupling to cables is considered. The voltage waveform predicted on interior cables follows the applied current waveform, as expected from the discussion of CFRP cylinders in Section 2.1. For the 200kA pulse the worst case computed gives 4.7kV on one cable for the open-circuit voltage, and 2kA for the short-circuit current. The methods of calculating the coupling from skin-currents into cables will be discussed later).

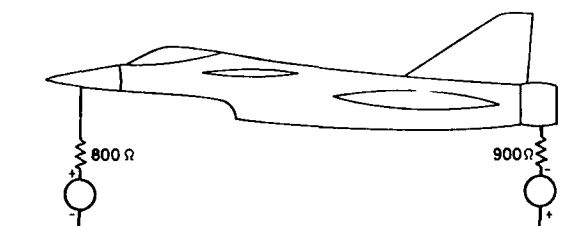


Figure 6. THREDE simulation of a direct lightning strike

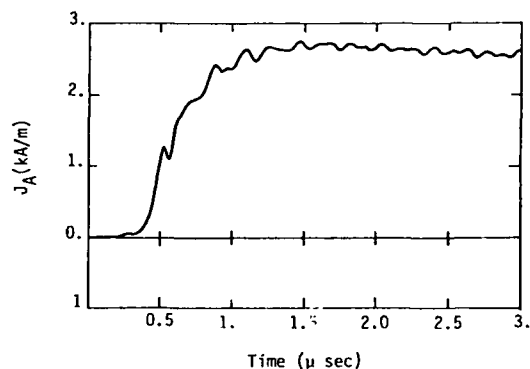


Figure 7. Axial current density on the top of the fuselage (LEMP).

The LEMP from stepped leaders and return strokes is also computed, but the former cause only about 10V signals and is considered negligible. The return stroke is represented by the transmission-line model of Uman, which assumes a very high velocity of 2.4×10^8 m/s along a 4km channel. A double exponential current pulse of 200kA amplitude flows, and the stroke is assumed to be as close (20m) as the length of the aircraft - a very pessimistic assumption. Horizontal E-fields of 800kV/m result.

When incident from the top, the axial current density in the skin of the fuselage is found to be almost 3kA/m. Figure 7 shows the waveshape, which is predominantly of the same form as the incident field with a high-frequency component due to a dipole mode of oscillation added. The skin current would be expected to be proportional to the incident wave field strength. However, at the side, at the shadow boundary, only the dipole resonance mode appears because the incident field H_1 is perpendicular to the metal surface and $\underline{n} \times \underline{H}_1 = 0$ (see Section 3.2).

On the same cable as before, the peak voltage due to LEMP was 1kV and the peak short-circuit current 180A, compared to 4.7kV and 2kA for the severe direct strikes. A computation on the effect of a thin coating of flame sprayed aluminium suggests that these LEMP values would be reduced by a factor 5 by the coating, a useful reduction in the hazard.

Although results are obtained for direct strikes and for LEMP from nearby strikes, it should be noted that the slow direct strike lightning current model cannot be analysed directly. THREDE can compute only about 10^3 time points without instability, and the intervals i.e. the time-steps between these points are determined by the grid size used. This allows only about 1 μ s computing time for this problem, even though THREDE is a highly developed code. Moreover, it is definitely not a user-oriented code. The data input, debugging procedures and the overcoming of numerical instabilities require specialist skills. The same comments apply to most other scattering codes also.

Finite element techniques are being developed (Mei 1974) but have not yet been applied to aircraft.

3.4 The Electric Field Integral Equation

Both time domain and frequency-domain solutions have been obtained for this equation, some of which are summarised by Bevensee et al (1978). The approach is appropriate to stick models, or to wire grid models. Figure 8 shows the model of a Learjet used by Strawe et al (1978) with the WIRANT code.

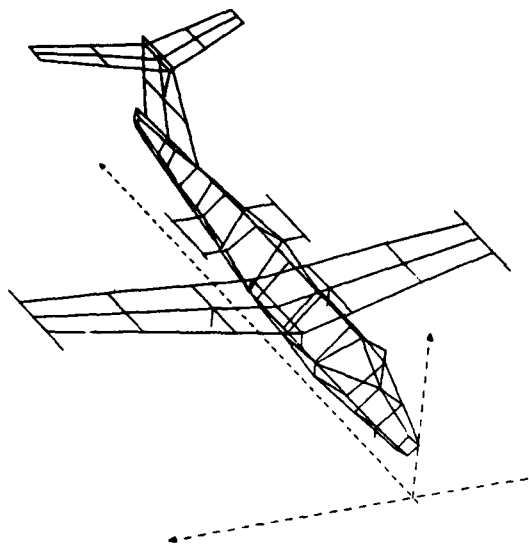


Figure 8. WIRANT model of Learjet.

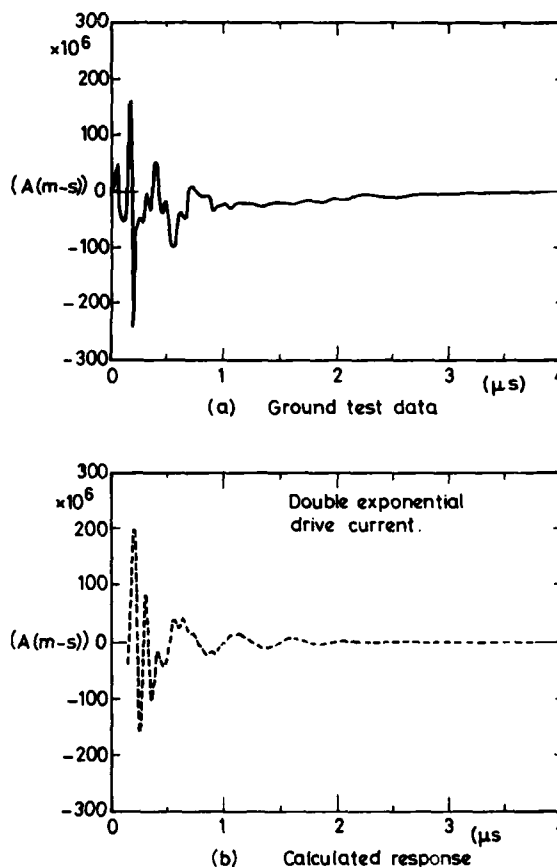


Figure 9. Right wing sensor skin current density (time derivative).

Diffusion through the metal skin is ignored here, because much stronger fast-flux coupling through breaks in the skin is possible: gaps exist around flaps, windows, ailerons etc. Skin currents and surface charges are sources of induced voltages and currents in the aircraft cabling, which are treated as multiwire transmission lines (Strawe 1972). The detailed models of the penetration mechanisms are described, and references given for the analytical treatments. Circuit models as used in NEMP are applied in this work to assess the LEMP hazard to the electronic equipment on the aircraft.

The Learjet is modelled as a wire grid (see Figure 8) to represent a lightning strike in flight but as a stick model for a lightning simulation test on the ground, because the power supply and return conductors must be represented and the number of equations that can be handled is limited.

The test current waveform actually used is reproduced well by a double-exponential waveform and better by a triple-exponential. A comparison of the surface current observed by dH/dt sensors on the aircraft with those predicted from the currents in the wires show good agreement for amplitude, and in the general character of the response. Figure 9 shows measured and calculated time derivatives of the skin current density at the aft body sensor. Some high frequency behaviour is not reproduced because details are not well modelled. The power supply cables influence the resonance response of the cables within the aircraft, and internal battery power is recommended for future tests.

Strawe (1978) also made calculations using WIRANT on a hypothetical all-composite F-18 aircraft, and obtained results consistent with those of Perala described in Section 3.1, though for different conditions. He obtained very high values, up to 32kV on one cable.

The stick model obviously has poor geometrical resolution and azimuthal variations cannot be included. Circumferential currents cannot be computed nor, in the scattering problem, the source term ($2n \times H_1$). Better resolution is obtained with the wire grid model, but the results are sensitive to the radii chosen for the grid wires. Care is needed in interpreting the wire currents and charges in terms of surface currents and charge densities, and large computer store size is needed. For example, the NEMP code CHAOS3 (Garthwaite and Armour 1978, 1980) operates in the frequency domain with about 750 wire segments, which allows the use of about ten wires per wavelength around the perimeter of a fuselage. The code has been tested against the analysis of simple geometries, by comparison with experiments on actual aircraft, and by comparison with other computational approaches. The accuracy achieved is 30-40%. The limitations of wire-grid modelling have been discussed by Lee, Marin and Castillo (1976), and their requirements are partially met in CHAOS by making the total surface area of all the wires equal to the surface area being represented. This makes the mesh inductance approximately the same as the aircraft inductance. Field penetration with 10 wires per wavelength is sufficiently small. Some problems with capacitance remain, and larger aircraft would be more difficult to model. The code has not been applied to lightning hazards but this should present no great difficulty.

3.5 The Magnetic Field Integral Equation Approach

This has been formulated in the time domain (Perala 1974) and the frequency domain (Sancer et al 1976). Only the latter has been applied to aircraft, making use of cylinders of elliptical cross-section to model wings and fuselage. No application to LEMP has been made, and adding a current injection scheme in order to represent an attached stroke is not trivial. This approach assumes perfect electrical conductivity and cannot take account of the resistance of the aircraft.

3.6 Miscellaneous Techniques

Hybrid methods in which electric field integral equations are combined with the magnetic field integral approach are known (Bennett and Ross 1978, Bevensee et al 1978). None have been applied to LEMP problems. An analytical approximation to the electric field integral equation has been applied to a simple six-stick model of an aircraft, (Bedrosian 1977). This results in a relatively simple programme which could be used by non-specialists. It has not been applied to lightning problems as yet.

Another class of solutions rely on geometrical scattering theory. These would not be useful for lightning problems, for they apply when the wavelengths being scattered are much smaller than the dimensions of the scattering body.

Bevensee et al (1978) give a large number of references to EMP codes in general and others are quoted by Bennett and Ross (1978). The US AFWL Interaction Notes on EMP should be consulted for more recent information.

3.7 Fourier Spectra of Lightning Currents and Fields

The excitation of resonances on the outer surface of an aircraft is likely to be much less for LEMP than for NEMP because of the lower frequencies in the former. The near-field LEMP from a severe lightning stroke as calculated by Perala et al (1979) from a model by Uman is shown in Figure 10 together with an approximate analytic representation of the form

$$\frac{E}{E_0} = \frac{e^{\alpha t - e^{\beta t}}}{1 + e^{-\nu}} (t - t_0) \quad (10)$$

where

$$\alpha = 4 \times 10^4, \quad \beta = 2.5 \times 10^6, \quad \nu = 1 \times 10^7, \quad t_0 = 4 \times 10^{-7}.$$

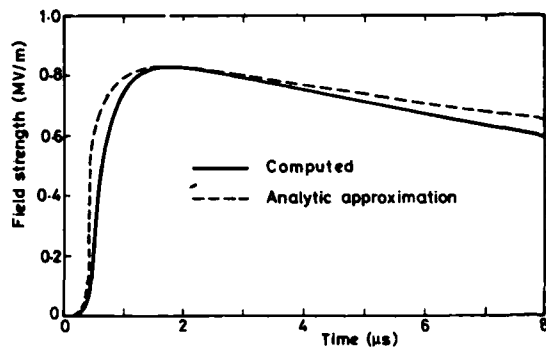


Figure 10.

Computed LEMP at 18m from lightning channel compared with analytic approximation.

The analytic expression exaggerates the high frequency content, but the Fourier spectrum of the LEMP approximation does not extend nearly as far as a typical NEMP, which can be represented by a double exponential.

$$\frac{E}{E_0} = e^{-\alpha t} - e^{-\beta t} \quad (11)$$

where $\alpha = 4 \times 10^4$, $\beta = 4 \times 10^8$

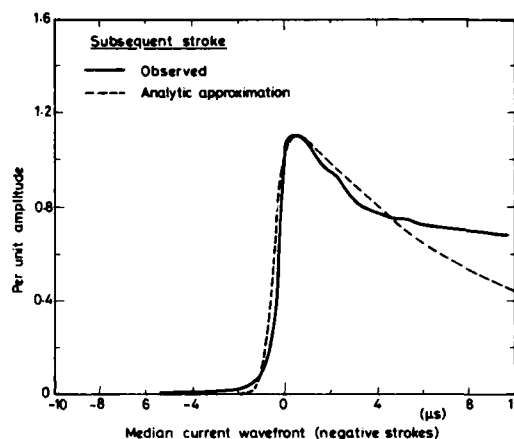
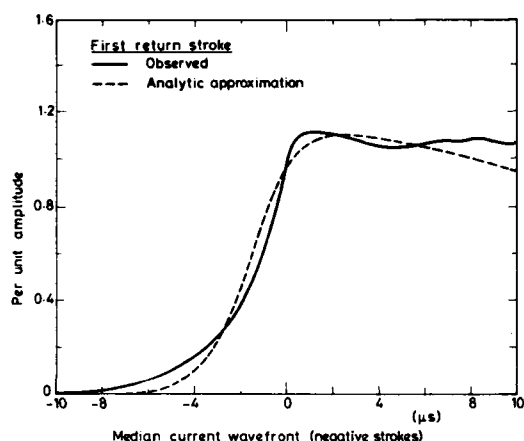


Figure 11. Observed median current waveforms compared with analytic approximations for (a) first (b) subsequent strokes.

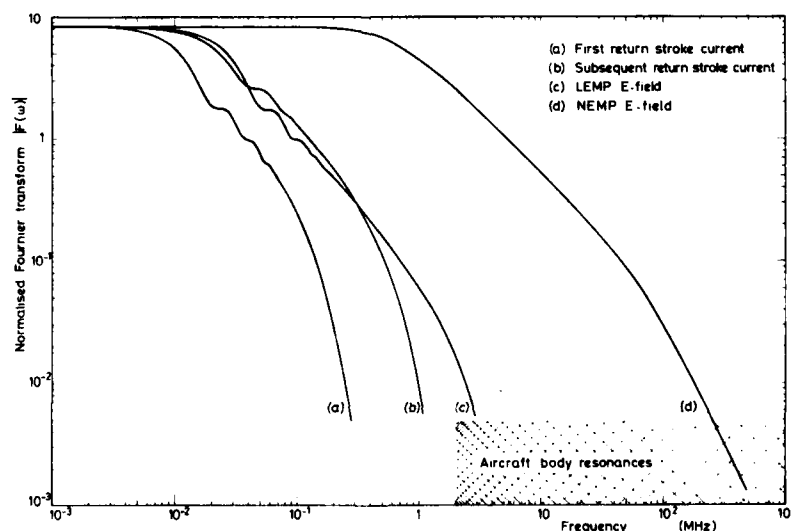


Figure 12. Fourier spectra of analytic approximations to lightning fields and currents.

The two spectra are compared in Figure 12. Aircraft resonances lie above about 2MHz even for large aircraft, as shown in the figure.

It is interesting to compare the LEMP spectrum with that of the current themselves. Figure 11(a) compares the median current waveform for the first return stroke with a representation of the same form as (10), where

$$\alpha = 2 \times 10^4, \beta = 7 \times 10^6, \nu = 5 \times 10^6, t_0 = 7.5 \times 10^{-6}$$

Figure 11(b) compares the median current in subsequent strokes with a similar analytic expression, where

$$\alpha = 1 \times 10^5, \beta = 2 \times 10^6, \nu = 2 \times 10^6, t_0 = 1.5 \times 10^{-6}.$$

The Fourier spectra of the analytic approximations to the current forms is given in Figure 12. The frequency range is again much less than that for NEMP.

It should be noted that even in return strokes the median current waveforms and the LEMP waveforms calculated from models of the return stroke omit much detail. Higher frequency components appear at the peak of the current pulse, and branching adds complexity to the pulse shape. The twisted shape of the channel will further modify the radiated waveform. Other phases of the flash, such as the leader pulses or intra-cloud discharges, are known to be sources of HF and VHF radiation. However, all measurements show a falling-off in radiated energy with frequency, so the greatest hazard occurs at low frequencies.

The geometrical distribution of the current around an aircraft will be different for a direct strike and for a nearby strike. Inductive sharing dominates (Section 2.1) for direct strikes when the aircraft skin is highly-conducting. In nearby strikes, when LEMP is incident on one side of the aircraft, we recall that the body resonances are prominent at the boundary between the side of the scattering body illuminated by the EMP radiation and the dark side, that is, along the edges of the shadow (Section 3.1). Currents following the waveshape of the incident radiation are small at these shadow edges.

4. COUPLING TO THE INTERIOR OF THE AIRCRAFT

4.1 Diffusion Flux (Resistive) Coupling

For lightning current pulses in an all-aluminium-alloy aircraft this type of coupling is not generally important. It produces very slowly-rising voltage pulses of small amplitude along the inner surface of the skin of the aircraft or, during the current redistribution around the cross-section, in any conducting loop where the diffusion flux ϕ_D penetrates. It is important in resistive materials such as CFRP, titanium or stainless steel as discussed in Section 2.1.

Estimates of the magnitude of the effect in three-dimensional structures may be made with sufficient accuracy by representing the structure around the region of interest as a cylinder of appropriate cross-section (usually non-circular, as in Figure 2).

For very resistive skin materials, the voltage pulse in the skin has the same form as the current pulse. The internal flux changes at a rate $d\phi_D/dt$ roughly equal to ϕ_D/τ where τ is the redistribution time. For large practical CFRP structures having thin skins with thicker spars of CFRP present τ is of the order of $1\mu s$, and also for panels of CFRP in aluminium-alloy skins τ will be near this value. The magnitude of ϕ_D is generally smaller than that of the aperture flux ϕ discussed below, and $d\phi_D/dt$ is much smaller than $d\phi/dt$. The magnitude of the $d\phi_D/dt$ voltages is less than the resistive voltages in the skin.

4.2 Aperture Flux (Fast-Flux) Coupling

The coupling of flux through a slot in a cylinder is discussed in Section 2.2, where empirical correction factors for slots of finite lengths are mentioned. These are then apertures of rectangular shape in a cylindrical body, and the flux in the cavity behind the apertures is calculated in this section for fields whose frequency is too low to excite resonances. The magnetic field due to an aperture may be calculated for any frequency by obtaining the skin current that would have flowed if the aperture were closed, and then determining the field of this finite patch of skin current. The geometry of the cavity behind the aperture must be taken into account. The actual field due to the aperture is then the reverse of this field pattern, and is clearly calculable from the local skin current density only, (see for example McCormick et al 1978).

The rate of change of the flux in the cavity is determined by the rate of change of the outer flux around the aircraft, scaled according to the magnitude of the aperture field. Intracloud discharges and return strokes in ground flashes give significant rates of change of flux, and the voltages induced in circuits within the aperture can be very large, as noted in Section 2.2. If, for example, the inductance of a length of fuselage is $0.02\mu H/m$ and the rate of rise of current in it is $10^{11} A/s$ then the peak field on the outside of the aircraft is $20kV/m$. At a point near the cavity wall, on the 1λ contour of the flux plot within the cavity, this peak field would be $200V/m$, and the waveshape would be proportional to dI/dt . Wires running across the mouth of the cavity would have fields of $5-10kV/m$ induced in them. Wallace (1978) gives details of numerical calculations of these induced fields.

For return stroke current pulses the energy at frequencies capable of exciting cavity resonances is negligible, so this type of calculation is appropriate. Radiation from lightning flashes as a whole extends up to $1GHz$, though with decreasing energy at higher frequencies, so cavity resonances will be weakly excited at some stage. The methods of solving the general problem of aperture coupling are reviewed by Brittingham (1976).

Butler et al (1978) and Bevensee et al (1978) deal with this general problem also. It is not likely that the excitation of cavity resonances by changing magnetic fields will be very important in lightning studies.

4.3 Aperture Electric Field Coupling

When the charge distribution on an aircraft is changed rapidly, as for example during the process of leader attachment, the E-field normal to the surface also changes. Apertures allow the E-field lines to enter the aircraft and terminate on cables or conductors within it. Changes are induced in this way on screens and wires, and if the E-field changes rapidly currents flow in the screens or wires.

The electrostatic field distribution within a cavity can be computed, and the effect of changing E-fields outside on interior conductors can be found. This is a form of capacity coupling. The field within the cavity can be regarded as due to an array of electric dipoles covering the area of the cavity, and again the local charge density on the surface determines the interior field.

The equipotentials within and around a circular cylinder carrying a slot will be the same as the flux surfaces shown in Figure 3. The normal E-field at the bottom of the cavity E_n is about two orders of magnitude below the field E_0 at the exterior surface in this example. The highest rate of change of E_0 is likely to be the maximum field on the surface divided by the transit time of EM waves along the aircraft. The breakdown field in air for corona onset is about 3 MV/m and the transit time for a 20m aircraft is about 70ns so $dE_0/dt \approx 10^{14}$ V/m-s as a maximum. This might occur during the leader attachment phase. The greatest fields at the bottom of the cavity of Figure 3 are likely to be about 30kV/m with $dE_n/dt \approx 10^{12}$ V/m-s and a displacement current density of about 100 A/m². Part of the displacement current will flow in screens or exposed wires which intercept the E-field lines.

5. COUPLING INTO CABLES AND WIRES

5.1 Direct Injection

Any conductor penetrating the skin to external equipment such as an aerial may carry the lightning pulse into the aircraft. The equivalent circuit must be drawn for lightning frequencies and an analysis performed of the injected current and voltage waveforms to determine likely hazards. Transmission line theory will be required for long cable runs and for multiwire cable bundles; (McCormick 1979, Perala et al 1979, Strawe et al 1978). The general references for EMP (Section 3.1) should be consulted also.

5.2 Induced Voltages and Currents

The voltage induced in a loop of area A by a transverse flux ϕ changing at a rate $d\phi/dt$ is simply $d\phi/dt$ or $A dB/dt$ where B is the flux density. The loop inductance and resistance must be estimated to give the impedance, and the equivalent generator is then defined.

The effective loop areas of some typical cables are given below in Table 2. (Blount et al 1974): work at Culham Lightning Studies Unit supports these results also.

Table 2

Type	Area for 1m length (m ²)
Common Mode; any wire	5×10^{-2}
Differential Signal; straight pair	2.5×10^{-2}
twisted pair	3×10^{-5}
shielded twisted pair	3×10^{-6}

The current I is induced by a normal field E_n within a cavity, changing at a rate dE_n/dt , in a wire of effective area S will be

$$I = \epsilon_0 \frac{dE_n}{dt} S$$

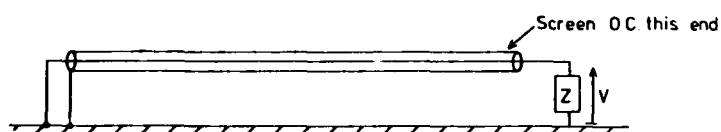
The capacity between the wire and the exterior couples the field changes outside to the wire, so that the source impedance is capacitive.

Given the nature of the source impedance and the voltage or current waveform produced the effects on internal circuits can be analysed as in 5.1 above.

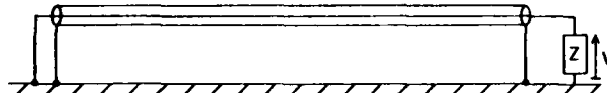
5.3 Screening of Internal Circuits

Some common screening connections, with comments, are given in Figures 13 and 14 which are self-explanatory. Ground-return circuits (Figure 13) are liable to disturbance by resistive voltages (IR) in the skin, and by magnetic flux-induced voltages in loops. Two-wire circuits are at hazard only from the latter.

Capacity coupled displacement currents will flow in the screen also, and these are an additional hazard.



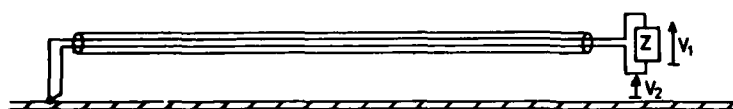
(a) This screen is useless against $\frac{d\Phi}{dt}$ and $I \times R$ voltages



(b) This screen - well bonded - eliminates $\frac{d\Phi}{dt}$ voltages but not $I \times R$.

Figure 13

Screening circuits with
airframe return



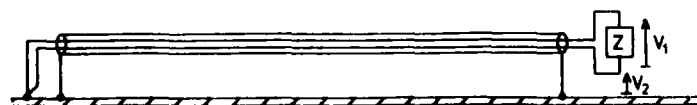
a) $V_1 = 0$ because the screen prevents flux threading between the wires. V_2 is unaffected



b) $V_1 = 0$ as for a) above. This screen aids electrostatic screening. V_2 is unaffected.



c) $V_1 = 0$ as above, $V_{\text{wire} - \text{screen}} \neq 0$, $V_3 = V_2$ in (b) above



d) $V_1 = 0$ as above, V_2 is $I \times R$ voltage only, the $\frac{d\Phi}{dt}$ component is eliminated.

Figure 14

Screening two-wire circuits

6. FINAL COMMENTS

The current and charge distribution on the skin of an aircraft produced by a lightning flash is difficult to calculate, though some valuable techniques have been developed both for direct and nearby strikes. Very large computer storage is required for this work. Induced voltages and currents on interior wiring due to a given distribution of fields and currents on the skin can be more readily determined.

Ground simulations of lightning give controlled conditions which can be analysed experimentally. The currents and voltages induced in the skin and in internal wiring can be measured, and need to be compared with theoretical predictions using the numerical approaches now available. The boundary conditions for the magnetic and electric field configurations must be properly arranged (Burrows, Luther and Pownall 1977, Burrows 1978). Some pioneer work on E-field excitation has been done by Butters et al (1978). In direct strike simulation the applied current pulse must have an appropriate Fourier spectrum, with no false high-frequency components (Hanson 1977, Burrows, Luther and Pownall 1977). The coupling to the aircraft must be made through a high impedance (Perala 1979).

7. ACKNOWLEDGEMENTS

The author wishes to thank B.J.C. Burrows of the Culham Lightning Studies Unit, T.E. Armour of AWRE, Aldermaston, R.A. Perala of Electro Magnetic Applications, Inc. and John C. Corbin Jr. of the USAF for useful discussions and the provision of valuable references. C.C.R. Jones and R. Forbes of Culham Lightning Studies Unit provided the analytic approximations and Fourier spectra described. This lecture was prepared with the support of the Procurement Executive of the UK Ministry of Defence.

REFERENCES (first mention only)SECTION 1

J.C. Corbin (1978), Vulnerability Assessment of Aircraft Systems to Indirect Lightning Effects, Conference on Certification of Aircraft for Lightning and Atmospheric Electricity Hazards, ONERA, Chatillon, France.

SECTION 2.1

R.H. Evans (1975) unpublished.
B.J.C. Burrows (1975), Induced Voltages, Measurement Techniques and Typical Values, Lightning and Static Electricity Conference, Culham, UK.
C.L. Thomas (1974) in Software for Numerical Mathematics, ed. D.J. Evans (London: Academic Press).
K. Khalafallah (1974) Time Constant for Magnetic Field Diffusion into a Hollow Cylindrical Conductor, Culham Laboratory Report CLM-R141.
B.J.C. Burrows (1979) unpublished.
B.J. Wallace, B.J.C. Burrows, R.T. Zeitler, A.J. Ludwig and K.G. Miles (1978), Composite Forward Fuselage Systems Integration, Volume II, AFFDL-TR-78-110.

SECTION 3.1

M. Born and E. Wolf (1959), Principles of Optics, Pergamon Press, London, (Chap. 13).
C.L. Bennett and G. Ross (1978), Time Domain Electromagnetics and its Application, IEEE Proceedings 66, 299-318.

SECTION 3.2

F.A. Fisher and J.A. Plumer (1977), Lightning Protection of Aircraft, NASA Reference Publication 1008.

SECTION 3.3

K.S. Yee (1966), Numerical Solution of Initial Boundary Value Problems Involving Maxwell's Equations in Isotropic Media, IEEE Trans. on Antennas and Propagation, AP-14, 302.
D.E. Hareweather (1971), Transient Currents Induced on a Metallic Body of Revolution by EMP, IEEE Trans. EMC, EMC-13 41-44.
R. Holland (1977), THREDE - A Free-Field Coupling and Scattering Code, Mission Research Corporation Report AMRC-R-85.
R.A. Perala, K. Lee and R. Cook (1979), Induced Effects of Lightning on an All-Composite Aircraft, Proc. Third Symp. on EMC, Rotterdam.
Space Shuttle Lightning Protection Criteria Document, NASA, Lyndon B. Johnson Space Center, Houston, Texas, JSC07636, Sept. 1973.
C.F. Wagner and A.R. Hileman (1962), Surge Impedance and its Application to the Lightning Stroke, IEEE Trans., Feb. 1962.
R.K. Mei (1974) Unimoment Method of Solving Antenna and Scattering Problems, IEEE Trans. on Antennas and Propagation AP-22, 760.

SECTION 3.4

R.M. Bevensee, J.N. Brittingham, F.J. Deadrick, T.N. Lehman, R. Edmund and A.J. Poggio (1978), IEEE Trans. on Antennas and Propagation, AP-26, 156.
D.F. Strawa, M. O'Byrne and S. Sandberg (1978) Electromagnetic Coupling Analysis of Learjet Aircraft, Techn. Report, AFFDL-TR 78-121, AFSC, Wright-Patterson, AFB, Ohio, USA.

D.F. Strawa et al (1977), Investigation of Effects of Electromagnetic Energy on Advanced Composite Aircraft Structures, Contract N00019-76-C-0497 unpublished.

F.G.L. Garthwaite, T.W. Armour and J. Moore (1978), Calculation of Surface Current Distributions on Aircraft Structures, Nuclear EMP Meeting, University of New Mexico, USA.
F.G.L. Garthwaite and T.W. Armour (1980), Wire-Grid Modelling and the Response of Aircraft to EMP, NATO Seminar on EMP Vulnerability of Military Systems, Shrivenham, UK.
K.S.H. Lee, L. Martin and J.P. Castillo (1976), Limitations of Wire-Grid Modelling of a Closed Surface, IEEE Trans. EMC, EMC-18 123.

SECTION 3.5

R.A. Perala (1974), Integral Equation Solution for Induced Surface Currents of Bodies of Revolution, IEEE Trans. on EMC, EMC-16, 172.
M.I. Sancer, S. Siegal and A.D. Varvatisis (1976), Foundation of the Magnetic Field Integral Equation Code, EMP Interaction Note 320, ed. C.E. Baum, AFWL, Kirtland AFB, NM, USA.

SECTION 3.6

G. Bedrosian (1977), Stick-Model of the Total Axial Current and Linear Charge Density on the Surface of an Aircraft, EMP Interaction Note 327, ed. C.E. Baum, AFWL, Kirtland AFB, NM, USA.

SECTION 4.2

W.S. McCormick, K.J. Maxwell and R. Finch (1978), Analytical and Experimental Validation of the Lightning Transient Analysis Technique, Techn. Report AFFDL-TR-78-47, AFSC, WPAFB, Ohio, USA.
J.N. Brittingham (1976), A Literature Review of EMP Effects on Apertures, Lawrence Livermore Laboratory Report, UCID-17321, Livermore, CA.
C.M. Butler, Y. Rahmat-Samii and R. Mittra (1978), Electromagnetic Penetration through Apertures in Conducting Surfaces, IEEE Trans. Antennas and Propagation, AP-26, 82-93.

SECTION 5.1

W.S. McCormick (1979), The Analysis and Identification of Flux-Induced Voltage Transients on Low-Loss Transmission Lines, IEEE Trans. EMC, EMC-21, 13-19.

SECTION 5.2

R.L. Blount, R.D. Gadbois, D.L. Suiter and J.A. Zill (1974), ASTP Simulated Lightning Test Report, JSC-09221, NASA.

SECTION 6

B.J.C. Burrows, C.A. Luther and P. Pownall (1977), Induced Voltages in Full-Size Aircraft at 10^{11} A/s, IEEE Internat. Symp. EMC, Seattle, Wash. USA, 207-214.
B.J.C. Burrows (1978), Tests on Actual Aircraft for Electromagnetic Effects, Conference on Certification of Aircraft for Lightning and Atmospheric Electricity Hazards, ONERA, Chatillon, France.
W.G. Butters, R.J. Lauber and K.S. Zeisel (1978), Evaluation of Lightning Induced Transients in Aircraft using E, V and I Shock Excitation Techniques, McDonnell Aircraft Company Report, MDC A5683.
A.W. Hanson (1977), Recent Developments in High Current Testing Techniques for Lightning Simulation, IEEE Internat. Symp. EMC, Seattle, Wash. USA, 385-389.

PROTECTION OF AIRCRAFT AVIONICS FROM LIGHTNING INDIRECT EFFECTS

by
J. Anderson Plumer
Lightning Technologies, Inc.
560 Hubbard Avenue
Pittsfield, Massachusetts 01201
U.S.A.

SUMMARY

Once the magnitudes of possible lightning-induced voltages in aircraft electrical circuits have been determined and the vulnerability of associated avionic components has been assessed, the systems and components that are in need of protection can be identified. In general, protection can be applied either by designing the aircraft wiring so as to be less susceptible to lightning-induced effects, or by applying surge protective devices at the avionics terminals to clamp the induced transients to levels that can be tolerated. In some cases a combination of these approaches is necessary. This paper describes how to estimate the magnitudes of voltages and currents induced on shielded and unshielded wiring, and how shields may be utilized to reduce the level of these effects in sensitive circuits. It reviews circuit design practices that also can be utilized to minimize induced effects, and reviews the various types of surge suppression devices that are available and the advantages and disadvantages of each. It concludes with a discussion of transient coordination and methods of verification.

ESTIMATION OF VOLTAGES AND CURRENTS INDUCED ON UNPROTECTED WIRING

The first step in design of protection for avionics is to estimate the magnitude of the induced effects that must be protected against. In principle, the induced voltages and currents appearing on aircraft wiring may be calculated from the geometry of the aircraft wiring and knowledge of the strength and orientation of the internal magnetic and electric fields. However, calculation of the voltages and currents on actual aircraft wiring may never be practical because of the mechanical complexity of most wiring harnesses. For estimation purposes, calculations may be performed for simplified geometries. Such calculations will illustrate the scope of the problem and indicate the direction of practices that minimize the voltages and currents, and hence minimize the risk of circuit damage or upset.

The simplest geometry to consider is that of a conductor, or group of conductors, placed adjacent to a metal surface and exposed to a uniform magnetic field oriented to produce maximum voltage in the wiring. The geometry is shown in Figure 1.

If only common-mode voltages are considered and only cable systems short enough that transmission line effects need not be considered, the induced voltage will be

$$e = \frac{d\phi}{dt} = \mu_0 A \frac{dH}{dt} \quad (1)$$

where

- A = area of the loop involved in meters squared
- $\mu_0 = 4\pi \times 10^{-7}$ in henries per meter (permeability of free space)
- ϕ = total flux linked in webers
- H = magnetic field intensity in amperes per meter
- t = in seconds
- e = in volts

Expressed in inch units:

$$e = 8.11 \times 10^{-10} l h \frac{dH}{dt} \quad (2)$$

where

- l = length of cable bundle in inches
- h = height above ground plane in inches
- H = magnetic field intensity in amperes per meter
- t = in seconds

It must be emphasized that the voltage so calculated is that existing between the entire group of conductors (comprising the cable) and the aircraft structure. The voltage will divide between the loads at the ends of the cable inversely as the impedance of the loads. For worst case analysis, consider one end of the cable grounded with the other end open-circuited. In this case, all of the voltage will appear at the open circuit end of the cable.

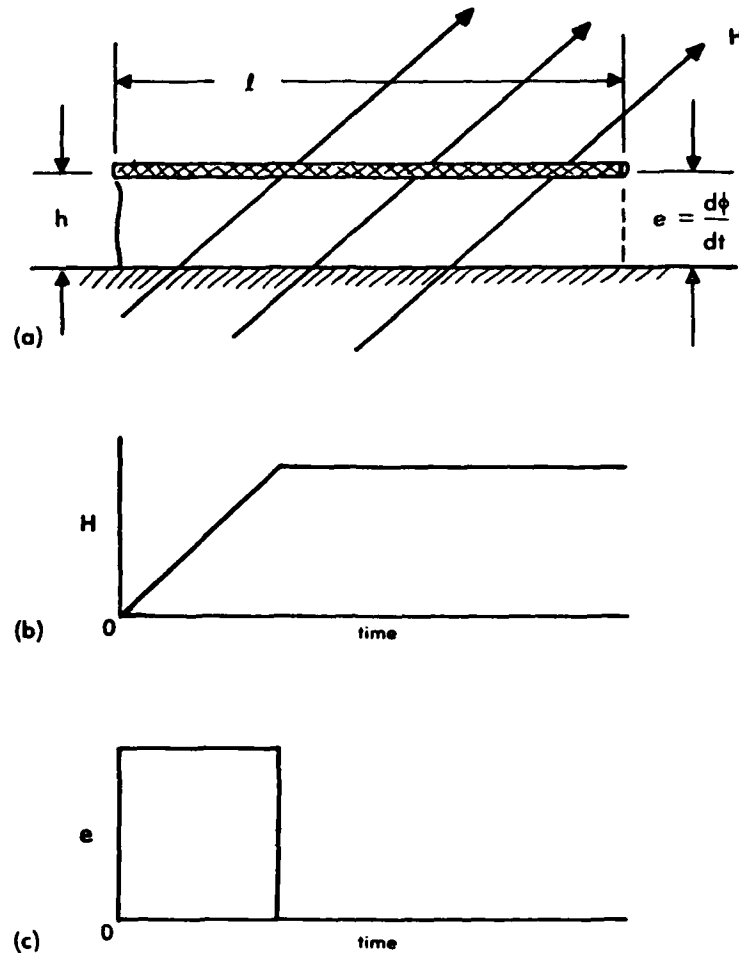


Figure 1 - Response to a Changing Magnetic Field: Open Circuit Voltage.

- (a) Geometry
- (b) Magnetic field waveshape
- (c) Voltage waveshape

Line-to-line or circuit voltages will be less, generally by a factor of 10 to 200, or 20 to 46 dB, down from the common-mode voltages because individual conductors are usually close together and are often twisted, thus reducing the total loop area.

The maximum cable current is that which flows when both ends of the cable are connected to the vehicle structure through a low or zero impedance. Such an impedance may be an overall shield grounded at each end, or it may be a group of semiconductor circuits, each having low input impedance. In the first case, the current will flow on the overall shield with the current on the input circuits determined by the shielding properties of the shields. In the second case, the current will flow directly through the input semiconductors and their bias sources.

The short circuit current that flows (Figure 2) may be determined from the familiar expression

$$e = L \frac{dI}{dt} \quad (3)$$

whence

$$I = 1/L \int e dt \quad (4)$$

where

I = Amperes

L = self-inductance of cable in henries

e = open circuit induced voltage in volts

t = time in seconds

Cable inductance may be estimated from the expression

$$L = 2 \times 10^{-7} \log_e \frac{4h}{d} \text{ H/m} \quad (5)$$

or

$$5.08 \times 10^{-9} \log_e \frac{4h}{d} \text{ H/in.} \quad (6)$$

where

h = height above a ground plane

d = conductor diameter

The induced voltage, e , which drives the current, is proportional to the cable height, h , but the cable inductance, which impedes the flow of current, is proportional to the logarithm of the cable height.

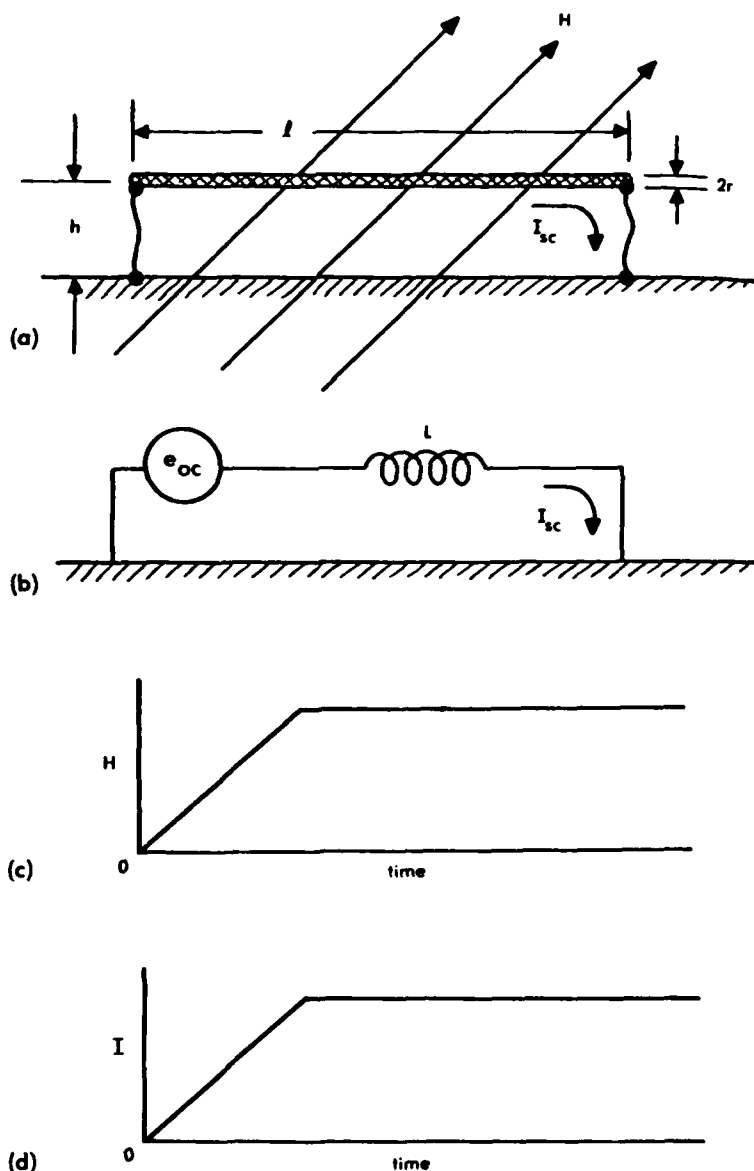


Figure 2 - Response to a Changing Magnetic Field: Short Circuit Current.

- (a) Geometry
- (b) Equivalent circuit
- (c) Magnetic field waveshape
- (d) Current waveshape

Transmission Line Effects

Conductors always have associated with them some distributed capacitance and inductance, the values of which are determined by the size of the conductors and the distance of the conductors from adjacent ground planes and other conductors. When these are considered, the effect of a changing magnetic field is to produce an oscillatory open circuit voltage. As shown in Figure 3, these oscillations will be superimposed on an underlying voltage proportional to the rate of change of the magnetic field. When the internal magnetic field is of complex waveshape (as is the usual case) and not the idealized ramp function shown in Figures 1b and 3b, the resulting open circuit voltage may be of a very complex nature. While the maximum voltage may be difficult to predict, given the complex nature of the superimposed oscillations, the amplitude of the envelope can at least be approximated from Equations 1 and 2. The frequency of the superimposed oscillations tends to be inversely proportional to the conductor length. Conductors, such as shields, grounded at one end, tend to ring as quarter-wave dipoles: for example, a conductor 10 m long tends to ring at 7.5 MHz. Even this simple relationship is difficult to apply, since one conductor is seldom free of the influence of adjacent conductors.

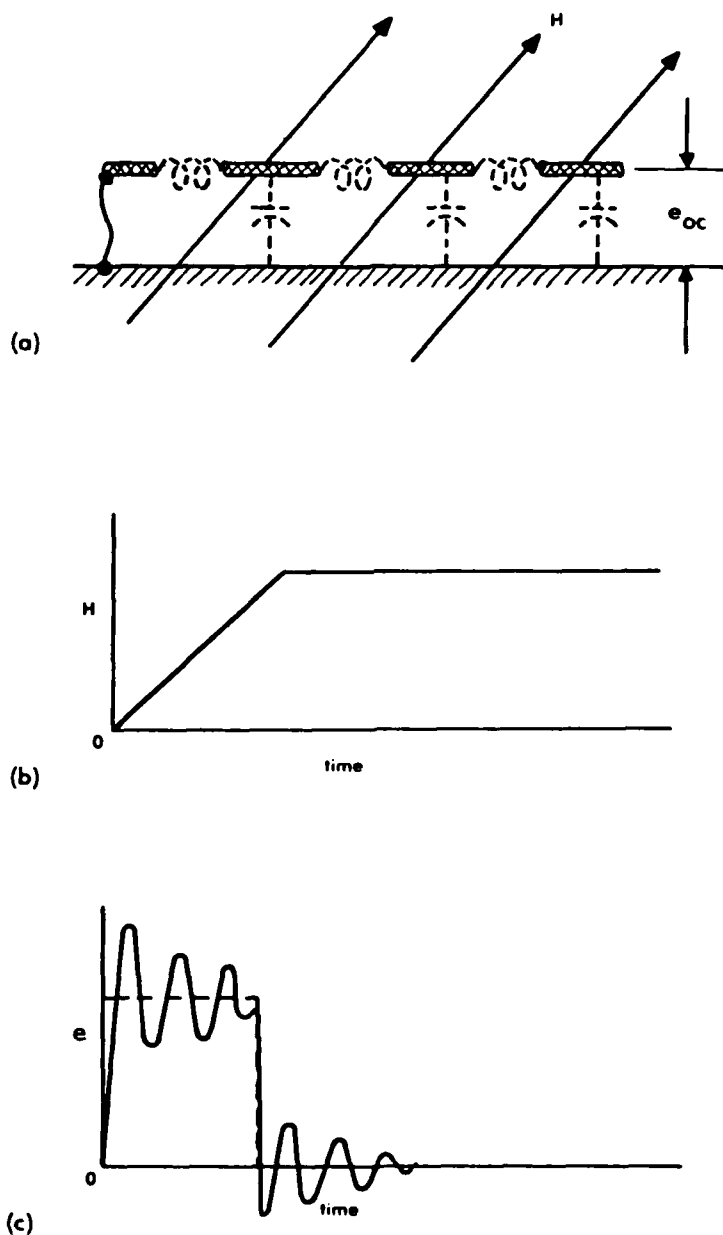


Figure 3 - Oscillatory Voltage Response Excited by a Changing Magnetic Field.

- (a) Geometry
- (b) Magnetic field waveshape
- (c) Voltage waveshape

Aircraft wiring is grouped into bundles, the bundles usually containing both short and long conductors. The assembly, even if exposed to a magnetic field of simple wave-shape will oscillate in a complex manner. Generally there will be one dominant frequency with several frequencies, usually higher, superimposed. Each will have its own characteristic decrement. Almost the only reliable generalization is that the cables associated with large aircraft will be longer than the cables associated with small aircraft and will characteristically oscillate at lower frequencies. On fighter aircraft, measurements of induced voltages have shown the characteristic frequencies to be in the range 1 to 10 MHz.

Currents measured on bundles of conductors tend to be oscillatory, like the voltages, as long as the conductors are part of a wiring group employing a single-point ground concept. If the conductors are part of a wiring group employing a multiple-point ground concept, the conductor currents tend not to be oscillatory but to follow the underlying shape of the internal magnetic field.

Magnetic Field Zones

From the foregoing it can be seen that the task of assessing the possible induced voltage or current levels in a conductor or shield depends on knowing the magnetic field levels inside the aircraft. Accurate determination of these fields at particular locations would be a formidable task. A possible solution to the problem lies in establishing characteristic zones. On a fighter aircraft, for example, the cockpit can be regarded as a magnetically open zone exposed primarily to aperture-coupled magnetic fields. Within reasonable limits, all fighter aircraft probably have approximately the same magnetic field in the cockpit. Another zone characteristic of fighters would be the avionics bays located in the fuselage. Many such bays tend to be alike, the differences, perhaps, relating mostly to the type of magnetic field structure fundamentally different from either the cockpit or the forward equipment bays. Accordingly, it should be possible to divide an aircraft into a relatively small number of typical zones; to assign a predominant magnetic field intensity to these zones, and to provide rather simplified tables of nomograms listing the characteristic transient likely to be induced in wiring of a given length.

The concept of dividing an aircraft into magnetic field zones was first used on the *Space Shuttle* (Reference 1). The zones so defined are shown in Figure 4 (Reference 2). The electromagnetic fields assigned to each of these zones were estimated by a group of engineers knowledgeable in the field. These magnetic fields were then refined during the course of an extensive analytical investigation. The magnetic field amplitudes assigned to each of these zones, based on the analytical study, are given in Table I (Reference 3).

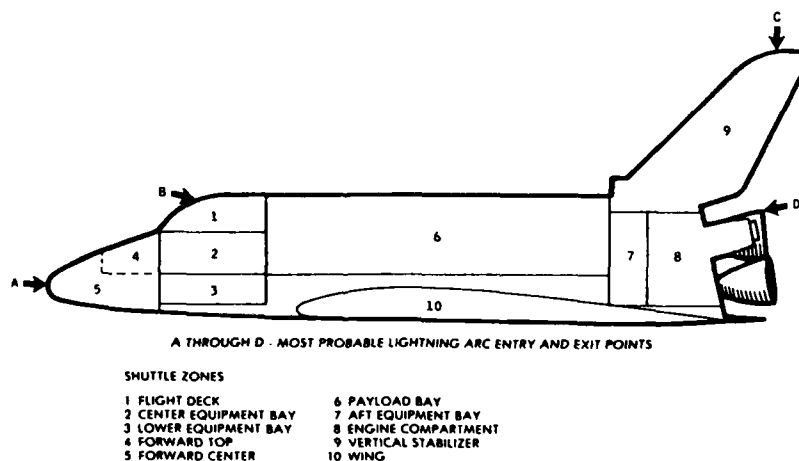


Figure 4 - Shielded Zones within the *Orbiter* Structure.

The fields were divided into two components, an A-component referring to fields coupled through apertures and a B-component referring to fields coupled by diffusion through metal surfaces. The A-component of the field would tend to have the same rapidly changing wave-shape as the external magnetic field, while the B-component would have a much slower wave-shape. In the *Space Shuttle* study the waveforms of the different components were taken to be as shown on Figure 5 (Reference 4). In each case the field intensity was based on a worst case 200 kA lightning current passing through the *Orbiter* vehicle. The field amplitudes of Table I were the maximum amplitudes calculated for any of the possible lightning current entry or exit points.

Analytical studies of field intensity could well be supplemented by experimental studies in which currents were circulated through an aircraft and the magnetic fields measured. Aircraft used for such studies should be in realistic condition in regard to the mechanical soundness of the structures, particularly relating to the access panels, but otherwise they need not contain complete electronic systems.

TABLE I - Magnetic Fields in Different Zones of the SPACE SHUTTLE

Zone	Aperture Fields A-component (A/m)	Diffusion Fields B-component (A/m)
1	1200	800
2	60	200
3	0	200
4	50	150
5	50	100
6	280	300
7	50	570
8	200	680
9	200	3700
10	65	300

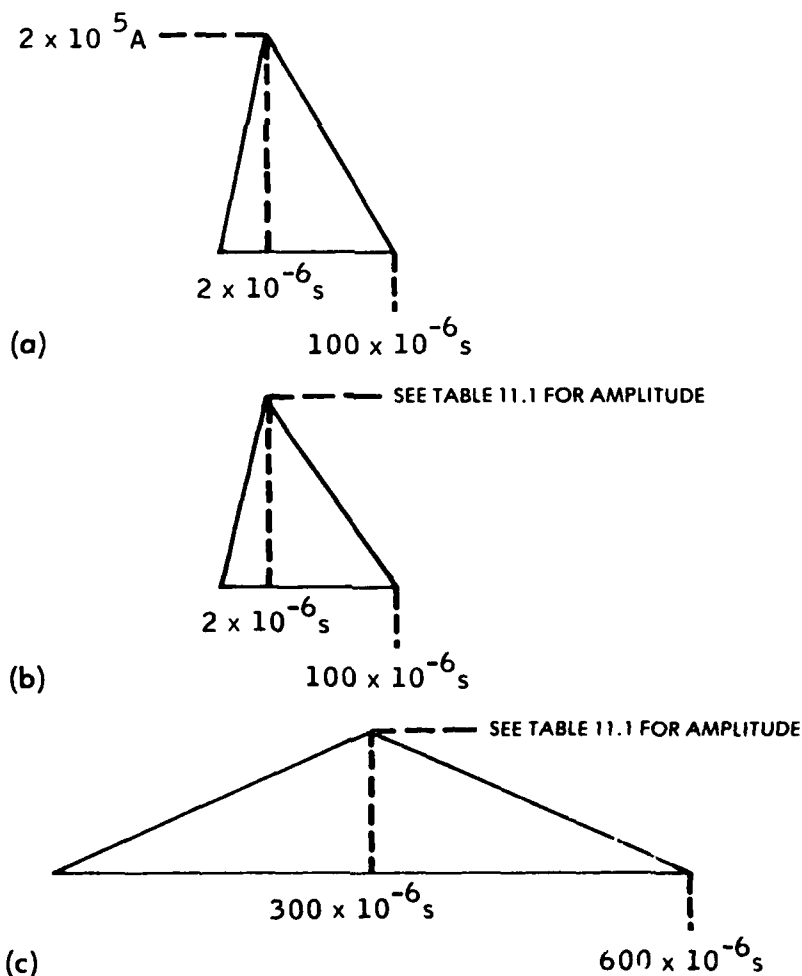


Figure 5 - Waveforms of aperture- and diffusion-coupled magnetic fields.
 (a) Lightning current
 (b) Aperture-coupled field, A-component
 (c) Diffusion-coupled field, B-component

Aids for Calculation of Estimated Voltages and Currents

The magnetic fields established for each zone may then be utilized to calculate the approximate voltage and current to be experienced by typical aircraft conductors or shields. For this purpose, the following additional assumptions are made:

- The conductor (or shield) is of length ℓ , diameter d , and spaced a height, h , above a ground plane which is the aircraft skin or a floor.
- The magnetic field is oriented to produce maximum voltages in the conductor.
- One end of the conductor is grounded.
- The magnetic fields are of the shape shown in Figure 5.

These are the same assumptions as those illustrated in Figures 1 and 2 and upon which Equations 1 and 2 were based. Under these assumptions

$$e_{oc} = K_1 \ell h H \quad (7)$$

where

$$K_1 = 0.63 \text{ if } \ell \text{ and } h \text{ are in meters}$$

$$K_1 = 0.63 \times 10^{-4} \text{ if } \ell \text{ and } h \text{ are in centimeters}$$

In all cases H is expressed in amperes per meter. The waveshape of the open circuit voltages would typically be proportional to the derivative of the H field, and hence oscillatory.

If we assume the conductor to be grounded at each end

$$I_{sc} = K_2 \ell h H \quad (8)$$

where K_2 is given by Figure 6. Conductor length does not influence short circuit current. The waveshape of the short circuit current tends to be the same as that of the magnetic field.

The height, h , of the cable bundle above a ground plane is difficult to specify because the ground plane is seldom purely a plane surface and because cable bundles are frequently strapped directly to a supporting structure. For purposes of this analysis, assume

- That the height, h , is measured to the nearest substantial metallic structural member
- That if the cable bundle is laid directly on that member, h equals one-half of the cable diameter
- That if the cable bundle is elevated above the metallic structural member, h equals the clear height above the member plus one-half the cable diameter. (If the cable height differs along its length, use an average height.)

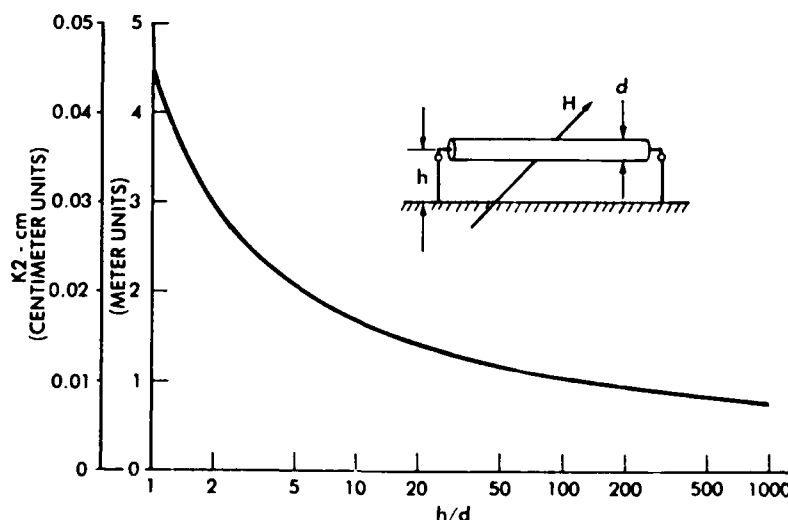


Figure 6 - K_2 - Metric Units.

Estimated Voltages and Currents in the Space Shuttle

Based upon Equation 1 to 8, Figure 5, and Table I, one may calculate the open-circuit induced voltages and short circuit currents that would be developed on typical wiring. The results are shown on Table II (Reference 5) for a conductor 4m in length within each of the 10 magnetic field zones established for the Space Shuttle and illustrated in Figure 4.

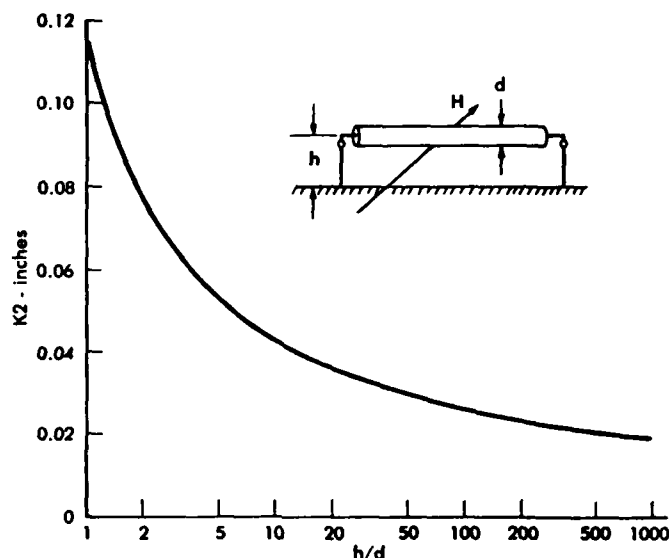


Figure 7 - K_2 - Inch Units.

Table II - OPEN CIRCUIT VOLTAGE AND SHORT CIRCUIT CABLE CURRENT IN THE VARIOUS ZONES OF THE SPACE SHUTTLE

Zone	h = 1 in. (0.0259 m) Voltage (volts)	Current (amperes)	h = 2 in. (0.0508 m) Voltage (volts)	Current (amperes)	h = 5 in. (0.1270 m) Voltage (volts)	Current (amperes)	h = 10 in. (0.254 m) Voltage (volts)	Current (amperes)
1	76.90	133.3	153.8	184.9	384.6	321.8	769.1	521.1
2	3.92	7.10	7.84	9.42	19.59	16.39	39.18	26.54
3	0.085	0.154	0.170	0.204	0.425	0.356	0.850	0.576
4	3.25	5.89	6.51	7.82	16.27	13.62	32.54	22.05
5	3.23	5.85	6.46	7.76	16.14	13.51	32.29	21.87
6	17.99	32.59	35.99	43.26	89.96	75.28	179.9	121.9
7	3.43	6.21	6.87	8.26	17.16	14.36	34.33	23.26
8	13.05	23.64	26.11	31.38	65.27	54.62	130.5	88.44
9	14.33	25.96	28.66	34.45	71.65	59.96	143.3	97.09
10	4.27	7.74	8.55	10.28	21.37	17.88	42.75	28.96

*All values based on cable length of 157.48 inches (4 m) and diameter of 1 inch (0.0254 m). For other lengths, scale the voltage proportionately.

The voltages and currents of Table II are the transients that will appear between unshielded conductors and the airframe, or between the shields of shielded conductors and the airframe. In either case the source impedance can be estimated by dividing the open circuit voltage (e_{oc}) by the short circuit current (i_{sc}) as follows:

$$Z_{\text{source}} = \frac{e_{oc}}{i_{sc}} \quad (9)$$

SHIELDING EFFECTIVENESS

Grounding of Shields

If a shield is to be effective against magnetic fields, it must be grounded to the airframe at either end. In this case, the short circuit current determined from Table II will flow in the shield, and this current will produce a magnetic flux that tends to cancel

the original flux. If one end of the shield is left ungrounded, the calculated induced voltage will appear between the ungrounded end of the shield and the airframe, and no circulating current or cancelling flux will appear.

To illustrate some of these effects let us consider a series of tests (Reference 6) that were made on a 5 m long length of RG-58/U coaxial cable. The cable was placed adjacent to a metal ground plane and a magnetic field passed between the cable and the ground plane. Measurements were made of the voltage between the center conductor and ground at each end of the cable. These voltages thus represent the common-mode voltages that would exist. The first set of results is shown in Figure 8. In an unshielded conductor or one in which the shield on a conductor is not used, equal and opposite voltages appear at the two ends if all of the loading impedances are balanced. The voltages at the two ends of the conductor are of equal amplitude but opposite polarity, as would be produced if the conductor were considered to have an equivalent voltage generator at its center, as shown in Figure 8c. If the load impedances at the ends are unbalanced by the addition of a 50Ω resistor at one end (Figure 9), the total voltage induced around the loop remains unchanged, but most of it appears at the end with the highest impedance. With reference to the equivalent circuit of Figure 9c, the fact that there is any voltage at V_2 implies the existence of some capacitive loading as well as the desired resistance load; otherwise there would be no voltage across V_2 .

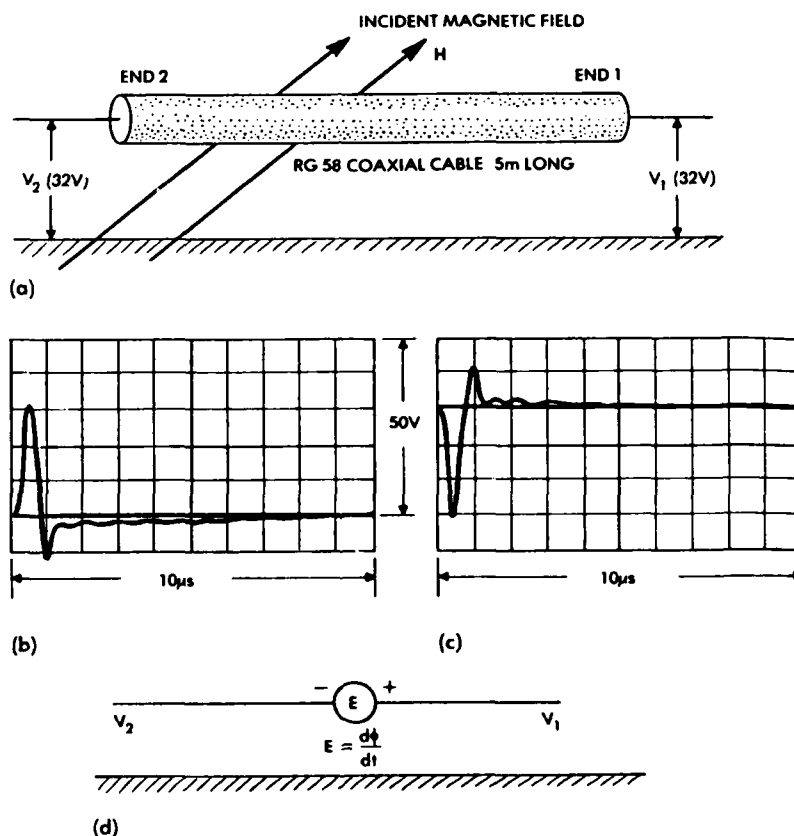


Figure 8 - Shield Not Grounded at Either End.

- (a) Test conditions
- (b) V_1
- (c) V_2
- (d) Equivalent circuit

Grounding the shield at one end, shown in Figure 10 does not significantly affect the common-mode voltage at the other end. The changing field induces a voltage between the open end of the shield and ground. The conductor is exposed to the same field, and there is thus the same voltage developed between the ends of the conductors as that between the ends of the shield. Because of the unbalanced load impedances, all this voltage must appear between the conductor and ground at end 1. Leaving aside considerations of unequal load impedance, the shield can reduce voltage at one end only by increasing it at the other end. This effect is shown in Figure 11. The reason the shield reduces the line-to-ground voltage at V_2 is that the capacitance between shield and conductor at the ungrounded end loads the signal conductor, just as did the 50Ω resistor of Figure 10.

Grounding the shield at both ends, as shown in Figure 12, produces an entirely different response. If the shield is grounded at both ends, the voltage induced by the changing magnetic field in the shield produces a flow of current through the shield.

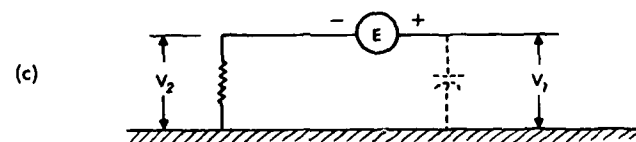
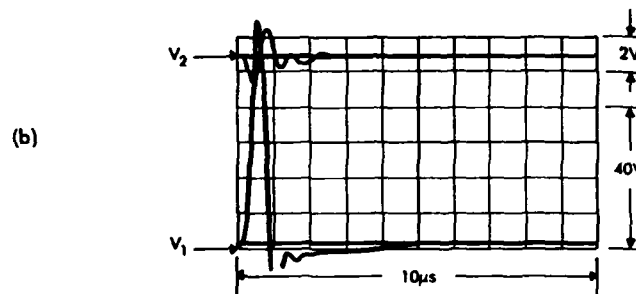
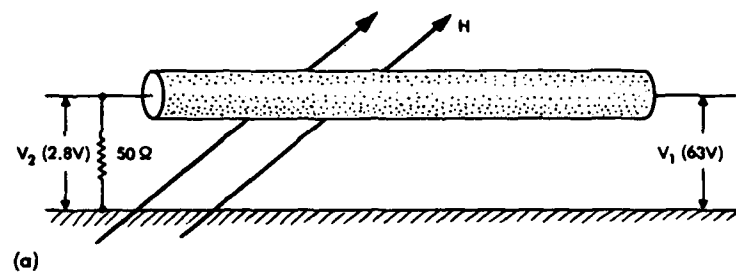


Figure 9 - Unequal Load Impedances
(a) Test conditions, (b) Voltages, (c) Equivalent circuits

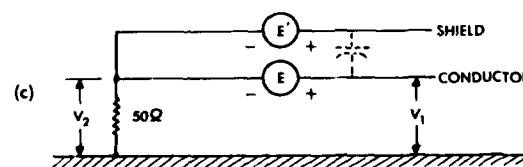
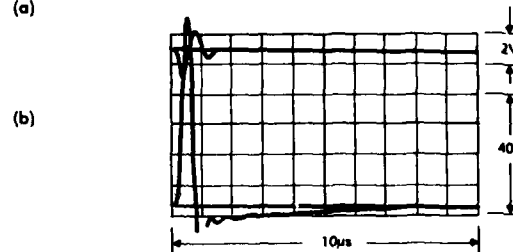
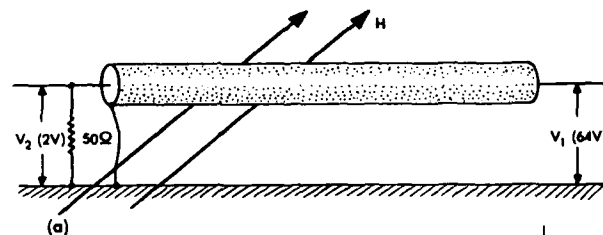


Figure 10 - Shield Grounded at One End.
(a) Test conditions, (b) Voltage, (c) Equivalent circuits

$$E' = \frac{d\phi}{dt} = \mu A \frac{dH}{dt} \quad (10)$$

$$I = \frac{1}{L_s} \int E' dt = \frac{\mu A}{L} H \quad (11)$$

where

E' = Voltage induced between ends of the shield

I = Current on the shield

L = Self-inductance of the shield

I = current on the shield

L = self-inductance of the shield

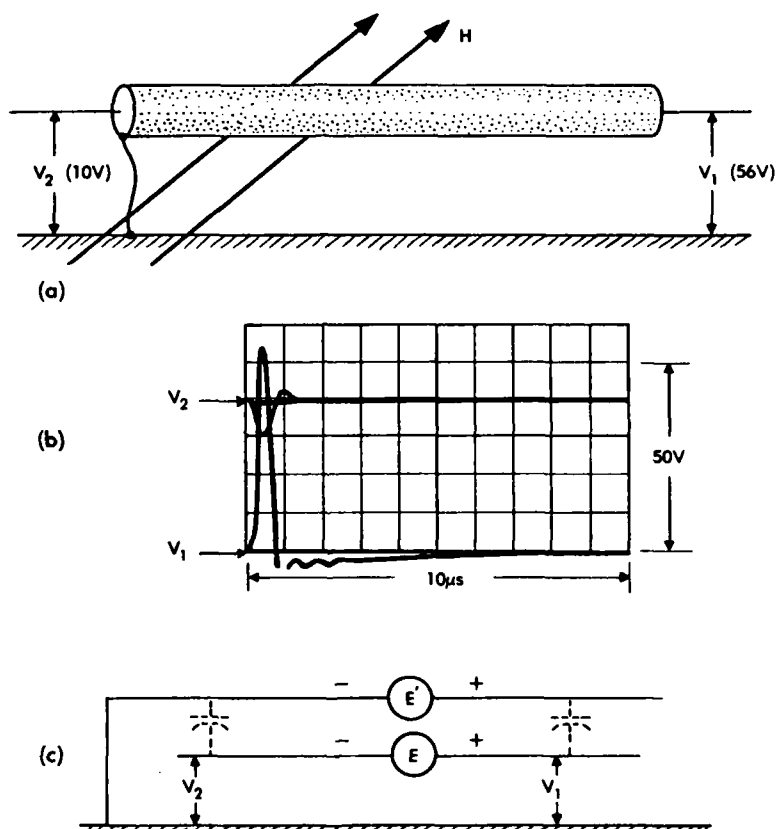
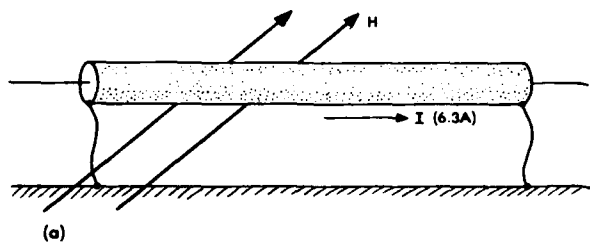


Figure 11 - Shield Grounded at One End.

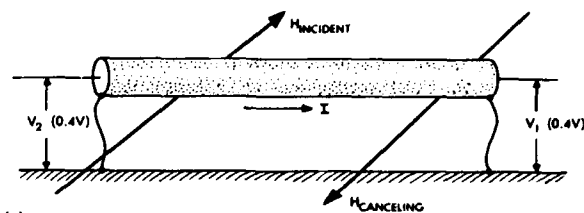
- (a) Test conditions
- (b) Voltages
- (c) Equivalent circuits

This shield current reduces the voltage induced between the signal conductor and ground, as shown in Figure 13. The reduction in voltages can be viewed equally well from two different standpoints.

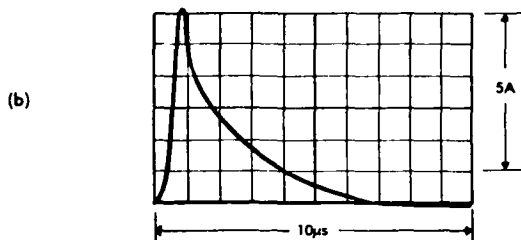
The first is that the shield current produces a magnetic field that tends to cancel the incident field. From this viewpoint the voltages on the signal conductors to ground depend only to the difference between the incident and the cancelling fields. Alternatively, the reduction in voltage can be viewed as the effect of the mutual inductance between the shield and the signal conductor. This latter approach is illustrated by the equivalent circuit of Figure 13c. The voltage between the ends of the conductor is the sum of that resulting from the voltage induced in the signal conductor, E , and that coupled through the mutual inductance between the shield and the signal conductor. Since the shield is grounded at both ends and able to carry a current, the voltage appearing across the primary inductance of the equivalent transformer is equal to the voltage E' induced between the ends of the shield by the incident field. Since the mutual coupling between the shield and the signal conductor is very nearly unity, the voltage induced in the secondary, or signal conductor, side of the equivalent transformer is about equal to the voltage originally induced in the shield. Accordingly, the voltages appearing at the ends of the conductor are much lower than they would be if the shield could not carry current.



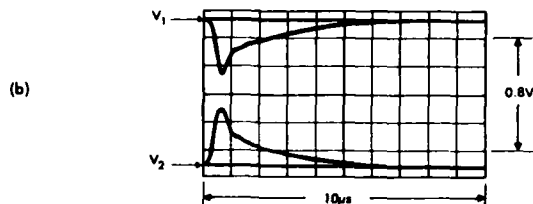
(a)



(a)



(b)



(b)

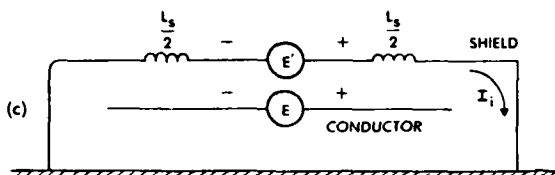


Figure 12 - Shield Grounded at Both Ends.

- (a) Test conditions
(b) Shield current
(c) Equivalent circuit

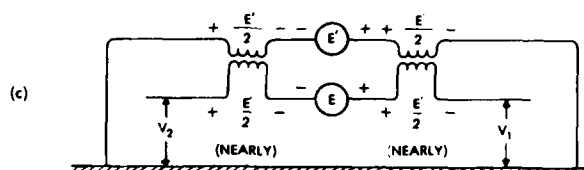
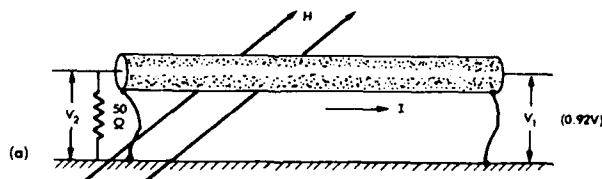


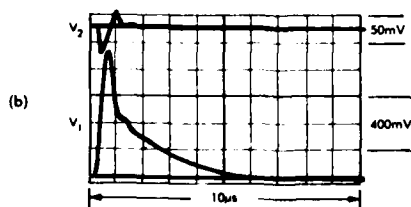
Figure 13 - Shield Grounded at Both Ends.

- (a) Test Conditions
(b) Conductor voltages
(c) Equivalent circuit

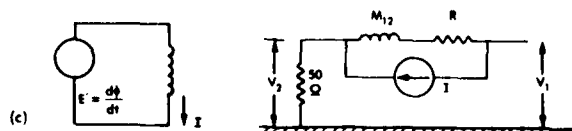
An alternative form of the equivalent circuit of Figure 13 is shown in Figure 14. There are two parts of the circuit, one relating the magnetic field to the current flowing on the shield and one relating the current on the shield to the voltage developed on the conductor. Both the measurements and the circuit indicate that voltage on the center conductor is affected by the relative impedance of the loads on the ends. A low impedance at one end pulls the voltage at that end down but raises the voltage at the other end. M_{12} and R represent transfer quantities, the values of which depend upon the type of shield.



(a)



(b)



(c)

Figure 14 - Shield Grounded at Both Ends.

- (a) Test conditions
(b) Conductor voltages
(c) Equivalent circuit

Shield Transfer Functions

If a shield were "perfect" the flow of current on the shield would not cause any voltage to be developed between the shield and the signal conductor. Factors exist, however, which prevent shields from being perfect. First, a shield always has resistance as shown in Figure 15. Current flowing through the resistance of the shield produces an electric field on the internal surface of the shield. The nature of the coupling between this internal field and the signal conductor depends upon the connections at the ends of the cable and upon the distributed inductance and capacitance of the circuit internal to the cable. As a simple case, imagine the left-hand end of the signal conductor to be shorted to the shield. The internal electric field would then be completely coupled to the signal conductor, and the voltage between the signal conductor and the shield at the right-hand end of the cable would be equal in magnitude to the total internal electric field along the length of the shield. This simple type of coupling is valid for low-frequency or slowly changing shield currents. For shield currents sufficiently slow that this model applies, the waveshape of the internal electric field is the same as the shield current, being related by Ohm's Law:

$$E = IR \quad (12)$$

Generally the coupling is not as simple as this. If the overall shield is a solid-walled cylinder, as shown in Figure 16, the internal electric field depends upon the product of the resistivity of the shield material and the density of the current on the internal surface of the shield. This internal current density, J_i , will not, in general, be the same as the density of the current on the external surface of the cylinder. Because of the phenomenon of skin effect, the current density on the inner surface of the shield will rise more slowly than does the external current. The rate at which current density on the inner surface increases will be directly proportional to the permeability of the field material and to the square of the wall thickness and inversely proportional to the resistivity of the wall material. Cables with solid-wall shields and cable trays of solid metal with tightly fitting covers will typically exhibit this type of behavior.

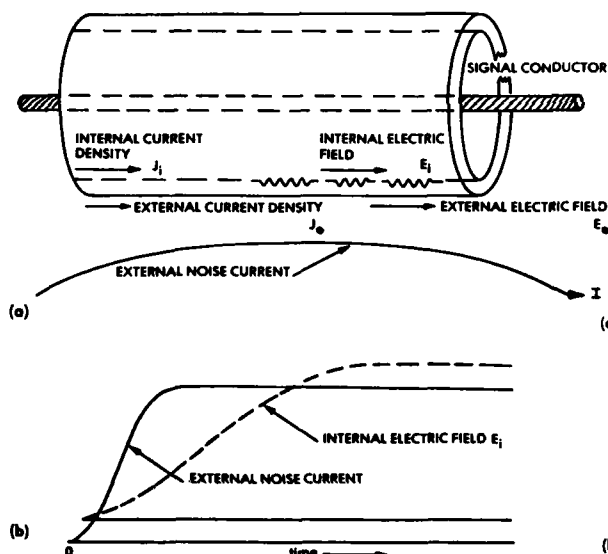


Figure 15 - Coupling Resulting from Resistance Effects.

- (a) Current and field polarities
- (b) Current and field waveshapes.

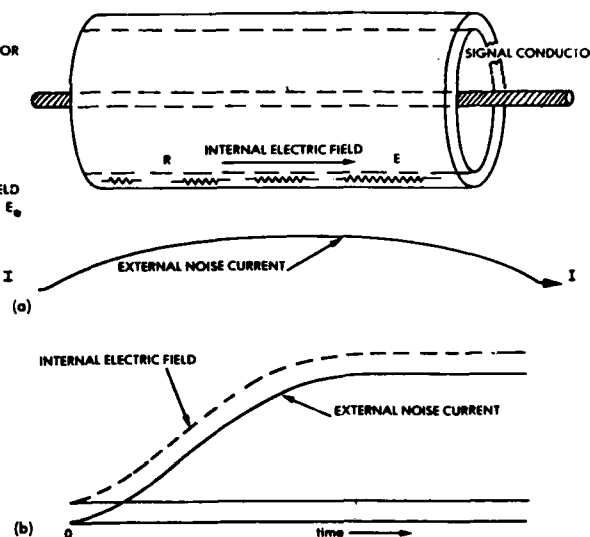


Figure 16 - Coupling via Diffusion through a Solid Wall.

- (a) Current and field polarities
- (b) Current and field waveshapes.

A different type of behavior is commonly observed on cables with braided shields, shown in Figure 17. The shields do not provide a perfect conducting cylinder, for they have a number of small holes which permit leakage. As a first approximation, one may visualize the external field lines looping in and out of the holes in the braided shield, as shown in Figure 17b. The leakage field produces a net magnetic field circumferentially around the inside surface of the shield, inducing a voltage between the center conductor(s) and the shield. The total induced voltage appearing between a conductor and the shield, then, is proportional to the resistance of the cable shield, to the rate of change of the shield current, and to the number of holes in the cable.

Another source of coupling is via capacitive leakage through the holes in the shield, as shown in Figure 18a. If the shield is held at ground potential by deliberate grounds, if the signal conductor is held near ground potential by external loads and if the shielded cable is subjected to an external and changing electric field, dielectric flux will pass through the holes in the cable from the external source and onto the signal conductor. The flow of these dielectric, or displacement, currents through the external load

impedances produces a voltage between the signal conductor and the shield. An alternate source of coupling, shown in Figure 18b, involves the voltage on the shield itself. Noise currents flowing through the external impedance of the shield may, if the shield is not perfectly grounded, produce a voltage between the shield and any external ground structure. External impedances between the signal conductor and the shield, as well as the inherent capacitance between the shield and the signal conductor, force the signal conductor to assume nearly all the same potential as the shield. Because the signal conductor is then at a potential different from the surrounding ground, dielectric flux can pass from the signal conductor through the holes in the shield and to ground, the dielectric currents again giving rise to a voltage between the signal conductor and the shield.

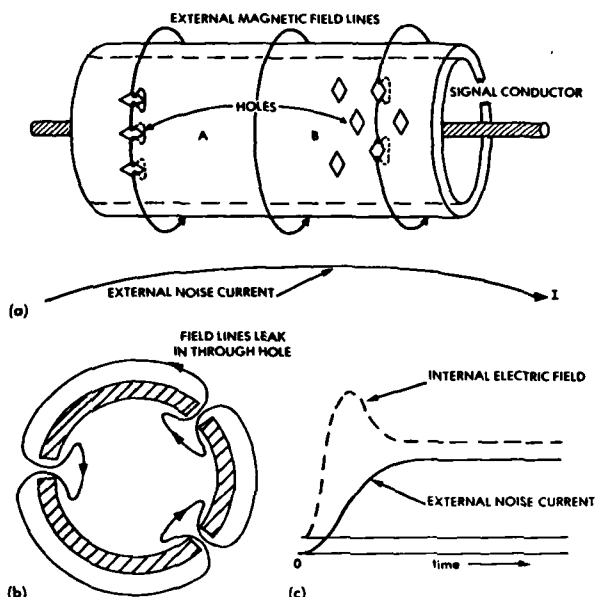


Figure 17 - Coupling via Magnetic Leakage through Holes.
(a) Current and field polarities
(b) Field leakage through holes: end view
(c) Current and field waveshapes

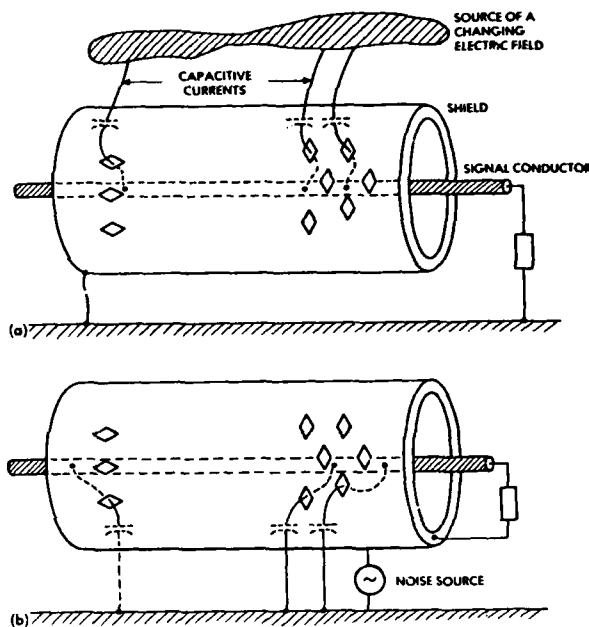


Figure 18 - Coupling via Capacitive Leakage through Holes.
(a) Coupling from an external source
(b) Coupling from voltage on the shield

In most cases the effects of magnetic leakage are probably more important than the effects of capacitive leakage.

The factors that affect the voltage which may appear between a signal conductor and the shield of a cable, as distinct from the voltages that may appear between the signal conductor and ground; are, then, the resistance of the shield, the degree to which the shield allows magnetic fields to leak to the inside, and the degree to which the shield allows electric fields to leak to the inside. These latter two characteristics may be expressed in terms of an equivalent transfer inductance of the shield and an equivalent transfer capacitance. These effects may be expressed in terms of the equivalent circuits shown in Figure 19. Figure 19a shows the equivalent circuit by which noise current on the shield of the cable may be related to the voltage induced between the signal conductor and the shield. In the frequency domain, this may be expressed as

$$V_s = I_n (Z_d + j\omega M_{12}) \quad (13)$$

As will be seen momentarily, the term Z_d may frequently be treated simply as the dc resistance of the cable shield, shown in Figure 19b, in which case the relation between current and voltage become simply

$$V_s = I_n (R_{dc} + j\omega M_{12}) \quad (14)$$

Treatment of capacitive effects yields the equivalent circuit shown in Figure 19c, in which the relation between loop current induced on the signal conductor and external noise voltage becomes

$$I_s = E_n j\omega C_{12} \quad (15)$$

Vance (Reference 7) gives an excellent dissertation on how the transfer inductance M_{12} and transfer capacitance C_{12} may be related to the characteristics of the braided shield.

The transfer impedance of a shielded cable is not a factor commonly specified either by the manufacturer or by procurement specifications. Even among cables of the same nominal type, this transfer impedance may vary considerably between the cables supplied by

different manufacturers. The most straightforward method of determining the transfer characteristic of a shielded cable is to make actual measurements of the conductor voltages that are produced by currents which are circulated through the shield.

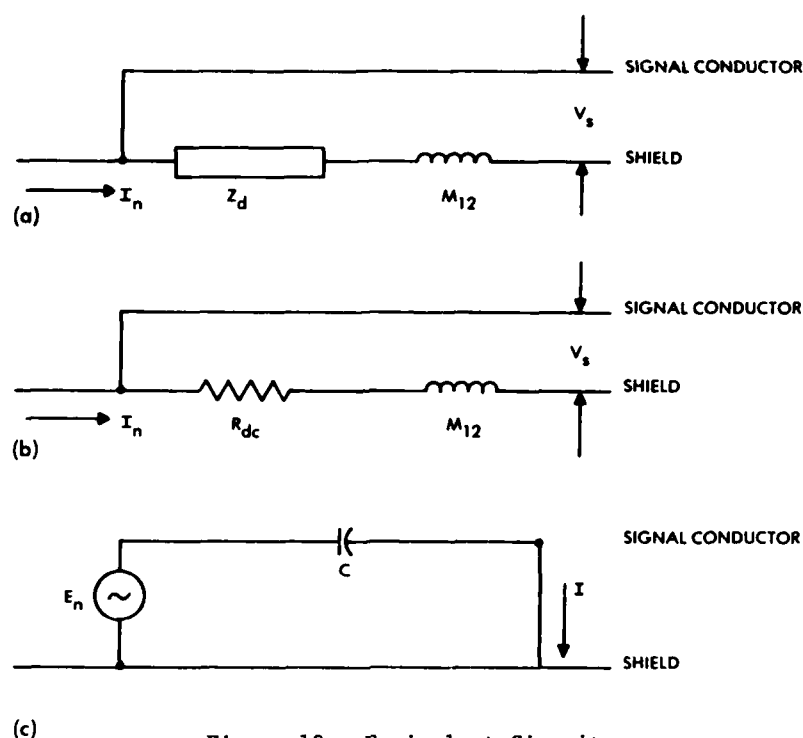


Figure 19 - Equivalent Circuits
 (a) Transfer impedances
 (b) Transfer impedance simplified
 (c) Transfer admittance

Methods of Grounding of Shields

The way in which a shield is grounded to the airframe may have a significant effect on the level of induced voltage that appears on the shielded conductors. A common treatment of a shield at a connector is to insulate the shield with tape and connect it to the back shell through a pigtail. Such treatment is shown in Figure 20a. Equally common practice is to insulate a panel connector from a panel with an insulating block and to ground the panel connector either to the panel through a pigtail or, more commonly, to an internal ground bus. A very common treatment of a shield at a connector, shown in Figure 20c, is for the shield to be connected to one of the connector pins and grounded internally through a pigtail, either to the panel or to an internal ground bus.

There are two fundamental drawbacks to pigtail grounding. The first, shown in Figure 21a, is that the shield current, being constricted to a path of small diameter, sets up a more intense magnetic field at the surface of the conductor than it would if the conductor were larger. If the shield current is carried to ground on a shell concentric with the conductors within the shield, shown in Figure 21b, there is much less voltage introduced into the conductors for the following reasons:

- The length of the path through which the shield current must flow is shorter.
- The field intensity external to the shield is reduced by virtue of the inherently larger diameter of the path upon which the current flows.
- The field intensity inside the shield is low - nearly zero.

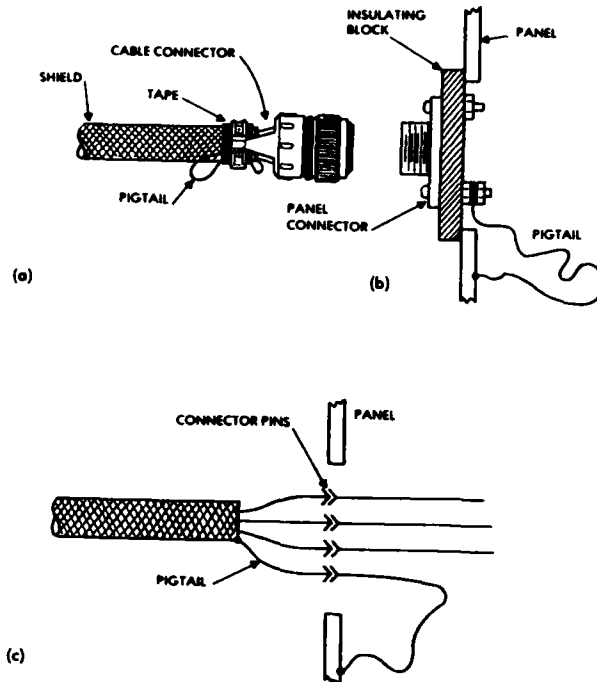


Figure 20 - Common Treatment of Shields at Connectors.
 (a) Pigtail connections to a backshell
 (b) Pigtail grounding to a panel connector
 (c) Shield carried on a connector pin

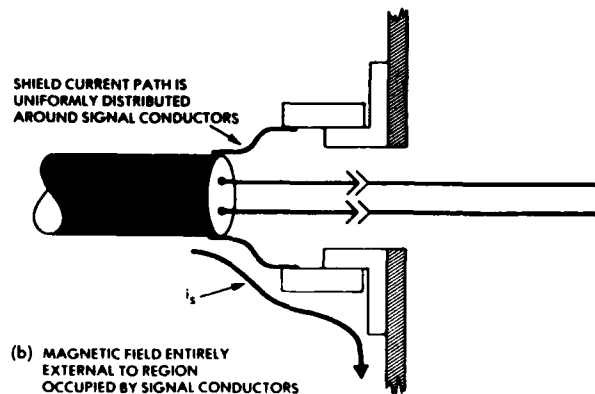
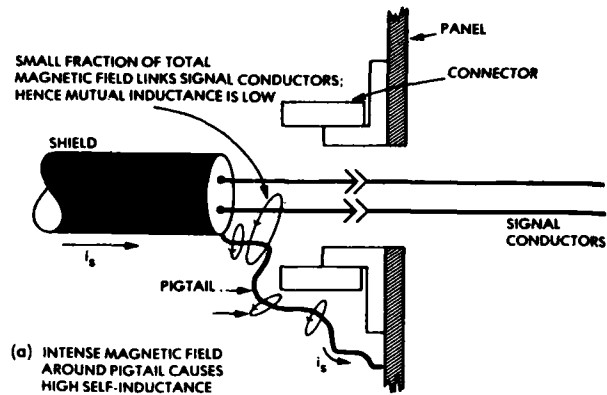


Figure 21 - Grounding of Shields.
 (a) Pigtails
 (b) 360° peripheral

SYSTEM DESIGN TO PROTECT AGAINST INDIRECT EFFECTS

Goals

Design to minimize the indirect effects of lightning should aim to accomplish the following goals:

1. Achieve a design that prevents the indirect effects from causing irreversible physical damage.
2. Eliminate that interference which provides an imminent hazard to the safety of the vehicle or its crew or one that presents a severe risk of preventing the completion of the aircraft's mission. For example, indirect effects that cause warning lights to appear might be acceptable whereas indirect effects that lead to the tripping of circuit breakers would be unacceptable, even if it were possible to reset the circuit breakers. Immediately after a lightning flash the pilot of the aircraft might have enough things to do that he should not be called upon to reset circuit breakers. Also, interference that leads to the scrambling of one channel of a redundant digital control system is probably acceptable, but interference that causes all computers to shut down is unacceptable, particularly if the computers are shut down in a disorderly manner which results in the internally stored programs becoming scrambled.
3. Design avionic equipment that can accept transient signals on input and output terminals at the outset rather than relying on retrofit programs to protect existing systems.
4. Design avionic systems around the capabilities of existing and proven protective devices or techniques.
5. Conduct trade-offs between the cost of providing electronic equipment capable of withstanding lightning-induced transients and the cost of shielding interconnecting wiring from the electromagnetic effects of lightning.
6. Take as much advantage as possible of the inherent shielding that aircraft structures are capable of providing and avoid placing equipment and wiring in locations that are most exposed to the electromagnetic fields produced by lightning.

Ways to accomplish some of these goals are discussed in the following paragraphs.

Protection Through Location of Avionic Equipment

While the designer may not have much choice in the matter, it is often possible to minimize indirect effects by locating electronic equipment in zones where the fields produced by lightning currents are lowest. For example, since the most important type of coupling from the outside electromagnetic environment to the inside of the aircraft is through apertures, it follows that equipment should be located as far from major apertures as possible. This means that equipment should be located as far from such access doors as possible, since access doors with their imperfectly conducting covers are a major source of electromagnetic leakage. In practice this may be more easily said than done, however, because frequently the purpose of access doors is to provide ready access to electronic equipment.

Protection Through Location of Wiring

The designer may have somewhat more control over the routing of wiring used to interconnect avionics than he does over the location of the equipment itself. Wiring should also be located away from apertures and away from regions where the radius of curvature of structural members or the outer skin is smallest. Also, wiring should be located as close to a ground plane or structural member as possible. If the structural member is shaped or can be shaped to provide a groove or trough, it will provide more inherent shielding than it will if the wiring is placed on the edge of the member. Some examples of typical structural members and the best places for wiring are shown in Figure 22. In each case the structural member is assumed to be carrying current along its axis.

Some basic principles to follow are these:

1. The closer a conductor is placed to a metallic ground plane, the less is the flux that can pass between the conductor and the ground plane.
2. Magnetic fields are concentrated around protruding structural members and diverge in inside corners. Hence, conductors located atop protruding members will intercept more magnetic flux than conductors placed in corners, where the field intensity is weaker.
3. Fields will be weaker on the interior of a U-shaped member than they will be on the edges of that member.
4. Fields will be lowest inside a closed member.

Some examples of cable routing are shown on Figure 23.

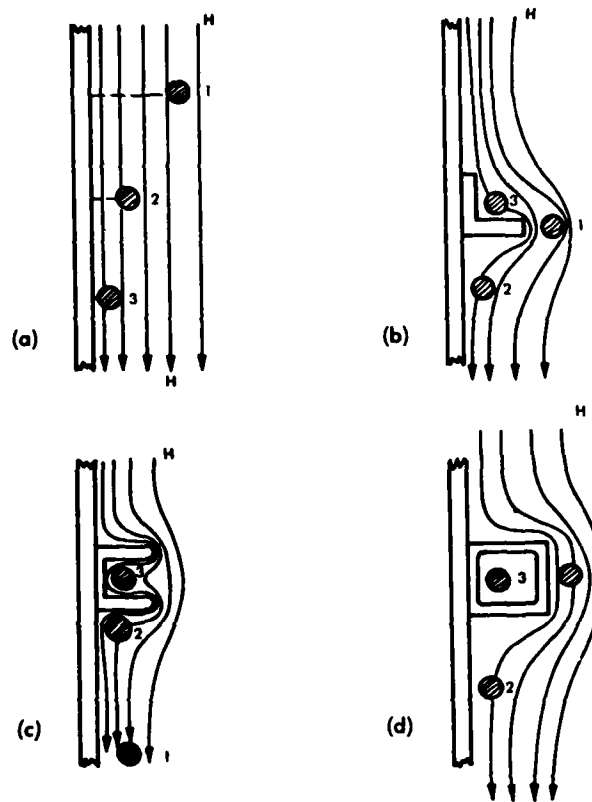


Figure 22 - Flux Linkages vs Conductor Position.
 (a) Conductors over a plane (b) Conductors near an angle
 (c) Conductors near a channel (d) Conductors near a box
 In each case pictured
 Conductor 1 - highest flux linkages: worst
 Conductor 2 - intermediate linkages: better
 Conductor 3 - lowest linkages: best

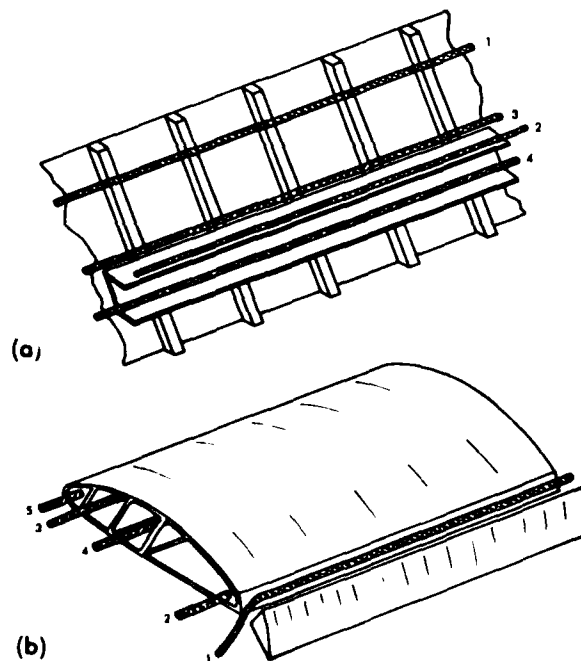


Figure 23 - Conductor Routing.
 (a) A fuselage structure (b) A wing structure
 In each case pictured
 Conductor 1 - highest flux linkages: worst
 Conductor 4 - lowest flux linkages: best

A cable clamped to stiffeners, as at Position 1 of Figure 23, will effectively be spaced away from the metal skin by the height of the stiffeners. A conductor along the outside edge of the U-shaped member, as shown by conductor 2 in Figure 23a, may or may not be better placed than conductor 1: effectiveness depends on how closely the conductor is attached to the side of the U-shaped member. Conductor 3, placed along the edge where the U-shaped member is attached to the stiffeners would probably be in a lower field environment than would either conductor 1 or conductor 2. Conductor 4, located in the interior of the U-channel, would be in the lowest field region and hence in the most effective position. Similar considerations apply to conductors located in structures like wings or stabilizers.

A conductor located along the outside trailing edge of the wing, as shown by conductor 1 in Figure 23b, will pick up much more flux than will any conductor located on the inside, probably by several orders of magnitude. Hence conductor 2, located on the inside of the trailing edge, would be better placed. Conductors 3 and 4, in that order, would be in the regions of lowest magnetic flux. A conductor that could be run inside a major structural member, as shown by conductor 4, will be exposed to a minimum amount of magnetic flux. Conductor 5, located at the forward edge of the wing, would be in a well-shielded region if the forward edge of the wing were metal, but it would be in a high field region and therefore vulnerable if the forward edge were a nonmetallic covering. However, even if the covering were metallic, conductor 5 would not be in as protected a region as that of either conductor 3 or conductor 4.

Windshield posts, shown in Figure 24, tend to concentrate the current flowing on the exterior surface of the vehicle, particularly if a flash is swept back contacting the windshield post directly or the eyebrow region above the windshield. Since the current is concentrated, the magnetic field intensity inside the crew compartment tends to be very high. The situation is aggravated by the fact that the windshields, unlike other regions where the field might have to diffuse through the metal surfaces, act as large apertures and so allow the internal magnetic flux to build to its peak values very rapidly. Instruments and wiring on the control panels are thus in a region of inherently high magnetic field strength. Conductors that run from overhead control panels (position A) to other instruments (position B) are often run along the windshield center posts. They are thus in a region of the most concentrated magnetic fields likely to be found on an aircraft, and accordingly they may have induced in them the highest voltages.

Protection Improvement Through Shielding

The effectiveness of shields has been discussed in a previous paragraph. It is almost always necessary to make some use of shielding on interconnecting wiring for protection of the most sensitive circuits. Shielding against magnetic fields requires the shield to be grounded at both ends in order that it may carry a circulating current. It is the circulating current that cancels the magnetic fields that produce common-mode voltages. There is some merit in grounding such a shield at multiple points, since frequently the cable will be exposed to a significant amount of magnetic field over only a small portion of its total length. If the shield is multiple-grounded, the circulating currents will tend to flow along only one portion of the cable whereas, if it is grounded at only the two ends, current is constrained to flow the entire length of the cable.

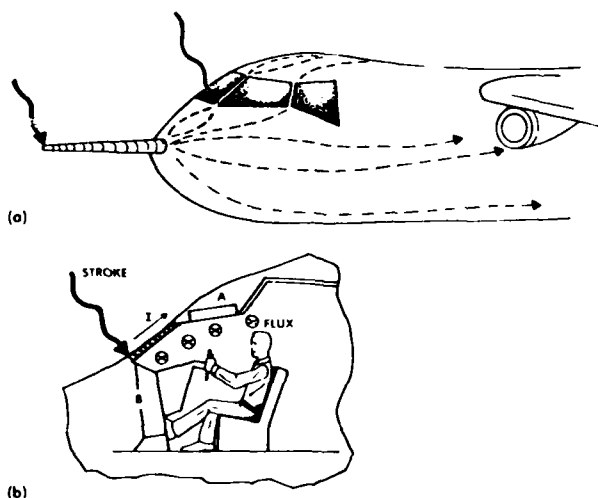


Figure 24 - Current Flow Along Windshield Posts.
(a) External current flow
(b) Internal magnetic fields

The requirement that a shield intended for protection against lightning effects must be grounded at both ends raises the perennial controversy about single-versus multiple-point grounding of circuits. For many legitimate reasons sensitive circuits need to be shielded against electromagnetic interference (EMI) from neighboring systems and power system return currents. The shields intended for EMI protection are grounded at only one end. But in this practice a fundamental concept often overlooked is that the physical length of such shields must be short compared to the wavelength of the interfering signals. Lightning-produced interference, however, is usually broad band and includes significant amounts of energy at quite high frequencies, frequencies higher than those the typical low-frequency shields are intended to handle. The dichotomy between the requirements for shielding against everyday, low-frequency interference is usually too great for both sets of requirements to be met by the use of only one shield system.

In these cases, both sets of requirements can be met only by having one shield system to protect against lightning-generated interference. The lightning shield can usually consist of an overall braided shield or conduit over a group of conductors with this overall shield being grounded to the aircraft structure at least at the ends. Within the overall shield may be placed whatever types of circuits are needed. Frequently these circuits will have a shielded conductor of their own. In a coordinated shielded system the designers of individual circuits should have the option of grounding such inner shields as their own requirements dictate, but they should not have the power of dictating the treatment of the overall shield.

Protection Through Circuit Design

One of the most important considerations in the control of lightning-related interference through proper circuit design lies in the fundamental observation that a device with a broad band-width can intercept more noise energy than can a narrow band-width device. Some of the considerations that derive from this observation are shown in Figure 25. The noise produced by lightning has a broad frequency spectrum. Considering for the moment only the spectrum of the lightning current, the observation is frequently made that most of the energy associated with the lightning current is contained in the low-frequency region, below 10 or 20 kHz. Before any sense of security is derived from that observation, it should be remembered that equipment is damaged or caused to malfunction in accordance with the total amount of energy intercepted. In a lightning flash there may be plenty of energy in the megahertz and multimegahertz region to cause interference. The energy that is available for damage or interference may well be concentrated in certain frequency bands by the characteristic response of the aircraft or the wiring within the aircraft.

Without reference to any specific frequency regions, however, the energy spectrum of the lightning-generated interference on electrical wiring within an aircraft will still be a broad spectrum. A receptor with a broad pass band, shown in Figure 25a, will inherently collect more energy than will a receptor with narrow pass band, shown in Figure 25b. The narrower the pass band, the better. In this respect analog circuits have an inherent advantage over digital circuits, since a narrow-pass band digital circuit is almost a contradiction in terms. If possible, circuits should not have a pass band that includes DC, shown in Figure 25c, because, when DC is excluded, the circuits will inherently be able to reject more of the energy associated with the flow of current through the resistance of the structure.

The studies of types of interference produced in aircraft by the flow of lightning current have shown that the lightning energy excites oscillatory frequencies on aircraft wiring, particularly if the wiring is based on a single-point ground concept. Those characteristic frequencies have tended to be in the range of several hundred kilohertz to a few megahertz. If at all possible, the pass bands of electronic equipment should not include these frequencies, as does the hypothetical pass band shown in Figure 25d. Higher or lower pass bands would inherently be better than the one shown. As an extreme example, shown in Figure 25e, fiber optic signal transmission operating in the infrared region avoids the frequency spectrum associated with lightning-generated interference almost completely.

Basic considerations about circuit design and signal transmission are shown in Figure 26. First, as shown on Figure 26a, signal circuits should avoid the use of the aircraft structure as return path. If the structure is used as a return path, the resistively generated voltage drops will be included in the path between transmitting and receiving devices. On the other hand, signal transmission over a twisted-pair circuit with signal grounds isolated from the aircraft structure tends to couple lower voltages in the signal path. It must not be forgotten, however, that the use of twisted-pair transmission lines does not eliminate the common-mode voltage to which electronic systems may be subjected. Common-mode voltages applied to the unbalanced transmission path, as in Figure 26b, can lead to line-line voltages which may at times be as high as the common-mode voltage.

Differential transmission and reception devices, shown in Figure 26c, can offer a many-fold improvement in the ability to reject the common-mode voltages produced by lightning.

In general it is preferable that wiring interconnecting two different pieces of electronic equipment not interface directly with the junctions of semiconductors, as shown in Figures 26a and 26c. Even modest amounts of resistance connected between the junctions and the interfacing wires, shown in Figure 26d, can greatly improve the ability of semiconductors to resist the transient voltages and currents. Transmission through balanced transmission lines and transformers, coupled with input protection for semiconductors, probably provides the greatest amount of protection against the transients induced on control wiring.

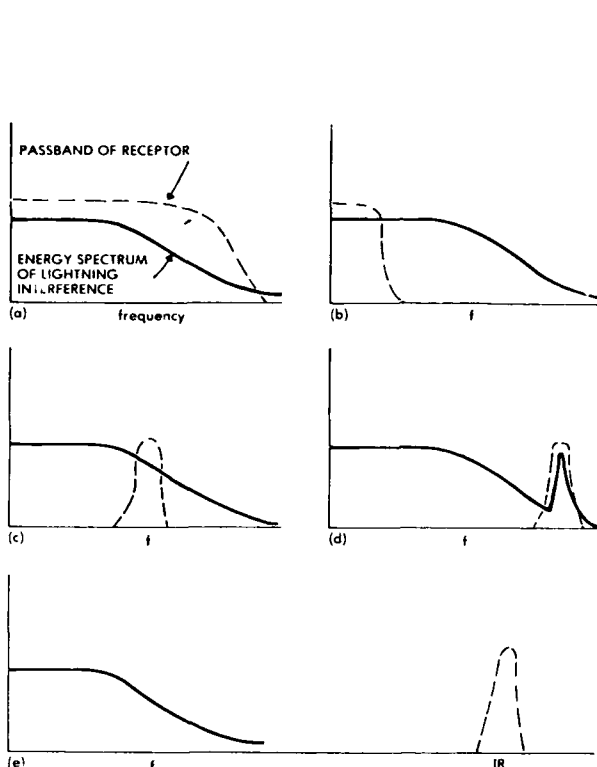


Figure 25 - Frequency Considerations.

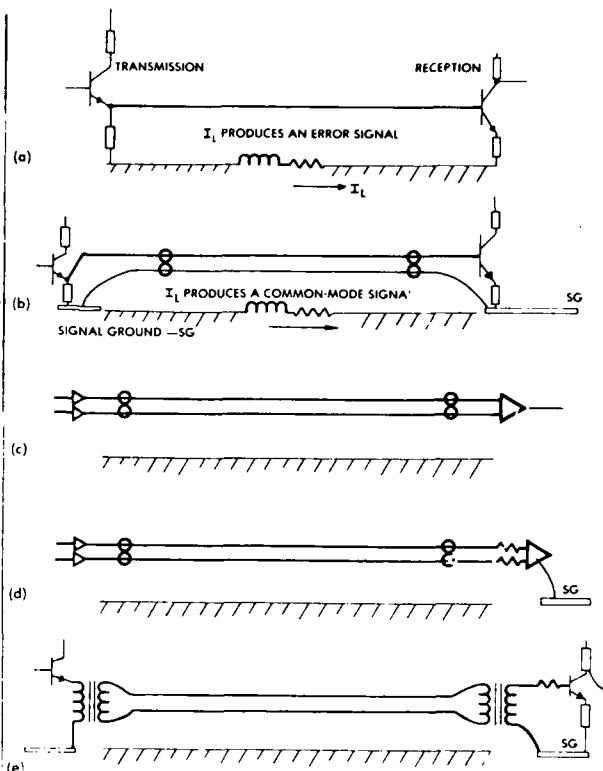


Figure 26 - Considerations Regarding Circuit Design.

Protection Through Use of Surge Protective Devices

Surge protective devices can sometimes be used to limit the amount of electrical energy that a wire can couple into a piece of electronic equipment. While one can seldom eliminate interference through the use of protective devices, suppressors judiciously used can virtually eliminate physical damage to electronic devices.

There are two basic types of protection devices: those which, on sensing an overvoltage, switch to a low-impedance state and thus cause the impressed voltage across them to collapse to a low value; and those which, on sensing an overvoltage tend (by virtue of their nonlinear voltage-current relation) to suppress the voltage to a safe level without collapsing it. Examples of the first type are spark gaps, and examples of the second type are Zener diodes and varistors. There are also devices which, on sensing an overvoltage, interrupt the power flow to the load. If this interruption is accomplished by electromechanical means, they should not be considered transient protection devices because they are inherently slow to respond.

Switching devices inherently offer greater surge-power handling capability than most Zener or varistor types of devices. The instantaneous power dissipated in a transient protective device is the product of the surge current flowing through the device and the voltage across the device. For a constant surge current, a switching device like a spark-gap, across which the voltage is low while in the conducting state, will have less power released in it than a device like a Zener diode, across which the surge voltage remains high. For a given surge-power handling capability, a spark gap will thus be smaller physically than a Zener diode or varistor device.

Another fundamental difference between switching devices (spark gaps) and nonswitching devices (Zener diodes or varistors) relates to their recovery characteristics after the surge has passed. If a circuit protected by a spark gap is connected to a source of energy (a power bus, for example) the energy source must usually be disconnected from the circuit before the spark gap can switch back from its low-impedance conducting state to its high-impedance nonconducting state. Generally, this requires opening a circuit breaker. A Zener diode or varistor effectively ceases to conduct as soon as the surge voltage has passed.

All types of overvoltage protection devices inherently operate by reflecting a portion of the surge energy to its source and by diverting the rest into another path, all with the intention of dissipating the surge energy in the resistance of the ground and interconnecting leads. The alternative to reflecting the energy is to absorb the surge energy in an unprotected load. Reflection and diversion of the surge energy are not without their hazards. Some are the following:

- The reflected energy can possibly appear on other unprotected circuits.
- Multiple reflections may cause the transient to last longer than it would otherwise.

- The spectral density of the energy may be changed, either high or low frequencies being enhanced. Interference problems on other circuits may well be increased even though the risk of damage to the protected circuit is reduced.

Most commonly the appropriate type of transient protective device to be used depends on the amount of surge energy to be dealt with. Generally, this energy decreases the further away one gets from the stroke. The surge energy to be expected can also be related crudely to the normal operating power of the circuit involved. One would normally expect lower surge levels on low-voltage signal circuits than on medium-power control circuits, and even lower levels than those on main-power distribution buses. Thus, one might logically use Zener diodes on individual circuit boards, varistors on terminal boards, and spark gaps on leads running to prime entry and exit points.

There are basically four generic types of transient protective devices applicable to lightning hardening of avionic systems. These types are gas-filled spark gaps, Zener diodes, varistors, and dielectrics. The latter are currently in development, but the others are readily available commercially. Each type has both advantages and disadvantages.

Spark Gaps

Spark gaps are generally composed of two metal electrodes separated by a dielectric and held at a fixed distance from each other. The gap may be sealed in a container. Sparkover voltage is determined by dielectric composition, density, and electrode geometry, and is also dependent on the surge voltage waveshape. If the voltage wave is increasing rapidly, the sparkover voltage will be higher than it is on a slowly rising voltage wave. Commercially available spark gaps frequently contain minute amounts of tritium or other radioactive elements to reduce the dependence of sparkover voltage on voltage waveshapes.

The advantages of spark gaps are as follows:

- They are simple and reliable.
- They have very low-voltage drop during the conducting state. When the gap is carrying maximum current, the voltage across the gap is typically 10 to 20 V. If more current tries to flow, the arc channel increases in diameter and holds the same arc-drop. A low arc-drop indicates relatively lower power absorption during the conducting phase.
- They have large power-handling capability. Gas-filled gaps have the highest peak current-handling capabilities of any transient protection device, and almost any gap can handle the maximum surge currents induced by lightning.
- They have high impedance and low capacitance. The low-shunt capacity and leakage current characteristics of gas-filled spark gaps minimize insertion problems for operating frequencies below 1 GHz.
- They provide bilateral operation, having the same characteristics on either polarity.

The disadvantages of spark gaps include the following:

- They have relatively high sparkover voltage.
- Simple gaps do not extinguish follow current. This is a most important point to consider if they are to be used on a power circuit. The arc must be extinguished by removing the voltage with a circuit breaker or fuse) or by inserting resistance rapidly into the circuit by an additional element, such as a silicon carbide or zinc oxide varistor. Through suitable designing, gaps can be made self-extinguishing for applied voltages up to about 100 V.
- They may have a large dependence of sparkover voltage on the waveshape of the voltage. Specifications relating to the impulse ratio or volt-time effects should be carefully considered.
- Since spark gaps reflect more energy than they absorb, external resistive components may be required to minimize ringing.

Zener Diodes

This category includes all single-junction semiconductor devices such as rectifiers, in addition to Zener diodes. While other semiconductor devices, such as PNP devices and bipolar transistors, may have application as surge arrestors, they will not be covered here because of the limited pertinent data available.

Zener diodes are basically polarized devices which exhibit an avalanche breakdown when the applied voltage in the reverse bias direction exceeds the device's specified breakdown, or Zener voltage of the device. Operated in an opposed series configuration diodes can be used as effective suppression devices. Since Zener diodes are designed to operate in the breakdown mode, they usually can perform more effectively as terminal protection devices than can signal diodes. While the energy-handling capabilities of Zener diodes are modest when compared with those of spark gaps, they are very well adapted for protection of individual components or circuit boards.

The advantages of Zener diodes include the following:

- They are of small size.
- They are easily mounted.
- They have low "firing" voltage.
- They have low dynamic impedance when conducting.
- They are self-extinguishing. When applied voltage drops below the Zener level, they cease conduction.
- They exhibit low volt-time turnup, or impulse ratio.

The disadvantages of Zener diodes include the following:

- They may be expensive.
- They are not bilateral. To protect against both polarities, two diodes in series back-to-back configuration are necessary.
- Diodes have relatively high-junction capacitance; therefore, they may cause significant signal loss at operating frequencies above 1 MHz. Special diode assemblies may extend the useful frequency to approximately 50 MHz.
- They do not switch state between a conducting and a nonconducting mode. The voltage across the diode does not switch to a low value when conducting but remains at the Zener voltage. This characteristic accounts for their ability to cease conduction when the voltage falls below the Zener level, but it has a disadvantage thermally. During conduction, the power absorbed by the diode is the product of the current through the diode and the voltage across the diode. The power absorbed for constant current, thus, is directly proportional to the diode voltage.

Partially offsetting this disadvantage, however, is the phenomenon that surge energy absorbed in the diode is energy that cannot be reflected back into the system to cause trouble elsewhere.

- They provide lower energy capabilities than do spark gaps. Since the Zener action takes place across a narrow P-N junction, the mass of the projecting junction is small and hence cannot store much energy. As a result, diode networks cannot be used where extremely high transient current or energy is predicted. For most hardening applications, this is not a serious limitation, since the induced surge-current levels are in the 1 to 100 A range at those locations where Zener diodes are most likely to be used.
- They are not available for voltages below about 5V.
- They are not normally available for voltages above a few hundred volts.

Forward-Conducting Diodes

In a forward-conducting state, a diode conducts little current below about 0.3V for germanium and 0.6V for silicon. They can, as a result, be placed directly across a low-voltage line and afford substantial protection.

The advantages of forward-conducting diodes include the following:

- They are of small size.
- They are not costly.
- They provide protection at very low-voltage levels.
- They have excellent surge-current ratings.

The disadvantages of forward-conducting diodes include the following:

- They are not bilateral. For protection of both polarities, two diodes in parallel must be used. Some vendors supply dipolar diodes for protection purposes.
- Conduction may occur on normal signals with attendant signal-clipping and frequency multiplication effects. Diodes must be used in series to raise voltage levels.
- They have relatively high capacitance.

Nonlinear Resistors

This category includes nonlinear resistors (varistors) that may be characterized by the expression

$$I = KV^N \quad (16)$$

where N and K are device constants dependent on the varistor material.

Varistors may be constructed of silicon carbide, selenium, or metal oxide. This section will concentrate on the metal oxide varistor (Reference 9).

The advantages of metal oxide-based nonlinear resistors include the following:

- They are bilateral devices.

- They are of small size.
- They are easily mounted. One common configuration is very similar in appearance to a disk ceramic capacitor.
- They are self-extinguishing. When applied voltage drops below the voltage for which the device is rated, they conduct very little current.
- They have an inherently fast response and low-impulse ratio.
- They provide high power-handling capability. The current- and energy-handling capability is second only to certain types of spark gaps. This device gives a higher ratio of energy absorbed to energy reflected than conventional gaps give. Moreover, the energy is absorbed throughout the bulk of the material and is not concentrated in a narrow P-N junction.

The disadvantages of nonlinear resistors include the following:

- They have low impedance and high capacitance. The zinc oxide varistor is characterized by high-shunt capacity, limiting its use to frequencies below 1 MHz. While it has a much higher idling current than have either gaps or diodes the standby power dissipation is in the milliwatt region and is usually not a significant limitation.
- They are not suitable for operating voltages below 20 to 30 V. Operating voltage is proportional to material thickness. Good surge protection of low-voltage circuits would require an impractically thin piece of material.

Improvement Through Transient Coordination

Transient coordination is a concept which, when reduced to its simplest terms, implies that *transient control levels* be assigned both to those that design electronic equipment and those that design wiring to interconnect this equipment. The task that is to be assigned the equipment designer is to produce equipment that will be able to withstand transients on all of the input and output wiring. The transient control levels describe the type of transients that the equipment must withstand and to which it may be subjected as part of an acceptance or proof test. The task that is to be assigned to the designer of interconnecting wiring is to assure that no external threat such as lightning or switching of inductive devices, shall induce transients higher than the control level which the avionics was designed to withstand. The control levels to which both designers must work can be defined in terms of open circuit voltage, and source impedance, or in terms of open circuit voltage and short circuit current.

The assignment of such tasks implies that there be a referee who assigns the appropriate control levels and oversees the work to ensure that both designers fulfill the tasks assigned. This referee may be called the system integrator. The transient control level philosophy is illustrated in Figure 27. The aims are as follows:

1. To insure that the actual transient level produced by lightning (or any other source of transient) will be less than that associated with the transient *control* level number assigned to the wiring designer. The wiring designer's job would be to analyze the electromagnetic threat that lightning would present and to use whatever techniques of circuit routing or shielding would be necessary to ensure that the actual transients induced by lightning did not exceed the values specified for that particular type of circuit.
2. The transient *design* level controlling the type of circuit or circuit protection techniques used, and assigned to the avionics designer, would be higher than the transient control level by a margin reflecting how important it was that lightning did not in fact interfere with the piece of avionics under design. A margin is necessary because any single lightning flash might produce an actual transient level higher than the assigned transient control level, which would have been derived for a predicted average in spite of the wiring designer's good intentions. Prediction of actual transient levels is an imperfect art.
3. The job of the avionics designer would be to ensure that the vulnerability levels of the equipment that he is to supply would be higher than the assigned transient design level. The vulnerability level is that level of transient which, if applied to the input or output circuit under question, would cause the equipment to be damaged.

There are several ways in which the levels might be set. In the first, the system integrator would set the desired transient level, then set the required margin, which in turn would set the transient control level. Whatever the rationale by which the system integrator sets the transient design level, that level would become a part of the purchase specifications and would, presumably, not be subject to variation by the vendor of the avionics. As an alternative, the avionics designer might determine by suitable testing the vulnerability and susceptibility levels of his equipment and provide a guarantee as to the level of transients that his equipment could withstand. That level would then be the transient design level. After the system integrator had set the desired safety margin, the appropriate transient control level for the wiring designer would have been established. One approach to the setting of margins appears in the Space Shuttle Criteria Document (Reference 11).

The numbers that would be assigned to the transient design level probably should be expressed in terms of the maximum voltage appropriate to a high-impedance circuit (open

circuit voltage) or the maximum current appropriate to a low-impedance circuit (short circuit current). In order for the transient coordination philosophy to have most impact, there should be a limited number of levels. One set of levels that has been proposed (Reference 12) is shown in Table III. With each level there is associated an open circuit voltage and a short circuit current; the two are related by a standard transient-source impedance, shown in Figure 28 (Reference 13).

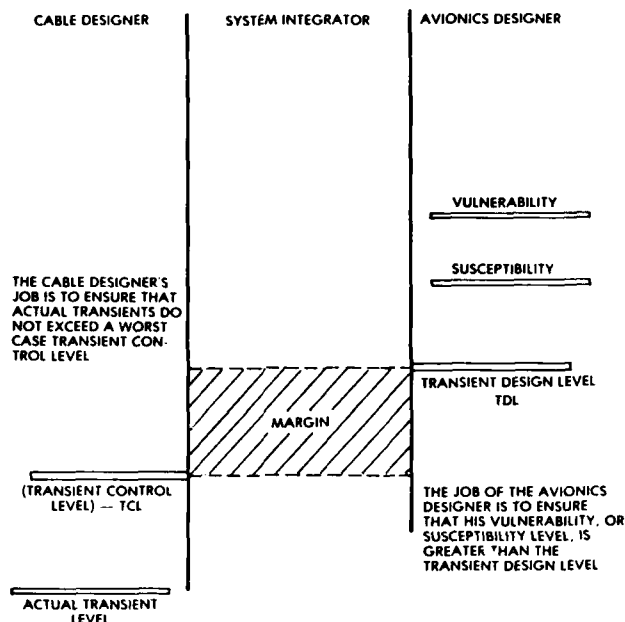


Figure 27 - The Transient Coordination Philosophy.

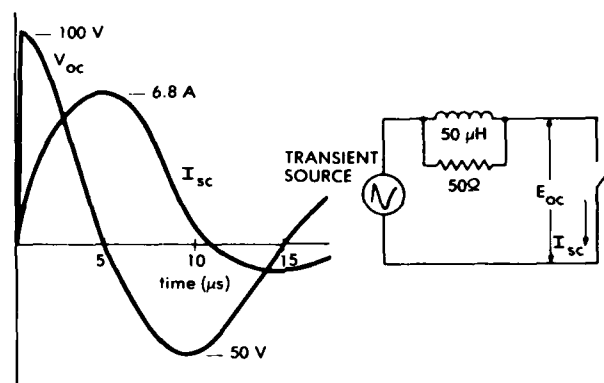


Figure 28 - Short Circuit Current (I_{sc}) Resulting from a Transient Source with V_{oc} Open Circuit Voltage and 50 Ω /50 μHz Source Impedance.

TABLE III - PROPOSED TRANSIENT CONTROL LEVELS

Proposed Transient Control Level Number	Open Circuit Voltage Level (volts)	Short Circuit Current Level (amperes)
1	10	0.68
2	25	1.7
3	50	3.4
4	100	6.8
5	250	17
6	500	34
7	1000	68
8	2500	170
9	5000	340

An alternative set of levels for which some voltages are numerically equal to the voltages in existing specifications is presented in Table IV.

TABLE IV - ALTERNATIVE TRANSIENT CONTROL LEVELS

Proposed Transient Control Level Number	Open Circuit Voltage Level (volts)	Short Circuit Current Level (amperes)
1	15	1
2	30	2
3	60	4
4	150	10
5	300	20
6	600	40
7	1500	100
8	3000	200
9	6000	400

REFERENCES

1. "Space Shuttle Lightning Protection Criteria Document", JSC-07636, National Aeronautics and Space Administration, Lyndon B. Johnson Space Center, Houston, Texas (1973).
2. "Space Shuttle Lightning Protection Criteria Document", JSC-07636, Revision A, National Aeronautics and Space Administration, Lyndon B. Johnson Space Center, Houston, Texas (1975) p. F-7.
3. "Space Shuttle Program Lightning Protection Criteria Document", Revision A, p. F-6.
4. "Space Shuttle Program Lightning Protection Criteria Document", Revision A, p. F-8.
5. "Space Shuttle Program Lightning Protection Criteria Document", Revision A, p. F-6.
6. F.A. Fisher, "Effects of a Changing Magnetic Field on Shielded Conductors", Lightning Protection Note 75-2, Internal General Electric Memorandum, High Voltage Laboratory, Corporate Research and Development, General Electric Company, Pittsfield, Mass. (1975).
7. E.F. Vance, "Coupling to Cables", DNA Handbook Revision, Chapter 11, Stanford Research Institute, Menlo Park, California (1974).
8. E.F. Vance, pp. 1-133 to 11-136.
9. "Transient Voltage Suppression Manual", Semiconductor Products Department, General Electric Company, Electronics Park, Syracuse, New York (1976).
10. J.A. Cooper and L.J. Allen, "The Lightning Arrester Connector: A New Concept in System Electrical Protection", IEEE International Electromagnetic Compatibility Symposium Record, IEEE 72CH0638-EMC, Institute of Electrical and Electronics Engineers, New York New York, (1972).
11. "Space Shuttle Program Lightning Protection Criteria Document" JSC-07636, Revision A, pp. D-2 to D-5.
12. F.A. Fisher and F.D. Martzloff, "Transient Control Levels: A Proposal for Insulation Coordination in Low-Voltage Systems", IEEE Transactions on Power Apparatus and Systems, PAS-95, 1, Institute of Electrical and Electronics Engineers, New York, New York, (1976) pp. 120-129.
13. F.A. Fisher and F.D. Martzloff, "Transient Control Levels", p. 128.

LIGHTNING EFFECTS ON AIRCRAFT: A COCKPIT PERSPECTIVE

by
J. Anderson Plumer
Lightning Technologies, Inc.
560 Hubbard Avenue
Pittsfield, Massachusetts 01201
U.S.A.

SUMMARY

Lightning strikes can be expected to occur to all types of aircraft in spite of the best efforts of the flight crews to avoid areas where lightning and other thunderstorm environments may be present. Aircraft specifically intended for flight in instrument flight rules (IFR) conditions may experience more lightning strikes than those intended primarily for use in clear weather conditions, but lightning strikes can occasionally propagate several kilometers from the originating charge cell and strike an aircraft in clear air. Knowledge of the flight and weather conditions during which aircraft are most likely to encounter strikes and some of the effects to be alert for may help pilots react safely to these events, and minimize the possibility of subsequent hazards. Most strikes have occurred when the aircraft is flying at between 3000 and 5000 meters altitude, where the outside air temperature is within 5 degrees of 0°C and there exists a light-to-moderate amount of precipitation. Strikes to aircraft have, however, occurred at altitudes as high as 12,000 m and also when the aircraft are parked on the ground. In most cases, the original lightning leader does not know where it will terminate and the aircraft is struck simply because it happens to be in the vicinity. If an aircraft approaches a highly electrified region, however, it may actually trigger a strike, especially if the aircraft is large and causes a significant perturbation in the nearby electric field. Typical conditions in which strikes have been experienced by large and small aircraft are described, together with effects as experienced by flight crews.

AIRCRAFT-LIGHTNING STRIKE MECHANISM

At the beginning of lightning-flash formation, when a stepped-leader propagates outward from a cloud charge center, the ultimate destination of the flash at an opposite charge center in another cloud or on the ground has not yet been determined. The difference of potential which exists between the stepped-leader and the opposite charge center(s) establishes an electrostatic force field between them, represented by imaginary equipotential surfaces. These are shown as lines in the two-dimensional drawing of Figure 1. The field intensity, commonly expressed in kilovolts per meter, is greatest where equipotential surfaces are closest together. It is this field that is available to ionize air and form the conductive spark which is the leader. Because the direction of electrostatic force is normal to the equipotentials and strongest where they are closest together, the leader is most likely to progress toward the most intense field regions.

If an aircraft happens to be in the neighborhood, it will assume the electrical potential of its location. Since the aircraft is a thick conductor and all of it is at this same potential, it will divert and compress adjacent equipotentials, thus increasing the electric field intensity in the vicinity of the aircraft, and especially between it and other charged objects, such as the leader. If the aircraft is far away from the leader, its effect on the field near the leader is negligible; however, if the aircraft is within several tens or hundreds of meters from the leader, the increased field intensity in between may be sufficient to attract subsequent leader propagation toward the aircraft. As this happens, the intervening field will become even more intense, and the leader will advance more directly toward the aircraft.

The highest electric fields about the aircraft will occur around extremities, where the equipotential lines are compressed closest together, as shown in Figure 2. Typically, these are the nose and wing and empennage tips, and also smaller protrusions, such as antennas or pitot probes. When the leader advances to the point where the field adjacent to an aircraft extremity is increased to about 30 kV/cm, the air will ionize and electrical sparks will form at the aircraft extremities, extending in the direction of the oncoming leader. Several of these sparks, called *streamers*, usually occur simultaneously from several extremities of the aircraft. These streamers will continue to propagate outward as long as the field remains above about 7 kV/cm (Reference 1). One of these streamers

will meet the nearest branch of the advancing leader and form a continuous spark from the cloud charge center to the aircraft. Thus, when the aircraft is close enough to influence the direction of the leader propagation, it will very likely become attached to a branch of the leader system.

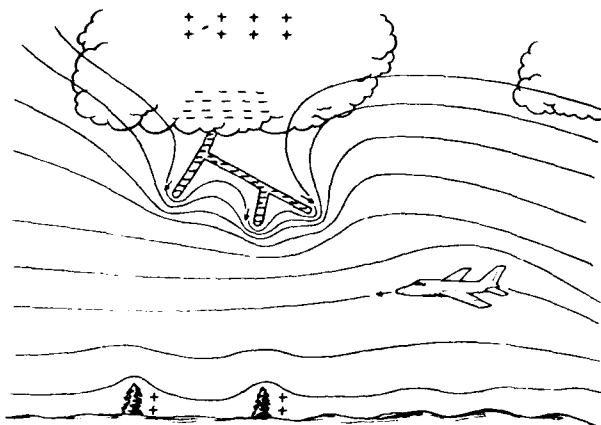


Figure 1 - Aircraft Influence on Stepped-leader Direction.

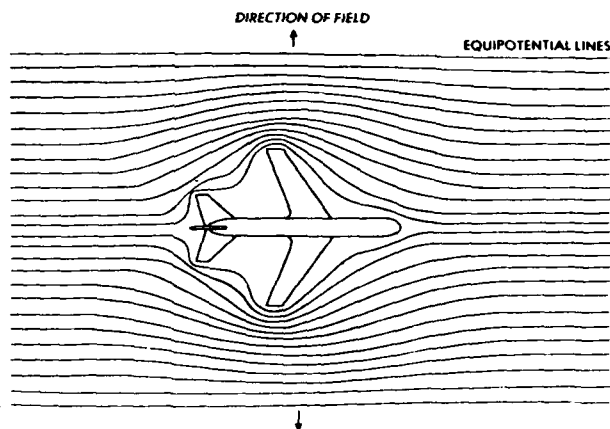
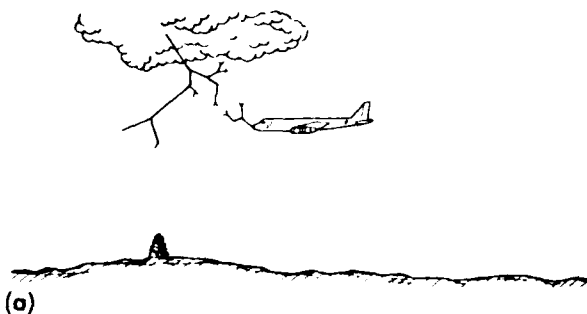


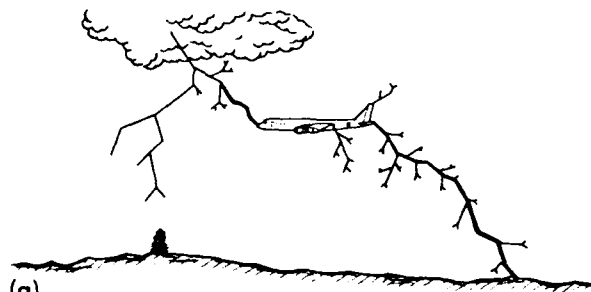
Figure 2 - Compression of Electric Field Around an Aircraft.

When the aircraft is attached to the leader, some charge (free electrons) will flow onto the aircraft, but the amount of charge which can be taken on is limited by the aircraft size. Thus, the aircraft merely becomes an extension of the path being taken by the leader on its way to an ultimate destination at a reservoir of opposite polarity charge. Streamers may propagate onward from two or more extremities of the aircraft at the same time. If so, the oncoming leader will have split, and the two (or more) branches will continue from the aircraft independently of each other until one or both of them reach their destination. This process of attachment and propagation onward from an aircraft is shown on Figure 3.

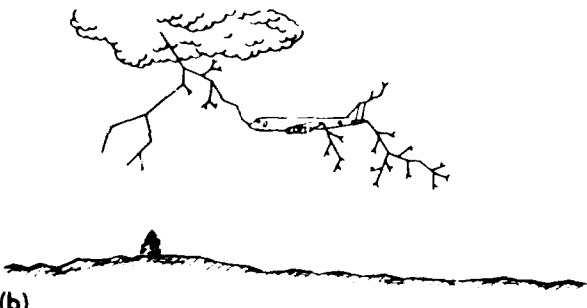
When the leader has reached its destination and a continuous ionized channel between charge centers has been formed, recombination of electrons and positive ions occurs back up the channel, and this forms the high-amplitude return stroke current. This stroke current and any subsequent stroke or continuing current components must flow through the aircraft, which is now part of the conducting path between charge centers, as shown in Figure 4(a).



(a)

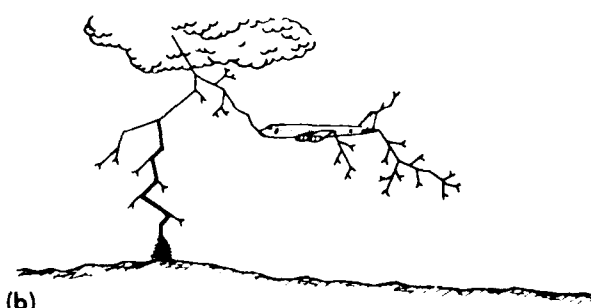


(a)



(b)

Figure 3 - Stepped-leader Attachment to an aircraft.
(a) Stepped-leader approaching aircraft
(b) Stepped-leader attachment and continued propagation from an aircraft



(b)

Figure 4 - Return Stroke Paths.
(a) Return stroke through the aircraft
(b) No return stroke through the aircraft

If another branch of the original leader reaches the ground before the branch which has involved the aircraft, the return stroke will follow the former, and all other branches will die out, as shown in Figure 4(b). No substantial currents will flow through the aircraft in such a case, and any damage to the aircraft will be slight.

Precipitation Static

The preceding analysis began with the assumption that the aircraft is at the potential of its position in an electric field established by the cloud and ground charge centers. In dry air this is correct, but if the aircraft is flying through dry precipitation in the form of sleet, hail, or snow, the impact of these particles on the aircraft will cause a charge to separate from the particle and join the aircraft, leaving the aircraft with a preponderance of positive or negative charge (depending on the form of precipitation), thereby changing its potential with respect to its surroundings. This phenomenon is known as *triboelectric charging* and has been extensively studied by Tanner and Nanevich, and others (Reference 2). It is commonly referred to as *precipitation static*, or *P-static*.

The P-static charging process is easily capable of raising the aircraft to a potential of 50 kV, or more, with respect to its surroundings, a charge sufficient to cause ionization of sharp extremities. The ionization radiates broadband electromagnetic radiation (EMR) throughout the low- and high-frequency spectrum. This EMR is often received as interference, or *static*, by the aircraft communications or low-frequency automatic direction finding (LF-ADF) receivers.

The EMR results from a continuous series of minute streamer-like discharges of ionized air in the immediate (i.e., 10 cm) vicinity of sharp extremities. These discharges also produce a continuous ultraviolet glow visible at night and called *St. Elmo's Fire* or *corona*.

P-static discharging (corona) will occur initially from the sharpest extremities, where the surrounding field first reaches the ionization potential for air. If more P-static charge enters the aircraft than is bled off by the discharges at these extremities, the aircraft potential will increase until the field surrounding extremities of large radii also becomes intense enough to ionize air. Thus, as the aircraft potential increases, the radiated EMR from static discharging becomes more intense, and so does the associated static in communications receivers.

P-static persists for as long as the aircraft is being charged by impact with dry precipitation, such as sleet or snow. It is rarely reported in rain. It is thus a continuous phenomenon lasting from several seconds to many minutes. Once the aircraft has left such a region, the static in communications receivers quickly clears up, and the aircraft potential reverts to that of its surroundings-established again by its location in the ambient cloud-ground electric field. Because of its low capacitance, an aircraft cannot retain enough P-static charge to produce a startling flash of several meters (or more) in length or a loud report, such as is often heard when lightning strikes the aircraft. Nevertheless, pilots often report a "static discharge" from the aircraft, and proceed to describe the symptoms of a lightning strike: i.e., a long, bright flash or spark extending outward from the aircraft, usually accompanied by a loud report, such as that which would be produced by a shotgun going off outside the cockpit.

Thus, the P-static process cannot contribute much to the formation of a lightning leader or to the process of leader attachment to an aircraft. It is true that an approaching streamer is most likely to attach to a point from which an opposing streamer has developed, but the intense field produced by an advancing leader would overcome that produced by the P-static process and draw streamers of its own from most locations where P-static discharges were occurring.

The P-static discharging process may be intensified when the aircraft is in a region where the ambient electric field is relatively intense, as is the case when a lightning flash is imminent. When the flash occurs (whether or not it intercepts the aircraft), the main charge centers are neutralized and the field collapses, thereby reducing the intensity of P-static discharging. This is the reason that pilots frequently report that P-static interference gradually intensifies until a lightning flash occurs and then diminishes instantaneously. This experience reinforces the pilot's impression that the flash is a sudden static discharge from the aircraft alone. For this reason P-static interference should be looked upon by pilots as an indicator that a lightning strike may be imminent (i.e. within a few seconds or minutes). P-static interference is, in fact, reported prior to the lightning strike in about half of the lightning strike incidents described in recent airline lightning-strike reports (Reference 3).

Aircraft Triggering of Lightning Strikes

A question that is often asked is whether an aircraft can initiate or *trigger* a lightning strike that would not have occurred if the aircraft were not present, or at least would not have occurred *at that time* if the aircraft had not been present. While there is insufficient scientific data upon which to base a conclusive answer to this question, the following factors suggest that the aircraft does not often trigger a flash.

1. Aircraft often fly through electrified regions without being struck, while lightning flashes are occurring nearby.

2. The stepped-leader must begin from a charge source capable of furnishing it with several coulombs of charge. Thus, the potential (voltage) of this center, and the surrounding field intensity, would seem to be much greater than that about an aircraft, leaving the implication that, unless the aircraft is very close to the charge center, it can have little influence on the surrounding field or on the process of leader initiation.
3. Laboratory breakdown tests of long high-voltage air gaps, thought to be similar to lightning leader formation, show that initial ionization always begins at one of the electrodes and not from an object suspended in the gap (Reference 4). Such an object significantly influences the voltage level at which breakdown begins only if it is close enough to one electrode to influence the field about this electrode.

It is more probable that the aircraft does not become involved until after leader propagation has begun. If the leader happens to approach the aircraft, the field intensification produced by the presence of the aircraft becomes much more significant, and the leader may now be attracted to the aircraft.

There is some evidence (Reference 5) that jumbo jet (wide-body) aircraft do trigger their own flashes, but this is not yet conclusive, since accumulated flight hours are not yet as great as those for conventional aircraft. If large-body aircraft are in fact triggering flashes, it is probably because their larger sizes make a more noticeable perturbation on the electric field near the cloud charge centers from which leaders begin.

The aircraft motion has little influence on the propagating leader because the aircraft is moving much slower, about 10^2 m/s, than the leader, which is advancing at 10^5 to 10^6 m/s. Thus, the aircraft appears stationary to the leader during the leader formation process.

Swept Strokes

After the aircraft has become part of a completed flash channel, the ensuing stroke and continuing currents which flow through the channel may persist for up to a second or more. Essentially, the channel remains in its original location, but the aircraft will move forward a significant distance during the life of the flash. Thus, whereas the initial entry and exit points are determined by the mechanisms previously described, there may be other, subsequent, attachment points that are determined by the motion of the aircraft through the relatively stationary flash channel. In the case of a fighter aircraft, for example, when a forward extremity such as the pitot boom becomes an initial attachment point, its surface moves through the lightning channel, and thus the channel appears to sweep back over the surface, as illustrated in Figure 5. This occurrence is known as the swept-flash phenomenon. As the sweeping action occurs, the type of surface can cause the lightning channel to attach and dwell at various surface locations for different periods of time. If part of the surface, such as the radome, is nonmetallic, the flash may continue to dwell at the last metallic attachment point (aft end of the pitot boom) until another exposed metallic surface (the fuselage) has reached it; or the channel may puncture the nonmetallic surface and reattach to a metallic object beneath it (the radar dish). Whether puncture or surface flashover occurs depends on the amplitude and rate of rise of the voltage stress created along the channel, as well as the voltage-withstand strength of the non-metallic surface and any air gap separating it from enclosed metallic objects. When the lightning arc has been swept back to one of the trailing edges, it may remain attached at that point for the remaining duration of the lightning flash. An initial attachment point at a trailing edge, of course, would not be subjected to any swept-stroke action.

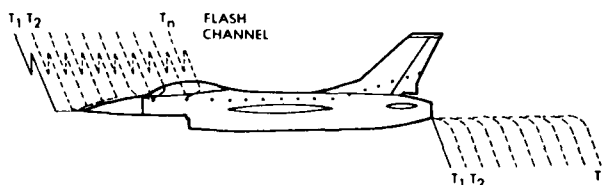


Figure 5 - Typical Path of Swept-flash Attachment Points.

The aircraft cannot fly out of, or away from, the channel. This is because the potential difference between charge centers (cloud and earth or another cloud) is sufficient to maintain a very long channel until the charges have neutralized each other and the flash dies. The aircraft is a very small (and highly conductive) part of the channel and cannot move sufficiently far away from the vicinity of the channel to become detached from it during the brief lifetime of a lightning flash.

From the cockpit perspective, the sweeping channel may appear as a swirling, luminous column stretching alongside the cabin and extending away from it, toward the region from whence it came. When the return stroke and subsequent strokes pass through the channel, a very bright flash and loud bang may be experienced in the cockpit. The flash may cause temporary blindness of the eyes, for periods of up to 30 seconds, especially if the strike occurs at night. The experiences of several pilots are illustrative of these effects:

"I will describe two events briefly, the first in an old propeller plane in extreme turbulence--the second event more recent in smooth air in a modern 4-engine jet.

1. The date: about 1953, aircraft type: DC-6B (4 piston engines), no radar, aircraft in scheduled passenger/belly freight configuration. Time: early afternoon Place: over Garden City, Kansas. Cloud condition: line of building cumulonimbus, bottoms perhaps 6,000 to 8,000 ft. tops 30,000 ft. plus. Crew: two pilots, 1 flight engineer.

The event: aircraft in 'clean' configuration entered large building cumulonimbus clouds. In the first few seconds only a few minor bumps and some frost and ice on the windshield occurred. The aircraft then 'hit' a wall of hail. Noise of the hail made cockpit communication dependent upon shouting. Aircraft attitude longitudinally was to a degree maintained by almost full fore and aft elevator movement with the help of full to idle power on all four engines. Aircraft altitude rose from an entry altitude of 16,000 ft. to an exit (from the cloud) altitude of 24,000 ft. During this forward and upward transit thru the cloud the aircraft 'rolled' around its longitudinal axis several times from about 10 degrees beyond the vertical each way, this in spite of full aileron input to prevent this. Airspeed was able to be bracketed approximately between 100 and 200 MPH. Hailstones were marble-size.

Electrical phenomena: During the entire transit thru the hail (perhaps 3 to 4 minutes), I noticed that a redish lightning discharge off the nose area kept recurring approximately every 2 to 3 seconds. As we began to fly out of the cloud and the hail began to let up, the discharge frequency abated. No discharge noise or anything audible associated with the discharges could be heard above the roar and general commotion. No damage, burn or tear or puncturing occurred. Our metro later reported a tornado over Garden City at the time we transited the cloud although we surely didn't encounter the funnel.

2. The date: about 1974, aircraft type: Boeing 707 (4 jet engines), with radar aircraft in scheduled passenger/belly freight configuration, on a ferry flight. Time: early evening, Place: between Philadelphia and Washington, D.C. heading toward N.Y. Cloud conditions: a line of low-level thunderstorms with small 'do-nut' defined centers (on radar) with bottoms perhaps 5,000 ft. and tops perhaps 29,000 ft. Crew: 2 pilots and 1 flight engineer. Being dark there was visible lightning, mostly cloud to cloud but some cloud to ground.

The event: aircraft in 'clean' configuration at an approximate altitude of 18,000 ft. entered a cloudy area between two active small cells. The aircraft speed was about 230 knots indicated. As we entered the cloud the windshield lit up with dancing static. The air became quite smooth and suddenly a large blue glow appeared off the nose. Lifting my seat so I could better look down onto the nose area, I saw the typical big 'bushel basket' of shimmering pale blue (corona) collecting onto the radar dome. I immediately lowered my seat and squinted my eyes and told the two pilots to 'watch your eyes, sometimes this "goes off" with a big spark more than once.' I had no more than said this when the big flash went off. The noise inside the aircraft was a big 'grunt' or 'whump', as though the aircraft had been mounted by an elephant. I asked, 'Is everyone all right?' The co-pilot, who had been flying the aircraft on instruments and who had been hunched down, responded that he was O.K. I glanced at the navigation instruments and they all agreed (on some of our 707's, an iron piece above and between the windshields sometimes becomes magnetized). The captain who had his seat raised and had been looking out and down onto the (corona) when it went off turned about in his seat and said that he couldn't see anything. (His normal vision returned in about 30 seconds). He later mentioned that he had never seen such a static build-up before and wanted to get a good look at it. We shortly thereafter flew out of the clouds and the static build-up did not recur. Maintenance at JFK had the aircraft out of service for 2 to 3 days replacing popped-out small inspection panels, many in the empennage area.

In general:

1. Electrical discharges occur both in rough/violent as well as smooth air, amidst hailstones, or dry ice crystals.
2. There may or may not be electrical discharge damage or magnetizing of parts of the aircraft or affectation of compass type instrumentation.
3. Squinting one's eyes and slightly lowering them into the cockpit (at night) will give more than enough protection against the sudden 'brightness' of any discharge.
4. Protecting one's eyes during daylight flight is not necessary.
5. There is a loud 'whump' inside as the charge discharges and an 'arcing' sound out front. (The 'whump' around me and the big flash both simultaneously occur.) I simply seem to be 'aware' that the spark made an arcing sound at the same instant -- (like striking an arc with an electric welder).

6. Reports from passengers say that immediately before a discharge, the trailing edges of wings, flaps, etc. were pouring off electrical 'fire'. (This report was made at night time.)

7. Aside from the aspects of electrical display: any pod-slung aircraft flying through an area of thunderstorms on radar is in a risky regime at best. A pod-slung aircraft having lost its radar in a thunderstorm area is in immediate grave danger due to its inability to stay together in violent turbulence found inside the typical 'electrical storm' or thunderstorm". (Reference 6).

- - - - -

"On December 14, 1972, about 2:30 a.m. I was flying at 11,000 feet in moderate rain at about 0°C. We were on instruments and in clouds. The screws on my windshield bar were discharging corona both left and right for a distance of about six inches in a near horizontal pattern. As the rain struck the windshield, bright discharges came down the windshield from the top metal fuselage edge to the base, in opposition to the rain drops. I had never witnessed the phenomenon but my copilot, an airline pilot, said he had seen the phenomenon several times before.

Our attention was directed to the tail of the airplane, a Twin Comanche, which was bathed in white light. I thought at first we must be above the overcast in moonlight; however, this was not the case. The entire back of the airplane, including the tail surfaces, were illuminated with a steady white light as if under powerful white incandescent lighting. This light grew in intensity just prior to running into heavier precipitation, at this time sleet. The light did not pulsate. If corona was discharging off my wicks, it was not visible from my cockpit position. No discharges were coming off the wing wicks. My copilot had never before witnessed this phenomenon". (Reference 7).

- - - - -

"It was a ferry flight to Farragut, ID. Enroute there were many scattered thunder showers. As we approached Billings, Montana, the build-up was becoming more and more noticeable. We had severe radio static. Communication was impossible with Billings. To reduce static somewhat I reduced RPM. That was when we were struck directly on the nose section. Seconds of just blank, then a hurried look at gauges, radios, instruments and personnel. The Radio Operator said a ball of flame passed down the isle through the door. The passenger said the ball of flame about the size of a basket-ball rolled down the isle even with the right wing, out through the fuselage, down the wing and off the tip. After landing at Billings the aircraft was checked completely for any skin damage. None was found, but there was 70 ft. of trailing antenna burned off the radio station spool.

Although this is thirty-five years late, I can say a lightning strike, (experienced from the cockpit) will leave a permanent impression as well as respect for the same". (Reference 8).

SYNOPTIC METEOROLOGICAL CONDITIONS OUTSIDE THE COCKPIT

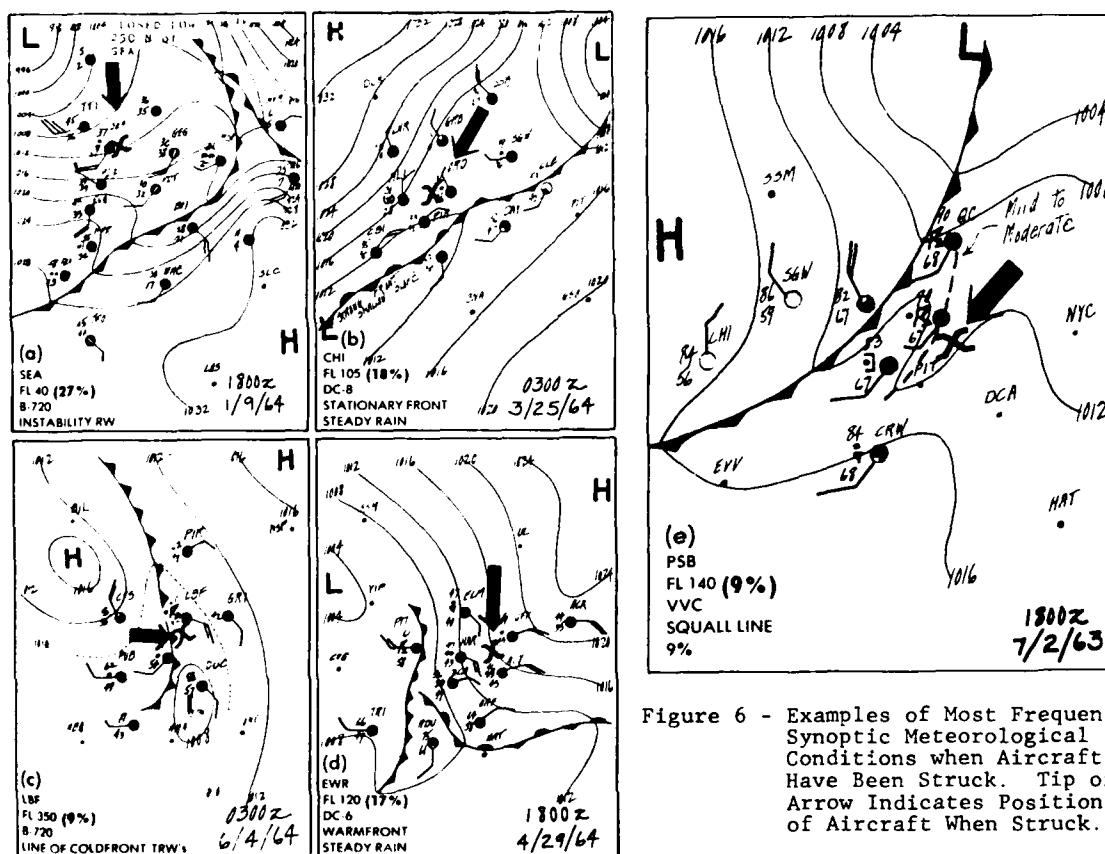
The experiences discussed thus far might imply that an aircraft must be within or very near a cloud to receive a lightning strike and, since electrical charge separation is associated with precipitation, that most strikes would occur when the aircraft is in regions of precipitation. Strike incident reports show that these conditions often do exist, but other lightning strikes occur to aircraft in a cloud when there is no evidence of precipitation nearby, or even to aircraft flying in clear air a supposedly safe distance from a thundercloud. Regulatory Agency and operator advisory procedures instruct pilots to circumvent thunderclouds or regions of precipitation evident either visibly or on radar, but strikes to aircraft flying 40 kilometers (25 miles) from the nearest radar returns of precipitation have been reported. Occasionally a report of a "bolt from the blue" with no clouds anywhere around, is received. It is highly improbable, however, that these reports are correct because it does not seem possible for electrical charge separation of the magnitude necessary to form a lightning flash to occur in clear air. In most well-documented incidents, a cloud is present somewhere (i.e. within 40 kilometers) when the incident occurs.

Perhaps of most interest to pilots are the area weather conditions which prevailed at the time of reported strikes. There is no universal data bank for this type of data, but a useful summary has been made by H. T. Harrison (Reference 9) of the synoptic meteorological conditions prevailing for 99 United Air Lines lightning-strike incidents occurring between July 1963 and June 1964. Table I lists the synoptic type and percentage of incidents (~ number of cases) occurring in each type. Examples of the most predominant synoptic conditions are presented in Figure 6 (a), (b), (c), (d), and (e) (Reference 10).

Table I - SYNOPTIC TYPES INVOLVED WITH
99 ELECTRICAL DISCHARGES

JULY 1963 to JUNE 1964

Synoptic Type	Percentage
Airmass instability	27
Stationary front	18
Cold front	17
Warm front	9
Squall line or instability line	9
Orographic	6
Cold LOW or filling LOW	5
Warm sector apex	3
Complex or intense LOW	3
Occluded front	1
Pacific surge	1

Figure 6 - Examples of Most Frequent
Synoptic Meteorological
Conditions when Aircraft
Have Been Struck. Tip of
Arrow Indicates Position
of Aircraft When Struck.

Harrison has summarized this data by saying that any conditions which will cause precipitation may also be expected to cause electrical discharges (lightning), although he adds that no strikes were reported in the middle of warm front winter snowstorms. Data reporting projects of Plumer and Perry (Reference 11) show that lightning strikes to aircraft in the United States and Europe occur most often during the spring and summer months, when thunderstorms are most prevalent.

It is also important to note that many strike incidents have been reported where no bona fide thunderstorms have been visually observed or reported. The United Air Lines flight crews stated that no thunderstorms were reported in the area in 42% of the lightning strike incidents documented in the aforementioned summary, as shown in Table II.

TABLE II - PERCENTAGES OF STRIKE INCIDENTS
VS REPORTED THUNDERSTORMS

Thunderstorms Reported in Vicinity	33%
Thunderstorms Reported in General Area	24%
No Thunderstorms Reported	42%

Figure 7 shows the immediate environment of the aircraft at the times of the 214 strikes reported in the project of Plumer and Hourihan (Reference 13). In over 80% of the strikes reported, each aircraft was within a cloud and was experiencing precipitation and some turbulence. With precipitation present, turbulence is to be expected, since vertical air currents acting against precipitation are thought to be the cause of electrical charge separation.

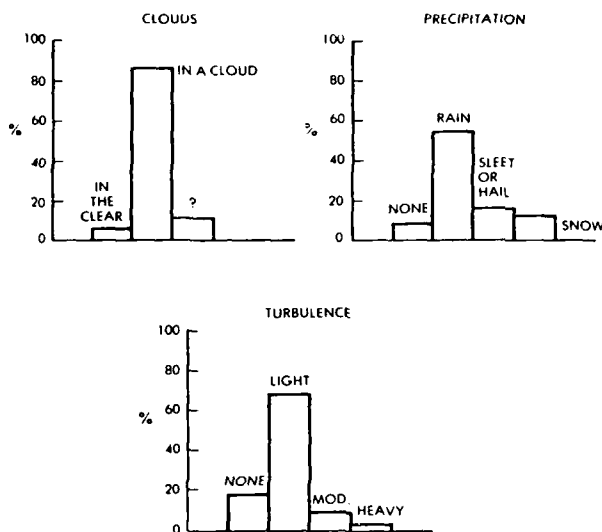


Figure 7 - Environmental Conditions at Time of Strike.

Incident reports also show that most aircraft strikes occur when an aircraft is near the freezing level of 0°C . Freezing temperatures (and below) are thought to be required for the electrical charge separation process to function. Of course, strikes to aircraft at temperatures higher than $+10^{\circ}\text{C}$ have occurred when the aircraft was close to (or on) the ground, where the ambient air temperature may be as high as about $+25^{\circ}\text{C}$, and strikes at temperatures below 0°C have occurred at high altitudes.

EFFECTS IN THE COCKPIT

Avionics and Electric Power Systems

In most cases the only noticeable effect of lightning currents having passed through an aircraft are the small pit marks left where the lightning flash attached to the aircraft. There may be some effects on flight instruments or other avionic systems and pilots should be aware of these possibilities.

For example, if there is a pitot tube on the nose radome, as is the case on most fighters, the probe is attractive to lightning. Usually the pitot probe is grounded to the airframe by a wire inside the radome. Sometimes this ground wire is too thin to carry severe lightning currents and it has exploded on several occasions, with damage similar to that of Figure 8. Sometimes the aluminum tubes which bring pitot static pressure back to the instruments have acted as the ground conductor, but the intense magnetic fields surrounding lightning currents often crimp such tubes, cutting off instrument air. To make matters even worse, the power cord which brings electric power out to the probe heater may also be exposed to the lightning magnetic fields. These fields may induce severe surge voltages in the heater power circuit. Since the heater is usually powered from the aircraft's essential power distribution bus, other equipment powered from this source is exposed to the same surge. The immediate result has been damage to a variety of other electronic equipment and has led, in a few cases, to loss of the entire aircraft. Much more is known today about how to protect against these effects, so that radomes and pitot systems in the aircraft now being built are not likely to be as vulnerable. The consequence of these effects may be loss of instruments that depend on pitot probe air data, and disruption of other electronic systems that receive power from the same source. Pilots should be aware of these consequences after strikes to the nose or other locations where instrument probes are located.

Because they are usually located on wing tips or other extremities, navigation lights are also frequently struck by lightning. Normally, the flash attaches to the metal lamp housing and does little damage, but once in a while it will break the globe and light bulb, exposing another path whereby lightning currents may enter an aircraft's power distribution system. This, like the probe heater situation described above, is another of the more hazardous lightning effects for it may cause loss of instruments or communication equipment needed in bad weather. The circuit breakers for this equipment will usually pop but not before the lightning surge has already passed by and caused whatever damage it may.

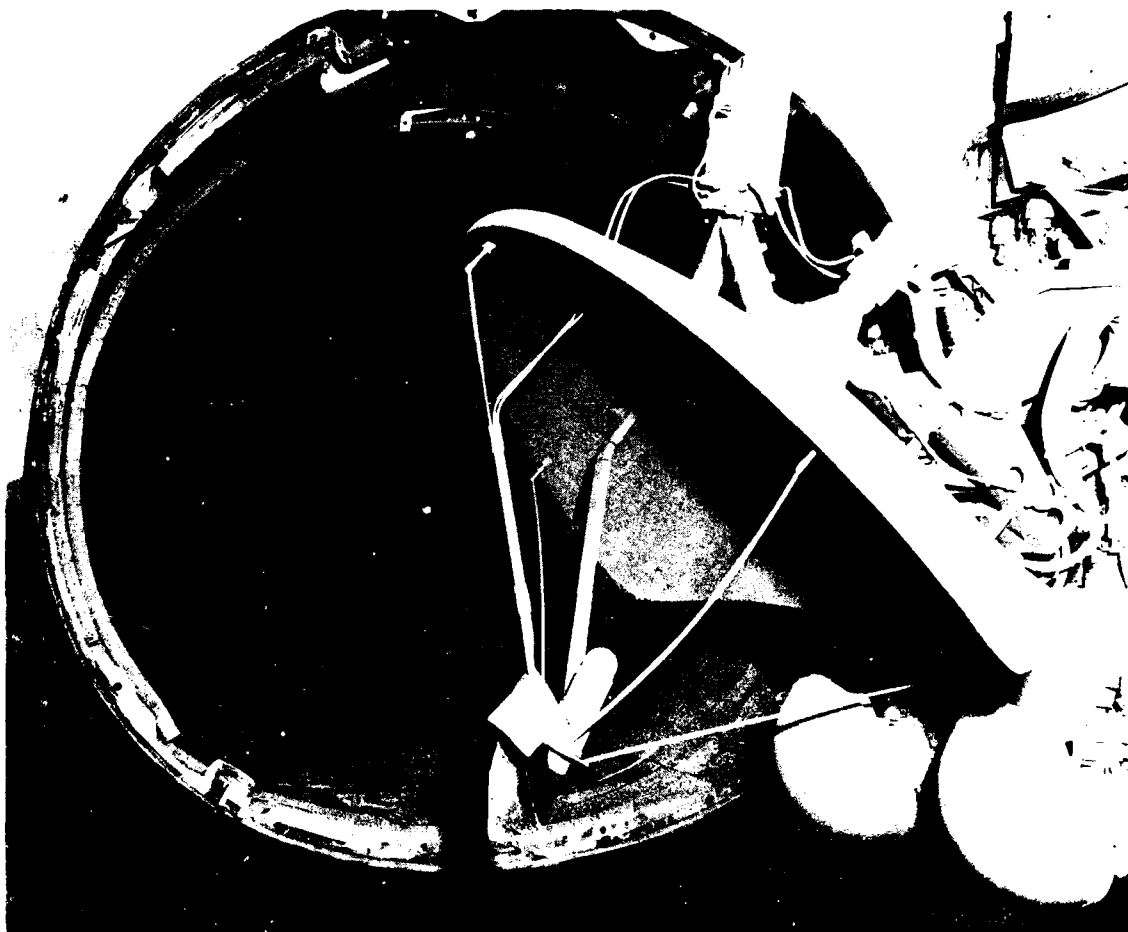


Figure 8 - Lightning Damage to Pitot Probe Instrument Air Tubes and Heater Power Harness.

Surge arrestors are available to suppress these surges before they get this far, but until recently they have not been incorporated in most aircraft electronic systems. When circuit breakers pop during a lightning strike event the flight crew should try to reset them, but should also be aware that some equipment may already be damaged.

As discussed earlier, precipitation static charging and/or discharging phenomena may also accompany lightning strikes. This phenomena, commonly called "P-static", occurs when an aircraft is flying through rain, sleet, hail, or snow. The impact of these particles on the aircraft causes a charge to separate from the particle and join the aircraft, leaving the aircraft with a preponderance of positive or negative charge (depending on the form of precipitation) and thereby elevating its potential with respect to its surroundings. Since the aircraft has capacity for only a small amount of this charge, some of it will begin to leak off in the form of ionization at sharp extremities. This ionization continues as long as the aircraft is flying in P-static charging conditions (precipitation) and is visible as a bluish corona (St. Elmo's fire) at night. Unfortunately, this ionization radiates broadband electromagnetic radiation (EMR) throughout the low and high frequency radio bands. This EMR is often received as interference, or "static" by the aircraft communication or low-frequency automatic direction finding (LF-ADF) or communication receivers, and may render this equipment temporarily unusable. The static dischargers usually found on tips and trailing edges reduce this interference by making it easier for the charge to leave the aircraft, but they are not always 100% effective, especially in heavy precipitation. Since the conditions that produce P-static may also produce lightning, a strike should be considered possible when P-static occurs.

Engine Effects

Flameouts or compressor stalls of fuselage-mounted engines of military fighter and other small aircraft must also be expected when lightning strikes occur. For example, from a recent group of 10 strikes reported to business-jet aircraft in the U.S. (Reference 13) four resulted in flameout of one engine and a fifth caused both engines to stop. It was possible to re-start the engine in flight in all but two of these instances, in which restarts were not possible until after the aircraft had landed. The aircraft that

lost both engines was struck at 31,500 feet and in spite of repeated attempts, the engines would not start again until the aircraft had descended to 13,000 feet. One instance of a turbo-prop engine flaming out has also been reported, with an in-flight re-start being obtained shortly afterwards.

Study of these incident reports and discussions with the operators involved reveals that the engine flameouts are probably caused by the disruption of inlet air which results when the hot lightning channel is swept in front of an engine as illustrated in Figure 9.



Figure 9 - How a Lightning Strike Causes Engine Flameouts.

Lightning flashes, of course, initially attach to extremities such as the nose or wing tips, but since the aircraft is moving, the lightning channel will become elongated and re-attach to other spots aft of the initial attachment point as illustrated in the insert of Figure 9. Items mounted on the fuselage, including the engines, may thus be exposed to the lightning channel even if they are not struck in the first place.

A typical lightning channel is a long, tortuous column of luminous, electrically conductive air. It may be a foot or more in diameter, and at its center, temperatures as high as 30,000°K and pressures of many atmospheres may be reached. This channel may disrupt the orderly flow of air into a small jet engine, sufficient to cause a compressor stall or flame-out. The reasons that lightning-related engine flameouts do not occur to transport category aircraft with fuselage-mounted engines are (1) that the flash has died before being swept the longer distance back to the engine intakes, and (2) that the intakes themselves are larger and a flash might not disrupt sufficient air to stall the engine.

Some operators have considered whether the engine flameouts might be due to a lightning related disruption of electric power or to some other indirect effect of the lightning strike. Since no damage to engine electronics or fuel pumps has been reported it appears that such effects are not the cause. Also, while loss of electric power was indeed reported in a number of incidents, they don't happen to be the ones that involved engine flameouts. The difficulty in obtaining inflight re-starts after these flameouts may be the result of flooding, since precipitation was also reported in four out of the five incidents. Rain was reported in two of the three cases of re-start difficulty.

As for protection against flameouts, there is no protective device or design change presently known that would improve the situation, although these incident reports have prompted researchers to begin discussions of how the effect might be simulated in the laboratory - a first step toward learning more about the intensities of temperature and overpressure required to disrupt these engines, and the extent to which they are related to engine power settings. Fortunately, some comfort can be derived from the fact that in most cases only one engine flames out. This is logical because the lightning flash usually sweeps along only one side of the fuselage. In the case where both engines flamed out, the strike must have swept along both sides at once. In this case the lightning strike must have entered one side of the fuselage and exited from the other side, as shown in Figure 10.

Therefore, at least until more is learned about the flameout problem, the best advice for operators of small aircraft is:

- Be aware that lightning may cause flameouts (to turbo-props as well as turbo-jet aircraft)
- Avoid areas of heavy precipitation, and
- Be familiar with in-flight re-start procedures

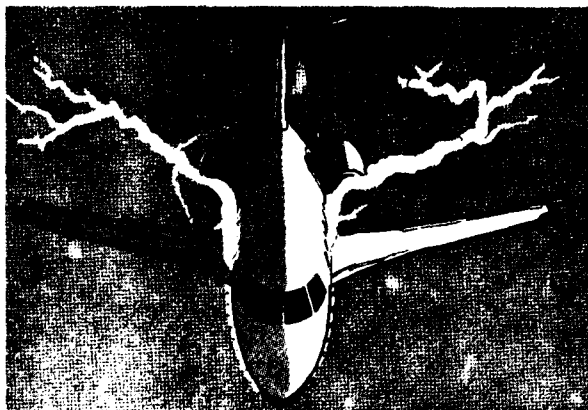


Figure 10 - Possible Cause of Dual Engine Flameouts.

- The strike enters one side and exits from the other.

Personnel

The most hazardous effect that cockpit or cabin occupants are likely to receive from a lightning strike is temporary blindness from the bright flash, if the strike occurs near a window. This blindness usually (but not always) occurs at night and may persist for up to 30 seconds, during which time it may not be possible to read flight instruments. If there are two pilots, one may minimize this problem by keeping his eyes lowered and focused on instruments when flying in an electrified region. Increasing the intensity of instrument lights may help in reducing eye sensitivity before the flash occurs, thereby making the instruments easier to regain afterwards.

Some pilots also report receiving a mild electric shock when lightning strikes occur, especially when positioned beneath a bubble-type canopy. Since most cockpits are fabricated of conducting materials, the electric potentials of objects in the cockpit remain very nearly the same with respect to one another - even during the lightning strike - and pilots are not in danger of being electrocuted. The strong electric fields which can pass through the canopy or windows as the leader approaches, however, may give rise to streamers from the pilot's helmet or shoulders, causing a slight shock if the currents which feed these streamers pass through his body. Just as often though, the shock is simply his startled reaction to the loud bang accompanying the strike.

The effects on occupants may be much more serious, however, within a non-metallic airplane, such as a glider. In such a craft, the control cables may be the only electric conductors present and may place the pilot in a direct path between lightning attachment points, with fatal consequences.

REFERENCES

1. C.T. Phelps, "Field Enhanced Propagation of Corona Streamers," Journal of Geophysical Research 76, 24 (August 1971), pp. 5799-5806.
2. R.L. Tanner and J.E. Nanevich, "An Analysis of Corona-Generated Interference in Aircraft," Proceedings of the IEEE 52, 1, Institute of Electrical and Electronics Engineers, New York, New York (January 1964) pp. 44-52.
3. B.I. Hourihan, "Data from the Airlines Lightning Strike Reporting Project", Summary Report GPR-75-004, High Voltage Laboratory, Environmental Electromagnetics Unit, Corporate Research and Development, General Electric Co., Pittsfield, Mass. (1975), p.5.
4. R.H. Golde, "Lightning Protection" (London: Edward Arnold, 1973), p. 25.
5. E.T. Pierce, "Triggered Lightning and Some Unsuspected Lightning Hazards," American Association for the Advancement of Science 138th Annual Meeting, 1971, Stanford Research Institute, Menlo Park, California (January 1972), pp. 14-28.
6. Pilot J.S. Brattain, Gardena, California, USA.
7. Pilot G.A. Brewer, Marion, Massachusetts, USA.
8. Pilot A.H. Lowell, San Jose, California, USA.
9. H.T. Harrison, "UAL Turbojet Experience with Electrical Discharges", UAL Meteorological Circular No. 57, United Air Lines, Chicago, Illinois, (January 1965), pp. 27-48.

REFERENCES - continued

10. H.T. Harrison, "UAL Turbojet Experience", pp. 30, 37, 39, 43, 47.
11. J.A. Plumer and B. L. Perry, "An Analysis of Lightning Strikes in Airline Operation in the USA and Europe," Proceedings of the 1975 Conference on Lightning and Static Electricity at Culham Laboratory, England, (April 1975) Session IV: Aircraft Applications, the Royal Aeronautical Society of London (December 1975), pp. 2, 10.
12. B.I. Hourihan, "Data from the Airlines Lightning Strike Reporting Project".
13. J.A. Plumer, "Lightning Strike Feedback: Some Trends Emerge", Flight Operations, February 1979, pp. 23-29.

BASIC PHENOMENOLOGY OF ELECTRICAL DISCHARGES AT ATMOSPHERIC PRESSURE

by Joseph TAILLET

Office National d'Etudes et de Recherches Aéronautiques (ONERA)

92320 CHATILLON (FRANCE)

SUMMARY

Starting from a short reminder of a few fundamental laws of plasma physics, the mechanism of the three types of discharges induced by static charging (spark, corona and surface streamers) is described in detail. From this mechanism, the radioelectric noise emitted by these discharges is predicted.

This lecture is intended for an introduction to the analysis of the disturbances produced by this radiation and to the study of hardening methods, which constitutes the subject of an associated lecture of the same series.

I - INTRODUCTIONI.1 - Aim of the lecture

When an aircraft is subjected to static charging, noisy disturbances are experienced in its radiocommunication and radionavigation systems. Even if the related noise is called "static" in technical jargon, the associated energy is electromagnetic and not electrostatic in the strict sense. As a matter of fact, it is the transformation of the electrostatic energy stored over the aircraft surfaces into electromagnetic energy, as a consequence of the initiation of a gas discharge, which produces the disturbances.

This is why it has been found interesting, before studying the disturbances experienced in flight by the aircraft avionic systems and the various methods of alleviation (or suppression) of these disturbances to review in their broad lines the physical characteristics of electrical discharges resulting from aircraft charging.

I.2 - Gas discharges at low and high pressures

When the electric field applied to an air gap exceeds a threshold value, the gaseous insulation breaks down and an electric current bridges the gap. The passage of electric current through gases is a consequence of ionization, i.e transformation of neutral molecules or atoms into ion-electron pairs, under the influence of collisions with electrons, photons or fast neutral particles. The study of electrical discharges in gases deals with the collective properties of ionized gases, which depend both on a number of elementary reactions between the species present and on statistical exchanges of momentum, energy, electric charge, electric current, heat flux, etc... within the fluid. The behaviour of conventional electrical discharges at low pressure is well known; the behaviour of the very inhomogeneous discharges at high pressure is still largely unexplained. The electrical discharges of interest to us are produced in air at atmospheric or subatmospheric pressure, and, in this range, the phenomena are well described, but quantitative analysis is lacking; nevertheless, a good feeling for the essential rules which explain their evolution can be gained from the knowledge of low pressure discharges and from the consideration of some scaling parameters. These scaling parameters are pd , the product of the gas pressure by the gap width and E/p , the ratio of the electric field to the gas pressure. The first parameter is used to define low pressure ($pd < 600$ MKSI) and high pressure discharges ($pd > 600$ MKSI). The second parameter is characteristic of the energy given by the electric field to the electron population of the gas discharge, and, consequently, of the state of ionization of the gas. When temperature is taken into account, p shall be replaced by n , number density of gas particles. [1] [2] [3] [4].

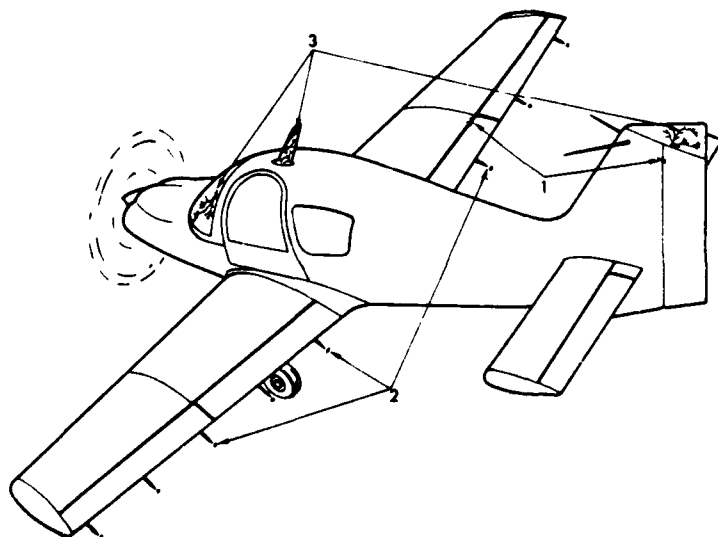
I.3 - Discharges due to aircraft charging

Fig. 1 - Discharges resulting from aircraft charging.

- 1) - Spark.
- 2) - Corona
- 3) - Surface streamer.

Three types of discharges can result from aircraft charging : (Fig. 1) :

- 1 - Sparks, flashing between conducting bodies at different potentials.
- 2 - Coronas, produced on conducting points or edges with a small radius of curvature.
- 3 - Surface streamers, flashing over insulating surfaces.

The scope of this lecture is to analyze the physical mechanism of these three types of discharges, in air and near atmospheric pressure, and to deduce from this mechanism their electromagnetic radiation in order to predict the disturbances to be expected from their interference with the communication and navigation systems.

1.4 - General properties of ionized gases

This paragraph is intended for defining the usual terminology used in gas discharge studies, and for stressing the fundamental mechanisms and the essential properties relevant to discharges due to aircraft charging. [1] [5].

1.4.1 - Elementary phenomena (Fig. 2)

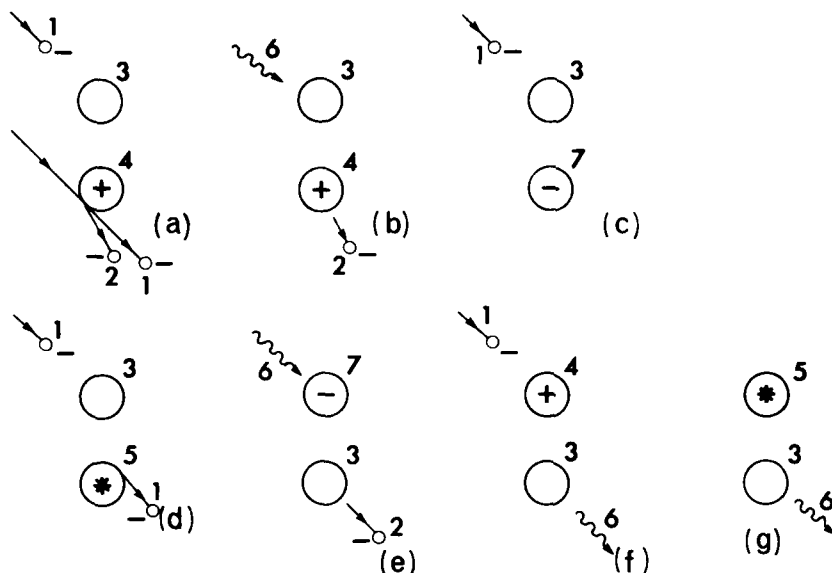


Fig. 2 - Elementary phenomena
Schematic representation of some elementary phenomena

- a) - Ionization by electron impact.
- b) - Photo-ionization.
- c) - Attachment.
- d) - Excitation.
- e) - Photo-detachment.
- f) - Recombination.
- g) - De-excitation.

- 1) - Primary electron.
- 2) - Secondary electron.
- 3) - Neutral.
- 4) - Positive ion.
- 5) - Excited neutral.
- 6) - Photon.
- 7) - Negative ion.

The charge carriers in ionized gases are the electrons, the positive ions and the negative ions. The positive ions are produced when a molecule or an atom loses by ionization one or several electrons, as a consequence of a collision with an electron or with a photon (photo-ionization). Electron collisions are usually the main source of ionization in low and high-pressure gas discharges. The negative ions are produced by attachment of an electron to an electronegative molecule or atom (O_2 , O , SF_6 , Cl ,... are electronegative species). The reciprocal of ionization is recombination, and the reciprocal of attachment is detachment. They are classified as elementary phenomena, since they are produced by reaction of individual particles (electrons, ions, photons or neutrals).

Other elementary phenomena of interest for our problem are excitation of atoms or molecules by electron collisions, and radiative de-excitation. Excitation brings the molecule to an excited vibrational state, and the atom or the molecule to an excited electronic state. De-excitation brings the molecule or the atom back to the ground state or to a lower state of excitation. It can be collisional or radiative. Collisional excitation, followed by radiative de-excitation and photo-ionization plays an important role in streamer propagation. Radiative de-excitation and radiative recombination are the two sources of the visible radiation emitted by gas discharges.

1.4.2 - Diffusion and drift (Fig. 3)

In the ionized gas, the electrons and the ions are subjected to diffusion and drift. Diffusion is a stochastic migration of particles from a region of high number density to a region of low number density, which is accounted for by kinetic theory. Diffusion is particularly important for light particles, such as the electrons, which have a high thermal velocity (random velocity, due to the kinetic energy corresponding to their temperature). This is why, when positive ions and electrons are produced, the electrons have the tendency to diffuse and the positive ions to lag behind them. Drift is an ordered motion of charged particles under the influence of electric forces. For a given electric field, drift velocity is proportional to the mobility of the charge carriers, a quantity itself proportional to their charge and inversely proportional to their mass and to their collision frequency with the neutral particles.

If an electron is introduced in a gaseous medium subjected to a high electric field, the electron is accelerated and produces an ion-electron pair by collision with a neutral atom or molecule. The secondary electrons drift away and ionize in the same way as the parent electron: a multiplication of which is called the avalanche charge carriers is produced by this mechanism. The ions stay relatively at rest whereas the electrons drift and pile up at the avalanche head, which progresses towards the anode and diffuses laterally as a function of the free diffusion coefficient of the electrons (Fig. 4).

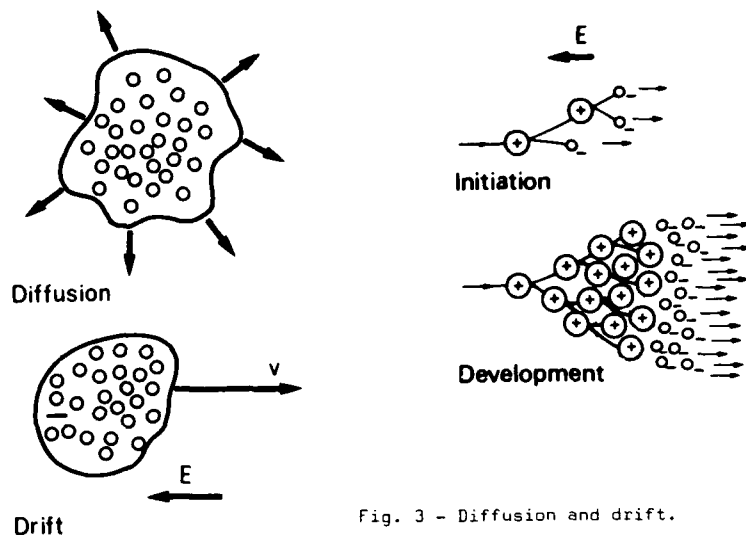


Fig. 4 - Avalanche initiation and development.

1.4.3 - Elastic collisions and energy exchange

At atmospheric pressure, the collision frequency with the neutral particles is very high ; between two collisions, neutral and charged particles have a mean free path of a small fraction of a micron ; the collisions of interest here are the elastic collisions between two particles, characterized by exchange of momentum and conservation of total kinetic energy ; collisions inducing an elementary reaction (excitation, ionization, etc...) are called inelastic and do not conserve total kinetic energy. An elastic collision with a neutral particle is very similar to a collision of two hard spheres (Fig. 5) ; for example, an electron, having a much smaller mass than the atoms and molecules, rebounds elastically in such a collision and exchanges essentially no energy with the gas particles ; an ion, having the same mass, will rapidly share its kinetic energy with the neutrals.



Fig. 5 - (a) - Hard spheres collision and (b) - Coulomb collision.

1.4.4 - Space charge effects : first transition

When the number density of the charged particles in an ionized gas is sufficiently high, the motion of the charge carriers is controlled not only by the externally applied electric fields, but also by the electric fields due to the presence of space charge (Fig. 6a). This space charge is defined by

$$\rho = e (n^+ - n^-)$$

where n^+ and n^- are the number densities of the positive and negative charge carriers, and e is the electronic charge (in this formula, the ions are supposed singly charged).

The space charge electric field \vec{E} is defined by the Poisson equation :

$$\text{div } \vec{E} = \frac{\rho}{\epsilon_0}$$

where ϵ_0 is the free space permittivity.

An important consequence of the existence of space charge electric fields is the modification brought to the diffusion regime. When the electrons are diffusing, they leave a positive space charge of ions ; if this space charge is sufficient, the attraction exerted on the electrons slows down the diffusion : free diffusion is then replaced by ambipolar diffusion, which is slower. The charged particles number density spatial distribution is then as follows : the center of the ionized volume is a plasma, characterized by $n^+ = n^-$, surrounded by a sheath of positive space charge left over by the departed electrons (Fig. 6b) ; in the asymptotic case of no collision (very low pressure), the thickness of this sheath is related to a specific length called the Debye radius, which is the distance needed by an electron originally having the thermal velocity to be stopped by a space charge $\rho = ne^+$. Sheaths are formed in particular at the boundary between gas discharge and wall or electrode.

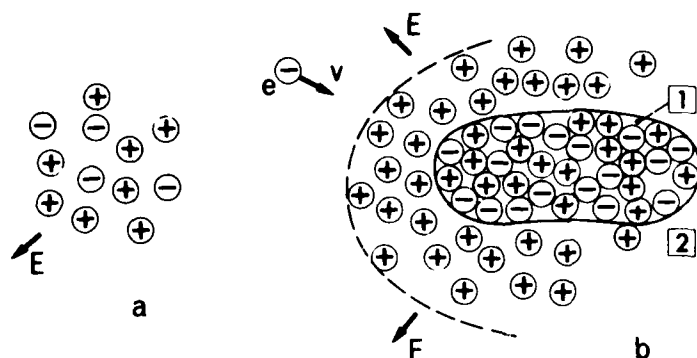


Fig. 6 - (a) - Space charge field
(b) - Plasma and sheath
1) - Plasma = center of the ionized volume characterized by $n^+ \approx n^-$.
2) - Sheath of positive space charges.

From the above fundamental principles, one can deduce that a first transition appears in gas discharges when a threshold is reached above which space charge plays an important role.

1.4.5 - Coulomb collisions and heating : second transition

A second transition appears in gas discharges if the number density of the charged particles is further increased. In the above description of elastic collisions, we have neglected the long-range electrostatic forces between charged particles (not the macroscopic forces resulting from space charge, and accounted for by the Poisson equation, but the individual attractive and repulsive forces due to mutual interactions of ions and electrons). These forces increase as the charged particles approach each other and this behaviour appears as a new type of collision, which is called Coulomb collision (Fig. 5). The cross section of Coulomb collisions is large in gas discharges (it becomes small in the very high temperature plasmas studied for thermonuclear fusion), but, as the density of charge carriers is generally much smaller than the neutral density, Coulomb collisions are often negligible in gas discharges. This is no longer the case above a given threshold of number density of charged particles; conditions are then obtained for energy equilibration between electrons and ions. Below the threshold, the energy acquired from the electric field by the electrons is essentially transferred to the gas by inelastic collisions, i.e. change of the internal energy of the neutrals and creation of ions. Above the threshold, this energy is shared with the ions, which lose this energy by colliding elastically with the neutrals: if this happens somewhere in the discharge, the gas is heated, the pressure is instantly increased locally, and relaxes in the form of a shock wave, with a local decrease in neutral density, hence an increase of E/n , the parameter which controls the energy transfer from the electric field to the electrons and consequently the electron drift velocity. If the field is not reduced by the external circuit, this induces an instability with an exponentially increased current. This second transition is related to an increase of current and conductivity of the gas discharge, which becomes an electric arc.

One can therefore distinguish two thresholds in the evolution of a gas discharge :

- a first transition, due to space charge accumulation, when a plasma controlled by the Poisson equation is formed ;
- a second transition, accompanied by high currents and reduced plasma resistivity, when Coulomb collisions realize a strong coupling between the electrical energy of the field and the kinetic energy of the plasma which becomes more or less fully ionized by thermal effect.

The corresponding regimes can be steady or unstable; the instability is generally stronger for high pressure discharges than for low pressure discharges, which are more easily described. This is why an example related to the low pressure case is given below to illustrate the existence of the two transitions listed above.

1.5 - Description of a typical low pressure discharge

Figure 7 shows a typical low pressure discharge, as produced between two electrodes within a glass vessel filled with a gas at reduced pressure. The figure caption enumerates the various zones which can be found along such a discharge. Special attention shall be devoted to the negative glow, where an anisotropic flow of high energy accelerated electrons produces, through excitation of neutrals, visible and U.V. radiations typical of non-equilibrium plasmas, and to the positive column, where the electrons are thermalized at a temperature higher than the gas temperature and produce essentially visible light. The positive column is a two temperature fluid (ions and neutrals at room temperature and electrons at about 1 eV).

The curve plotted in Fig. 8 is the voltage-current characteristic typical of this low pressure glow discharge. A resistor R is inserted in series with the gas discharge (Fig. 7); the curve of Fig. 8 is obtained experimentally by reducing the value of R .

- a) - When R is very large, the current corresponds to charges produced by external ionization (cosmic rays) and collected on the electrodes by the action of the electric field.
- b) - When R decreases, ionization proceeds by avalanches [6]. This regime was discovered and described by Townsend. Besides ion-electron production in gases, secondary electron production on the cathode surface is necessary for having a self-sustained discharge.

This production is due to bombardment of the cathode by the positive ions generated in the discharge. In this regime, the number density is very low and no appreciable light is emitted (dark-discharge region).

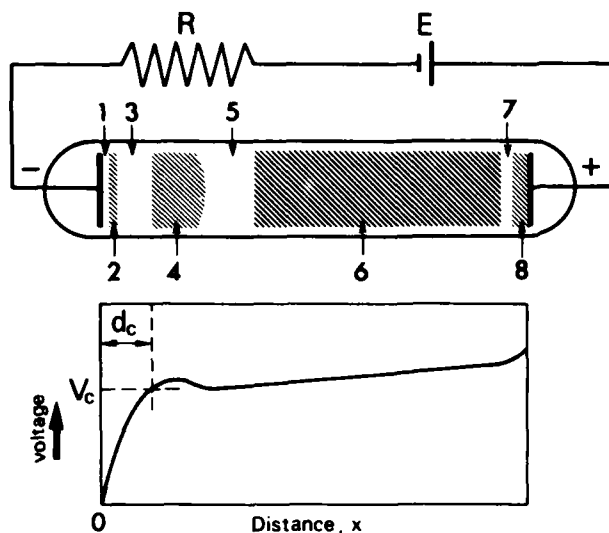
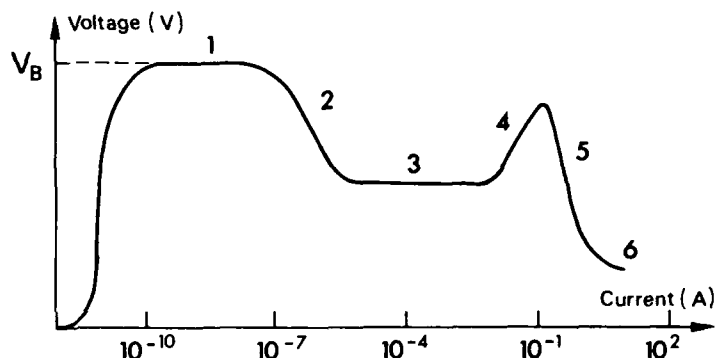


Fig. 7 - Low-pressure discharge

- 1) - Aston dark space.
- 2) - Cathode glow.
- 3) - Cathode dark space.
- 4) - Negative glow.
- 5) - Faraday dark space.
- 6) - Positive column.
- 7) - Anode dark space.
- 8) - Anode glow.
- d_c = cathode region length.
- V_c = cathode fall.

Fig. 8 - Low-pressure discharge characteristic.

- 1) - Dark discharge region = Townsend regime.
- 2) - Dark-to-glow transition.
- 3) - Normal-glow region.
- 4) - Abnormal-glow region.
- 5) - Glow-to-arc transition.
- 6) - Arc region.



- c) - When R is further decreased, a plasma is formed at dark-to-glow transition. Electron diffusion being reduced by space charge fields, the voltage needed to sustain the discharge decreases. A visible glow appears as a consequence of the increase of carriers density and current (normal glow region).
- d) - The discharge is non-uniform in space, and the main voltage drop is located close to the cathode. Decreasing R increases this voltage drop, hence V increases (abnormal glow region).
- e) - In a low pressure discharge, electrode phenomena are all important: by still further decreasing R , heating of the cathode by ion bombardment changes the electron emission process from secondary electron emission to thermionic emission; a large electron current is thus emitted and the voltage drop decreases. Ionization increases and glow-to-arc transition is reached.

I.6 - Analogy between low and high pressure discharges

Note that on the one hand the secondary emission in the Townsend regime and the thermionic emission at the glow-to-arc transition are important mainly to low pressure discharges; on the other hand, the two transitions appear both in low pressure and in high pressure discharges:

- sparks and surface streamers are initiated by avalanches, like Townsend discharges; when pd is large, dark-to-glow transition is obtained with the creation of streamers; glow-to-arc transition is reached after formation of a hot channel which in long sparks and lightning is called the leader;
- corona discharges are initiated by avalanches, followed by an unstable glow, which is time-modulated by regularly distributed pulses or by streamers. Glow-to-arc transition can be reached in laboratory coronas, but not in coronas initiated over an aircraft structure, except in the case of lightning initiation or surface discharges.

The following paragraphs will describe in more detail the physical mechanisms of high pressure discharges.

II - PHYSICAL MECHANISM OF THE SPARK DISCHARGE

II.1 - Physical mechanism of the spark [7] [8]

When the voltage between two conductors separated by a narrow gap is increased up to a critical voltage V_B (V_B depending upon the atmospheric pressure for a given couple of conductors), the gaseous insulation in the gap breaks down in the region where the electric field is maximum. The sequence of events producing the breakdown depends on pd (p : gas pressure, d : gap width). In any case, initiation of breakdown is due to a stray electron penetrating the zone where it can be accelerated by the electric field up to the point where ionization occurs. This primary electron can be produced locally by cosmic rays, but more likely by chance detachment from a negative ion [9]; electrons produced by cosmic rays in the field-free atmosphere are, as a matter of fact, readily attached to the oxygen molecules to form negative ions. The released electron is accelerated by the electric field up to values such that

ionization can result from a collision. The initial electron therefore produces an avalanche, which progresses in the direction of the anode with a drift velocity of about 10^5 ms⁻¹ at atmospheric pressure, (see Fig. 4).

In spark discharge research, an important parameter is the overvoltage, or percentage of the voltage applied to the gap above the minimum breakdown voltage. When the breakdown is produced by static charging, this overvoltage is likely to be small (as compared to the case of application of a step voltage to the gap). For this reason, the sparks obtained by static charging belong to the low overvoltage case; the dark discharge period can last microseconds, during which successive avalanches increase the total current continuously up to values of the order of a microampere.

When pd is smaller than approximately 600 MKSI, the ionized medium has the character of a low pressure discharge [10]. A diffuse channel bridges the gap from cathode to anode, since secondary electrons are emitted from this cathode as a result of ion and photon bombardment. Starting from the dark discharge, a diffuse glow is ignited as soon as the carriers density is sufficient to create a significant space charge. When this happens, the ions produced in the channel, which are slower, tend to keep the secondary electrons from diffusing freely, and a plasma surrounded by a positive space charge sheath is formed. The field distortion produced by the space charge can sometimes induce convective instabilities, called ionization waves; propagation of these waves along the channel increases plasma density behind them.

When the plasma reaches a density such that ion-electron collisions come into play, energy is transferred to the neutrals; the total pressure increases first in the discharge region, then relaxes by production of a more or less cylindrical shock wave. In a time of the order of 500 ns, the neutral density decreases in the discharge core and E/n increases, giving rise to a more intense ionization along a constricted channel. This is the second transition (glow-to-arc). Thermal emission from the cathode reduces the voltage drop in the arc, and the current is essentially limited by the circuit inductance. This arc is extinguished only when the supply of free charges in the condenser formed by the two conductors has been fully exhausted. [11].

If $pd > 600$ MKSI, the critical density for dark-to-glow transition is reached locally at the avalanche head when the gap is still far from being bridged by the discharge. The convective instability mentioned above develops in the form of streamers, a type of discharge which will be described later in the paragraph related to surface streamers. In this case, the discharge channel has the typical character of a high-pressure discharge, and is called a long spark. [12]. Long sparks are produced, for example, by flash-over of high voltage lines; they are not likely to be obtained in the case of aircraft charging, except over insulating surfaces, as developed further on. This is why we will assume that typical sparks obtained between two unconnected metallic panels by aircraft charging are essentially of the low pressure type.

It is interesting to note a few orders of magnitude related to the spark mechanism. Avalanche development (dark discharge) can last microseconds; the current is smaller than a microampere. Plasma development (glow discharge) can last tens of microseconds in some cases, or hundreds of nanoseconds in some other cases, depending on the overvoltage. The current increases up to values of the order of several amperes before reaching the glow-to-arc transition. When an arc is formed, the current can well reach values of thousands of amperes; the arc regime can last tens of microseconds.

During discharge development, dI/dt goes through two or more maxima corresponding to the various transitions (dark-to-glow, glow-to-arc, secondary emission to thermal emission). When the arc is ignited, I and $\frac{dI}{dt}$ are pseudo-periodic and their amplitude is large compared to their values during the initiation phase.

11.2 - Electromagnetic radiation due to a spark

The main characteristics of the spark current are that its path closes through conductors having large dimensions compared to the spark length itself. The radiating circuit is formed by the conductors traversed by the current, and is closed by the channel, which lasts as long as the electromagnetic energy stored in the system is not dissipated. Apart from the radiation emitted during the breakdown itself (before the transition to the arc), which corresponds to a broad band spectrum if the breakdown time is short and is not important if the breakdown time is long, energy is radiated within the bandwidth of the RLC circuit excited by the discharge. It consists essentially of a damped sine-wave at a frequency which, in many cases, is in the radio frequency range.

An example of this situation, which is borrowed from the field of space technology, is the damped sine wave at about 1 MHz injected along a ground line during the first phase of the F11 flight of the EUROPA II launcher in November 1971. As this ground line was connected with the ground line of the guidance computer of the launcher, unfortunately the radiation of this sine wave stopped the computer, and the launcher was lost. This sine wave originated when an ungrounded shield located in the fairings of the launcher acquired a static charge sufficient for producing, at reduced pressure, a spark in a 1 mm wide gap located between shield and ground line. Fig. 9 is a plot of the corresponding current as a function of time, as reproduced in similar equipment. As a matter of fact, the gap suffered a successive breakdowns, each of them producing the same damped waveform; the first one was sufficient to jeopardize the flight [13].

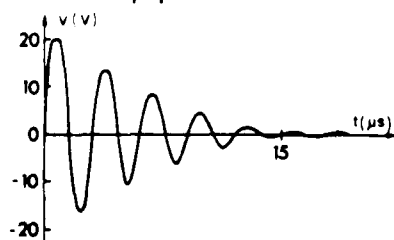


Fig. 9 - Damped sine wave following spark breakdown as observed during EUROPA II F11 flight.

II.3 - Conclusion

The high peak values of I and $\frac{dI}{dt}$ reached during the oscillation of the RLC circuit shorted out by the spark are likely to radiate, at radio frequency, powerful electromagnetic fields. Apart from the possible damage to the low-level integrated circuits, these fields can saturate the electronics with a corresponding loss of signal during a time generally much longer than the damped wave itself; if the spark occurs with a relaxation frequency, as a result of a steady charging, a strong audio noise at the same frequency can be produced, disturbing the communications.

Sparks are avoided by proper bonding of all the metallic panels of the aircraft structure. This bonding can be checked by various ways on the ground. Unefficient bonding can be revealed by watching the radiated waveforms under simulated (on the ground) or real (in-flight) charging conditions: appearance of damped sine waves is an unequivocal sign of poor bonding.

III - PHYSICAL MECHANISM AND RADIATION OF THE CORONA DISCHARGE

A key feature of the corona discharge is the inhomogeneity of the electrostatic field. This discharge occurs in a gaseous medium in the vicinity of an electrode of small radius of curvature subjected to an intense electric field, the so-called "stressed electrode". The opposite electrode can be a large blunt electrode located at some distance, or can be virtual: in the case of aircraft charging, corona is established between points of maximum curvature of the aircraft structure and the environment, as a consequence of electric field amplification near these points.

Observation of an operating corona discharge shows that a feeble glow appears in the vicinity of the stressed electrode; for commercial passive dischargers as used on aircraft, the glow is a small spot a fraction of a millimeter in diameter adjacent to the metallic point. Observation with an image intensifier shows that this spot is sometimes embedded in a brush discharge of larger dimensions. Time resolution could bring further information, showing that the glow is steady or slightly unstable, and that the brush discharge is composed of a very great number of branches appearing in succession as narrow channels about 20 microns in diameter moving forward at a speed of about $5 \cdot 10^5 \text{ ms}^{-1}$; as a matter of fact, only the tip of the channel, about .2 mm long, is visible. These branches are called streamers.

The following problems will be examined here:

- a) - Onset of corona discharges.
- b) - Operating regimes for positive and negative coronas in air.
- c) - Average current of a corona discharge.
- d) - Correlation distances of corona discharges.
- e) - Corona microdischarges.
- f) - Electromagnetic radiation of a corona discharge.
- g) - Radioelectric noise measurements.

III.1 - Onset of corona discharges [4] [6]

Corona discharges are initiated as soon as the voltage of the stressed electrode with respect to the auxiliary electrode exceeds a threshold voltage V_T , (and therefore as soon as the electric field at a given reference point of the aircraft exceeds a threshold field E_T). The current increases abruptly from a very small value characteristic of collection of atmospheric ions (10^{-14} A) to a value consistent with avalanche development.

If the stressed electrode is negative (cathode), avalanches can be initiated by a "seed" electron in the region close to the electrode. Avalanches develop in a direction away from the cathode, out to that distance at which the ionization process is compensated by attachment (Fig.10). Ionization being preponderant in high fields, and attachment in low fields, it has been shown that there is a critical distance corresponding to a field of about 25 kV cm^{-1} ; in between the stressed electrode and this distance, ionization prevails; beyond this distance, attachment is so important that there are no more free electrons. This severely limits the active zone of a corona discharge. If the stressed electrode is positive (anode), avalanches develop towards the anode, beginning at a location which depends on the "seed" electrons (Fig.11). As in the case of negative corona, these electrons are efficient only if introduced (or produced) in the "initiation volume" where ionization is more important than attachment. Being limited by the 25 kV cm^{-1} field intensity surface, this volume increases with the potential applied to the stressed electrode, and vanishes if the electric field is everywhere smaller than 25 kV cm^{-1} . This is the physical explanation of the existence of the threshold field E_T .

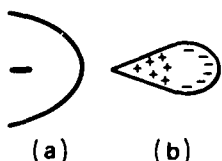


Fig. 10 - Onset of negative corona
a) - Electrode.
b) - Avalanche.

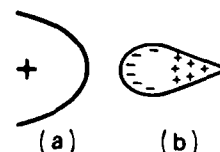


Fig. 11 - Onset of positive corona
a) - Electrode
b) - Avalanche.

The threshold voltage variations with pressure are described by Paschen-type curves [2]. As a consequence, in the pressure range of interest for aircraft charging, i.e. atmospheric and slightly subatmospheric, E_T is proportional to the pressure. In airflow, the pressure to be considered is the ambient pressure developed right at the point; corona discharges generated on passive dischargers located at the trailing edge of aircraft wings have a lower threshold field at high altitude (decrease of atmospheric pressure) and at high speed, when a depression is obtained in the wake of the wing. The value of the threshold field E_{TS} (kV cm⁻¹) at the surface of the stressed electrode is given by Peek's law [15]:

$$E_{TS} = E_0 \delta \left[1 + \frac{k}{\sqrt{r\delta}} \right]$$

where $E_0 = 31 \text{ kV cm}^{-1}$

$$\delta = \frac{0.392 p}{273 + T} \quad (p \text{ Torr, } T = ^\circ\text{C})$$

$$k = 0.308 \text{ cm}^{-1}$$

r = stressed electrode radius (cm).

From the E_{TS} , one can calculate the aircraft threshold potential if the geometry is known.

III.2 - Operating regimes for positive and negative coronas in air [14] [16] [17]

III.2.1 - a) - The stressed electrode is an anode (positive corona)

If the stressed electrode voltage is increased above the onset voltage, the avalanches initiated in the high field region generate, near the anode, a plasma which decreases the field by its conductivity (dark-to-glow transition). Radiative de-excitation in this plasma produces photons, and hence photoionization in the close environment.

If the secondary electrons generated by this process are produced within an appreciable volume, they are continuously attracted by the anode and contribute to form the glow region: the corresponding current is a DC current.

The secondary electrons produced in the close vicinity of the primary avalanche can also generate new avalanches converging on the avalanche head. The carriers produced by these avalanches pile up in front of the head, up to the point where a plasma is formed which merges with the head (dark-to-glow transition). This is equivalent to a forward displacement of the avalanche head. Electrons are partly absorbed by the anode, and a net positive space charge is left at the avalanche head. This process increases the electric field in front of the head, and reduces this field at its back, where plasma is accumulated. This is the physical mechanism of streamer propagation. It has been shown, by spectroscopic observations (stark effect), that the space charge electric field located just in front of a streamer head can reach ten times the breakdown field at atmospheric pressure [17]. This is why streamers can propagate in macroscopic electric fields well below the breakdown field: the streamer head itself generates the electric field necessary for the propagation of ionization; a streamer is an ionization wave, and the optically observed propagation speed is actually the phase velocity of this wave (Fig.12).

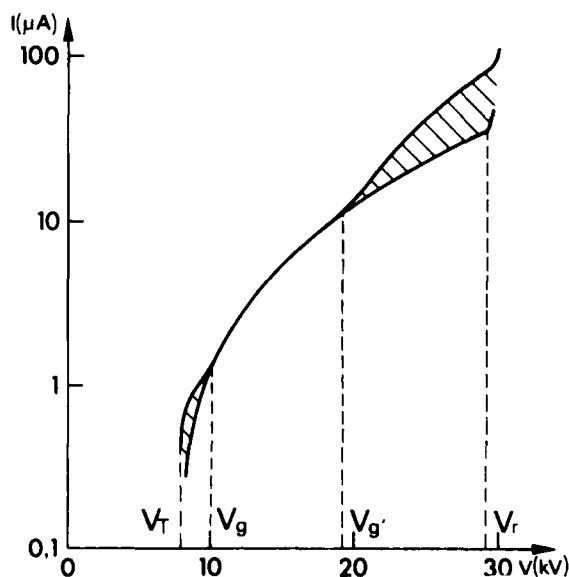
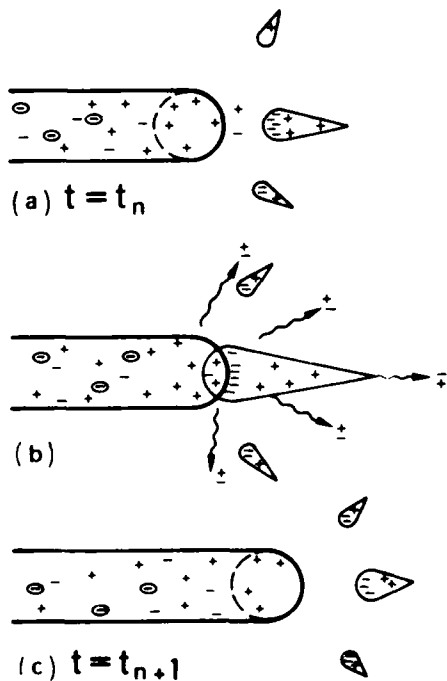


Fig. 13 - Current potential curve of the positive corona.

Fig. 12 - Streamer propagation

- a) - Streamer at the time t_n - Development of avalanches behind the head.
- b) - Merging of avalanches with the streamer head.
- c) - Streamer at the time t_{n+1} .

In a positive corona discharge, both glow and streamers can be found. Fig. 13 shows a typical current-potential curve as observed by Buchet et al. [18]. The shaded regions characterize the streamer contributions to the current. One can observe three voltage regimes :

- a) - from onset voltage V_0 to a first limit V_g , one finds a very unstable glow discharge composed of a superposition of small amplitude bursts and a number of large pulses due to streamers (called pre-onset streamers) ;
- b) - from V_g to a second limit V_g' , only a pulseless glow persists ;
- c) - from V_g' to V_r (breakdown voltage), a stable impulsive discharge, with pulses regularly spaced in time, develops on top of the glow discharge. The glow-to-arc transition cannot be reached by aircraft charging (except in the case of lightning or surface discharge).

The frequency of the pulses associated with the streamers is of the order of several kilohertz ; Fig. 14 shows this frequency as a function of corona voltage, for a stressed anode 170 microns in diameter located at 20 mm from a plane cathode [18].

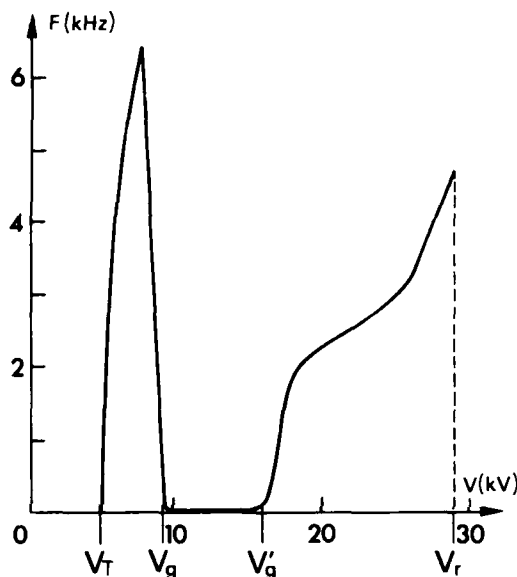


Fig. 14 - Pulse frequency as a function of potential in the positive corona.

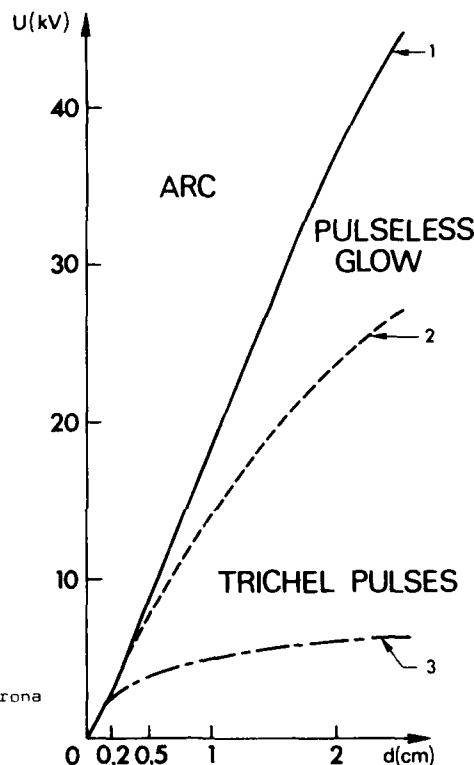


Fig. 15 - Operating regimes of the negative corona discharge in air.

- 1) - Glow-to-arc transition.
- 2) - Trichel-to-glow transition.
- 3) - Onset.

III.2.2 - The stressed electrode is a cathode (negative corona)

In this case, the ions produced by the avalanches are attracted by the cathode and increase the field near the stressed electrode ; the electrons moving away from the cathode in the lower field region attach themselves to neutral atoms or molecules, generating a negative-ion space charge which moves relatively slowly towards the anode ; this weakens the field in the direct vicinity of the space charge zone. Accumulation of the negative-ion space charge produces a quenching of the current pulse ; the current resumes only when this space charge has disappeared by diffusion and drift (laboratory case), and eventually has been swept away by the airflow (aircraft case).

The negative corona is characterized by two voltage regimes (Fig. 15).

- a) - From onset to a threshold voltage V_0 , the current appears essentially in the form of pulses superimposed on a D.C. component. Near onset (autostabilization regime), random sequences formed by a large pulse followed by small pulses are obtained. When the voltage is increased, the number of small pulses increases in the sequence and these pulses become more regular. When the voltage is further increased, the large pulses disappear and the sequences merge into a continuous succession of regularly spaced pulses of same amplitude. The repetition frequency of these pulses, called Trichel pulses, increases with the applied voltage, but their charge stays constant. Fig. 16 shows that, for relatively low currents, the relaxation frequency of the Trichel pulses is a linear function of the average current. It decreases, and the charge of the pulse increases correlatively, when the radius of the stressed electrode increases [20]. This can be observed in the case of aircraft passive dischargers : when they have been operating for a long time, their point, usually 20 to 60 microns in diameter, becomes slightly blunted, and the relaxation frequency decreases.

Fig. 17 displays the curves giving the relaxation frequency as a function of the average current for a point-to-plane corona discharge (conical rhodium point with an angle of 12° at the tip of a cylinder 3 mm in diameter ; point-to-plane distance 2,5 cm). The relationship is no longer linear if the entire current range is considered. For a given average current, decreasing the pressure reduces the

relaxation frequency : Fig. 16 shows that the pulse width increases correlatively [21]. This effect has been observed in-flight when altitude increases [22]. The relaxation frequency also increases with aircraft speed, as the time necessary for sweeping out the space charge decreases with airflow velocity.

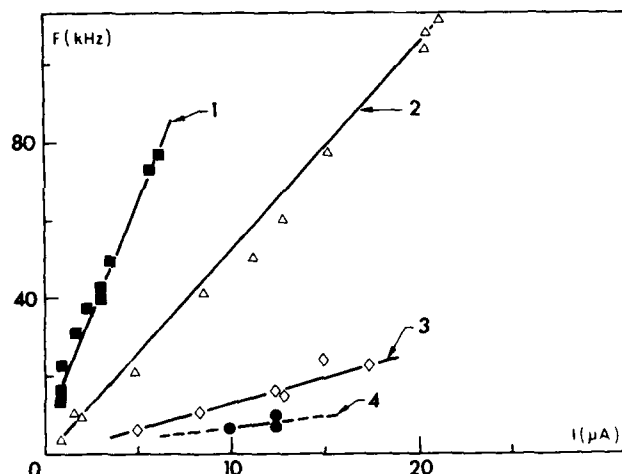


Fig. 16 - Trichel pulses frequency for different points as a function of average current.

- 1) - For sharp point.
- 2) - For .5 mm point.
- 3) - For 1.5 mm point.
- 4) - For 4.73 mm point.

Fig. 17 - Relaxation frequency of Trichel pulses as a function of average current and pressure.

- $P \approx 750$ mm Hg
- $P_0 \approx 650$ mm Hg
- $P_1 \approx 550$ mm Hg
- $P_2 \approx 450$ mm Hg
- $P_3 \approx 350$ mm Hg
- $P_4 \approx 250$ mm Hg
- $P_5 \approx 150$ mm Hg
- P_6

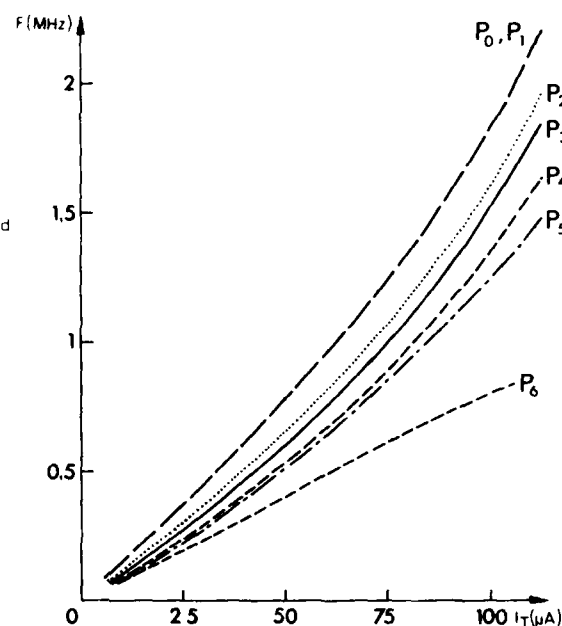
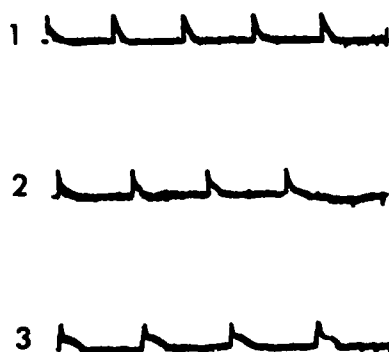


Fig. 18 - Variation of trichel pulse shape with pressure.

p : pressure in mm Hg.
 f : repetition frequency in MHz.

- 1) - $p \approx 750$ $f \approx 0,94$
- 2) - $p \approx 650$ $f \approx 0,85$
- 3) - $p \approx 450$ $f \approx 0,75$.



At atmospheric pressure, the amplitude of a typical Trichel pulse can reach 1 mA. Its rise time is 3,5 ns ; its decay time constant is approximately 35 ns. Its relaxation frequency varies from several kiloHertz to more than one MegaHertz.

- b) - Above the voltage V_g , the pulses merge to form a pulseless glow discharge. V_g is a slightly decreasing function^g of pressure.

When voltage is further increased, negative corona can reach glow-to-arc transition. This is obtained by aircraft charging only in the case of lightning or surface streamer. (see Fig. 16).

Fig. 19 shows curves of the average-current versus the applied voltage of a negative corona discharge operating at various pressures [21]. The zones corresponding to the Trichel and pulseless glow operating regimes are bounded by the dotted lines. The shape of the curves is analyzed in the next paragraph.

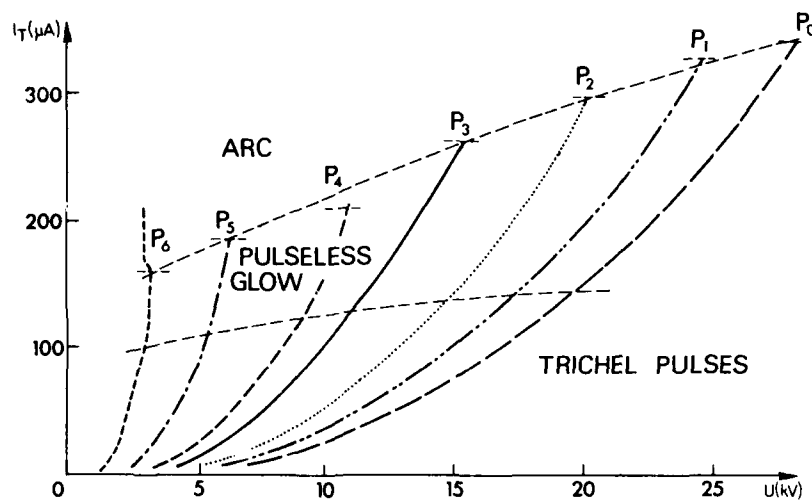


Fig. 19 - Average current and operating regimes for a negative corona in air, as a function of voltage and pressure

$P_0 \approx 750$ mm Hg
 $P^0 = 650$ mm Hg
 $P_1 = 550$ mm Hg
 $P_2 = 450$ mm Hg
 $P_3 = 350$ mm Hg
 $P_4 = 250$ mm Hg
 $P_5 = 150$ mm Hg.
 P_6

III.3 - Average current of a corona discharge

Outside of the active zone of corona discharges in air, electrons are attached to atoms or molecules to form negative ions. The active zone of either corona polarity, positive or negative, is therefore shielded by a space charge sheath of ions of low mobility compared to the electrons. The current continuity from stressed electrode to outer electrode (real or virtual) is ensured through this sheath, when current pulses are generated in the active zone, by the sum of an average ionic conduction current and of a displacement current (of zero net value). The fact that negative or positive ions have nearly the same mobility explains that the average current characteristics are nearly the same for negative or positive coronas in pulsed or steady regimes: continuity of the average current makes it possible to analyze the behaviour of the conducting medium through the sheath only, where the current results from mobility of heavy carriers in a steady field distribution.

This problem was studied by Townsend in the case of the steady regime, with the Poisson Equation $\text{div } \mathbf{E} = \frac{\rho}{\epsilon_0}$ and the relationship relating current density \mathbf{j} to charge density ρ , field \mathbf{E} and carriers mobility μ : $\mathbf{j} = \mu \rho \cdot \mathbf{E}$. \mathbf{E} includes space charge and externally applied fields.

Townsend found that the current I of the discharge can be related to μ , E_T and E (E_T : threshold field) by the following expression:

$$I = C \mu V (E - E_T)$$

Loeb gives a slightly different formula:

$$I = C \mu (E - E_T)^2 \cdot i - \frac{8r}{d}$$

where r is the radius of the point and d the gap width.

In case of aircraft charging, $r \ll d$ and the Loeb formula becomes:

$$I = C \mu (E - E_T)^2 \cdot i \approx C \mu (E - E_T)^2$$

E and E_T can be defined at any reference point of the configuration, the constant C obviously depending on the choice of this reference point. Fig. 20 shows a characteristic obtained in a typical experiment, E being the field measured at a reference point on the trailing edge of the model of a wing where a passive discharger was fitted. In this case, $C\mu$ was equal to $3.06 \cdot 10^{-4}$ with I in microamperes and E_T and E in V cm^{-1} .

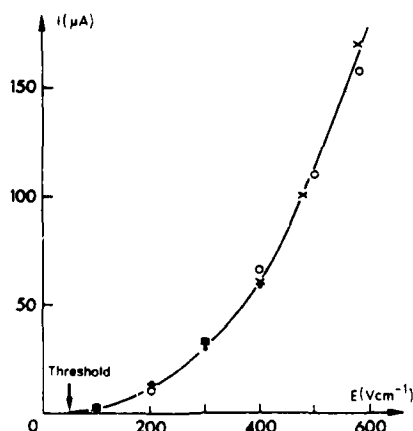


Fig. 20 - Average current as a function of the electric field at a reference point for a negative corona sustained at the tip of a discharger.

The influence of air speed on the average current has been studied by Chapman. The following formula applies in the most general case :

$$I = \epsilon_0 \left[K_1 \mu (E - E_0)^2 + K_2 v (E - E_0) + K_3 \frac{v^2}{\mu} \right]$$

where μ is the mobility, E the applied field, E_0 the threshold field, v the airflow speed ; the coefficients K_1 , K_2 and K_3 have the dimension of a length.

The third term is generally negligible and the second term dominates as soon as $v > 20 \text{ ms}^{-1}$; in the case of corona discharge carried by an aircraft in flight the average current is essentially proportional to v :

$$I \approx \epsilon_0 K_2 (E - E_0) v$$

III.4 - Correlation distances between corona discharges

As aforesaid, the average current of a corona discharge is controlled by the space charge accumulated in the vicinity of the active region of the discharge. Positive or negative coronas have an average current which is controlled by space charge sheaths extending far from the active region, when no auxiliary electrode is present to collect this charge (case of aircraft charging). If a second discharge is located close enough to the first one, its current is controlled and can be quenched by the space charge of the first discharge ; the two discharges are then correlated. This can be seen in two ways :

- 1) - the total current carried by two corona discharges is reduced when their distance is smaller than, for example, 30 cm. This distance is the correlation distance of the two discharges. At a larger distance, the two discharges act independently. This defines a D.C correlation distance, relevant to average values of the corona current.
- 2) - oscilloscopic observation of the Trichel pulses of a two-point negative corona discharge shows that the pulses are produced in a regular alternance, the pulse produced in one point quenching the other, and alternately. Such a configuration is typical of a popular model of aircraft passive discharger (Dayton-Granger discharger) where the two points are located at a distance of a few millimeters from each other. This defines a pulse correlation distance, relevant to instantaneous values of the corona current [24].

These observations can be explained in the following way :

the space charge region around the cathode of a negative corona can be divided into two zones :

- . a first zone, at a small distance from the electrode, where electrons diffusing from the active zone during each pulse increase, by fast bursts, the negative space charge before being attached to neutral atoms or molecules ;
- . a second zone, at a large distance from the stressed electrode, where only negative ions can be found. Here, the space charge is slowly transported by diffusion and drift of negative ions formed in the first zone, and the bursts of space charge present in the first zone decay to a negligible value by smearing out in a continuous background.

The existence of these two zones is therefore the origin of the two types of correlation distance found experimentally, with typical values of tens of centimeters for the DC type and of several millimeters for the pulse type.

The D.C correlation distance between two corona discharges decreases with air speed, and the pulse correlation distance increases with pulse amplitude. At the trailing edge of an aircraft, corona produced on discharger tips are located on a line perpendicular to airflow. Airflow sweeps away the space charge and reduces its lateral extension : the transverse DC correlation distance between two dischargers consequently is decreased at high speed.

If by some arrangement the total charge released during a Trichel pulse is reduced, the pulse correlation distance is also reduced ; this can be obtained by reducing both pulse amplitude and pulse duration. The next paragraph shows how to take advantage of this effect.

III.5 - Corona microdischarges

It was recently pointed out by Brunet [25] that if a corona discharge is initiated at the tip of a very thin carbon fiber, the discharge pulse is of very small amplitude. This results from two conditions specific to carbon fibers with a diameter less than about ten microns :

- a) - the capacitance of their tip is very small ;
- b) - their resistance is very high.

As a consequence of these conditions, the corona discharge is rapidly quenched, not as usual by accumulation of space charge, but by the voltage drop of the electric circuit : the accumulated charge disappears so rapidly during the pulse that the field decreases below threshold. This quenching is therefore of electrical origin and not of physical origin, and it is experienced for any polarity and for any type of gas, including rare gases. The pulse amplitude can be made, for example, one hundred times smaller than for ordinary Trichel pulses (i.e. 10 μA instead of 1 mA). On the one hand, to carry the same current, more points are needed, which might seem impractical ; but, on the other hand, the correlation distance between two pulses is largely decreased, and this makes it possible to work with a composite material rod made of aligned carbon fibers embedded in an insulating resin. If a large number of closely spaced carbon fiber tips are exposed to a high field, the space charge released by each pulse over a tip is so small that inhibition of the corona discharges is limited to neighbouring

fibers and lasts only a short time. Many microdischarges can appear at the same time in uncorrelated areas. If we consider the composite rod as a whole, the emitted current is a stochastic succession of very short pulses. It will be shown farther on that the associated spectrum doesn't show any of the characteristic frequency lines specific to relaxation, as is the case for Trichel pulses or for positive streamers in conventional corona discharges.

III.6 - Electromagnetic radiation of corona discharges

Corona discharges, having in most cases a pulsed component, generate electromagnetic radiation which interferes with the communication and navigation systems of the aircraft. Coupling between corona discharges and the antennas of the communication and navigation systems has been studied by Tanner and Nanevich, who have given the conditions for minimizing the coupling [26]. This problem is analyzed in the lecture by J. Nanevich in this series, and will not be treated here. We will restrict our attention to the study of the spectrum of the electromagnetic radiation generated at the source, which is the same as the spectrum of the corona current.

As a corona discharge can operate in a number of different regimes according to the polarity and to the value of the average current, it is advisable to analyze the cases associated with intense generation of electromagnetic radiation. This is why the pulseless glow is not considered here. Positive corona, characterized by two unstable regimes associated with pre-onset and pre-breakdown streamers, is worthy of attention; though negative corona is more interesting, as aircraft charging is negative in about 90 % of the cases. In this paragraph, we will predict the spectrum of the electromagnetic noise emitted by a negative corona discharge in the Trichel regime. Qualitative arguments will be given to evaluate the relative importance of electromagnetic radiation generated in negative, positive, and micro-discharge coronas.

III.6.1 - Power spectrum of a corona pulse

A typical corona pulse is shown in Fig. 21. It has a rise time of about 3.5 ns and a decay time constant of 35 ns. The waveform can be assimilated to a sum of two exponentials, a positive exponential with a time constant of 35 ns, and a negative exponential with a time constant which can be computed from the condition that the resulting curve must have a maximum equal to 1 at about 3.5 ns. The corresponding function is :

$$I = a [e^{-\alpha t} - e^{-\beta t}] \quad \text{with} \quad \begin{aligned} a &= 1,136 \\ \alpha &= 2,86 \cdot 10^7 \\ \beta &= 1,06 \cdot 10^9 \end{aligned}$$

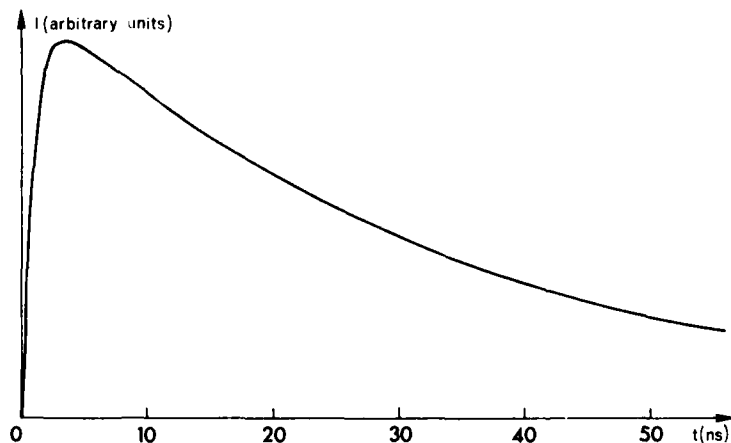
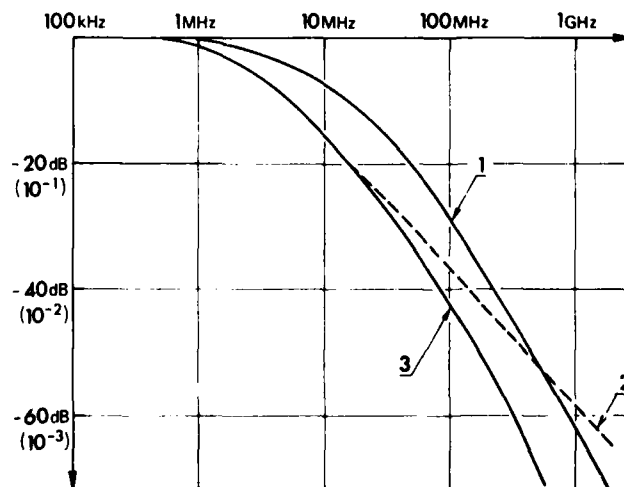


Fig. 21 - Typical corona pulse.

Fig. 22 - Spectra of a typical corona pulse.
1) - Standard pulse having a rise time of 3.5 ns and a decay time constant τ of 35 ns
2) - Single exponential, $\tau = 100$ ns.
3) - Standard pulse having a rise time of 10 ns and $\tau = 100$ ns.



The Fourier power spectrum of this function is :

$$P(\omega) = \frac{(\alpha - \beta)^2 (\omega^2 - \alpha\beta)^2 + \omega^2 (\alpha^2 - \beta^2)^2}{(\alpha^2 + \omega^2)^2 (\beta^2 + \omega^2)^2}$$

Fig. 22 shows the corresponding relative amplitude of the components of the spectrum of the pulse, for the standard pulse defined above and for a standard pulse having a rise time of 10 ns and a decay time constant of 100 ns. This pulse is a reference pulse mentioned by J. Robb [27]. For a pulse having a negligible rise time and a 100 ns decay time constant, the amplitude spectrum is represented by the dashed line. This line has a slope of 6 dB/octave, whereas the asymptotic slope of the spectrum of the corona pulse is 12 dB/octave. This shows that corona-produced disturbances are essentially below a frequency of about 100 MHz. Automatic direction finders (200 - 1750 kHz) and Omega navigation equipment (10 - 14 kHz) are particularly vulnerable; DME (1 GHz) and VOR-ILS receivers (100 - 300 MHz) are less disturbed; MLS (5 GHz to 15 GHz) will be quite insensitive to static charging effects.

III.6.2 - Power spectrum of negative and position corona discharges

Trichel pulses form a regular sequence of exponential pulses like our standard corona pulse ; the corresponding spectrum is obtained by multiplication of the above spectrum and the spectrum of an infinite sequence of unit impulses occurring at the repetition frequency f of the Trichel pulses. This spectrum consists of a comb of frequency lines separated by f , with a maximum amplitude limited by an envelope which is the spectrum of the individual corona pulse (Fig. 23)

Maximum interference with avionic equipment results from maximum overlapping of these frequency lines onto the bandwidth ΔF of the considered equipment. If the spacing of the lines is large, and the bandwidth ΔF narrow, overlapping could in principle be avoided in steady conditions. But as a matter of fact, random variations of charging will induce corresponding variations in pulse recurrence and therefore associated changes in line separation and position : it is not possible to avoid overlapping, and the resulting interference, for all the charging conditions to be encountered in flight.

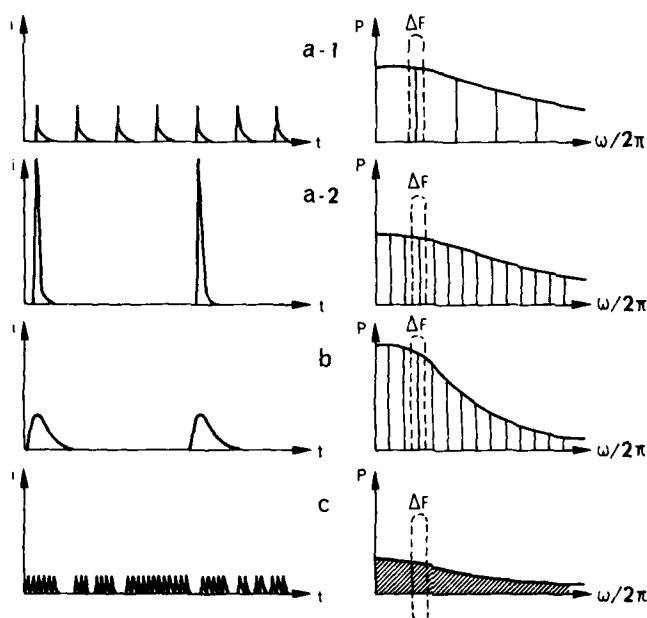


Fig. 23 - Current pulses and corresponding power spectra of corona discharges.

a₁ - Negative corona (Trichel pulses).
a₂ - Positive corona (ideal pulses).
b) - Positive corona (real pulses).
c) - Corona microdischarges.
 ΔF is the bandwidth of the disturbed receiver.

It is interesting to compare the amplitude of spectral lines for positive and negative coronas carrying the same average current. Positive corona is characterized by pulses or relatively large peak-value with a low repetition frequency. If the pulse rise and decay times were the same in positive and negative coronas, the average current I would be $I = f \cdot a$ where f is the repetition frequency and a the peak value. The generated power P would be $P = f a^2$ or $P = \frac{I^2}{f}$. The number of lines in the radiated spectrum bandwidth Δf would be $\frac{\Delta f}{f}$; the power per line, $P_L = \frac{I^2}{f} \times \frac{f}{\Delta f} = \frac{I^2}{\Delta f}$ would be independent of the repetition frequency, i.e. the same for positive and negative coronas (Fig. 23a). Actually, the positive pulse has generally a longer rise time (≈ 35 ns) and a longer decay time constant ; in the spectrum, the low frequency side is therefore enhanced, and, on the one hand, positive corona may be more damaging for the VLF and the RF equipment (Omega navigation, Automatic Direction Finder, etc...); on the other hand, if frequency lines are close together, more than one line can be overlapping the bandwidth ΔF of the equipment, particularly at the high frequency side (the bandwidth ΔF generally being a given fraction of the working frequency F). For this reason, positive corona is considered as more disturbing than negative corona (Fig. 23b).

III.6.3 - Power spectrum of corona microdischarges

If the same total power is distributed over the whole spectrum and not only onto discrete lines, the envelope amplitude is greatly reduced. Maximum interference is therefore reduced in the same proportions. This is obtained if the corona pulses, instead of being regularly spaced in time, form a random sequence. For this reason, corona microdischarges are particularly suitable to reduce the radiated noise : they emit a random sequence of uncorrelated micropulses. Their spectrum is similar to the single pulse spectrum (Fig. 23c). More work is needed to establish a consistent theory of the electromagnetic behaviour of corona microdischarges ; however, experimental results obtained in the laboratory show that an improvement of the order of 40 dB or more can be achieved for the same average current with carbon fiber dischargers.

III.6.4 - Radioelectric noise measurements in the laboratory : experimental arrangement

To measure, in the laboratory, the radioelectric noise generated by a corona discharge, and in particular to compare various passive dischargers, a set-up similar to the device shown in Fig. 24 can be used. This set-up comprises a grounded metallic profile simulating the trailing edge of the aircraft wing, and an arrangement, composed of a high-voltage electrode and two guard rings, for applying the D.C. electric field to the corona point fitted at the back of the profile. This device can be used at reduced pressure or located in a wind tunnel. A reference antenna picks up the noise radiated by the corona ; the best arrangement has been found to be formed by two small plane plates parallel to wing surfaces near the trailing edge. As the significant wavelengths are large compared to the set-up dimensions, the problem is essentially quasistatic, and interference is due to capacitive coupling : each of the antenna is coupled with the discharge by the capacity between plate and active zone of the corona. If comparison between dischargers is sought, care should be taken to locate the corona discharges at the same place.

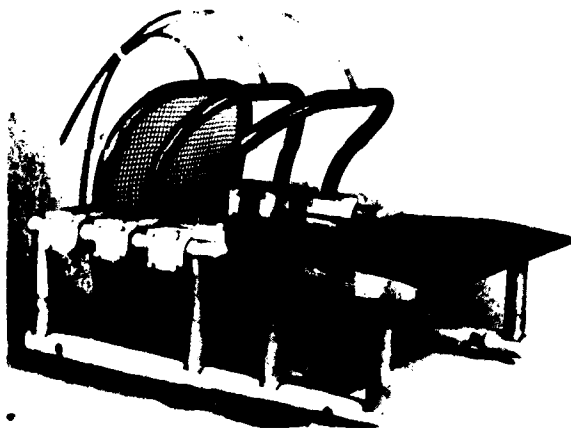
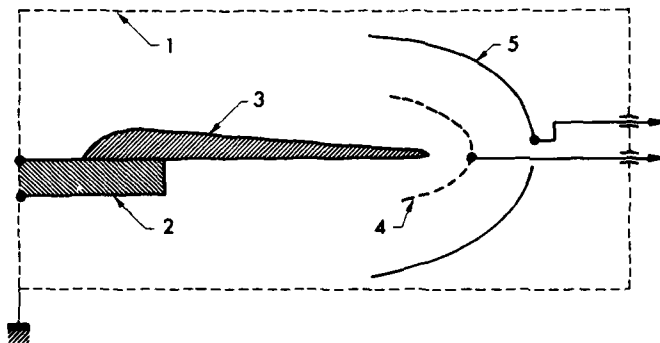


Fig. 24 - Experimental set-up for measuring the radioelectric noise of passive dischargers.

Fig. 25 - Simplified sketch of a shielded set-up for passive discharger noise measurements.

- 1) - Faraday cage.
- 2) - Support.
- 3) - Discharger.
- 4) - High-voltage terminal T.
- 5) - Antenna.



The described equipment is not shielded against external radiation, and cannot be used for measurements of very small radiated powers. This is why we will describe a second set-up, shown in Fig. 25, which has been built at ONERA. Here, all the equipment is enclosed in a shielded Faraday cage. The metallic profile and the corona point have the same arrangement as in the preceding set-up. The high voltage terminal T is a plexiglass paraboloid located in front of the point ; the paraboloid is covered by a thin resistive layer (1 MΩ per square mesh) which is transparent to electromagnetic radiation but acts as an equipotential surface for the electrostatic field. The receiving capacitive antenna A is a metallic paraboloid located behind T.

III.6.5 - Experimental results [28]

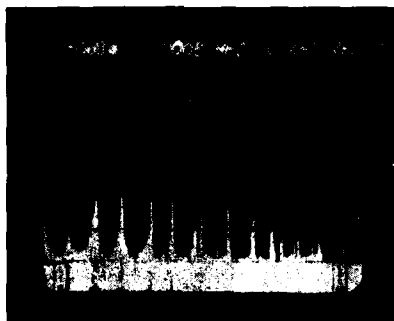
The following results, which have been found by using this equipment, are illustrative of the preceding paragraph :

a) - Fig. 26 shows a characteristic spectrum obtained by using a conventional corona discharge in the Trichel regime.

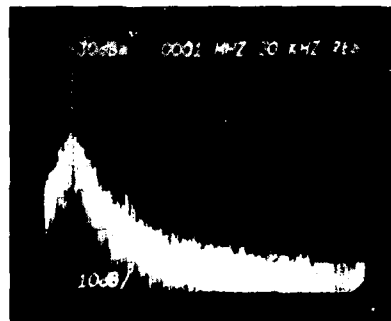
b) - Fig. 27 shows a characteristic spectrum obtained by using a microdischarge system (carbon fiber dischargers) with the same average intensity as in Fig. 26.

c) - Fig. 28 compares the noise generated by various dischargers.

These results demonstrate the improvements obtained by the various methods of uncoupling, and particularly, by the microdischarge devices. Detailed discussion of these measurements involves consideration of the theory developed in reference [26].



2MHz \longleftrightarrow 2MHz
Fig. 26 - Radioelectric noise spectrum of a corona sustained on a conventional discharger for an average current of 75 μ A.



500kHz \longleftrightarrow 500kHz
Fig. 27 - Radioelectric noise spectrum of corona microdischarges sustained on a carbon fiber discharger for an average current of 75 μ A.

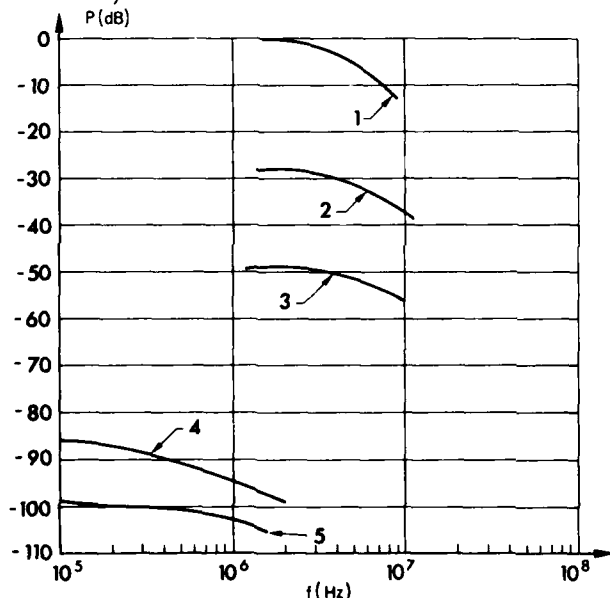


Fig. 28 - Power spectra of noise radiated by dischargers of different types in operation.
1) - Unprotected corona discharge (reference).
2) - Resistive uncoupling.
3) - Orthogonal uncoupling.
4) - Corona microdischarge.
5) - Optimized discharger.

III.6.6 - Conclusion

When aircraft experience charging in flight, operation of dischargers is necessary to get rid of the electric charge; corona discharges sustained at the tip of the dischargers can produce interference which affects the avionic equipment. To reduce this interference which changes in a difficultly predictable way with the charging current, reduction of the coupling with the antennas, according to the theory developed by Nanevich and Tanner (resistive and orthogonal uncoupling), is the method most in use today [26]. A further improvement can be obtained by using corona microdischarges together with resistive and orthogonal uncoupling [28].

IV - PHYSICAL MECHANISM AND RADIATION OF SURFACE STREAMERS

IV.1 - Physical mechanism of surface streamers

Surface streamers are generated if static charge accumulates on a highly insulating surface (canopy, antenna cover, radome, fairings). Generally, the surface streamer assumes the form of a tree-like discharge, the stem being attached to a point of the surrounding metallic frame, and the branches spreading over the insulating surface. The branches act as charge collectors and the stem brings the current to the aircraft structure. The streamer is localized in a thin air layer adjacent to the insulating surface.

The physical mechanism of surface streamers has some points in common with the physical mechanism of long sparks; the differences arise from the fact that surface streamers propagate in an initial surface charge; in this respect, they resemble more closely the streamers propagating through charged clouds during thunderstorms. It has been found experimentally that typical parameters of surface streamers are in the same range as lightning pre-breakdown parameters - one order of magnitude larger than long sparks parameters.

IV.1.1 - Onset of surface streamers

When electric charge accumulates on an insulating surface, the potential of this surface increases, with respect to the potential of the conducting surfaces located at the periphery (the metallic frame of a windshield, for example). The associated electric field depends on the geometry. Fig. 29 shows a charged dielectric slab placed on a grounded metallic plate. Here, the electric field is essentially localized within the dielectric slab, the external field being partially neutralized by the image charge (in the metallic plate) of the surface layer. If the dielectric slab is far from metallic bodies, intense normal and longitudinal components of the field can develop in the air around the slab. In any case, maximum field will be found at small radius of curvature points of the conducting frame in which the slab is fitted. If onset conditions are attained at these points for a corona discharge, the first step of the surface streamer is reached: initiation of a corona discharge, avalanche formation and pre-onset streamers or Trichel pulses. Note that pre-onset streamers are obtained with negative charging and Trichel pulses with positive charging.

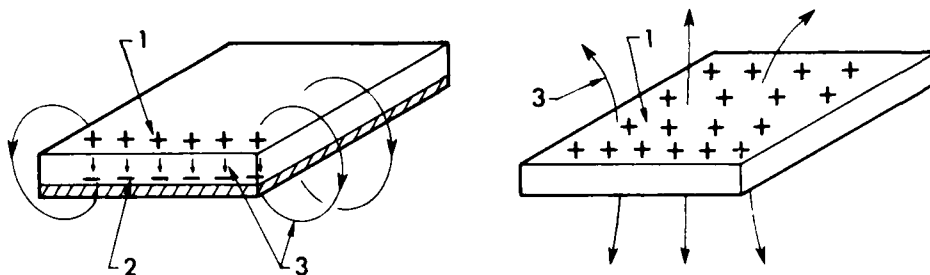


Fig. 29 - Static charge and field distribution on a dielectric slab placed on a metallic plane.

1) - Static charges layer. 2) - Image charges layer. 3) - Fields lines.

IV.1.2 - Development of surface streamers

Surface streamers therefore start in the form of corona streamers. However, as the growth of surface streamers show the brush-like discharges characteristic of corona streamers (Fig. 30), nevertheless, the evolution of the surface streamers involves new mechanisms which are characteristic of spark discharges. In this sense, the usual term "surface streamer" can be misleading and we will use the term "surface discharge".



Fig. 30 - Photograph of a negative surface streamer.

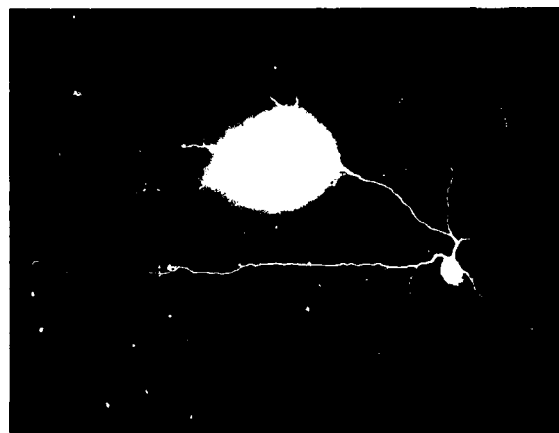


Fig. 31 - Photograph of a positive surface streamer.

Analysis of surface discharges in space and time reveals the following characteristics:

a) - a surface discharge is a tree-like discharge; the branches are the first step of the discharge with streamer charges and are called leaders; the following period of the discharge is called a surface charge or avalanche similar to the discharge of a spark (see Fig. 32). Figure 32 shows the typical structure of a positive surface discharge in air, initiated from a point electrode (cathode):

1) - the development of the discharge is stepwise: a period of pre-onset streamers with the pre-onset forward steps of the pre-onset leaders;

Quantitative analysis and interpretation of the physical mechanisms of these discharges are still lacking. Little effort has been devoted to this subject since the pioneering work of Frenkel [3]. However, from the results obtained by Hallenbeck and others [4] and [5] in the case of leaders and sparks, the following conclusions can be tentatively proposed [6] [7]:

a) - corona streamers are essentially unstable discharges in which the first step is the formation of space charge is all important in these discharges, but plasma conductivity is still low and a significant

voltage drop is experienced along the ionized channel produced behind the streamer (order of magnitude : channel resistance of $10^6 \Omega \text{ cm}^{-1}$) ;

b) - merging of many streamer channels increases the total current along the common trunk. This can be sufficient to heat the neutral gas, already excited by streamer propagation, up to the point where a small decrease of neutral density in the core of the channel is initiated : E/N increases in their core and ionization is enhanced ; the glow discharge sustained in this core has a higher conductivity than the streamer corona branches, and, at the beginning, is similar to the positive column of the low pressure discharge. This can be the explanation for leader formation (order of magnitude : leader resistance of $10^3 \Omega \text{ cm}^{-1}$) ;

c) - if the total current is sufficient in the leader main trunk, resistivity decreases up to the point where glow-to-arc transition is reached (order of magnitude from $10^2 \Omega \text{ cm}^{-1}$ to $10^{-2} \Omega \text{ cm}^{-1}$).

In this model we have followed a suggestion by Marode who has shown that, in sparks, the thermal instability characterized by a constriction of the discharge appears well below glow-to-arc transition. This instability can be initiated after streamer development if the initial conditions are such that discharge quenching by attachment (or recombination) is not completely achieved before the decrease of neutral density and the resulting E/n increases [30]. No explanation has yet been proposed for the step length and duration.

IV.1.3 - Order of magnitude of surface discharges

Surface discharges can carry currents of hundred of amperes, and $\frac{dI}{dt}$ can reach values of 10^8 As^{-1} . Their duration is of the order of few hundred nanoseconds. Leader tip velocity is about 10^8 cm s^{-1} . Voltage drop in the leader channel depends on the local current ; it varies from $5 \cdot 10^6 \text{ V/m}$ near the head to 50 V/cm at the point of attachment to the metallic frame.

IV.2 - Electromagnetic radiation of a surface discharge

To the best of the author's knowledge, detailed information about radiation of surface discharges is inexistent. Extensive work is needed before modeling surface discharges and predicting their electromagnetic behaviour are possible. During an experiment performed at ONERA, high power pulses with durations of a few nanoseconds and recurrence period of 20 ns have been found. It is too early to give a comprehensive model to explain this experiment.

If these discharges are sustained along a dielectric layer covering a metallic panel, their current flows essentially parallel to the conducting surface ; therefore, according to the Tanner criterium, they are poorly coupled with the antennas ; however, one can easily obtain, by simulation, evidence of strong disturbances experienced by the electronic equipment : the reason could be the very high values of dI/dt obtained during the discharge, and the influence of end effects ; as a matter of fact, the discharge current flows in a closed loop which is magnetically coupled to the aircraft structure, inducing an electrical response in all the equipment.

If the discharge is established along the dielectric cover of an antenna, the current loop is closed during streamer and leader propagation by displacement currents parallel to the RF electric field, and the coupling is very strong. Saturation of electronic equipment is readily obtained in this case.

IV.3 - Conclusion

Unlike the corona discharges obtained at the tips of the dischargers which are necessary for normal operation of aircraft, the surface discharges are harmful and should be eliminated. This is possible by the proper choice of reduced resistivities for the various dielectric surfaces of the aircraft.

V - GENERAL CONCLUSION

The analysis of the physical mechanism and of the radioelectric behaviour of the three types of discharges obtained by aircraft charging has led to the following conclusions :

- a) - sparks and surface streamers are generators of powerful radioelectric disturbances. They should be carefully avoided. Proper bonding eliminates sparks and specific surface treatments suppress surface discharges ;
- b) - coronas are necessary for getting rid of the accumulated static charge. On the one hand, attention should be given to reducing as much as possible the coupling between coronas discharges and antennas of the avionic system. On the other hand, use of corona microdischarges can bring a further improvement in static noise reduction.

R E F E R E N C E S

- [1] - HOWATSON AM - An Introduction to Gas Discharges. Pergamon Press - London (1976).
- [2] - LLEWELLYN JONES F. - Ionization and Breakdown in Gases. Methuen and Co - London (1957).
- [3] - MEEK J.M. and CRAGGS J.D. (editors) - Electrical Breakdown in Gases. John Wiley & Sons, London (1978)
- [4] - REES J.A. (editor) - Electrical Breakdown in Gases. Halsted Press, John Wiley & Sons, New York (1973).
- [5] - REES J.A. - Fundamental Processes in the Electrical Breakdown in Gases. Chapter 1 of ref. [3].
- [6] - LLEWELLYN JONES F. - Ionization Avalanches and Breakdown. Methuen & Co, London (1967).
- [7] - DUTTON J. - Spark Breakdown in uniform fields. Chapter 3 of ref. [3].
- [8] - CRAGGS J.D. - Spark Channels. Chapter 10 of ref. [3].
- [9] - WATERS R.T., JONES R.E. and BULCOCK C.J. - Proc. IEE 112 (1965), p. 1431.
- [10] - LLEWELLYN JONES F. and PARKER A.B. - Spark mechanism in air, Paper 6 of ref. [4].
- [11] - HAYDON S.C - Spark channels, Paper 14 of ref. [4].
- [12] - ALLIBONE T.E - The long sparks. Physics of Lightning, GOLDE R.H. Academic Press, London, (1977).
- [13] - TAILLET J. - JBIS 27, 185 (1974).
- [14] - GOLDMAN M. and GOLDMAN A. - Corona Discharges. Gaseous Electronics, HIRSH M.N and OSKAM H.J, Academic Press, New York, (1978).
- [15] - PEEK F.W. - Dielectric Phenomena in High-Voltage Engineering. Mc. Craw-Hill, New York (1929).
- [16] - SIGMOND RS - Corona Discharges, Chapter 4 of ref. [3].
- [17] - LOEB L.B. - Electrical Coronas. University of California Press, Berkeley (1965).
- [18] - HARTMANN G. - Thesis, University Paris-Sud France, (1977).
- [19] - BUCHET G., GOLDMAN M. and GOLDMAN A. - C.R. Acad. Sci. Paris 263 B, 356 (1966).
- [20] - LOEB L.B. and KIPP A.F. - J. Appl. Phys. 10, 142 (1939).
- [21] - PEYROUS R. - CNAM Thesis, University of Pau, France (1974).
- [22] - NEWMAN N.M. and ROBB J.D. - Aircraft Corona Variation with altitude. Proc. National Electronic Conference - Vol. 8 (1953).
- [23] - CHAPMAN S. - Geophys. Res. 75, 12 (1970).
- [24] - LAMA W.L. and GALLO C.F. - J. Phys. D. Appl. Phys. 6, 1963 (1973).
- [25] - BRUNET A. - IFL C. Illegitim on Corona Discharges, London, (Dec. 1979)
- [26] - TANNER R.L., VANEVICH J.E. - Proc. IEEE, 52, 1 (1964), p. 44.
- [27] - ROBB J.D., TANNER R.L. - AFAL - TR - 72 - 325. ILS/VOR Navigation and Approach Errors From Precipitation Static Interference. "Air Force Avionics" Laboratory (December 1972).
- [28] - BOULAY J. - La Recherche Aéronautique (1979-2), p. 101.
- [29] - TLEPLER M. - Ann. d. Phys. 53, (1917), p. 217. Archiv für Electrotechnik, X, 5, 6 (1921).
- [30] - MARODE E., BASTIEN F., BAKKER M. - Appl. Phys. 50, 50, 1 (1979), p. 140.
- [31] - GALLIMBERTI I. - J. de Phys., XIVE CIPIG - Vol. 2 (1979).

STATIC CHARGING EFFECTS ON AVIONIC SYSTEMS

J. E. Nanevitz
Associate Director, Electromagnetic Sciences Laboratory
SRI International,
333 Ravenswood Avenue
Menlo Park, California 94025

ABSTRACT

Electrical discharges can occur on an aircraft as the result of static electrification, either of the aircraft as a whole or of parts of the aircraft. The character of discharges at typical aircraft operating altitudes is such that radio frequency (RF) noise is generated in the portion of the electromagnetic spectrum normally used for aircraft communication and navigation systems. The noise sources excite the aircraft structure and can couple electromagnetic noise signals into antennas and electronic systems wiring. Under some circumstances, the noise can be sufficiently severe that critical systems are disabled when they are most needed.

The electromagnetic character of the various noise sources--corona discharge, surface streamers, and spark discharges--will be discussed. Available data include the results of flight tests and laboratory discharge simulations. In general, the source data exist both as time-domain waveforms and as frequency-domain spectra. The differences between the noise signals generated by the different sources will be discussed, and the dependence of noise levels on aircraft-charging current will be indicated.

Results of laboratory determinations of coupling between source locations and antennas will be presented together with the results of flight-test experiments conducted to verify the coupling information. Finally, the source data will be combined with the coupling information to predict the equivalent noise fields to be expected at typical antenna locations on aircraft. These noise fields are compared to atmospheric noise levels to determine the degree of system performance degradation that can result from precipitation-static noise.

I INTRODUCTION

A. General

As aircraft began to be operated under all-weather conditions, the effects of electrostatic charging were observed.^{1,2} In general, it was found that when aircraft were operated in precipitation, radio noise would often occur and disable onboard communication and navigation systems just when they were most needed. This relationship between electromagnetic interference "static" and precipitation led to the name "precipitation static."

Careful study of the problem immediately after World War II indicated that the noise resulted from frictional charging occurring when precipitation particles struck the aircraft and deposited charge on its surfaces.³ This charging, in turn led to electrical discharges of the sort discussed by Dr. Taillet in the previous paper. It was determined that it was the radio noise from these discharges that disabled the communication and navigation equipment.

Subsequent studies led to a better understanding of the various mechanisms involved in the charging and discharging processes and techniques were developed to mitigate the undesirable effects of the charging/discharging processes. Indeed, conventional metal-skinned aircraft equipped with analog-type electronics could operate successfully under all weather conditions.

B. Motivation for Continued Study of Static Charging

As each new aircraft is developed, there is a constant effort to improve its performance over that of its predecessors. To achieve this goal, the designer is driven to use new materials in the fabrication of the airframe and to equip it with the latest avionics systems. Changes in either of these areas can affect the susceptibility of the overall system to static charging. It is important that the designer be aware of the impact on system static susceptibility of changes in design.

In an all-metal aircraft equipped with analog avionics systems, the primary source of noise is corona discharge from the aircraft extremities. Since the skin of the aircraft is a good electromagnetic shield, noise couples to avionics systems primarily through their associated antennas located on the exterior of the aircraft. The use of new materials such as dielectrics and composites changes the way in which charge is deposited on the aircraft and generally degrades its electromagnetic shielding. Thus, unless care is exercised, the electromagnetic noise levels on the interior of the new aircraft may be substantially higher than they were on conventional all-metal aircraft.

Also significant, is the fact that the original avionics systems were based on vacuum tube analog circuitry which was quite immune to damage and catastrophic upset by electromagnetic noise pulses. The new systems, on the other hand, use digital avionics which are far more susceptible to damage and upset. In addition, momentary loss of avionics systems in the older generations of aircraft generally meant a temporary inconvenience in that the aircraft could be flown by the pilot during the period of outage. In future generations of aircraft, it appears that improved performance will be achieved through increased reliance on stability-augmentation devices--possibly to the extent that the aircraft will be so unstable that the pilot will no longer be able to fly it without the avionics systems. Thus, a loss of a critical avionics system may jeopardize the entire aircraft.

Since the addition of fixes to provide immunity from the effects of static electrification always implies cost and weight penalties, the designer needs accurate information about the processes and their effects to prevent overdesign or underdesign of the protection schemes.

II ELECTROMAGNETIC NOISE COUPLING

The generation and coupling of electromagnetic interference is most readily attacked by breaking down the overall processes into the three steps illustrated in Figure 1. A source of noise exists on the aircraft and excites electromagnetic coupling paths to couple interference into the victim circuit. With the breakdown shown in the figure, it is possible to consider the three facets of the problem independently.

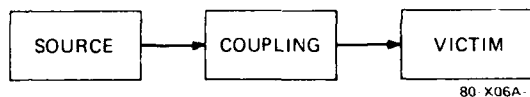


FIGURE 1 GENERATION AND COUPLING OF ELECTROMAGNETIC INTERFERENCE

The noise sources can be characterized as Dr. Taillet has done for the corona discharge, the spark, and the surface streamer.⁴⁻¹⁰ This information on source characteristics together with information on charging rates and discharge location, permits the engineer to consider a noise source of prescribed intensity and electromagnetic character to be located at a defined position on the aircraft.

Next, the electromagnetic coupling between the source location and the victim circuit of interest must be considered. Sometimes, as in the case of corona discharge directly from an antenna, the coupling path is obvious and is amenable to a simple analysis. In other cases, these coupling mechanisms are more subtle and it may be necessary to resort to experiment to define the coupling over the frequency range of interest.^{5,6,8}

By combining the source and coupling information, it is possible to determine the signal coupled to the victim circuit.⁶ If the coupled signal level is lower than the susceptibility level of the victim system under consideration by a reasonable margin, no interference will occur. If the coupled noise signal level exceeds the susceptibility limits of the victim, appropriate noise reduction measures must be taken.

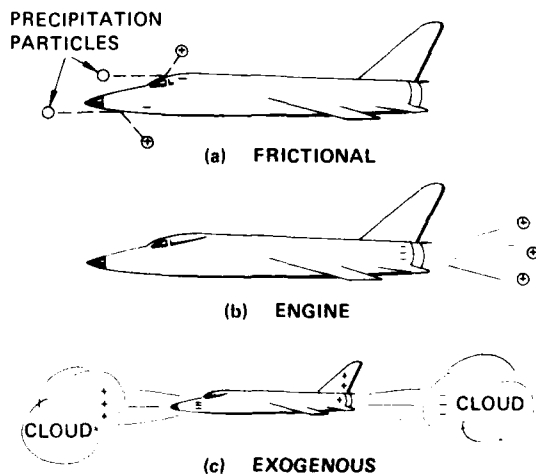
Considering the noise generation and coupling problem in the light of Figure 1 serves to emphasize the fact that controlling the interference can be attacked in three different ways. First, one can take steps to eliminate or reduce the intensity of the noise source. Indeed, this approach is generally the simplest to implement in the case of surface streamering and sparking.^{7,8} Second, an effort can be made to reduce the coupling between the source and victim. Examples of this approach include the addition of shielding and the installation of decoupled corona discharges.^{5,11} Third, the basic hardness of the victim can be improved. Since this approach often involves changes in circuit design or system design philosophy, it frequently cannot be applied.

A further consequence of viewing the interference problem in the light of Figure 1 is the recognition that the nature of the interference signal at the victim may be quite different from the source signal. The fact that the amplitude may be lower at the victim is intuitively obvious. Less widely recognized is the fact that the time waveform of the noise pulse arriving at the victim often may be quite different from that generated by the source. In general, the source consists of a succession of short pulses which excite currents on the aircraft structure and wiring. Electromagnetic resonances in the structure and wiring can cause the pulse arriving at the victim to be stretched out in time.

III EFFECTS STEMMING FROM CHARGING OF ENTIRE AIRCRAFT

A. Electrification Processes

The various ways in which static electrification of an aircraft can occur are illustrated in Figure 2. Figure 2(a) illustrates frictional electrification; as uncharged precipitation particles strike the aircraft, they acquire a positive charge, leaving an equal and opposite negative charge on the aircraft and raising its potential to tens or hundreds of thousands of volts.^{1,8} Charging occurs both on the metal structure of the aircraft and on dielectric surfaces such as the windshield. As is discussed in more detail in Section IV, dielectric surfaces can thus become charged with respect to the airframe.^{7,8,9} Engine charging, illustrated in Figure 2(b), occurs when flight vehicles are operated at low altitudes.^{5,10} Processes, as yet incompletely understood, occur within the engine combustion chamber and cause a predominantly positive charge to be expelled with the engine exhaust. This causes an equal and opposite (negative) charge to be imparted to the aircraft, charging it to potentials of tens or hundreds of thousands of volts. Exogenous charging, illustrated in Figure 2(c), occurs when the vehicle flies in a region of electric field, such as that generated between oppositely charged regions of clouds; this field can cause discharges to occur from the extremities of the vehicle.



80-X06A-2

FIGURE 2 CHARGING PROCESSES

The operational conditions under which static electrification can occur depend somewhat on the class of vehicle. Since airplanes encounter severe charging during operation in clouds in horizontal flight, electrification can continue for considerable periods of time on all-weather missions. On jet aircraft operating at low altitude, engine charging can be an additional source of long-term electrification. Helicopters become

charged while flying through naturally occurring clouds. In addition, a hovering helicopter can stir up snow or dust thereby generating its own cloud of particles to produce frictional static charging problems in regions where conventional aircraft do not.

A typical record generated at an altitude of 25,000 ft during the flight of a jet fighter through cirrus clouds is shown in Figure 3. At the top of the record is a trace showing the charging current arriving on an electrically-isolated probe installed on the front of the aircraft. The total current arriving on the aircraft is proportional to the particle probe current. The middle trace in Figure 3 shows the time history of the aircraft potential. It is evident that the aircraft potential varies directly with charging current. The lower trace in the figure indicates the current leaving a discharger mounted on the tip of the trailing edge of one of the wings. The discharge current evidently follows the variations in aircraft potential.

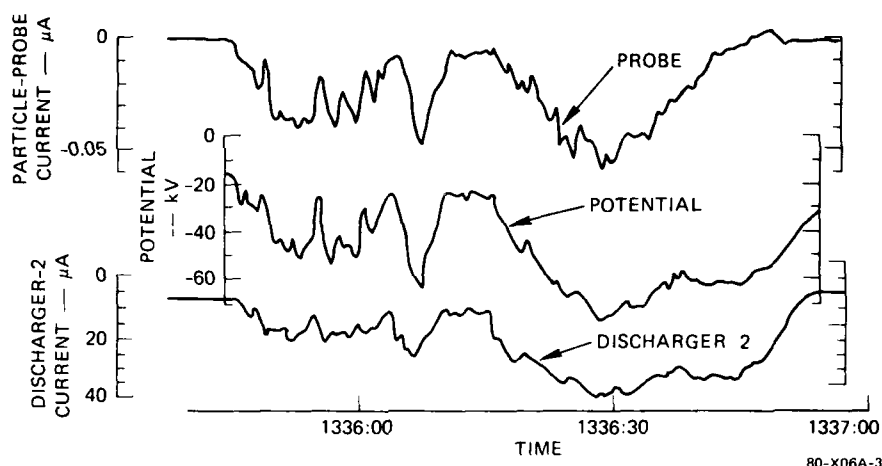


FIGURE 3 PRECIPITATION CHARGING OF JET FIGHTER AIRCRAFT

It is interesting to note the rapidity with which all of the measured parameters in Figure 3 vary. Charging current and aircraft potential go from minimum to maximum in 1 or 2 s. It is also of interest that negative charge is arriving on the aircraft. The aircraft charges to a negative potential, and negative charge leaves the aircraft via the dischargers. It should be noted that during the period shown on the record, the peak aircraft voltage was 80 kV, and that the maximum current leaving the instrumented discharges was roughly 45 μ A. These magnitudes are typical for flights through cirrus clouds. Finally, the record indicates that even when the aircraft potential is as low as 25 kV, the discharge current does not go to zero.

A record of engine charging during the takeoff of a jet fighter aircraft is shown in Figure 4. The wheels leave the ground at $t=0$. At $t=0.5$ s, the aircraft potential has reached -64 kV, and the discharge current is 13 μ A. As the aircraft climbs, we see that the airplane potential and discharge current gradually decrease. This decrease in engine charging during climbout is characteristic of all aircraft and also occurs on rockets.

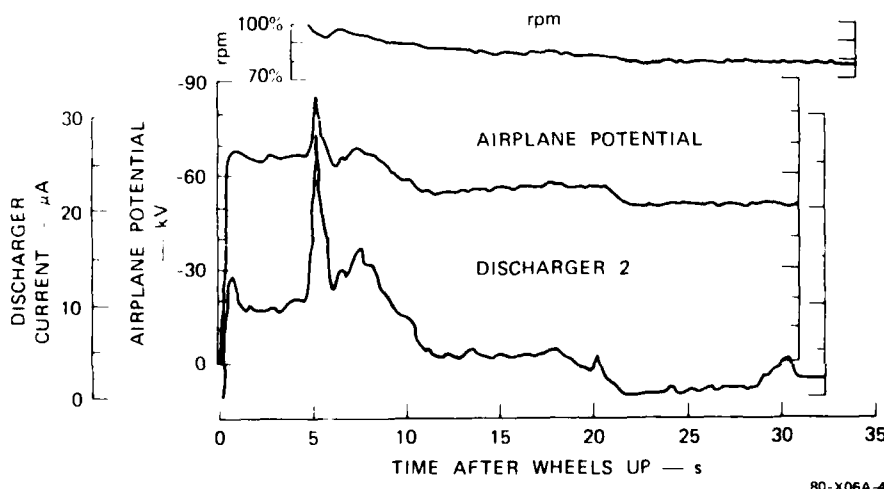
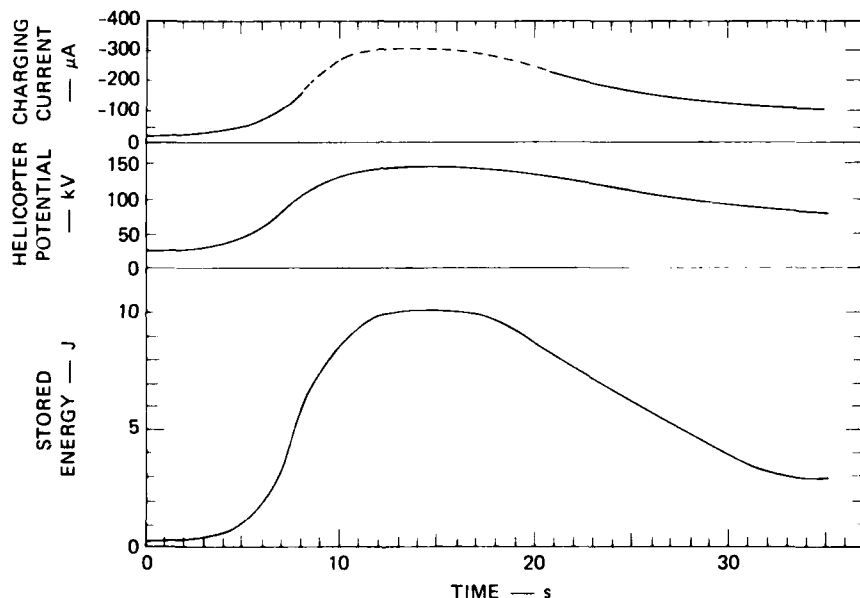


FIGURE 4 ENGINE CHARGING DURING TAKEOFF OF JET FIGHTER AIRCRAFT

The sensitivity of engine charging current to changes in throttle setting is illustrated in an interesting manner in Figure 4 by the period of increased charging and airplane potential 5 s after takeoff. Here discharger currents were briefly increased by a factor of two or more. The changes in charging are associated with a power change evidenced by an abrupt 6% reduction in engine RPM. Such behavior was also observed during flight tests on a 707 aircraft.

In comparing Figures 3 and 4 we note that the aircraft potentials in the two cases are of comparable magnitude, but that the discharge current is substantially less under engine charging conditions. Precipitation charging currents are even higher than those shown in Figure 3 when the aircraft is flown in different cloud types--for example, through frontal snow. Thus, noise elimination methods adequate for precipitation charging will certainly be adequate under conditions of engine charging. It should be noted that the record of Figure 4 was generated during a takeoff in clear weather. Thus engine charging will cause electromagnetic interference problems on every takeoff and landing unless the proper protective steps are taken.

Frictional charging of a different type of aircraft is shown in Figure 5. This figure shows a record of charging current and helicopter potential measured on a Chinook helicopter hovering in a dusty environment. $T=0$ denotes roughly where take-off occurred, and the hover altitude of 50 ft was established at approximately 15 s.¹⁵ In this figure the charging current rapidly increases to about $300\mu\text{A}$ and then at about $t=17$ seconds slowly begins to decay. This decay is due to the rotor wash blowing the dust away from the measurement site. It should be noted that the helicopter potential reached a maximum value of 140 kV and then gradually decayed to roughly 75 kV. Since the self capacitance of a hovering Chinook helicopter is roughly 1000 pF, these potentials correspond to stored energies of 10 J and 3 J, respectively.



80-X06A-5

FIGURE 5 HELICOPTER POTENTIAL AND CHARGING CURRENT AS A FUNCTION OF TIME AFTER LIFTOFF IN A DUSTY ENVIRONMENT

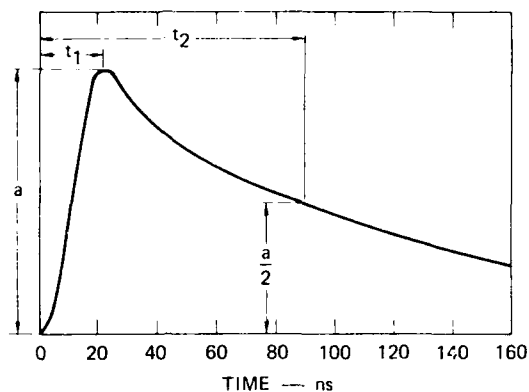
B. Effects on Vehicle Operation

1. Electromagnetic Noise

Although the vehicle charging processes discussed above produce virtually no difficulty, the vehicle voltage can become so high that electrical discharges occur (as illustrated in Figures 3 and 4). The discharge of the accumulated static electricity is harmful because it produces electromagnetic noise.

As was indicated by Dr. Taillet, the corona discharge at aircraft operating altitudes consists of a series of short pulses such as the one shown in Figure 6. The precise amplitude and time structure are a function of aircraft altitude and discharge point radius. Laboratory measurements on a corona discharge from a sheared metal edge (simulating the trailing edge of an airfoil) indicate that, at atmospheric pressure, the pulse repetition frequency (prf) is on the order of 10^5 pulses per second when the discharge current is $100\mu\text{A}$.⁵ Thus each pulse carries away 10^{-11} Coul. of charge. Since a precipitation particle deposits roughly 10^{-11} Coul. of charge, each corona pulse removes the charge deposited by 100 precipitation particles. Since the capacitance of a large aircraft such as the 707 is 100 pF, the charge carried away by a single corona pulse changes the aircraft potential by 1 volt.

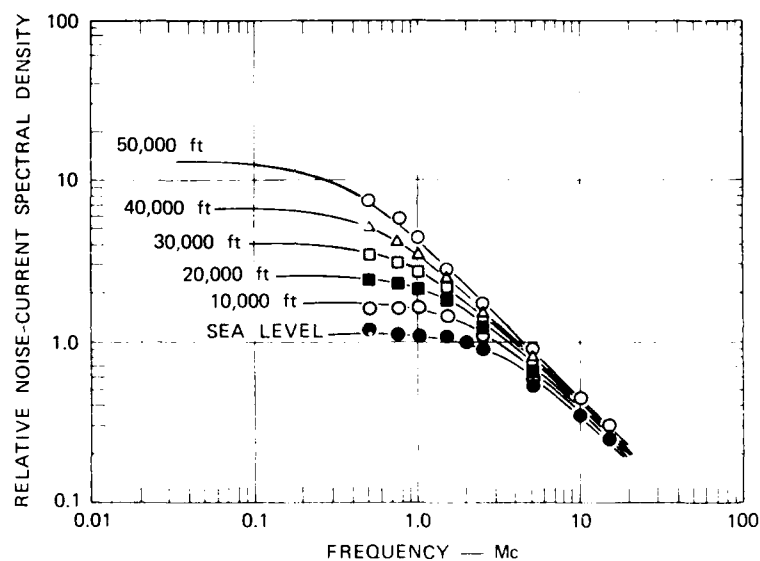
Although data regarding corona pulse form and other characteristics provide insight into the corona discharge process, corona noise calculations are most easily carried out using noise spectral data of the sort shown in Figure 7.^{5,6} These data present measured spectral characteristics for the entire aircraft operating altitude range. It should be noted that the corona source is most energetic at low frequencies, but that it contains appreciable energy well into the HF band.



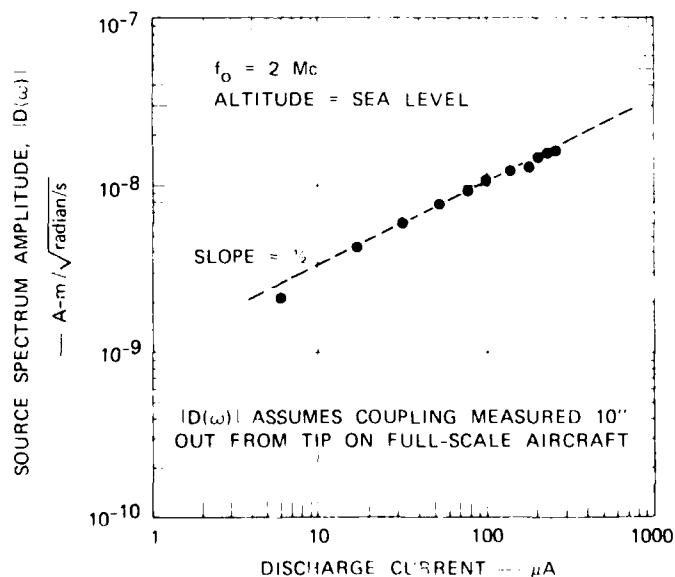
6 HERE

80-XU6A-6

FIGURE 6 TIME STRUCTURE OF NEGATIVE POINT CORONA PULSE, PRESSURE = 200 mm/Hg



(a) NORMALIZED SPECTRUM SHOWING ALTITUDE EFFECTS



(b) RELATIONSHIP OF ABSOLUTE NOISE LEVEL TO DISCHARGE CURRENT

80-X06A-7

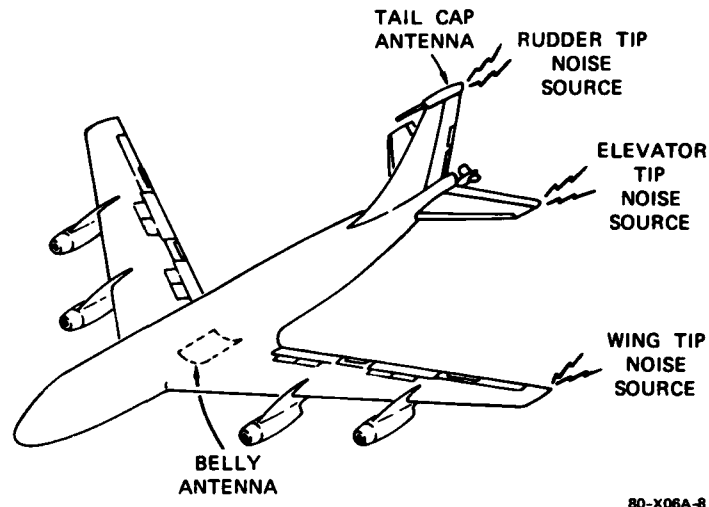
FIGURE 7 CORONA-NOISE-SOURCE SPECTRUM CHARACTERISTICS

When the source characterization work leading to Figure 7 was under way, aircraft used the VHF and UHF bands strictly for line-of-sight communication and navigational aids were operated at received signal levels sufficiently high that corona noise at these frequencies was not of concern. Accordingly no effort was made to extend the corona spectrum studies above 14 MHz. This is unfortunate since it is now planned that satellite communication links operating at low received signal levels will be employed on aircraft. To accurately assess their vulnerability, it would be useful to have corona spectral data extending to VHF and UHF.

In general, the corona noise source on an aircraft is located in one place, and the affected antenna or system is located in another. It is therefore necessary to define the coupling between the noise source and the victim system. This was done experimentally for two antenna locations on the 707 aircraft as illustrated in Figure 8.^{8,9} The antennas used in making the measurements were a small tail-cap and a flush belly antenna located in a fairing at the root of the wing. Coupling was measured between each of these antennas and the noise source regions at each of the airfoil extremities. The results of the measurements are shown in Figure 9.

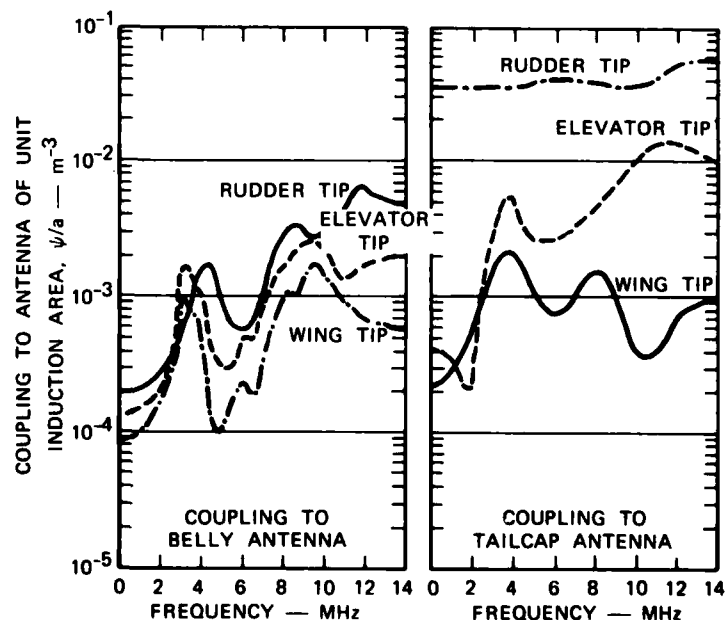
Although the coupling-measurement technique used inevitably includes the test-antenna characteristics in the measured results, the form of the coupling as a function of frequency is not affected by the details of the test antenna, provided the antenna dimensions are small compared to a wavelength at the frequencies of interest. In this case, only the magnitude of the coupling function will be affected by a change in the antenna. The data shown in Figure 9 have therefore been adjusted to represent the coupling to an antenna having unity induction area, a , in response to a low-frequency, vertically-polarized signal.

The variation with frequency of the coupling to the various points is of considerable interest, since it shows the effect of the various electromagnetic resonances of the aircraft. For example, the peak in coupling between the belly antenna and the tips of the tail surfaces occurs at approximately 3 MHz. At this frequency, the path distance from a point just aft of the wings to a tip of one of the tail surfaces is one-quarter wavelength. The presence of the resonance peaks in the coupling function serves to emphasize the fact that the pulses arriving at the antenna terminals will differ from the pulses generated by the corona discharges at the extremities in that they will be stretched out in time by aircraft resonances. It is also interesting to note that discharges from



80-X06A-8

FIGURE 8 ANTENNA AND CORONA-NOISE SOURCE LOCATIONS FOR KC-135 COUPLING MEASUREMENTS



80-X06A-9

FIGURE 9 MEASURED COUPLING FACTORS FOR ANTENNAS ON BOEING 707 PROTOTYPE AIRCRAFT

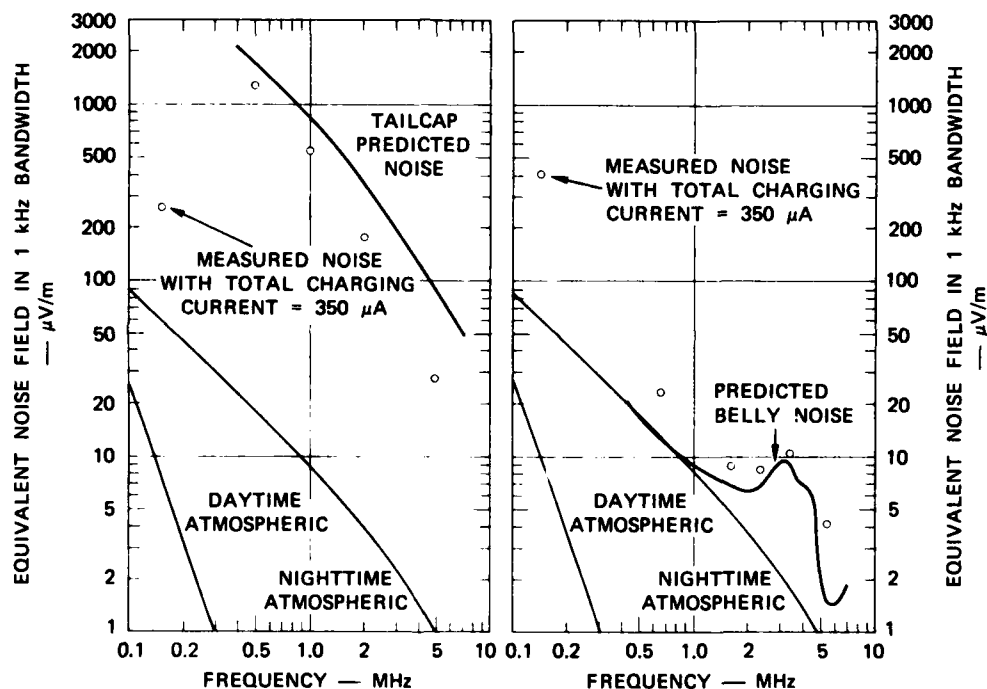
the rudder tip are strongly coupled to the tailcap antenna. Discharges from the fin will therefore generate the dominant corona noise signals in the tailcap.

The data of Figure 9 can be applied without restriction to aircraft of similar shape but different size. In general, the same resonances will occur on the scaled aircraft, but they will occur at the scaled frequency. The magnitude of the coupling must also be scaled with aircraft size.^{5,6}

Actually, the data of Figure 9 are the only coupling data presently available for conventional aircraft and have been scaled and applied to other aircraft with remarkably good results even when the scaled aircraft were not very similar to the 707. Limited coupling studies have been carried out for a helicopter but have not been published.¹⁴ Additional coupling data covering a wider variety of aircraft configurations and antenna locations are badly needed.

In the case of helicopters, corona discharges occur from the tips of the blades, so that coupling to the blade tips is of interest. Since this varies with blade position, the corona noise intensity is modulated at the rotor frequency.¹⁴ In general, the coupling varies with antenna location and displays resonances of the same general sort observed in Figure 9.

By combining data of the sort shown in Figures 7 and 9, it is possible to predict the corona discharge noise levels. This was done for the case of the 707 aircraft and the results are shown in Figure 10 along with the results of flight test noise measurements.^{5,6} It is evident that the two sets of data are in good agreement for both antennas.



80-X06A-10

FIGURE 10 CORONA DISCHARGE NOISE IN 707 ANTENNAS

The corona noise level in the tailcap antenna is substantially above the accepted value of nighttime atmospheric noise.¹⁵ Since the system designer can achieve improved performance to the point where the system input-noise figure is reduced to the atmospheric noise level, it must be assumed that optimized systems are now or will be operating at the atmospheric noise level. Thus, the tailcap corona noise severely degrades the performance of such a system. It should also be observed that 40 dB of noise reduction is required to reduce corona noise to the nighttime atmospheric noise level cited in Reference 15. Even greater noise reduction is required to approach daytime atmospheric levels.

Although the belly antenna noise levels shown in Figure 10 are comparable to the nighttime atmospheric noise at certain frequencies, it is important to note that a 350 μ A charging current is typical of the charging conditions found in light cirrus, and that currents up to 3 MA were measured in flight. Under these conditions, the noise levels will be 10 dB higher. Thus at least 30 dB of noise reduction is required to reduce corona noise to the nighttime atmospheric noise level at all frequencies.

Because of the way in which charging current, and noise coupling scale with aircraft size, corona noise problems are generally more severe on smaller aircraft.^{5,6}

2. Shock Hazard

Although the electromagnetic noise generated by corona discharges from helicopter blades can cause operational problems, another serious problem occurs in connection with their operation. As a result of the static charge on helicopters, ground cargo handlers may receive severe shocks upon touching lowered cargo hooks.^{16,17} The static charge on the helicopter can also ignite flammable materials or initiate sensitive electro-explosive devices.

To assess the significance of the helicopter charge levels shown in Figure 5, it is necessary to be able to relate them to a person's response to different levels of stored energy.¹⁸ To this end the test helicopter was configured as shown in Figure 11 and hovered 25 ft over a concrete pad.¹⁸ This test was conducted by raising the helicopter up to some potential, V , using the internal power supply. The (barefooted) person beneath the helicopter then touched the simulated cargo hook and noted his response. Helicopter voltages, discharge energies, and the subject's observations about the shock levels experienced are shown in Table 1.^{19,20} It can be seen from this table that the subject's comments agree well with data published by Dalziel.^{19,20} The data in Table 1 also demonstrates that the tolerable helicopter voltage is substantially below the helicopter potentials measured in Figure 5.

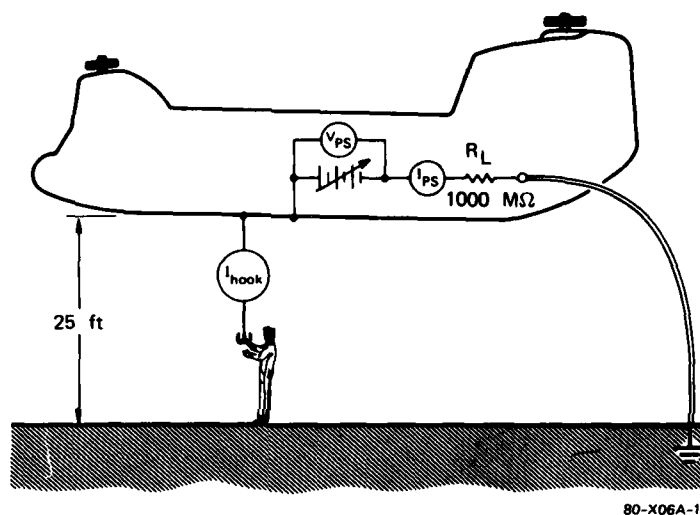


FIGURE 11 AIRCRAFT CONFIGURATION USED TO MEASURE PHYSIOLOGICAL RESPONSE TO ELECTRIC SHOCK

Table I

PHYSIOLOGICAL RESPONSE OF SUBJECT EVALUATING ELECTRIC-SHOCK FROM CHARGED HELICOPTER

Aircraft Voltage (kV)	Helicopter Discharge Energy* (mJ)	Comments
2.5	3	
5.0	12.5	
6.0	20	(Dalziel threshold)
7.5	28	"Slight shock"
10.0	50	"Shock in fingers"
12.5	78	
15.0	112	"Sensible shock"
17.5	152	"Shock felt in wrist"
20.0	200	"Distinct shock felt in wrist and ankles"
23.7	250	"(Dalziel: Strong shock, not dangerous)"

*NOTE: Assumed helicopter capacitance 1000 pF.

Defining lethal levels of impulse shock is difficult in view of the scarcity of data and the complex way in which electrical shock affects the body. Ventricular fibrillation, the most common cause of death in electric shock cases, occurs at intermediate levels of current. Below this level, only unpleasant sensations are felt, while very strong short shocks will stop a fibrillating heart. Dalziel describes a case in Sweden in which a 22 year-old man was killed as the result of receiving the residual charge from the capacitors of a high-voltage filter supplying a 150-kW transmitter. The energy received by the victim was estimated to be 24 J. The same paper discusses other cases in which people received comparable or higher shocks and survived with burns, unconsciousness, or severe headaches. The conservative interpretation of Dalziel's data is that the peak potentials and stored energies in Figure 5 are not acceptable for cargo handling operations, and that means for controlling the helicopter potential must be provided.

IV EFFECTS STEMMING FROM DIFFERENTIAL CHARGING OF PARTS OF AIRCRAFT

A. Electrification Processes

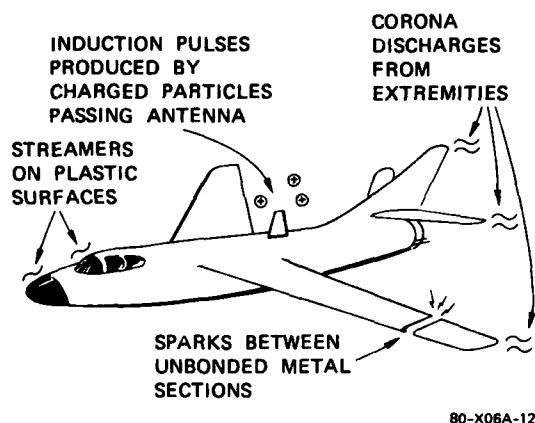


FIGURE 12 NOISE SOURCES

In Figure 2(a) it is indicated that impinging precipitation particles deposit charge on the frontal surfaces of the aircraft. Charge deposited on metal surfaces is free to flow over the airframe and redistribute itself as required by the governing boundary conditions. Charge deposited on dielectric surfaces such as the windshield or radome is bound where it arrives since these surfaces are not electrical conductors. Thus it is possible for these frontal dielectric regions to charge to a potential different from that of the airframe.^{7,8} Charge continues to be deposited on the dielectric raising its potential until a streamer (a sparklike discharge) occurs across the dielectric surface to the airframe. The processes involved in the streamer discharge, and its electromagnetic properties, have been discussed by Dr. Taillet. Since streamer discharges are short in duration and involve the transport of charge over a long distance, they act as a strong source of RF interference.

An important source of interference that often occurs inadvertently on airplanes is associated with sparking between unbonded adjacent metal sections of the aircraft.²¹ For example, consider Figure 12, which shows a break in the wing; charging processes on the airframe will raise the potential of the inboard section with respect to the outboard section until a spark occurs in the gap. This spark produces a short current pulse, which is also a source of noise. In flight, the current required for corona discharge

charge from the isolated wing tip is supplied from the remainder of the airplane. In fact, it is possible for charge arriving on the radome of the aircraft in Figure 12 to generate noise by three different processes before it finally leaves the aircraft. First the charge accumulates until it produces a streamer over the radome. Next it can generate a spark in the gap shown in the wing. Finally it generates noise where it is discharged in the corona from the wing tip.

B. Effects on Vehicle Operation

1. Streamer Noise

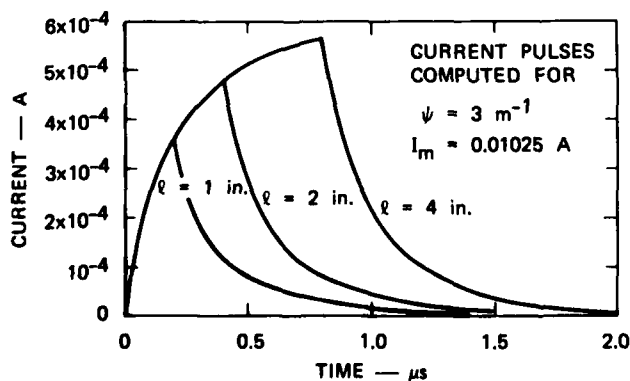


FIGURE 13 TYPICAL CURRENT PULSES INDUCED BY STREAMER DISCHARGES

Typical pulses induced in a wire located immediately below the dielectric surface on which streamers are occurring are shown in Figure 13.^{7,8} It is evident from the figure that the time waveform of the pulse depends on the length of the streamer discharge.

Assuming that the wire is terminated in an impedance of 1000 ohms the current pulses of Figure 14 will generate voltage pulses of 0.4 V. This pulse amplitude is sufficient to upset a variety of circuits. In particular, it should be noted that great care should be exercised not to route cables associated with digital systems under dielectrics located on aircraft frontal surfaces.

To investigate the effects of streamer discharge noise on narrow-band systems such as radio receivers, it is convenient to express the source function in terms of a noise frequency spectrum as was done for the case of corona noise in Section III B-1. The results of streamer-noise-source spectrum calculations for several arrangements of the dielectric region are shown in Figure 14 for the case of

unity coupling ($\psi = 1 \text{ m}^{-1}$) and a charging current to the dielectric region of $I_{dc} = 1 \mu\text{A}$. It is evident from Figure 14(b) that in spite of the differences in the physical arrangements considered, the three spectra are almost identical in the frequency range considered. This result is significant in that details of the geometry of the dielectric region and details of antenna location do not noticeably affect the form or magnitude of the resulting noise spectrum. Thus, we can be quite loose in defining the precise streamer geometry and still obtain valid noise data.

To further explore the effects on the noise spectrum of varying streamer geometry, calculations were carried out to determine the noise spectra generated by a given charging current on regions of a given shape but of varying size. The results of such calculations indicate that increasing the size of the region (this increases streamer length) increased the low-frequency content of the noise spectrum. This is in keeping with the results shown in Figure 13 where it is indicated that increasing the length of the streamers stretches the induced-current pulse, thereby increasing its low-frequency content.

A spark noise source (isolated at the ends of high resistance leads to avoid modifying the electromagnetic coupling fields) was used in the work of Ref. 22 to measure the coupling between three antennas located in the fuselage of an aircraft, and the surface of a radome located on the nose. The measurements were made using an oscilloscope connected to the antenna terminals, and represent the low-frequency coupling, which is of primary interest because streamer noise spectra fall off rapidly with increasing frequency above 1 MHz. The results of these measurements are reproduced in Figure 15.

It is interesting to note that the magnitude of the coupling from the fuselage antennas to the radome (Figure 15) is of the same order as the coupling of the belly antenna to the airfoil extremities (shown in Figure 9). Also, we should note that for a given discharge current the source intensity (at low frequencies) for streamer discharges shown in Figure 14 is roughly the same as for corona shown in Figure 7. It should be observed, however, that all of the current arriving on a vehicle is discharged as corona, whereas only a small fraction of the total charging current (that arriving on the dielectric surface in question) contributes to the streamer-noise generation process. Thus, except for antennas located in the immediate vicinity of a frontal dielectric surface (in which case coupling is high), streamer noise is generally less of a problem than corona noise.

2. Discharges from Windshields

Modern windshields often incorporate an optically-transparent electrically-conductive layer below the outer ply. Electrical power applied to the conductive layer heats it and de-ices the windshield. Wires lead from the de-icing layer to control circuitry and to the aircraft power system. The presence of this highly-conductive layer immediately below the outer ply allows the storage of great amounts of charge on the windshield.^{25,26} Ground crew personnel have been shocked and knocked off aircraft by touching the windshield shortly after the aircraft landed. Fighter pilots occasionally receive shocks when their fingers extend onto the windshield as they support themselves by the windshield frame while getting up from the forward seat.

Occasionally massive discharges occur in which most of the charge on the windshield is discharged. These discharges have caused the de-icing control circuitry to be damaged. In other instances, less energetic but more frequent discharges have induced signals in de-icer control wiring which, in turn, coupled interference pulses into avionic systems causing them to malfunction.

3. Spark Discharges

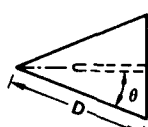
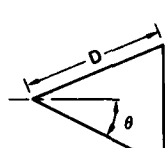
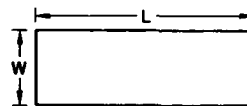
As Dr. Taillet has indicated, spark discharges involve processes capable of generating high-amplitude, fast-risetime pulses containing energy extending from the LF through the VHF range. Operational experience with this noise source has generally involved instances in which various electrical conductors became unbonded in subtle ways. Examples of three such instances on operational aircraft are shown in Figure 16.

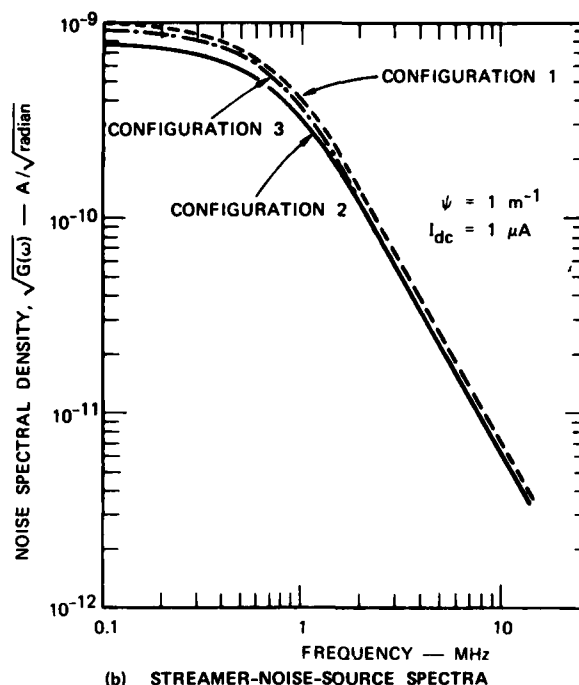
In the example of Figure 16(a), an airline began to experience p-static of sufficient intensity to adversely affect VOR navigation and VHF communications. Minute cracks were found in the lightning diverter strips on the nose radome due to weathering of the thin aluminum foil. Whenever precipitation charging was experienced, charge deposited on the radome surface would flow to the isolated portion of the diverter strip and accumulate until the voltage across the gap became high enough to initiate a spark. Each spark discharges the isolated strip completely, so considerable charge is transferred; therefore, each spark is an extremely energetic noise source. The dimensions of the diverter strips, furthermore, are such that at VHF they are a large fraction of a wavelength long; thus, at VHF a defective diverter system degenerates into an efficient antenna system driven by a spark noise source.

In the example of Figure 16(b), a particular B-707 aircraft of an international airline experienced severe p-static on its radios. All efforts to solve the problem failed, and the problem threatened to ground the aircraft as unsafe for long-range flight. Finally, an outboard wing inspection panel was discovered to have been repainted during a previous inspection; when it was reinstalled on the aircraft, the mounting screws had not penetrated the paint, which left an isolated section. Precipitation charging of the isolated panel charged it to a high potential with respect to the airframe so that sparking occurred across the insulating gap. Thus, the insulated panel was, in effect, an electric dipole antenna driven by a spark noise source.

The example of Figure 16(c) occurred early in the application of the ortho-decoupled dischargers to jet transports. Two airlines flying DC-8 aircraft reported bad P-static on discharger-equipped aircraft. The design of the DC-8 vertical fin is such that a bonding strap must be used to bridge from the metal main structure of the forward part of the fin to the dischargers mounted on the insulating plastic trailing edge. Damage to the electrical bond was found so that current flowing from the airframe to the discharger produced sparks across the gap in the discharger bonding system. This resulted in a spark-excited radiating system on the vertical fin of the aircraft.

Perhaps most significant in Figure 16 is the fact that such minor departures from the design configuration are ultimately found to be responsible for the generation of sparking noise. This degree of attention to detail is always necessary in tracking down noise sources on aircraft.

1. TRIANGULAR DIELECTRIC, ANTENNA WIRE ON BACK
- 
2. TRIANGULAR DIELECTRIC, ANTENNA DISTANT
- 
3. RECTANGULAR DIELECTRIC, ANTENNA DISTANT
- 
- (a) DIELECTRIC SHAPES AND ANTENNA ARRANGEMENTS FOR WHICH STREAMER STATISTICAL CALCULATIONS WERE CARRIED OUT



80-X06A-14

FIGURE 14 STREAMER-NOISE-SOURCE SPECTRA FOR SEVERAL PHYSICAL CONFIGURATIONS OF THE DIELECTRIC REGION

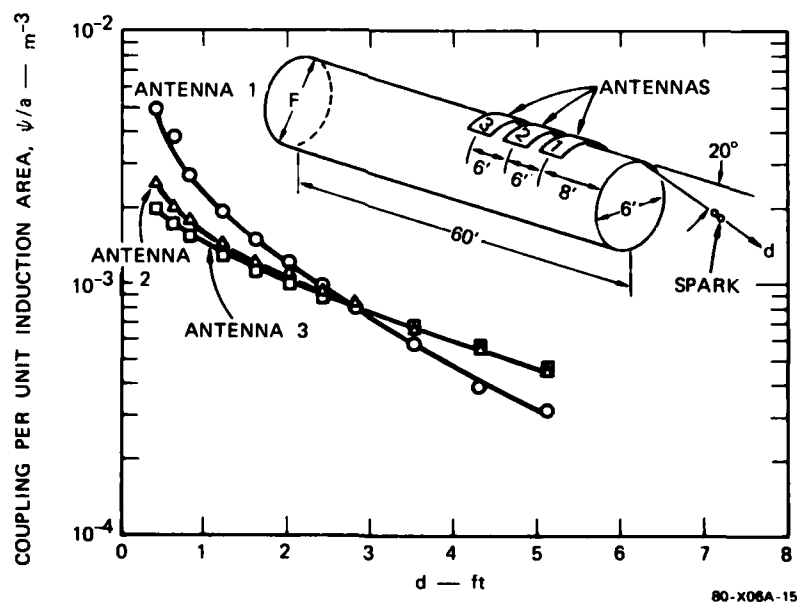
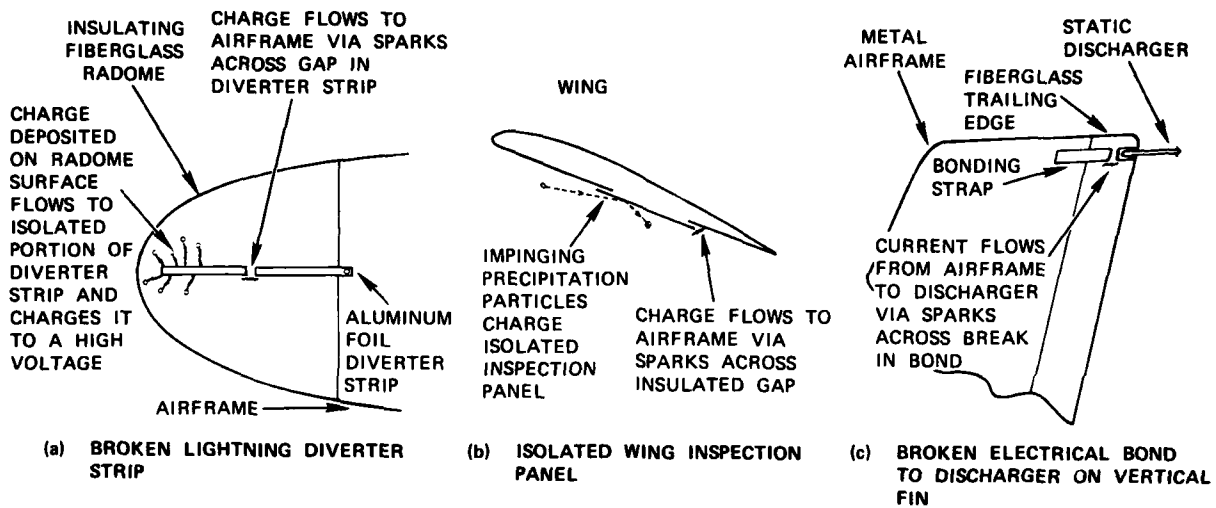


FIGURE 15 NOISE COUPLING TO RADOME

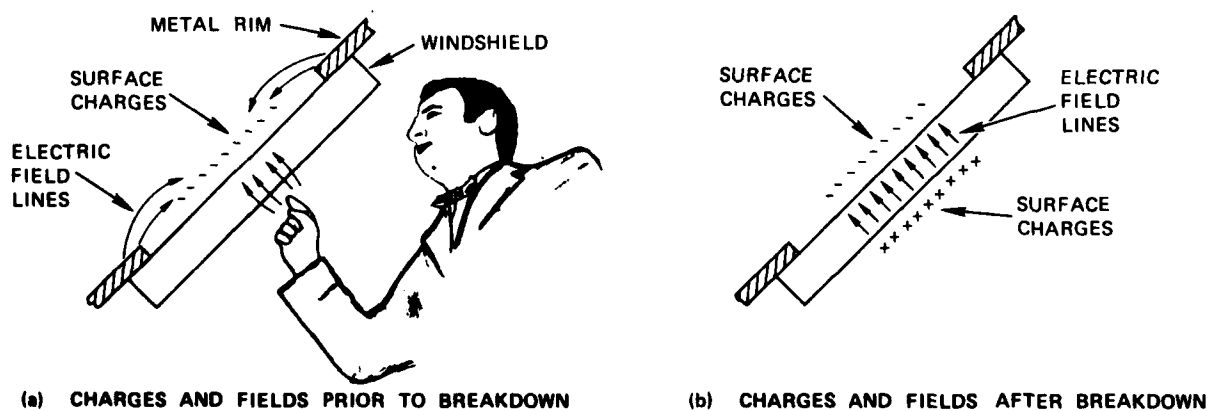
4. Discharges to Interior of Aircraft

Thus we have discussed the charging of dielectric surfaces on aircraft ultimately resulting in surface discharges on the outside surface of the dielectric to relieve the deposited charges. It must be recognized that field lines originating on the surface charges can penetrate the dielectric and terminate on objects inside the aircraft as is illustrated by the pilot's fingers in Figure 17(a), as well as terminating on the metal rim surrounding the dielectric surface. If the pilot reaches toward the windshield he will initiate a breakdown between his finger and the back of the windshield which deposits charge on the inside of the windshield as shown in Figure 17(b). Once the situation in Figure 17(b) is established, additional negative charge can accumulate on the outside of the windshield, and, if the pilot points at the windshield a second time, a second breakdown can occur.



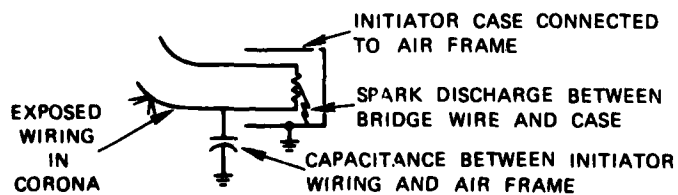
80-X06A-16

FIGURE 16 EXAMPLES OF SPARKING-NOISE SOURCES ON OPERATIONAL AIRCRAFT (after Moore)



80-X06A-17

FIGURE 17 WINDSHIELD CHARGING SITUATION RESULTING IN SHOCK TO PILOT



80-X06A-18

FIGURE 18 SQUIB INITIATION BY CORONA DISCHARGE

This same mechanism can initiate electro-explosive devices as is shown in Figure 18. Charge on the dielectric surface induces a corona discharge from the initiation wiring and deposits charge on the bridgewire circuit. The charge on this circuit ultimately causes a spark discharge between the bridgewire and case. The spark fires the initiator.

As is discussed by Taillet (29), discharges to the wiring on the interior of a vehicle can also cause computer malfunction with serious consequences.

V CONCLUSIONS

Static electrification during aircraft operation charges the aircraft as a whole, and produces potential differences between insulated parts of the aircraft and the main airframe. As a result of this electrification, a number of discharge processes can be activated. The consequences of these resulting discharges vary from the annoying to catastrophic, depending upon which avionic system is affected and the time during the mission when the discharge occurs. Accordingly, it is important that careful consideration be given to static electrification and its consequences during the design and development of an aircraft system.

REFERENCES

1. H. G. Hucke, "Precipitation Static Interference," Proc. IRE, Vol. 27, May 1939.
2. R. C. Ayers and J. O. Jarrard, Trans-World Airlines Inc., "Aircraft Precipitation Static Investigation," 1944, Contract W 33-106 SC-70.
3. Ross Gunn, et al, "Army-Navy Precipitation Static Project," Proc IRE, Vol. 34, 1946.
4. R. L. Tanner, Stanford Research Institute, "Radio Interference from Corona Discharges," 1953, Technical Report 37, SRI Project 591, Air Force Contract AF 19(604)-266.
5. R. L. Tanner and J. E. Nanevicz, Stanford Research Institute, "Precipitation Charging and Corona-Generated Interference in Aircraft," 1961, Technical Report 73, Air Force Contract AF 19(604)-3458.
6. R. L. Tanner and J. E. Nanevicz, "An Analysis of Corona-Generated Interference in Aircraft," Proc. IEEE, Vol. 52, January 1964.
7. R. L. Tanner and J. E. Nanevicz, Stanford Research Institute, "Radio Noise Generated on Aircraft Surfaces," 1956, Final Report, Air Force Contract AF 33(616)-2761.
8. J. E. Nanevicz, Stanford Research Institute, "A Study of Precipitation Static Noise Generation in Aircraft Canopy Antennas," 1957, Tech. Report 62, Air Force Contract AF 19(604)-1296.
9. J. E. Nanevicz and E. F. Vance, Stanford Research Institute, "Studies of Supersonic Vehicle Electrification," 1970, Lightning and Static Electricity Conference, Air Force Avionics Laboratory, Wright-Patterson AFB, Ohio.
10. J. E. Nanevicz, SRI International, "Flight-Test Studies of Static Electrification on a Supersonic Aircraft," 1975 Conference on Lightning and Static Electricity at Culham Laboratory, England, The Royal Aeronautical Society, England.
11. J. E. Nanevicz and R. L. Tanner, "Some Techniques for the Elimination of Corona Discharge Noise in Aircraft Antennas," Proc. IEEE, Vol. 52, January 1964.
12. J. E. Nanevicz, "Results of Titan III Flight Electrostatic Experiments," 1972, Lightning and Static Electricity Conference Papers, 12-15 December 1972, Las Vegas, Nevada, AFAL, AFSC, WPAFB, Ohio, AFAL-TR-72-325.
13. J. E. Nanevicz, D. G. Douglas, S. Blair Poteate, B. J. Solak, Stanford Research Institute, "Experimental Investigation of Problems Associated with Discharging Hovering Helicopters," 1972, Lightning and Static Electricity Conference, Air Force Avionics Laboratory, Wright-Patterson AFB, Ohio, AFAL-TR-72-325.
14. J. E. Nanevicz and D. G. Douglas, SRI International, "Supporting Laboratory Studies for the Development of Rotor-Blade Treatments to Minimize Electrostatically Generated Noise on the HLH Helicopter," 1974, Final Report SRI Project 2868, Contract DAAJ01-71-C-0840, p40.
15. Reference Data for Engineers, Fourth Edition, International Telephone and Telegraph Corporation, New York, 1956.
16. J. M. Seibert, U.S. Army Transportation Research Command, "Helicopter Static Electricity Measurements," 1962, Interim Report.
17. S. Baron, U.S. Army, "Measurement Program to Determine Static Electricity Charging Currents in Helicopter Main Rotor Blades," 1964, Technical Report 64-14, Contract DA 44-177-TC-844.
18. D. G. Douglas, J. E. Nanevicz, and B. J. Solak, SRI International, "Passive Potential Equilization Between the Cargo Handler and a Hovering Helicopter," 1975 Conference on Lightning and Static Electricity at Culham Laboratory, England, The Royal Aeronautical Society, England.
19. C. F. Dalziel, "A Study of the Hazards of Impulse Currents," Proc. AIEE, October 1953, pp. 1037-1043.
20. C. F. Dalziel and W. R. Lee, "Lethal Electric Current," IEEE Spectrum, February 1969, pp. 44-50.
21. J. E. Nanevicz, E. F. Vance, R. L. Tanner, and G. R. Hilbers, Stanford Research Institute, "Development and Testing of Techniques for Precipitation Static Interference Reduction," 1962, Final Report, Air Force Contract AF 33(616)-6561.
22. J. E. Nanevicz, E. F. Vance, W. C. Wadsworth, and J. A. Martin, Stanford Research Institute, "Low Altitude Long-Range All-Weather Vehicle Interference Investigation; Part I: Laboratory Studies," (1965) AFAL-TR-65-239, Part I, Contract AF 33(615)-1934, SRI Project 5082.
23. R. E. Wittman, Air Force Materials Laboratory, "A Review of Air Force Experience with Static Electricity Problems on Aircraft Windshields," 1972, Lightning and Static Electricity Conference, Air Force Avionics Laboratory, Wright-Patterson AFB, Ohio, AFAL-TR-72-325.

24. M. M. Newman, J. D. Robb, and J. R. Stahmann, Lightning and Transients Research Institute, "Windshield Static Electrification Problems--Commercial Aircraft Experience and Protection," 1972, Lightning and Static Electricity Conference, Avionics Laboratory, Wright-Patterson AFB, Ohio, AFAL-TR-72-325.
26. R. O. Brick, The Boeing Company, Commercial Airplane Group, "Windshield Related Electrostatic Problems--Electrification Studies on the 747," 1972, Lightning and Static Electricity Conference, Air Force Avionics Laboratory, Wright-Patterson AFB, Ohio, AFAL-TR-72-325.
27. K. A. Moore, "Precipitation Static Noise Problems on Operational Aircraft," 1969, Lightning and Static Electricity Conference, 3-5 December 1968, Technical Report, Air Force Avionics Laboratory, Wright-Patterson AFB, Ohio AFAL-TR-68-290, Part II.
28. J. E. Nanevicz, SRI International, "Advanced Materials Aspects and Concepts for Development of Antistatic Coatings for Aircraft Transparencies," 1973, Final Report, Contract F33615-72-C-2113, SRI Project 2393.
29. J. Taillet, "Methods for Reducing Electrostatic Hazards in Space Launchers," Lightning and Static Electricity Conference, Culham Laboratory, England, 14-17 April 1975, The Royal Astronautical Society, England.

ALLEVIATION TECHNIQUES FOR EFFECTS OF STATIC CHARGING ON AVIONICS

J. E. Nanevich

Associate Director, Electromagnetic Sciences Laboratory
SRI International
333 Ravenswood Avenue
Menlo Park, California 94025

LIST OF SYMBOLS

- \underline{E}_1 = electric field that would be produced in region T_2 by the application of a Voltage (V_1) to the antenna terminals
- I_z = short-circuit antenna noise current
- \underline{J}_2 = current density in region T_2 produced by motion of noise-producing charge
- T_2 = spatial region of interest in which \underline{J}_2 is non-zero
- V_1 = voltage applied to antenna terminals to produce field \underline{E}_1 .
- \underline{x} = three-dimensional field--or current--vector

ABSTRACT

It is productive to consider electromagnetic problems in terms of the source, the coupling process, and the victim system. Elimination of precipitation static can also be considered in these terms.

Since the radio interference of concern stems from noise-producing discharges resulting from aircraft charging, it is tempting to try to eliminate the source of the problem by eliminating the aircraft charging itself. Unfortunately, it has not been possible to devise workable schemes to eliminate the charging.

Accordingly, noise reduction schemes intended to eliminate the source are confined to the elimination of surface streamer discharges on electrically-insulating frontal surfaces by coating the surfaces with electrically-conductive material. This procedure allows the charging current to flow off the surface as rapidly as it arrives without generating noise.

Another technique for eliminating surface-streamer noise at the source is simply to relocate insulating materials (i.e., antenna-insulating materials) to regions at the aft of the aircraft where they will not be charged by impinging precipitation particles or to install particle deflectors upstream of the dielectric surface.

Successful techniques for the control of corona discharge noise involve forcing the discharge to occur from special discharging devices installed at high field regions on the aircraft where corona discharges are likely to occur naturally. The dischargers are designed to reduce the corona source intensity and to decouple the discharge source from the airframe. Practical dischargers are capable of reducing corona discharge noise by as much as 60 dB.

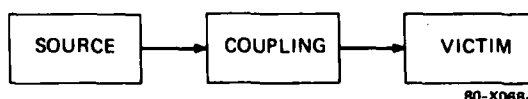
Noise generated by sparking between sections of the metal structure can be eliminated by electrical bonding of all portions of the structure.

Descriptions of techniques demonstrated by laboratory and flight tests to be successful in controlling precipitation-charging interference are given below.

I INTRODUCTION

As was indicated in the previous paper, static charging of aircraft in flight results in electrical discharge processes which can have deleterious effects on avionic systems. When operational problems developed from the effects of static charging, various programs were conducted to identify the responsible mechanisms and to develop alleviation techniques.

The alleviation problem can be approached by a consideration of the generic manner in which electromagnetic interference is generated and coupled into electronic systems. Figure 1, reproduced here from the previous paper, indicates that the problem may be considered in three separate stages: a source of interference exists on the aircraft and excites the various coupling paths which transfer the interference to the victim system.



80-X068-1

FIGURE 1 GENERATION AND COUPLING OF ELECTROMAGNETIC INTERFERENCE

Conceptually, the alleviation process can be applied at any one or all of these stages. One can concentrate on the elimination of the noise source, minimizing the coupling between the sources and the victim, or rendering the victim system inherently immune to interference. In the case of static charging effects, the approaches to alleviation techniques have included each of these basic areas.

II ATTEMPTS TO ELIMINATE CHARGING

As soon as it became evident that "precipitation static" was caused by frictional charging of the aircraft or parts of the aircraft, the possibility of devising coatings to eliminate the charging or at least to reduce its magnitude to acceptable levels arose. The possibility was pursued to a substantial extent in the work reported by Gunn.¹ Unfortunately, the charge separation occurring when two bodies are brought into contact and then separated depends upon the properties of the contacting surfaces and not upon the underlying bulk materials. Thus it was found that a coating which reduced charging substantially when it was first applied to an aircraft had its desirable properties destroyed when the leading edges of the wings were wiped down with a cloth having traces of oil. Also, it was found that the static charging properties of ice varied substantially with temperature so that a coating which might be satisfactory at one temperature would be ineffective at another temperature. A further consideration for not pursuing charging-control coatings is that they would have no effect on engine charging. Thus even if a successful coating could be developed, other alleviation techniques would have to be developed for engine charging. In light of these difficulties, it was decided that it would be most fruitful to pursue alleviation techniques which did not depend on controlling the charging process.

In subsequent programs, measurements have been made of important charging parameters such as the charge transferred to the aircraft by an individual precipitation particle, the total charging current to an aircraft as a function of cloud type, the way in which charging current varies with aircraft size, and the location of current discharge from an aircraft. These measurements were all directed at quantifying the noise problem and understanding the discharge processes involved, and not at attempting to control the charging.

III ALLEVIATION OF PROBLEMS STEMMING FROM CHARGING OF THE WHOLE AIRCRAFT

As was indicated in the previous section, it is not possible to eliminate the aircraft charging which leads to the corona discharges responsible for most of the precipitation static interference. Thus, it is not possible to completely eliminate the corona "source" in Figure 1. Successful attempts to alleviate the effects of corona discharge have focussed on controlling the nature of the corona discharge to reduce the source strength and/or devising ways to minimize the coupling between the source and the victim. Indeed, the most successful techniques employ both approaches.

A. Passive Discharging

The properties of the static electric fields around an electrically-conducting body are such that the highest fields will occur at the extremities--the airfoil tips on a conventional aircraft. Thus, corona discharges will occur from the regions of the airfoil tips under conditions of precipitation charging. Figure 2 shows the results of laboratory measurements of aircraft voltage needed to induce corona from different parts of the wing. The lower curve shows that a discharge at the tip can be initiated with roughly half the voltage required to initiate corona from a point 50 in. inboard of the wing tip.

The fact that corona discharges tend to occur in a few well-localized regions on the aircraft indicated that it should be possible to force all of the discharge current normally experienced in flight to leave via specially-designed dischargers installed in these same regions. If the dischargers were designed to control source intensity and noise coupling, a substantial corona noise reduction could be achieved.

The upper curve in Figure 2 indicates that the space charge generated by corona from a discharger installed along an airfoil trailing edge has the effect of shielding the region in its vicinity and making the trailing edge less prone to corona discharge. Thus, only a limited number of dischargers would need to be installed along the trailing edge to handle all of the charging current to the aircraft.

The development of a highly-successful discharger for use on jet aircraft proceeded generally as follows: The problem of corona noise generation and its coupling into antenna systems was considered in light of a reciprocity theorem which may be derived in much the same manner as the familiar Lorentz reciprocity theorem.²⁻⁵ For the conditions outlined in Figure 3, the coupling theorem states that

$$I_2(\omega) = \frac{1}{V_1(\omega)} \int_{T_2} \underline{E}_1(\underline{x}, \omega) \cdot \underline{J}_2(\underline{x}, \omega) dV \quad (1)$$

Eq. (1) may be interpreted as follows: if the space and time distribution of the current density, \underline{J}_2 , produced by the disturbance are known, and if the field \underline{E}_1 in the region T_2 produced by a voltage V_1 applied to the antenna terminals can be determined, then it is possible to compute the short-circuit current induced in the antenna terminals. (Essentially the coupling theorem states that the noise current generated in a receiving antenna by a discharge is proportional to the RF field that would exist at the location of the discharge if the same antenna were used for transmitting).

In applying the coupling theorem to the problem of discharging an aircraft, we may consider \underline{J}_2 to be the discharge current. The coupling theorem then suggests several ways in which the noise content of the antenna current I_2 can be reduced or eliminated:

1. By letting the noise content of \underline{J}_2 approach zero
2. By letting the ratio $\frac{\underline{E}_1}{V_1}$ approach zero (reducing the coupling)
3. By letting \underline{J}_2 be perpendicular to \underline{E}_1 (reducing the coupling).

It should be noted that, perversely, the regions of high dc field, such as the airfoil extremities where the corona discharges occur and where the dischargers must be located, also correspond to regions of high RF coupling fields. For example, consider the field in a small region about the trailing edge of a wing Figure 4 (a). It is evident that the field configuration, either RF or static, is determined by the shape of the conductor forming the field boundary. To develop a decoupled discharger, therefore, it is necessary to devise a scheme for causing a difference between the two fields. In particular, we would like to have a high dc field imposed upon the discharge point and at the same time to have the RF field at the point equal to zero.

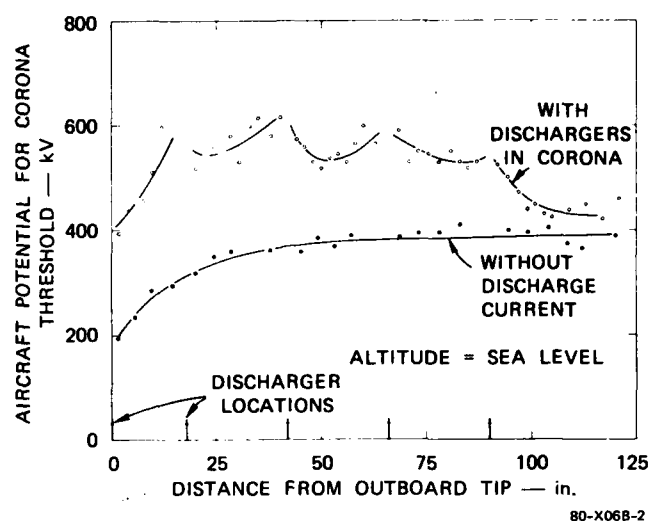
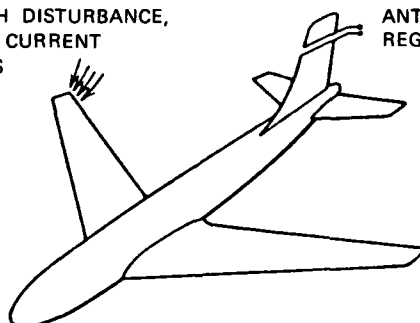


FIGURE 2 THRESHOLD POTENTIALS OF POINTS ALONG TRAILING EDGE OF WING ON KC-135

REGION T_2 IN WHICH DISTURBANCE, CHARACTERIZED BY CURRENT DENSITY J_2 , OCCURS

ANTENNA TERMINALS REGION T_1



$$I_2 = \frac{1}{V_1} \int_{T_2} E_1 \cdot J_2 dv$$

SITUATION 1:

VOLTAGE V_1 IS APPLIED TO TERMINALS T_1 PRODUCING FIELD E_1 AT ALL POINTS OF SPACE AND IN PARTICULAR IN THE REGION T_2 .

SITUATION 2:

DISTURBANCE OCCURS IN THE REGION T_2 . CURRENT DENSITY J_2 IS THEREFORE FINITE IN T_2 . IN RESPONSE TO THE DISCHARGE A CURRENT I_2 FLOWS IN THE SHORT-CIRCUITED ANTENNA TERMINALS T_1 .

80-X06B-3

FIGURE 3 ILLUSTRATION OF NOISE-COUPING THEOREM

How this was done in the case of the flush-mounted, decoupled discharger is evident from Figure 4 (b), which shows a cross-section of the trailing edge of an airfoil surface in which the rearmost portion is electrically isolated from the remainder of the surface. It is evident that there are two lines along the conductor on which the field is zero, and a considerable region over which the field is very small. If a discharge could be made to occur at the point of zero field, it would be coupled into the receiving system. In order for a discharge to occur at the point of zero field, however, the isolated section must be maintained at the same dc potential as the remainder of the aircraft. The requirements that the trailing edge be isolated at RF and directly connected at dc can be very closely approximated by connecting the trailing edge to the airframe through a very high resistance. If the value of the connecting resistance is high compared to the capacitive reactance between the isolated trailing edge and the remainder of the airfoil, the RF field will remain essentially as depicted in Figure 4(b), while the dc field in the immediate vicinity of the trailing edge will be of the form indicated in Figure 4(c), which differs only slightly from that illustrated in Figure 4(a). Fortunately, the dc current through the connecting resistance is small, so that the voltage drop is not significant except at very high discharging rates.

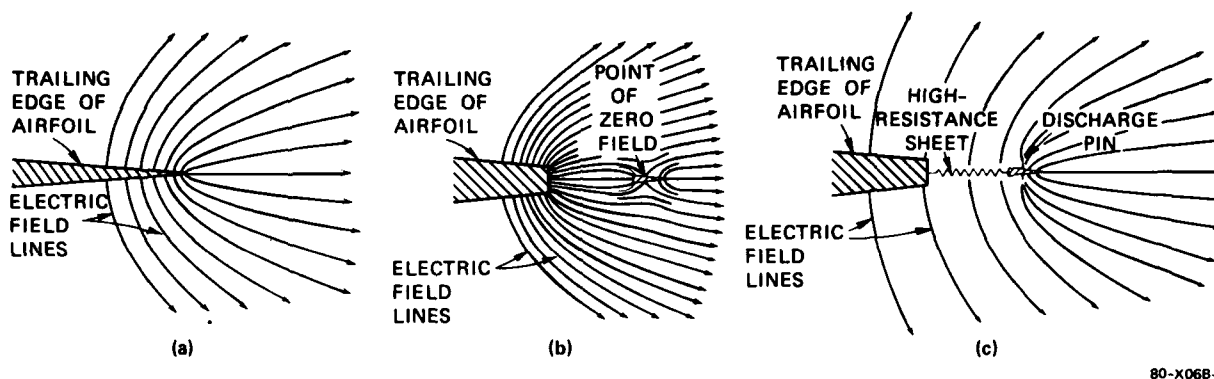


FIGURE 4 ILLUSTRATING DECOUPLED DISCHARGER EVOLUTION

A practical flush-mounted discharger (employed in a series of flight tests in 1957-59 on the Boeing 707 prototype^{2,6}) embodying the techniques just discussed is illustrated in Figure 5. Observe that the discharge is forced to occur in the region of minimum reciprocal field due to installation of low-threshold needles in this region. Since the discharge occurs from the points of the needles, the discharge current flows at approximately right angles to the reciprocal field lines. The discharge is thus orthogonally decoupled as well as being decoupled by virtue of the minimum in the reciprocal field. Finally, if very sharp points are used, the amplitudes of the individual current pulses are small, yielding a reduced noise content in the discharge current. In the practical design then, all three of the noise-reduction methods are employed, although the majority of the noise reduction results from the decoupling techniques.

Although tests of the flush dischargers were encouraging, it was found that they had a rather high corona threshold potential. Furthermore, because it is an integral part of the airfoil trailing edge, the flush-mounted discharger is rather expensive to install on a retrofit basis. Consequently, another design was considered—particularly for retrofit installations.

Production versions of the retrofit decoupled dischargers that were finally developed are shown in Figure 6. Although two physically different dischargers are shown, they are identical in principal and differ only in that Type A (shown in the lower part of the figure) is designed to mount at the trailing edges of airfoils parallel to the windstream, while Type B (shown in the upper part of the figure) is designed to mount on the outboard tips of airfoils at right angles to the airstream. Essentially, the discharger consists of a rod of high-resistance material with a tungsten discharge point located at the point of minimum coupling near the end of the rod. The aft end of the rod is hemispherically rounded and coated with a dielectric to prevent corona from occurring at the tip where the coupling is relatively high. The rod fits into a metallic socket on the mounting base which protrudes aft of the trailing edge and serves as a lightning diverter, thus tending to protect the trailing edge from direct lightning strikes.

Type-B dischargers are required on the outboard portions of the airfoils, the vortices generated in these regions produce localized pressure reductions which reduce the corona threshold sufficiently so that discharges can occur from sections of relatively large radius. The type-B dischargers produce a column of space charge along the wing tip which reduces the dc field in this region and prevents discharges from the wing tip itself.

B. Active Discharging of Conventional Aircraft

Although passive techniques described above have been developed to discharge current from an aircraft without coupling appreciable interference into the receiving system, these dischargers require appreciable airplane potential to discharge the required current (for example, 130 kV to discharge 1 mA from a KC-135). In many applications it is important that the airplane potential be essentially zero. It is necessary, for example, to minimize VTOL aircraft potentials to prevent personnel hazards and to ensure safe handling of flammable or explosive cargo. On other large jet aircraft, mission requirements often necessitate the installation of devices that protrude beyond the mold lines of the aircraft and that have low corona threshold. Unless the design of the protruding device is such that it can support a passive discharger, corona noise will be generated if the aircraft potential is not maintained below the corona-threshold

Because of its relatively simple geometry, the theoretical decoupling of the Type-A discharger can be calculated.^{2,6} For rods such as those illustrated in the lower part of Figure 6, with a total rod resistance of 20 M ohm the calculation indicated that the noise at a frequency of 500 kHz should be reduced by 55.6 dB (the noise reduction increases 20 dB per octave with increasing frequency). The noise reduction afforded by the dischargers as determined from flight test data obtained on the instrumented Boeing 707 prototype was at least 50 dB. Laboratory measurements indicate that 60-dB noise reductions are obtainable in practice.

Other discharger configurations were conceived, and their performance was predicted in light of the coupling theorem of Eq. (1). The results of laboratory measurements to verify the analyses are shown in Figure 7. It is evident from the figure that the An/ASA-3 relies both on control of the amplitude of the corona pulses and on the provision of decoupling and is a highly-successful design. Unfortunately, the wick cannot survive the aerodynamic environment typical of jet aircraft.

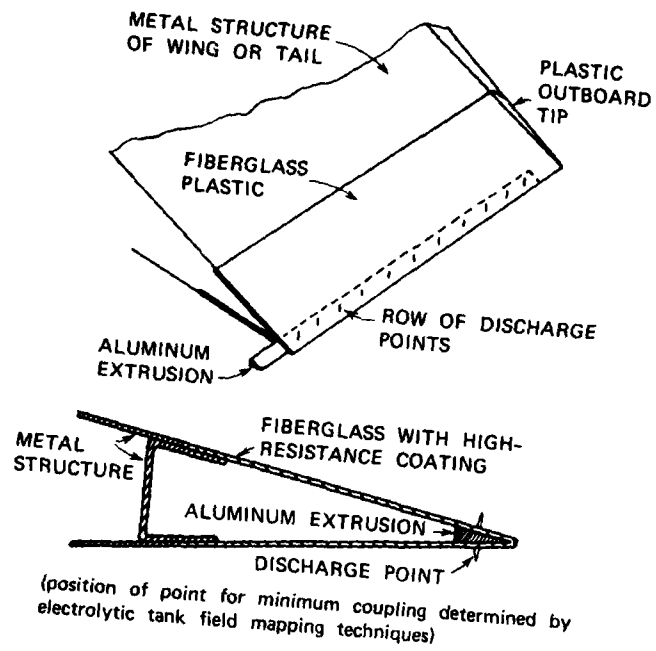


FIGURE 5 CONSTRUCTION OF FLUSH-MOUNTED DECOUPLED DISCHARGER

80-X068-5

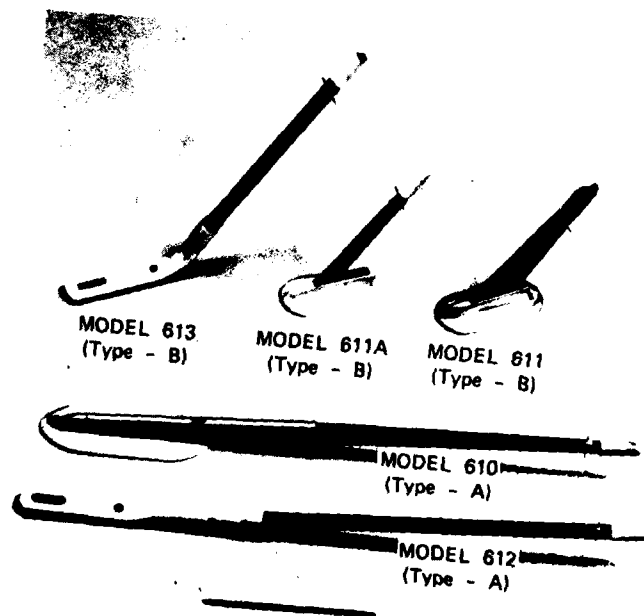
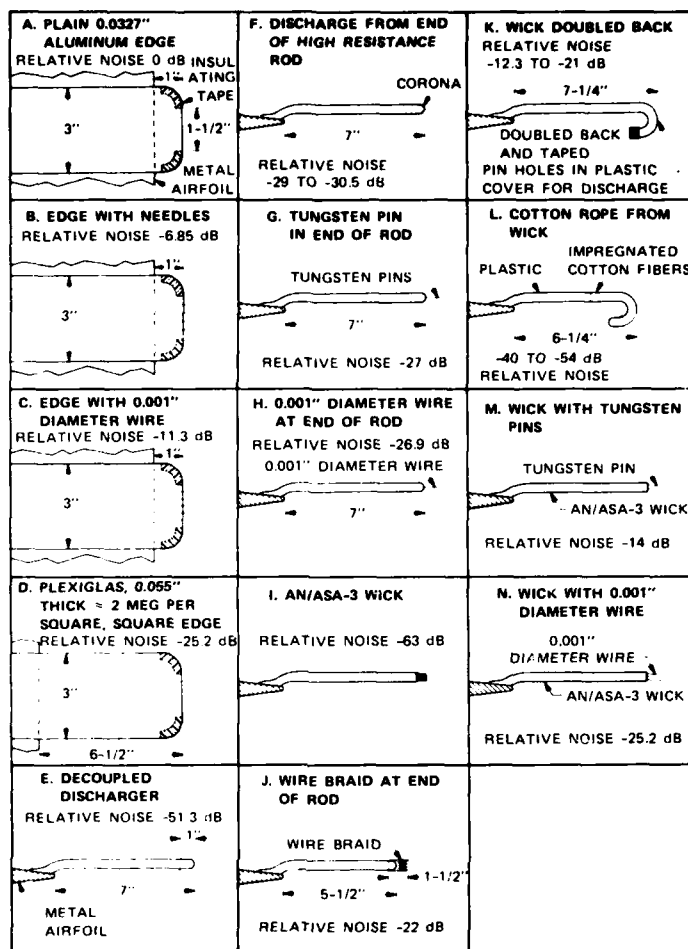


FIGURE 6 PRODUCTION MODELS OF TYPE - A AND TYPE - B ORTHO-DECOUPLED DISCHARGERS

80-X068-6

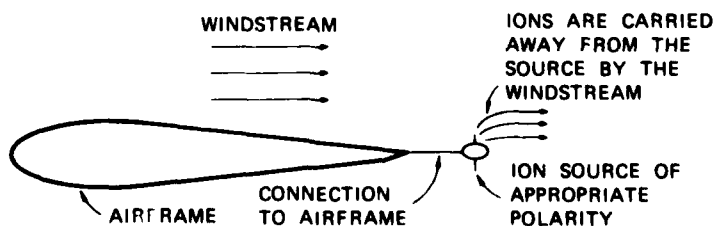


80-X068-7

FIGURE 7 RESULTS OF MEASUREMENTS OF NOISE GENERATED WHEN A GIVEN CURRENT IS DISCHARGED FROM A PROPOSED DISCHARGER. Noise levels are expressed relative to the noise generated when the same current is discharged from the edge of a 0.0327-in.-thick aluminum sheet simulating the trailing edge of an airfoil.

of the protruding device. Another situation in which it would be desirable to control aircraft potential occurs during airborne refueling operations when one would like to reduce the potential difference between the two aircraft involved, to minimize the possible hazards of fuel ignition. In order to maintain the aircraft potential at some arbitrary value (including zero), an active, or dynamic, discharger system is required.

Such a system was developed for the Air Force and evaluated in flight tests on a Boeing 707 aircraft.^{7,8} Essentially, the system consists of an ion source that injects ions of the appropriate sign into the windstream about the aircraft, as is indicated schematically in Figure 8. If the aircraft were stationary, these ions would be recirculated back to the airframe. In flight, however, the windstream carries the injected ions away from the aircraft in much the same way as the belt of a Van de Graff generator transports charge. At aircraft operating altitudes, ion mobility is very low, so that the windstream is able to overcome high electric fields in moving ions away from the aircraft. In the system tested, a corona discharge was used as the ion source.



80-X068-8

FIGURE 8 ILLUSTRATION OF ACTIVE DISCHARGER FUNCTIONING

It is convenient to break down the active-discharger system tested into four subsystems: a set of corona points exposed to the windstream and serving as the ion source, a high-voltage power supply to excite the corona points, a controller to maintain the proper power-supply voltage and discharge current, and a sensor to detect the aircraft potential and provide an error signal to the controller. This breakdown of subsystems is shown in block form in Figure 9. The airplane is represented by its free-space capacitance, C_a , charged to potential V_a . The electric field sensed by the field-meter sensor located on the skin of the airplane is proportional to the airplane potential. The controller servo-system uses the field-meter signal as an input and adjusts the high-voltage unit in such a way as to minimize the airplane voltage.

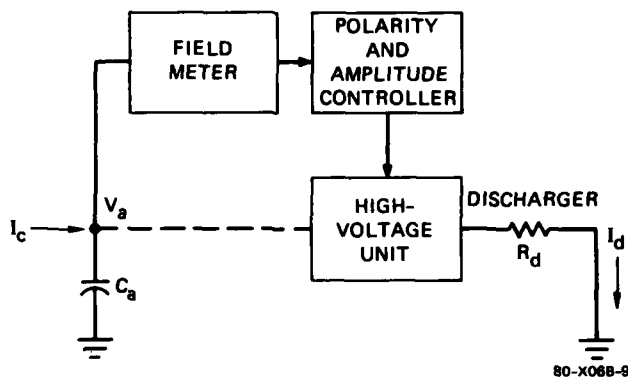


FIGURE 9 BLOCK DIAGRAM OF CONTROL SYSTEM

Various practical considerations dictated the final physical and electrical form of the individual parts of the system. For example, consideration of space charge limitation of the current that can be discharged from an airplane dictated that the entire stationary wing trailing edge region outboard of the flaps on both wings would be required to discharge the requisite currents. This in turn meant that one could not use one power supply and discharging element for negative polarity and a second such combination for positive polarity. Instead, it was necessary to use the same discharging element for either polarity. The foregoing arguments dictated the development of a variable, reversible high-voltage power supply. It is not possible to use two unipolar high-voltage supplies back to back to obtain the range $-V$ to 0 to $+V$, since the rectifiers in these supplies are back to back, thus preventing dc current flow.

Previous flight-test experience indicated that voltages in excess of 60 kV would probably not be practical in a high-altitude airborne system. Thus the power supply was designed to have an output voltage range of -60 to 0 to $+60$ kV. To permit the dynamic discharger system to be used on aircraft larger than the KC-135, on which the charging current will be higher, the power-supply system was designed to permit 10 mA to be supplied continuously.

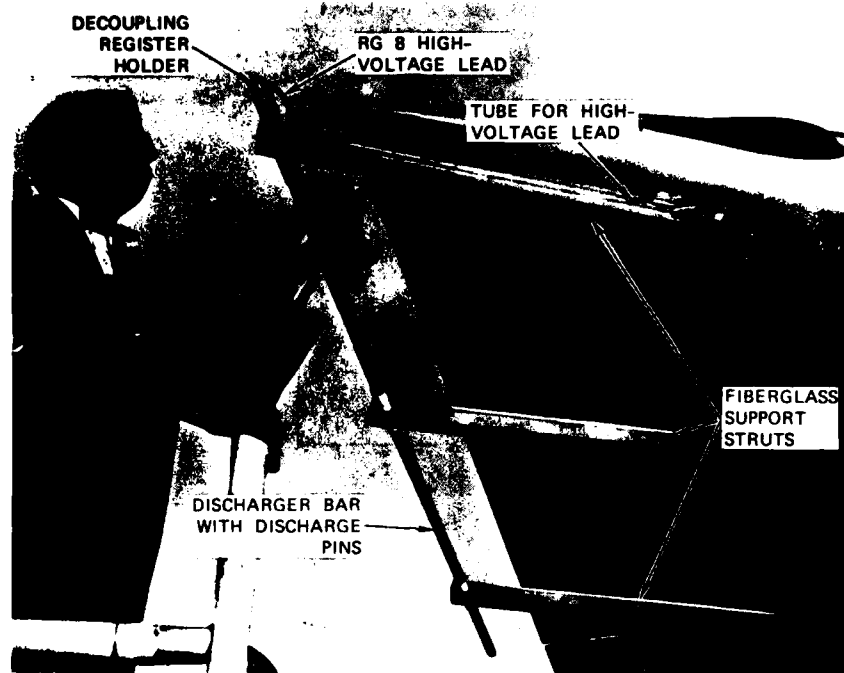
Since two discharging elements (located on opposite wingtips) must be used on each aircraft, it was necessary either to run high-voltage leads from a common power supply or to provide a separate power supply for each discharging element. The latter approach was taken and two power supplies, one mounted on each wing tip, were employed in the active discharger system tested.

A photograph of the final system installed on the test aircraft is shown in Figure 10. The discharging element is shown installed behind the trailing edge of the wing. (The discharging element actually used the flush-mounted decoupled discharger of Figure 5). The power supply for each wing was housed at the tip of the wing and covered by the normal wing cap. The electric field meter sensor used to measure aircraft potential was mounted in the belly of the aircraft just aft of the wheel well.

Functioning of the active discharger under precipitation charging conditions is illustrated in the record of Figure 11. At the beginning of the record, the system was operated with manual control of the power-supply voltages as is indicated by the bottom trace. The power-supply voltage was roughly -20 kV, and the airplane voltage was -60 kV.

At the time indicated by the step in the lower trace, the operating mode was changed to place the power supply in each wing under automatic control. This switching generated the short transient at this time. The transient was accompanied by current discharged from the instrumented passive discharger at the top of the fin. It should be noted that the transient was completely settled in roughly 1 s, at which time the total discharging current was roughly $800 \mu\text{A}$. After this time the airplane voltage remained essentially at zero. At $T = 06:48:37.4$ the precipitation conditions changed so that the charging current decreased, causing both the power-supply voltages and power-supply currents to gradually decrease between $T = 06:48:38$ and $06:48:41$. In this time interval, the supply voltages and supply currents varied in a random manner in agreement with the charging current to the airplane, and the airplane potential remained constant at zero. At $T = 06:48:41$, both power supplies were turned off, permitting the airplane voltage to rise to a value of 130 kV, at which time the primaries to both supplies were turned on again, generating a transient that persisted for roughly 1½ s. The airplane potential remained at zero until, at $T = 06:48:45.5$, the power-supply primaries were again switched off to produce still a third transient. In conclusion, the data of Figure 11 indicated: (1) that the system is capable of maintaining essentially zero airplane potential with individual power-supply currents as high as $400 \mu\text{A}$ (total discharge current = $800 \mu\text{A}$), (2) that it is able to follow variations in charging current, and (3) that its stability under conditions of precipitation charging is very good.

Tests in higher charging conditions indicated that the active discharger system was capable of meeting the design goal of discharging maximum experienced charging rates while maintaining aircraft potential below the threshold voltage of any part of the aircraft structure.



80-X068-10

FIGURE 10 ACTIVE DISCHARGER INSTALLATION ON RIGHT WING TIP OF 707 TEST AIRCRAFT

In general, the use of an active system on large aircraft is attractive because of the large number of passive dischargers required to properly handle the high charging current to these aircraft. Although one might suppose that using an active-discharge system on a fighter-type aircraft is extremely impractical these aircraft often pose problems that offer almost no other alternative. For example, prominent pitot tubes and the external stores commonly found on fighters have such low corona thresholds that functioning of passive-discharge installations is severely compromised. Thus a simple, lightweight active-discharger system could find application on fighter aircraft.

Since one of the applications envisioned for the system was to eliminate the voltage difference between aircraft during refueling operations, it could be desirable to test the system's ability to accomplish this objective. To carry out this test, it would be necessary to fabricate a special, compact field-meter sensor head to mount on the refueling boom of the test aircraft to permit the potential difference between the two aircraft to be sensed.

C. Helicopter Dischargers

The shock hazard to ground cargo-handling personnel motivated efforts to develop active discharging systems to control helicopter potential. It was recognized that two major problem areas needed to be addressed before a satisfactory helicopter discharge system could be developed. The first was a means to discharge the required current without having it recirculate back to the helicopter. (There is no net high-velocity air flow around the hovering helicopter to carry charge away from its vicinity). The second was the development of a satisfactory scheme to sense the potential difference between the helicopter and ground without providing a ground contact.

A system involving discharge electrodes immersed in the engine exhaust was demonstrated to be capable of carrying away the requisite current. Experiments in which charged aerosol drops were used to carry away charge with minimum recirculation also showed promise.

Unfortunately, flight tests performed with helicopters hovering in a dusty environment demonstrated that the charge on the dust cloud produced intense electric fields in its vicinity and that helicopter potential sensing would not be possible without making contact with the ground. This result led to the idea that the use of passive techniques and a study of their limitations should be pursued. The passive discharging method, a technique whereby the helicopter is earthed through ground contact with a wire or conductive rope, is very attractive because of its simplicity, low cost, and ease of use. However, it was believed, largely as the result of low-voltage measurements of desert soil conductivities, that few soil materials could be relied upon to provide a sufficiently low grounding resistance to adequately discharge a large helicopter. In order to determine the grounding resistance achievable with various materials, a series of high-voltage contact-resistance measurements were made. The measurements, performed by connecting a high-voltage power supply through a microammeter to a ground stake at one end and a contact element at the other, were made on arid desert surfaces such as sand, rock, concrete, and macadam after a 159-day drought. The measurements showed a surprising characteristic: the resistance decreased nonlinearly as the applied voltage increased as shown in Figure 12. This nonlinear behavior was apparently due to the electrical breakdown of insulating films on the materials, and the low resistances (for even moderate voltages) indicated that the passive discharging technique could be used successfully.

In order to demonstrate the usefulness of this technique under a wide variety of conditions, several different types of grounding apparatus were tested over various surfaces using a hovering instrumented helicopter illustrated in Figure 13. Table I shows the results of tests performed over various "clean" surfaces where the charging current would not be

expected to be very great. (Charging for this series of tests was provided by the 0-to-200-kV power supply carried in the helicopter.) It can be seen from this table that the residual helicopter potential, after contact, was quite low.

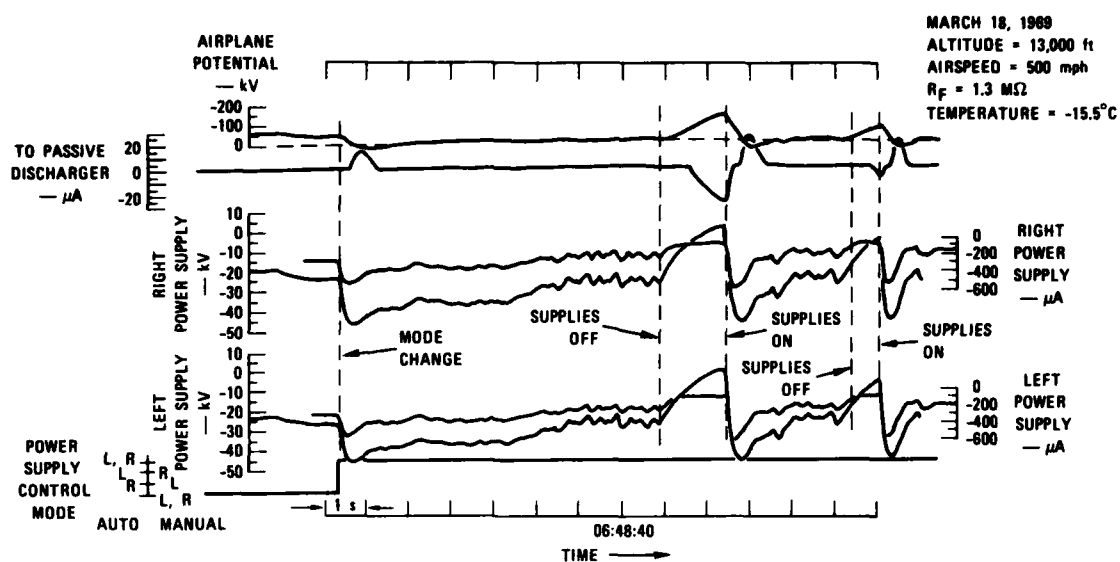


FIGURE 11 ACTIVE DISCHARGER OPERATION UNDER MODERATE PRECIPITATION CHARGING CONDITIONS

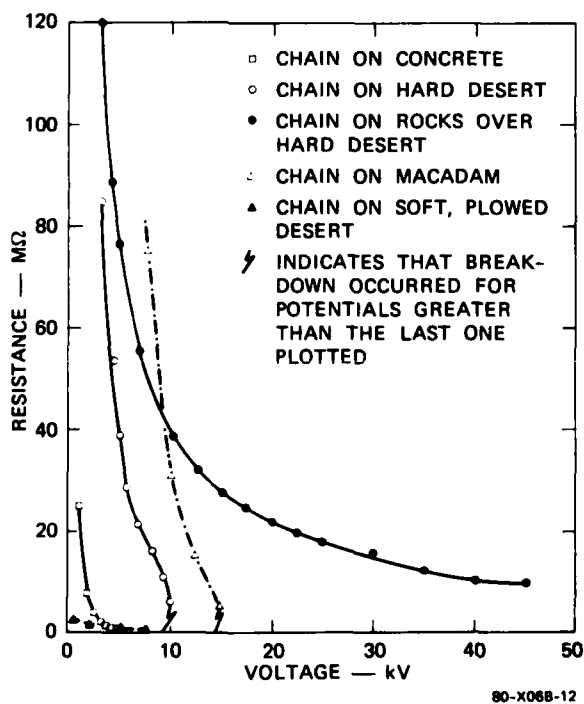


FIGURE 12 RESISTANCE AS A FUNCTION OF VOLTAGE FOR VARIOUS GROUND SURFACE MATERIALS

Table 1

EFFECTS OF VARIOUS SURFACES AND SURFACE CONDITIONS ON
GROUNDING-ELEMENT PERFORMANCE

Surface Material	Initial Aircraft Potential (kV)	Dry Surface			Wet Surface		
		I_{ps} (μA)	I_{hook} (μA)	$V_{residual}$ (kV)	I_{ps} (μA)	I_{hook} (kV)	$V_{residual}$ (μA)
Macadam (asphalt) 100	50	150	125	9	160	155	0
	300	265	15	325	315	0	
	150	500	430	17	525	500	0
Hard desert	50	180	170	0	160	135	0
	100	325	315	0	350	335	0
	150	500	500	0	500	500	0
Concrete	50	150	140	5	160	155	0
	100	325	300	7	350	325	0
	150	500	485	8	525	500	0

In another similar test, the aircraft was flown into an area of freshly disked sand and various discharging elements were dropped to the ground to test their effectiveness in discharging the helicopter. (For these tests, the internal power-supply voltage was disconnected, and charging occurred entirely as the result of frictional electrification by the impinging dust particles). The passive discharging technique was again demonstrated to be successful, as shown in Table 2. It is appropriate to point out that only desert soil materials were available for these tests. The "wet" surfaces of Table 1 were obtained by pouring gallons of water over the otherwise dry surfaces. Although the arid surfaces provided a severe test of the passive discharge technique, the results of these tests should not be interpreted as representative of all surface materials. It is possible that some other surfaces, such as dry snow, might not demonstrate the same behavior as the desert materials.

The "before-and-after grounding" potentials and currents reported in Table 2 were measured by a large, toroidal parallel-plate, infinite-impedance voltmeter/ammeter carried aloft in the helicopter during these tests, and connected to earth by a long piece of cable designed to withstand voltages in excess of 200 kV. The voltmeter, illustrated in Figure 13, consisted of a field meter mounted in one of a pair of parallel conducting plates (the lower one was connected to the airframe). A voltage applied to the upper plate generated a static electric field between the two plates which was measured by the field meter. The voltmeter was calibrated with a 0-to-200-kV power supply and periodically checked for leakage current and to ensure that it was indeed, "infinite" impedance.

Table 2

SUMMARY OF NATURAL TRIBOELECTRIC-ENVIRONMENT GROUNDING
MEASUREMENTS

(Discharging Element Dropped into Dry, Plowed Desert)

Grounding-Line "System"	I_{chg} (μA)	I_{hook} (μA)	V_{acft} (kV)	V_{resid} (kV)
14-M resistor, light chain, A/C discharger	90	79	55	1.1
14-M resistor, heavy chain, corona brush	76	31	70	2.6
14-M resistor, spiked resistor, 10 inc.-dia. ball	135	125	85	4.8
Heavy chain, corona brush	133	128	78	0
Light chain, A/C discharger	110	106	67	0.2
Spiked resistor, 10-in.-dia. ball	150	140	98	1.5
Heavy chain	180	180	98	0.9

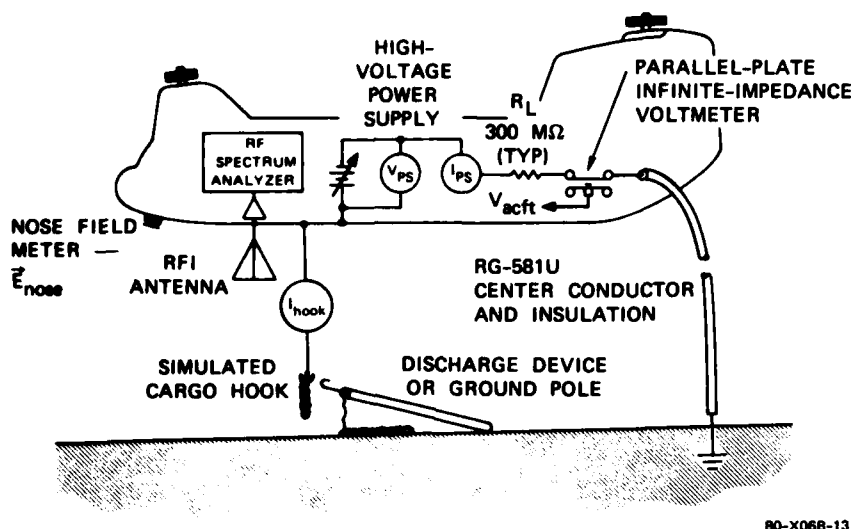


FIGURE 13 GENERAL AIRCRAFT CONFIGURATION USED DURING TESTS

IV ALLEVIATION OF PROBLEMS STEMMING FROM DIFFERENTIAL CHARGING OF PARTS OF THE AIRCRAFT

A. Preventing Charging

Although it is not possible to prevent charging of the vehicle as a whole, it is possible to locate critical areas such as dielectric covers over antennas in such a way that they will not be struck by precipitation particles in flight. For example, flush-mounted ADF sense antennas located in the belly of aircraft have proven to be free of streamer-discharge noise.

If a small area of dielectric is involved, as in the case of an insulator at the base of a blade antenna, it is often possible to provide a particle deflector ahead of the insulator.

B. Avoid the Use of Dielectric Frontal Surfaces

In some cases, a small region of dielectric on a frontal surface can generate and couple sufficient noise to completely disable a system. For example, a paper by the author¹⁴ describes a program in which an aircraft ADF system consistently malfunctioned under modest charging conditions. The problem was traced to an aerodynamic plug in the end of a "towel rail" antenna bar which had been fabricated of plastic instead of aluminum used in the development prototype. Charging of this 1-in.-dia. plug generated sufficient streamer noise in the antenna on which it was mounted to disable the ADF system. Replacing the plastic plug with a metal one cleared up the noise problem in this fleet of aircraft.

This example illustrates a problem frequently encountered in tracking down sources of malfunction similar to that described above. The designer of the antenna was questioned regarding the materials used in antenna fabrication. (The antenna design incorporated sophisticated features such as metal shields on the stand-off masts to prevent streamers). He indicated that all leading-edge surfaces were made of metal. However, it was not until the aerodynamic plug was exposed to charging by a directed stream of lycopodium powder that the change of material used in making the plug was discovered. Accordingly, it necessary for the troubleshooter to have available a means for simulating dielectric charging using either the lycopodium powder technique or the cleaner ion gun or bonding sensor techniques described by Dr. Taillet in the next paper.

C. Prevent the Accumulation of Charge on Dielectrics

When dielectrics must be used on frontal surfaces, it is possible to coat their outer surface with electrically-conducting material to drain away charge as rapidly as it arrives on the frontal surface. If the dielectric is only a structural member such as a wing leading edge, the conductivity of the coating can be as high as is convenient. Flame-sprayed coatings which apply a substantial thickness of metal have been used for these matters.

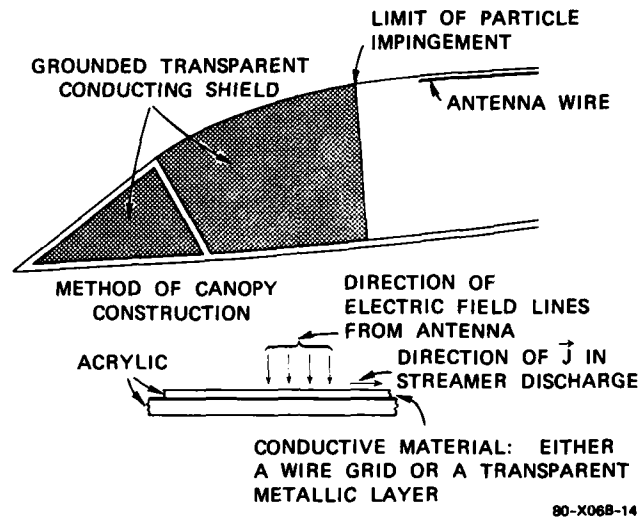
Other dielectric frontal surfaces such as radomes must be transparent to RF radiation, but their optical properties are unimportant. These surfaces can be coated with a layer of high-resistance conductive paint. Appropriate paints are usually made of a mixture of carbon black and graphite added to a paint vehicle such as lacquer or epoxy. Approximately 45% by weight of carbon material must be added to the paint vehicle to render it conductive. Analysis of the fields generated by current flow through the conductive layer¹⁵ indicates that surface resistivities as high as roughly 1000 MΩ/square are acceptable even under high precipitation-charging conditions. Thus, it is possible to provide static discharging without causing appreciable attenuation of the radar signal.

Optical surfaces such as windshields must also be located on frontal surfaces. These can be rendered conductive by coating them with a thin optically-transparent film of a material such as stannous oxide. Unfortunately these films are fragile and are abraded by the impinging precipitation particles. It has been found that the durability of the

conducting layer on a glass windshield can be improved substantially by baking the glass after the layer is applied. Unfortunately, polycarbonate windshields cannot be baked and so no satisfactory technique exists for controlling their charging.

D. Discharge Decoupling Technique

A dielectric treatment which should be effective in substantially reducing streamer noise is illustrated in Figure 14 for the case of an aircraft canopy. The forward region of the canopy where precipitation particle impingement occurs is treated by installing a grounded conducting sheet between the layers of acrylic radome material. The conducting sheet may be either a grid formed of thin wires or a deposited metal film such as those used for windshield defrosting.



80-X068-14

FIGURE 14 A POSSIBLE CANOPY TREATMENT TO REDUCE NOISE

Although the conducting shield shown in Figure 14 does not eliminate streamer discharges on the canopy surface, its presence forces the reciprocal field from the antenna to be normal to the canopy surface. (See the discussion in connection with Eq. 1 in Section III A.) Since the streamer current density is directed along the canopy surface, the discharge will couple no signal into the antenna. Actually it is too optimistic to expect that the coupling fields will be precisely orthogonal to the discharge current density at all points on the canopy surface, and, since streamering is an extremely energetic mechanism, some streamer noise should be expected in the antenna in spite of the shielding. From the results of the laboratory shielding experiments, however, it appears reasonable to assume that, through the use of a conducting shield, streamer noise can be reduced by as much as 26 dB.

E. Bonding

As was indicated in the previous paper, unbonded metal sections on an aircraft can result in extremely serious interference to systems. Unfortunately, it is also true that most of the troublesome instances of unbonded metal structure occurred inadvertently (broken lightning diverters, painted inspection panels, etc.), and were not evident even during a careful search by reasonably sophisticated personnel. They were finally pinpointed as the result of extremely careful observation and systematic measurement of the bonding resistance of suspected structures. In this regard, it appears that techniques such as the use of lycopodium power or the use of ions (discussed by Dr. Taillet in the next paper) offer a powerful tool for the location of unbonded metal structures.

V HARDENING OF VICTIM

A. Active Noise-Limiting Circuits

In general, the precipitation static interference from any of the noise mechanisms is caused by the occurrence of a succession of short discrete pulses. This feature of the interference motivated the search for techniques to sense the arrival of the noise pulse and to disable or blank the radio receiver for the duration of the pulse. Tests on a blander of relatively recent design indicate that noise reductions of up to 20 dB are achievable at a corona discharge level of 100 A with the corona occurring directly from the antenna.¹⁷ As the discharge current is increased to values typical of a 707 aircraft (1 MA or more), more pulse overlap will occur and it is to be expected that the blander will be less effective.

An analysis has been made of the effects of aircraft resonances on the wave shape arriving at an antenna removed from the noise source.¹⁸ This work indicates that the pulses will be stretched out in time by the aircraft resonances. Thus, there will be even more pulse overlap and the blander may be expected to be less effective than it is when the noise pulses are generated on the antenna itself. In general, it is concluded from the analysis that the blander will be most effective when used on small aircraft.

Since corona noise reductions of up to 60 dB can be obtained with passive dischargers, there has been little application of blankers to the control of precipitation static interference.

B. Shielding of Systems from Sources

In conventional, metal-skinned aircraft the skin provides substantial shielding of the electronics from the source. Accordingly, most effects of static charging were manifested on systems equipped with deliberate outside antennas such as communication and navigation receivers.

Occasionally, problems arose in systems not associated with deliberate antennas. An example is the damage experienced by windshield de-icer controllers from massive discharges on the windshield. Also, there have been instances in which the high currents on the de-icer circuitry coupled signals into nearby avionic system wiring.

As more plastic and composite materials are used on aircraft, care must be exercised that the reduced shielding resulting from the use of these materials is taken into account during the design of interconnecting wiring for the avionic systems.

VI CONCLUSIONS

The various mechanisms by which static charging of aircraft affects avionic systems have been identified, and techniques have been developed to mitigate the effects in most cases. Since the application of the alleviation techniques and their effectiveness depend on aircraft design, it is important that designers be aware of the effects that their new designs will have on the susceptibility of avionic systems to static charging.

For example, the application of passive dischargers to control corona noise required that the dischargers be installed at the aircraft extremities where corona discharges normally occur. If the aircraft design includes many protrusions, such as nose-mounted pitot tubes on which dischargers cannot be installed, the corona noise level on the aircraft cannot be controlled with passive dischargers. Similarly, the use of regions of dielectric on the surface of the aircraft increases the number of streamer noise sources on the vehicle.

Deviations from good static electric design sometimes cannot be avoided. In these cases the designer must be prepared to accept higher electromagnetic noise levels for his avionic systems, or he must incorporate specially-designed static control techniques.

REFERENCES

1. Ross Runn et al., "Army-Navy Precipitation Static Project," Proc. IRE, Vol. 34 (1946).
2. R. L. Tanner and J. E. Nanevicz, Stanford Research Institute, "Precipitation Charging and Corona-Generated Interference in Aircraft," Technical Report 73, Contract AF 19(604)-3458 (1961).
3. R. L. Tanner and J. E. Nanevicz, Stanford Research Institute, "An Analysis of Corona-Generated Interference in Aircraft," Proc. IEEE, Vol. 52 (January 1964).
4. J. E. Nanevicz and R. L. Tanner, Stanford Research Institute, "Some Techniques for the Elimination of Corona Discharge Noise in Aircraft Antennas," Proc. IEEE, Vol. 52 (January 1964).
5. R. L. Tanner, Stanford Research Institute, "Radio Interference From Corona Discharges," 1953, Technical Report 37, Contract AF 19(604)-266, SRI Project 591.
6. J. E. Nanevicz, E. F. Vance, R. L. Tanner, and G. R. Hilbers, Stanford Research Institute, "Development and Testing of Techniques for Precipitation Static Interference Reduction," 1962, Final Report, Contract AF 33(616)-6561.
7. J. E. Nanevicz et al., Stanford Research Institute, "Experimental Development of Dynamic Static Discharger System for Large Jet Aircraft," 1967, Contract AFAL-TR-67-313, SRI Project 6129.
8. J. E. Nanevicz and G. R. Hilbers, Stanford Research Institute, "Flight Test Evaluation of an Active Discharger System," 1970, Interim Technical Report 1 (Phase II), Contract F33615-68-C-1359, SRI Project 7104.
9. J. E. Nanevicz, D. G. Douglas, S. Blair Poteate, and B. J. Solak, Stanford Research Institute, "Experimental Investigation of Problems Associated with Discharging Hovering Helicopters," 1972, Contract AFAL-TR-72-325.
10. Rudolf G. Buser, Helmuth M. Kaunzinger, and Hans E. Inslerman, U.S. Army Electronics Command, Fort Monmouth, New Jersey, "Aerosol Discharge Systems for Heavy Lift Helicopters," 1972, Contract AFAL-TR-72-325.
11. B. J. Solak, J. E. Nanevicz, G. J. Wilson, and C. H. King, Stanford Research Institute, "Helicopter Cargo Handling--Electrostatic Considerations," 1972, Contract AFAL-TR-72-325, Lightning and Static Electricity Conference.
12. G. J. Born and E. J. Durbin, Instrumentation Control Laboratory Department of Aerospace and Mechanical Sciences, Princeton University, "A Passive Discharge System for the Electrically Charged Hovering Helicopter," 1972, Lightning and Static Electricity Conference, Contract AFAL-TR-72-325.
13. D. G. Douglas, J. E. Nanevicz, and B. J. Solak, SRI International, "Passive Potential Equalization Between the Cargo Handler and a Hovering Helicopter," 1973, Conference on Lightning and Static Electricity at Culham Laboratory, England, The Royal Aeronautical Society, England.
14. J. E. Nanevicz, Stanford Research Institute, "Investigation of Static Noise Problems on the HS-125 Aircraft," 1976, Final Report, Contract P.O. S-16724, SRI Project 674.
15. J. E. Nanevicz, SRI International, "Advanced Materials and Concepts for the Development of Antistatic Coatings for Aircraft Transparencies," 1973, Final Report, Contract F33615-72-C-2113, SRI Project 2393.

16. "The Properties and Application of Sierracote," Technical Paper presented by the Sierracin Corp., at the WADC-University of Dayton Joint Conference on Transparent Materials for Aircraft Enclosures, December 12, 1956.
17. G. J. Paladino and R. H. Sugarman, American Electronic Laboratories, Inc., "Integrated Receiver Interference Reduction Techniques," 1972, AFAL-TR-69-109, Contract F33615-67-C-1433.
18. A. Vassiliadis, Stanford Research Institute, "A Study of Corona Discharge Noise in Aircraft Antennas," 1960, AFCRL-TN-60-1107, Technical Report 70, Contract AF19(604)-3458.

AIRCRAFT STATIC CHARGING TESTING

by Joseph TAILLET

Office National d'Etudes et de Recherches Aéronautiques (ONERA)
92320 CHATILLON (FRANCE)

*
* *
*

SUMMARY

Aircraft protection against static charge accumulation involves minimum-noise electrostatic dischargers, perfect bonding of all conductors, antistatic painting of radomes and antenna covers, and conductive coatings of canopies. This paper deals with a procedure proposed for :

a) - characterizing in the laboratory the effects of aircraft charging on the operation of unprotected navigation and communication systems ; b) - assessing in the laboratory the validity of the above-mentioned methods of protection ; c) - checking in the factory the correct application of these methods ; d) - routine testing between flights, in the field, of the good condition of the protecting devices and treated surfaces.

It is hoped that careful application of this procedure will, in the near future, increase the reliability of navigation/communication systems during their operational use.

1 - INTRODUCTION

Static charge accumulation on aircraft structures can bring about three types of discharges : sparks between conductors, streamers over the insulating surfaces, and coronas at the sharp points and edges. All these discharges induce radioelectric noise on navigation/communication equipment, reducing its operational performance and impairing flight safety. [1].

The principles of a good protection against these harmful effects are well known [2]. Sparks can be avoided by a careful bonding of all the metallic parts of the aircraft. Superficial electric charges developed by friction or collected on insulators can be evacuated before initiation of a flash-over, if the surface resistance is kept below a certain value by using conductive paints or coatings on windshields, canopies, radomes and fairings. Lastly, the coupling between corona discharges and antennas of the communication/navigation systems can be drastically reduced by a careful choice of the configuration, the positions and the voltage threshold of the passive dischargers used for draining the static charges from the aircraft.

However, the practical application of these principles is today a matter of empiricism. On the one hand, apart from the possibility of performing a full in-flight experiment [3] [4], there is not yet a standard method for characterizing on a real aircraft, treated or untreated, all the disturbances induced in navigation/communication systems by the accumulation of charges. On the other hand, the in-flight experiment is an expensive task : the complexity of the full avionics system with its many interfering subsystems, the non-reproducibility of the meteorological situation from flight to flight, the inconvenience of recording, storing, packing and correlating a huge quantity of data, might turn such an experiment into a heavy burden with scanty results if these experiments have not been prepared by previous tests on the ground.

The situation is still worse if we go from the laboratory to the factory or to the airfield. No tool exists to verify, at the production stage, if the protection methods have been correctly applied during the construction of the aircraft ; no standard testing procedure has been elaborated for trial by the buyer. At the exploitation stage, no airline is in a position to routinely carry out maintenance tests between flights for verifying the good condition of the protective devices and of the treated surfaces. Meanwhile, from the field engineers to the pilots, everybody is convinced that such verification is badly needed : the dangerous disturbance induced in vital equipment by the discharges of static electricity is an universal worry.

The present lecture constitutes a step towards the definition of a standard procedure for testing aircraft charging phenomena and protections, in the laboratory, in the factory and in the field. Until such a procedure is operational and universally adopted by the research institutions, the aerospace industries and the airlines, a full protection against communication/navigation disturbances is not ensured during flights in very adverse atmospheric conditions.

In this paper, solutions are proposed for meeting the requirements of a safe protection. In order to apply the test method quickly and efficiently, specific instruments have been designed and implemented at ONERA, and are already available on the market in France. A general description of their performance is given below.

2 - TEST PROCEDURE REQUIREMENTS

The proposed test method shall fulfil the following functions :

a) - check the bonding between metallic surfaces, even if these surfaces are covered by an insulating coating ;

- b) - measure the value of surface resistance of semi-conductive coatings or resistive paints deposited over insulating substrate, even if these coatings are covered by a layer of highly insulating material ;
- c) - simulate tribo-electric charging or charge collection separately on any surface element of the aircraft, in order to determine the location and the nature of the more sensitive spots, and to assess the effect of the charging of these elements on the navigation/communication systems ;
- d) - verify that the coupling between dischargers and antennas is minimum, i.e. that the position of the dischargers is optimized, and that the noise collected by the antennas for a given discharge current is in conformity with the value announced in the specifications and has not increased because of some deterioration experienced by the dischargers.

During all this testing procedure, the aircraft shall be electrically grounded, or, if global operation of the dischargers is required, it shall be insulated by dielectric slabs placed below the wheels. This insulation shall be matched with the voltage limit due to the operation of the dischargers, in order to avoid flashover between aircraft and ground. A high resistance bleeder shall be used, for safety, to discharge the aircraft below the threshold voltage of the dischargers.

If any voltage generator is used for operations (c) or (d), its output impedance shall be kept very high, to insure safe operation.

Operations (a) and (b) are to be performed without damaging the superficial layer of paint.

Operation (c) shall be clean, i.e. without projection of particles or aerosols which could change the electrical properties of the surfaces or those of the environment. It shall be sufficiently well resolved in space to separate the effects of the charging of various elements (radome, fairings, antenna covers, canopies) on each navigation/communication system, and to permit the observation of local sparks due to a faulty bonding.

The validity of simulation (c) shall be confirmed by visual/auditory observation of the behavior of the navigation/communication instruments. Under such simulation tests and for a given electrostatic protection, an experienced pilot, seated in the cockpit, wearing earphones and watching the displays, shall identify the situation as similar to a real flight with different atmospheric conditions.

3 - VERIFICATION OF BONDING

The first step in testing aircraft on the ground for static charging is the drafting of a check-list of all the metallic parts of the structure. Bonding of all these pieces should be checked, even if they are clamped or riveted together. The presence of insulating gaskets -teflon gaskets, for example- or even corrosion of the rivets can impair the bonding. A reference point should be selected in the structure : the terminal generally provided for grounding the aircraft during refueling can be used, as well as the negative electrode of the power supply. Resistance between all the pieces included in the check-list and this reference point should be measured. If the pieces are not painted, an ohmmeter can be used. If they are covered by an insulating layer of paint, the only way of checking the bonding is with a capacitive method. For example, by using an electrode in contact with the insulating layer of paint, an alternating current at audio frequency is injected through the layer into the metallic piece. The second electrode of the audio generator is connected to the reference point. A high impedance sensing electrode measures, through the same layer, the A.C. voltage of the piece. If this voltage is not negligible with respect to the forcing electrode voltage, the bonding is not correct. The two electrodes can be arranged on the same measuring head, which can be used in the same way as a medical doctor uses a stethoscope (Fig. 1). This method takes advantage of the fact that, for static electricity elimination, bonding requirements are by no means stringent : two conductors can be considered as bonded if the resistance of their connection is lower than $10^5 \Omega$. Two problems arise when the design of the correlative instrument is considered :

- a) - the response should be independent of the thickness of the layer of paint, and of the pressure exerted by the operator on the measuring head ;
- b) - the device should be able to discover a poor bonding even in the case where the piece has a large capacitance with respect to the reference metallic structure.

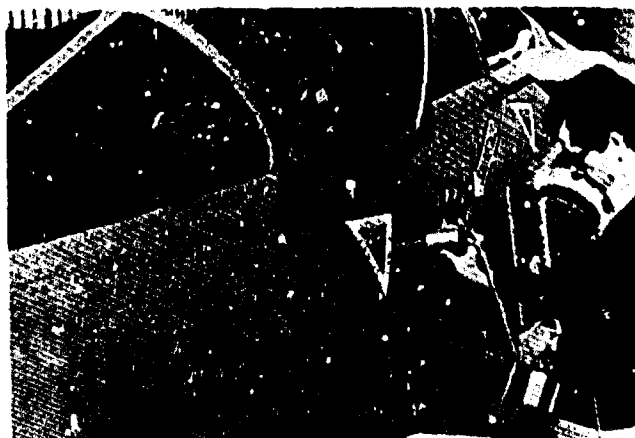


Fig. 1 - Checking the bonding of an Alphajet with the CORAS.

The solution results from a compromise between sensitivity and reasonable elimination of false alarms, which determines the choice of the operation frequency. The study of such a device was performed at ONERA and has led to the manufacture of a standard instrument sold under the trade name CORAS, which is being adopted by aircraft manufacturers in Europe (AMD-BA, DORNIER, AEROSPATIALE).

4 - SURFACE RESISTANCE MEASUREMENTS

The second step in testing aircraft on the ground for static charging is the drafting of the check list of all the insulating items appearing on the surface, and more particularly of the dielectric pieces exposed to triboelectric charging (radomes, windshields, canopies, fairings, antenna covers, plastic wing-tip, glass-fiber flaps, pneumatic deicing devices). If these pieces are not coated with a resistive layer, they can be the source of charge accumulation. The first effect of charge accumulation is corona initiation at the small radius of curvature points of the metallic pieces close to the charged dielectric. A second effect, which arises in the case of unprotected dielectric antenna caps, is corona initiation followed by sparking between the enclosed antenna and the dielectric cover (this implies local breakdown of the dielectric). A third effect is the initiation of a surface streamer.

The check-list should include measurements of surface resistances and measurements of the bonding of these surfaces. Dielectric surfaces are considered as having a good antistatic protection if their surface resistance (resistance of a square mesh) is below a threshold value ; they are unprotected if their surface resistance is above this value. They are bonded or unbonded according to whether the value of the resistance between a line located on their periphery and the reference point is below or above a threshold value.

Antistatic coatings are generally covered by an insulating layer of protective paint ; this is why only a capacitive method can be used to perform the measurement of surface resistance. This can be made if CORAS is used. The CORAS has a second head especially designed for that purpose. The surface resistance is measured in the same way as the resistance of a shunt ; the current is measured, and forced through the protective paint by two concentric ring electrodes ; two high impedance amplifiers connected to two intermediate rings measure the voltage. The electrode arrangement is located in the mobile head of the CORAS.

After the measurements have been performed, the various metallic pieces are classified as bonded or unbonded, and the various dielectric items are classified as treated or untreated by antistatic coating, and if they are treated, as bonded or unbonded. This classification is then used for making a decision about further protection. If some cases are still ambiguous, the decision can be delayed until ground simulation of static charging is performed.

5 - SIMULATION OF TRIBOELECTRIC CHARGING

If the aircraft to be tested were perfectly conducting over all its surface area, the charges induced by friction or collected in the atmosphere would be distributed according to the surface geometry. In this case, it would be sufficient, for performing a check on corona discharges location and on the associated R.F. noise, for example, to connect the surface to a high voltage generator, with the aircraft insulated. As field configuration can be roughly computed from model measurements, this kind of test is necessary only to verify that the passive dischargers are performing correctly, i.e. that all the corona discharges are located at their tips. We will come back to this type of measurement in the next section.

The real problem comes from the fact that no aircraft is perfectly conducting over all its surface, as radomes, canopies, windshields, fairings and antenna covers are insulating when not specifically treated to acquire total or partial surface conductivity. We want to have the following two answers.

- a) - For a given untreated dielectric surface, what are the consequences of a given local charging current on the operation of the navigation/communication systems of the aircraft ? This includes the anomalies induced, on the corresponding antenna, by charging both its dielectric cover and the other antenna covers.
- b) - If the same dielectric surface has been treated, is the applied treatment sufficient for complete elimination of all the observed anomalies, over the whole range of charging currents likely to be experienced in flight ?

By stressing that the source of radioelectric disturbances is essentially due to local coronas or streamers associated with the redistribution of charges accumulated on the insulating surfaces [5], [6], [7], it is easy to see that local charging of these surfaces will produce approximately the same effect if the aircraft structure is grounded through a high resistance or if the aircraft is in flight. This remark opens the way to a very important test, i.e. the observation of the effects of local streamers on the performance of navigation/communication systems, and for a complete verification of streamers disappearance when the insulating surfaces have been duly treated. What one needs for performing this test is a good source for locally charging the insulating surfaces.

Taking into account the order of magnitude of the charging current to be simulated, and also its very nature (surface charging by low energy and not by energetic particles), two types of processes can be used :

- a) - triboelectric charging, using a two-phase flow of air with a suspension of uncharged fine particles ; this method has yielded interesting results in the laboratory [7] [8] ; however the particles are not drained by the airflow as in flight, and their accumulation on the surfaces raises a serious problem, which is why this method has not been used in this work ;
- b) - charge collection using an injector of charged particles ; this method is good as long as an efficient charge injector is used ; it is this method that has been applied at ONERA, as described below.

Instead of using very high voltage generators, ONERA has extended a method first proposed by Whewell, Bright and Makin [9] following previous work by Marks, Baretto and Chu [10]. In the corresponding device, low mobility charged microparticles of ice, obtained by condensation and freezing of water vapour in humid air expanding in a supersonic nozzle, and driven by fluid friction in the jet, are used as charge carriers. This principle is applied to inject charges upon an insulating surface, in spite of the associated repulsive electric field. Note that the microparticles of ice sublime after leaving the supersonic region of the jet; this simulation method is therefore clean in the sense that the local properties (surface resistance and breakdown voltage) are not modified when the charge injector is operating. This device is marketed under the trade name INJECO.

Figure 2 is a schematic representation of the INJECO device. Figure 3 is a photograph of the instrument. Its main characteristics are listed in Table 1. Figure 4 shows how this injection is performed when testing a real aircraft; a first operator applies the charged flow upon a given antenna cover and, at the same time, a second operator watches the displays associated with the navigation equipment of the aircraft and estimates the noise collected by the communication receivers. Visual observation of induced sparking or streamers can also be performed (Fig. 5). The charging current sign and intensity can be controlled, ranging from low to high for simulation of weather conditions between fair and extreme. The difference between the cases of untreated and treated surfaces is striking and points out the importance of having a carefully applied surface treatment; associated with the surface resistance and bonding measurements, this simulation also permits a quantitative correlation of the reduction of the surface resistances (or the improvement of the bonding) with the decrease of the noise induced by aircraft charging on navigation/communication systems.

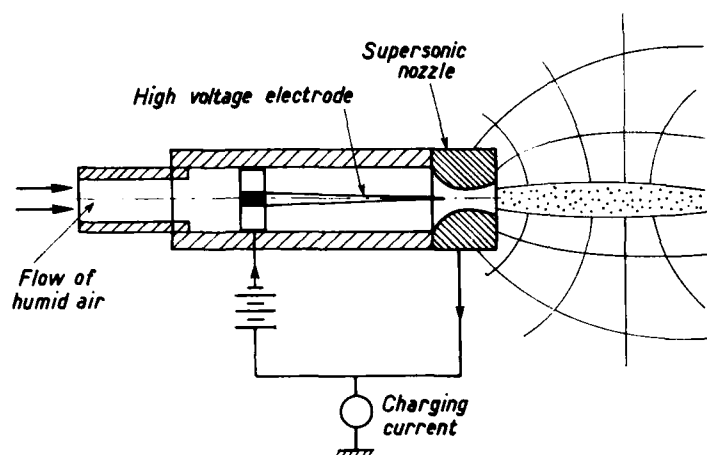


Fig. 2 - Diagram of the INJECO device.



Fig. 3 - INJECO with its power supply.



Fig. 4 - Simulating static charging with an aircraft on the ground.



Fig. 5 - Surface streamer produced by charging the fuselage.

Table 1 - INJECO characteristics.

Characteristics

Generating pressure	5 atm
Flow rate	20 Nm ³ /h
Power supply voltage	± 10 kV
Nozzle diameter	2.3 mm
Current	0 to 80 μA
Two polarities	

To apply this method one needs a supply of compressed air with a pressure of 6 atm, and a power supply with a voltage of 10 kV, positive and negative. Both can be readily operated in the laboratory, in the factory and on the airfield. As shown in Figure 3, the injection nozzle is of light weight, and can be easily used to charge any part of the aircraft. An important detail must be pointed out : in this experiment, the radioelectric disturbances are produced by local discharges following charge accumulation on insulating surfaces. Assessment of the noise produced by these discharges is possible only if the injector itself does not transmit any discharge noise ; this property is an important advantage of the described device and its achievement was the result of a careful design involving a difficult optimization process.

Apart from measurements performed on communication links (audio noise) and on subsystems especially instrumented for noise evaluation, a standard procedure for evaluation of performance of navigation systems is the following. It applies to automatic direction finders (ADF) in the HF range and to VHF navigation and landing aids (VOR, ILS).

A beacon, radiating at high power if located outside of the hangar where the test is performed, or at low power if located inside, is operated in conjunction with the equipment to be tested ; it gives a signal which results in a definite position of the pointer on the display. The operator on the pilot seat watches the display ; the second operator applies the charging flow of the INJECO upon various parts of the aircraft. The following measurements are performed for each sensitive spot :

- a) - value of the injected current corresponding to saturation of the ADF servo loop ;
- b) - value of the injected current corresponding to a given variation of the pointer's position for the VOR-ILS systems ;
- c) - value of the injected current corresponding to the disappearance of the flags.

6 - VERIFICATION OF THE DISCHARGERS

This verification directly follows the method introduced by Tanner and Nanevitz [1]. To avoid RF current circulation in ground lines, the aircraft reference terminal is connected to ground through a 20 MΩ resistor ; insulation of the structure is realized by thick dielectric slabs located under the wheels. To reduce the aircraft-to-ground capacitance, these slabs should be at least 4 inches thick. This operation is recommended for small aircraft, and may be difficult for large commercial aircraft. (Fig. 6)

The first step in this verification is the evaluation of the coupling between coronas and antennas. It can be performed with a corona probe which is constituted by an insulating tube having at its tip a point-to-plane arrangement (radius of the stressed tungsten electrode 50 μm ; point-to-plane distance 1 mm) where a negative corona is excited (average current 150 μA). Reference [1] describes in detail a slightly different arrangement.

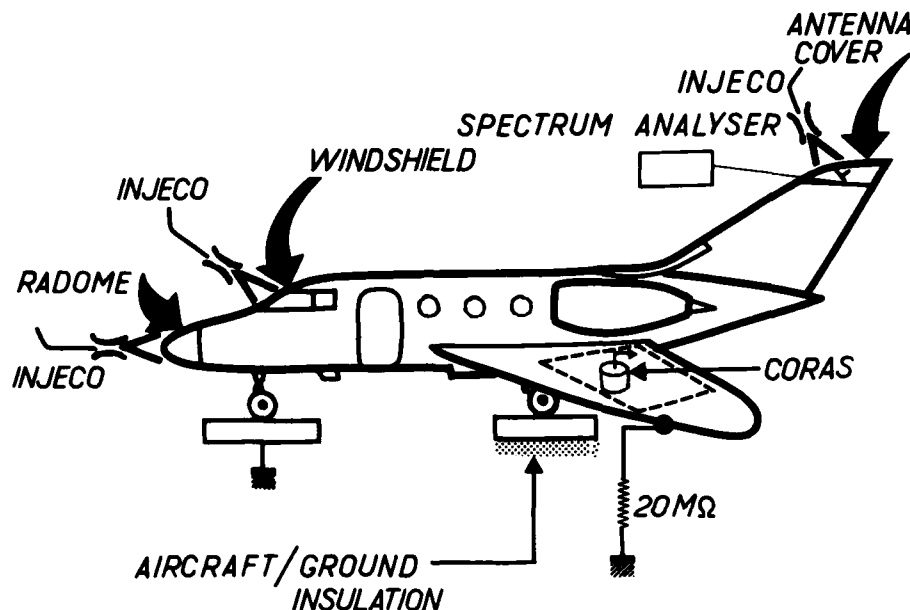


Fig. 6 - Block diagram of the experimental set-up used for aircraft testing.

The method consists of moving the reference discharge from point to point and of reading the noise current at the antenna terminals by connecting an appropriate receiver to these terminals. Next, the receiver is connected to parallel plate coupling electrodes, into which the probe is inserted. The coupling to reference point is determined from the coupling for the parallel plate electrodes (which can be computed) and the attenuation necessary to equalize the receiver noise outputs (see ref. [1]).

The second step consists in the measurement of the noise induced by the coronas excited at the tip of the dischargers. To perform this measurement, it is not necessary to apply a high voltage to the dischargers, nor to divert their average current through a microammeter; if an INJECO is used, by spreading positive charges over a discharger from a distance of about 10 cm, all the current is collected by the discharger tip. The average current can be read directly on the INJECO meter, and this simulation is made with the discharger connected to the structure as in its normal operation. This measurement can be performed by connecting a receiver to the antenna terminals and reading the noise current, or by evaluating the disturbances produced in the avionic equipment.

A third step, which is necessary only for making sure that no corona can be sustained over all the aircraft except at the dischargers tips, involves the connexion of the entire insulated aircraft to a high voltage power supply. During this check, the aircraft kerosene tanks should be full, or, if not, under nitrogen pressure. The connexion to the high voltage terminal is made through a high value resistor. In these conditions, the measurements can be safely performed by personnel working inside the aircraft. The verification consists in watching the various instruments while the high voltage is progressively raised. It is recommended in this case to instrument at least one discharger (for having a value of its average current) and to limit the maximum voltage of the power supply under a safety upper bound determined by the total maximum current of the dischargers. The insulating slabs should afford twice this voltage without flashover. If the disturbances produced during this check exceed the effect predicted from the sum of the noise induced by the various dischargers, a stray discharge is operating somewhere and should be discovered.

7 - ASSESSMENT OF THE ANTISTATIC PROTECTION OF THE AIRCRAFT

From the list established according to the method developed in § 3 and 4, and from the measurements performed according to the method described in § 5, recommendations are written up and decisions can be made about desirable improvements in bonding and antistatic coating. After completion of these improvements, a new check is made according to § 3, 4 and 5. Verification of dischargers performance, and, if necessary, optimization of their operation is then performed according to the method described in § 6.

The methodology described here has been applied in Europe to the following aircraft :

- Falcon 10
- Alpha-jet
- CESSNA 177
- CESSNA 337
- Mercure.

Its application of the AIRBUS is currently under study.

8 - CONCLUSION

This lecture has presented a procedure for evaluating the vulnerability of protected or unprotected aircraft to static charging, and for assessing the validity of the protection methods.

It is hoped that careful application of this test procedure will, in the near future, increase the reliability of navigation/communication systems during operational use.

REFERENCES

- [1] - R.L. TANNER and J.E. NANEVICZ - "An Analysis of Corona generated interference in Aircraft" - Proc. IEEE, 52, 1 (1964), p. 44-52.
- [2] - J.E. NANEVICZ, R.L. TANNER - "Some Techniques for the Elimination of Corona Discharge Noise in Aircraft Antennas" - Proc. IEEE, vol. 52, n° 1 (1964), p. 53-64.
- [3] - R.L. TRUAX - "Electrostatic Charging and Noise Quieting" - AFAL TR 72-325 (1972) Part II, p. 2763-2777.
- [4] - J.E. NANEVICZ, E.F. VANCE, R.L. TANNER, G.R. HILBERS - "Development and Testing of Techniques for Precipitation Static Interference Reduction" - Final Report, ADS TDR 62-38, SRI Project 2848, Stanford Res. Inst. Cal. (January 1962).
- [5] - R.L. TANNER and J.E. NANEVICZ - "Radio Noise Generated on Aircraft Surfaces" - Final Report, Contract AF33 (616) - 2761, SRI Project 1267, Stanford Res. Inst. Cal. (September 1956).
- [6] - R.C. TWOMEY - "Laboratory Simulated Precipitation Static Electricity and its Effects on Aircraft Windshield Subsystems" - IEEE Int. Symp. on Electromagnetic Compatibility, Seattle, Wash., Aug. 2-4, 1977, p. 201-206.
- [7] - M.B. MUNSELL and D.W. CLIFFORD - "R.F. Measurements of Electrostatic Discharges Produced by Triboelectric Charging of Non-Metallic Structures" - IEEE Int. Symp. on Electromagnetic Compatibility, Seattle, Wash., Aug. 2-4, 1977, p. 228-231.
- [8] - J.B. CHOWN, J.E. NANEVICZ - "Static Electricity Problems - VLF/Loran systems" - AFAL TR 72-325 (1972), Part 1, p. 59-71.
- [9] - B.R. WHEWELL, A.W. BRIGHT, B. MAKIN - "The Application of Charged Aerosol to the Discharge of Static from Aircraft" - 1st Int. Conf. on Static Electricity, Vienna, Austria (1970).
- [10] - A. MARKS, E. BARETTO and C.K. CHU - "Charged Aerosol Energy Converter" - AIAA Journal, Vol. 2, n° 1 (1964), p. 45-51.

Atmospheric Electricity - Aircraft Interactions

This Bibliography with Abstracts has been prepared to support AGARD Lecture Series No. 110 by the Scientific and Technical Information Branch of the U.S. National Aeronautics and Space Administration Washington, D.C., in consultation with the Lecture Series director, Mr. G. A. Dubro.

UTTL: Conference on Lightning and Static Electricity, Abingdon, Oxon, England, April 14-17, 1975. Proceedings. Conference sponsored by RAES, IEE, and SAE. London. Royal Aeronautical Society. 1975. 590 p. Papers are presented describing experimental and theoretical studies of lightning phenomena and their consideration in aircraft design. Some of the topics covered include lightning strike point studies on scale models, flight test studies of electrification on a supersonic aircraft, charge generation by commercial aircraft fuels and filter-separators, effects of simulated lightning strikes on mechanical strength of CFRP laminates and sandwich panels, passive potential equalization between the cargo handler and a hovering helicopter, radome protection, and electrical discharges caused by satellite charging at synchronous orbit altitudes. Individual items are announced in this issue. 75/00/00 75A14402

UTTL: Society of Automotive Engineers and U.S. Air Force Avionics Laboratory. Lightning and Static Electricity Conference. San Diego, Calif., December 9-11, 1970. Proceedings. SOCIETY OF AUTOMOTIVE ENGINEERS, INC., SOCIETY OF AUTOMOTIVE ENGINEERS AND U.S. AIR FORCE AVIONICS LAB., LIGHTNING AND STATIC ELECTRICITY CONFERENCE. SAN DIEGO, CALIF., DEC. 9-11, 1970. PROCEEDINGS. 70/00/00 71A19926

UTTL: Federal Aviation Administration Florida Institute of Technology Workshop on Grounding and Lightning Technology. CORP: Florida Inst. of Tech., Melbourne. CSS: (Dept. of Electrical Engineering.) Workshop held at Melbourne, Fla., 6-8 Mar. 1979. The articles presented were entitled: (1) Lightning Effects on General Aviation Aircraft; (2) A New Approach to Lightning Positioning and Tracking; (3) Design, Development and Fabrication of Devices for the Protection of Electronic Equipment Against Lightning; (4) Lightning Fatalities: Can They be Prevented?; and (5) Lightning Test Waveforms and Techniques for Aerospace Vehicles and Hardware. AD-A070779 FAA-RD-79-6-SUPPL-1A 79/05/00 79N30477

UTTL: Proceedings of the 2nd Annual Workshop on Meteorological and Environmental Inputs to Aviation Systems: Executive Summary. A/FROST, W.; B/CAMP, D. W.; C/CONNOLLY, J. W.; D/ENDERS, J. H.; E/SOWAR, J. F.; F/BURTON, M. L. PAA: A/(Tenn. Univ. Space Inst.); C/(NOAA, Rockville, Md.); D/(NASA, Washington); E/(FAA, Washington); F/(FAA, Washington) CORP: National Aeronautics and

UTTL: Conference on Certification of Aircraft for Lightning and Atmospheric Electricity Hazards. Chatillon-sous-Bagneux, Hauts-de-Seine, France, September 14-21, 1978. Proceedings. Conference supported by ONERA, U.S. Air Force, U.S. Navy, and NATO; Chatillon-sous-Bagneux, Hauts-de-Seine, France. Office National d'Etudes et de Recherches Aeronautiques, 1979. 221 p. In English and French. (For individual items see A79-51127 to A79-51148). The Conference focused on the theory of lightning phenomena, basic waveforms, lightning attachment and swept stroke testing, fuel vapor ignition and direct effects testing, indirect effects testing and lightning protection methodology, and static electricity. Specifically, papers were presented on laboratory tests to determine lightning attachment points with small aircraft, simulation of swept lightning strokes, laboratory tests to determine the possibility of ignition of fuel vapors by lightning, laboratory tests to determine the physical damage by lightning, test on actual aircraft for electromagnetic effects, direct effects protection methods for thin skins/composites, protection methods for hardware, static electricity phenomena and problems, fuel electrification, and aircraft testing. 79/00/00 79A51126

UTTL: Lightning. Volume 1 - Physics of lightning. Volume 2 - Lightning protection. A/GOLDE, R. H. London and New York, Academic Press, 1977. Vol. 1. 539 p.; vol. 2. 395 p. (For individual items see A78-16270 to A78-16274). Point discharges, cloud discharges, earth flashes, ball lightning and long sparks are discussed; lightning protection of aircraft, power transmission lines and telecommunications systems is also considered. Subjects treated in the papers include the measurement of lightning current amplitude and wave shape, lightning spectroscopy, atmospherics and radio noise generated by lightning, techniques for measuring the electric field and field-change associated with thunderstorms, protection of rockets from lightning hazards during launch, forecasting of lightning hazards, protection of power distribution systems, and insulation to prevent lightning overvoltage in power lines. 77/00/00 78A16269

Space Administration. Marshall Space Flight Center, Huntsville, Ala. In Tenn. Univ. Space Inst. Proc. of the 2nd Ann. Workshop on Meteorol. and Environ. Inputs to Aviation Systems p 1-14 (SEE N79-17413 08-47)
A summarization of committee findings relative to the five topic areas of severe storms, turbulence, icing, visibility and lightning is given. 78/03/00 79N17414

UTTL: Airborne measurement of electromagnetic environment near thunderstorm cells. TRIP-76 A/NANEVICZ, J. E.; B/ADAMO, R. C.; C/BLY, R. T., JR. CORP: Stanford Research Inst., Menlo Park, Calif. The increasing use of digital equipment and nonmetallic structures on aerospace vehicles has focused new attention on the potential electromagnetic threat posed by the lightning and thunderstorm environment. To better define this threat, a quick reaction airborne lightning measurement effort was undertaken. Digital 'snapshot' data and continuous analog spectrum analyzer data were alternately recorded on an instrumented NASA Learjet during 29 flights. Recorded events included one direct lightning strike and many nearby strikes, as well as 'incipient lightning' streamers and non-lightning-associated signals. A comparison with nuclear EMP waveforms is given, indicating nearby lightning to be a far more energetic threat than EMP at low frequencies, and that it is non-negligible at 10 MHz and above. NASA-CR-157642 AD-A060875 AFFDL-TR-77-62 77/08/00 79N15514

UTTL: Federal Aviation Administration - Georgia Institute of Technology Workshop on Grounding and Lightning Protection CORP: Georgia Inst. of Tech., Atlanta. Workshop held at Atlanta, 2-4 May 1978. A state-of-art review and background research reveals a number of opinions as to the preferred techniques of grounding of electronic equipment and systems. These techniques become important when protection must be provided for transients induced by lightning, electromagnetic pulses and other sources. AD-A058797 FAA-RD-78-83 78/05/00 79N12332

UTTL: Lightning protection of aircraft A/FISHER, F. A.; B/PLUMER, J. A. CORP: General Electric Co., Pittsfield, Mass. NASA-RP-1008 77/10/00 78N11024

UTTL: Conference on Lightning and Static Electricity A/HARRIS, M. S. CORP: Office of Naval Research, London (England). Conf. held at Abingdon Engl., 14-18 Apr. 1975
A four-day international conference on lightning and static electricity was sponsored by the Royal Aeronautical Society and the U.S. Atomic Energy Agency's Culham Laboratory at Culham on 14-18 April 1975. The meeting was primarily devoted to describing effects of lightning and static electricity on aircraft and components, laboratory simulation of these effects, and methods to prevent aircraft damage. This report discusses some of the European papers presented in the five sessions of the conference: Fundamental Aspects and Test Criteria, Fuels, Structures and Materials, Aircraft Application, and Missiles and Spacecraft. AD-A011443 ONRL-C-11-75 75/00/00 76N10624

UTTL: Lightning and Static Electricity Conference CORP: Air Force Avionics Lab., Wright-Patterson AFB, Ohio. Conf. held at Las Vegas, Nev., 12-15 Dec. 1972; sponsored by AFAL and SAE
The document contains the text of unclassified papers presented at the 1972 Conference on Lightning and Static Electricity, held 12-15 December 1972. The papers document the discussion of the theoretical aspects of both lightning and atmospheric electrification. In addition, the practical control of adverse effects is addressed relative to aerospace vehicles and installations. Sessions include fundamental aspects, missiles and spacecraft, aircraft, advanced composites, fuels, and lightning simulation. AD-752551 AFAL-TR-72-325 72/12/00 73N17552

UTTL: Lightning and Static Electricity Conference, Part 2 - Conference papers CORP: Air Force Systems Command, Wright-Patterson AFB, Ohio. CSS: (AVIONICS LAB.) CONF. HELD AT MIAMI BEACH, FLA., 3-5 DEC. 1968 SPONSORED BY AF AND THE SOC. OF AUTOMOTIVE ENGR. AD-693135 AFAL-TR-68-290-PT-2 69/05/00 70N19027

Lightning A/Uman, Martin A. McGraw-Hill New York. 1969 QC966.U4 551.5632 LC-68-8036 72V16139

Atmospheric electricity A/Chalmers, John Alan. Pergamon Press Oxford, New York. 1967 QC961.C46 1967 551.56 LC-68-29669 72V12403

REPORT DOCUMENTATION PAGE

1. Recipient's Reference	2. Originator's Reference	3. Further Reference	4. Security Classification of Document								
	AGARD-LS-110	ISBN 92-835-1361-4	UNCLASSIFIED								
5. Originator	Advisory Group for Aerospace Research and Development North Atlantic Treaty Organization 7 rue Ancelle, 92200 Neuilly sur Seine, France										
6. Title	ATMOSPHERIC ELECTRICITY AIRCRAFT INTERACTION										
7. Presented at	a Lecture Series under the sponsorship of the Avionics Panel and the Consultant and Exchange Programme of AGARD, on 9-10 June 1980 in London, UK; 12-13 June 1980 in Munich, Germany and 24-25 June 1980 at Menlo Park, California, USA.										
8. Author(s)/Editor(s)			9. Date								
Various			May 1980								
10. Author's/Editor's Address			11. Pages								
Various			236								
12. Distribution Statement	This document is distributed in accordance with AGARD policies and regulations, which are outlined on the Outside Back Covers of all AGARD publications.										
13. Keywords/Descriptors	<table border="0"> <tr> <td>Avionics</td> <td>Flight control</td> </tr> <tr> <td>Airborne equipment</td> <td>Electromagnetic interference</td> </tr> <tr> <td>Lightning</td> <td>Static electricity</td> </tr> <tr> <td>Atmospheric electricity</td> <td></td> </tr> </table>			Avionics	Flight control	Airborne equipment	Electromagnetic interference	Lightning	Static electricity	Atmospheric electricity	
Avionics	Flight control										
Airborne equipment	Electromagnetic interference										
Lightning	Static electricity										
Atmospheric electricity											

14. Abstract

The potential susceptibility of aircraft to atmospheric electricity hazards (such as lightning and static charging phenomena) appears as an increasing threat to future aircraft for two reasons: on the one hand, more and more sensitive solid-state electronics and micro-processors will be used in the future on flight critical equipment, as can be anticipated from advanced guidance and control hardware developments; on the other hand, new structural materials, such as dielectrics and composites, will be extensively used for aircraft, leading to potential problems due to surface charges and reducing the electromagnetic shielding protection offered by the conventional metallic skins on present-day vehicles.

Starting with fundamentals of atmospheric electricity phenomena, the Lecture Series reviews the hazards, criteria, testing and avionics protection, and provides insights from both pilot and design perspectives. In view of the above, this Lecture Series should be of interest to aircraft manufacturers, airline operators, government and industrial research establishments, and avionics engineers.

<p>AGARD Lecture Series No.110 Advisory Group for Aerospace Research and Development, NATO ATMOSPHERIC ELECTRICITY - AIRCRAFT INTER-ACTION Published May 1980 236 pages</p> <p>The potential susceptibility of aircraft to atmospheric electricity hazards (such as lightning and static charging phenomena) appears as an increasing threat to future aircraft for two reasons: on the one hand, more and more sensitive solid-state electronics and microprocessors will be used in the future on flight critical equipment, as can be anticipated from advanced guidance and control hardware developments: on the other hand,</p> <p>P.T.O.</p>	<p>AGARD-LS-110</p> <p>Avionics Airborne equipment Lightning Atmospheric electricity Flight control Electromagnetic interference Static electricity</p>	<p>AGARD Lecture Series No.110 Advisory Group for Aerospace Research and Development, NATO ATMOSPHERIC ELECTRICITY - AIRCRAFT INTER-ACTION Published May 1980 236 pages</p> <p>The potential susceptibility of aircraft to atmospheric electricity hazards (such as lightning and static charging phenomena) appears as an increasing threat to future aircraft for two reasons: on the one hand, more and more sensitive solid-state electronics and microprocessors will be used in the future on flight critical equipment, as can be anticipated from advanced guidance and control hardware developments: on the other hand,</p> <p>P.T.O.</p>	<p>AGARD-LS-110</p> <p>Avionics Airborne equipment Lightning Atmospheric electricity Flight control Electromagnetic interference Static electricity</p>
<p>AGARD Lecture Series No.110 Advisory Group for Aerospace Research and Development, NATO ATMOSPHERIC ELECTRICITY - AIRCRAFT INTER-ACTION Published May 1980 236 pages</p> <p>The potential susceptibility of aircraft to atmospheric electricity hazards (such as lightning and static charging phenomena) appears as an increasing threat to future aircraft for two reasons: on the one hand, more and more sensitive solid-state electronics and microprocessors will be used in the future on flight critical equipment, as can be anticipated from advanced guidance and control hardware developments: on the other hand,</p> <p>P.T.O.</p>	<p>AGARD-LS-110</p> <p>Avionics Airborne equipment Lightning Atmospheric electricity Flight control Electromagnetic interference Static electricity</p>	<p>AGARD Lecture Series No.110 Advisory Group for Aerospace Research and Development, NATO ATMOSPHERIC ELECTRICITY - AIRCRAFT INTER-ACTION Published May 1980 236 pages</p> <p>The potential susceptibility of aircraft to atmospheric electricity hazards (such as lightning and static charging phenomena) appears as an increasing threat to future aircraft for two reasons: on the one hand, more and more sensitive solid-state electronics and microprocessors will be used in the future on flight critical equipment, as can be anticipated from advanced guidance and control hardware developments: on the other hand,</p> <p>P.T.O.</p>	<p>AGARD-LS-110</p> <p>Avionics Airborne equipment Lightning Atmospheric electricity Flight control Electromagnetic interference Static electricity</p>

<p>new structural materials, such as dielectrics and composites, will be extensively used for aircraft, leading to potential problems due to surface charges and reducing the electromagnetic shielding protection offered by the conventional metallic skins on present-day vehicles.</p> <p>Starting with fundamentals of atmospheric electricity phenomena, the Lecture Series reviews the hazards, criteria, testing and avionics protection, and provides insights from both pilot and design perspectives. In view of the above, this Lecture Series should be of interest to aircraft manufacturers, airline operators, government and industrial research establishments, and avionics engineers.</p> <p>The material in this publication was assembled to support a Lecture Series under the sponsorship of the Avionics Panel and the Consultant and Exchange Programme of AGARD, presented on 9-10 June 1980 in London, UK; 12-13 June 1980 Munich, Germany and 24-25 June 1980 Menlo Park, California, USA.</p> <p>ISBN 92-835-1361-4</p>	<p>new structural materials, such as dielectrics and composites, will be extensively used for aircraft, leading to potential problems due to surface charges and reducing the electromagnetic shielding protection offered by the conventional metallic skins on present-day vehicles.</p> <p>Starting with fundamentals of atmospheric electricity phenomena, the Lecture Series reviews the hazards, criteria, testing and avionics protection, and provides insights from both pilot and design perspectives. In view of the above, this Lecture Series should be of interest to aircraft manufacturers, airline operators, government and industrial research establishments, and avionics engineers.</p> <p>The material in this publication was assembled to support a Lecture Series under the sponsorship of the Avionics Panel and the Consultant and Exchange Programme of AGARD, presented on 9-10 June 1980 in London, UK; 12-13 June 1980 Munich, Germany and 24-25 June 1980 Menlo Park, California, USA.</p> <p>ISBN 92-835-1361-4</p>
<p>new structural materials, such as dielectrics and composites, will be extensively used for aircraft, leading to potential problems due to surface charges and reducing the electromagnetic shielding protection offered by the conventional metallic skins on present-day vehicles.</p> <p>Starting with fundamentals of atmospheric electricity phenomena, the Lecture Series reviews the hazards, criteria, testing and avionics protection, and provides insights from both pilot and design perspectives. In view of the above, this Lecture Series should be of interest to aircraft manufacturers, airline operators, government and industrial research establishments, and avionics engineers.</p> <p>The material in this publication was assembled to support a Lecture Series under the sponsorship of the Avionics Panel and the Consultant and Exchange Programme of AGARD, presented on 9-10 June 1980 in London, UK; 12-13 June 1980 Munich, Germany and 24-25 June 1980 Menlo Park, California, USA.</p> <p>ISBN 92-835-1361-4</p>	<p>new structural materials, such as dielectrics and composites, will be extensively used for aircraft, leading to potential problems due to surface charges and reducing the electromagnetic shielding protection offered by the conventional metallic skins on present-day vehicles.</p> <p>Starting with fundamentals of atmospheric electricity phenomena, the Lecture Series reviews the hazards, criteria, testing and avionics protection, and provides insights from both pilot and design perspectives. In view of the above, this Lecture Series should be of interest to aircraft manufacturers, airline operators, government and industrial research establishments, and avionics engineers.</p> <p>The material in this publication was assembled to support a Lecture Series under the sponsorship of the Avionics Panel and the Consultant and Exchange Programme of AGARD, presented on 9-10 June 1980 in London, UK; 12-13 June 1980 Munich, Germany and 24-25 June 1980 Menlo Park, California, USA.</p> <p>ISBN 92-835-1361-4</p>